METABOLIC REGULATION OF DRUG RESISTANCE AND PATHOGENICITY IN AQUATIC PATHOGENS

EDITED BY: Bo Peng, Xinhua Chen and Hetron M. Munang'andu
PUBLISHED IN: Frontiers in Microbiology

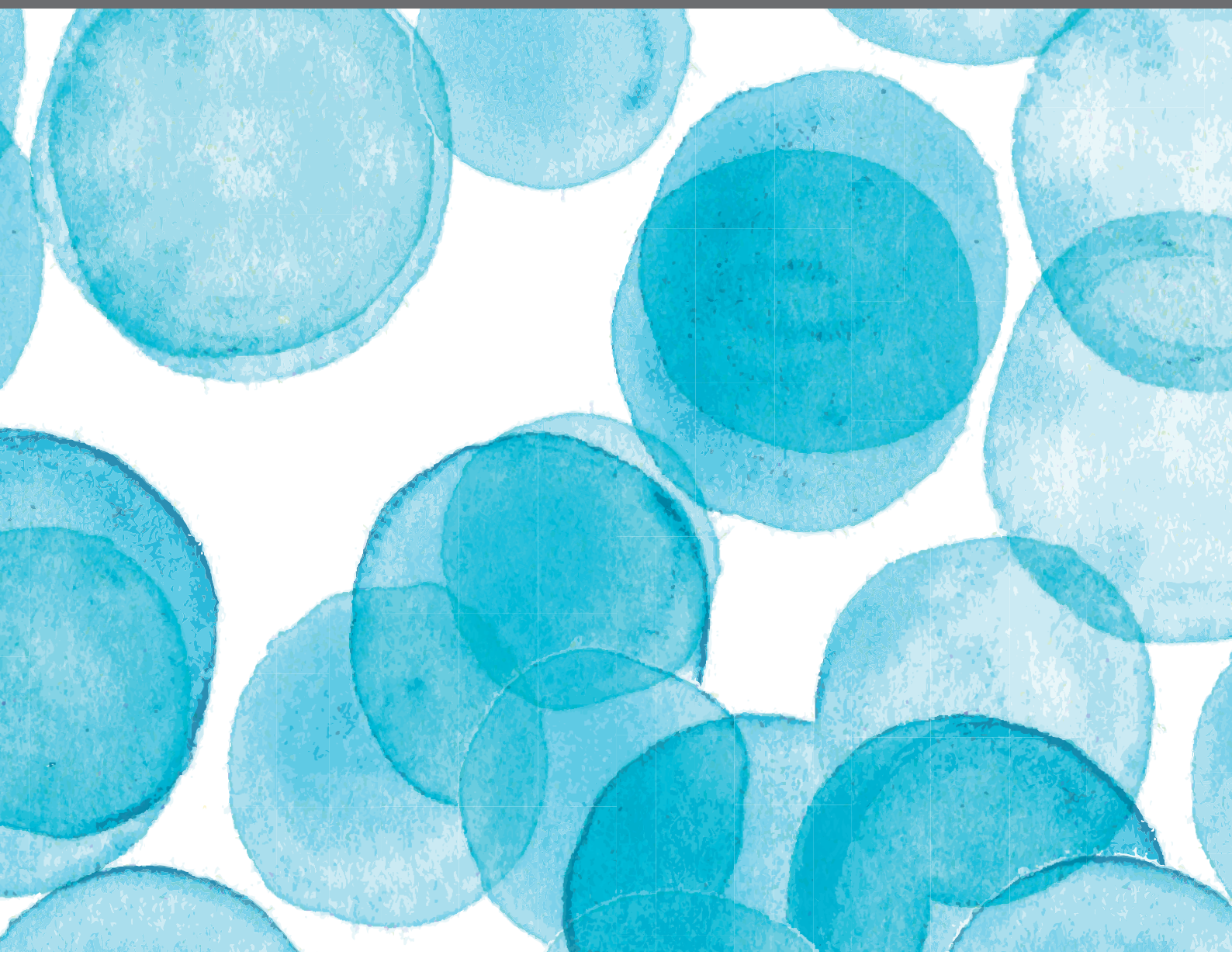

frontiers Research Topics

frontiers

ISSN 1664-8714
ISBN 978-2-88974-584-5
DOI 10.3389/978-2-88974-584-5

About Frontiers

Frontiers is more than just an open-access publisher of scholarly articles: it is a pioneering approach to the world of academia, radically improving the way scholarly research is managed. The grand vision of Frontiers is a world where all people have an equal opportunity to seek, share and generate knowledge. Frontiers provides immediate and permanent online open access to all its publications, but this alone is not enough to realize our grand goals.

Frontiers Journal Series

The Frontiers Journal Series is a multi-tier and interdisciplinary set of open-access, online journals, promising a paradigm shift from the current review, selection and dissemination processes in academic publishing. All Frontiers journals are driven by researchers for researchers; therefore, they constitute a service to the scholarly community. At the same time, the Frontiers Journal Series operates on a revolutionary invention, the tiered publishing system, initially addressing specific communities of scholars, and gradually climbing up to broader public understanding, thus serving the interests of the lay society, too.

Dedication to Quality

Each Frontiers article is a landmark of the highest quality, thanks to genuinely collaborative interactions between authors and review editors, who include some of the world's best academicians. Research must be certified by peers before entering a stream of knowledge that may eventually reach the public - and shape society; therefore, Frontiers only applies the most rigorous and unbiased reviews.
Frontiers revolutionizes research publishing by freely delivering the most outstanding research, evaluated with no bias from both the academic and social point of view. By applying the most advanced information technologies, Frontiers is catapulting scholarly publishing into a new generation.

What are Frontiers Research Topics?

Frontiers Research Topics are very popular trademarks of the Frontiers Journals Series: they are collections of at least ten articles, all centered on a particular subject. With their unique mix of varied contributions from Original Research to Review Articles, Frontiers Research Topics unify the most influential researchers, the latest key findings and historical advances in a hot research area! Find out more on how to host your own Frontiers Research Topic or contribute to one as an author by contacting the Frontiers Editorial Office: frontiersin.org/about/contact

METABOLIC REGULATION OF DRUG RESISTANCE AND PATHOGENICITY IN AQUATIC PATHOGENS

Topic Editors:
Bo Peng, Sun Yat-sen University, China
Xinhua Chen, Fujian Agriculture and Forestry University, China
Hetron M. Munang'andu, Nord University, Norway

Citation: Peng, B., Chen, X., Munang'andu, H. M., eds. (2022). Metabolic Regulation of Drug Resistance and Pathogenicity in Aquatic Pathogens. Lausanne: Frontiers Media SA. doi: 10.3389/978-2-88974-584-5

Table of Contents

frontiers in Microbiology

EDITORIAL
published: 03 February 2022
doi: 10.3389/fmicb.2021.832756

Editorial: Metabolic Regulation of Drug Resistance and Pathogenicity in Aquatic Pathogens

Bo Peng[1]*, *Xinhua Chen*[2,3]* and *Hetron Mweemba Munang'andu*[4]*

[1] State Key Laboratory of Biocontrol, Guangdong Key Laboratory of Pharmaceutical Functional Genes, School of Life Sciences, Southern Marine Science and Engineering Guangdong Laboratory (Zhuhai), Higher Education Mega Center, Sun Yat-sen University, Guangzhou, China, [2] Key Laboratory of Marine Biotechnology of Fujian Province, Institute of Oceanology, Fujian Agriculture and Forestry University, Fuzhou, China, [3] Laboratory for Marine Biology and Biotechnology, Qingdao National Laboratory for Marine Science and Technology, Qingdao, China, [4] Department of Production Medicine and Science, Section of Experimental Bio-Medicine, Norwegian University of Life Sciences, Ås, Norway

Keywords: metabolic regulation, antibiotic resistance, pathogenicity, aquaculture, bacterial pathogen

Editorial on the Research Topic

Metabolic Regulation of Drug Resistance and Pathogenicity in Aquatic Pathogens

Aquaculture is an important sector in the food industry able to provide micronutrients to humans, especially in the context of the decline of wild stock of aquatic animals. One big challenge for aquaculture is the infectious diseases that are hard to treat due to the emergence of antibiotic-resistant bacteria (ARB). However, this aspect of ARB has been largely ignored in the past. So that antibiotics are overused to control infectious diseases caused by ARB. Therefore, strategies should be developed to not only manage the antibiotic resistance, but also develop alternative means to control bacterial infection in an antibiotic-independent way, e.g., anti-infective strategy.

Microbial metabolism plays central roles in regulating biological processes including drug resistance and pathogenicity. Bacterial pathogens become resistant to antimicrobials using different mechanisms such as mutations in the cell wall leading to restrictions of drug permeability hindering access to target sites, active efflux of the drug from cells, acquisition of alternative pathways inhibiting drug entry, as well as modification of drug targets (Van Hoek et al., 2011). Metabolic alterations that render microbes to become more pathogenic or refractory to antimicrobials are important mediators of pathogenicity or drug resistance. Therefore, rewiring these metabolic alterations is the key to finding effective strategies for preventing drug resistance and reducing the virulence of pathogens in aquatic organisms. To address these knowledge gaps, this Research Topic aimed at gathering contributions to the Frontiers Research Topic on "*Metabolic Regulation of Drug Resistance and Pathogenicity in Aquatic Pathogens*" for which we were honored to serve as Guest Editors. We gathered a total of 12 articles that present state-of-the-art knowledge on the Research Topic. As outlined below, the articles gathered were broadly grouped into metabolic regulation of (i) drug resistance, and (ii) pathogenicity.

The use of high throughput sequencing (HTS) technologies permits identification of numerous antimicrobial resistance (AMR) genes and pathways that regulate drug resistance. Thus, there exist several platforms and databases for identification of AMR genes as shown by Sakulworakan et al. who analyzed the resistome of *Aeromonas veronii* isolated from diseased tilapia and detected 20 antibiotic resistance genes (ARG)s of which 16 were shared among *A. veronii* populations worldwide. Fu et al. used the data-independent acquisition (DIA) quantitative proteomics method and found a total of 594 differentially expressed genes (DEGs) between the mutant (Δ*yeeY*) and wild-type strain under Furazolidone (FZ) treatment. Using the bacterial drug resistance gene database (CARD), 34 AMR genes were found to be regulated by the YeeY mutant. Several biological

OPEN ACCESS

Edited and reviewed by:
Rustam Aminov,
University of Aberdeen,
United Kingdom

***Correspondence:**
Bo Peng
pengb26@mail.sysu.edu.cn
Xinhua Chen
chenxinhua@tio.org.cn
Hetron Mweemba Munang'andu
hetroney.mweemba.munangandu
@nmbu.no

Specialty section:
This article was submitted to Antimicrobials, Resistance and Chemotherapy, a section of the journal Frontiers in Microbiology

Received: *10 December 2021*
Accepted: *31 December 2021*
Published: *03 February 2022*

Citation:
Peng B, Chen X and Munang'andu HM (2022) Editorial: Metabolic Regulation of Drug Resistance and Pathogenicity in Aquatic Pathogens. Front. Microbiol. 12:832756. doi: 10.3389/fmicb.2021.832756

pathways such as the secretion system and protein transport were involved in FZ resistance. Liu et al. reviewed the methods used for combating antibiotic tolerance and distinguished antibiotic resistance from tolerance. They showed that exogenous metabolites including amino acids, tricarboxylic acid cycle (TCA cycle) metabolites, and nucleotides effectively activate bacterial metabolism and convent the tolerant cells to sensitive cells.

Gene deletions and knockout systems are the key to elucidating the functional roles of genes that regulate drug metabolism. Fu et al. used gene deletion antibiotics susceptibility assays to show that the YeeY mutant encoded vital genes that regulate FZ resistance in *A. hydrophila*. By comparing protein profiles of *ahslyA* knockout and wild type in *A. hydrophila* strains expressed by the transcriptional regulators (TRs) enoxacin (ENX), Li Z. et al. showed that *ahslyA* deletion upregulated antibiotic resistance proteins of *A. hydrophila* upon ENX stress, pointing to the vital role of *ahslyA* in regulating antibiotic resistance in bacteria. Similarly, Wang et al. showed that deletion of *Hfq* in *A. veroni*i led to increased trimethoprim resistance accompanied by downregulation of the efflux pump related genes acrA and acrB while complementation of acrA and acrB in Δhfq reversed the resistance. This study demonstrated that Hfq mediated trimethoprim resistance by elevating the efflux pump expression. Altogether, these studies underscore the importance of mutational changes in regulating drug metabolism.

Antibiotic resistance or tolerance is strongly correlated with bacterial metabolism, which is an attractive spot for developing intervening approaches for control antibiotic resistance. Ortiz-Severín et al. showed that nutrient scarcity can lead to antibiotic resistance. They showed that all *Piscirickettsia salmonis* strains grown in nutrient-limited media were resistant to ampicillin, erythromycin, penicillin G, streptomycin, spectinomycin, polymyxin B, ceftazidime, and trimethoprim in a nutrient deficiency dependent manner. Ampicillin resistance was linked to decrease in bacterial metabolism that included the TCA cycle, pentose-phosphate pathway, energy production, and nucleotide metabolism. Contrariwise, some chemical formulations and metabolites have been shown to enhance bacteria susceptibility to drug treatment. For example, Gao et al. showed that *A. hydrophila*, *Vibrio harveyi*, *V. fluvialis*, *V. alginolyticus*, *E. tarda*, and *Streptococcus iniae* can be rapidly killed during their stationary growth phase after immersion in gentamicin- or neomycin-containing ion-free solutions. They noted that hypoionic shock enhanced bacterial uptake of gentamicin in an ATP-dependent manner thereby enhancing the killing effect of *A. hydrophila* in infected zebrafish (*Danio rerio*). In another study, Srinivasan et al. showed that naringin (NA) can be used as an anti-quorum sensing (QS) compound resulting in reduced biofilm formation in *A. hydrophila*. In zebrafish infected with *A. hydrophila* the recovery rate increased upon NA treatment. Altogether, these studies show that factors that influence bacteria growth such as nutrient scarcity, metabolites like NA as well as compounds like hypo-ionic solutions have a significant influence on bacteria susceptibility or resistance to antimicrobials.

Discovery of novel genes that regulate pathogenicity is essential for understanding the cellular mechanisms of disease establishment. Li D. Y. et al. identified a novel T6SS effector, named EvpQ, encoded by mobile genetic elements in the *E. piscicida* genome. Sequence analysis reveals that EvpQ shares a conserved domain of C70 family cysteine protease with the T3SS effector AvrRpt2 of phytopathogenic *Erwinia amylovora*. Discovery of the EvpQ gene in the T6SS effector is bound to enhance our understanding of the pathogenicity of T6SS in edwardsiellosis.

Elucidating gene functions that regulate bacteria pathogenicity is sometimes better explained using gene knockouts or mutant strains. After characterizing the type II TA system based on the YefM-YoeB gene of *E. piscicida* where YoeB is the toxin shown to arrest bacterial growth restored by the adding the antitoxin YefM, Ma et al. constructed *yoeB* and *yefM-yoeB* in-frame mutant strains of which *yefM-yoeB* was shown to reduce resistance against oxidative stress and antibiotics while its deletion enhanced bacterial high temperature tolerance, biofilm formation, and host serum resistance. In addition, *yefM-yoeB* was shown to enhance bacterial host cells adhesion, dissemination, and virulence in fish tissues. In another study, Hu et al. investigated the effect of the *tonB* gene on the virulence of *Pseudomonas plecoglossicida* by knocking down the *tonB* with RNAi. The differences between the wild-type and *tonB*-RNAi strains showed that *tonB* regulates virulence through motility, chemotaxis, adhesion, and biofilm formation in *P. plecoglossicida* infections. These studies demonstrated the use of gene knockdown and other mutational changes to underpin the functional roles of genes regulating pathogenicity.

Novel platforms for microbial gene analysis are highly needed for elucidating networks that regulate microbial virulence and drug resistance. Xie et al. developed an online network platform called AbviresDB, integrating co-functional multiple sources of data from *Acinetobacter baumannii*. They used the k-shell decomposition approach to analyze the co-functional network and showed that genes involved in basic cellular physiological function such as drug resistance genes had high k-shell values while non-essential genes like virulence genes had lower k-shell values. They showed that ABviresDB platform can be used for visualization of each gene in the network having the potential for drug resistance and pathogenesis research.

Altogether, this Research Topic outlines metabolic regulations that can be exploited to overcome drug resistance and pathogenicity of pathogens infecting aquatic organisms. We are confident that the information availed in the articles will advance our understanding of the metabolic regulation of drug resistance and pathogenicity. We also envisage that data presented in these articles will contribute to developing preventive measures against drug resistance and to reducing the prevalence of infectious diseases of aquatic organisms.

AUTHOR CONTRIBUTIONS

All authors listed have made a substantial, direct, and intellectual contribution to the work and approved it for publication.

FUNDING

This work was sponsored by grants from NSFC project (Nos. 32061133007 and U1905204), China Agriculture Research System (CARS-47), Project supported by Innovation Group Project of Southern Marine Science and Engineering Guangdong Laboratory Zhuhai (No. 311020006), and Research Council of Norway RCN (No. 320692).

ACKNOWLEDGMENTS

We highly acknowledge the contributions of every author and reviewers that made their contribution to this Research Topic.

REFERENCES

Van Hoek, A. H., Mevius, D., Guerra, B., Mullany, P., Roberts, A. P., and Aarts, H. J. (2011). Acquired antibiotic resistance genes: an overview. *Front. Microbiol.* 2:203. doi: 10.3389/fmicb.2011.00203

Conflict of Interest: The authors declare that the research was conducted in the absence of any commercial or financial relationships that could be construed as a potential conflict of interest.

frontiers in Microbiology

ORIGINAL RESEARCH
published: 09 September 2020
doi: 10.3389/fmicb.2020.577376

The LysR-Type Transcriptional Regulator YeeY Plays Important Roles in the Regulatory of Furazolidone Resistance in *Aeromonas hydrophila*

Yuying Fu[1,2], Lishan Zhang[1,2], Guibin Wang[1,2,3], Yuexu Lin[1,2], Srinivasan Ramanathan[1,2], Guidi Yang[1,2], Wenxiong Lin[1,2] and Xiangmin Lin[1,2,4]**

[1] Fujian Provincial Key Laboratory of Agroecological Processing and Safety Monitoring, School of Life Sciences, Fujian Agriculture and Forestry University, Fuzhou, China, [2] Key Laboratory of Crop Ecology and Molecular Physiology (Fujian Agriculture and Forestry University), Fujian Province University, Fuzhou, China, [3] State Key Laboratory of Proteomics, Beijing Proteome Research Center, National Center for Protein Sciences (Beijing), Beijing Institute of Lifeomics, Beijing, China, [4] Key Laboratory of Marine Biotechnology of Fujian Province, Institute of Oceanology, Fujian Agriculture and Forestry University, Fuzhou, China

OPEN ACCESS

Edited by:
Bo Peng,
Sun Yat-sen University, China

Reviewed by:
Shanmuganathan – Balakrishnan,
Upstate Medical University,
United States
Suganthy Natarajan,
Alagappa University, India

***Correspondence:**
Wenxiong Lin
lwx@fafu.edu.cn
Xiangmin Lin
xiangmin@fafu.edu.cn

Specialty section:
This article was submitted to Antimicrobials, Resistance and Chemotherapy, a section of the journal Frontiers in Microbiology

Received: 29 June 2020
Accepted: 19 August 2020
Published: 09 September 2020

Citation:
Fu Y, Zhang L, Wang G, Lin Y, Ramanathan S, Yang G, Lin W and Lin X (2020) The LysR-Type Transcriptional Regulator YeeY Plays Important Roles in the Regulatory of Furazolidone Resistance in Aeromonas hydrophila. Front. Microbiol. 11:577376. doi: 10.3389/fmicb.2020.577376

Aeromonas hydrophila is an aquatic pathogen of freshwater fish. The emergence of widespread antimicrobial-resistance strains of this pathogen has caused increasing rates of fish infections. Our previous research reported that *A. hydrophila yeeY*, a LysR-type transcriptional regulator (LTTR), negatively regulated furazolidone (FZ) resistance. Although, it's intrinsic regulatory mechanism is still unclear. In this study, a data-independent acquisition (DIA) quantitative proteomics method was used to compare the differentially expressed proteins (DEPs) between the Δ*yeeY* and wild-type strain under FZ treatment. When compared to the control, a total of 594 DEPs were identified in Δ*yeeY*. Among which, 293 and 301 proteins were substantially increased and decreased in abundance, respectively. Bioinformatics analysis showed that several biological pathways such as the secretion system and protein transport were mainly involved in FZ resistance. Subsequently, the antibiotics susceptibility assays of several gene deletion strains identified from the proteomics results showed that YeeY may regulate some important genes such as *cysD*, *AHA_2766*, *AHA_3195,* and *AHA_4275*, which affects the FZ resistance in *A. hydrophila*. Furthermore, 34 antimicrobial resistance genes (ARGs) from the bacterial drug resistance gene database (CARD) were found to be directly or indirectly regulated by YeeY. A subsequent assay of several ARGs mutants showed that Δ*AHA_3222* increased the susceptibility of *A. hydrophila* to FZ, while Δ*cysN* and Δ*AHA_3753* decreased the susceptibility rate. Finally, the chromatin immunoprecipitation (ChIP) PCR and an electrophoretic mobility shift assay (EMSA) have revealed that the genes such as *AHA_3222* and *AHA_4275* were directly and transcriptionally regulated by YeeY. Taken together, our findings demonstrated that YeeY may participate in antimicrobial resistance of *A. hydrophila* to FZ, which provides a new target for the development of novel antimicrobial agents in the future.

Keywords: *Aeromonas hydrophila*, DIA based proteomics, YeeY, furazolidone, antimicrobial resistance

INTRODUCTION

Aeromonas hydrophila is a well-known pathogen of freshwater fish, which is widely distributed in aquatic habitats including surface water, oceans, sewage and even chlorinated water (Liu et al., 2019). The number of reported cases caused by *A. hydrophila* has been grown worldwide. Therefore, this pathogen has received an increasing attention to combat their infections. Further, a several earlier studies have reported that *A. hydrophila* is a causative agent of hemorrhagic septicemia and motile aeromonad septicemia (MAS) in fish (Zahran et al., 2018; Abdelhamed et al., 2019). Outbreaks of *A. hydrophila* in humans have been recorded since 1992, which thought to be related to diarrhea, septicemia and soft-tissue wound infections in humans (de la Morena et al., 1993; Soltan Dallal et al., 2016). Further, a tons of antibiotics are used in aquaculture each year for controlling the infections in aquaculture worldwide, which causes a significant bacterial antibiotic resistance (Dahanayake et al., 2019). Therefore, the fish vaccines are used to the control the spread of diseases connected with *A. hydrophila*. However, only a few aquatic vaccines have obtained the national veterinary drug certifications in China, meaning that control measures are far from meeting the needs of the *status quo* (Wang Q. et al., 2020). Thus, it is necessary to understand the mechanism of antibiotic resistance in this pathogen to develop new and novel therapeutic agents.

It is generally agreed that the production of enzymes that inactivate antibiotics, changes in the target of antibiotics, increases in the permeability of cell membrane pore proteins and activation of efflux pumps are classic mechanisms of bacterial resistance (Das et al., 2020). Moreover, the previous studies have documented the outer membrane proteins (e.g., LamB and OmpA), fatty acid biosynthesis and the central metabolism of *A. hydrophila* also play an important roles in antibiotic resistance (Lin et al., 2014; Li et al., 2016; Yao et al., 2016). Nevertheless, specific mechanisms of antibiotic resistance are still largely elusive; although the proteins involved in antibiotic resistance yet need to be discovered.

LysR-type transcriptional regulators (LTTRs) are belonging to the transcription regulation families, which are widespread in prokaryotes. They are generally reported to be involved in bacterial antibiotic resistance. For example, the LTTR protein CidR was reported to positively regulate the *Staphylococcus aureus cidABC* operon, which enhances murein hydrolase activity and affects antibiotic tolerance against penicillin, vancomycin and rifampicin (Yang et al., 2005). A another LTTR protein OxyR regulates the cell division superfamily (RND) efflux pump gene *acrB* in *Klebsiella pneumoniae* and thereby confers resistance to chloramphenicol, erythromycin, nalidixic acid and trimethoprim (Rice et al., 2005). Since, LTTRs control diverse multi-functional genes and proteins as a well-known transcriptional regulator family, the antibiotic resistance regulatory functions of LTTRs are needed to be further investigated.

YeeY in *A. hydrophila* ATCC 7966 belongs to the LTTRs family that encodes a putative HTH-type transcriptional regulator. A multiple sequence alignment analysis showed that it's DNA binding domain with an HTH motif at the N terminal and a regulatory domain at the C terminal is highly conserved with those of other LTTRs (Kim et al., 2018). Interestingly, the deletion of *yeeY* (*AHA_3980* as well) has displayed multidrug characteristics, which significantly increased resistance to chloramphenicol, chlortetracycline, ciprofloxacin, furazolidone and balofloxacin. So, it clearly suggests that the YeeY act as a negative transcriptional regulator during antibiotic stresses (Fu et al., 2019). However, the intrinsic antibiotic resistance mechanism regulated by *A. hydrophila* YeeY remains unclear.

In this study, to further understand the role of YeeY in antibiotic resistance, we compared the differentially expressed proteins (DEPs) between Δ*yeeY* and wild-type strains under the stress of FZ using data-independent acquisition (DIA) quantitative proteomics technology. The bioinformatics analysis showed that the deletion of *yeeY* affected several key biological processes and metabolic pathways. Several DEPs were subsequently validated by Western blotting and several related genes were deleted and their antimicrobial susceptibilities were evaluated. Furthermore, the outcome of chromatin immunoprecipitation (ChIP) PCR and electrophoretic mobility shift assay (EMSA) were suggested that some antimicrobial resistance related genes were directly and transcriptionally upregulated by YeeY. Overall, the obtained results of this study provide a novel understanding on the regulatory role of LTTRs YeeY in antibiotic resistance of *A. hydrophila* against FZ.

MATERIALS AND METHODS

Bacterial Strain and Sample Preparation

A. hydrophila ATCC 7966 (WT), *yeeY* deleted strain (Δ*yeeY*), the rescue strain (Δ*yeeY* + *pACYC184-yeeY*), a negative control strain (Δ*yeeY* + *pACYC184*) and other gene deletion strains were constructed and stored in our laboratory as previously described (Pang et al., 2018). Bacterial strains were cultured overnight in Luria-Bertani (LB) medium at 30°C on a shaker at 200 rpm and then transferred to 100 mL LB medium at a ratio of 1:100 with a final concentration of 1.5 μg/mL of FZ treatment. The cells were collected by centrifugation at 8000 g for 15 min at 4°C when the OD of the bacteria culture reached 1.0 at 600 nm. After washed three times with pre-cooled PBS buffer, the cell pellets were resuspended in lysis buffer (6 M urea, 2 M thiourea, 100 mM Tris–HCl pH 8.5, protease inhibitor) and then ultrasonically disrupted by sonication on ice for 15 min at 30% power with intervals of 9 s. Then, the whole proteins were isolated by centrifuging at 12000 × *g* for 30 min at 4°C and the concentrations were determined by the Bradford method.

Trypsin Digestion

A total of 50 μg protein of each sample was reduced with dithiothreitol (DTT), alkylated by iodoacetamide (IAA) and then digested with trypsin at a ratio of 1:50 for 16–18 h at 37°C. Subsequently, the digested peptides were desalted using a Sep-Pak Vac C18 Column (Waters Inc., Milford, MA) and dried using a CentriVap Concentrator (Labconco, Inc., Kansas City, MO) (Sun et al., 2019; Wisniewski, 2019; Yao et al., 2019).

DIA Based LC-MS/MS Analysis

The digested peptides were resuspended in 25 μL of 0.1% formic acid (FA) containing iRT standard peptide (Biognosys) and then submitted to analysis on an Q Exactive HF mass spectrometer (Thermo Scientific, United States) with an EASY-nano-LC1200 chromatographic system (Thermo Scientific, United States) as previously described (Doerr, 2014). Briefly, peptides were loaded onto a C18 Trap column EASY-nano-LC at a rate of 4.5 μL/min with 12 μL phase A (2% acetonitrile and 0.1% FA) at a maximum pressure of 280 bars and then eluted using a C18 column with a runtime of 120 min at a rate of 600 nL/min using phase A (2% acetonitrile and 0.1% FA) and phase B (98% acetonitrile and 0.1% FA) with the following gradient elution program: 0–18 min, 6–12% B; 18–77 min, 12–20% B; 77–109 min, 20–32% B; 109–110 min, 32–90% B; 111–120 min, 90% B hold. The data were collected in the nano-spray ion source with an ion-spray voltage of 2.1 kV and an ion source temperature of 320°C. The scan range was 350 to 1400 m/z at a resolution of 60000 FWHM (at m/z 200) with automatic gain control (AGC) set to 3 E^6 (maximum injection time of 20 ms). Further, the MS/MS was scanned at a resolution of 15000 FWHM (at m/z 200) with an isolation window of 1.6 Da with AGC set to 5 E^4 (maximum injection time of 45 ms). DIA was scanned at a resolution of 30000 FWHM (at m/z 200) with a set of 45 variable overlapping windows covering the precursor mass range of 350–1400 m/z.

A confidential spectral library generated as previously study was used for spectral library (Wang G. B. et al., 2020). The DIA-generated data were imported into Spectronaut Pulsar X for protein qualitative and quantitative analyses using the following parameters: the iTR curve preceded local (non-linear) regression and protein identification was performed with Precursor Q value Cutoff 0.01 software. The identified proteins with at least two peptides matching and the peptide and protein FDR (false discovery rate) less than 0.01 were further analyzed.

Bioinformatics Analysis

The Gene Ontology (GO) annotations and Kyoto Encyclopedia of Genes and Genomes (KEGG) pathways of DEPs were analyzed with DAVID online software[1] (Li H. L. et al., 2020; Zhang et al., 2020). The GO and KEGG results were displayed in a diagram using GOCircle and GOChord plot functions of the GOplot R package. The predicted antibiotic resistance of DEPs was analyzed with the Comprehensive Antibiotic Research Database (CARD[2]) and visualized with loop heat map using the TBtool software (Chen et al., 2019, 2020).

Western Blotting Validation

To validate the proteomics results, several specific antibodies were developed in house and Western blotting was performed as described previously (Li L. et al., 2020). Protein samples from each group were run on SDS-PAGE gels and transferred to PVDF membranes (Millipore, Billerica, MA, United States) for 15 min at 25 V using a Trans-Blot SD Cell (Bio-Rad, Hercules, CA, United States). After that, the PVDF membranes were washed three times with PBST and blocked in 5% skim milk with PBS buffer containing 0.05% Tween 20 (PBST) for 1 h and then probed with primary antibody before being incubated for 1 h at room temperature. Then, the membranes were washed with PBST five times and incubated in HRP goat anti-mouse or anti-rabbit IgG for 1 h at room temperature. Finally, the PVDF membranes were washed five times with PBST, exposed using the ECL system and visualized with a ChemiDoc^{TM} MP imager (Bio-Rad, Hercules, CA, United States). The band signals were quantified with Image J software.

Antibiotics Susceptibility Assay

The antibiotics susceptibility assay was performed as described previously (Yao et al., 2018; Zhang et al., 2019). Briefly, the mutant and WT strains were incubated at 30°C for overnight and then diluted to ratio of 1:100 with fresh LB medium. After being treated with a series of concentrations of 0.25, 0.5, 1.0, and 2.0 μg/mL of FZ, the samples were divided into a HONEYCOMB® Sterile 100 well plate and the OD_{600} value was determined at 16 h using a Bioscreen C instrument (Oy Growth Curves AB Ltd., Helsinki, Finland).

ChIP-PCR

To further investigate the regulations between transcriptional regulator YeeY and candidate genes, ChIP-PCR was performed as previously described with slight modifications (Shen et al., 2020). Briefly, Δ*yeeY* containing *pACYC184-His-yeeY* or *pACYC184-His* were incubated at 30°C for overnight and then collected by centrifugation at 6000 g for 10 min at 4°C. After being washed three times with pre-cooled PBS buffer, the pellets were resuspended in 40 μL of 1% formaldehyde containing PBS buffer and placed on ice for 5 min; then, 3 M glycine solution was added for 15 min to terminate the crosslinking reaction. After crosslinking, the chromatin was collected and resuspended in 40 μL PBS buffer. After that, the chromatin was fragmented by sonication on ice for 20 min at 30% power with intervals of 9 s on ice to obtain an average length of 300 to 500 bps. Then, the nickel beaver beads were incubated with the crosslinking products for 2 h at 4°C and then the immunoprotein was eluted using 400 μL of 500 mM imidazole. After immunoprecipitation, 10% SDS and 2 μL of 100 mg/mL proteinase K was added to the precipitate and the samples were stored at 37°C. Next, the crosslinking was reversed and the DNA was extracted using phenol, chloroform and isoamyl alcohol at a ratio of 25:24:1 and then dissolved in 100 μL sterile water. Finally, the purified DNA was analyzed by ChIP-PCR using the primers listed in **Table 1**.

EMSA

To investigate the binding of YeeY to the target genes' promoters, the EMSA was performed as described previously

[1]https://david.ncifcrf.gov/

[2]http://arpcard.mcmaster.ca

TABLE 1 | Primer sequences used for ChIP-PCR and EMSA in this study.

Primer	Oligonucleotide sequence (5′ → 3′)	Purpose
AHA_3222-F	atgcggatcctgttggt	ChIP-PCR
AHA_3222-R	tcatgcccggtggtc	ChIP-PCR
P_{AHA_3222}-F	tgagcgcaacgcaataagcttTGTTATTCCCCTCAAAAGACGC	ChIP-PCR
P_{AHA_3222}-R	gagctgtacaagtaaggatccACCCAAGTCGGATCAGAGCG	ChIP-PCR
AHA_4275-F	ttgatatttgagacacttactatgattgc	ChIP-PCR
AHA_4275-R	ttaccagcggtagttgatgc	ChIP-PCR
P_{AHA_4275}-F	tgagcgcaacgcaataagcttTGAGTTGTTTCTGATTTCTTATTATTGG	ChIP-PCR
P_{AHA_4275}-R	gagctgtacaagtaaggatccCAATGGGGATCCCCGATG	ChIP-PCR
AHA_3222-F2	gctatttaaactctgcccaccagcttgcatactggtgggcagcgtcttttgaggggaataaca-Cy5	EMSA
AHA_3222-R2	tgttattcccctcaaaagacgctgcccaccagtatgcaagctggtgggcagagtttaaatagc	EMSA
AHA_3222-F3	gctatttaaactctgcccaccagcttgcatactggtgggcagcgtcttttgaggggaataaca	EMSA
AHA_4275-F2	tagcatgtcgctgctttattcgcctgaggaaccgggctaccggcatgaccgggcaccaataataa gaa-Cy5	EMSA
AHA_4275-R2	ttcttattattggtgcccggtcatgccggtagcccggttcctcaggcgaataaagcagcgacatgcta	EMSA
AHA_4275-F3	tagcatgtcgctgctttattcgcctgaggaaccgggctaccggcatgaccgggcaccaataataagaa	EMSA

(Heravi and Altenbuchner, 2014; Cheng et al., 2019). First, the recombinant proteins of pET-32a-YeeY were obtained via a prokaryotic expression system. Briefly, the *pET-32a* plasmid containing *yeeY* was transformed into *E. coli* BL21 (DE3). The recombinant proteins were induced with IPTG (isopropyl β-D-1-thiogalactopyranoside, 0.05 mM) at 30°C for 6 h and then purified using Ni-TNA column as described in previous study (Li et al., 2017). Second, two DNA probes were synthesized by PCR using two pairs of single-strand primers (**Table 1**) in which the upstream primer was labeled by Cy5-labeled oligonucleotides at the 5′ end, whereas two cold probes as a competitor were synthesized with the primers without the Cy5-labeled at the upstream primer 5′ end (**Table 1**). To ensure the specificity of the probes, we randomly selected pET-32a-Hcp, which was kept in our laboratory as a negative control and then the recombinant proteins pET-32a-YeeY and pET-32a-Hcp were incubated with probe and binding buffer (1 M pH 7.5 Tris–HCl, 5 M NaCl, 1 M KCl, 1 M $MgCl_2$, 0.5 M pH 8.0 EDTA, 10 mg/mL BSA), respectively for 30 min at 4°C in the dark. Finally, the mixture was separated by PAGE gels and then scanned using Odyssey@ CLX (LI-COR, United States).

RESULTS

The Deletion of *A. hydrophila yeeY* Increases the Antibiotics Resistance to FZ

The antimicrobial susceptibility rate of deletion and rescued strains were assessed when challenged with a series of FZ concentrations by a percentage of survival (**Figure 1**). At lower FZ concentrations (0.25 and 0.5 μg/mL), no significant differences were observed in the susceptibility rate of Δ*yeeY* or Δ*yeeY* + *pACYC184* when compared to the wild-type and Δ*yeeY* + *pACYC184-yeeY* strains, respectively. However, at the higher doses of FZ (1 to 2 μg/mL), the Δ*yeeY* strain showed significantly increased susceptibility rate, whereas the rescued strain showed decreased susceptibility rate when compared to the controls.

Quantitative Proteomics of DEPs Between WT and Δ*yeeY* in Response to FZ

To further understand the effects of *yeeY* deletion on protein expression in *A. hydrophila*, whole protein samples between WT and Δ*yeeY* under 1.5 μg/mL of FZ antibiotic stress were extracted and then digested to peptides by trypsin to quantify in the protein levels by using DIA-based proteomics method. Each sample was independently repeated three times as biological replicates. Consequently, a total of 2066 proteins were identified with a considerable conservative threshold (protein and peptide false discovery rate <1%; listed in **Supplementary Table S1**) by LC-MS/MS. The protein MS intensities of WT and Δ*yeeY* were highly correlated among biological replicates (Pearson correction factor > 0.9) suggesting that the quantification analysis had high reliability (**Figure 2A**). Besides, as shown in the volcano plot, 593 DEPs were identified, including 293 increased and 300 decreased in abundance with fold change (FC) > 2 and p-value < 0.05 (**Figure 2B**).

Go Enrichment of DEPs Under FZ Stress

GO analysis of DEPs between WT and Δ*yeeY* strains under FZ stress was performed with DAVID and visualized using the GOplot package in the R software. In the biological process (BP) classification clusters, the significantly enriched GO terms were oxidation-reduction process (5.6%, 25 increased and 8 decreased in abundance), aerobic respiration (2.5%, 11 increased and 4 decreased in abundance), energy derivation by oxidation of organic compounds (3.7%, 17 increased and 5 decreased in abundance), tricarboxylic acid cycle (2.2%, 9 increased and 4 decreased in abundance), cellular respiration (3.2%, 15 increased and 4 decreased in abundance) and cellular catabolic process (5.4%, 9 increased and 23

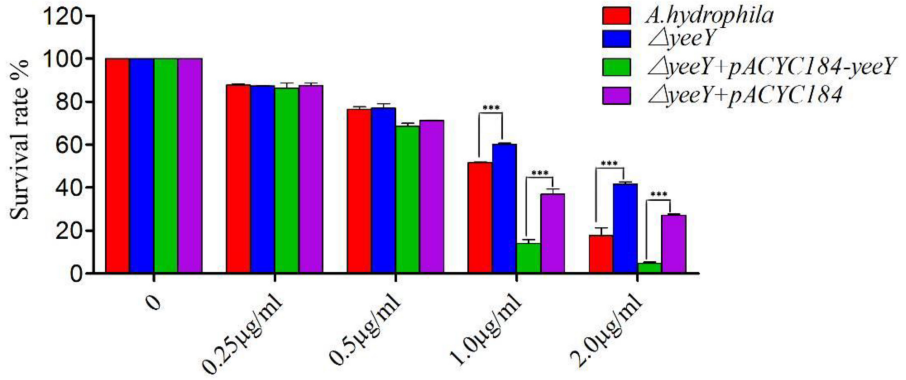

FIGURE 1 | The antibiotics susceptibility of Δ*yeeY* derivatives to FZ. The survival rates of Δ*yeeY*, wild-type, Δ*yeeY* carrying *pACYC184-yeeY* (rescued strain) and Δ*yeeY* carrying an empty vector when exposed to various FZ concentrations.

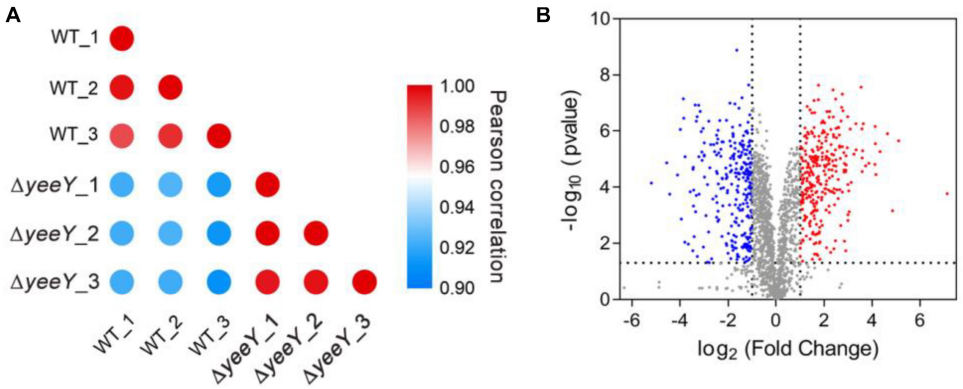

FIGURE 2 | DIA based quantitative proteomics data analysis. **(A)** Correlation coefficients were used to analyze the associations of protein strength in three biological replications; **(B)** Volcano map comparing the abundance ratios of proteins with significant differences in expression (Fold change > 2; $p < 0.05$). The blue dots in the figure represent differentially down-regulated proteins; the red dots represent differentially increasing abundance proteins and the gray color represents non-differentially expressed proteins.

decreased in abundance) (**Figure 3A**). In the molecular functioning (MF) classification clusters, the significantly enriched GO terms were oxidoreductase activity, electron carrier activity, metal ion binding, tetrapyrrole binding and cation binding. Of these clusters, many proteins were increased in abundance in tetrapyrrole binding, electron carrier activity and heme-binding (**Figure 3B**). In the cell component (CC) classification clusters, the most significantly enriched GO terms were external encapsulating structure, cell envelope, cell outer membrane, external encapsulating structure part and outer membrane and envelope. Further, the protein expression showed that *lamB* had the highest fold change, while the *hgpB* exhibited the lowest expression in the CC enrichment (**Figure 3C**).

KEGG Enrichment of DEPs in FZ Stress

KEGG pathways enrichment analysis was further performed for the DEPs between the WT and Δ*yeeY* under FZ stress. The results showed that the most representative pathways were carbon metabolism (19 proteins increased and 23 proteins decreased in abundance), microbial metabolism in diverse environments (29 proteins increased and 29 proteins decreased in abundance), biosynthesis of antibiotics (33 proteins increased and 21 proteins decreased in abundance), TCA cycle (11 proteins increased and 3 proteins decreased in abundance), bacterial secretion system, protein export and pyruvate metabolism (**Figure 4**). Meanwhile, many pyruvate metabolism-related proteins were decreased in abundance, whereas bacterial secretion system and protein export-related proteins were found to be largely enriched with increased abundance. In general, most of these proteins are involved in key metabolic functions and protein export and these processes may contribute to FZ resistance.

Western Blotting Validation of Proteomics Results

To validate the proteomics results, two increased abundance proteins (AhyI and Hcp) and three decreased abundance proteins (A0KGN7, A0KLX0 and A0KFG8) were selected and

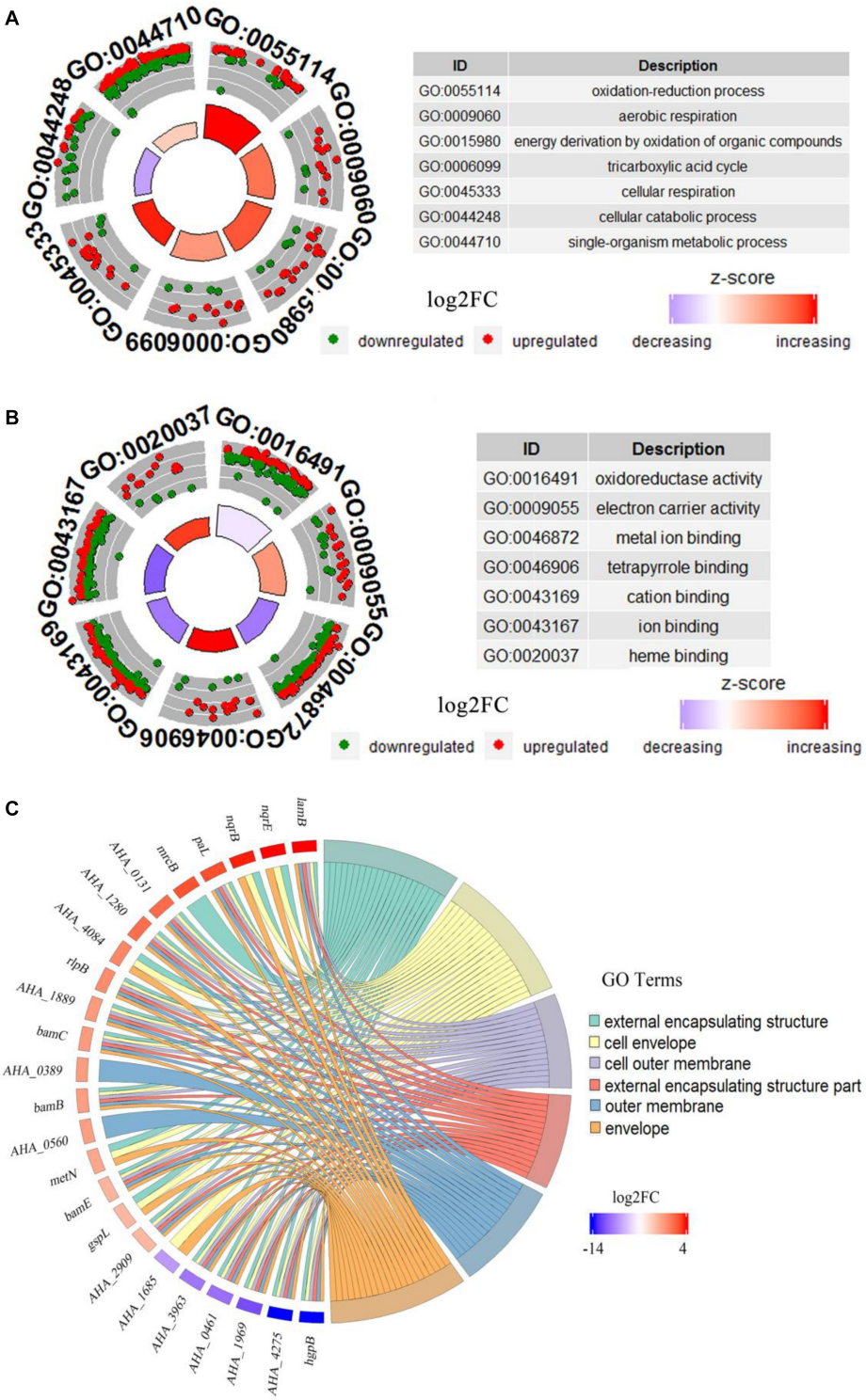

FIGURE 3 | Bioinformatics analysis of DEPs between WT and Δ*yeeY* under FZ stress. **(A)** The cluster analysis of GO annotation in biological processes; **(B)** The cluster analysis of GO annotation in molecular functions; **(C)** The chord chart analysis of GO annotation in cellular components.

analyzed by Western blotting using the primary antibodies that were previously developed by our group. The Western blotting results showed that Acyl-homoserine lactone synthase (AhyI) and hemolysin co-regulated protein (Hcp) were increased in abundance in Δ*yeeY*, while oligopeptide ABC transporter (A0KFG8), phosphate acetyltransferase

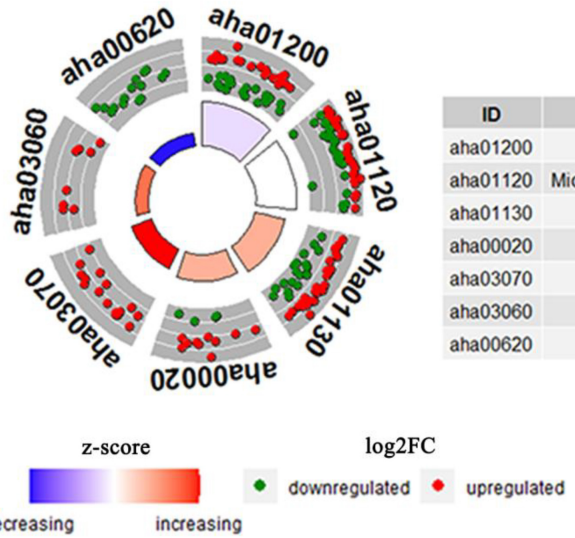

ID	Description
aha01200	Carbon metabolism
aha01120	Microbial metabolism in diverse environments
aha01130	Biosynthesis of antibiotics
aha00020	Citrate cycle (TCA cycle)
aha03070	Bacterial secretion system
aha03060	Protein export
aha00620	Pyruvate metabolism

FIGURE 4 | The cluster enrichment analysis of KEGG metabolic pathway of DEPs between WT and Δ*yeeY* under FZ stress. The three circles from outside to inside are indicated GO terms; a scatter plot of the expression levels (log_2FC) for the genes in each, where red dots represent increasing abundance while green dots represent down-regulated; and a bar plot where the bar height indicates the significance of the KEGG pathway ($log_{10}p_{value}$) and the color indicates the z-score gradient.

(A0KGN7) and cytochrome c553 (A0KLX0) were down-regulated in Δ*yeeY*, compared to the WT strain under FZ stress (**Figure 5A**). All experiments were repeated at least three times, then the target bands intensity were quantified using Image J software and visualized with histogram (**Figure 5B**). Our data showed that the Western blotting results were relatively consistent with the mass spectrometry data, which indicates that our proteomics results were reliable.

Survival Capability Assay of Related Mutants in Response to FZ Stress

To further understand the roles of YeeY on the altered proteins under FZ resistance, the antimicrobial susceptibilities of seven deletion mutants (Δ*ahyI*, Δ*cysD*, Δ*mrcA*, Δ*AHA_0389*, Δ*AHA_2766*, Δ*AHA_2831* and Δ*AHA_4275*), which were stored in our laboratory, were evaluated based on survival rate in a series of FZ concentrations treatment. Among these, *cysD*, *mrcA* and *AHA_4275* genes were involved in metabolic pathways and microbial metabolism in diverse environments. Further, the *cysD* gene was also involved in the biosynthesis of antibiotics and *AHA_2766* was involved in the part of metabolic pathways. The results showed that Δ*AHA_2766* and Δ*AHA_4275* had significantly increased survival rate, while Δ*cysD* and Δ*mrcA* had decreased survival rate when compared to the survival rate of the wild-type strain. Although *ahyI* and *AHA_0389* were showed increasing abundance in the proteomics results, whereas these two deleted mutants were showed no significant differences in survival rates, compared to the WT strain. Interestingly, Δ*AHA_2831* was showed increased survival rate in lower concentrations of antibiotics (0.25 to 0.5 μg/mL), while it was showed sharply decreased survival rate in 1.0 μg/mL of FZ. In general, our results indicated that *AHA_2766*, *AHA_4275*, *mrcA* and *cysD* may be regulated by YeeY and may be involved in FZ resistance (**Figure 6**).

The Roles of CARD Drug-Resistant Genes on FZ Resistance

To further understanding the effect of *A. hydrophila* YeeY on antimicrobial resistance genes (ARGs), all DEPs from proteomics analysis were submitted to ARGs detection by searching the CARD that provides well-known ARGs from diverse bacterial species. A total 30 resistance genes were found to be directly or indirectly regulated by YeeY under FZ stress, of which 22 and 12 proteins were increased and decreased in abundance, respectively (**Figure 7A**, **Table 2**). Subsequently, the antimicrobial susceptibilities of four resistance deletion mutants (Δ*cysN*, Δ*secD*, Δ*AHA_3222* and Δ*AHA_3753*), which were kept in our laboratory, were evaluated based on survival rate when treated with a series of FZ concentrations (**Figure 7B**). The results showed that the survival rates of Δ*AHA_3222* and Δ*secD* were increased while those of Δ*cysN* and Δ*AHA_3753* were significantly decreased under the stress of FZ. Therefore, our results indicated that the genes *cysN*, *AHA_3222* and *AHA_3753* were regulated by YeeY, which may participate in the resistance process of *A. hydrophila* to FZ.

AHA_3222 and *AHA_4275* Were Directly Regulated by YeeY in FZ Resistance

The data of this study indicates that YeeY may affect the FZ resistance of *A. hydrophila* via regulating the expression of some proteins, such as *cysN*, *mrcA*, *AHA_3222* and *AHA_4275*. Therefore, we have validated this possibility using ChIP-PCR technique. The *A. hydrophila* chromatin was isolated and

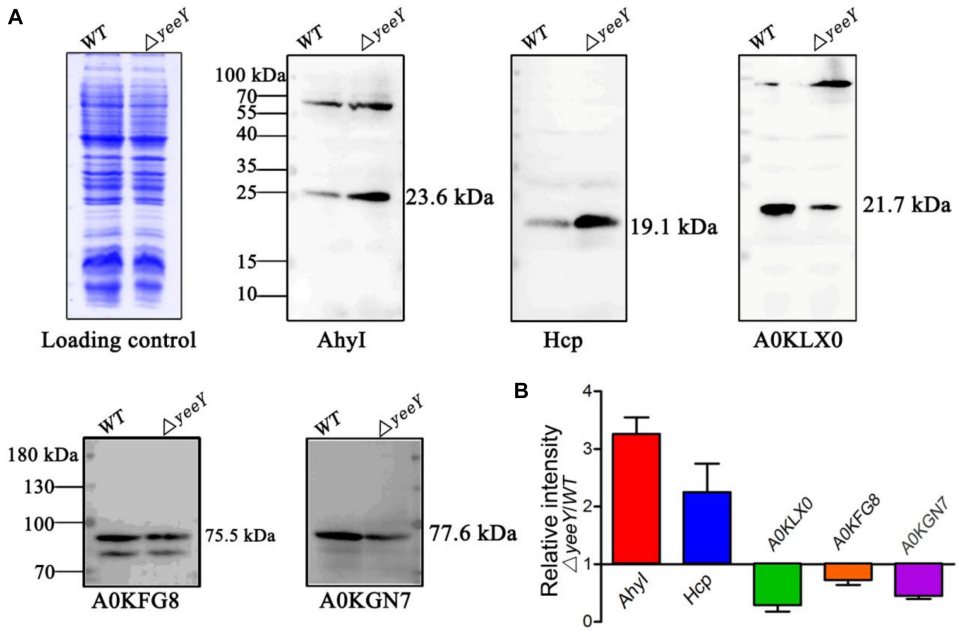

FIGURE 5 | Western blotting analysis of the selected DEPs between WT and Δ*yeeY* under FZ stress. **(A)** The CBB-stained SDS-PAGE map of *A. hydrophila* WT and Δ*yeeY* under 1.0 μg/ml FZ treatment on the left acted as a loading control; **(B)** Gray level analysis of western blotting band signals by image J software.

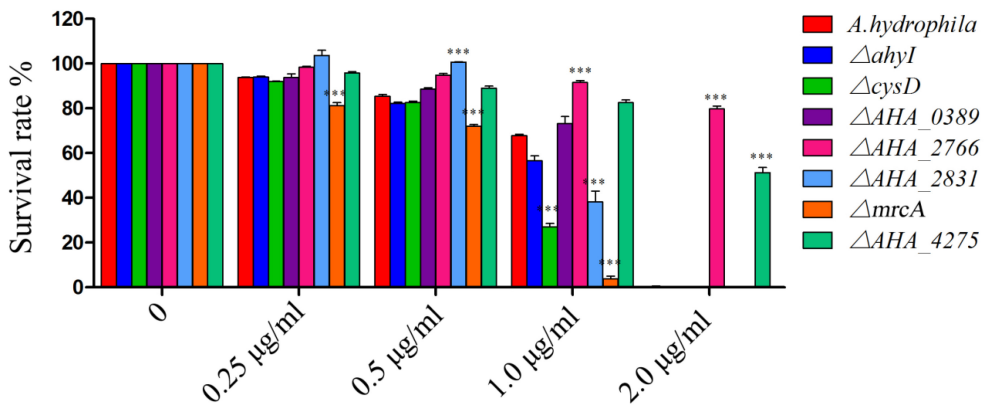

FIGURE 6 | Survival capability assay of selected gene deleted strains under different doses of furazolidone treatment. ***means $p < 0.001$.

immunoprecipitation with anti-His antibody and the acquired recovered DNA was used as a template for PCR with the target gene and its predicted promoter region primer pairs. The results showed that only the predicted promoter regions of *AHA_3222* and *AHA_4275* produced product in the Δ*yeeY*: *pACYC184-His-yeeY* IP sample, whereas *AHA_3222* and *AHA_4275* could not be amplified (**Figures 8A,B**). So, it is suggesting that *AHA_3222* and *AHA_4275* may be directly targeted by YeeY. To further confirm these results, EMSA was performed to investigate the binding of YeeY to *AHA_3222* and *AHA_4275* promoters *in vitro*. The results showed that promoter fragments of both genes were bound by YeeY (**Figures 8C–E**). Therefore, the outcome of EMSA clearly suggested that *AHA_3222* and *AHA_4275* can be directly regulated by YeeY.

DISCUSSION

A. hydrophila is an important aquatic bacterial pathogen in freshwater aquaculture and it has been reported that the threat of infection caused by this pathogen in fish and even in humans is on the rise worldwide (Awan et al., 2018). Although, the antibiotic treatment is an effective tactic to control the bacterial diseases in aquaculture, side however the effects such as antibiotic residue and antibiotic resistance cannot be ignored. Further, more than two million people who are infected with antibiotics resistant bacterial pathogens each year in the United States on average 23000 people die, meaning that antibiotic resistance has become one of the greatest threats faced by modern medicine (Laxminarayan et al., 2013). Therefore, elucidating the antibiotic

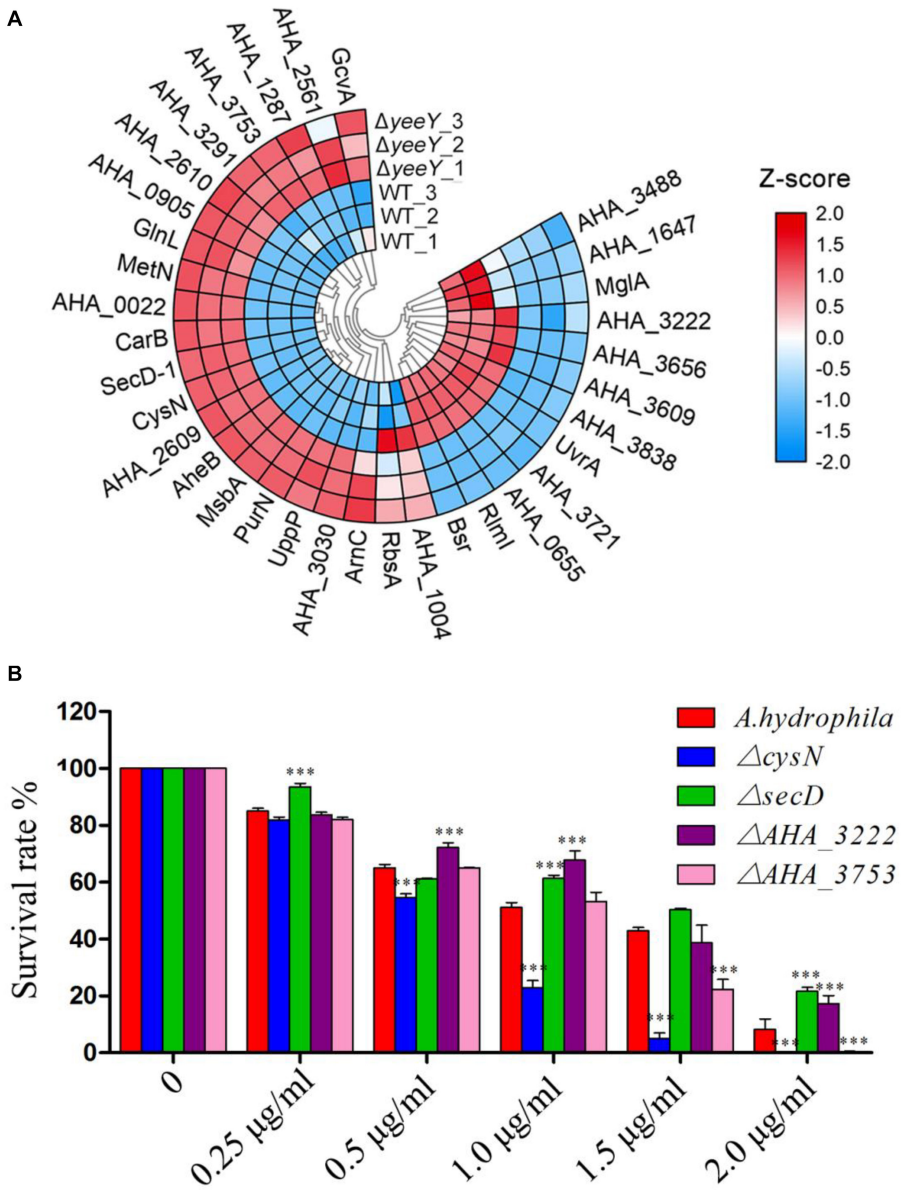

FIGURE 7 | CARD ARGs analysis of DEPs between WT and Δ*yeeY* under FZ stress. **(A)** Loop heat map analysis of ARGs in Δ*yeeY* differentially expressed genes. The colors of squares indicate the z-scores, red represents increased and blue represents decreased. The outer cycle of the heat map represents the gene names of DEPs in Δ*yeeY*; **(B)** survival capability assay of four ARG deleted strains under different doses of furazolidone treatment.

resistance mechanism of *A. hydrophila* is of great significance for the development of new antibiotic therapeutic strategies in the future. YeeY, an LTTR, was reported to be associated with the rapid emergence of persistence in *E. coli* (Girgis et al., 2012). However, the biological function of this protein is still largely unknown, especially concerning antibiotic resistance. Although furazolidone has been prohibited in many parts of the world due to its toxic and carcinogenic side effects, we found that the minimal inhibitory concentration (MIC) of FZ was decreased when the YeeY was overexpressed and the absence of *yeeY* led to an increase the FZ resistance in our previous work (Fu et al., 2019). To further understand the biological behavior of YeeY on antibiotic resistance, differentially expressed proteins between Δ*yeeY* and WT strains were compared under FZ stress by DIA-quantitative proteomics in this study. A total of 594 DEPs were identified in Δ*yeeY*, with 293 proteins that were increased in abundance and 301 were decreased in abundance.

Of these DEPs, 15 outer membrane proteins were affected by the loss of *yeeY* under the FZ stress when compared to the wild-type strain. Among them, the proteins such as LamB, OprM, and OmpA were increased in abundance, whereas A0KQZ1 (*AHA_4275*) and A0KN35 (*AHA_2766*) were decreased in abundance. The OmpA has been reported to play an important role in the transport of antibiotics. For example, the

TABLE 2 | DEPs related to ARGs between Δ*yeeY* and WT *A. hydrophila* under FZ stress by DIA-LC-MS/MS.

Accession	Gene	Description	Matched peptides	*P*-value	log2(Δ*yeeY*/*WT*)
A0KEF9	*tatA*	Sec-independent protein translocase protein TatA	3	5.43E-05	1.762
A0KEY7	*glnL*	Nitrogen regulation protein NR(II)	14	0.000149	2.754
A0KF41	*secY*	Protein translocase subunit SecY	7	1.43E-07	2.724
A0KG12	*AHA_0655*	Arginine ABC transporter, ATP-binding protein	9	4.24E-07	−2.348
A0KGQ2	*AHA_0905*	Aerobic respiration control sensor protein	26	1.74E-05	3.720
A0KGR2	*metN*	Methionine import ATP-binding protein MetN	13	1.65E-05	1.348
A0KGY7	*arnC*	Undecaprenyl-phosphate 4-deoxy-4-formamido-L-arabinose transferase	11	0.008264	2.845
A0KHD7	*gcvA*	Glycine cleavage system transcriptional activator	11	0.03694	1.501
A0KHS7	*AHA_1287*	HlyD family secretion protein	15	0.000332	1.685
A0KJ22	*secD-1*	Protein translocase subunit SecD	28	3.11E-07	2.377
A0KJ23	*secF-1*	Protein-export membrane protein SecF	8	2.73E-05	2.495
A0KKF0	*rlmI*	Ribosomal RNA large subunit methyltransferase I	13	4.55E-06	−1.337
A0KLC0	*AHA_2561*	Transcriptional regulator	10	0.036697	1.818
A0KLG5	*bsr*	Broad specificity amino-acid racemase	18	4.43E-06	−2.302
A0KLG7	*AHA_2609*	Oligopeptide ABC transporter, ATP-binding protein OppF	19	1.4E-05	1.330
A0KLG8	*AHA_2610*	Oligopeptide ABC transporter, ATP-binding protein OppD	14	0.000151	1.074
A0KLT0	*carB*	Carbamoyl-phosphate synthase large chain	52	9.59E-06	1.054
A0KLY2	*msbA*	Lipid A export ATP-binding/permease protein MsbA	22	9.88E-06	2.219
A0KM25	*purN*	Phosphoribosylglycinamide formyltransferase	5	8.26E-06	1.522
A0KMB3	*aheB*	Efflux pump membrane transporter	30	8.17E-06	1.915
A0KMN1	*AHA_3030*	ABC transporter, CydDC cysteine exporter (CydDC-E) family, permease/ATP-binding protein CydC	16	0.000171	2.044
A0KN35	*mrcA*	Penicillin-binding protein 1A	31	2.64E-05	1.993
A0KN62	*AHA_3222*	DNA-binding response regulator	7	0.007093	−1.178
A0KND1	*AHA_3291*	DNA-binding response regulator	10	0.002697	1.812
A0KNE6	*secG*	Protein-export membrane protein SecG	3	0.000126	2.184
A0KNW1	*AHA_3488*	ABC transporter, ATP-binding protein	5	0.036196	−1.357
A0KP35	*cysN*	Sulfate adenylyltransferase subunit 1	25	1.62E-06	2.398
A0KP36	*cysD*	Sulfate adenylyltransferase subunit 2	11	1.7E-05	2.395
A0KP78	*AHA_3609*	Transcriptional regulator, MarR family	6	0.000606	−1.397
A0KPB1	*AHA_3656*	Chloramphenicol acetyltransferase	3	3.86E-05	−1.009
A0KPG8	*AHA_3721*	Transcriptional regulator, MarR family	8	1.96E-05	−1.082
A0KPK0	*AHA_3753*	LysR-family transcriptional regulator	7	0.000149	1.924
A0KPT0	*AHA_3838*	Chemotaxis protein CheV	14	1.94E-05	−1.429
A0KQ38	*uvrA*	UvrABC system protein A	48	7.36E-05	−1.032
A0KQI1	*uppP*	Undecaprenyl-diphosphatase	2	8.05E-05	2.085
A0KQZ1	*AHA_4275*	Ferrichrome receptor	15	4.47E-07	−3.322
A0KQZ7	*yidC*	Membrane protein insertase YidC	26	3.61E-06	2.757
A0KR20	*AHA_0022*	RND transporter, hydrophobe/amphiphile efflux-1 (HAE1) family, MFP subunit	15	1.06E-05	1.720

MICs of chloramphenicol, aztreonam and nalidixic acid were decreased when the *ompA* was disrupted in *A. baumannii* (Smani et al., 2014). Further, in our previous study, we have observed that the MBCs (minimum bactericidal concentrations) of ceftriaxone sodium, apramycin, neomycin sulfate and gentamicin in Δ*AHA_2766* were increased more than 4-fold, whereas the MBCs of norfloxacin and chloramphenicol in Δ*AHA_4275* were decreased at least 2-fold (Li et al., 2019). Therefore, we have evaluated the antibiotic susceptibility of these both mutants to FZ antibiotic in this study. The survival test showed that the survival rates of Δ*AHA_2766* and Δ*AHA_4275* were significantly higher, compared to the wild strains under various doses of FZ. It suggests that *A. hydrophila* YeeY may regulate several antibiotic resistance-related outer membrane proteins during FZ stress.

MrcA (penicillin-binding protein 1a, PBP1a) and MrcB (penicillin-binding protein 1b, PBP1b) were both increased in abundance in Δ*yeeY* strain under FZ stress. Both proteins are essential for cell wall peptidoglycan biosynthesis and maintenance of cell growth. More both of these proteins are considered as antibiotic targets by beta-lactams (Kumar et al., 2012; King et al., 2017). Apart from their involvement in beta-lactams resistance, these both proteins were increased in abundance within the chlortetracycline (CTC) resistant strain in our previous study, whereas their actual functions in CTC

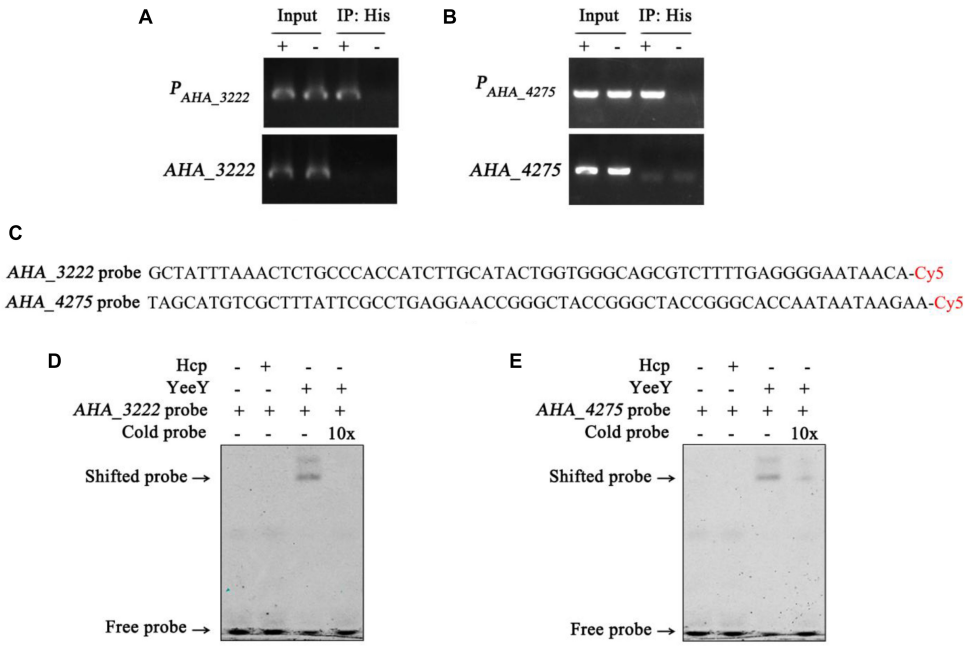

FIGURE 8 | The binding of YeeY with the promoters of *AHA_3222* and *AHA_4275*. **(A,B)** ChIP-PCR analysis of the binding of YeeY and the promoter fragments of *AHA_3222* and *AHA_4275*. The promoter fragments of both genes are marked as P_{AHA_3222} and P_{AHA_4275}, respectively; **(C)** the nucleotide sequences of *AHA_3222* and *AHA_4275* DNA probes; **(D,E)** EMSA analysis of the binding of YeeY and the promoter fragments of *AHA_3222* and *AHA_4275*, respectively; The Cold probes competition were performed with 10 × unlabeled probes.

resistance are still unknown (Li et al., 2018). In this study, the survival rate of Δ*mrcA* was decreased under high doses of FZ, which suggesting that the MrcA may be involved in FZ resistance as well. This finding indicates that YeeY may negatively regulate penicillin-binding protein against FZ stress.

The KEGG analysis showed that the bacterial secretion system was enriched in increased abundance proteins, including general secretion pathway (*gspC*, *gspG*), type II secretion system T2SS (*gspM*, *gspL*), type VI secretion system T6SS (*AHA_1826*, *AHA_1827*, *AHA_1840*, *AHA_1841*, and *AHA_1845*), Sec secretion system (*secD*, *yidC*, *secE*, *secF*, *secG*, *secY*, and *lepB*) and Tat-dependent system (*tatA*). Some studies have documented that the bacterial secretion system related proteins are involved in antibiotics resistance. For example, T6SS functioned not only as a virulence system, which also contributed to antimicrobial resistance in *A. baumannii* ATCC 19606, it was proved that upon the T6SS core component *vgrG* was deleted, the antimicrobial resistance to ampicillin, chloramphenicol and β-lactam antibiotics was altered (Wang et al., 2018). It indicated that T6SS may be closely related to furazolidone resistance in *A. hydrophila* since *AHA_1827* was highly homolog to *A. baumannii* ATCC 19606's gene *vgrG* by comparative amino acid sequence analysis. Besides, beta-lactamase, a target of beta-lactam antibiotics, was transported through the Sec and Tat-dependent secretion systems (Pradel et al., 2009). Thus, protein transport may be an adaptive strategy in the FZ resistance in *A. hydrophila*.

The DEPs were also involved in complex cellular metabolic processes, especially the TCA cycle and sulfur metabolism. It was reported that the down-regulation of bacterial energy generation systems such as the TCA cycle may be a potential antibiotic resistance tactic in many bacterial species (Rosato et al., 2014; Peng et al., 2015; Su et al., 2018). However, many proteins associated with the TCA cycle, such as SucA, SucB, SucC, SucD, GltA, IcD, and SdhA were increased in abundance in this study, indicating that the role of the TCA cycle in FZ resistance in *A. hydrophila* may be alleviated by YeeY regulation. Sulfur, an essential element, exists in hundreds of metabolites with various oxidation states that are not only related to the virulence and antioxidant stress of *Mycobacterium tuberculosis* but also play important roles in rifampicin resistance. In the current study, four sulfur metabolism-related proteins (CysD, CysI, CysH, and CysN) were increased in abundance in Δ*yeeY* under FZ stress. The survival assay showed that the survival rate of Δ*cysD* and Δ*cysN* mutant strains were decreased when compared to the wild-type strain, which suggesting that sulfur metabolism is also a part of the mechanism of bacterial resistance by YeeY regulation. Taken together, these findings suggest that bacterial intracellular metabolism may be an important bacterial resistance strategy.

Also, we estimated the FZ susceptibilities of four well-known ARGs homologs (*AHA_3222*, *AHA_3753*, *cysN,* and *secD*) from the CARD by measuring the survival rates of their gene deletion strains under different concentrations of FZ. According to the annotation of CARD, *cysN* is related to tetracycline resistance; *AHA_3222* homolog is related to fluoroquinolone and acridine dye resistance; *AHA_3753* homolog is related to cephalosporin and *secD* is related to cephalosporin. There is considerable research documenting the antibiotic resistance

properties of these ARGs or their homologs. For example, both SecD and SecF belong to the resistance-nodulation-cell division (RND) family of multidrug exporters and they are involved in the export of antimicrobial resistance proteins in *Staphylococcus aureus* (Quiblier et al., 2011). *AHA_3222* is a DNA-binding response regulator and its homologous protein ArlR (98% identity) in *S. aureus* was reported to positively regulate the expression of the efflux pump gene NorA and to be involved in bacterial multidrug resistance (Fournier et al., 2000); In addition to these, *Mycobacterium tuberculosis* sulfur metabolism genes including CysN were found to participate in certain antibiotics resistance as well (Hatzios and Bertozzi, 2011). In the current proteomics results, the protein level of *AHA_3222* (A0KN62) was decreased, while CysN and *AHA_3753* (A0KPK0) were increased in the Δ*yeeY* strain under FZ stress. Moreover, the survival of Δ*AHA_3222* was increased, while those of Δ*cysN* and Δ*AHA_3753* were decreased. It indicates that YeeY may positively regulate *AHA_3222* and negatively regulate *cysN* and *AHA_3753* by direct or indirect pathways contributing to survival under FZ stress. In addition, we found SecD was increased in the proteomics analysis, whereas the deletion of *secD* showed increased survival rate under FZ stress. This apparent inconsistency could be the result of a tradeoff between adaption and survival. As an important component of the Sec system for protein secretion, the deletion of *secD* could sharply reduce the membrane permeability and thereby prevent antibiotics entry. However, the loss of some important proteins such as outer membrane proteins will be disadvantageous for survival in the long term. Thus, the regulation of *secD* should be complex or there may be other transcriptional regulators involved.

Additionally, ChIP-PCR and EMSA were performed to explore the relationships of the LTTR protein YeeY with those genes. Interestingly, we found that YeeY can directly regulate *AHA_3222*, which may regulate the expression of efflux pump-related genes involved in bacterial multidrug resistance. Further, it also can directly regulate the outer membrane related gene (*AHA_4275*) during FZ stress. In general, our results provide evidence that the YeeY protein can bind directly with certain ARGs' promoters that contribute to FZ resistance in *A. hydrophila*.

CONCLUSION

In this study, we found that *A. hydrophila* YeeY could directly and positively regulate the ARG such as *AHA_3222* and *AHA_4275* and could indirectly or directly regulate several drug resistance-related genes as well as genes involved in key energy biosynthetic pathways such as metabolism and the bacterial secretion system. Overall, the outcomes of this study gave a view to understand the complicated regulatory mechanisms of transcription factors on bacterial physiological functions. More, it provided a new target for the treatment of pathogenic bacteria and the development of new antimicrobial agents.

DATA AVAILABILITY STATEMENT

All datasets generated for this study are included in the article/**Supplementary Material**.

AUTHOR CONTRIBUTIONS

XL and WL conceived and supervised the project. YF constructed strains, performed the experimental work, and drafted the manuscript. LZ and GW contributed to quantitative proteomics and data analysis. YL, SR, and GY improved the manuscript. All authors reviewed and approved the final manuscript.

FUNDING

This work was sponsored by grants from NSFC projects (Nos. 31670129, 31470238, and 31802343) and China Postdoctoral Science Foundation (No. 2019M662214).

ACKNOWLEDGMENTS

We acknowledge the support of the program for Innovative Research Team in Fujian Agricultural and Forestry University (No. 712018009), Key Laboratory of Marine Biotechnology of Fujian Province (2020MB04), and the Fujian-Taiwan Joint Innovative Center for Germplasm Resources and Cultivation of Crop (FJ 2011 Program, No. 2015-75, China). We also thank Mr. Sheng Yang for providing technical guidance on ChIP-PCR and EMSA.

SUPPLEMENTARY MATERIAL

The Supplementary Material for this article can be found online at: https://www.frontiersin.org/articles/10.3389/fmicb.2020.577376/full#supplementary-material

TABLE S1 | Identification and quantification results between WT and Δ*yeeY* using DIA method in 1.5 g/mL FZ stress.

REFERENCES

Abdelhamed, H., Banes, M., Karsi, A., and Lawrence, M. L. (2019). Recombinant ATPase of virulent *Aeromonas hydrophila* protects channel catfish against motile *Aeromonas septicemia*. *Front. Immunol.* 10:1641. doi: 10.3389/fimmu.2019.01641

Awan, F., Dong, Y., Wang, N., Liu, J., Ma, K., and Liu, Y. (2018). The fight for invincibility: environmental stress response mechanisms and *Aeromonas hydrophila*. *Microb. Pathog.* 116, 135–145. doi: 10.1016/j.micpath.2018.01.023

Chen, C., Chen, H., Zhang, Y., Thomas, H. R., Frank, M. H., He, Y., et al. (2020). TBtools, a toolkit for biologists integrating various HTS-data handling tools with a user-friendly interface. *BioRxiv* [Preprint]. doi: 10.1101/289660

Chen, C. Y., Clark, C. G., Langner, S., Boyd, D. A., Bharat, A., McCorrister, S. J., et al. (2019). Detection of antimicrobial resistance using proteomics and the comprehensive antibiotic resistance database: a case study. *Proteomics Clin. Appl.* 14:e1800182. doi: 10.1002/prca.201800182

Cheng, Z. X., Guo, C., Chen, Z. G., Yang, T. C., Zhang, J. Y., Wang, J., et al. (2019). Glycine, serine and threonine metabolism confounds efficacy of complement-mediated killing. *Nat. Commun.* 10:3325. doi: 10.1038/s41467-019-11129-5

Dahanayake, P. S., Hossain, S., Wickramanayake, M., and Heo, G. J. (2019). Antibiotic and heavy metal resistance genes in *Aeromonas* spp. isolated from marketed Manila Clam (*Ruditapes philippinarum*) in Korea. *J. Appl. Microbiol.* 127, 941–952. doi: 10.1111/jam.14355

Das, B., Verma, J., Kumar, P., Ghosh, A., and Ramamurthy, T. (2020). Antibiotic resistance in *Vibrio cholerae*: understanding the ecology of resistance genes and mechanisms. *Vaccine* 38(Suppl. 1), A83–A92. doi: 10.1016/j.vaccine.2019.06.031

de la Morena, M. L., Van, R., Singh, K., Brian, M., Murray, M. E., and Pickering, L. K. (1993). Diarrhea associated with *Aeromonas* species in children in day care centers. *J. Infect. Dis.* 168, 215–218. doi: 10.1093/infdis/168.1.215

Doerr, A. (2014). DIA mass spectrometry. *Nat. Methods* 12:35. doi: 10.1038/nmeth.3234

Fournier, B., Aras, R., and Hooper, D. C. (2000). Expression of the multidrug resistance transporter NorA from *Staphylococcus aureus* is modified by a two-component regulatory system. *J. Bacteriol.* 182, 664–671. doi: 10.1128/jb.182.3.664-671.2000

Fu, Y. Y., Cai, Q. L., Wang, Y. Q., Li, W. X., Yu, J., Yang, G. D., et al. (2019). Four LysR-type transcriptional regulator family proteins (LTTRs) involved in antibiotic resistance in *Aeromonas hydrophila*. *World J. Microbiol. Biotechnol.* 35:127. doi: 10.1007/s11274-019-2700-3

Girgis, H. S., Harris, K., and Tavazoie, S. (2012). Large mutational target size for rapid emergence of bacterial persistence. *PNAS* 109, 12740–12745. doi: 10.1073/pnas.1205124109

Hatzios, S. K., and Bertozzi, C. R. (2011). The regulation of sulfur metabolism in *Mycobacterium tuberculosis*. *PLoS Pathog.* 7:e1002036. doi: 10.1371/journal.ppat.1002036

Heravi, K. M., and Altenbuchner, J. (2014). Regulation of the *Bacillus subtilis* mannitol utilization genes: promoter structure and transcriptional activation by the wild-type regulator (MtlR) and its mutants. *Microbiology* 160, 91–101. doi: 10.1099/mic.0.071233-0

Kim, Y., Chhor, G., Tsai, C. S., Winans, J. B., Jedrzejczak, R., Joachimiak, A., et al. (2018). Crystal structure of the ligand-binding domain of a LysR-type transcriptional regulator: transcriptional activation via a rotary switch. *Mol. Microbiol.* 110, 550–561. doi: 10.1111/mmi.14115

King, D. T., Wasney, G. A., Nosella, M., Fong, A., and Strynadka, N. C. (2017). Structural insights into inhibition of *Escherichia coli* penicillin-binding protein 1b. *J. Biol. Chem.* 292, 979–993. doi: 10.1074/jbc.M116.718403

Kumar, A., Sarkar, S. K., Ghosh, D., and Ghosh, A. S. (2012). Deletion of penicillin-binding protein 1b impairs biofilm formation and motility in *Escherichia coli*. *Res. Microbiol.* 163, 254–257. doi: 10.1016/j.resmic.2012.01.006

Laxminarayan, R., Duse, A., Wattal, C., Zaidi, A. K., Wertheim, H. F., Sumpradit, N., et al. (2013). Antibiotic resistance-the need for global solutions. *Lancet Infect. Dis.* 13, 1057–1098. doi: 10.1016/S1473-3099(13)70318-9

Li, H., Zhu, Q. F., Peng, X. X., and Peng, B. (2017). Interactome of *E. piscicida* and grouper liver proteins reveals strategies of bacterial infection and host immune response. *Sci. Rep.* 7:39824. doi: 10.1038/srep39824

Li, H. L., Li, Y. J., Sun, T. S., Du, W., Zhang, Z. J., Li, D. C., et al. (2020). Integrative proteome and acetylome analyses of murine responses to *Cryptococcus neoformans* infection. *Front. Microbiol.* 11:575. doi: 10.3389/fmicb.2020.00575

Li, L., Su, Y. B., Peng, B., Peng, X. X., and Li, H. (2020). Metabolic mechanism of colistin resistance and its reverting in Vibrio alginolyticus. *Environ. Microbiol.* doi: 10.1111/1462-2920.15021

Li, W. X., Ali, F., Cai, Q. L., Yao, Z. J., Sun, L. N., Lin, W. X., et al. (2018). Quantitative proteomic analysis reveals that chemotaxis is involved in chlortetracycline resistance of *Aeromonas hydrophila*. *J. Proteomics* 172, 143–151. doi: 10.1016/j.jprot.2017.09.011

Li, W. X., Yao, Z. J., Sun, L. N., Hu, W. J., Cao, J. J., Lin, W. X., et al. (2016). Proteomics analysis reveals a potential antibiotic cocktail therapy strategy for *Aeromonas hydrophila* infection in biofilm. *J. Proteome Res.* 15, 1810–1820. doi: 10.1021/acs.jproteome.5b01127

Li, Z. Q., Wang, Y. Q., Li, X. Y., Lin, Z. P., Lin, Y. X., Srinivasan, R., et al. (2019). The characteristics of antibiotic resistance and phenotypes in 29 outer-membrane protein mutant strains in *Aeromonas hydrophila*. *Environ. Microbiol.* 21, 4614–4628. doi: 10.1111/1462-2920.14761

Lin, X. M., Kang, L. Q., Li, H., and Peng, X. X. (2014). Fluctuation of multiple metabolic pathways is required for *Escherichia coli* in response to chlortetracycline stress. *Mol. Biosyst.* 10, 901–908. doi: 10.1039/c3mb70522f

Liu, J. Q., Xie, L. F., Zhao, D., Yang, T. T., Hu, Y. F., Sun, Z. L., et al. (2019). A fatal diarrhoea outbreak in farm-raised *Deinagkistrodon acutus* in China is newly linked to potentially zoonotic *Aeromonas hydrophila*. *Transbound Emerg. Dis.* 66, 287–298. doi: 10.1111/tbed.13020

Pang, H. Y., Qiu, M. S., Zhao, J. M., Hoare, R., Monaghan, S. J., Song, D. W., et al. (2018). Construction of a Vibrio alginolyticus hopPmaJ (hop) mutant and evaluation of its potential as a live attenuated vaccine in orange-spotted grouper (*Epinephelus coioides*). *Fish Shellfish Immunol.* 76, 93–100. doi: 10.1016/j.fsi.2018.02.012

Peng, B., Su, Y. B., Li, H., Han, Y., Guo, C., Tian, Y. M., et al. (2015). Exogenous alanine and/or glucose plus kanamycin kills antibiotic-resistant bacteria. *Cell. Metab.* 21, 249–262. doi: 10.1016/j.cmet.2015.01.008

Pradel, N., Delmas, J., Wu, L. F., Santini, C. L., and Bonnet, R. (2009). Sec- and Tat-dependent translocation of beta-lactamases across the *Escherichia coli* inner membrane. *Antimicrob. Agents Chemother.* 53, 242–248. doi: 10.1128/AAC.00642-08

Quiblier, C., Zinkernagel, A. S., Schuepbach, R. A., Berger-Bachi, B., and Senn, M. M. (2011). Contribution of SecDF to *Staphylococcus aureus* resistance and expression of virulence factors. *BMC Microbiol.* 11:72. doi: 10.1186/1471-2180-11-72

Rice, K. C., Nelson, J. B., Patton, T. G., Yang, S. J., and Bayles, K. W. (2005). Acetic acid induces expression of the *Staphylococcus aureus* cidABC and lrgAB murein hydrolase regulator operons. *J. Bacteriol.* 187, 813–821. doi: 10.1128/JB.187.3.813-821.2005

Rosato, R. R., Fernandez, R., Paz, L. I., Singh, C. R., and Rosato, A. E. (2014). TCA cycle-mediated generation of ROS is a key mediator for HeR-MRSA survival under beta-lactam antibiotic exposure. *PLoS One* 9:e99605. doi: 10.1371/journal.pone.0099605

Shen, L., Yang, S., Yang, F., Guan, D., and He, S. L. (2020). CaCBL1 acts as a positive regulator in pepper response to *Ralstonia solanacearum*. *Mol. Plant Microbe Interact.* 33, 945–957. doi: 10.1094/MPMI-08-19-0241-R

Smani, Y., Fabrega, A., Roca, I., Sanchez-Encinales, V., Vila, J., and Pachon, J. (2014). Role of OmpA in the multidrug resistance phenotype of *Acinetobacter baumannii*. *Antimicrob. Agents Chemother.* 58, 1806–1808. doi: 10.1128/AAC.02101-13

Soltan Dallal, M. M., Mazaheri Nezhad Fard, R., Kavan Talkhabi, M., Aghaiyan, L., and Salehipour, Z. (2016). Prevalence, virulence and antimicrobial resistance patterns of *Aeromonas* spp. isolated from children with diarrhea. *Germs* 6, 91–96. doi: 10.11599/germs.2016.1094

Su, Y. B., Peng, B., Li, H., Cheng, Z. X., Zhang, T. T., Zhu, J. X., et al. (2018). Pyruvate cycle increases aminoglycoside efficacy and provides respiratory energy in bacteria. *PNAS* 115, E1578–E1587. doi: 10.1073/pnas.1714645115

Sun, L. N., Yao, Z. J., Guo, Z., Zhang, L. S., Wang, Y. Q., Mao, R. R., et al. (2019). Comprehensive analysis of the lysine acetylome in *Aeromonas hydrophila* reveals cross-talk between lysine acetylation and succinylation in LuxS. *Emerg. Microbes Infect.* 8, 1229–1239. doi: 10.1080/22221751.2019.1656549

Wang, G. B., Wang, Y. Q., Zhang, L. S., Cai, Q. L., Lin, Y. X., Lin, L., et al. (2020). Proteomics analysis reveals the effect of *Aeromonas hydrophila* sirtuin CobB on biological functions. *J. Proteomics* 225:103848. doi: 10.1016/j.jprot.2020.103848

Wang, J. F., Zhou, Z. H., He, F., Ruan, Z., Jiang, Y., Hua, X. T., et al. (2018). The role of the type VI secretion system vgrG gene in the virulence and antimicrobial resistance of *Acinetobacter baumannii* ATCC 19606. *PLoS One* 13:e0192288. doi: 10.1371/journal.pone.0192288

Wang, Q., Ji, W., and Xu, Z. (2020). Current use and development of fish vaccines in China. *Fish Shellfish Immunol.* 96, 223–234. doi: 10.1016/j.fsi.2019.12.010

Wisniewski, J. R. (2019). Filter aided sample preparation-A tutorial. *Anal. Chim. Acta* 1090, 23–30. doi: 10.1016/j.aca.2019.08.032

Yang, S. J., Rice, K. C., Brown, R. J., Patton, T. G., Liou, L. E., Park, Y. H., et al. (2005). A LysR-type regulator, CidR, is required for induction of the

Staphylococcus aureus cidABC operon. *J. Bacteriol.* 187, 5893–5900. doi: 10.1128/JB.187.17.5893-5900.2005

Yao, Z. J., Guo, Z., Wang, Y. Q., Li, W. X., Fu, Y. Y., Lin, Y. X., et al. (2019). Integrated succinylome and metabolome profiling reveals crucial role of s-ribosylhomocysteine lyase in quorum sensing and metabolism of *Aeromonas hydrophila*. *Mol. Cell. Proteomics* 18, 200–215. doi: 10.1074/mcp.RA118.001035

Yao, Z. J., Li, W. X., Lin, Y. X., Wu, Q., Yu, F. F., Lin, W. X., et al. (2016). Proteomic analysis reveals that metabolic flows affect the susceptibility of *Aeromonas hydrophila* to antibiotics. *Sci. Rep.* 6:39413. doi: 10.1038/srep39413

Yao, Z. J., Sun, L. N., Wang, Y. Q., Lin, L., Guo, Z., Li, D., et al. (2018). Quantitative proteomics reveals antibiotics resistance function of outer membrane proteins in *Aeromonas hydrophila*. *Front. Cell. Infect. Mi* 8:390. doi: 10.3389/fcimb.2018.00390

Zahran, E., Abd El-Gawad, E. A., and Risha, E. (2018). Dietary Withania somnifera root confers protective and immunotherapeutic effects against *Aeromonas hydrophila* infection in *Nile tilapia* (*Oreochromis niloticus*). *Fish Shellfish Immunol.* 80, 641–650. doi: 10.1016/j.fsi.2018.06.009

Zhang, L. S., Li, W. X., Sun, L. N., Wang, Y. Q., Lin, Y. X., and Lin, X. M. (2020). Quantitative proteomics reveals the molecular mechanism of *Aeromonas hydrophila* in enoxacin stress. *J. Proteomics* 211:103561. doi: 10.1016/j.jprot.2019.103561

Zhang, S., Wang, J., Jiang, M., Xu, D., Peng, B., Peng, X. X., et al. (2019). Reduced redox-dependent mechanism and glucose-mediated reversal in gentamicin-resistant *Vibrio alginolyticus*. *Environ. Microbiol.* 21, 4724–4739. doi: 10.1111/1462-2920.14811

Conflict of Interest: The authors declare that the research was conducted in the absence of any commercial or financial relationships that could be construed as a potential conflict of interest.

frontiers in Microbiology

REVIEW
published: 22 October 2020
doi: 10.3389/fmicb.2020.577564

Combating Antibiotic Tolerance Through Activating Bacterial Metabolism

Yuan Liu[1,2,3,4†], Kangni Yang[1†], Haijie Zhang[1], Yuqian Jia[1] and Zhiqiang Wang[1,3,4*]*

[1]College of Veterinary Medicine, Yangzhou University, Yangzhou, China, [2]Institute of Comparative Medicine, Yangzhou University, Yangzhou, China, [3]Jiangsu Co-innovation Center for Prevention and Control of Important Animal Infectious Diseases and Zoonoses, Yangzhou University, Yangzhou, China, [4]Joint International Research Laboratory of Agriculture and Agri-Product Safety, The Ministry of Education of China, Yangzhou University, Yangzhou, China

The emergence of antibiotic tolerance enables genetically susceptible bacteria to withstand the killing by clinically relevant antibiotics. As is reported, an increasing body of evidence sheds light on the critical and underappreciated role of antibiotic tolerance in the disease burden of bacterial infections. Considering this tense situation, new therapeutic strategies are urgently required for combating antibiotic tolerance. Herein, we provide an insightful illustration to distinguish between antibiotic resistance and tolerance, and highlight its clinical significance and complexities of drug-tolerant bacteria. Then, we discuss the close relationship between antibiotic tolerance and bacterial metabolism. As such, a bacterial metabolism-based approach was proposed to counter antibiotic tolerance. These exogenous metabolites including amino acids, tricarboxylic acid cycle (TCA cycle) metabolites, and nucleotides effectively activate bacterial metabolism and convert the tolerant cells to sensitive cells, and eventually restore antibiotic efficacy. A better understanding of molecular mechanisms of antibiotic tolerance particularly *in vivo* would substantially drive the development of novel strategies targeting bacterial metabolism.

Keywords: antibiotic resistance, antibiotic tolerance, antibiotic efficacy, bacteria, metabolism, metabolites

OPEN ACCESS

Edited by:
Hetron Mweemba Munang'andu, Norwegian University of Life Sciences, Norway

Reviewed by:
Jason H. Yang, Rutgers, The State University of New Jersey, United States
Linsheng Liu, The First Affiliated Hospital of Soochow University, China

***Correspondence:**
Yuan Liu
liuyuan2018@yzu.edu.cn
Zhiqiang Wang
zqwang@yzu.edu.cn

†*These authors have contributed equally to this work*

Specialty section:
This article was submitted to Antimicrobials, Resistance and Chemotherapy, a section of the journal Frontiers in Microbiology

Received: *29 June 2020*
Accepted: *25 September 2020*
Published: *22 October 2020*

Citation:
Liu Y, Yang K, Zhang H, Jia Y and Wang Z (2020) Combating Antibiotic Tolerance Through Activating Bacterial Metabolism. Front. Microbiol. 11:577564. doi: 10.3389/fmicb.2020.577564

INTRODUCTION

Discovery and wide application of antibiotics save millions of lives in the past decades (Marston et al., 2016). Indeed, antibiotics are not only special drugs for infectious diseases, but also as an important cornerstone for the vigorous development of surgical medicine (Ramakrishna et al., 2014). The fortuitous discovery of penicillin by Fleming in 1929 offers an unprecedented regimen for infections caused by Gram-positive bacteria such as *Staphylococcus aureus*, and the identification of streptomycin in 1943 enables the effective control of tuberculosis by *Mycobacterium tuberculosis*. As such, these previous endeavors paved the way for the coming of the golden era of antibiotics. However, just as the saying goes, "*Where there is oppression, there is resistance*", bacteria have evolved versatile means to antagonize antibiotic killing, such as antibiotic resistance (Aminov, 2009). Antibiotic resistance is commonly conferred by the emergence of resistance genes in bacteria, and could spread by plasmid-mediated horizontal transfer during inter- and intra-species. However, it was increasingly observed that bacteria could survive under extensive antibiotic treatments without genotypic changes. This phenomenon

was termed antibiotic tolerance, which was first described by Tomasz et al. (1970). To be specific, they depicted *Streptococcus pneumoniae* with a deficient autolytic system protecting the pathogen from lysis by penicillin. Recently, growing evidence demonstrated that antibiotic tolerance profoundly diminishes antibiotic efficacy both *in vitro* and in clinic (Handwerger and Tomasz, 1985; Fridman et al., 2014). Tolerant bacteria are phenotypically resistant but genetically susceptible to antibiotic treatment (Wiuff et al., 2005; Windels et al., 2019). Traditional testing measures for antibiotic resistance such as minimum inhibitory concentration (MIC) assay (Andrews, 2001) and PCR analysis are not applicable for the detection of antibiotic tolerance. As a consequence, antibiotic tolerance is generally overlooked in clinical practice, existing as a "hidden bomb" that threatens antibiotic efficacy and human health worldwide. Besides, it has been suggested that antibiotic tolerance facilitates the emergence and evolution of antibiotic resistance (Levin-Reisman et al., 2017).

Thus far, several strategies have been proposed for addressing the antibiotic resistance crisis, including novel antibiotics, combinations therapy, and other alternatives to antibiotics. However, these therapies are limited for drug-resistant bacteria but not effective against tolerant bacteria. As such, there is an urgent need to mine distinct strategies to combat antibiotic tolerance, not only for improving treatment outcomes but also to address the crisis caused by antibiotic resistance at the root. Given that phenotypic tolerance is highly sensitive to environmental conditions, which either directly interfere with antibiotics or alter bacterial physiology, thus we reasoned that bacterial metabolic networks-based strategies might be a feasible approach to counteract antibiotic tolerance.

In this review, we first systematically compare the difference between antibiotic resistance and tolerance. Subsequently, we discuss the close relationship between bacterial metabolism and antibiotic tolerance. Based on this, bacterial metabolic network-based approaches were proposed to deal with antibiotic tolerance, by which bacterial metabolic state was re-activated. These findings suggest that bacterial metabolism regulators can serve as potential antibiotic adjuvants, thus providing a distinctly different perspective in the fight against antibiotic tolerance.

DISTINGUISHING BETWEEN ANTIBIOTIC RESISTANCE AND TOLERANCE

Although both antibiotic resistance and tolerance provide a surviving advantage for bacteria after exposure to antibiotics, they are utterly different biology phenomena (**Figure 1**). Resistance is the inheritable capability of microbes to survive high levels of antibiotics and can be determined by the MIC test (Mouton et al., 2018). Be more specific, higher concentrations of antibiotics are required for resistant bacteria when to act as effectively as sensitive bacteria. Tolerance, on the one hand, is more widely used to describe the ability of microorganisms to be briefly exposed to high levels of antibiotics but displaying unaltered MIC values, whether inherited or not (Brauner et al., 2016). On the other hand, their underlying molecular mechanisms are different. The majority molecular mechanisms of antibiotic resistance have been identified through the ongoing study of antibiotic-resistant bacterial strains, including mutations of drug target, deactivation of antibiotic by hydrolases or modified enzyme, and decreased intracellular antibiotic accumulation due to reduced permeability or over-activation of efflux pumps (Blair et al., 2015). These resistance determinants are commonly conferred by resistance genes that are located on chromosomes or mobilized plasmids. For example, metallo-β-lactamases (MBLs) such as NDM-1 could hydrolyze carbapenems in a Zn^{2+}-dependent manner (Walsh et al., 2011), whereas Tet(X) and its variants selectively hydroxylate the tigecycline at C11a and confer high-levels of tigecycline resistance (He et al., 2019; Sun et al., 2019). Besides, mobile colistin resistance (*mcr*)-encoded phosphoethanolamine transferase catalyzes the addition of the cationic moiety to the phosphate groups of lipopolysaccharides (LPSs; Liu et al., 2016), resulting in decreased affinity between colistin and LPS. By contrast, antibiotic tolerance refers to genetically susceptible bacteria but phenotypically tolerant to antibiotic killing (Liu et al., 2019b). Typically, bacterial metabolism-mediated tolerance can be identified in two types: tolerance by "slow growth" or "by lag" (Fridman et al., 2014; Brauner et al., 2016). Slow growth-mediated tolerance occurs at a steady-state (Thonus et al., 1982), yet tolerance by lag is a transient state owing to stressful or starvation conditions (Fridman et al., 2014). Notably, antibiotic tolerance can either be inherited such as an inherently slow growth rate in specific strain, or noninherited under the circumstance of poor growth conditions or within biofilms or host cells (Kitano and Tomasz, 1979; Bernier et al., 2013).

It has been proved that tolerance applies only to bactericidal antibiotics, rather than bacteriostatic antibiotics. Because all bacteria are expected to survive after short-term exposure to bacteriostatic antibiotics, which will not be fatal, but only prevent bacterial growth (Ocampo et al., 2014). As tolerant bacteria and non-tolerant bacteria have the same MIC value, the MIC test is not applicable to evaluate antibiotic tolerance. Although minimum bactericidal concentration (MBC, the antibiotic concentration that is required to kill ≥99.9% of bacterial cells) and MBC/MIC ratio were also proposed as a measure of antibiotic tolerance, these metrics are only reliable for drug-induced tolerance but correlate poorly with other types of tolerance (Keren et al., 2004; Pasticci et al., 2011). Recently, a quantitative indicator based on the time-kill curves, which is called the minimum duration for killing (MDK; Brauner et al., 2017), has been designed to eliminate a certain percentile of the bacterial population. Tolerant bacteria and susceptible strain usually have a similar MIC value, but the MDK_{99} (the minimum duration for killing for 99% bacterial cells) for a tolerant strain is remarkably higher than that in a susceptible strain (Balaban et al., 2019). Nevertheless, antibiotic tolerance has not been fully characterized, owing to the lack of definite quantitative indicators.

Phenotype tolerance to antibiotic treatment exacerbates the lack of effective antibacterial therapy against chronic infections (Fauvart et al., 2011). Based on the mechanism of antibiotic resistance, traditional methods of dealing with drug-resistant bacteria act on critical biosynthesis processes such as membrane

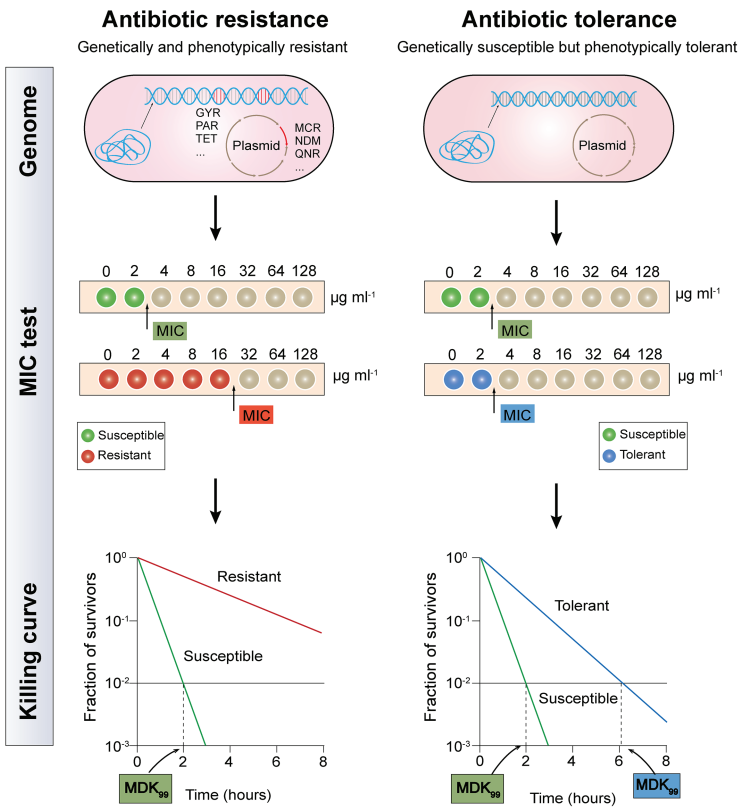

FIGURE 1 | Distinguishing between antibiotic resistance and antibiotic tolerance (Brauner et al., 2016). Antibiotic resistance (the left half of diagram) is characterized by both bacterial genetic and phenotypic resistance; the MIC for a resistant bacteria strain is substantially higher than the MIC for a susceptible bacteria strain; the minimum duration for killing for 99% bacterial cells (MDK_{99}) for a resistant bacteria strain is substantially higher than the MDK_{99} for a susceptible bacteria strain. Antibiotic tolerance (the right half of diagram) is characterized by genetic sensitivity but phenotypic tolerance; the MIC for a tolerant bacteria strain is similar to the MIC for a susceptible bacteria strain; MDK_{99} for a tolerant bacteria strain is 3-fold higher than the MDK_{99} for a susceptible bacteria strain.

synthesis, DNA replication and transcription, and protein synthesis (Liu et al., 2019a), which have limited efficacy in the fight against tolerant bacteria. Thus, novel strategies are urgently needed to combat tolerant bacteria.

CORRELATION BETWEEN ANTIBIOTIC TOLERANCE AND BACTERIAL METABOLISM

As prior mentioned, "tolerance by slow growth" and "tolerance by lag" have been identified as two representative mechanisms for tolerance formation, which are both ultimately attributed to changes in the metabolic status of bacteria (Brauner et al., 2016). In other words, reduced metabolism is one of the crucial drivers for the emergence of antibiotic tolerance. Metabolically dormant bacteria constitute a growing threat to many effective treatment regimens, the treatment of *Pseudomonas aeruginosa* with aminoglycosides was taken as an example, the bactericidal activity of aminoglycosides requires proton motive force (PMF)-dependent transport to allow sufficient cell penetration (Allison et al., 2011). When the central carbon metabolism is perturbed by the addition of carbon source metabolites, the sensitivity of *P. aeruginosa* to tobramycin also changed. In these metabolites, glyoxylate acts as an inducer of antibiotic tolerance by retarding TCA cycle activity and cellular respiration, thereby decreasing transmembrane PMF and drug internalization (Meylan et al., 2017). Similarly, in the study of antibiotic tolerance in *M. tuberculosis* (Mtb), isocitrate lyase mediates broad antibiotic tolerance by remodeling Mtb's TCA cycle, including increased glyoxylate shunt activity and suppressed TCA cycle (Nandakumar et al., 2014). Consistent with this observation, another quantitative proteomics analysis also demonstrated that the decrease in energy metabolism and central carbon are associated with levofloxacin tolerance in naturally occurring waterborne pathogen *Vibrio alginolyticus* (Cheng et al., 2018).

Marked antibiotic tolerance can also be produced by a metabolic downshift coinciding with nutrient deprivation (Braeken et al., 2006; Traxler et al., 2008). When bacteria are exposed to nutrient constraints, they respond by activating a strict response (SR) that changes their state (Boutte and Crosson, 2013), in this regard, the bacterial protein synthesis and other metabolic activities are remarkably shut down. By way of example, *P. aeruginosa* in a nutritionally restricted environment showed tolerance to multiple antibiotics owing to the activation of SR (Nguyen, 2011; Khakimova et al., 2013; Martins et al., 2018).

Besides, a recent study investigated the relative contribution of growth rate and metabolic state of bacteria to antibiotic lethality (Lopatkin et al., 2019). As a result, they found that bacterial metabolic state was more correlated with the antibiotic lethality than growth rate. Similarly, another study demonstrated that the lethal mechanism of beta-lactams is not simply inhibiting penicillin-binding proteins (PBPs), they result in futile cycling of cell wall synthesis and degradation, suggesting that dysfunction of bacterial metabolism is related to antibiotic lethality (Cho et al., 2014b). Collectively, these examples suggest that antibiotic tolerance is closely associated with low levels of metabolism in bacteria, thus it may be possible to restore the sensitivity of tolerant bacteria to antibiotics by altering the metabolic state of bacteria (**Figure 2**).

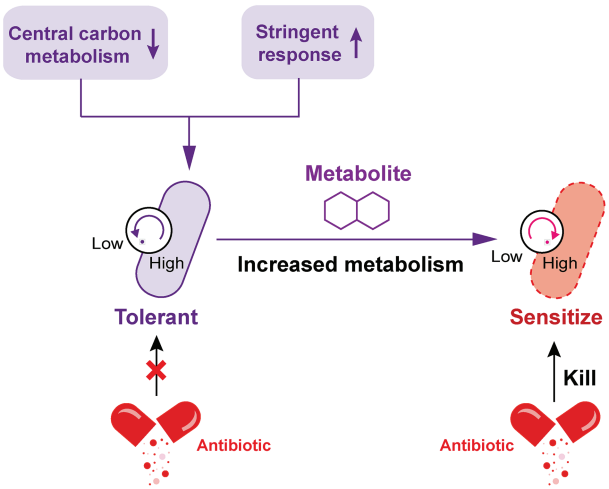

FIGURE 2 | Increased metabolism restores the susceptibility of tolerant bacteria to antibiotics. The decrease of central carbon metabolism level and activation of stringent response drive the inhibition of bacterial metabolic state, which leads to the formation of antibiotic tolerance. By contrast, the addition of specific exogenous metabolites is able to improve the bacterial metabolic state; tolerant bacteria were subsequently converted to metabolically active bacteria and restore susceptibility to antibiotic killing.

BACTERIAL METABOLISM-BASED STRATEGIES AGAINST ANTIBIOTIC TOLERANCE

Since the metabolic state of bacteria correlates with their susceptibility to antibiotic treatment, instead the development of new drugs or adjuvant strategies, modulating bacterial metabolic activity provides a universal strategy to potentiate bactericidal antibiotic killing (Stokes et al., 2019). The metabolic state of a bacterium is closely related to its environment including nutrients, so it is a proposed method to change the metabolic state and restore antibiotic sensitivity by adding exogenous metabolites such as amino acids, tricarboxylic acid (TCA) cycle metabolites and nucleotides during bacterial growth.

Amino Acid Supplementation

Amino acids are one of the most active macromolecules in the construction of living organisms and are the basic materials for the construction of cells and the repair of tissues (Wu, 2013). It has been reported that the combination of multiple amino acids and antibiotics can reinforce antibiotic activity through increasing PMF, upregulating pyruvate cycle (P cycle) or stimulating bacterial respiration, the production of reactive oxygen species (ROS), or host immune response (**Figure 3**).

There are a series of evidence indicate that increasing the transmembrane PMF stimulates the internalization of aminoglycoside antibiotics (Allison et al., 2011; Radlinski et al., 2019). In particular, the PMF is the sum of two components: the electric potential ($\triangle\psi$) and the transmembrane proton gradient ($\triangle$pH; Farha et al., 2013). It has been widely acknowledged that the uptake of aminoglycoside is mainly dependent on $\triangle\psi$, whereas uptake of tetracyclines is driven by $\triangle$pH (Taber et al., 1987; Stokes et al., 2020). For example, fructose or mannitol was found to stimulate the production of PMF *via* increasing $\triangle\psi$ (Allison et al., 2011). Lebeaux et al. found that the bactericidal activity of aminoglycosides against antibiotic-tolerant *Escherichia coli* could be reversed through the supplementation with the basic amino acid, *L*-arginine, which results in increased environmental pH and PMF, as well as the uptake of drugs (Lebeaux et al., 2014).

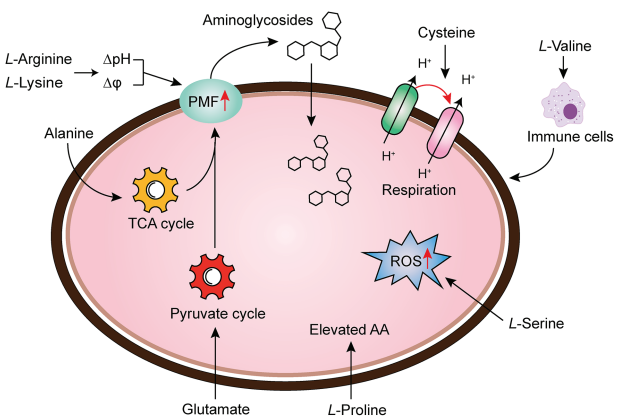

FIGURE 3 | Amino acid supplementation reverses antibiotic tolerance (Liu et al., 2019b). Potentiation of antibiotic efficacy against antibiotic tolerance by exogenous amino acid supplementation results from enhanced amino acid metabolism, proton motive force (PMF), reactive oxygen species (ROS), bacterial cellular respiration, or host immunity.

Controversially, differing from the above notion, they demonstrated that the effect of *L*-arginine on gentamicin against bacterial infection probably relies on transmembrane $\triangle$pH rather than $\triangle\psi$. Furthermore, the beneficial effect of *L*-arginine on aminoglycosides against various pathogens has been verified in both *in vitro* and *in vivo* rat models. Similarly, another basic amino acid *L*-lysine was also found to sensitive both Gram-negative bacteria (*Acinetobacter baumannii*, *E. coli*, and *Klebsiella pneumoniae*), and a Gram-positive bacterium (*Mycobacterium smegmatis*) to aminoglycosides *via* promoting

the transmembrane proton gradient (ΔpH), which in turn enhances PMF and stimulates the uptake of aminoglycosides (Deng et al., 2020). Despite the mechanistic difference in basic amino acids and other metabolites, an increase in PMF is of great importance for the restoration of aminoglycosides activity.

In bacteria, the PMF results from the extrusion of protons by the electron transport chain are highly dependent on the electron donor such as NADH, which produced from the TCA cycle. Therefore, activation of the TCA cycle is also crucial for the bactericidal activity of aminoglycoside antibiotics. In 2015, by comparing the metabolome differences between kanamycin-resistant *Edwardsiella tarda* LTB4 and wild-type strains, Peng et al. (2015) revealed that the alanine and glucose abundance significantly decreased in resistant bacteria. Inspired by this unique phenomenon, they investigated whether kanamycin-resistant *E. tarda* LTB4 cells would restore their sensitivity to aminoglycoside antibiotics when cultured with exogenous alanine and/or glucose. Subsequent studies indicated that the addition of exogenous alanine and/or glucose activated the TCA cycle of the tolerant bacteria and enhanced PMF, thereby increasing their sensitivity to kanamycin, both *in vitro* and in a mouse model of urinary tract infection (Peng et al., 2015). Following this line of thought, the author further showed that glutamate, another depressed biomarker, also promoted the inactivation of drug-resistant bacteria by kanamycin. Mechanical studies indicated that exogenous glutamate reverted the phenotype of antibiotic resistance in both *E. tarda* and *E. coli* by modulating flux through the P cycle, emphasizing that the P cycle is a common pathway of respiration and energy production. More specifically, these results robustly implied that strengthening the P cycle is conducive to respiration and metabolism of bacteria (Su et al., 2018).

To the best of our knowledge, the treatment of Tuberculosis (TB) caused by the bacillus Mtb is a lengthy and arduous process (approximately six mouth), which majorly due to the presence of a small population of tolerant bacteria (Dheda et al., 2016; Furin et al., 2019). Meanwhile, this process may result in the emergence of multidrug-resistant (MDR) TB, which aggravates the infections inevitably (Lobue and Mermin, 2017). Thus, a shorter treatment option would be beneficial (Tiberi et al., 2018). A recent study revealed that the upregulation of bacterial cellular respiration enhanced the antibiotic susceptibility to Mtb cells (Vilcheze et al., 2017). They showed that the addition of cysteine can enhance the effect of isoniazid killing against exponentially growing Mtb cells, and prevent the emergence of drug-resistant mutants. In-depth investigations showed that small thiols could shift the menaquinone/menaquinone balance toward a reduced state, thus stimulating Mtb respiration and potentiating killing by isoniazid or rifampicin. Also, the INH/thiol combination was more effective both *in vitro* and infected murine macrophages by Mtb compared with monotherapy. Additionally, the authors also found that ROS concentrations were higher in INH/Cys-treated Mtb leading to DNA damage, although cysteine is not primarily ROS-mediated as a potentiator, the involvement of ROS production indeed correlates with some specific antibiotic killing. In agreement with this observation, when *L*-serine interacts with fluoroquinolones such as ofloxacin or moxifloxacin in Gram-negative bacteria, the bacteria can produce increased NADH and interfere with Fe-S clusters related to the Fenton's reaction, thereby stimulating the over-production of endogenous ROS and ultimately enhancing the bactericidal action of drugs (Duan et al., 2016). Apart from these mechanisms, the immune modulation of amino acids to host cells has also been revealed. To illustrate, the metabolomic analysis of *K. pneumonia* infected mice showed that *L*-valine was a key metabolite to promote the survival of mice challenged by *K. pneumoniae*; moreover, this similar effect could be observed with other Gram-negative pathogens such as *E. coli*, *P. aeruginosa*, or MRSA, further implying that *L*-valine may be one of the metabolites that regulate immune functions (Chen et al., 2017). It has also been verified that the addition of exogenous *L*-proline has a significant impact on the mortality of tilapia infected by *Streptococcus agalactiae* at higher water temperatures, among which the addition of exogenous *L*-proline can enhance the anti-infection ability of tilapia through triggering its immune response (Zhao et al., 2015). Collectively, these findings provide new insight into the unique functions of amino acids as metabolic modulators in reverting antibiotic tolerance.

TCA Related Metabolites Supplementation

The TCA cycle, as the common and ultimate metabolic pathway of the three major nutrients, and the hub of the metabolism of carbohydrate lipid and amino acid, is an integral part of the metabolism of bacteria (Salway, 2018). Recently, a series of studies revealed that boosting the TCA cycle could alter the metabolic state of bacteria, and thereby improving antibiotic efficacy (**Figure 4**). In 2017, Meylan et al. found that when *P. aeruginosa* was co-cultured with carbon source metabolites in different central metabolic pathways, there were significant differences in the bactericidal activity of tobramycin, implying that the sensitivity of *P. aeruginosa* to tobramycin was related to the disorder of central carbon metabolism. Consistently, lower TCA cycle metabolites such as fumarate, succinate, α-ketoglutarate, and pyruvate significantly sensitized stationary-phase cells to tobramycin. Mechanistic investigations showed that fumarate activated cellular respiration and generated more PMF by stimulating the TCA cycle as a tobramycin potentiator, which was consistent with the prior findings that aminoglycosides' sensitivity is associated with PMF and drug internalization levels (Meylan et al., 2017). By contrast, glyoxylate-treated cells bypass the generation of two reducing equivalents (NADH and $FADH_2$), thereby displaying a lower TCA cycle and decreased cellular respiration, which eventually lead to decreased antibiotic efficacy. In 2018, Su et al. found that glutamate promoted the inactivation of drug-resistant bacteria by kanamycin, and the underlying mechanism revealed a previously unknown prevalent pathway termed P cycle (Su et al., 2018). In the further study of the P cycle, excess carbon sources such as oxaloacetate and pyruvate also improved kanamycin's lethality to *E. tarda* through the same mechanism, indicating that P cycle is a vital pathway for bacterial respiration and energy production.

Another example is quinolone antibiotics, which kill pathogens by targeting the DNA of bacteria, hindering the DNA cyclotron enzyme, further causing the irreversible damage of bacterial DNA

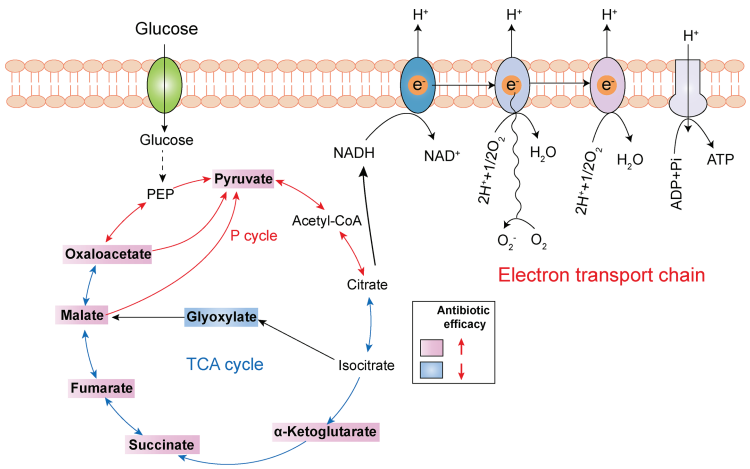

FIGURE 4 | Tricarboxylic acid (TCA) cycle metabolites supplementation restores antibiotic efficacy. The addition of exogenous TCA metabolites (pink background) facilitates pyruvate cycle (red line) or TCA cycle (blue line) and upregulates bacterial electron transport chain, thus improving antibiotic efficacy. However, glyoxylate supplementation (blue background) inhibits TCA cycle and downstream respiration, thereby triggering antibiotic tolerance.

(Mitscher, 2005; Kottur and Nair, 2016; Mohammed et al., 2019). There are also studies showing that the bactericidal effect of quinolones is affected by the density of the cell population, which is called density-dependent persistence (DDP). As the consumption of certain metabolites, such as carbon catabolism and oxidative phosphorylation, has been implicated in DDP, the supplementation of glucose and appropriate terminal electron receptors (such as fumarate) in stationary-phase cultures sensitized cells to quinolone killing by stimulating respiratory metabolism (Gutierrez et al., 2017).

In addition to *in vitro* experimental studies, *in vivo* assay also showed that the benefit of elevated TCA cycle in preventing animal infections. For instance, exogenous malate was confirmed to boost the TCA cycle and increase the enzymatic activities of α-ketoglutaric dehydrogenase (KGDH) and succinate dehydrogenase (SDH; Yang et al., 2018, 2020). Consequently, increased survival of zebrafish to *Vibrio alginolyticus* infection was observed. Besides, a recent study utilized reprogramming metabolomics to explore the metabolic mechanisms of colistin resistance in *V. alginolyticus*. They found that colistin-resistant *V. alginolyticus* was characterized by decreased central carbon metabolism and energy metabolism. By contrast, the addition of metabolites such as pyruvate reverted colistin activity against resistant *V. alginolyticus* both *in vitro* and in zebrafish (Li et al., 2020).

Nucleotide Supplementation

Nucleotides, as one of the essential metabolites of organisms, are widely distributed in the human body and have a variety of biological functions, such as constituting nucleic acid, storeing energy, delivering drugs, and participating in metabolism and physiological regulation (Poijärvi-Virta, 2006; Cho et al., 2014a; Roy et al., 2016). As mentioned earlier, the lethality of bactericidal antibiotics in bacteria correlates with altered bacterial metabolism, including the increased abundance of carbon metabolites in the center of cells and the disruption of nucleotide pools. Accumulated observations imply that the dysfunction of nucleotide metabolism is also associated with bactericidal antibiotic activity, regardless of their macromolecular targets. For example, a study manifested that the killing of β-lactams and quinolones is predominantly elicited by specific oxidation of the guanine to 8-oxyguanine in the nucleotide pool and its subsequent activity in nucleic acid transactions, leading to the overproduction of DinB (DNA polymerase IV) in *E. coli*, which eventually leads to bacterial death (Foti et al., 2012). Besides, the oxidation of deoxynucleotide cytosine triphosphate (dCTP) was also found to lead to antibiotic lethality against stationary-phase *mycobacteria* (Fan et al., 2018).

In cells, nucleotides synthesis is made up of purine and pyrimidine synthesis pathway. On the basis of 5-phosphoribosyl pyrophosphate (PRPP), the *de novo* pathway enzymes produce purine and pyrimidine nucleotides through scratch simple molecules such as CO_2 and amino acids (West, 2014; Lane and Fan, 2015). Meanwhile, the nucleotide end products would produce internal feedback inhibition on nucleotide biosynthesis pathways (**Figure 5A**). In 2019, Yang et al. develop a "white-box" machine-learning approach combining biochemical screening and network modeling to explore metabolic mechanisms of antibiotic lethality and to provide novel mechanistic insights. These results showed that adenine supplementation inhibited the biological activity of purines, reduced the demand for ATP and the metabolic activity of central carbon, and thus reduced the lethality of antibiotics. In contrast, pyrimidine such as uracil supplementation inhibited pyrimidine biosynthesis and in turn promoted purine biosynthesis pathway by PRPP accumulation and, consequently, increased antibiotic lethality (**Figure 5B**; Yang et al., 2019). Consistently, our recent study demonstrated that thymine can potentiate killing by bactericidal antibiotics against multiple Gram-negative bacteria *via* upregulating bacterial metabolism (Unpublished). Given those results, it is probable that pyrimidines may potentially serve as novel antibiotic adjuvants by promoting purine biosynthesis and altering the metabolic status of bacteria.

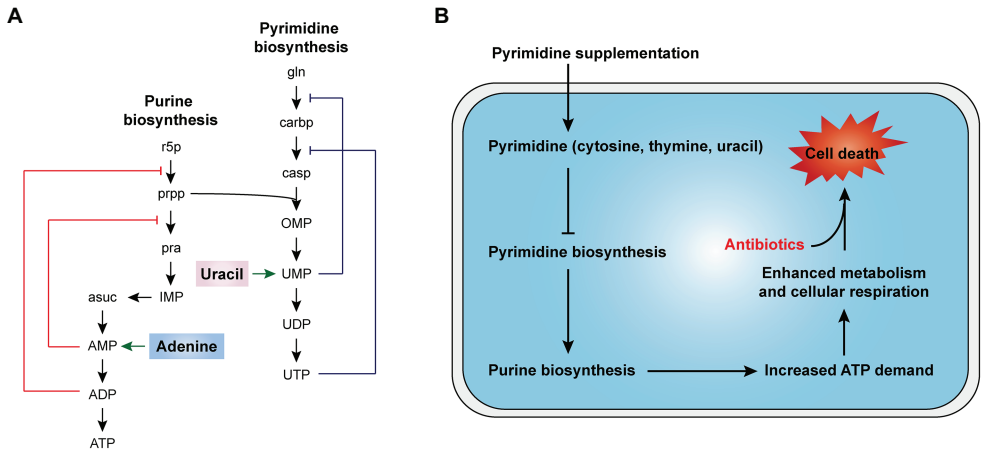

FIGURE 5 | Nucleotides supplementation activates bacterial metabolism (Yang et al., 2019). **(A)** Purine and pyrimidine biosynthesis pathways and feedback inhibition by products. **(B)** The addition of exogenous pyrimidine (cytosine, thymine, and uracil) displays a feedback inhibition on the pyrimidine biosynthesis and triggers purine biosynthesis, thus increasing ATP demand, which drives increased activity through central carbon metabolism and cellular respiration, ultimately restoring the killing of antibiotics against tolerant bacteria.

CONCLUSION AND PROSPECTS

Antibiotic tolerance plays an important but underappreciated role in the evolution of antibiotic resistance. However, at present, there are no standard methods to distinguish between antibiotic tolerance and resistance accurately. Therefore, there is a strong need to deepen mechanisms of action of antibiotic tolerance and identify feasible coping strategies. A collection of studies on the tolerance formation mechanism demonstrates that it is tightly related to the metabolic state of bacteria. The primary manifestation is that antibiotics act on the important metabolic pathway of bacteria, thus changing the metabolic state of bacteria. In turn, the metabolic state of bacteria will also affect the efficacy of antibiotics. Inspired by this notion, we hypothesized that the addition of exogenous compounds to alter the metabolic state of bacteria might recover their sensitivity to antibiotics. As expected, the feasibility and effectiveness of this approach have been partially proved. It has been suggested that various exogenous amino acids, TCA cycle metabolites, and nucleotides can enhance the efficacy of bactericidal antibiotics through activating bacterial metabolism. Besides, other metabolites that enter upper glycolysis such as glucose, mannitol, and fructose could also potentiate antibiotic activity (Allison et al., 2011; Peng et al., 2015; Zeng et al., 2017). Meanwhile, some exogenous compounds have been found to modulate bacterial metabolism and thereby affect antibiotic activity. For example, artemisinin and structural analogs can improve the therapeutic effect of isoniazid on *M. tuberculosis* by inhibiting the dormancy pathway (Zheng et al., 2017). As such, the utilization of these exogenous metabolites as potential antibiotic adjuvants is an emerging and scalable strategy for developing novel antibiotic therapies. In this review, we distinguish the difference between antibiotic tolerance and drug resistance, and discuss the relationship between antibiotic tolerance and bacterial metabolism. Meanwhile, we provide an overview of strategies to restore bacterial sensitivity to antibiotics based on the metabolic network for existing tolerant bacteria according to different metabolite types.

However, the current researches on improving antibiotic efficacy based on the bacterial metabolic network also have some limitations. First, although the metabolic state of bacteria is a uniform characteristic defining antibiotic efficacy across in various physiologic states, the same metabolites did not increase the sensitivity of each pathogen, it is important to note that these strategies must be tuned on a pathogen-by-pathogen basis to be successful. For example, the sensitivity of aminoglycoside to *E. coli* can be enhanced with the addition of four metabolites (glucose, fructose, mannitol, and pyruvate), but fructose was the only one that increased the efficacy of gentamicin against tolerant *S. aureus* (Allison et al., 2011), suggesting that we should consider the characteristics of different pathogens in the process of screening and verifying metabolites that can be used as adjuvant of antibiotics to find species-specific therapeutic strategies. Another serious limitation is that most of the studies targeting tolerance have been proved *in vitro*, with only a few studies that have tested the strategy of using metabolites as antibiotic adjuvants *in vivo* animal models, whereas *in vivo* trials are essential for the application of new antibiotic strategies to actual clinical treatment. Notably, the dynamic changes of metabolites in the physiological environment of resistant bacterial infections cannot be obtained by *in vitro* experiments alone (Yang et al., 2017). It is important to note that several studies have shown that engineered bacterial sensor strains can be used to characterize *in vivo* infection dynamics and to verify the therapeutic effect of antibiotics (Certain et al., 2017). These sensor strains can be customized to detect and report on an array of environmental conditions, bacterial stress responses, and growth behaviors. This progress is worthy of further exploration for the *in vivo* efficacy of metabolites as novel antibiotic adjuvants.

Despite the gaps in our search for new approaches to reverse antibiotic tolerance by metabolite-based approaches, these findings discussed in this review provide a variety of strategies and ideas for exploring novel therapeutic regimens for combating antibiotic tolerance, and in future studies, the complex metabolic networks of bacteria should be more fully utilized.

AUTHOR CONTRIBUTIONS

All authors listed have made a substantial, direct, and intellectual contribution to the work, and approved it for publication.

FUNDING

This work was supported by the National Key Research and Development Program of China (2018YFA0903400), National Natural Science Foundation of China (32002331), Natural Science Foundation of Jiangsu Province of China (BK20190893), Agricultural Science and Technology Independent Innovation Fund of Jiangsu Province (CX(20)3091), China Postdoctoral Science Foundation (2019M651984), A Project Funded by the Priority Academic Program Development of Jiangsu Higher Education Institutions (PAPD), and Lift Engineering of Young Talents of Jiangsu Association for Science and Technology.

REFERENCES

Allison, K. R., Brynildsen, M. P., and Collins, J. J. (2011). Metabolite-enabled eradication of bacterial persisters by aminoglycosides. *Nature* 473, 216–220. doi: 10.1038/nature10069

Aminov, R. I. (2009). The role of antibiotics and antibiotic resistance in nature. *Environ. Microbiol.* 11, 2970–2988. doi: 10.1111/j.1462-2920.2009.01972.x

Andrews, J. M. (2001). Determination of minimum inhibitory concentrations. *J. Antimicrob. Chemother.* 48, 5–16. doi: 10.1093/jac/48.suppl_1.5

Balaban, N. Q., Helaine, S., Lewis, K., Ackermann, M., Aldridge, B., Andersson, D. I., et al. (2019). Definitions and guidelines for research on antibiotic persistence. *Nat. Rev. Microbiol.* 17, 441–448. doi: 10.1038/s41579-019-0196-3

Bernier, S. P., Lebeaux, D., Defrancesco, A. S., Valomon, A., Soubigou, G., Coppée, J. Y., et al. (2013). Starvation, together with the SOS response, mediates high biofilm-specific tolerance to the fluoroquinolone ofloxacin. *PLoS Genet.* 9:e1003144. doi: 10.1371/journal.pgen.1003144

Blair, J. M. A., Webber, M. A., Baylay, A. J., Ogbolu, D. O., and Piddock, L. J. V. (2015). Molecular mechanisms of antibiotic resistance. *Nat. Rev. Microbiol.* 13, 42–51. doi: 10.1038/nrmicro3380

Boutte, C. C., and Crosson, S. (2013). Bacterial lifestyle shapes stringent response activation. *Trends Microbiol.* 21, 174–180. doi: 10.1016/j.tim.2013.01.002

Braeken, K., Moris, M., Daniels, R., Vanderleyden, J., and Michiels, J. (2006). New horizons for (p)ppGpp in bacterial and plant physiology. *Trends Microbiol.* 14, 45–54. doi: 10.1016/j.tim.2005.11.006

Brauner, A., Fridman, O., Gefen, O., and Balaban, N. Q. (2016). Distinguishing between resistance, tolerance and persistence to antibiotic treatment. *Nat. Rev. Microbiol.* 14, 320–330. doi: 10.1038/nrmicro.2016.34

Brauner, A., Shoresh, N., Fridman, O., and Balaban, N. Q. (2017). An experimental framework for quantifying bacterial tolerance. *Biophys. J.* 112, 2664–2671. doi: 10.1016/j.bpj.2017.05.014

Certain, L. K., Way, J. C., Pezone, M. J., and Collins, J. J. (2017). Using engineered bacteria to characterize infection dynamics and antibiotic effects in vivo. *Cell Host Microbe* 22, 263.e4–268.e4. doi: 10.1016/j.chom.2017.08.001

Chen, X. H., Liu, S. R., Peng, B., Li, D., Cheng, Z. X., Zhu, J. X., et al. (2017). Exogenous L-valine promotes phagocytosis to kill multidrug-resistant bacterial pathogens. *Front. Immunol.* 8:207. doi: 10.3389/fimmu.2017.00207

Cheng, Z. X., Yang, M. J., Peng, B., Peng, X. X., Lin, X. M., and Li, H. (2018). The depressed central carbon and energy metabolisms is associated to the acquisition of levofloxacin resistance in *Vibrio alginolyticus*. *J. Proteome* 181, 83–91. doi: 10.1016/j.jprot.2018.04.002

Cho, H., Cho, Y. Y., Bae, Y. H., and Kang, H. C. (2014a). Nucleotides as nontoxic endogenous endosomolytic agents in drug delivery. *Adv. Healthc. Mater.* 3, 1007–1014. doi: 10.1002/adhm.201400008

Cho, H., Uehara, T., and Bernhardt, T. G. (2014b). Beta-lactam antibiotics induce a lethal malfunctioning of the bacterial cell wall synthesis machinery. *Cell* 159, 1300–1311. doi: 10.1016/j.cell.2014.11.017

Deng, W., Fu, T., Zhang, Z., Jiang, X., Xie, J., Sun, H., et al. (2020). L-lysine potentiates aminoglycosides against *Acinetobacter baumannii* via regulation of proton motive force and antibiotics uptake. *Emerg. Microbes Infect.* 9, 639–650. doi: 10.1080/22221751.2020.1740611

Dheda, K., Barry, C. E. 3rd, and Maartens, G. (2016). Tuberculosis. *Lancet* 387, 1211–1226. doi: 10.1016/S0140-6736(15)00151-8

Duan, X., Huang, X., Wang, X., Yan, S., Guo, S., Abdalla, A. E., et al. (2016). L-serine potentiates fluoroquinolone activity against *Escherichia coli* by enhancing endogenous reactive oxygen species production. *J. Antimicrob. Chemother.* 71, 2192–2199. doi: 10.1093/jac/dkw114

Fan, X. -Y., Tang, B. -K., Xu, Y. -Y., Han, A. -X., Shi, K. -X., Wu, Y. -K., et al. (2018). Oxidation of dCTP contributes to antibiotic lethality in stationary-phase mycobacteria. *Proc. Natl. Acad. Sci. U. S. A.* 115, 2210–2215. doi: 10.1073/pnas.1719627115

Farha, M. A., Verschoor, C. P., Bowdish, D., and Brown, E. D. (2013). Collapsing the proton motive force to identify synergistic combinations against *Staphylococcus aureus*. *Chem. Biol.* 20, 1168–1178. doi: 10.1016/j.chembiol.2013.07.006

Fauvart, M., De Groote, V. N., and Michiels, J. (2011). Role of persister cells in chronic infections: clinical relevance and perspectives on anti-persister therapies. *J. Med. Microbiol.* 60, 699–709. doi: 10.1099/jmm.0.030932-0

Foti, J. J., Devadoss, B., Winkler, J. A., Collins, J. J., and Walker, G. C. (2012). Oxidation of the guanine nucleotide pool underlies cell death by bactericidal antibiotics. *Science* 336, 315–319. doi: 10.1126/science.1219192

Fridman, O., Goldberg, A., Ronin, I., Shoresh, N., and Balaban, N. Q. (2014). Optimization of lag time underlies antibiotic tolerance in evolved bacterial populations. *Nature* 513, 418–421. doi: 10.1038/nature13469

Furin, J., Cox, H., and Pai, M. (2019). Tuberculosis. *Lancet* 393, 1642–1656. doi: 10.1016/S0140-6736(19)30308-3

Gutierrez, A., Jain, S., Bhargava, P., Hamblin, M., Lobritz, M. A., and Collins, J. J. (2017). Understanding and sensitizing density-dependent persistence to quinolone antibiotics. *Mol. Cell* 68, 1147.e3–1154.e3. doi: 10.1016/j.molcel.2017.11.012

Handwerger, S., and Tomasz, A. (1985). Antibiotic tolerance among clinical isolates of bacteria. *Annu. Rev. Pharmacol. Toxicol.* 25, 349–380. doi: 10.1146/annurev.pa.25.040185.002025

He, T., Wang, R., Liu, D., Walsh, T. R., Zhang, R., Lv, Y., et al. (2019). Emergence of plasmid-mediated high-level tigecycline resistance genes in animals and humans. *Nat. Microbiol.* 4, 1450–1456. doi: 10.1038/s41564-019-0445-2

Keren, I., Kaldalu, N., Spoering, A., Wang, Y., and Lewis, K. (2004). Persister cells and tolerance to antimicrobials. *FEMS Microbiol. Lett.* 230, 13–18. doi: 10.1016/S0378-1097(03)00856-5

Khakimova, M., Ahlgren, H. G., Harrison, J. J., English, A. M., and Nguyen, D. (2013). The stringent response controls catalases in *Pseudomonas aeruginosa* and is required for hydrogen peroxide and antibiotic tolerance. *J. Bacteriol.* 195, 2011–2020. doi: 10.1128/JB.02061-12

Kitano, K., and Tomasz, A. (1979). *Escherichia coli* mutants tolerant to beta-lactam antibiotics. *J. Bacteriol.* 140, 955–963. doi: 10.1128/JB.140.3.955-963.1979

Kottur, J., and Nair, D. T. (2016). Reactive oxygen species play an important role in the bactericidal activity of quinolone antibiotics. *Angew. Chem. Int. Edit.* 55, 2397–2400. doi: 10.1002/anie.201509340

Lane, A. N., and Fan, T. W. (2015). Regulation of mammalian nucleotide metabolism and biosynthesis. *Nucleic Acids Res.* 43, 2466–2485. doi: 10.1093/nar/gkv047

Lebeaux, D., Chauhan, A., Létoffé, S., Fischer, F., de Reuse, H., Beloin, C., et al. (2014). pH-mediated potentiation of aminoglycosides kills bacterial

persisters and eradicates in vivo biofilms. *J. Infect. Dis.* 210, 1357–1366. doi: 10.1093/infdis/jiu286

Levin-Reisman, I., Ronin, I., Gefen, O., Braniss, I., Shoresh, N., and Balaban, N. Q. (2017). Antibiotic tolerance facilitates the evolution of resistance. *Science* 355, 826–830. doi: 10.1126/science.aaj2191

Li, L., Su, Y. B., Peng, B., Peng, X. X., and Li, H. (2020). Metabolic mechanism of colistin resistance and its reverting in *Vibrio alginolyticus*. *Environ. Microbiol.* doi: 10.1111/1462-2920.15021 [Epub ahead of print]

Liu, Y., Ding, S., Shen, J., and Zhu, K. (2019a). Nonribosomal antibacterial peptides that target multidrug-resistant bacteria. *Nat. Prod. Rep.* 36, 573–592. doi: 10.1039/c8np00031j

Liu, Y., Li, R., Xiao, X., and Wang, Z. (2019b). Bacterial metabolism-inspired molecules to modulate antibiotic efficacy. *J. Antimicrob. Chemother.* 74, 3409–3417. doi: 10.1093/jac/dkz230

Liu, Y. -Y., Wang, Y., Walsh, T. R., Yi, L. -X., Zhang, R., Spencer, J., et al. (2016). Emergence of plasmid-mediated colistin resistance mechanism MCR-1 in animals and human beings in China: a microbiological and molecular biological study. *Lancet Infect. Dis.* 16, 161–168. doi: 10.1016/S1473-3099(15)00424-7

Lobue, P. A., and Mermin, J. H. (2017). Latent tuberculosis infection: the final frontier of tuberculosis elimination in the USA. *Lancet Infect. Dis.* 17, e327–e333. doi: 10.1016/S1473-3099(17)30248-7

Lopatkin, A. J., Stokes, J. M., Zheng, E. J., Yang, J. H., Takahashi, M. K., You, L., et al. (2019). Bacterial metabolic state more accurately predicts antibiotic lethality than growth rate. *Nat. Microbiol.* 4, 2109–2117. doi: 10.1038/s41564-019-0536-0

Marston, H. D., Dixon, D. M., Knisely, J. M., Palmore, T. N., and Fauci, A. S. (2016). Antimicrobial resistance. *JAMA* 316, 1193–1204. doi: 10.1001/jama.2016.11764

Martins, D., McKay, G., Sampathkumar, G., Khakimova, M., English, A. M., and Nguyen, D. (2018). Superoxide dismutase activity confers (p)ppGpp-mediated antibiotic tolerance to stationary-phase *Pseudomonas aeruginosa*. *Proc. Natl. Acad. Sci. U. S. A.* 115, 9797–9802. doi: 10.1073/pnas.1804525115

Meylan, S., Porter, C. B. M., Yang, J. H., Belenky, P., Gutierrez, A., Lobritz, M. A., et al. (2017). Carbon sources tune antibiotic susceptibility in *Pseudomonas aeruginosa* via tricarboxylic acid cycle control. *Cell Chem. Biol.* 24, 195–206. doi: 10.1016/j.chembiol.2016.12.015

Mitscher, L. A. (2005). Bacterial topoisomerase inhibitors: quinolone and pyridone antibacterial agents. *Chem. Rev.* 105, 559–592. doi: 10.1021/cr030101q

Mohammed, H. H. H., Abuo-Rahma, G., Abbas, S. H., and Abdelhafez, E. M. N. (2019). Current trends and future directions of fluoroquinolones. *Curr. Med. Chem.* 26, 3132–3149. doi: 10.2174/0929867325666180214122944

Mouton, J. W., Muller, A. E., Canton, R., Giske, C. G., Kahlmeter, G., and Turnidge, J. (2018). MIC-based dose adjustment: facts and fables. *J. Antimicrob. Chemother.* 73, 564–568. doi: 10.1093/jac/dkx427

Nandakumar, M., Nathan, C., and Rhee, K. Y. (2014). Isocitrate lyase mediates broad antibiotic tolerance in *Mycobacterium tuberculosis*. *Nat. Commun.* 5:4306. doi: 10.1038/ncomms5306

Nguyen, D. (2011). Active starvation responses mediate antibiotic tolerance in biofilms and nutrient-limited bacteria. *Science* 334, 982–986. doi: 10.1126/science.1211037

Ocampo, P. S., Lázár, V., Papp, B., Arnoldini, M., Abel Zur Wiesch, P., Busa-Fekete, R., et al. (2014). Antagonism between bacteriostatic and bactericidal antibiotics is prevalent. *Antimicrob. Agents Chemother.* 58, 4573–4582. doi: 10.1128/AAC.02463-14

Pasticci, M. B., Moretti, A., Stagni, G., Ravasio, V., Soavi, L., Raglio, A., et al. (2011). Bactericidal activity of oxacillin and glycopeptides against *Staphylococcus aureus* in patients with endocarditis: looking for a relationship between tolerance and outcome. *Ann. Clin. Microbiol. Antimicrob.* 10:26. doi: 10.1186/1476-0711-10-26

Peng, B., Su, Y. B., Li, H., Han, Y., Guo, C., Tian, Y. M., et al. (2015). Exogenous alanine and/or glucose plus kanamycin kills antibiotic-resistant bacteria. *Cell Metab.* 21, 249–262. doi: 10.1016/j.cmet.2015.01.008

Poijärvi-Virta, P. (2006). Prodrug approaches of nucleotides and oligonucleotides. *Curr. Med. Chem.* 13, 3441–3465. doi: 10.2174/092986706779010270

Radlinski, L. C., Rowe, S. E., Brzozowski, R., Wilkinson, A. D., Huang, R., Eswara, P., et al. (2019). Chemical induction of aminoglycoside uptake overcomes antibiotic tolerance and resistance in *Staphylococcus aureus*. *Cell Chem. Biol.* 26, 1355.e4–1364.e4. doi: 10.1016/j.chembiol.2019.07.009

Ramakrishna, S., Kwaku Dad, A. B., Beloor, J., Gopalappa, R., Lee, S. K., and Kim, H. (2014). Gene disruption by cell-penetrating peptide-mediated delivery of Cas9 protein and guide RNA. *Genome Res.* 24, 1020–1027. doi: 10.1101/gr.171264.113

Roy, B., Depaix, A., Périgaud, C., and Peyrottes, S. (2016). Recent trends in nucleotide synthesis. *Chem. Rev.* 116, 7854–7897. doi: 10.1021/acs.chemrev.6b00174

Salway, J. G. (2018). The Krebs uric acid cycle: a forgotten Krebs cycle. *Trends Biochem. Sci.* 43, 847–849. doi: 10.1016/j.tibs.2018.04.012

Stokes, J. M., Lopatkin, A. J., Lobritz, M. A., and Collins, J. J. (2019). Bacterial metabolism and antibiotic efficacy. *Cell Metab.* 30, 251–259. doi: 10.1016/j.cmet.2019.06.009

Stokes, J. M., Yang, K., Swanson, K., Jin, W., Cubillos-Ruiz, A., Donghia, N. M., et al. (2020). A deep learning approach to antibiotic discovery. *Cell* 180, 688–702. doi: 10.1016/j.cell.2020.01.021

Su, Y. B., Peng, B., Li, H., Cheng, Z. X., Zhang, T. T., Zhu, J. X., et al. (2018). Pyruvate cycle increases aminoglycoside efficacy and provides respiratory energy in bacteria. *Proc. Natl. Acad. Sci. U. S. A.* 115, E1578–E1587. doi: 10.1073/pnas.1714645115

Sun, J., Chen, C., Cui, C. Y., Zhang, Y., Liu, X., Cui, Z. H., et al. (2019). Plasmid-encoded tet(X) genes that confer high-level tigecycline resistance in *Escherichia coli*. *Nat. Microbiol.* 4, 1457–1464. doi: 10.1038/s41564-019-0496-4

Taber, H. W., Mueller, J. P., Miller, P. F., and Arrow, A. S. (1987). Bacterial uptake of aminoglycoside antibiotics. *Microbiol. Rev.* 51, 439–457. doi: 10.1128/MMBR.51.4.439-457.1987

Thonus, I. P., Fontijne, P., and Michel, M. F. (1982). Ampicillin susceptibility and ampicillin-induced killing rate of *Escherichia coli*. *Antimicrob. Agents Chemother.* 22, 386–390. doi: 10.1128/aac.22.3.386

Tiberi, S., Du Plessis, N., Walzl, G., Vjecha, M. J., Rao, M., Ntoumi, F., et al. (2018). Tuberculosis: progress and advances in development of new drugs, treatment regimens, and host-directed therapies. *Lancet Infect. Dis.* 18, e183–e198. doi: 10.1016/S1473-3099(18)30110-5

Tomasz, A., Albino, A., and Zanati, E. (1970). Multiple antibiotic resistance in a bacterium with suppressed autolytic system. *Nature* 227, 138–140. doi: 10.1038/227138a0

Traxler, M. F., Summers, S. M., Nguyen, H. T., Zacharia, V. M., Hightower, G. A., Smith, J. T., et al. (2008). The global, ppGpp-mediated stringent response to amino acid starvation in *Escherichia coli*. *Mol. Microbiol.* 68, 1128–1148. doi: 10.1073/pnas.1704376114

Vilcheze, C., Hartman, T., Weinrick, B., Jain, P., Weisbrod, T. R., Leung, L. W., et al. (2017). Enhanced respiration prevents drug tolerance and drug resistance in *Mycobacterium tuberculosis*. *Proc. Natl. Acad. Sci. U. S. A.* 114, 4495–4500. doi: 10.1073/pnas.1704376114

Walsh, T. R., Weeks, J., Livermore, D. M., and Toleman, M. A. (2011). Dissemination of NDM-1 positive bacteria in the New Delhi environment and its implications for human health: an environmental point prevalence study. *Lancet Infect. Dis.* 11, 355–362. doi: 10.1016/S1473-3099(11)70059-7

West, T. P. (2014). Pyrimidine nucleotide synthesis in *Pseudomonas nitroreducens* and the regulatory role of pyrimidines. *Microbiol. Res.* 169, 954–958. doi: 10.1016/j.micres.2014.04.003

Windels, E. M., Michiels, J. E., Van Den Bergh, B., Fauvart, M., and Michiels, J. (2019). Antibiotics: combatting tolerance to stop resistance. *MBio* 10, e02095–e02119. doi: 10.1128/mBio.02095-19

Wiuff, C., Zappala, R. M., Regoes, R. R., Garner, K. N., Baquero, F., and Levin, B. R. (2005). Phenotypic tolerance: antibiotic enrichment of noninherited resistance in bacterial populations. *Antimicrob. Agents Chemother.* 49, 1483–1494. doi: 10.1128/AAC.49.4.1483-1494.2005

Wu, G. (2013). Functional amino acids in nutrition and health. *Amino Acids* 45, 407–411. doi: 10.1007/s00726-013-1500-6

Yang, J. H., Bhargava, P., Mccloskey, D., Mao, N., Palsson, B. O., and Collins, J. J. (2017). Antibiotic-induced changes to the host metabolic environment inhibit drug efficacy and alter immune function. *Cell Host Microbe* 22, 757.e3–765.e3. doi: 10.1016/j.chom.2017.10.020

Yang, M. J., Cheng, Z. X., Jiang, M., Zeng, Z. H., Peng, B., Peng, X. X., et al. (2018). Boosted TCA cycle enhances survival of zebrafish to *Vibrio alginolyticus* infection. *Virulence* 9, 634–644. doi: 10.1080/21505594.2017.1423188

Yang, J. H., Wright, S. N., Hamblin, M., Mccloskey, D., Alcantar, M. A., Schrubbers, L., et al. (2019). A white-box machine learning approach for revealing antibiotic mechanisms of action. *Cell* 177, 1649.e9–1661.e9. doi: 10.1016/j.cell.2019.04.016

Yang, M. J., Xu, D., Yang, D. X., Li, L., Peng, X. X., Chen, Z. G., et al. (2020). Malate enhances survival of zebrafish against *Vibrio alginolyticus* infection in the same manner as taurine. *Virulence* 11, 349–364. doi: 10.1080/21505594.2020.1750123

Zeng, Z. H., Du, C. C., Liu, S. R., Li, H., Peng, X. X., and Peng, B. (2017). Glucose enhances tilapia against *Edwardsiella tarda* infection through metabolome reprogramming. *Fish Shellfish Immunol.* 61, 34–43. doi: 10.1016/j.fsi.2016.12.010

Zhao, X. L., Han, Y., Ren, S. T., Ma, Y. M., Li, H., and Peng, X. X. (2015). L-proline increases survival of tilapias infected by *Streptococcus agalactiae* in higher water temperature. *Fish Shellfish Immunol.* 44, 33–42. doi: 10.1016/j.fsi.2015.01.025

Zheng, H., Colvin, C. J., Johnson, B. K., Kirchhoff, P. D., Wilson, M., Jorgensen-Muga, K., et al. (2017). Inhibitors of *Mycobacterium tuberculosis* DosRST signaling and persistence. *Nat. Chem. Biol.* 13, 218–225. doi: 10.1038/nchembio.2259

Conflict of Interest: The authors declare that the research was conducted in the absence of any commercial or financial relationships that could be construed as a potential conflict of interest.

frontiers in Microbiology

ORIGINAL RESEARCH
published: 02 November 2020
doi: 10.3389/fmicb.2020.598380

Integrated Co-functional Network Analysis on the Resistance and Virulence Features in *Acinetobacter baumannii*

Ruiqiang Xie[1], *Ningyi Shao*[1] *and Jun Zheng*[1,2]*

[1] *Faculty of Health Sciences, University of Macau, Macau, China,* [2] *Institute of Translational Medicine, University of Macau, Macau, China*

Acinetobacter baumannii is one of the most troublesome bacterial pathogens that pose major public health threats due to its rapidly increasing drug resistance property. It is not only derived from clinic setting but also emerges from aquaculture as a fish pathogen, which could pass the resistant genes in the food chain. Understanding the mechanism of antibiotic resistance development and pathogenesis will aid our battle with the infections caused by *A. baumannii*. In this study, we constructed a co-functional network by integrating multiple sources of data from *A. baumannii* and then used the k-shell decomposition to analyze the co-functional network. We found that genes involving in basic cellular physiological function, including genes for antibiotic resistance, tended to have high k-shell values and locate in the internal layer of our network. In contrast, the non-essential genes, such as genes associated with virulence, tended to have lower k-shell values and locate in the external layer. This finding allows us to fish out the potential antibiotic resistance factors and virulence factors. In addition, we constructed an online platform ABviresDB (https://acba.shinyapps.io/ABviresDB/) for visualization of the network and features of each gene in *A. baumannii*. The network analysis in this study will not only aid the study on *A. baumannii* but also could be referenced for the research of antibiotic resistance and pathogenesis in other bacteria.

Keywords: *Acinetobacter baumannii*, integrated network, k-shell decomposition, antibiotic resistance, virulence factor

OPEN ACCESS

Edited by:
Bo Peng,
Sun Yat-sen University, China

Reviewed by:
Chen Ming,
Icahn School of Medicine at Mount Sinai, United States
Miao Liu,
Harvard Medical School, United States
Hai Xia Xie,
Chinese Academy of Sciences, China

***Correspondence:**
Jun Zheng
junzheng@um.edu.mo

Specialty section:
This article was submitted to Antimicrobials, Resistance and Chemotherapy, a section of the journal Frontiers in Microbiology

Received: *24 August 2020*
Accepted: *06 October 2020*
Published: *02 November 2020*

Citation:
Xie R, Shao N and Zheng J (2020) Integrated Co-functional Network Analysis on the Resistance and Virulence Features in Acinetobacter baumannii. Front. Microbiol. 11:598380. doi: 10.3389/fmicb.2020.598380

INTRODUCTION

Acinetobacter baumannii, an opportunistic gram-negative bacterial pathogen, has emerged as the most common cause of nosocomial and difficult-to-treat infections (Asif et al., 2018). It has become especially troublesome due to the quick emergence and wide spread of antibiotic resistance. In fact, *A. baumannii* has developed resistance to almost all antibiotics clinically used and the infections by multidrug-resistant strains are very common (Xie et al., 2018; Theuretzbacher et al., 2020). In addition, *A. baumannii* persistence could also contribute to the treatment failure of its infection (BarthJr., Rodrigues et al., 2013; Zou et al., 2018, 2020; Ji et al., 2019). In fact, death caused by drug-resistant *A. baumannii* infections has increased by approximately 60% in the past 6 years (Allen et al., 2020). The threats by *A. baumannii* have recently been emphasized by WHO, which has

listed *A. baumannii* as the priority 1 pathogen for research and development on new antimicrobial treatment (World Health Organization [WHO], 2017). Thus, it is urgent to find new approaches to battle with the infection caused by *A. baumannii*, whereas understanding the factors contributing to its antibiotic resistance will help this endeavor.

In addition to the cause of well-known nosocomial infections, *A. baumannii* has recently been recognized as an emerging fish pathogen, raising the public concern of *A. baumannii* transmission from aquatic culture to human through food chain (Dekic et al., 2018). In fact, *A. baumannii*, including antibiotic resistant *A. baumannii*, has been isolated from a wide range of aquatic environments and diverse fish species (Musa et al., 2008; Xia et al., 2008; Rauta et al., 2011; Brahmi et al., 2016). Behera et al. isolated *A. baumannii* from diseased fish—*Labeo rohita*—and found that intraperitoneal transmission of isolated *A. baumannii* to fish resulted in significant mortality, further confirming that *A. baumannii* is a fish pathogen (Behera et al., 2017). Thus, *A. baumannii* not only threatens human health but also could cause loss in fishery.

To successfully establish a niche in the infected host, bacteria have to be equipped with virulence factors (Cornejo et al., 2017). In addition to the wide existence of drug resistance, the virulence factors of *A. baumannii* contributed greatly to the successful infection in host (Harding et al., 2018; Morris et al., 2019). Biofilm formation, motility, and the secretion systems are common virulence factors for bacterial pathogens, including *A. baumannii* (Harding et al., 2018). Despite extensive research work that has been conducted, the pathogenesis of *A. baumannii* is still yet to be fully understood. Identification and shortlist of potential virulence factors would greatly contribute to the study and understanding on *A. baumannii* infections.

Biological network represents a typically biological system reflecting the direct and indirect connection of different molecular factors. These molecular factors, including genes or proteins, play important roles in the biological process, cellular function, and signaling cascades of the organisms (Vidal et al., 2011). Network topological structure could provide important information from its nodes or edges with the parameters of the centrality, betweenness, and degree. The hub nodes or influential nodes generally play pivotal roles in the complex biological network (Cho et al., 2012) and tend to correspond to proteins that are essential (Zotenko et al., 2008). Recently, the k-shell decomposition method was illustrated to be effective to identify influential nodes in the network (Pei et al., 2014). In general, analyzing the network structure and understanding the topological properties could discover novel nodes in the complex biologic system and provide new insights for elucidation of the molecular mechanism (Yan et al., 2018). For example, through a genome-scale co-functional network analysis, Lee et al. successfully identified several novel genes associated with antibiotic resistance or virulence in *Klebsiella pneumoniae* (Lee et al., 2019).

In this study, we have developed a new strategy to understand the connection of different molecular factors in *A. baumannii*. We integrated the co-expression, operon organization, and the corresponding protein structural data of genes in *A. baumannii* and constructed an integrated network. Our analysis showed that genes involved in basic cellular physiological function, including genes for antibiotic resistance, tended to have high k-shell values and locate in the internal layer of our network. In contrast, the non-essential genes, such as genes associated with virulence, tended to have lower k-shell values and locate in the external of our network. Based on this finding and the protein structure similarity to known resistance and virulence factors, we have identified a list of potential factors involved in antibiotic resistance and bacterial virulence. Furthermore, the *A. baumannii* virulence and resistance database (ABviresDB) was constructed to visualize the network and the features of each gene in *A. baumannii*. The ABviresDB supports several functions for *A. baumannii* research, including searching, browsing, data downloading, feedback, help, and analysis. We expect that our study would contribute to the future research on the antibiotic resistance and virulence of *A. baumannii*.

MATERIALS AND METHODS

Data Source

The genomic data from *A. baumannii* ATCC 17978 were used for our analysis. The gene expression data were sourced from GEO database (**Supplementary Table S1**). The gene and its promoter as well as the operon information were integrated from the ProOpDB (Taboada et al., 2012) and DOOR2 (Mao et al., 2014) database. The structure family data were extracted from the Superfamily 1.75 (Gough et al., 2001). The pathway information of genes in *A. baumannii* was accessed from KEGG (Kyoto Encyclopedia of Genes and Genomes) database.

Network Analysis

The centrality in the co-functional network was analyzed using R package igraph (Csardi and Nepusz, 2006). Briefly, the basic features of the co-functional network, including the degree and the number of edges connected to a node, were calculated. Betweenness refers to the number of shortest paths that pass through a node. Closeness means the quantitative index of the centrality of one node. The parameters including degree, betweenness, and closeness were also calculated with the R package igraph.

The k-shell decomposition is a well-established method for analyzing the structure of complex networks (Wei et al., 2015). It assigns an integer index to each node that represents the location of the node in the network based on its connectivity patterns (Carmi et al., 2007). The implementation of the k-shell algorithm was accessed from a previous study and performed in our network analysis with the default cut-off value (Ahmed et al., 2018). The hub node is defined as the node with high value of k shell and high degree. The average degree was calculated by summing the degree of each node and dividing the number of nodes for each shell. The network visualization was applied by R package of networkD3 (Allaire et al., 2017). The network property was analyzed by Cytoscape v3.7.2 (Shannon et al., 2003).

Statistical Analysis

Linear regression was applied to calculate the relationship between the degree and the k-shell values of nodes by using R program. The functional annotation was used to determine the enrichment of the interested groups of clustered genes. The functional enrichment was carried out by hypergeometric test with DAVID 6.7 (Huang da et al., 2009). The gene expression data of different samples were normalized using Z-score transformation. The co-expression network was constructed based on Pearson's correlation coefficient for calculating the correlation of two genes. The cut-off of the Pearson correlation coefficient was set as its absolute value of 0.8 for high correlation and $p < 0.05$. The Clusters of Orthologous Groups (COGs) of the protein were predicted by EggNOG database (Huerta-Cepas et al., 2017).

RESULTS

The Integrated Regulatory Network in *A. baumannii* Infections

To examine the relationship between gene-to-gene interaction at a system level, we curated multiple sources of datasets corresponding to the gene expression, operon organization, and the structural similarities of the corresponding protein to construct a co-functional network (**Figure 1**). First, to demonstrate the high co-expression relationship between the gene pairs, an absolute value of correlation coefficient, which was greater than 0.8, was set to build the gene co-expression network. The co-expression network was fitted with power-law form (R^2 = 0.892). The heatmap of the correlation coefficient between genes described the whole expression profile of genes in *A. baumannii* (**Figure 2A**). The gene pairs with highly correlated expression presumably have similar physiological functions or biological features. Next, the operon network was constructed based on the genes from the same operon organization, which demonstrated the co-transcription regulation relationship between genes (**Figure 1**). Lastly, to find the relationship of the corresponding proteins with a similar structure or the same domain, the protein family encoded by each gene was sourced and integrated to construct a co-family network for gene pairs from the same protein family. Subsequently, we mapped these subnetworks to construct a co-functional network which was fitted with power-law form (R^2 = 0.773, **Supplementary Figure S1**).

The k-shell decomposition was used to analyze the co-functional network and each gene was assigned to different layers based on the k-shell values. The genes in the internal layers have high k-shell values. In contrast, the genes in the peripheral layers have relatively low k-shell values. We analyzed the top 500 genes based on their k-shell values and found that these genes were mainly clustered in the COGs function of transcription and metabolism that presumably act as the basic physiological function in cell activity (**Supplementary Figure S2**). In addition, our results found that the k-shell value significantly correlated with its degree (**Figure 2B**, linear regression R^2 = 0.819). The degree of nodes in internal network has a high value compared with that in the peripheral network (**Figure 2C**).

We further analyzed the betweenness of the co-functional network and found that the nodes with the top high betweenness were mainly clustered in the internal co-functional network (**Figure 2D**). The genes with the betweenness on the top 100,

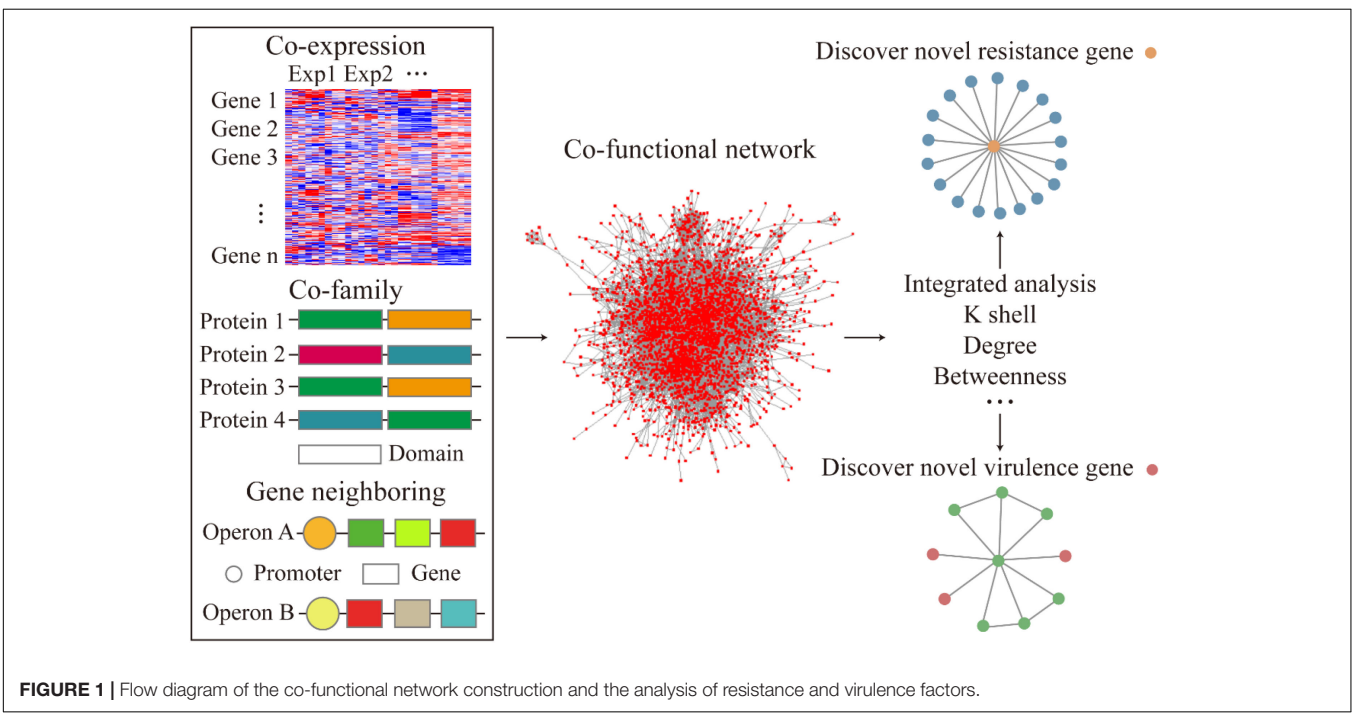

FIGURE 1 | Flow diagram of the co-functional network construction and the analysis of resistance and virulence factors.

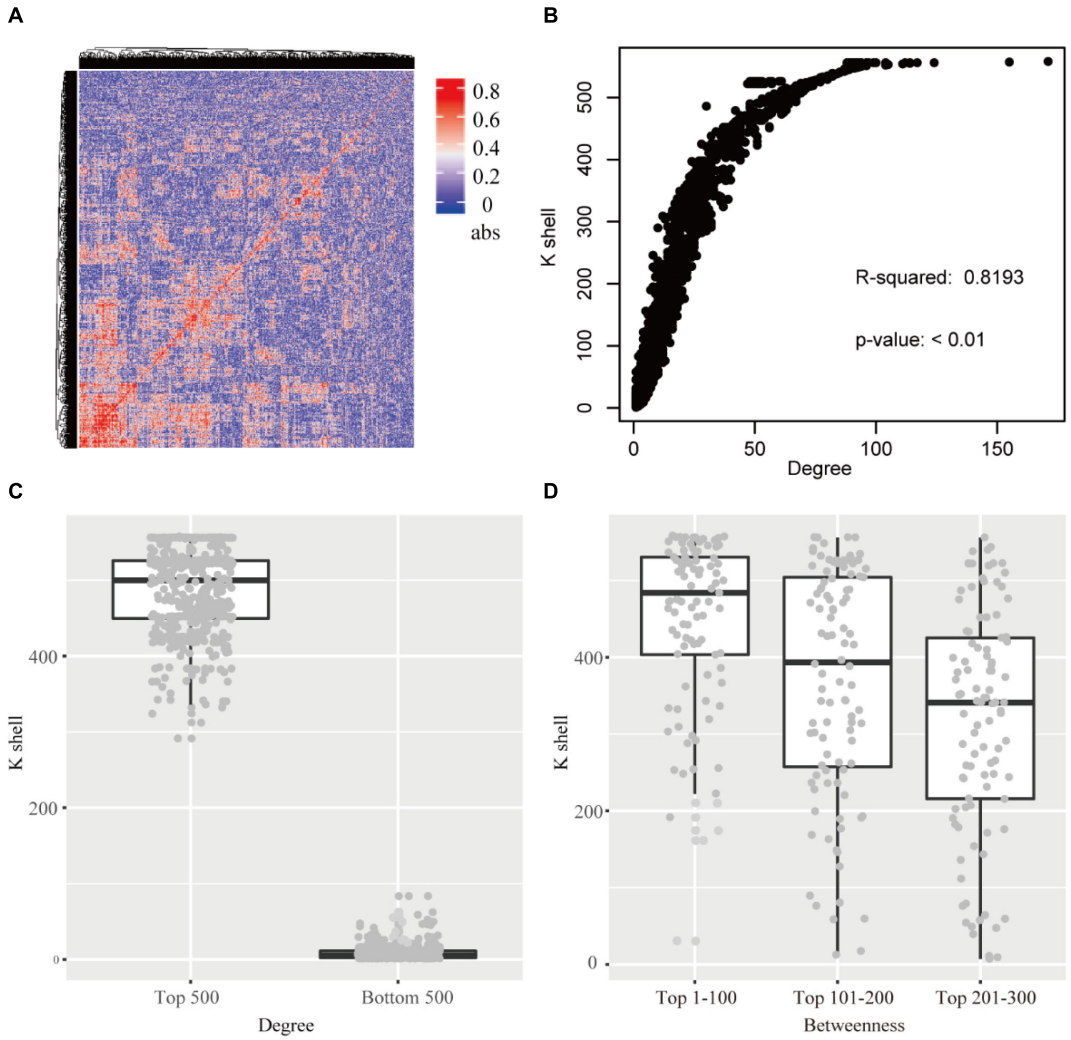

FIGURE 2 | (A) The heatmap of the correlation for each gene pair. abs: the absolute value of the correlation. **(B)** The relationship of k-shell value and degree for each gene. **(C)** The genes of top 500 and bottom 500 degree and the corresponding k-shell layers. **(D)** The genes of top 300 betweenness and the corresponding k-shell layers.

which have the high k-shell value of 447 in average, were significantly enriched in the fatty acid biosynthesis pathway ($p < 0.01$, FDR < 0.05).

The majority of genes (or corresponding proteins) having similar structure or function tended to be clustered in the same layer of k-shell decomposition (**Figure 3**). For example, the genes for proteins with the structure of phosphate binding protein in the k shell of 556 were enriched in ABC transporters pathway ($p < 0.01$, FDR < 0.01). The genes for proteins with the structure of ABC transporter ATPase domain-like, which participated in nucleotide binding and were enriched in ABC transporter pathway ($p < 0.01$, FDR < 0.01), were mainly found in the k shell of 526 (**Supplementary Table S2**). Nevertheless, we were still able to find that certain genes for proteins with similar structure or function could be clustered in different k-shell layers (**Supplementary Figure S3**). For example, the genes for proteins with the structure of tetracycline repressor-like domain, which mainly involve in metabolic process and transcription activity, were found in the k shell of 317, 368, and 383 (**Supplementary Table S3**).

The Resistance Feature and the Potential Resistance Factors

Antibiotic resistance has become a major concern over the world, especially for *A. baumannii* infection. We analyzed the known resistance factors from the efflux pumps and proteins related drug resistance (**Table 1**). The genes that have been reported as resistance in literature and that the corresponding proteins associating with the protein family of efflux pump, such as the ATP binding cassette (ABC) transporters, resistance-nodulation-division (RND) transporters, small multidrug resistance (SMR) family, and major facilitator superfamily (MFS), were considered

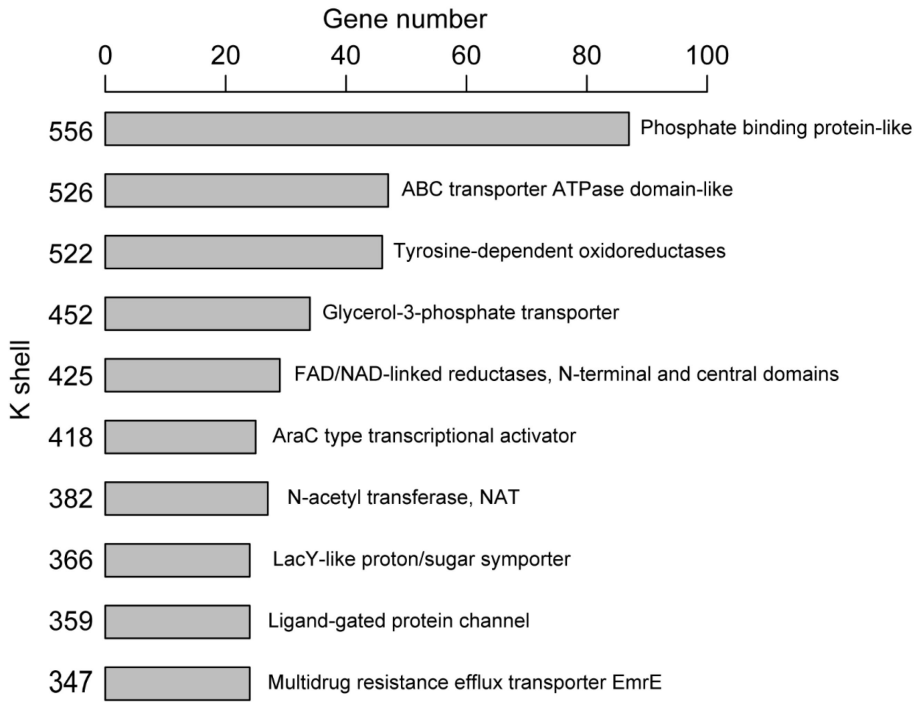

FIGURE 3 | The clustered genes in the same k-shell layer with similar structure.

TABLE 1 | The key resistance genes and selected candidates representing resistance genes in the internal layer of the co-functional network.

Gene name	K-shell	Degree	Betweenness	Product
A1S_0536*	526	49	2,712	Macrolide transport protein
A1S_1242	526	53	9,207	Multidrug ABC transporter transmembrane protein
A1S_3146	366	30	8,106	Multidrug ABC transporter
A1S_1750*	380	30	15,127	AdeB
A1S_2660	314	25	17,889	RND efflux transporter
A1S_0116	246	21	17,817	RND superfamily transporter
A1S_2736	380	30	9,089	RND family drug transporter
A1S_0710	347	26	2,535	SMR family drug transporter
A1S_2298	347	25	0	SMR family efflux pump
A1S_1331*	537	83	72,166	Major facilitator superfamily transporter
A1S_0964	452	37	0	Major facilitator superfamily fosmidomycin/multidrug transport protein
A1S_1516	484	62	47,616	Putative antibiotic resistance
A1S_2198	452	37	0	Putative multidrug resistance protein
A1S_0908	255	18	2,763	RND family multidrug resistance secretion protein
A1S_1772*	366	27	1,546	MFS family transporter
A1S_1773*	255	18	1,544	RND family drug transporter

Detailed information in ***Supplementary Tables S4–S8.*** **Reported resistance factor.*

as resistant genes (Abdi et al., 2020b). Such genes were found to have high values of k shell and clustered in the internal layer of the co-functional network (**Figure 3**). For example, the proteins with the structure of ABC transporter ATPase domain-like were enriched in the k shell of 526. The ABC transporters play an important role in the resistance of *A. baumannii*. The gene of A1S_0536 from ABC transporter pathway, which has a k-shell number of 526, was previously demonstrated to contribute to the resistance to tigecycline, imipenem, and amikacin (Lin et al., 2017). Therefore, other genes, that were enriched in the layer of k shell 526 and that simultaneously the corresponding proteins contain a structure similar to ABC transporter ATPase domain, are likely the potential resistance factors in *A. baumannii* (**Supplementary Table S4**).

RND transporters are well known as the major drug efflux pumps in antibiotic resistance (Van Bambeke et al., 2000).

The RND transporter AcrB associates with the resistance to a variety of antibiotics (Zgurskaya and Nikaido, 1999; Higgins, 2007). The RND transporter A1S_1750 (AdeB), which contains multidrug efflux transporter AcrB transmembrane domain and was layered in k shell of 380, contributes to multidrug resistance of *A. baumannii* (Abdi et al., 2020a). Thus, it is likely that the genes such as A1S_2736, A1S_2660, and A1S_0116, which have a similar structure of multidrug efflux transporter AcrB transmembrane domain and are simultaneously located in the internal layers of network, are the potential resistance factors (**Supplementary Table S5**). Similarly, the small multidrug resistance transporter EmrE confers drug resistance to antibiotics (Higgins, 2007). We speculate that the genes with k shell of 347, 358, and 414, which contain the structure of multidrug resistance efflux transporter EmrE, are the potential resistance factors (**Supplementary Table S6**).

The major facilitator superfamily (MFS) transporters are important factors for antibiotic resistance in *A. baumannii* (Abdi et al., 2020b). The MFS transporter A1S_1331 has a k-shell value of 537, which contains the antibiotic related structure of Glycerol-3-phosphate transporter (Lemieux et al., 2004). It was shown to be responsible for fosfomycin resistance in *A. baumannii* (Sharma et al., 2017). Many genes, which products are predicted to be the MFS transporters, are located in the internal layer of our network. They are likely the potential resistance factors (**Supplementary Table S7**).

In addition, some genes that were predicted to be the putative resistance factors, multidrug efflux pump and drug transport genes, which were layered in the internal co-functional network, were also considered as potential resistance genes (**Supplementary Table S8**). For example, the gene A1S_1516 in the k shell of 484 is a putative antibiotic resistance factor and it has a high betweenness parameter (**Table 1**). It may play a potential important role in the antibiotic resistance in *A. baumannii*.

The Virulence Feature and the Potential Virulence Factors

A. baumannii has become one of the most troublesome pathogens not only because of its resistance property but also its virulence feature. The genes that have been reported to contribute to bacterial virulence in the literature and the genes encoding the related protein family, such as genes for biofilm formation, type II secretion system (T2SS), or type VI secretion system (T6SS), were considered as the virulence factors (**Table 2**). We found that the virulent factors tended to be in the peripheral layer of the co-functional network (**Table 2**). For example, the virulence factors A1S_1343, A1S_1193, A1S_2840 (Outer membrane protein A), A1S_1347, and A1S_2989 (Choi et al., 2008; Jacobs et al., 2010; Eijkelkamp et al., 2014; De Silva et al., 2018) are located in the peripheral layer of the network with a k-shell number of 166, 46, 76, 18, and 4, respectively (**Table 2**). Outer membrane protein A (OmpA) has been studied intensively and well characterized in the virulence of *A. baumannii* (McConnell et al., 2013). We speculate that the genes encoding proteins with a similar structure of OmpA (OmpA-like) and located in the peripheral layer in our co-functional network, such as A1S_1033, A1S_1305, A1S_0884, and A1S_2987, are the potential virulence factors for *A. baumannii* (**Supplementary Table S9**).

The biofilm formation is strongly associated with the virulence of *A. baumannii*. Therefore, the biofilm formation–related genes (Harding et al., 2018), including A1S_2213, A1S_2214, A1S_2215, A1S_2216, A1S_2217, and A1S_2218, which have k-shell values of 21–48, were considered as the potential virulence factors (**Supplementary Table S10**).

TABLE 2 | The key virulence genes and selected candidates representing virulence genes in the peripheral layer of the co-functional network.

Gene name	K-shell	Degree	Betweenness	Product
A1S_2840*	76	13	17,992	Outer membrane protein A
A1S_0884	47	8	2,356	Putative outer membrane protein
A1S_2987	46	7	2,247	Putative lipoprotein precursor
A1S_1033	46	7	2,856	Putative antigen
A1S_1193*	46	6	0	OmpA/MotB
A1S_1305	46	7	926	Putative outer membrane lipoprotein
A1S_2989*	4	1	0	Putative phospholipase D protein
A1S_1343*	166	15	3,345	PaaC
A1S_1347*	18	2	0	PaaX
A1S_2213	52	7	8,964	CsuE
A1S_2214	21	4	0	CsuD
A1S_2215	23	6	349	CsuC
A1S_2216	21	4	0	CsuB
A1S_2217	21	5	1,100	CsuA
A1S_2218	48	4	2,992	CsuA/B
A1S_2601	13	4	3,858	Putative outer membrane protein A
A1S_2602	3	1	0	Hypothetical protein

Detailed information in ***Supplementary Tables S9–S13.*** **Reported virulence factor.*

Furthermore, we analyzed the genes from T2SS or T6SS (Harding et al., 2018). Most of the genes in these two secretion systems were involved in the peripheral layer of the network and considered as the potential virulence factors (**Supplementary Tables S11, S12**). For example, the genes from T2SS, including A1S_0271, A1S_0270, A1S_0369, A1S_0370, A1S_1563, A1S_1564, and A1S_1565, were layered in k shell of 8, 52, 9, 90, 7, 4, and 74, respectively. The genes from the T6SS, including A1S_0550, A1S_1288, A1S_1289, A1S_1296, and A1S_1310, have a k shell of 9, 7, 22, 32, and 5, respectively.

In addition, the genes of A1S_2601 and A1S_2602, the production of which are from the protein family of virulence factor P.69 pertactin (Emsley et al., 1996) and were layered in k shell 13 and 3, are likely the potential virulence factors (**Supplementary Table S13**). Outer membrane proteins play important roles in bacteria virulence (Lin et al., 2002). The outer membrane proteins in the peripheral layer of the co-function network might also contribute to virulence (**Supplementary Table S13**).

The Online Platform ABviresDB

We constructed an *A. baumannii* virulence and resistance database ABviresDB (see footnote) to illustrate the analyzing results and developing efforts for further research. The database of ABviresDB provides the comprehensive information for the resistance and virulence features through our co-functional network analysis. The candidate of resistance and virulence genes from our analysis could be accessed in ABviresDB.

The features of ABviresDB and its main functions as well as the corresponding statistical information are summarized at its homepage. With the website provided, users can browse all the genes of *A. baumannii* for their detailed information, such as the gene region, gene length, gene product, protein family information, network features, and their candidatures as resistance and virulence factors. Meanwhile, the subnetwork of the interested gene and its connections could be illustrated and shown. Researchers can access the relationship between the interested genes and resistance/virulence factors for further study.

In addition, we provide the browse page for users to choose the interested browsing way and item. The "download" page of the website provides access to data of the genes and our analysis results. Users also can browse the help page for the instructions to use this database. ABviresDB supports the feedback or comments from users to improve our database.

DISCUSSION

Network analysis is a powerful tool to study complex biological systems, which are normally caused by a combination of genetic and environmental factors (Cho et al., 2012). The development of bacterial resistance involves the complex network of physiological interactions of molecules that adjust the expression profiling. Similarly, bacterial infection is a complex process that coordinates the virulence gene expression at the right environmental circumstance (Crofts et al., 2018). Identification of resistance and virulence factor by traditional molecular technologies is normally labor intensive. Network analysis has been successfully used to analyze the antibiotic resistance and virulence in selected bacteria (Lee et al., 2019). Here, we use the integrated network analysis to construct a co-functional network to investigate the resistance and virulence factors in *A. baumannii*, one of the most threatening bacterial pathogens to humans currently because of its widespread antibiotic resistance. The k-shell decomposition method (Wei et al., 2015) was applied to analyze the co-functional network, and we revealed that genes implicated in basic cellular physiological function, including genes for antibiotic resistance, tended to have high k-shell values and locate in the internal layer of our network. In contrast, the non-essential genes, such as genes associated with virulence, tended to have low k-shell values and locate in the external of our network. Based on the feature of individual genes in the co-functional network, a list of candidates for antibiotic resistance and virulence was proposed.

Antibiotics generally target an essential cellular function of bacteria (Durao et al., 2018). To survive in the presence of such antimicrobials, bacteria have to develop a mechanism to protect themselves from their own antimicrobials or other antimicrobial agents during the evolution (Galan et al., 2013). In fact, bacteria have developed antibiotic resistance at least a few million years ago, long before the antibiotics were discovered and utilized by human beings. The selective pressure of antibiotics drives the evolution of drug resistance in bacteria by *de novo* mutagenesis in the target gene (Durao et al., 2018). In addition, bacteria could also acquire multiple efflux pumps to reduce the intracellular concentration of a drug (Nikaido and Pages, 2012). The concerted action is to prevent the drug from taking effect. Efflux pumps, which were focused by our study, can confer diverse drug resistance as the intrinsic resistance or acquired resistance mechanism, and display broad physiological functions (Sun et al., 2014). For example, an intrinsic resistance determinant KpnGH in *K. pneumoniae*, which is the MFS efflux pump, is involved in crucial physiological functions. Its corresponding mutant demonstrated reduced growth and increased susceptibility to cell envelope stressors (Srinivasan et al., 2014). The involvement of broad physiological functions suggested that the antibiotic resistance genes of efflux pumps may have more connections in the network, which was supported by our observation: the known resistance genes in efflux pumps were hub genes in the internal network (**Table 1**). This finding is consistent with several previous studies showing that the resistance factors were likely to be the hub nodes or the key connected nodes in the network (Miryala et al., 2019, 2020; Naha et al., 2020). Thus, based on the structural similarity of a protein to efflux pump and its location as a hub gene, we would be able to identify potential resistance factors, which could help us to understand the drug resistance mechanisms in bacteria. The genes closely linked to the resistance factors in the co-functional network might also associate with antibiotic resistance. Those factors that we identified might contribute to antibiotic resistance once the genes are highly induced at certain circumstances or any mutagenesis enhancing their expression level occurs.

Different from antibiotic resistance, the evolution of bacterial virulence was context dependent and highly affected by its host though the host–pathogen interactions (Diard and Hardt, 2017). The process of acquisition or loss of virulence factors involves the interaction of bacteria with or its transmission between its host (Diard and Hardt, 2017). Therefore, the virulence factors may have more links with the external environment. This might explain why virulence factors locate in the peripheral layer of the co-functional network. If the genes in the peripheral layer of the co-functional network associate with known virulence factors, such as T2SS or T6SS, they would have higher chance to be the virulence factors and contribute to the pathogenesis of *A. baumannii*. Therefore, the k-shell value and the localization of gene from our con-functional network would guide experimental research and help find virulence factors for understanding the infection mechanism of *A. baumannii*. Although we are trying to identify novel factors involved in antibiotic resistance or virulence, our analyses were based on the similarity of genes/proteins to known protein architecture that is involved in antibiotic resistance and virulence. Thus, novel factors that have no similarities with such known resistance or virulence factors might not be able to be identified.

In summary, we have integrated the co-expression, operon organization, and structural data of the corresponding protein of gene in *A. baumannii* and built a co-functional network. We discovered that the factors for antibiotic resistance in the bacteria were enriched in the internal layer of the network whereas the virulence factors tended to be in the peripheral layer of the network. This finding could help researchers on *A. baumannii* to fish out the potential antibiotic resistant factors and virulent factors. For such purpose, a database of ABviresDB was developed. The database provides a platform to access the comprehensive information of *A. baumannii* from our analysis, which we expect to help the research work on antibiotic resistance and bacterial pathogenesis of *A. baumannii*. In addition, the approach of network analysis used in our study could also guide the research on antibiotic resistance and pathogenesis in other bacteria.

DATA AVAILABILITY STATEMENT

The original contributions presented in the study are included in the article/**Supplementary Material**, further inquiries can be directed to the corresponding author.

AUTHOR CONTRIBUTIONS

RX and JZ designed the integrated co-functional network analysis strategy and did the data collection, analysis and interpretation. RX, NS, and JZ drafted the manuscript. All authors provided important intellectual revision of the manuscript.

FUNDING

This study was funded by the University of Macau (File Nos. MYRG2016-00073-FHS, MYRG2016-00199-FHS, and MYRG2019-00050-FHS) and the Science and Technology Development Fund, Macau SAR (File Nos. 0058/2018/A2 and 0113/2019/A2).

SUPPLEMENTARY MATERIAL

The Supplementary Material for this article can be found online at: https://www.frontiersin.org/articles/10.3389/fmicb.2020.598380/full#supplementary-material

REFERENCES

Abdi, S. N., Ghotaslou, R., Asgharzadeh, M., Mehramouz, B., Hasani, A., Baghi, H. B., et al. (2020a). AdeB efflux pump gene knockdown by mRNA mediated peptide nucleic acid in multidrug resistance *Acinetobacter baumannii*. *Microb. Pathog.* 139:103825. doi: 10.1016/j.micpath.2019.103825

Abdi, S. N., Ghotaslou, R., Ganbarov, K., Mobed, A., Tanomand, A., Yousefi, M., et al. (2020b). *Acinetobacter baumannii* efflux pumps and antibiotic resistance. *Infect. Drug Resist.* 13, 423–434. doi: 10.2147/IDR.S228089

Ahmed, H., Howton, T. C., Sun, Y., Weinberger, N., Belkhadir, Y., and Mukhtar, M. S. (2018). Network biology discovers pathogen contact points in host protein-protein interactomes. *Nat. Commun.* 9:2312. doi: 10.1038/s41467-018-04632-8

Allaire, J., Gandrud, C., Russell, K., and Yetman, C. (2017). *networkD3: D3 Javascript Network Graphs from R. R Package Version 0.4*.

Allen, J. L., Tomlinson, B. R., Casella, L. G., and Shaw, L. N. (2020). Regulatory networks important for survival of *Acinetobacter baumannii* within the host. *Curr. Opin. Microbiol.* 55, 74–80. doi: 10.1016/j.mib.2020.03.001

Asif, M., Alvi, I. A., and Rehman, S. U. (2018). Insight into *Acinetobacter baumannii*: pathogenesis, global resistance, mechanisms of resistance, treatment options, and alternative modalities. *Infect. Drug Resist.* 11, 1249–1260. doi: 10.2147/IDR.S166750

Barth, V. C. Jr., Rodrigues, B. A., Bonatto, G. D., Gallo, S. W., Pagnussatti, V. E., Ferreira, C. A., et al. (2013). Heterogeneous persister cells formation in *Acinetobacter baumannii*. *PLoS One* 8:e84361. doi: 10.1371/journal.pone.0084361

Behera, B., Paria, P., Das, A., Bhowmick, S., Sahoo, A., and Das, B. J. A. (2017). Molecular characterization and pathogenicity of a virulent *Acinetobacter baumannii* associated with mortality of farmed Indian Major Carp Labeo rohita (Hamilton 1822). *Aquaculture* 471, 157–162. doi: 10.1016/j.aquaculture.2017.01.018

Brahmi, S., Touati, A., Cadiere, A., Djahmi, N., Pantel, A., Sotto, A., et al. (2016). First Description of Two Sequence Type 2 *Acinetobacter baumannii* Isolates Carrying OXA-23 Carbapenemase in Pagellus acarne Fished from the Mediterranean Sea near Bejaia, Algeria. *Antimicrob. Agents Chemother.* 60, 2513–2515. doi: 10.1128/AAC.02384-15

Carmi, S., Havlin, S., Kirkpatrick, S., Shavitt, Y., and Shir, E. (2007). A model of Internet topology using k-shell decomposition. *Proc. Natl. Acad. Sci. U.S.A.* 104, 11150–11154. doi: 10.1073/pnas.0701175104

Cho, D. Y., Kim, Y. A., and Przytycka, T. M. (2012). Chapter 5: network biology approach to complex diseases. *PLoS Comput. Biol.* 8:e1002820. doi: 10.1371/journal.pcbi.1002820

Choi, C. H., Hyun, S. H., Lee, J. Y., Lee, J. S., Lee, Y. S., Kim, S. A., et al. (2008). *Acinetobacter baumannii* outer membrane protein A targets the nucleus and induces cytotoxicity. *Cell Microbiol.* 10, 309–319. doi: 10.1111/j.1462-5822.2007.01041.x

Cornejo, E., Schlaermann, P., and Mukherjee, S. (2017). How to rewire the host cell: a home improvement guide for intracellular bacteria. *J. Cell Biol.* 216, 3931–3948. doi: 10.1083/jcb.201701095

Crofts, A. A., Giovanetti, S. M., Rubin, E. J., Poly, F. M., Gutierrez, R. L., Talaat, K. R., et al. (2018). Enterotoxigenic *E. coli* virulence gene regulation in human infections. *Proc. Natl. Acad. Sci. U.S.A.* 115, E8968–E8976. doi: 10.1073/pnas.1808982115

Csardi, G., and Nepusz, T. (2006). The igraph software package for complex network research. *InterJ. Complex Syst.* 1695, 1–9.

De Silva, P. M., Chong, P., Fernando, D. M., Westmacott, G., and Kumar, A. (2018). Effect of Incubation Temperature on Antibiotic Resistance and Virulence Factors of *Acinetobacter baumannii* ATCC 17978. *Antimicrob. Agents Chemother.* 62:e01514-17. doi: 10.1128/AAC.01514-17

Dekic, S., Klobucar, G., Ivankovic, T., Zanella, D., Vucic, M., Bourdineaud, J. P., et al. (2018). Emerging human pathogen *Acinetobacter baumannii* in the natural aquatic environment: a public health risk? *Int. J. Environ. Health Res.* 28, 315–322. doi: 10.1080/09603123.2018.1472746

Diard, M., and Hardt, W. D. (2017). Evolution of bacterial virulence. *FEMS Microbiol. Rev.* 41, 679–697. doi: 10.1093/femsre/fux023

Durao, P., Balbontin, R., and Gordo, I. (2018). Evolutionary mechanisms shaping the maintenance of antibiotic resistance. *Trends Microbiol.* 26, 677–691. doi: 10.1016/j.tim.2018.01.005

Eijkelkamp, B. A., Stroeher, U. H., Hassan, K. A., Paulsen, I. T., and Brown, M. H. (2014). Comparative analysis of surface-exposed virulence factors of *Acinetobacter baumannii*. *BMC Genomics* 15:1020. doi: 10.1186/1471-2164-15-1020

Emsley, P., Charles, I. G., Fairweather, N. F., and Isaacs, N. W. (1996). Structure of *Bordetella pertussis* virulence factor P.69 pertactin. *Nature* 381, 90–92. doi: 10.1038/381090a0

Galan, J. C., Gonzalez-Candelas, F., Rolain, J. M., and Canton, R. (2013). Antibiotics as selectors and accelerators of diversity in the mechanisms of resistance: from the resistome to genetic plasticity in the beta-lactamases world. *Front. Microbiol.* 4:9. doi: 10.3389/fmicb.2013.00009

Gough, J., Karplus, K., Hughey, R., and Chothia, C. (2001). Assignment of homology to genome sequences using a library of hidden Markov models that represent all proteins of known structure. *J. Mol. Biol.* 313, 903–919. doi: 10.1006/jmbi.2001.5080

Harding, C. M., Hennon, S. W., and Feldman, M. F. (2018). Uncovering the mechanisms of *Acinetobacter baumannii* virulence. *Nat. Rev. Microbiol.* 16, 91–102. doi: 10.1038/nrmicro.2017.148

Higgins, C. F. (2007). Multiple molecular mechanisms for multidrug resistance transporters. *Nature* 446, 749–757. doi: 10.1038/nature05630

Huang da, W., Sherman, B. T., and Lempicki, R. A. (2009). Bioinformatics enrichment tools: paths toward the comprehensive functional analysis of large gene lists. *Nucleic Acids Res.* 37, 1–13. doi: 10.1093/nar/gkn923

Huerta-Cepas, J., Forslund, K., Coelho, L. P., Szklarczyk, D., Jensen, L. J., von Mering, C., et al. (2017). Fast genome-wide functional annotation through orthology assignment by eggNOG-mapper. *Mol. Biol. Evol.* 34, 2115–2122. doi: 10.1093/molbev/msx148

Jacobs, A. C., Hood, I., Boyd, K. L., Olson, P. D., Morrison, J. M., Carson, S., et al. (2010). Inactivation of phospholipase D diminishes *Acinetobacter baumannii* pathogenesis. *Infect. Immun.* 78, 1952–1962. doi: 10.1128/IAI.00889-09

Ji, X., Zou, J., Peng, H., Stolle, A. S., Xie, R., Zhang, H., et al. (2019). Alarmone Ap4A is elevated by aminoglycoside antibiotics and enhances their bactericidal activity. *Proc. Natl. Acad. Sci. U.S.A.* 116, 9578–9585. doi: 10.1073/pnas.1822026116

Lee, M., Pinto, N. A., Kim, C. Y., Yang, S., D'Souza, R., Yong, D., et al. (2019). Network integrative genomic and transcriptomic analysis of carbapenem-resistant *Klebsiella pneumoniae* strains identifies genes for antibiotic resistance and virulence. *mSystems* 4:e00202-19. doi: 10.1128/mSystems.00202-19

Lemieux, M. J., Huang, Y., and Wang, D. N. (2004). Glycerol-3-phosphate transporter of *Escherichia coli*: structure, function and regulation. *Res. Microbiol.* 155, 623–629. doi: 10.1016/j.resmic.2004.05.016

Lin, J., Huang, S., and Zhang, Q. (2002). Outer membrane proteins: key players for bacterial adaptation in host niches. *Microbes Infect.* 4, 325–331. doi: 10.1016/s1286-4579(02)01545-9

Lin, M. F., Lin, Y. Y., Tu, C. C., and Lan, C. Y. (2017). Distribution of different efflux pump genes in clinical isolates of multidrug-resistant *Acinetobacter baumannii* and their correlation with antimicrobial resistance. *J. Microbiol. Immunol. Infect.* 50, 224–231. doi: 10.1016/j.jmii.2015.04.004

Mao, X., Ma, Q., Zhou, C., Chen, X., Zhang, H., Yang, J., et al. (2014). DOOR 2.0: presenting operons and their functions through dynamic and integrated views. *Nucleic Acids Res.* 42, D654–D659. doi: 10.1093/nar/gkt1048

McConnell, M. J., Actis, L., and Pachon, J. (2013). *Acinetobacter baumannii*: human infections, factors contributing to pathogenesis and animal models. *FEMS Microbiol. Rev.* 37, 130–155. doi: 10.1111/j.1574-6976.2012.00344.x

Miryala, S. K., Anbarasu, A., and Ramaiah, S. (2019). Systems biology studies in *Pseudomonas aeruginosa* PA01 to understand their role in biofilm formation and multidrug efflux pumps. *Microb. Pathog.* 136:103668. doi: 10.1016/j.micpath.2019.103668

Miryala, S. K., Anbarasu, A., and Ramaiah, S. (2020). Role of SHV-11, a class a beta-lactamase, gene in multidrug resistance among *Klebsiella pneumoniae* strains and understanding its mechanism by gene network analysis. *Microb. Drug Resist.* 26, 900–908. doi: 10.1089/mdr.2019.0430

Morris, F. C., Dexter, C., Kostoulias, X., Uddin, M. I., and Peleg, A. Y. (2019). The mechanisms of disease caused by *Acinetobacter baumannii*. *Front. Microbiol.* 10:1601. doi: 10.3389/fmicb.2019.01601

Musa, N., Lee, S. W., Shaharom, F., and Wee, W. (2008). Surveillance of bacteria species in diseased freshwater ornamental fish from aquarium shop. *World Appl. Sci. J.* 3, 903–905.

Naha, A., Kumar Miryala, S., Debroy, R., Ramaiah, S., and Anbarasu, A. (2020). Elucidating the multi-drug resistance mechanism of Enterococcus faecalis V583: a gene interaction network analysis. *Gene* 748:144704. doi: 10.1016/j.gene.2020.144704

Nikaido, H., and Pages, J. M. (2012). Broad-specificity efflux pumps and their role in multidrug resistance of Gram-negative bacteria. *FEMS Microbiol. Rev.* 36, 340–363. doi: 10.1111/j.1574-6976.2011.00290.x

Pei, S., Muchnik, L., Andrade, J. S. Jr., Zheng, Z., and Makse, H. A. J. S. R. (2014). Searching for superspreaders of information in real-world social media. *Sci. Rep.* 4:5547.

Rauta, P. R., Kumar, K., and Sahoo, P. K. (2011). Emerging new multi-drug resistant bacterial pathogen, *Acinetobacter baumannii* associated with snakehead *Channa striatus* eye infection. *Curr. Sci.* 101, 548–553.

Shannon, P., Markiel, A., Ozier, O., Baliga, N. S., Wang, J. T., Ramage, D., et al. (2003). Cytoscape: a software environment for integrated models of biomolecular interaction networks. *Genome Res.* 13, 2498–2504. doi: 10.1101/gr.1239303

Sharma, A., Sharma, R., Bhattacharyya, T., Bhando, T., and Pathania, R. (2017). Fosfomycin resistance in *Acinetobacter baumannii* is mediated by efflux through a major facilitator superfamily (MFS) transporter-AbaF. *J. Antimicrob. Chemother.* 72, 68–74. doi: 10.1093/jac/dkw382

Srinivasan, V. B., Singh, B. B., Priyadarshi, N., Chauhan, N. K., and Rajamohan, G. (2014). Role of novel multidrug efflux pump involved in drug resistance in *Klebsiella pneumoniae*. *PLoS One* 9:e96288. doi: 10.1371/journal.pone.0096288

Sun, J., Deng, Z., and Yan, A. (2014). Bacterial multidrug efflux pumps: mechanisms, physiology and pharmacological exploitations. *Biochem. Biophys. Res. Commun.* 453, 254–267. doi: 10.1016/j.bbrc.2014.05.090

Taboada, B., Ciria, R., Martinez-Guerrero, C. E., and Merino, E. (2012). ProOpDB: prokaryotic operon database. *Nucleic Acids Res.* 40, D627–D631. doi: 10.1093/nar/gkr1020

Theuretzbacher, U., Bush, K., Harbarth, S., Paul, M., Rex, J. H., Tacconelli, E., et al. (2020). Critical analysis of antibacterial agents in clinical development. *Nat. Rev. Microbiol.* 18, 286–298. doi: 10.1038/s41579-020-0340-0

Van Bambeke, F., Balzi, E., and Tulkens, P. M. (2000). Antibiotic efflux pumps. *Biochem. Pharmacol.* 60, 457–470. doi: 10.1016/s0006-2952(00)00291-4

Vidal, M., Cusick, M. E., and Barabasi, A. L. (2011). Interactome networks and human disease. *Cell* 144, 986–998. doi: 10.1016/j.cell.2011.02.016

Wei, B., Liu, J., Wei, D., Gao, C., and Deng, Y. (2015). Weighted k-shell decomposition for complex networks based on potential edge weights. *Phys. A Stat. Mech. Appl.* 420, 277–283. doi: 10.1016/j.physa.2014.11.012

World Health Organization [WHO] (2017). *WHO Publishes List of Bacteria for Which New Antibiotics are Urgently Needed*. Geneva: WHO.

Xia, L., Xiong, D. M., Gu, Z. M., Xu, Z., Chen, C. F., Xie, J., et al. (2008). Recovery of *Acinetobacter baumannii* from diseased channel catfish (*Ictalurus punctatus*) in China. *Aquaculture* 284, 285–288. doi: 10.1016/j.aquaculture.2008.07.038

Xie, R., Zhang, X. D., Zhao, Q., Peng, B., and Zheng, J. (2018). Analysis of global prevalence of antibiotic resistance in *Acinetobacter baumannii* infections disclosed a faster increase in OECD countries. *Emerg. Microbes Infect.* 7:31. doi: 10.1038/s41426-018-0038-9

Yan, J., Risacher, S. L., Shen, L., and Saykin, A. J. (2018). Network approaches to systems biology analysis of complex disease: integrative methods for multi-omics data. *Brief. Bioinform.* 19, 1370–1381. doi: 10.1093/bib/bbx066

Zgurskaya, H. I., and Nikaido, H. (1999). Bypassing the periplasm: reconstitution of the AcrAB multidrug efflux pump of *Escherichia coli*. *Proc. Natl. Acad. Sci. U.S.A.* 96, 7190–7195. doi: 10.1073/pnas.96.13.7190

Zotenko, E., Mestre, J., O'Leary, D. P., and Przytycka, T. M. (2008). Why do hubs in the yeast protein interaction network tend to be essential: reexamining the connection between the network topology and essentiality. *PLoS Comput. Biol.* 4:e1000140. doi: 10.1371/journal.pcbi.1000140

Zou, J., Kou, S. H., Xie, R., VanNieuwenhze, M. S., Qu, J., Peng, B., et al. (2020). Non-walled spherical *Acinetobacter baumannii* is an important type of persister upon beta-lactam antibiotic treatment. *Emerg. Microbes Infect.* 9, 1149–1159. doi: 10.1080/22221751.2020.1770630

Zou, J., Zhang, W., Zhang, H., Zhang, X. D., Peng, B., and Zheng, J. (2018). Studies on aminoglycoside susceptibility identify a novel function of KsgA to secure translational fidelity during antibiotic stress. *Antimicrob. Agents Chemother.* 62:e00853-18. doi: 10.1128/AAC.00853-18

Conflict of Interest: The authors declare that the research was conducted in the absence of any commercial or financial relationships that could be construed as a potential conflict of interest.

frontiers in Microbiology

ORIGINAL RESEARCH
published: 03 December 2020
doi: 10.3389/fmicb.2020.600622

Anti-quorum Sensing and Protective Efficacies of Naringin Against *Aeromonas hydrophila* Infection in *Danio rerio*

Ramanathan Srinivasan[1,2†], Kannan Rama Devi[3†], Sivasubramanian Santhakumari[3,4], Arunachalam Kannappan[3,5], Xiaomeng Chen[1,2], Arumugam Veera Ravi[3] and Xiangmin Lin[1,2,6]**

[1] Fujian Provincial Key Laboratory of Agroecological Processing and Safety Monitoring, School of Life Sciences, Fujian Agriculture and Forestry University, Fuzhou, China, [2] Key Laboratory of Crop Ecology and Molecular Physiology, Fujian Agriculture and Forestry University, Fujian Province University, Fuzhou, China, [3] Department of Biotechnology, Alagappa University, Karaikudi, India, [4] Department of Biochemistry and Molecular Biology, School of Life Sciences, Pondicherry University, Pondicherry, India, [5] Department of Food Science and Technology, School of Agriculture and Biology, Shanghai Jiao Tong University, Shanghai, China, [6] Key Laboratory of Marine Biotechnology of Fujian Province, Institute of Oceanology, Fujian Agriculture and Forestry University, Fuzhou, China

OPEN ACCESS

Edited by:
Bo Peng,
Sun Yat-sen University, China

Reviewed by:
Xiaofeng Shan,
Jilin Agriculture University, China
Rodolfo García-Contreras,
National Autonomous University of Mexico, Mexico

***Correspondence:**
Arumugam Veera Ravi
aveeraravi@rediffmail.com
Xiangmin Lin
xiangmin@fafu.edu.cn

† These authors have contributed equally to this work

Specialty section:
This article was submitted to Antimicrobials, Resistance and Chemotherapy, a section of the journal Frontiers in Microbiology

Received: 30 August 2020
Accepted: 12 November 2020
Published: 03 December 2020

Citation:
Srinivasan R, Devi KR, Santhakumari S, Kannappan A, Chen X, Ravi AV and Lin X (2020) Anti-quorum Sensing and Protective Efficacies of Naringin Against Aeromonas hydrophila Infection in Danio rerio. Front. Microbiol. 11:600622. doi: 10.3389/fmicb.2020.600622

It is now well known that the quorum sensing (QS) mechanism coordinates the production of several virulence factors and biofilm formation in most pathogenic microorganisms. *Aeromonas hydrophila* is a prime pathogen responsible for frequent outbreaks in aquaculture settings. Recent studies have also continuously reported that *A. hydrophila* regulates virulence factor production and biofilm formation through the QS system. In addition to the presence of antibiotic resistance genes, biofilm-mediated antibiotic resistance increases the severity of *A. hydrophila* infections. To control the bacterial pathogenesis and subsequent infections, targeting the QS mechanism has become one of the best alternative methods. Though very few compounds were identified as QS inhibitors against *A. hydrophila*, to date, the screening and identification of new and effective natural QS inhibitors is a dire necessity to control the infectious *A. hydrophila*. The present study endorses naringin (NA) as an anti-QS and anti-infective agent against *A. hydrophila*. Initially, the NA showed a concentration-dependent biofilm reduction against *A. hydrophila*. Furthermore, the results of microscopic analyses and quantitative virulence assays displayed the promise of NA as a potential anti-QS agent. Subsequently, the downregulation of *ahh1*, *aerA*, *lip* and *ahyB* validate the interference of NA in virulence gene expression. Furthermore, the *in vivo* assays were carried out in zebrafish model system to evaluate the anti-infective potential of NA. The outcome of the immersion challenge assay showed that the recovery rate of the zebrafish has substantially increased upon treatment with NA. Furthermore, the quantification of the bacterial load upon NA treatment showed a decreased level of bacterial counts in zebrafish when compared to the untreated control. Moreover, the NA treatment averts

the pathogen-induced histoarchitecture damages in vital organs of zebrafish, compared to their respective controls. The current study has thus analyzed the anti-QS and anti-infective capabilities of NA and could be employed to formulate effective treatment measures against *A. hydrophila* infections.

Keywords: *Aeromonas hydrophila*, biofilm, naringin, quorum sensing, virulence factors, zebrafish

INTRODUCTION

The genus *Aeromonas* is a challenging group of microorganisms to treat for physicians and microbiologists due to their notorious role in causing several infectious diseases (Janda and Abbott, 2010). It engages in a variety of human illnesses such as gastroenteritis, hemolytic uremic syndrome, bacteremia, septicemia, meningitis, peritonitis, wound infections, and respiratory tract and ocular infections (Li et al., 2020). This study mainly focuses on *Aeromonas hydrophila*, which is an important species in the genus *Aeromonas* that has posed a potential health threat to fishes and humans especially (Rama Devi et al., 2016). *A. hydrophila* has been recognized as an opportunistic pathogen causing infections in immunocompromised patients, and it was recently found to cause foodborne illness in healthy individuals (Daskalov, 2006). It produces a wide range of extracellular enzymes, which are thought to be key players in causing infections in immunocompromised individuals.

Biofilm is the favorite mode of growth for most bacteria. Biofilm is an assemblage of microbial cells on a surface with an enclosed polysaccharide matrix (Donlan, 2002). This biofilm formation is intimately related to a population-dependent gene expression system known as quorum sensing (QS), which utilizes small self-produced chemicals called autoinducers (AIs) (Fuqua et al., 2001; Srinivasan et al., 2016). Generally, *A. hydrophila* is known to produce three different types of AIs, such as N-butanoyl-homoserine lactone (C4-HSL), N-hexanoyl-homoserine lactone (C6-HSL), and AI-2, for their communication (Kozlova et al., 2008). In addition to biofilm formation, *A. hydrophila* secretes a wide array of virulence factors, such as aerolysin, cytotoxic enterotoxins, elastase, hemolysins, lipases, proteases, and an S layer under the control of QS system (Rama Devi et al., 2016). These virulence factors of *A. hydrophila* have the symptomatic potential to cause severe diseases in fishes and humans (Murray et al., 1988; Chopra and Houston, 1999; Cascón et al., 2000; Singh et al., 2009; Khajanchi et al., 2010; Shak et al., 2011).

The hemolysin production in *A. hydrophila* is controlled by two-component hemolytic systems like hemolysin (*ahh1*) and aerolysin (*aerA*) (Wang et al., 2003). These extracellular hemolysin enzymes invade the host cell membrane's lipid bilayer and lead to the leakage of cytoplasmic content. Furthermore, the extracellular hydrolytic enzyme elastase (*ahyB*) is an important virulence trait in *A. hydrophila*, which causes cell damage when associated with aerolysin (Song et al., 2004). Another extracellular hydrolytic enzyme in *A. hydrophila* is lipase, which affects the host's immune system functions by generating free fatty acids through lipolytic activity (Eftimiadi et al., 1987).

The use of antibiotics is the gold-standard treatment strategy to contain the human illness caused by *A. hydrophila* (Morris and Horneman, 2013). However, the current rise in antibiotic resistance among aeromonads has urged an interest in developing a promising alternative treatment strategy (Li et al., 2019). Since QS plays a key role in the pathogenesis and survival of *A. hydrophila*, targeting QS has become an alternate approach to contain *A. hydrophila* infection. Naringin (NA) [4′,5,7-trihydroxyflavanone-7-β-D-α-L-rhamnosyl(1→2)-β-D-glucoside] is a flavanone glycoside predominantly found in citrus fruits and particularly in grapefruit and sour orange (Peterson et al., 2006a,b). It is a prime bitter component in grapefruit and its level varies with different cultivars. In recent years, flavonoids from citrus fruits have gained much importance in drug development research because of their proven medicinal values (Rawson et al., 2014; Salvamani et al., 2014). The current study aimed to explore the anti-QS potential of NA against *A. hydrophila* and its efficacy in rescuing *Danio rerio* (animal model) from *A. hydrophila* infection.

MATERIALS AND METHODS

Bacterial Strain, Growth Condition, and Media

A. hydrophila MTCC 1739 was obtained from the Microbial Type Culture Collection & Gene Bank, Institute of Microbial Technology (IMTECH), Chandigarh, India. The test strain was routinely grown at 30°C in Luria Bertani (LB) broth with rotary shaking at 130 rpm. The OD of the test bacterial pathogen was adjusted to 0.4 at 600 nm (UV-visible spectrophotometer; Shimadzu, UV-2450, Japan) from the overnight culture (1×10^8 CFU/ml) and used as the standard cell suspension for all the *in vitro* assays.

Determination of Minimum Biofilm Inhibitory Concentration (MBIC)

The MBIC of NA was tested against *A. hydrophila* in a 24-well microtiter plate (MTP). NA at doubled dilution concentrations (93.75, 187.5, 375, 750, and 1,500 μg/ml) was added to the MTP wells containing 1 ml of LB broth, and 1% of *A. hydrophila* standard cell suspension was used as inoculum. The MTP was incubated for 24 h at 30°C in a static condition. Control was maintained without the addition of NA. After incubation, the planktonic cells and the spend media were discarded from the control and NA treated wells. Then, the wells were washed with sterile distilled water and allowed to air dry. Further, the wells were stained with 0.4% crystal violet (CV) (w/v) solution at room

temperature for 5 min. The unbound CV was washed with sterile distilled water and air dried. A total of 1 ml of 20% glacial acetic acid solution was added to all wells to extract the biofilm bound CV and read spectrophotometrically at 570 nm to quantify the biofilm biomass (Kannappan et al., 2019a). The percentage of biofilm inhibition was calculated by using the following formula:

$$\text{Percentage of inhibition} = [(\text{control OD}_{570\ \text{nm}} - \text{treated OD}_{570\ \text{nm}})/\text{control OD}_{570\text{nm}}] \times 100$$

MBIC was determined as the lowest concentration of NA that holds the maximum percentage of biofilm inhibition without any reduction in bacterial growth.

QS Inhibition Assay in *A. hydrophila*

A. hydrophila was grown at 30°C for 24 h in the absence and presence of NA (93.75–750 μg/ml). After incubation, the cultures were harvested, and cell-free culture supernatants (CFCS) were collected and then filter sterilized using a 0.22 μm membrane filter (Millipore Corp., United States) and used for further studies.

β-Hemolysin Quantification Assay

The extracellular hemolysin production in *A. hydrophila* was quantified using the method described by Scheffer et al. (1988). Briefly, 100 μl of both NA treated and untreated *A. hydrophila* CFCS were added with 900 μl of phosphate buffer saline (PBS; pH 7.4) containing 2% sheep erythrocytes. The mixture was left undisturbed for 20 min in ice. The mixture was then centrifuged, and the absorbance for the released hemoglobin in the supernatant was measured at 530 nm.

Lipase Assay

The lipase production was quantitatively evaluated by *p*-nitrophenyl palmitate as a substrate. A total of 100 μl of NA treated and untreated CFCS were added to 900 μl of substrate mixture containing 1 volume of 0.3% (w/v) *p*-nitrophenyl palmitate in isopropanol and 9 volume of 50 mM Na_2PO_4 buffer [0.2% sodium deoxycholate (w/v) and 0.1% gummi arabicum (w/v) (pH 8.0)]. The resultant mixture was incubated for 1 h at room temperature. Following incubation, 1 ml of 1 M sodium carbonate buffer was added to the mixture to terminate the reaction. The resultant mixture was then centrifuged at 10,000 rpm, and the absorbance for the supernatant was read at 410 nm using a spectrophotometer (Srinivasan et al., 2017).

Elastase Assay

Elastin Congo Red (ECR; Sigma, St. Louis, MO, United States) was used as a substrate to measure the elastolytic activity of *A. hydrophila*. ECR buffer (900 μl, 100 mM Tris, 1 mM $CaCl_2$, pH 7.5) containing 20 mg of ECR was added to 100 μl of filter-sterilized CFCS. The reaction mixture was incubated with shaking at 37°C for 3 h. After incubation, the insoluble ECR was separated by centrifugation at 10,000 rpm, and the supernatant was measured at 495 nm (Ohman et al., 1980).

In situ Microscopic Analysis

For microscopic visualization of *A. hydrophila* biofilm formation, the *A. hydrophila* cells could form biofilm on glass slides (1 × 1 cm) placed in 24 wells MTP supplemented with and without NA (93.75–750 μg/ml), and they were incubated for 24 h at 30°C in static condition. After incubation, the glass slides were washed with distilled water and processed as follows.

For light microscopic visualization, the glass slides were washed with distilled water and stained with a 0.4% CV solution for 3 min. The stained-glass slides were then washed with distilled water, air dried, and then mounted on a microscopic slide with the biofilm directed upwards and imaged using a light microscope (Nikon Eclipse Ti 100, Tokyo, Japan) at a magnification of ×400 (Sivaranjani et al., 2018).

For confocal laser scanning microscopic (CLSM) analysis, the glass slides were washed with distilled water and stained with 0.1% acridine orange solution (w/v) (Sigma, St. Louis, MO, United States) for 1 min. The stained-glass slides were washed with distilled water and air dried at room temperature. Then, the stained slides were imaged using CLSM (Model LSM 710, Carl Zeiss, Germany) at ×200 magnification (Bakkiyaraj and Karutha Pandian, 2010).

Fourier Transform Infrared (FT-IR) Spectral Analysis

A. hydrophila cells cultured in the presence and absence of NA was subjected to FT-IR spectral analysis to disclose the alterations in the cell membrane. An equal volume (1 mg) of lyophilized bacterial cells was mixed with potassium bromide (100 mg, KBr) powder and then ground to prepare bacterial pellets. These pellets were analyzed using an FT-IR spectrophotometer (Nicolet^{TM} iS5, Thermo Scientific, United States). The pellets were scanned at 4,000–400 cm^{-1}. Each spectrum represents a total of 16 scans with a spectral resolution of 4 cm^{-1}. KBr pellets without bacterial cells were used to reduce the background noise. The spectral readings were plotted as absorbance versus wavenumber and analyzed using OMNIC software (Kannappan et al., 2019b).

RNA Isolation and cDNA Conversion

The effect of NA at MBIC on the expression of key virulence genes in *A. hydrophila* was quantified. Total RNA was extracted from *A. hydrophila* cells harbored in the presence and absence of NA at MBIC using TRIzol reagent (Sigma, St. Louis, MO, United States). According to the manufacturer's instructions, extracted RNA was converted to cDNAs using a High-Capacity cDNA Reverse transcription kit (Applied Biosystems).

Comparative qRT-PCR Analysis

An equal volume of cDNA (2 ng) was combined individually with primers of the target gene (*aerA*, *ahh1*, *lip,* and *ahyB*) and reference gene (16S rRNA) of *A. hydrophila* (**Table 1**) and Power SYBR® Green PCR master mix (Applied Biosystems). The qRT-PCR was processed with Applied Biosystem's 7,500 sequence detection system. The PCR cycling conditions include an initial denaturation at 95°C for 5 min, denaturation at 95°C for 40 s, annealing at 57°C for 45 s and extension at 72°C for 40 s

TABLE 1 | List of primers used in the gene expression studies.

S. No	Gene	Gene name	Primer sequence (5′–3′)		Size (bp)	Accession numbers	References
			Forward	Reverse			
1	*ahh1*	Hemolysin	GCCGAGCGCCCAGAAGGTGAGTT	GAGCGGCTGGATGCGGTTGT	130	A0A3T-0ZZY5	Wang et al., 2003
2	*aerA*	Aerolysin	CAAGAACAAGTTCAAGTGGCCA	ACGAAGGTGTGGTTCCAGT	309	P09167	Wang et al., 2003
3	*lip*	Lipase	ATCTTCTCCGACTGGTTCGG	CCGTGCCAGGACTGGGTCTT	383	H6VYX6	Sen, 2005
4	16S rRNA	16S ribosomal RNA	ACTCCTACGGGAGGCAGCAG	ATTACCGCGGCTGCTGG	1,400	JN559379	Rama Devi et al., 2016

(40 cycles) and a final extension at 72°C for 10 min. Data were normalized with the reference gene and analyzed by the $2^{-\Delta\Delta CT}$ method (Kannappan et al., 2017a).

Effect of NA on the Growth of *A. hydrophila*

The effect of NA on the growth of *A. hydrophila* was assessed by cell density quantification assay. NA was added to the wells of MTP containing the above said concentrations, ranging from 93.75 to 1,500 μg/ml to 1 ml LB broth, to which 1% of standard cell suspension of *A. hydrophila* culture was inoculated and incubated at 30°C for 24 h. After 24 h of incubation, the cell density was quantified spectrophotometrically at 600 nm (Bakkiyaraj and Karutha Pandian, 2010).

In vivo Analysis

Animal Maintenance

Clinically healthy wild type adult zebrafish, *D. rerio* was collected from local ornamental fish farm, Madurai, Tamil Nadu, India. The collected zebrafish were acclimatized at 28 ± 2°C for 7 days in a sterilized glass aquarium and fed with commercial food pellets twice a day. Charcoal-filtered fresh water was used during the study period.

Determination of LC_{50}

After acclimatization, fish were randomly divided into seven groups (Control group and six experimental groups) with triplicates in 3L glass aquarium tanks (Size—length 240 mm, width 135 mm and height 130 mm) with optimum conditions. Each group contains six healthy fishes of 2.5–3.0 cm length and 3.0–6.0 gm weight. To estimate the lethal concentration 50% (LC_{50}), the fishes were exposed to NA at different concentrations (100, 110, 120, 130, 140, and 150 ppm). Control groups were maintained without NA. The concentrations of NA were maintained after every water exchange. Clinical disease symptoms and mortalities were recorded for 96 h. The LC_{50} concentration for 96 h was determined, and the one-tenth value of the LC_{50} concentration was taken as the sublethal concentration for further analysis (Westerfield, 2000).

Infectivity Challenge

The immersion route of infection is found to be a suitable experiment method for testing the bacterial virulence. Hence, in this study, the infectivity challenge was carried out in zebrafish according to the immersion challenge test described by Rasch et al. (2004). Zebrafish were immersed in *A. hydrophila* culture at a final concentration of 1×10^5 CFU/ml for 6 h. After immersion, the fish were transferred to their respective aquaria in triplicates. In total, five treatment groups were assigned, and their details are as follows: an uninfected treatment group (control), a post-challenge untreated control group and a post-challenge NA treatment group with three different concentrations (3.5, 7.0, and 14 ppm). Fishes in the uninfected treatment group were not exposed to the test pathogen. Fishes were fed with a normal diet and observed once in every 12 h up to 96 h to record the clinical symptoms and mortalities.

Quantification of Bacterial Load

To quantify the bacterial load, individual fish from each treatment group was homogenized and their slurries were made into suspensions. From serially diluted zebrafish slurries, 100 μl was spread onto Aeromonas isolation agar (Commercially purchased from HiMedia India, Catalog code—M884) plates in triplicate and incubated at 30°C for 24 h. Colonies with a distinctive green color were counted to calculate the average number of CFU/ml. Their fold changes were calculated by using the following formula:

$$\text{Fold change} = \frac{(\text{CFU/ml of control})}{(\text{CFU/ml of treated})}$$

Histopathology Analysis

Histopathology is a well-known technique to assess the qualitative changes in the tissue and the patterns of recovery during infection. For histopathological studies, zebrafish tissue specimens, such as gills, muscle, liver, intestine, and kidneys, were taken from uninfected, infected, and NA (14 ppm) treated groups. Tissue specimens were fixed in 10% neutral buffered formalin (NBF) for 24 h and embedded in paraffin wax, and all the tissues were sectioned at 3 μm thickness. All mounted sections were stained with hematoxylin and eosin (H&E) stain (Sheehan and Hrapchak, 1980).

Statistical Analysis

All the experiments were done in triplicate and repeated at least thrice. Values were expressed as mean ± SD. The statistical analyses were performed using GraphPad Prism v7.0. The

Tukey's multiple comparisons test (one-way analysis of variance) was used to compare the groups for all assays. The Student's *t*-test was used to compare the control and treated samples for qRT-PCR analysis. All the letters (a, b, c, d, and e) indicate statistically significant at $p \leq 0.0001$.

RESULTS

Determination of Minimum Biofilm Inhibitory Concentration of NA

To determine the MBIC, the biofilm biomass inhibition assay was performed with *A. hydrophila* in the presence of NA at doubling concentrations. The results revealed that NA inhibited the biofilm formation of *A. hydrophila* in a concentration-dependent manner (**Figures 1**, **2**). At 750 μg/ml concentration, the NA effectively reduced the *A. hydrophila* biofilm formation up to 55%, and this concentration was considered as MBIC. Therefore, the concentrations ranging from 93.75 to 750 μg/ml were selected for assessing the QS inhibitory potential of NA against *A. hydrophila*.

QS Inhibition Assay for *A. hydrophila*

Effect of NA on β-Hemolysin of *A. hydrophila*

Hemolysin is an exotoxin and the lytic activities on erythrocytes cause anemia in the host. The hemolytic activity in *A. hydrophila* was measured using sheep erythrocytes as substrate. The exposure of *A. hydrophila* to NA at different concentrations (93.75–750 μg/ml) significantly reduced the hemolysin production compared to that of the untreated control (**Figure 2**). The production of hemolysin was inhibited to 51% upon the treatment with 750 μg/ml concentration of NA.

Effect of NA on Lipase of *A. hydrophila*

The lipase is vital for bacterial nutrition and causes damage to the host plasma membrane. A significant decrease in lipase production was found in NA treated *A. hydrophila*. The highest test concentration (750 μg/ml) of NA inhibited a maximum of 49% of lipase production in *A. hydrophila* (**Figure 2**).

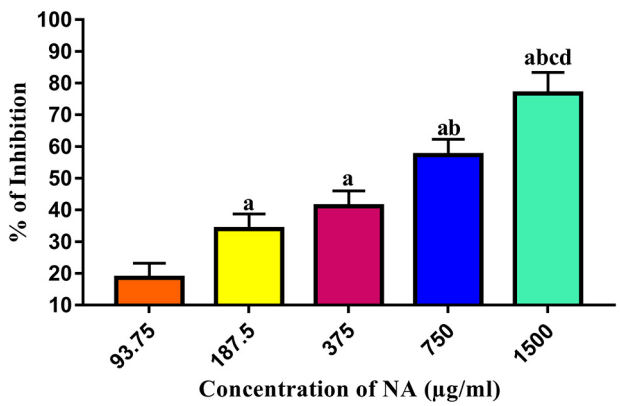

FIGURE 1 | Determination of MBIC of NA against *A. hydrophila* biofilm formation. Results indicate the mean values of three independent experiments and SD. The Tukey's multiple comparisons test (one-way analysis of variance) was used to compare the groups. [a]$p \leq 0.0001$ when compare to control, [b]$p \leq 0.0001$ when compare to 93.75 μg/ml, [c]$p \leq 0.0001$ when compare to 187.5 μg/ml, and [d]$p \leq 0.0001$ when compare to 375 μg/ml.

Effect of NA on Elastase of *A. hydrophila*

Elastase is one of the extracellular hydrolytic enzymes, which are thought to be a contributor of *A. hydrophila* pathogenesis. In an elastase assay, a concentration-dependent inhibition was observed in elastase production of test pathogen upon treatment with NA (**Figure 2**). The 750 μg/ml of NA treatment showed a 40% inhibition in *A. hydrophila* elastase production.

NA Affects Micro-Colony Formation and Biofilm Architecture Development

The microscopic visualization of biofilms demonstrated the effect of NA on *A. hydrophila* biofilm development. The light microscopic examination of *A. hydrophila* harbored NA (93.75–750 μg/ml) on a glass surface showed far less number of micro-colonies compared to the untreated control (**Figure 3**). The three-dimensional architecture of *A. hydrophila* biofilm in the absence and presence of NA was also studied using CLSM. The confocal images lucidly displayed continuous and well-structured biofilm architecture in untreated control glass slides (**Figure 3**). In contrast, the *A. hydrophila* slides treated with NA (93.75–750 μg/ml) exhibited disintegration of biofilms along with a significant decrease in the number of micro-colony formation.

Fourier Transform Infrared (FT-IR) Spectral Analysis

The FT-IR spectral observations exhibited modification in the cellular components of NA treated cells compared to the control cells. In this study, the four most prominent regions corresponding to cellular constituents of NA treated *A. hydrophila* cells were investigated. The predominant regions considered for analysis were 3,500–3,100, 3,000–2,750, 1,800–1,500, and 1,500–1,000 cm^{-1}, which corresponds to the hydration, fatty acids, and amide linkage from proteins and peptides and the mixed region, proteins, fatty acids and polysaccharides of bacterial cells, respectively.

In FT-IR spectra, NA treated *A. hydrophila* cells showed a declined peak of transmittance in the 3,500–3,100 cm^{-1} region, which indicates enhanced hydration in NA treated *A. hydrophila* cells than the control cells. The vast difference in the transmittance was observed in NA treated bacterial cells at 3,000–2,750 cm^{-1} region. It reflects a massive reduction in fatty acids in treated *A. hydrophila* cells. In 1,800–1,500 cm^{-1} region, NA treated *A. hydrophila* cells showed declension in the transmittance peak when compared to the control cells, which implies a reduction in proteins and peptides. The descending peak of transmittance was observed in treated *A. hydrophila* cells at 1,500–1,000 cm^{-1}, which signifies a considerable reduction in the mixed region for protein and fatty acids (**Figure 4**). The overall outcome of the FT-IR analysis revealed that NA treatment made considerable alterations in the cellular components of *A. hydrophila*.

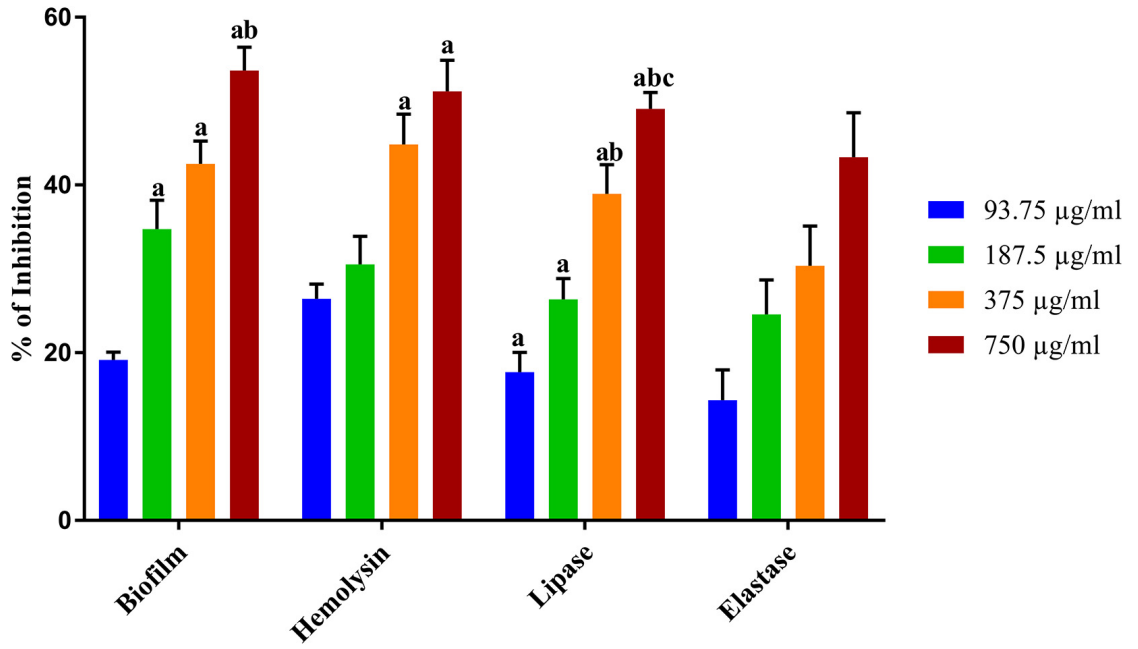

FIGURE 2 | Inhibitory effect of NA on the QS controlled virulence factors production. The graph illustrates percentages of biofilm, hemolysin, lipase, and elastase inhibition in *A. hydrophila* upon treatment with NA at different concentrations (93.75–750 µg/ml). Results indicate the mean values of three independent experiments and SD. The Tukey's multiple comparisons test (one-way analysis of variance) was used to compare the groups. $^{a}p \leq 0.0001$ when compare to control, $^{b}p \leq 0.0001$ when compare to 93.75 µg/ml, and $^{c}p \leq 0.0001$ when compared to 187.5 µg/ml.

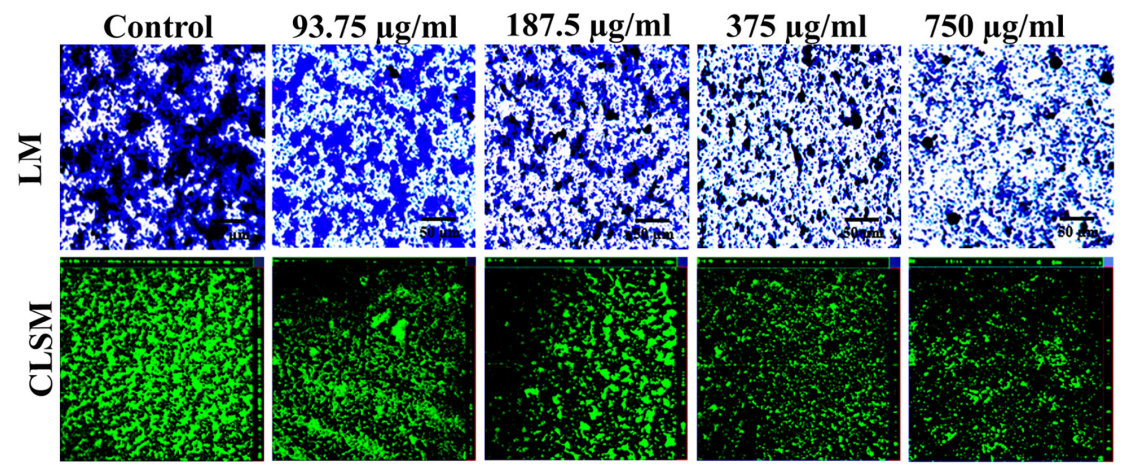

FIGURE 3 | Microscopic validation on the biofilm inhibitory effect of NA against *A. hydrophila*. The light microscopic (LM) and confocal laser scanning microscopic (CLSM) images of *A. hydrophila* biofilm formed in the presence (93.75–750 µg/ml) and the absence (control) of NA.

Impact of NA on Virulence Gene Expressions

Quantitative real time-PCR (qRT-PCR) has turned out into a precise technique used for gene expression analysis owing to its high specificity and sensitivity. In the present study, the qRT-PCR analysis was carried out to assess the differential gene expression of virulence-associated genes in *A. hydrophila* cells harbored with and without NA. The qRT-PCR results confirmed the downregulation of *ahyB, ahh1*, *lip*, and *aerA* genes up to 0. 5-, 0. 9-, 0. 9-, and 0.6-fold, respectively, upon treatment with NA (**Figure 5**).

NA Exhibits Non-bactericidal Activity

Growth of *A. hydrophila* was studied when exposed to NA at different concentrations ranging from 93.75 to 1,500 µg/ml. The spectrophotometric assessment of cell density has revealed no difference in their OD values between the control and the test concentrations of NA up to 750 µg/ml concentration. At the

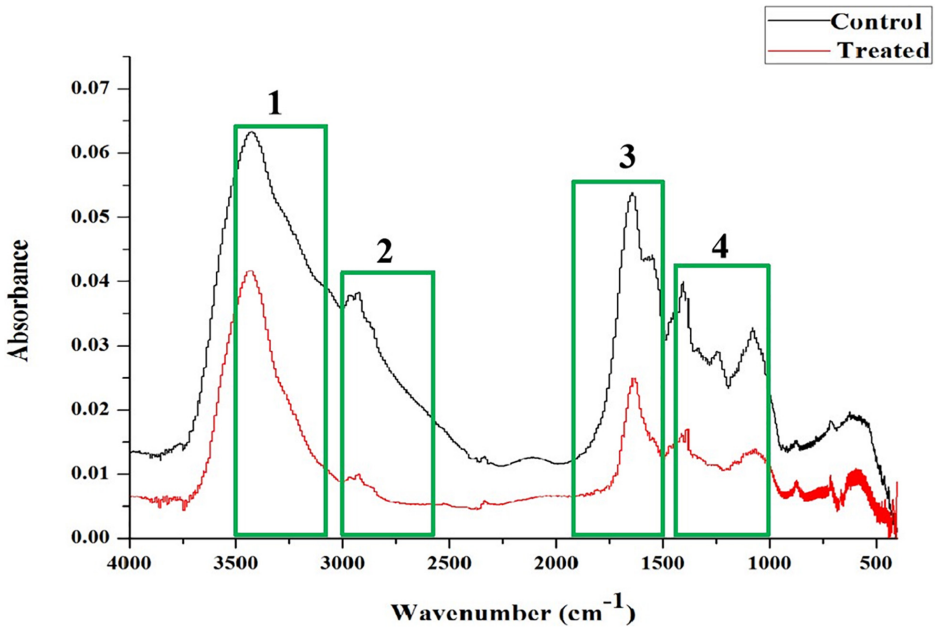

FIGURE 4 | FT-IR spectral analysis showed variation in the absorbance in *A. hydrophila* cells upon treatment with NA (750 μg/ml) compared to the untreated control cells. The regions taken for analysis were shown in the following boxes: (1) 3,500–3,100 cm^{-1} and hydration of microbial cells; (2) 3,000–2,750 cm^{-1} related to fatty acids; (3) 1,800–1,500 cm^{-1}: amide linkages within proteins and peptides; and (4) 1,500–1,000 cm^{-1} of a mixed region among proteins and fatty acids of microbial cells.

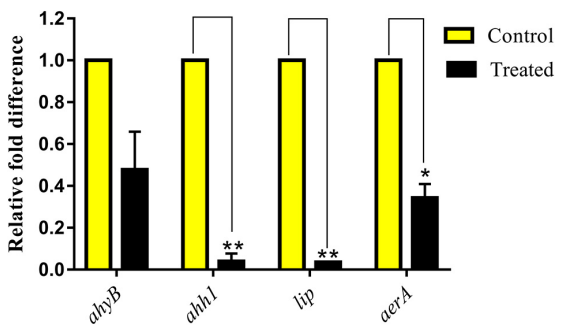

FIGURE 5 | Effect of NA at MBIC on the relative expression of virulence genes in *A. hydrophila*. NA treatment (750 μg/ml) downregulated the QS-controlled virulence genes expression in *A. hydrophila*. Results indicate the mean values of three independent experiments and SD. The Student's *t*-test was used to compare the control and treated data from qRT-PCR analysis. *$p \leq 0.0308$ and **$p \leq 0.0033$.

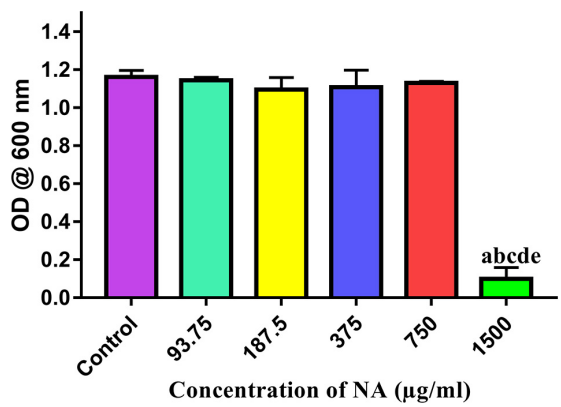

FIGURE 6 | Effect of different concentrations of NA (93.75–1,500 μg/ml) on the growth of *A. hydrophila*. Results indicate the mean values of three independent experiments and SD. The Tukey's multiple comparisons test (one-way analysis of variance) was used to compare the groups. $^{a}p \leq 0.0001$ when compare to control, $^{b}p \leq 0.0001$ when compare to 93.75 μg/ml, $^{c}p \leq 0.0001$ when compare to 187.5 μg/ml, $^{d}p \leq 0.0001$ when compare to 375 μg/ml, and $^{e}p \leq 0.0001$ when compare to 750 μg/ml.

highest concentration (1,500 μg/ml), NA exhibited significant antibacterial activity. This result evidenced the non-bactericidal nature of NA at the QS inhibitory concentration, which is 750 μg/ml (**Figure 6**).

In vivo Challenge Assay

Determination of LC_{50}

At 96 h of incubation, 140 ppm of NA kills half of the total population of zebrafishes. Hence, the same concentration was fixed as the LC_{50} value of NA (**Figure 7**). One-tenth of the LC_{50} value (14 ppm) was fixed as sub-lethal concentration and the same was used for further anti-infective studies.

Effect of NA on Rescuing Post *A. hydrophila* Challenged Zebrafishes

The effect of NA on the survival of zebrafishes challenged with *A. hydrophila* was assessed. The uninfected control group

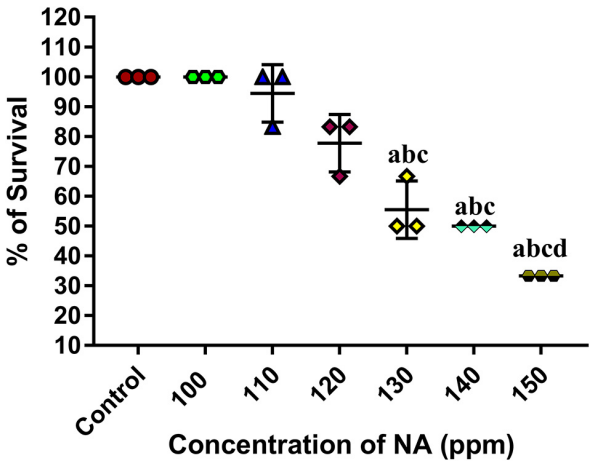

FIGURE 7 | Determination of LC_{50} value of NA on zebrafish. Results indicate the mean values of three independent experiments and SD. The Tukey's multiple comparisons test (one-way analysis of variance) was used to compare the groups. $^{a}p \leq 0.0001$ when compare to control, $^{b}p \leq 0.0001$ when compare to 100 ppm, $^{c}p \leq 0.0001$ when compare to 110 ppm, and $^{d}p \leq 0.0001$ when compare to 120 ppm.

showed 100% survival at 96 h. At 24 h of immersion challenge test, zebrafishes started to show clinical signs such as lethargy, increased respiration, abnormal swimming, abdominal ulceration, abdominal dropsy, and bulged eye. At 72 h past the post infection period, the infected control group showed mere survival (28%) of Zebrafishes, whereas the NA treatment (14 ppm) group showed survival of zebrafishes up to 60%. The survival percentage of post challenged zebrafish in the NA treatment group (14 ppm) exhibited 44% at 96 h. In contrast, the 3.5 and 7.0 ppm of NA treatment showed nearly similar level of survival rates to that of the infected group at 96 h (**Figure 8**).

A. hydrophila Adhesion to Zebrafish

The surface adhered cells of *A. hydrophila* were recovered from post-challenged zebrafishes to assess the influence of NA in treatment groups. It was found that the adherence of *A. hydrophila* cells on post challenged zebrafishes is much higher than the NA treated zebrafishes. The colony counts accounted from the NA treatment group showed a decreasing unit over the increasing concentration; the fold change was thus increased (**Figure 9**). The fold changes for 3.5, 7.0, and 14 ppm are 1. 3-, 4. 8-, and 49-fold in CFU counts, respectively, when compared to the untreated control.

Impact of NA on Histopathology of Post-challenged Zebrafish

The present study revealed that the post challenged zebrafish treated with NA manifest morphological alterations in gills, muscle, liver, and intestine and kidney tissue as follows.

Histopathology of Gills

Histological observations on gills of uninfected control zebrafish showed the typical architecture of gills filaments such as the primary lamellae and secondary lamellae with a scattering of mucus cells on both sides. The gills of post challenged untreated control zebrafish showed the most pronounced histopathological alterations such as lamellar lifting, fusion of secondary lamellar, excessive secretion of mucus on the surface of filaments, and proliferation of filamentary epithelium. However, the post-challenged NA treatment groups did not show any deformities in the gills structure. Gills of post challenged zebrafish treated with NA at 14 ppm concentration supported the typical architecture, as seen in the uninfected control fish (**Figure 10A**).

Histopathology of Muscle

The muscle of the uninfected control zebrafish showed normal arrangements of muscle fibers and muscle bundles. Degeneration and fragmentation of muscle fibers were spotted in the muscle tissue of post challenged zebrafish in the untreated control. However, the NA (14 ppm) treatment restored the normal architecture muscle tissue in post challenged zebrafish, which is similar to the histoarchitecture of muscle from the zebrafish in the uninfected control (**Figure 10B**).

Histopathology of Liver

Histopathological section of the liver in the uninfected control zebrafish exhibited a typical structural organization of hepatocytes with a homogenous cytoplasm and a large spherical nucleus. The liver obtained from post-challenged untreated control zebrafish showed severe fatty acid changes of hepatocytes, a focal area of necrosis, cytoplasmic vacuolation, and hepatocyte disruption. In the present investigation, the liver of NA (14 ppm) treated zebrafish post challenged with *A. hydrophila* showed less damage compared to the zebrafish in the untreated control group (**Figure 10C**).

Histopathology of Intestine

Histological sectioning of intestine from uninfected control zebrafish showed no changes in the intestine architecture. In contrast, histopathological sectioning of post challenged untreated control zebrafish showed anomalies such as an increased number of goblet cells (Hyperplasia), collapsed tunica mucosa and degeneration of epithelial cells. Unlike the uninfected control group, NA treatment restored those deformities rendered by *A. hydrophila* infection in the intestine region (**Figure 10D**).

Histopathology of Kidney

Upon NA treatment, zebrafish challenged with *A. hydrophila* showed hyaline droplets in a few renal tubules. In contrast, the post challenged zebrafish in the infection control group showed degeneration of renal tubule with the formation of hyaline droplets, degeneration of renal glomerulus, and renal hematopoietic necrosis to a very severe degree. Histological sectioning of the uninfected control zebrafish kidney showed the typical structural organization of the nephritic tubules with a well-organized glomerulus (**Figure 10E**).

DISCUSSION

QS is a gene regulation system dependent on cell density; it coordinates the expression of various virulence factors and

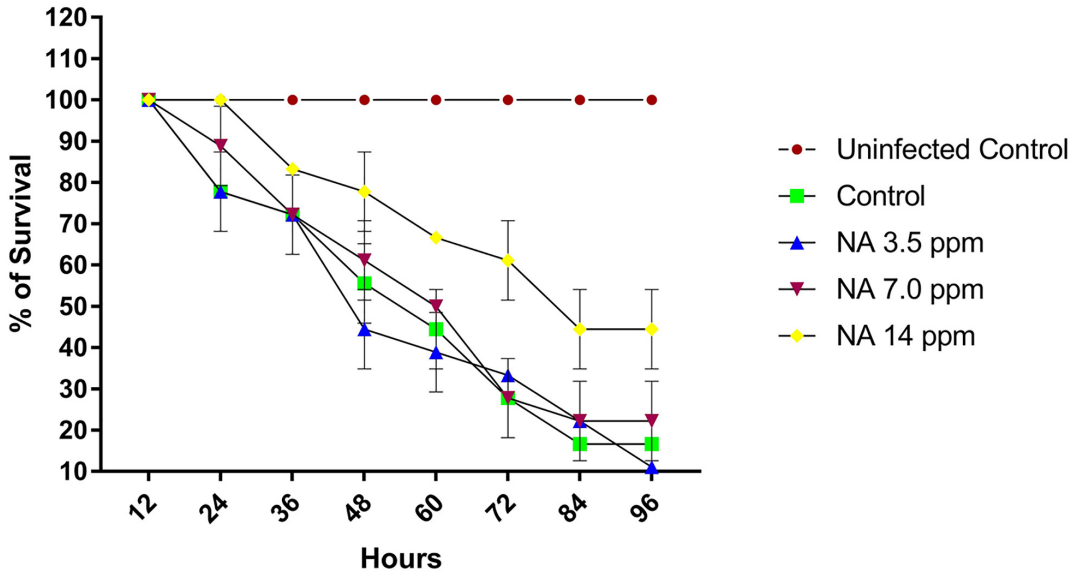

FIGURE 8 | The graph represents the survival percentage of post challenged zebrafishes upon treatment with and without NA at different sub-lethal concentrations (3.5, 7.0, and 14 ppm). Results indicate the mean values of three independent experiments and SD.

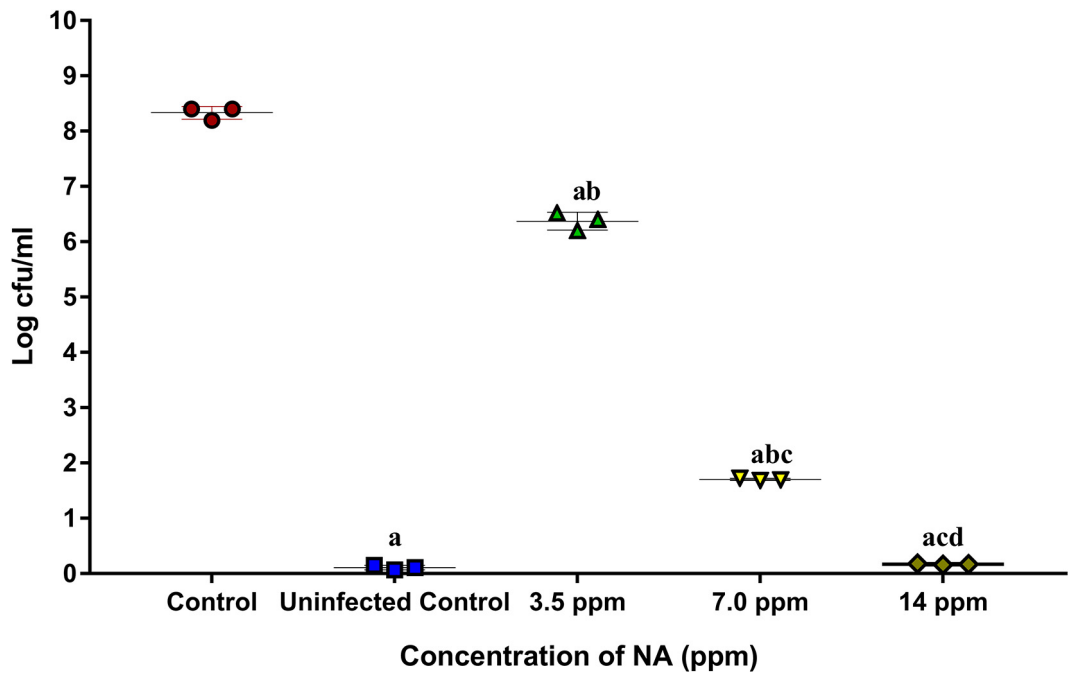

FIGURE 9 | The graph represents CFU counts of *A. hydrophila* in post challenged zebrafish upon treatment with (3.5, 7.0, and 14 ppm) and without NA. Results indicate the mean values of three independent experiments and SD. The Tukey's multiple comparisons test (one-way analysis of variance) was used to compare the groups. $^{a}p \leq 0.0001$ when compare to control, $^{b}p \leq 0.0001$ when compare to uninfected control, $^{c}p \leq 0.0001$ when compare to 3.5 ppm, and $^{d}p \leq 0.0001$ when compare to 7.0 ppm.

biofilm formation in most of the pathogenic microorganism. *A. hydrophila* is an opportunistic aquatic pathogen responsible for causing frequent outbreaks, and it also has an impact on humans while ingesting contaminated seafood (Rama Devi et al., 2016). Recent studies are also continuously reporting that *A. hydrophila* too regulates the virulence factors production and biofilm formation through QS system (Kozlova et al., 2008). In addition to the presence of antibiotic resistance genes, biofilm-mediated antibiotic resistance induces the severity of *A. hydrophila* infections. To control the bacterial pathogenesis

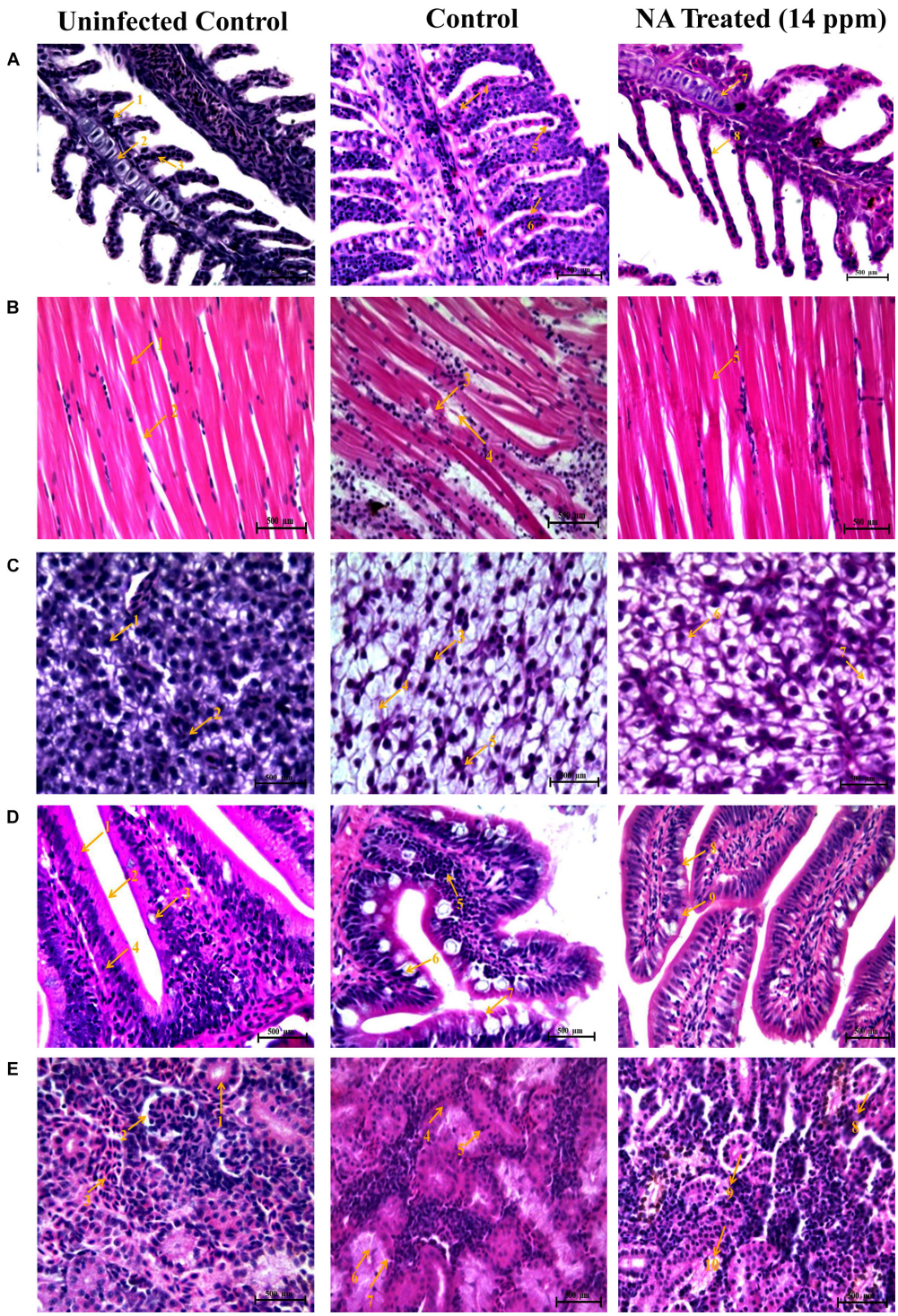

FIGURE 10 | Histopathology analysis of gills **(A)**. 1. Branchial blood vessels; 2. Primary lamella; 3. Secondary lamella; 4. Fusion of secondary lamella; 5. Lamellar lifting; 6. Proliferation of filamentary epithelium; 7. Normal branchial blood vessels; 8. Rescued & healthy secondary lamellae. Histopathology analysis of muscle **(B)**. 1. Muscle bundles; 2. Muscle fiber; 3. Degeneration of muscle bundles; 4. Swelling of muscle fiber; 5. Healthy muscle bundles. Histopathology analysis of liver **(C)**. 1. Hepatocytes; 2. Spherical nucleus; 3. Fatty acid changes in hepatocytes; 4. Cytoplasmic vacuolation; 5. Hepatocytes disruption; 6. Rescued and healthy hepatocytes; 7. Small cytoplasmic vacuolation. Histopathology analysis of intestine **(D)**. 1. Tunica mucosa; 2. External muscle layer; 3. Goblet cell; 4. Lymphocytes; 5. Degeneration of epithelial cells; 6. Hyperplasia of goblet cells; 7. Collapsed tunica mucosa; 8. Normal goblet cell; 9. Rescued and healthy tunica mucosa. Histopathology analysis of kidney **(E)**. 1. Renal glomerulus; 2. Bowman's space; 3. Normal distal tubules; 4. Congested distal tubules; 5. Hematopoietic necrosis; 6. Degeneration of renal glomerulus; 7. Reduced bowman's space; 8. Normal bowman's space; 9. Normal renal glomerulus; 10. Rescued and healthy distal tubulus.

and subsequent infection, targeting QS mechanism has become one of the attractive and best alternative methods.

Several studies are continuously reporting the QS inhibitory potential of phenolic plant extracts, clove oil, and natural compounds against *A. hydrophila* (Husain et al., 2013; Ponnusamy et al., 2013; Rodrigues et al., 2016). However, the necessities for developing new classes of effective QS inhibitors against infectious *A. hydrophila* strains are still in demand. Hence, the present study aimed to delineate the anti-QS and anti-infective potential of NA against *A. hydrophila*. Naringin, a non-toxic, polyphenolic compound, has a myriad pharmacological properties such as anti-oxidant, anti-diabetic, and anti-dyslipidemic effects (Jung et al., 2003; Murunga et al., 2016). Further, several studies have reported the antibacterial, antifungal, and QS-inhibitory potential of various plants and fruits extract containing NA as one of its ingredients (Negi and Jayaprakasha, 2001; Celiz et al., 2011; Hendra et al., 2011; Truchado et al., 2012). In contrast, only a very few studies have investigated the QS inhibitory potential of NA. Annapoorani et al. (2012) have reported NA as an effective inhibitor against *Serratia marcescens* QS mechanism. However, to the best of our knowledge, NA has not been previously reported for its anti-QS property against *A. hydrophila*. Hence, an attempt was taken in the present study to explore the anti-QS and anti-infective efficacy of NA against infectious *A. hydrophila*.

Targeting the QS-dependent biofilm formation is an effective alternative treatment strategy to control bacterial infections (Ramanathan et al., 2018). In this study, the obtained result from the biofilm inhibition assay revealed that NA inhibits biofilm formation of *A. hydrophila* in a concentration-dependent manner (**Figures 1**, **2**). Further, the 750 μg/ml concentration of NA was determined as MBIC up to these concentrations as thus taken for further assays. In line with the result, vanillin, a naturally occurring organic compound, has been reported for its anti-biofilm potential against *A. hydrophila* biofilm formation (Ponnusamy et al., 2013). The QS regulatory mechanisms of *A. hydrophila* are closely linked to biofilm formation along with the production of several virulence factors. *A. hydrophila* expresses diverse virulence enzymes production that contribute to its pathogenicity (Igbinosa et al., 2012). Hemolysins are one such group of multifunctional enzymes that involve pore formation in the target cell membrane (Asao et al., 1984). Lipase has been found to damage the plasma membrane of the host cells, and elastase secreted by *A. hydrophila* causes diseases in fish and humans (Stehr et al., 2003; Nam and Joh, 2007). The reduction in the virulence factors production directly evidenced the anti-QS potential of compounds against pathogenic bacteria. Compared to the normal circumstances, *A. hydrophila* harbored in the presence of NA at MBIC was shown to have a decreased extracellular virulence enzymes production level (**Figure 2**). This result falls in line with the previous findings, wherein the rosmarinic acid at its tested concentration effectively inhibited the production of QS controlled virulence factors such as hemolysin, lipase and elastase and biofilm formation in a pathogenic strains of *A. hydrophila* (Rama Devi et al., 2016).

Schuster and Markx (2013) have stated that the nature and architecture of biofilm prevent the penetration of antibiotics and inhibit their contact with bacterial cells. The anti-biofilm activity of NA was studied by the light microscopic and CLSM analyses. In this study, NA has inhibited the biofilm development of *A. hydrophila* and subsequently reduced the surface area coverage of biofilm. Unlike untreated control images, the images of the treatment group displayed a massive reduction in biofilm architecture development and micro-colony formation in *A. hydrophila* (**Figure 3**). The results of the light microscopic and CLSM analyses are in agreement with the findings of Alexpandi et al. (2019), wherein *Diplocyclos palmatus* methanolic leaf extract treated *S. marcescens* displayed the collapsed biofilm architecture with a reduction in the number of micro-colonies, compared to their respective untreated controls. This perspective of NA brings it one step closer to being an ideal QS inhibitor.

FT-IR is one of the most used techniques in molecular biology for the detection of alterations in the functional groups present in the cellular components, such as nucleic acids, proteins, lipids, and carbohydrates. Hence, the present study utilized the FT-IR technique to probe the variation in cellular components of *A. hydrophila* when treated with and without NA. The FT-IR spectra of NA treatment displayed the variations in the absorbance peaks correspond to the hydration of bacterial cells, reduction in the level of lipids, proteins, peptides, and polysaccharides compared to the control (**Figure 4**). Thus, the reduction in cell-bound peptides and polysaccharides directly substantiates the anti-biofilm potential of NA against *A. hydrophila*. Further, FT-IR spectral observations from the work of Kannappan et al. (2017b) is very much similar to the result observed in the present study, wherein the authors assessed the anti-biofilm activity of geraniol against *Staphylococcus epidermidis* RP62A (Kannappan et al., 2017b). Moreover, in this study, the anti-biofilm and anti-QS potential of NA were also assessed at the transcriptional level. The differential expressions of virulence-associated genes were quantified using qRT-PCR analysis. Among the genes used in the study, *ahh1 and aerA* are hemolytic toxin genes responsible for pore formation in host cells, which leads to apoptosis (Heuzenroeder et al., 1999; Wang et al., 2003). These two-component hemolytic systems (*ahh1 and aerA*) are considered to be the prime regulators for the expression of the Aeromonas virulence genes. Further, Wong et al. (1998) have stated that these two-component hemolytic systems should need to abolish for attenuating the virulence of *A. hydrophila* (Wong et al., 1998). The obtained expression data showed a perceptible downregulation of both the *ahh1* and *aerA* genes upon NA treatment (**Figure 5**). Therefore, it confirms that the NA treatment attenuated the major virulence of *A. hydrophila*. Moreover, the qRT-PCR analysis disclosed the downregulation of *lip* and *ahyB* genes upon treatment with NA (**Figure 5**). The downregulation of *lip* gene expression in this study goes in parallel with the earlier report of Rama Devi et al. (2016) where the rosmarinic acid downregulated the expression of the lipase gene in *A. hydrophila*. Overall, the gene expression analysis validated the outcome of physiological assays and elucidated the anti-QS potential of NA. It has also been well stated that ideal QS inhibitors should not interfere

with the growth of bacteria. To evidence the statement, the concentrations used in the MBIC assay were assessed for their growth inhibitory activity using cell density quantification assay. Up to a 750 μg/ml concentration, NA did not show any effect on the growth of *A. hydrophila*. At 1,500 μg/ml, NA completely suppress the *A. hydrophila* growth (**Figure 6**). It indicated that the NA at the tested concentration targets only the QS mediated gene expressions of *A. hydrophila* and not its growth. This result therefore publicized that NA is a potential QS inhibitor with no influence on the growth of *A. hydrophila*.

The outcomes of *in vitro* studies have suggested that NA inhibits the QS mediated biofilm and virulence factors production in *A. hydrophila*. To further manifest this, *in vivo* experiments were carried out using zebrafish (*D. rerio*) as a model organism. Zebrafish is a freshwater fish; it has been used for laboratory purposes due to its small size, short life cycle and high fecundity. In this study, the NA was applied in the aquaria water to treat *A. hydrophila* infection in Zebrafish. To determine the LC_{50} value of NA, the survival assay was performed with the different concentrations of NA (100–150 ppm). The obtained data displayed that the LC_{50} value of NA was 140 ppm (**Figure 7**). One-tenth of the LC_{50} value was thus taken as a sublethal concentration of NA for *in vivo* analysis. The *in vivo* colonization ability of *A. hydrophila* aids the successful establishment of infection in the host (Natrah et al., 2012). *A. hydrophila* infection in zebrafish was experimentally induced by immersing the fish in a suspension of the test bacterial pathogen. The result of *in vivo* infectivity assay showed that the NA reduced the infection rate and enhanced the survival of zebrafishes challenged with *A. hydrophila*, compared to the untreated control (**Figure 8**). The outcome of this result has clearly indicated that the NA treatment significantly enhanced the survival of zebrafishes from *A. hydrophila* infections. Further, Harikrishnan et al. (2009) have observed a similar enhanced survival rate of goldfish (*Carassius auratus*) challenged with *A. hydrophila* upon treatment with triherbal solvent extracts. Furthermore, the CFU counting assay validated the outcome of survival assay, in which the NA treatment showed a decreased level of CFU counts in zebrafish, compared to the untreated control (**Figure 9**). The outcome of these results is going parallel with the findings of Pachanawan et al. (2008), who studied the protective effect of flavonoids from ethanolic leaf extract of *Psidium guajava* against *A. hydrophila* in tilapia fish.

To confirm the anti-infective efficacy of NA, the histopathological analysis was documented for NA treated and untreated vital organs (gills, muscle, liver, intestine, and kidney) of zebrafish. Gills of fish are predominantly sensitive to chemical and physical changes in the aquatic environment. The liver can detoxify toxic compounds. The presence of toxic compounds at high concentrations cause structural damages in the liver cells (Bruslé and Anadon, 1996; Camargo and Martinez, 2007). The intestine of a fish is the primary site for food digestion and nutrient absorption. Furthermore, the liver and kidney are easily infected by contaminants in water (Thophon et al., 2003). In this study, the *A. hydrophila* infected fish showed acute hemorrhage and necrosis in vital organs such as the liver, intestine, and kidney due to the production of toxins and extracellular enzymes by *A. hydrophila*. This data have supported the outcome of Gado (1998) and Afifi et al. (2000), who have reported that the extracellular virulence enzymes and toxins produced by *A. hydrophila* leads to rapid death in fishes as a result of organ failure. Furthermore, the histological observations of vital organs from the zebrafish of uninfected control showed typical histoarchitecture. In contrast, the histological sectioning of post-challenged zebrafish from control group showed significant histological alterations by *A. hydrophila* infection in all vital organs such as fusion and increased thickness of secondary lamellar in gills, the structural damages observed in muscle sectioning, vacuolation in liver hepatic cells., increased goblet cell secretion and epithelial cell necrosis in intestine and tubule degeneration and hematopoietic tissue necrosis in kidney. A similar kind of annotations was previously observed by Gobinath and Ramanibai (2014), who have reported the adverse histological variations in different vital organs of *Labeo rohita* such as the gills, muscle, liver, and kidney upon *Vibrio cholerae* infection. In contrast to the untreated control, the NA treatment did not show any adverse pathological changes in vital organs of zebrafish. Moreover, the normal structural architecture was observed in NA treatment as like uninfected control (**Figure 10**). Therefore, the findings of this *in vivo* study revealed that the NA treatment increases the defending ability of zebrafish against *A. hydrophila* infection and in turn reduces the disease susceptibility.

In conclusion, for the first time, NA has proven to be a potential anti-QS and anti-infective agent against *A. hydrophila*. The results of microscopic, spectroscopic, and differential gene expression analyses have substantiated our perception over NA as an anti-QS agent. Furthermore, the *in vivo* experiments with zebrafish as model system have confirmed the anti-infective potential of NA. Overall, this study clearly reveals the *in vitro* and *in vivo* therapeutic potential of NA against *A. hydrophila* infection. Furthermore, clinical studies evaluating the potential of NA against *A. hydrophila* infection and elucidating the molecular mechanism behind anti-QS activity of NA, which could pave the way to develop NA as a potential drug candidate against *A. hydrophila* pathogenesis.

DATA AVAILABILITY STATEMENT

The original contributions presented in the study are included in the article/supplementary material, further inquiries can be directed to the corresponding author/s.

ETHICS STATEMENT

All the zebrafish experiments in this study were done in accordance with the guidelines of Committee for the Purpose of Control and Supervision of Experiments on Animal (CPCSEA) (cpcsea.nic.in/WriteReadData/userfiles/file/SOP_CPCSEA_inner_page.pdf), Government of India and general guidelines of Institutional Animal Ethics Committee, Alagappa University. Therefore, ethical approval is not required for the animal work in this study.

AUTHOR CONTRIBUTIONS

RS, KD, AR, and XL conceptualized and validated the study. RS and KD performed the methodology and the data curation, and wrote and prepared the manuscript for the final draft. RS and AK performed the formal analysis. RS, KD, SS, and AK investigated the study. AR and XL were responsible for the resources, supervised the study, and performed the funding acquisition. RS, AK, AR, and XL visualized the study. RS, KD, and AK wrote, reviewed, and edited the manuscript. All authors contributed to the article and approved the submitted version.

ACKNOWLEDGMENTS

RS thankfully acknowledges China Post-doctoral Science Foundation, China, for the financial support to carry out the Post-doctoral research work (Grant No. 2019M662214). This work was sponsored by grants from Program for Innovative Research Team in Fujian Agricultural and Forestry University, China (No. 712018009), NSFC projects, China (No. 31670129), Key Laboratory of Marine Biotechnology of Fujian Province (2020MB04), and the Fujian-Taiwan Joint Innovative Center for Germplasm Resources and Cultivation of Crop, China (FJ 2011 Program, No. 2015-75). Financial assistance rendered to KD in the form of a Basic Scientific Research Fellowship (BSRF) by the University Grants Commission, India [No. F. 4-1/2006(BSR)/7-326/2011(BSR)] is gratefully acknowledged. SS sincerely thanks the Science and Engineering Research Board (Statutory Body Established through an Act of Parliament: SERB Act 2008), Department of Science and Technology, Government of India, for financial support in the form of National Post-Doctoral Fellowship (NPDF Order No. PDF/2018/001518).

REFERENCES

Afifi, S., Al-Thobiati, S., and Hazaa, M. (2000). Bacteriological and histopathological studies on *Aeromonas hydrophila* infection of Nile tilapia (*Oreochromis niloticus*) from fish farms in Saudi Arabia. *Assiut Vet. Med. J.* 42, 195–205.

Alexpandi, R., Prasanth, M. I., Ravi, A. V., Balamurugan, K., Durgadevi, R., Srinivasan, R., et al. (2019). Protective effect of neglected plant *Diplocyclos palmatus* on quorum sensing mediated infection of *Serratia marcescens* and UV-A induced photoaging in model *Caenorhabditis elegans*. *J. Photochem. Photobiol. B Biol.* 201:111637. doi: 10.1016/j.jphotobiol.2019.111637

Annapoorani, A., Parameswari, R., Pandian, S. K., and Ravi, A. V. (2012). Methods to determine antipathogenic potential of phenolic and flavonoid compounds against urinary pathogen *Serratia marcescens*. *J. Microbiol. Methods* 91, 208–211. doi: 10.1016/j.mimet.2012.06.007

Asao, T., Kinoshita, Y., Kozaki, S., Uemura, T., and Sakaguchi, G. (1984). Purification and some properties of *Aeromonas hydrophila* hemolysin. *Infect. Immun.* 46, 122–127. doi: 10.1128/iai.46.1.122-127.1984

Bakkiyaraj, D., and Karutha Pandian, S. T. (2010). *In vitro* and *in vivo* antibiofilm activity of a coral associated actinomycete against drug resistant *Staphylococcus aureus* biofilms. *Biofouling* 26, 711–717. doi: 10.1080/08927014.2010.511200

Bruslé, J., and Anadon, G. (1996). The structure and function of fish liver. *Fish Morphol.* 76, 545–551.

Camargo, M. M., and Martinez, C. B. (2007). Histopathology of gills, kidney and liver of a Neotropical fish caged in an urban stream. *Neotrop. Ichthyol.* 5, 327–336. doi: 10.1590/s1679-62252007000300013

Cascón, A., Yugueros, J., Temprano, A., Sánchez, M., Hernanz, C., Luengo, J. M., et al. (2000). A major secreted elastase is essential for pathogenicity of *Aeromonas hydrophila*. *Infect. Immun.* 68, 3233–3241. doi: 10.1128/iai.68.6.3233-3241.2000

Celiz, G., Daz, M., and Audisio, M. C. (2011). Antibacterial activity of naringin derivatives against pathogenic strains. *J. Appl. Microbiol.* 111, 731–738. doi: 10.1111/j.1365-2672.2011.05070.x

Chopra, A. K., and Houston, C. W. (1999). Enterotoxins in *Aeromonas*-associated gastroenteritis. *Microb. Infect.* 1, 1129–1137. doi: 10.1016/s1286-4579(99)00202-6

Daskalov, H. (2006). The importance of *Aeromonas hydrophila* in food safety. *Food Control* 17, 474–483. doi: 10.1016/j.foodcont.2005.02.009

Donlan, R. M. (2002). Biofilms: microbial life on surfaces. *Emerg. Infect. Dis.* 8, 881–890. doi: 10.3201/eid0809.020063

Eftimiadi, C., Buzzi, E., Tonetti, M., Buffa, P., Buffa, D., Van Steenbergen, M., et al. (1987). Short-chain fatty acids produced by anaerobic bacteria alter the physiological responses of human neutrophils to chemotactic peptide. *J. Infect.* 14, 43–53. doi: 10.1016/s0163-4453(87)90808-5

Fuqua, C., Parsek, M. R., and Greenberg, E. P. (2001). Regulation of gene expression by cell-to-cell communication: acyl-homoserine lactone quorum sensing. *Annu. Rev. Genet.* 35, 439–468. doi: 10.1146/annurev.genet.35.102401.090913

Gado, M. (1998). Studies on the virulence of *Aeromonas hydrophila* in Nile Tilapia (*Oreochromis niloticus*). *Assiut Vet. Med. J.* 40, 190–200.

Gobinath, J., and Ramanibai, R. (2014). Histopathological studies in the Gill, Liver, and Kidney of the Freshwater Fish Labeorohita Fingerlings. *Int. J. Innov. Res. Scie.Eng. Technol.* 3:10296.

Harikrishnan, R., Balasundaram, C., Kim, M.-C., Kim, J.-S., Han, Y.-J., and Heo, M.-S. (2009). Innate immune response and disease resistance in *Carassius auratus* by triherbal solvent extracts. *Fish Shellfish Immunol.* 27, 508–515. doi: 10.1016/j.fsi.2009.07.004

Hendra, R., Ahmad, S., Sukari, A., Shukor, M. Y., and Oskoueian, E. (2011). Flavonoid analyses and antimicrobial activity of various parts of Phaleria macrocarpa (Scheff.) Boerl fruit. *Int. J. Mol. Sci.* 12, 3422–3431. doi: 10.3390/ijms12063422

Heuzenroeder, M. W., Wong, C. Y., and Flower, R. L. (1999). Distribution of two hemolytic toxin genes in clinical and environmental isolates of *Aeromonas* spp. correlation with virulence in a suckling mouse model. *FEMS Microbiol. Lett.* 174, 131–136. doi: 10.1111/j.1574-6968.1999.tb13559.x

Husain, F. M., Ahmad, I., Asif, M., and Tahseen, Q. (2013). Influence of clove oil on certain quorum-sensing-regulated functions and biofilm of *Pseudomonas aeruginosa* and *Aeromonas hydrophila*. *J. Biosci.* 38, 835–844. doi: 10.1007/s12038-013-9385-9

Igbinosa, I. H., Igumbor, E. U., Aghdasi, F., Tom, M., and Okoh, A. I. (2012). Emerging *Aeromonas* species infections and their significance in public health. *Sci. World J.* 2012:625023.

Janda, J. M., and Abbott, S. L. (2010). The genus *Aeromonas*: taxonomy, pathogenicity, and infection. *Clin. Microbiol. Rev.* 23, 35–73. doi: 10.1128/cmr.00039-09

Jung, U., Kim, H., Lee, J., Lee, M., Kim, H., Park, E., et al. (2003). Naringin supplementation lowers plasma lipids and enhances erythrocyte antioxidant enzyme activities in hypercholesterolemic subjects. *Clin. Nutr.* 22, 561–568. doi: 10.1016/s0261-5614(03)00059-1

Kannappan, A., Balasubramaniam, B., Ranjitha, R., Srinivasan, R., Packiavathy, I. A. S. V., Balamurugan, K., et al. (2019a). *In vitro* and *in vivo* biofilm inhibitory efficacy of geraniol-cefotaxime combination against *Staphylococcus* spp. *Food Chem. Toxicol.* 125, 322–332. doi: 10.1016/j.fct.2019.01.008

Kannappan, A., Srinivasan, R., Nivetha, A., Annapoorani, A., Pandian, S. K., and Ravi, A. V. (2019b). Anti-virulence potential of 2-hydroxy-4-methoxybenzaldehyde against methicillin-resistant *Staphylococcus aureus* and

its clinical isolates. *Appl. Microbiol. Biotechnol.* 103, 6747–6758. doi: 10.1007/s00253-019-09941-6

Kannappan, A., Gowrishankar, S., Srinivasan, R., Pandian, S. K., and Ravi, A. V. (2017a). Antibiofilm activity of *Vetiveria zizanioides* root extract against methicillin-resistant *Staphylococcus aureus*. *Microb. Pathog.* 110, 313–324. doi: 10.1016/j.micpath.2017.07.016

Kannappan, A., Sivaranjani, M., Srinivasan, R., Rathna, J., Pandian, S. K., and Ravi, A. V. (2017b). Inhibitory efficacy of geraniol on biofilm formation and development of adaptive resistance in *Staphylococcus epidermidis* RP62A. *J. Med. Microbiol.* 66, 1506–1515. doi: 10.1099/jmm.0.000570

Khajanchi, B. K., Fadl, A. A., Borchardt, M. A., Berg, R. L., Horneman, A. J., Stemper, M. E., et al. (2010). Distribution of virulence factors and molecular fingerprinting of *Aeromonas* species isolates from water and clinical samples: suggestive evidence of water-to-human transmission. *Appl. Environ. Microbiol.* 76, 2313–2325. doi: 10.1128/aem.02535-09

Kozlova, E. V., Popov, V. L., Sha, J., Foltz, S. M., Erova, T. E., Agar, S. L., et al. (2008). Mutation in the S-ribosylhomocysteinase (*luxS*) gene involved in quorum sensing affects biofilm formation and virulence in a clinical isolate of *Aeromonas hydrophila*. *Microb. Pathog.* 45, 343–354. doi: 10.1016/j.micpath.2008.08.007

Li, D., Ramanathan, S., Wang, G., Wu, Y., Tang, Q., and Li, G. (2020). Acetylation of lysine 7 of AhyI affects the biological function in *Aeromonas hydrophila*. *Microb. Pathog.* 140:103952. doi: 10.1016/j.micpath.2019.103952

Li, Z., Wang, Y., Li, X., Lin, Z., Lin, Y., Srinivasan, R., et al. (2019). The characteristics of antibiotic resistance and phenotypes in 29 outer-membrane protein mutant strains in *Aeromonas hydrophila*. *Environ. Microbiol.* 21, 4614–4628. doi: 10.1111/1462-2920.14761

Morris, J., and Horneman, A. (2013). *Aeromonas Infections*. Waltham, MA: UpToDate.

Murray, R., Dooley, J., and Whippey, P. (1988). Structure of an S layer on a pathogenic strain of *Aeromonas hydrophila*. *J. Bacteriol.* 170, 2625–2630. doi: 10.1128/jb.170.6.2625-2630.1988

Murunga, A. N., Miruka, D. O., Driver, C., Nkomo, F. S., Cobongela, S. Z., and Owira, P. M. (2016). Grapefruit derived flavonoid naringin improves ketoacidosis and lipid peroxidation in type 1 diabetes rat model. *PLoS One* 11:e0153241. doi: 10.1371/journal.pone.0153241

Nam, I.-Y., and Joh, K. (2007). Rapid detection of virulence factors of *Aeromonas* isolated from a trout farm by hexaplex-PCR. *J. Microbiol.* 45, 297–304.

Natrah, F., Alam, M. I., Pawar, S., Harzevili, A. S., Nevejan, N., Boon, N., et al. (2012). The impact of quorum sensing on the virulence of *Aeromonas hydrophila* and *Aeromonas salmonicida* towards burbot (*Lota lota* L.) larvae. *Vet. Microbiol.* 159, 77–82. doi: 10.1016/j.vetmic.2012.03.014

Negi, P., and Jayaprakasha, G. (2001). Antibacterial activity of grapefruit (*Citrus paradisi*) peel extracts. *Eur. Food Res. Technol.* 213, 484–487. doi: 10.1007/s002170100394

Ohman, D., Cryz, S., and Iglewski, B. (1980). Isolation and characterization of *Pseudomonas aeruginosa* PAO mutant that produces altered elastase. *J. Bacteriol.* 142, 836–842. doi: 10.1128/jb.142.3.836-842.1980

Pachanawan, A., Phumkhachorn, P., and Rattanachaikunsopon, P. (2008). Potential of *Psidium guajava* supplemented fish diets in controlling *Aeromonas hydrophila* infection in tilapia (*Oreochromis niloticus*). *J. Biosci. Bioeng.* 106, 419–424. doi: 10.1263/jbb.106.419

Peterson, J. J., Beecher, G. R., Bhagwat, S. A., Dwyer, J. T., Gebhardt, S. E., Haytowitz, D. B., et al. (2006a). Flavanones in grapefruit, lemons, and limes: a compilation and review of the data from the analytical literature. *J. Food Comp. Anal.* 19, S74–S80.

Peterson, J. J., Dwyer, J. T., Beecher, G. R., Bhagwat, S. A., Gebhardt, S. E., Haytowitz, D. B., et al. (2006b). Flavanones in oranges, tangerines (mandarins), tangors, and tangelos: a compilation and review of the data from the analytical literature. *J. Food Comp. Anal.* 19, S66–S73.

Ponnusamy, K., Kappachery, S., Thekeettle, M., Song, J., and Kweon, J. (2013). Anti-biofouling property of vanillin on *Aeromonas hydrophila* initial biofilm on various membrane surfaces. *World J. Microbiol. Biotechnol.* 29, 1695–1703. doi: 10.1007/s11274-013-1332-2

Rama Devi, K., Srinivasan, R., Kannappan, A., Santhakumari, S., Bhuvaneswari, M., Rajasekar, P., et al. (2016). In vitro and *in vivo* efficacy of rosmarinic acid on quorum sensing mediated biofilm formation and virulence factor production in *Aeromonas hydrophila*. *Biofouling* 32, 1171–1183. doi: 10.1080/08927014.2016.1237220

Ramanathan, S., Arunachalam, K., Chandran, S., Selvaraj, R., Shunmugiah, K., and Arumugam, V. (2018). Biofilm inhibitory efficiency of phytol in combination with cefotaxime against nosocomial pathogen *Acinetobacter baumannii*. *J. Appl. Microbiol.* 125, 56–71. doi: 10.1111/jam.13741

Rasch, M., Buch, C., Austin, B., and Slierendrecht, W. J. (2004). An inhibitor of bacterial quorum sensing reduces mortalities caused by vibriosis in rainbow trout (*Oncorhynchus mykiss*. Walbaum). *Syst. Appl. Microbiol.* 27, 350–359. doi: 10.1078/0723-2020-00268

Rawson, N. E., Ho, C.-T., and Li, S. (2014). Efficacious anti-cancer property of flavonoids from citrus peels. *Food Sci. Hum. Wellness* 3, 104–109. doi: 10.1016/j.fshw.2014.11.001

Rodrigues, A. C., Oliveira, B. D., Silva, E. R. D., Sacramento, N. T. B., Bertoldi, M. C., and Pinto, U. M. (2016). Anti-quorum sensing activity of phenolic extract from *Eugenia brasiliensis* (Brazilian cherry). *Food Sci. Technol.* 36, 337–343. doi: 10.1590/1678-457x.0089

Salvamani, S., Gunasekaran, B., Shaharuddin, N. A., Ahmad, S. A., and Shukor, M. Y. (2014). Antiartherosclerotic effects of plant flavonoids. *BioMed Res. Int.* 2014:480258.

Scheffer, J., König, W., Braun, V., and Goebel, W. (1988). Comparison of four hemolysin-producing organisms (*Escherichia coli*, *Serratia marcescens*, *Aeromonas hydrophila*, and *Listeria monocytogenes*) for release of inflammatory mediators from various cells. *J. Clin. Microbiol.* 26, 544–551. doi: 10.1128/jcm.26.3.544-551.1988

Schuster, J. J., and Markx, G. H. (2013). "Biofilm architecture," in *Productive Biofilms*, eds K. Muffler and R. Ulber (Berlin: Springer), 77–96. doi: 10.1007/10_2013_248

Sen, K. (2005). Development of a rapid identification method for *Aeromonas* species by multiplex-PCR. *Can. J. Microbiol.* 51, 957–966. doi: 10.1139/w05-089

Shak, J. R., Whitaker, J. A., Ribner, B. S., and Burd, E. M. (2011). Aminoglycoside-resistant *Aeromonas hydrophila* as part of a polymicrobial infection following a traumatic fall into freshwater. *J. Clin. Microbiol.* 49, 1169–1170. doi: 10.1128/jcm.01949-10

Sheehan, D. C., and Hrapchak, B. B. (1980). *Theory and Practice of Histotechnology*. Maryland Heights, MO: Mosby.

Singh, V., Somvanshi, P., Rathore, G., Kapoor, D., and Mishra, B. (2009). Gene cloning, expression and homology modeling of hemolysin gene from *Aeromonas hydrophila*. *Protein Expr. Purif.* 65, 1–7. doi: 10.1016/j.pep.2008.11.015

Sivaranjani, M., Srinivasan, R., Aravindraja, C., Karutha Pandian, S., and Veera Ravi, A. (2018). Inhibitory effect of α-mangostin on *Acinetobacter baumannii* biofilms–an *in vitro* study. *Biofouling* 34, 579–593. doi: 10.1080/08927014.2018.1473387

Song, T., Toma, C., Nakasone, N., and Iwanaga, M. (2004). Aerolysin is activated by metalloprotease in *Aeromonas veronii* biovar sobria. *J. Med. Microbiol.* 53, 477–482. doi: 10.1099/jmm.0.05405-0

Srinivasan, R., Devi, K. R., Kannappan, A., Pandian, S. K., and Ravi, A. V. (2016). Piper betle and its bioactive metabolite phytol mitigates quorum sensing mediated virulence factors and biofilm of nosocomial pathogen *Serratia marcescens in vitro*. *J. Ethnopharmacol.* 193, 592–603. doi: 10.1016/j.jep.2016.10.017

Srinivasan, R., Mohankumar, R., Kannappan, A., Karthick Raja, V., Archunan, G., Karutha Pandian, S., et al. (2017). Exploring the anti-quorum sensing and antibiofilm efficacy of phytol against *Serratia marcescens* associated acute pyelonephritis infection in Wistar rats. *Front. Cell. Infect. Microbiol.* 7:498. doi: 10.3389/fcimb.2017.00498

Stehr, F., Kretschmar, M., Kröger, C., Hube, B., and Schäfer, W. (2003). Microbial lipases as virulence factors. *J. Mol. Catal. B Enzymat.* 22, 347–355. doi: 10.1016/s1381-1177(03)00049-3

Thophon, S., Kruatrachue, M., Upatham, E., Pokethitiyook, P., Sahaphong, S., and Jaritkhuan, S. (2003). Histopathological alterations of white seabass, *Lates calcarifer*, in acute and subchronic cadmium exposure. *Environ. Pollut.* 121, 307–320. doi: 10.1016/s0269-7491(02)00270-1

Truchado, P., GiméNez-Bastida, J.-A., Larrosa, M., Castro-IbáÑEz, I., EspìN, J. C., TomáS-BarberáN, F. A., et al. (2012). Inhibition of quorum sensing (QS) in Yersinia enterocolitica by an orange extract rich in glycosylated flavanones. *J. Agric. Food Chem.* 60, 8885–8894. doi: 10.1021/jf301365a

Wang, G., Clark, C. G., Liu, C., Pucknell, C., Munro, C. K., Kruk, T. M., et al. (2003). Detection and characterization of the hemolysin genes in *Aeromonas hydrophila* and *Aeromonas sobria* by multiplex PCR. *J. Clin. Microbiol.* 41, 1048–1054. doi: 10.1128/jcm.41.3.1048-1054.2003

Westerfield, M. (2000). "The zebrafish book," in *A Guide for the Laboratory Use of Zebrafish (Danio rerio)*, 4th Edn, Eugene: Univ. of Oregon Press. Available online at: http://zfin.org/zf_info/zfbook/zfbk.html

Wong, C. Y., Heuzenroeder, M. W., and Flower, R. L. (1998). Inactivation of two haemolytic toxin genes in *Aeromonas hydrophila* attenuates virulence in a suckling mouse model. *Microbiology* 144, 291–298. doi: 10.1099/00221287-144-2-291

Conflict of Interest: The authors declare that the research was conducted in the absence of any commercial or financial relationships that could be construed as a potential conflict of interest.

frontiers in Microbiology

ORIGINAL RESEARCH
published: 01 March 2021
doi: 10.3389/fmicb.2021.646299

Edwardsiella piscicida YefM-YoeB: A Type II Toxin-Antitoxin System That Is Related to Antibiotic Resistance, Biofilm Formation, Serum Survival, and Host Infection

Dongmei Ma[1,2], Hanjie Gu[2], Yanjie Shi[2], Huiqin Huang[2], Dongmei Sun[1] and Yonghua Hu[2,3,4]**

[1] College of Life Science and Technology, Heilongjiang Bayi Agricultural University, Daqing, China, [2] Institute of Tropical Bioscience and Biotechnology, Hainan Academy of Tropical Agricultural Resource, CATAS, Haikou, China, [3] Laboratory for Marine Biology and Biotechnology, Pilot National Laboratory for Marine Science and Technology, Qingdao, China, [4] Hainan Provincial Key Laboratory for Functional Components Research and Utilization of Marine Bio-resources, Haikou, China

OPEN ACCESS

Edited by:
Bo Peng,
Sun Yat-sen University, China

Reviewed by:
Weiwei Zhang,
Ningbo University, China
Yoshihiro Yamaguchi,
Osaka City University, Japan

***Correspondence:**
Dongmei Sun
sdmlzw@126.com
Yonghua Hu
huyonghua@itbb.org.cn

Specialty section:
This article was submitted to Antimicrobials, Resistance and Chemotherapy, a section of the journal Frontiers in Microbiology

Received: *26 December 2020*
Accepted: *03 February 2021*
Published: *01 March 2021*

Citation:
Ma D, Gu H, Shi Y, Huang H, Sun D and Hu Y (2021) Edwardsiella piscicida YefM-YoeB: A Type II Toxin-Antitoxin System That Is Related to Antibiotic Resistance, Biofilm Formation, Serum Survival, and Host Infection. Front. Microbiol. 12:646299. doi: 10.3389/fmicb.2021.646299

The emergence of drug resistant bacteria is a tricky and confronted problem in modern medicine, and one of important reasons is the widespread of toxin-antitoxin (TA) systems in pathogenic bacteria. *Edwardsiella piscicida* (also known as *E. tarda*) is the leading pathogen threatening worldwide fresh and seawater aquaculture industries and has been considered as a model organism for studying intracellular and systemic infections. However, the role of type II TA systems are completely unknown in aquatic pathogenic bacteria. In this study, we identified and characterized a type II TA system, YefM-YoeB, of *E. piscicida*, where YefM is the antitoxin and YoeB is the toxin. *yefM* and *yoeB* are co-expressed in a bicistronic operon. When expressed in *E. coli*, YoeB cause bacterial growth arrest, which was restored by the addition of YefM. To investigate the biological role of the TA system, two markerless *yoeB* and *yefM-yoeB* in-frame mutant strains, TX01Δ*yoeB* and TX01Δ*yefM-yoeB*, were constructed, respectively. Compared to the wild strain TX01, TX01Δ*yefM-yoeB* exhibited markedly reduced resistance against oxidative stress and antibiotic, and markedly reduced ability to form persistent bacteria. The deletion of *yefM-yoeB* enhanced the bacterial ability of high temperature tolerance, biofilm formation, and host serum resistance, which is the first study about the relationship between type II TA system and serum resistance. *In vitro* infection experiment showed that the inactivation of *yefM-yoeB* greatly enhanced bacterial capability of adhesion in host cells. Consistently, *in vivo* experiment suggested that the *yefM-yoeB* mutation had an obvious positive effect on bacteria dissemination of fish tissues and general virulence. Introduction of a trans-expressed *yefM-yoeB* restored the virulence of TX01Δ*yefM-yoeB*. These findings suggest that YefM-YoeB is involved in responding adverse circumstance and pathogenicity of *E. piscicida*. In addition, we

found that YefM-YoeB negatively autoregulated the expression of *yefM-yoeB* and YefM could directly bind with own promoter. This study provides first insights into the biological activity of type II TA system YefM-YoeB in aquatic pathogenic bacteria and contributes to understand the pathogenesis of *E. piscicida*.

Keywords: *Edwardsiella piscicida*, toxin-antitoxin, YefM-YoeB, adversity, virulence

INTRODUCTION

Edwardsiella was isolated from infected humans and animals and identified as a new genus of Enterobacteriaceae in 1965 (Ewing et al., 1965). The *Edwardsiella* genus was classified into five species, including *E. piscicida*, *E. anguillarum*, *E. ictaluri, E. tarda*, and *E. hoshinae* (Abayneh et al., 2013; Leung et al., 2019). The front three species belong to fish pathogens. *E. piscicida* (formerly included in *E. tarda*) is recognized as one of the most severe pathogens in cultivating fishery (Leung et al., 2012). It can infect not only freshwater and marine fish at the same time, causing a large number of infections and deaths of fish, but also a zoonotic pathogen with a wide host range, including mammals and reptiles (Janda and Abbott, 1993; Mohanty and Sahoo, 2007; Park et al., 2012). In recent years, researches on the pathogenic mechanism of *E. piscicida* have become a research hotspot in the field of aquatic animal diseases. A variety of pathogenic factors and systems, such as adhesion factors, iron uptake regulators, antiserum ability, type III and VI secretion systems, hemolysin, catalase, cytotoxin, TAM, two-component system, density induction systems, flagellin, lysozyme inhibitors, intracellular survival mechanisms, and some environmental stress factors have been discovered and studied (Yin et al., 2018; Leung et al., 2019; He et al., 2020; Li et al., 2020; Yoon et al., 2020). However, toxin-antitoxin (TA) system, an important stress and antibiotic resistance factor/system, are totally unknown in *E. piscicida*.

The rapid rise in the emergence of drug-resistant bacteria is a tricky and confronted problem in modern medicine. One of important reasons for emergence of antibiotic-resistant bacteria is the widespread of TA systems in bacteria (Równicki et al., 2020). The first identified toxin-antitoxin (TA) systems were characterized as "plasmid addiction modules" (Ogura and Hiraga, 1983; Guo et al., 2019). Subsequently, TA systems were discovered to be extensive as genetic elements in bacteria and archaea, including chromosomally encoded TA systems. In the past 30 years, according to the nature of the antitoxin and the composition of the TA system, a total of six types of TA (Type I–Type VI) have been discovered (Page and Peti, 2016). Amongst these TA systems, type II TA systems are the most prevalent and most extensively studied (Równicki et al., 2020). They are usually composed of two co-transcribed genes, encoding stable toxin proteins and easily degradable antitoxin proteins. In normal growing cells, the antitoxin combines with its homologous toxin to produce a harmless protein-protein complex that prevents the toxin from exerting its toxicity (Yamaguchi et al., 2011). The antitoxin binds to the upstream of the TA operon to inhibit the expression of the operon, and the toxin acts as an auxiliary inhibitor combined with the antitoxin to strengthen this inhibition, so the level of intracellular TA complex is regulated by the antitoxin and TA complex together (Gerdes and Maisonneuve, 2012). Under certain stress conditions, the antitoxins are degraded by proteases to release stable toxin proteins, at the same time, the inhibition of the operon is lifted, resulting in the accumulation of toxins and the activation of toxic effects (Brzozowska and Zielenkiewicz, 2013; Schuster and Bertram, 2013).

Persisters are rare bacteria in a bacterial population that could resist to lethal antibiotics and that could account for the relapse of infections. Environmental stresses and growth phases influence the formation of persister cells (Bernier et al., 2013; Helaine et al., 2014). An important reason for the formation of persister cells is TA systems (Verstraeten et al., 2015). Currently, a number of type II TA systems have been identified, and they are widely present in all kinds of pathogens, such as *E. coli*, *Streptococcus pneumoniae*, *Pseudomonas aeruginosa*, and *Staphylococcus aureus* (Lobato-Márquez et al., 2016; Wood and Wood, 2016; Chan et al., 2018; Wen et al., 2018). Reports have shown that type II toxin-antitoxin systems can ensure the safety and stability of mobile genetic elements, induce the formation of persistent cells, participate in biofilm formation, stress response, and pathogenicity (Wang and Wood, 2011; Harms et al., 2016; Oron-Gottesman et al., 2016; Sun et al., 2017; Ma et al., 2019). Recently, an increasing number of studies are devoted to the role of type II TA systems in pathogenicity (Równicki et al., 2020).

Among type II TA systems, YefM-YoeB is one of most frequently encountered TA systems in many pathogenic bacteria. In *S. aureus*, there are two distinct oligomeric assemblies: heterotetramer (YoeB-YefM2-YoeB) and heterohexamer (YoeB-YefM2-YefM2-YoeB) (Xue et al., 2020). In *S. pneumoniae*, it is reported that YefM-YoeB participates in oxidative stress and biofilm formation (Chan et al., 2018). In *E. coli*, YoeB toxin is activated during thermal stress (Janssen et al., 2015) and YefM-YoeB is involved in the niche-specific colonization and stress resistance (Norton and Mulvey, 2012). Currently, there is no report about the type II TA systems in aquatic pathogenic bacteria and their roles are totally unknown. In this study, we for the first time identified and characterized a type II TA system, YefM-YoeB, in *E. piscicida*. We investigated the role of YefM-YoeB in adversity adaptation and pathogenicity. Our results suggested that the whole TA system YefM-YoeB was related to antibiotic resistance, persistence bacteria formation, oxidative resistance, biofilm formation, host serum resistance, and host infection. Antitoxin YefM negatively autoregulated its own expression and toxin YoeB remarkably enhance the regulatory effect of YefM. This study provides first insights into the biological activity of type II TA system in aquatic pathogenic bacteria and will help us understand the pathogenic mechanism.

MATERIALS AND METHODS

Bacteria and Growth Conditions

E. coli BL21 (DE3) was purchased from TransGen (Beijing, China). *E. coli* S17-1λpir was purchased from Biomedal (Seville, Spain). *E. piscicida* TX01 was isolated from diseased fish. Bacteria were cultured in Luria-Bertani broth (LB) at 37°C (for *E. coli*) or 28°C (for *E. piscicida*). Where indicated, Ampicillin, Kanamycin, chloramphenicol, tetracycline, and polymyxin B, were supplemented at the concentration of 100, 50, 30, 15, and 100 μg/mL (Fang et al., 2019).

Total RNA Isolation, cDNA Generation, and Co-transcription Analysis

Overnight cultures of *E. piscicida* were diluted 1:100 in LB and grown at 28°C to exponential phase. The genomic DNA and total RNA of bacteria were isolated with TIANamp Bacteria DNA Kit (TIANGEN, Beijing, China) and HP Total RNA kit (Omega Bio-Tek, United States). Total RNA was used to synthesize the cDNA with random primers and PrimeScript Reverse Transcriptase (Thermo Fisher Scientific, Wilmington, DE, United States). cDNA was used as template for PCR amplification, simultaneously, genomic DNA as a positive control and total RNA as a negative control for the PCR. The PCR were analyzed with the primers YoeBRTF/YoeBRTR for *yoeB* (control) and YefM-YoeBRTF/YefM-YoeBRTR for *yefM-yoeB*. Primers YefM-YoeBRTF/YefM-YoeBRTR were annealed to the 5′ end of *yefM* and 3′ end of *YoeB* coding region, respectively, and Gel electrophoresis was analyzed the PCR products amplified with genomic DNA, cDNA, and RNA. The primers used in this study were listed in **Table 1**.

TABLE 1 | Primers used in this study.

Primer	Sequence (5′–3′)
YoeBKOF1	GGATCCCGGTACGTCAGTTTTATCAAT(BamHI)
YoeBKOR1	CGGTGCTGGCCGTTTAGGGTAAAATTAATAG
YoeBKOF2	TAAACGGCCAGCACCGCCTCGTTTACAGT
YoeBKOR2	GGATCCGGGAGATGCCGAGCTTTCTG(BamHI)
YoeBKOF3	GTTCATGTCTTGTACGCGAAT
YoeBKOR3	CCACCGTAACCGTGTTACCT
YefM-YoeBKOF1	GGATCCAGAGGAGGTGATGCTGG(BamHI)
YefM-YoeBKOR1	CAGGCAACGTTGGTTACACGGTTC
YefM-YoeBKOF2	TAACCAACGTTGCCTGCCGCTTTC
YefM-YoeBKOR2	GGATCCCTGGGAATCCATGAGC(BamHI)
YefM-YoeBKOF3	TGTTACCTTCTCGGATGCC
YefM-YoeBKOR3	CAAGAGGGCCGGGATT
YefM-YoeBC-F	GATATCGAGGAGGTGATGCTGG(EcoR V)
YefM-YoeBC-R	GATATCTCATTTATCCCCGTAGTGAAAG(EcoR V)
YefM-YoeBP-F	GATATCGAGGAGGTGATGCTGG(EcoR v)
YefM-YoeBP-R	GATATCTCGCATCCTTAAGAGTGGT(EcoR V)
YefMPro-F	GAATTCATGCACACTGTTACCTTCTC(EcoRI)
YefMPro-F	CTCGAGATAGTCCACTGTGACAACTTCG(XhoI)
YefMF4	GGATCCATGCACACTGTTACCTTCTC(BamHI)
YefMR4	CATATGATAGTCCACTGTGACAACTTCG(NdeI)
YoeBF4	GGATCCTTGTCACAGTGGACTATTAATT(BamHI)
YoeBR4	CATATGTCATTTATCCCCGTAGTGAAAG(NdeI)
YoeBRTF	ATGTCACAGTGGACTATTAATTTTAC
YoeBRTR	TTATTTATCCCCGTAGTGAAAGC
YefM-YoeBRTF	GATACCATGAACCGTGTAACCAACA
YefM-YoeBRTR	TAGTGAAAGCGGCAGGCAAC

Endogenous Toxicity of YoeB Assay

The endogenous toxicity of the toxin YoeB was determined by growth in liquid and solid medium. To construct the overexpression plasmid pTYefM and pETYoeB, ORFs of *yefM* and *yoeB* were amplified with the primer pairs YefMF4/YefMR4 and YoeBF4/YoeBR4, respectively. The amplified fragments were inserted into the pBT3 (Zhang et al., 2008) and pET28a, resulting in pTYefM and pETYoeB, which express YefM and YoeB, respectively. pTYefM, pETYoeB, and pET were transformed into *E. coli* BL21 (DE3), which resulted in BL21/pETYoeB, BL21/pTYefM+pETYoeB, and BL21/pTYefM+pET. These strains were cultured in LB with or without 0.5 mM IPTG and bacterial growth curve was monitored for 12 h (Wen et al., 2018). Bacteria was cultured to the exponential phase, diluted serially and dripped onto the LB plate with or without 0.5 mM IPTG, then the plates were cultured at 28°C for 24 h. The experiment was performed three times.

Construction of yoeB and yefM-yoeB Mutation and yefM-yoeB Complementation

The primers used in this study were listed in **Table 1**. The construction of mutants was performed as reported as previously (Hu et al., 2014). To construct the *yoeB* knockout strain, TX01Δ*yoeB*, in-frame deletion of a 162 bp segment (residues 37–198) of *yoeB* was performed by overlap extension PCR as follows: the first overlap PCR was performed with the primer pair YoeBKOF1/R1, the second overlap PCR was performed with the primer pair YoeBKOF2/R2, and the fusion PCR was performed with the primer pair YoeBKOF1/R2. The PCR products amplified by primer pair YoeBKOF1/R2 were inserted into the suicide plasmid pDM4 at the BglII site, resulting in pDMYoeB. S17-1λpir was transformed with pDMYoeB and the transformants were conjugated with TX01 as described previously (Hu et al., 2014). The transconjugants were selected on LB agar plates supplemented with 10% sucrose. Colonies that grew up on LB plates with sucrose and was sensitive to chloramphenicol were analyzed by PCR with YoeBKOF3/YoeBKOR3. To confirm the in-frame deletion, the PCR products were subjected to DNA sequencing. To construct *yefM-yoeB* knockout strain, TX01Δ*yefM-yoeB*, deletion of a 403 bp segment (residues 67–469) of *yefM-yoeB* was performed by overlap PCR. The experiment was performed as described above. To constructed the complementary strain TX01Δ*yefM-yoeB*C, *yefM-yoeB* was amplified by PCR with primers YefM-YoeBC-F/R, was inserted into the plasmid pJR21 at the PmeI site, resulting in pJRYefM-YoeB. Then pJRYefM-YoeB was transformed into TX01Δ*yefM-yoeB* by conjugation. The complementary strain was named TX01Δ*yefM-yoeB*C.

Resistance to Environmental Stress and to Non-immune Fish Serum

For high temperature resistance, TX01, TX01Δ*yoeB*, TX01Δ*yefM-yoeB*, and TX01Δ*yefM-yoeB*C were cultured in LB medium to exponential phase, then bacteria were transferred to fresh LB medium and cultured at 28 and 40°C. Bacterial cell density was measured at different time points by determining absorbance at OD_{600} as previously described (Fang et al., 2019).

For oxidative stress assay, the TX01, TX01Δ*yoeB*, TX01Δ*yefM-yoeB,* and TX01Δ*yefM-yoeB*C in exponential phase were washed with PBS and resuspended in PBS. Approximately 10^5 bacterial cells were mixed with 250 μL 3.2 mM H_2O_2 or PBS (control). After incubating at 28°C for 60 min, the mixtures were serially diluted and plated in triplicate on LB agar plates. The plates were incubated at 28°C for 24 h, and the colonies that appeared on the plates were enumerated. The survival rate was calculated as follows: [(number of $H_2O_2^-$treated cells)/(number of control cells)] × 100% (Wang et al., 2019). The experiment was performed three times.

To determine the non-immune fish serum tolerance, bacteria in exponential phase was washed with PBS three times. Ten microliters of bacteria (including approximately 10^5 bacterial cells) were incubated with 50 μL non-immune fish serum or PBS (control) for 60 min. The mixtures were serially diluted and plated in triplicate on LB agar plates. The plates were incubated at 28°C for 24 h, and the colonies that appeared on the plates were enumerated. The survival rate was calculated as follows: [(number of serum-treated cells)/(number of control cells)] × 100% (Wang et al., 2019). The experiment was performed three times.

Biofilm Assay

TX01, TX01Δ*yoeB*, TX01Δ*yefM-yoeB*, and TX01Δ*yefM-yoeB*C were cultured in LB medium to exponential phase and diluted to 10^5 CFU/mL. Crystal violet staining of biofilm assay was performed as previously (Shi et al., 2019).

The observation of biofilms by confocal laser scanning microscopy (CLSM) was performed as described by Chan et al. (2018) and Shi et al. (2019). Briefly, TX01, TX01Δ*yoeB*, TX01Δ*yefM-yoeB*, and TX01Δ*yefM-yoeB*C were grown in LB medium on glass-bottom dishes for 24 h at 28°C. The dishes were rinsed to remove non-adherent bacteria and then stained with a LIVE/DEAD BacLight bacterial viability kit L-13152 (Invitrogen-Molecular Probes, Carlsbad, CA, United States) for observation of biofilms. The staining procedure involved incubation for 20 min at room temperature in the dark. The biofilms were observed using a Leica TCS-SP2-AOBS-UV confocal laser scanning microscope equipped with an argon ion laser. The experimental procedures were performed three times (Shi et al., 2019).

Drug Sensitivity Test

The antibiotic drug susceptibility test was carried out in accordance with the operating standards of the paper diffusion method (Kirby-Bauer, K-B) recommended by the Clinical Laboratory Standards Institute (CLSI). TX01, TX01Δ*yoeB,* and TX01Δ*yefM-yoeB* were cultivated to OD_{600} = 0.5 (log phase), prepared a bacterial suspension (10^8 CFU/mL) and plated it evenly on the MH solid plates. Thirty kinds of drug sensitive tablets (HANGWEI,Hangzhou, China) were attached to the plates, and three types of them were placed on each plate. After that, the plates were cultivated at 28°C for 24 h. Finally, the diameters of the inhibition zone on the plates were measured. The experiment was performed three times.

Persister Cell Formation Assay

In order to study whether *yefM-yoeB* has an effect on the persister formation, TX01, TX01Δ*yoeB,* and TX01Δ*yefM-yoeB* were cultured overnight and the culture solution was diluted with 1:100 in LB. Bacterial culture was incubated at 28°C on a shaker at 200 rpm until the absorbance at 600 nm reached 0.5 (logarithmic phase). Then, the bacteria were diluted serially with LB. The bacteria (including approximately 10^7 bacterial cells) were exposed to a lethal dose of 50 × MIC of chloramphenicol (Amraei et al., 2020). After incubation 1, 3, and 5 h, mixture was washed three times by PBS to remove the antibiotic. Then the bacteria were diluted 200-folds. The diluents were plated on LB plates and incubated at 28°C for 24 h. Colonies on the plates were counted. The experiment was performed three times.

Invasion of Host Cell Lines

The interaction of bacteria (TX01, TX01Δ*yoeB*, TX01Δ*yefM-yoeB*, and TX01Δ*yefM-yoeB*C) with Japanese flounder gill cells (FG cells) was performed as below. FG cells were cultured in 96-well cell culture plates to a monolayer and mixed with 100 μL strain (1×10^6 CFU/mL) at a multiplicity of infection (MOI) of 10:1. After incubation at 25°C for 1 and 2 h, the plates were washed three times with PBS. To determine the number of bacterial cells associated with the entire FG cell, the washed FG cells were lysed with 200 μL of 1% (vol/vol) Triton X-100 in PBS, and the number of bacteria was counted by dilution plating (Hu et al., 2014). The experiment was performed three times.

Bacterial replication in murine monocyte-macrophage cells (RAW264.7 cells, cultured at 37°C in 5% CO_2) was performed as previously (Wang et al., 2019). *E. piscicida* (1×10^6 CFU) was added into RAW264.7 cells cultured in Dulbecco's minimal Eagle's medium (DMEM) (Gibco, United States) containing 10% fetal bovine serum (FBS) (Gibco, United States) at a MOI of 10:1. After incubating at 28°C for 2 h, the plates were washed with PBS and extracellular *E. piscicida* was killed by adding gentamicin (100 μg/mL) for 2 h. Then, the cells were washed with PBS and cultured in fresh DMEM containing 10 μg/mL gentamicin for 0, 2, 4, and 6 h. For detecting the number of survival bacteria in RAW264.7 cells at different time point, cells were lysed and lysate were plated on LB agar plates as described above.

Fish and Experimental Challenges for Bacterial Dissemination *in vivo*

Healthy tilapia (average weight 13.5 g) were purchased from a commercial fish farm of Hainan. The fish were maintained at 25 ± 1°C in aerated water and fed daily with commercial dry pellets. Fish were acclimatized in the laboratory for 2 weeks before

experimental manipulation (Fang et al., 2019). To make sure that the fish were not infected by bacteria, randomly selected fish were tested for bacteria in the tissues, including blood, liver, kidney, and spleen. The fish were treated with tricaine methanesulfonate (MS-222) (Sigma, United States) to collect the tissue. For tissue dissemination analysis, TX01, TX01Δ*yoeB*, TX01Δ*yefM-yoeB*, and TX01Δ*yefM-yoeB*C were cultured in LB medium to an OD_{600} of 0.5. The cells were washed with PBS and resuspended in PBS to 10^7 CFU/mL. Five groups of fish (36 per group) were infected by intramuscularly (i.m.) with 50 μL TX01, TX01Δ*yoeB*, TX01Δ*yefM-yoeB*, TX01Δ*yefM-yoeB*C, and PBS, respectively. At 24 and 48 h post-infection (hpi), spleen from three fish were taken aseptically. The bacterial recovery from the spleen was determined as reported previously (Hu et al., 2014). The rest of the infected fish (30 per group) were used for mortality assay for 25 days. At each examined time points, the result of one experiment was from the average value of three fish. And three replicated experiments were performed.

Transcriptional Regulation of the Promoter of *yefM-yoeB*

The speculative promoter of *yefM-yoeB* (the 345 bp of upstream of the *yefM-yoeB* operon), P345, was cloned with the primer pair YefM-YoeBP-F/YefM-YoeBP-R and inserted into the SwaI site of pSC11, a promoter probe plasmid (Hu et al., 2009a), which resulted in pSCP345. pSCP345 was introduced into *E. coli* DH5α by transformation and cultured on LB agar plates adding 20 μg/mL X-Gal (5-bromo-4-chloro-3-indolyl-beta-d-galactopyranoside, Solarbio, Beijing, China) (Shi et al., 2019). To construct the overexpression plasmid pTYefM and pTYefM-YoeB, ORFs of *yefM* and *yefM-yoeB* were amplified with the primer pairs YefMF4/YefMR4 and YefMF4/YoeBR4, respectively. The amplified fragments were inserted into the pT3, resulting in pTYefM and pTYefM-YoeB, which express *yefM* and *yefM-yoeB*, respectively. *yefM*, *yefM-yoeB*, and pT (control) were transformed into DH5α/pSCP345, respectively, which resulted in DH5α/pSCP345/pTYefM, DH5α/pSCP345/pTYefM-YoeB, and DH5α/pSCP345/pT. The transformants were cultured on X-gal plates and used for β-galactosidase assay as reported previously (Hu et al., 2009b).

Expression and Purification of Recombinant YefM (rYefM)

To express the YefM protein, segments of *yefM* were amplified with the primer pair YefMPro-F/YefMPro-R and then the PCR segments were inserted into the protein expression plasmid pET32a, resulting in pET32aYefM. The expressions and purifications of rYefM protein and control protein rTrx were performed as previously (Shi et al., 2019). The Trx (thioredoxin), a tag protein of about 20 KDa in pET32a, can facilitate the soluble expression of exogenous protein.

Electrophoretic Mobility Shift Assay

An electrophoresis mobility shift assay (EMSA) was performed as below. The DNA fragment of the speculative promoter was amplified by PCR and labeled with carboxyfluorescein (Sangon, China). The labeled DNA was mixed with rYefM and incubated at 37°C for 30 min in 20 μL of binding buffer (1 M Tris–HCl, pH 8.0; 5 M NaCl; 0.1 M $MgCl_2$; 0.5 M EDTA; 1 M DTT; 80% glycerol) and the negative control was a mixture of rTrx and nucleic acid probe. The samples were then separated by electrophoresis in non-denaturing 8% polyacrylamide gels (Shi et al., 2019).

Statistical Analysis

Statistical analyses were performed with SPSS 25.0 software (SPSS Inc., Chicago, IL, United States). Data were analyzed with analysis of variance (ANOVA). Data are expressed as the mean ± standard error of the mean (SEM). Error bars indicate the Standard Error of Mean (SEM) ($n = 3$, biologically independent samples). Statistical significance was defined as $P < 0.05$ (Gu et al., 2021).

RESULTS

E. piscicida TX01 Harbor YefM-YoeB TA System in Its Genome

When scaning the whole genome of *E. piscicida* TX01 using TADB 2.0 (Xie et al., 2018), we found Toxin and antitoxin genes. The antitoxin (ETAE_RS07650), a 246 bp ORF, shows homology to the Phd/YefM family. The toxin (ETAE_RS17330), a 276 bp ORF, shows homology to Txe/YoeB family proteins. We named the TA system as YefM-YoeB. Protein BLAST search revealed that only two *Edwardsiella* species, including *E. piscicida*, *E. tarda*, but not *E. ictaluri*, *E. hoshinae,* and *E. anguillarum*, harbor YefM-YoeB TA module and share relatively high homology and similar genetic organization (**Figure 1A**). Sequence alignment showed that the YefM of *E. piscicida* shares 77.78, 55.26, and 38.75% sequence identities with YefM from *E. coil*, *S. aureus*, and *S. pneumoniae*, respectively (**Figure 1B**), while YoeB of *E. piscicida* shares 64.04, 44.44, and 45.28% sequence identities with YefM from *E. coil*, *S. aureus*, and *S. pneumoniae*, respectively (**Figure 1C**).

Classically, two genes of type II TA systems are expressed under one operon, where the antitoxin is located upstream to the toxin (Zander et al., 2020). Consistently, in *E. piscicida*, *yefM* and *yoeB* are adjacent and contain 20 bp overlap sequences. To verify the two genes are co-transcribed, specific primer pair YefM-YoeBRTF/YefM-YoeBRTR that stretch across *yefM* and *yoeB* were designed, and reverse transcription-polymerase chain reaction (RT-PCR) was conducted using total RNA, complementary DNA (cDNA), and genomic DNA (gDNA) of *E. piscicida* as templates. The results showed that the predicted PCR products of 447 bp were observed in cDNA and gDNA templates, but not in RNA template (**Figure 1D**), which indicates that *yefM* and *yoeB* are expressed in a bicistronic operon.

When TA system is working, the toxin protein exhibits its inhibitory effect on the growth of the bacteria, while the antitoxin protein eliminates the toxic effect (Chan et al., 2012). To check the interaction between YefM and YoeB, pTYefM, which expresses antitoxin YefM constitutively, and pETYoeB, which expresses YoeB inductively by IPTG, were constructed and transformed into BL21, respectively, or simultaneously.

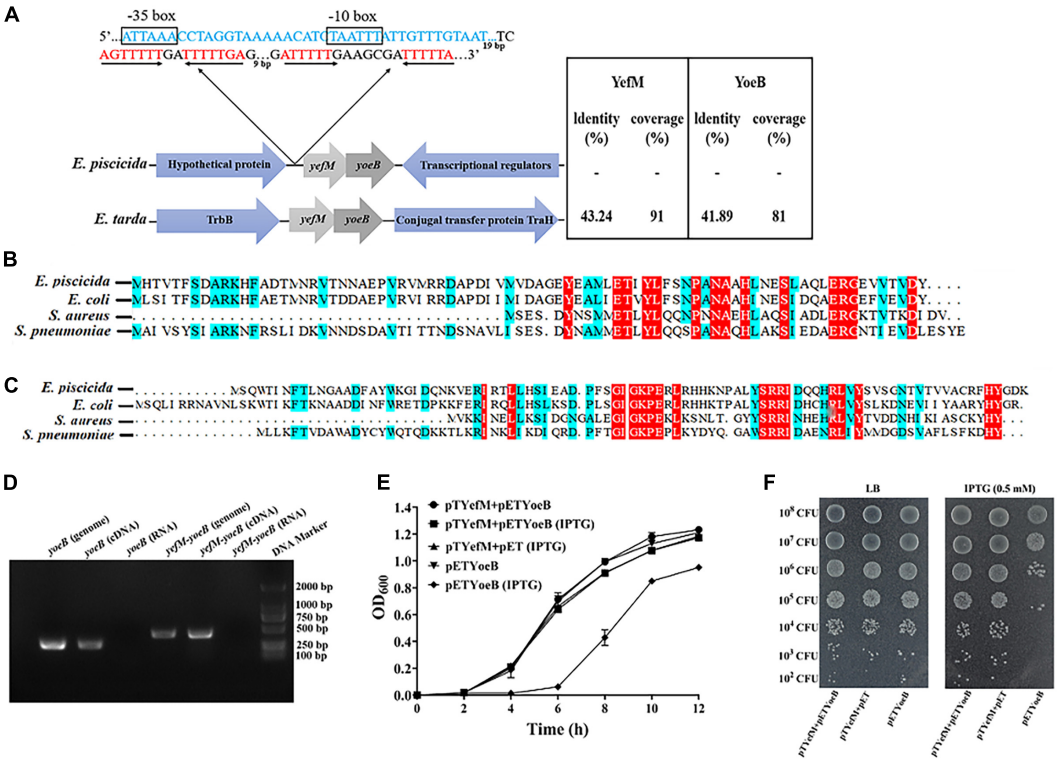

FIGURE 1 | Identification of type II TA system YefM/YeoB in *Edwardsiella piscicida*. **(A)** Genetic organization of YefM/YeoB operon in *Edwardsiella*. The amino acid sequences of *E. piscicida* YefM and YeoB were searched against *Edwardsiella* (taxid:635) database and two bacterial strains of *Edwardsiella* found in the protein BLAST search. Arrows represent genes and genetic context, sizes and spaces are only for representation and are not at actual scale. In the 5′-UTR of *yefM-yoeB*, a promoter region (blue sequence) we predicted and –10 and –35 region were boxed. Two mirror repeat sequences (red sequence) were found in downstream of predicted promoter region. **(B,C)** Sequence alignment of YefM and YoeB from *E. piscicida Escherichia coil*, *Staphylococcus aureus*, and *Streptococcus pneumoniae*, respectively. **(D)** Identification of *yefM* and *yeoB* co-transcription. Total RNA was isolated from *E. piscicida* at a turbidity of 0.8 at 600 nm and treated with DNase I. cDNA was synthesized and used as the template in PCR. PCR products were amplified with specific primer pair YoeBRTF/YoeBRTR for *yoeB* and with primer YefM-YeoBRTF and specific reverse primer YefM-YeoBRTR for *yefM-yoeB*. Genomic DNA was used as a positive control, and total RNA was used as a negative control. **(E)** Inhibition of cell growth by YeoB. Stains BL21/pETYeoB, BL21/pTYefM+Pet, and BL21/pTYefM+pETYeoB were cultured in LB medium with or without IPTG (0.5 mM). **(F)** BL21/pETYeoB, BL21/pTYefM+pET, and BL21/pTYefM+pETYeoB were cultured to the exponential phase, diluted serially and dripped onto the LB plate with or without 0.5 mM IPTG. Data are presented as means ± SEM (*N* = 3). N, the number of times the experiment was performed.

The growth curve assay was performed and the result showed that the growth of BL21/pETYoeB was similar to that of BL21/pTYefM+pETYoeB. However, when IPTG was added in the medium, the growth of BL21/pETYoeB was delayed markedly, but the growth of BL21/pTYefM+pETYoeB did not affected by IPTG (**Figures 1E,F**). This result indicates that YoeB has a toxic effect on BL21 cells, and the effect was neutralized by YefM. These findings show that YefM-YoeB is a characteristic type II TA system.

Construction of yoeB and *yefM-yoeB* Mutants

To examine their functional importance, the *yoeB* and *yefM-yoeB* were knocked out by markerless in-frame deletion of the operon from 37 to 198 bp and 67 to 469 bp, respectively. The resulting mutants were named TX01Δ*yoeB* and TX01Δ*yefM-yoeB*, respectively. However, we did not obtain the *yefM* mutant, which indicates the absence of YefM-type antitoxins seems to be lethal in different bacteria or at least to affect their growth (Yoshizumi et al., 2009). Next, we examined the effects of TX01Δ*yoeB* and TX01Δ*yefM-yoeB* on the information of persister cells, adversity adaptation, and pathogenicity of *E. piscicida*.

Effects of yoeB and yefM-yoeB Mutants on the Persister Cells Populations

Studies have proved that the majority of type II TA systems are related to the formation of persistence bacteria (Amraei et al., 2020), so we want to investigate the participation of YefM-YoeB in persister cells of *E. piscicida*. By means of the drug susceptibility test, we found that TX01, TX01Δ*yoeB*, TX01Δ*yefM-yoeB* were sensitive to chloramphenicol, ofloxacin, and furazolidone, among which chloramphenicol was the most sensitive antibiotic. Amongst the three strains, TX01Δ*yefM-yoeB* was more sensitive to the all three antibiotics than TX01Δ*yoeB*, which was comparative to TX01 (**Figures 2A,B**). Based on this result, we speculated that YefM-YoeB play a role in the resistance of bacteria against the three antibiotics. Chloramphenicol was

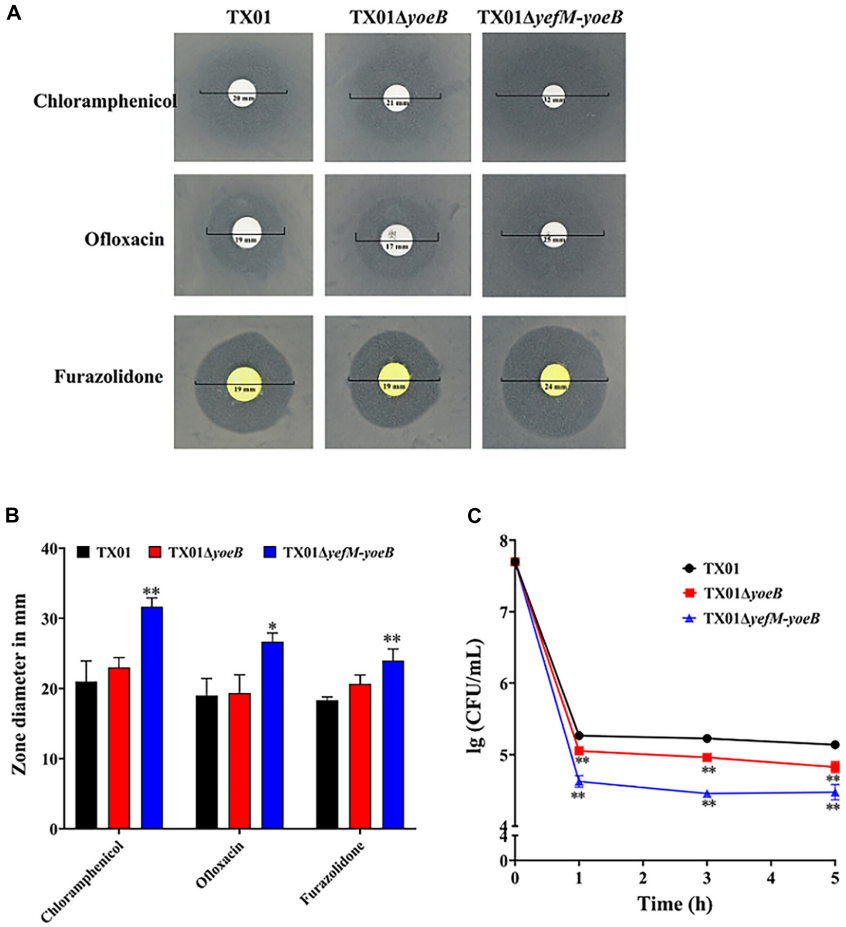

FIGURE 2 | Resistance of *Edwardsiella piscicida* to antibiotics and their ability to form persistent bacteria. **(A)** Drug sensitivity test of *E. piscicida*. Thirty drug sensitive papers were selected to determine the drug resistance of TX01, TX01Δ*yoeB*, TX01Δ*yefM-yoeB* by Kirby-Bauer. The three bacteria were sensitive to chloramphenicol, ofloxacin, and furazolidone, among which chloramphenicol was the most sensitive antibiotics. **(B)** The inhibition zone of chloramphenicol, ofloxacin, and furazolidone on TX01, TX01Δ*yoeB*, and TX01Δ*yefM-yoeB*. **(C)** Time-kill curves of different strains exposed to chloramphenicol. TX01, TX01Δ*yoeB*, TX01Δ*yefM-yoeB* were exposed to lethal concentration (240 μg/mL) of chloramphenicol for 1, 3, and 5 h, then viable bacteria were determined by culturing on the LB agar plates. Data are presented as the means ± SEMs ($N = 3$). N, the number of times the experiment was performed. $^{*}P < 0.05$; $^{**}P < 0.01$.

chosen for the test of bacterial persistence formation. Then the minimum inhibitory concentration (MIC) assay was conducted and the result showed that the MIC of chloramphenicol on TX01, TX01Δ*yoeB*, TX01Δ*yefM-yoeB* were all 4.8 μg/mL. Then the lethal concentration 240 μg/mL (50 × MIC) of chloramphenicol was used to treat these strains. Viable bacteria were determined and the result showed the number of persistence bacteria of TX01Δ*yoeB* and TX01Δ*yefM-yoeB* were significantly reduced by about twofolds and fivefolds compared to TX01, respectively (**Figure 2C**), indicating *yoeB* and *yefM-yoeB* play an important role in the formation of persister cell of *E. piscicida*.

Effects of *yoeB* and *yefM-yoeB* Mutants on Bacterial Resistance Against Environmental Stress

One of the functions of TA systems is to help bacteria adapt to adversity. High temperature is a kind of environmental pressure that bacteria often undergo. So we firstly examined the effect of YefM-YoeB on bacterial resistance against temperature stress. For this purpose, growth analysis was performed and the result showed that TX01, TX01Δ*yoeB*, and TX01Δ*yefM-yoeB* exhibited a comparative growth rate when bacteria were cultured in LB medium under normal condition (**Figure 3A**), which indicates deletion of *yoeB* and *yefM-yoeB* did not affect bacterial growth and propagation in normal condition. However, when cultured in LB medium at high temperature (40°C), TX01Δ*yefM-yoeB* displayed higher maximum cell density than TX01, while TX01Δ*yoeB* exhibited growth patterns similar to that of TX01 (**Figure 3B**). These results suggest that the deletion of *yoeB* did not affect bacterial tolerance to high temperature, but the deficiency of the whole TA system *yefM-yoeB* enhanced bacterial tolerance to high temperature stress.

Oxidative stress and acid stress are unavoidable challenge for pathogenic bacteria invading and living in the host. To check the role of this TA system in oxidative stress, TX01, TX01Δ*yoeB*,

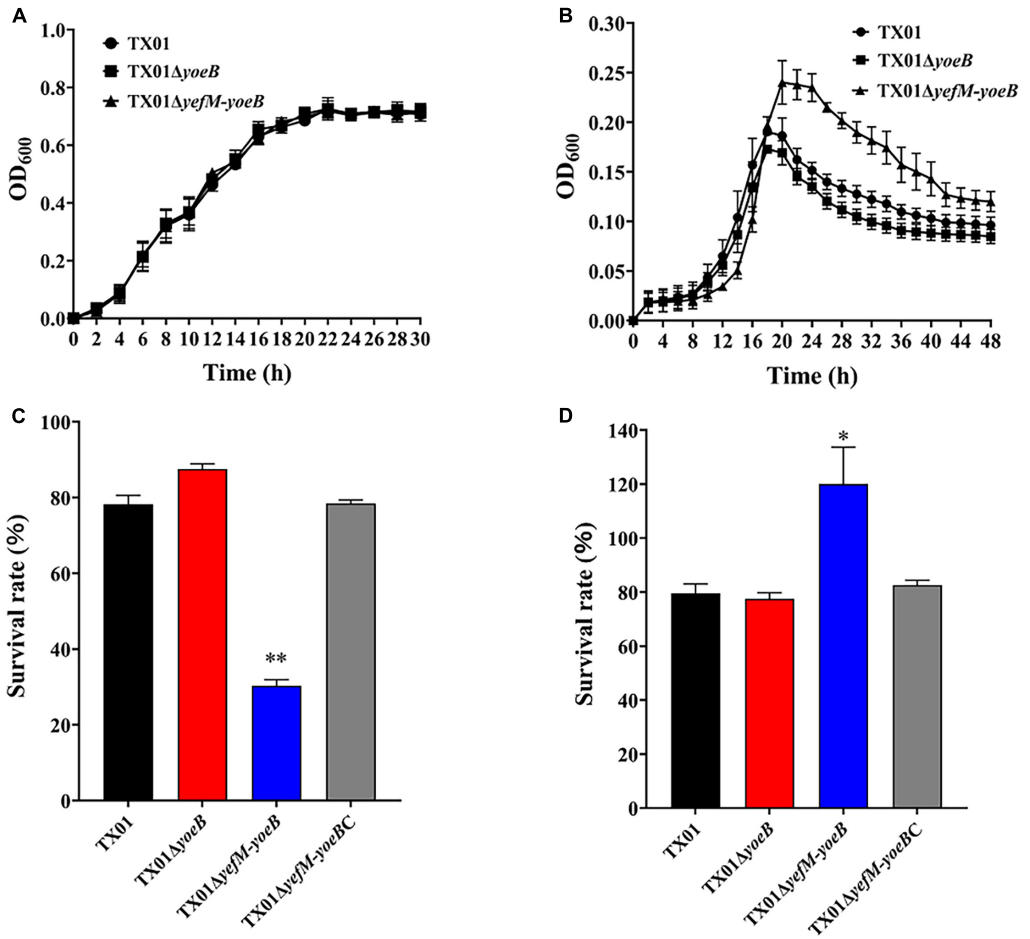

FIGURE 3 | Sensitivity of *Edwardsiella piscicida* to stress. **(A)** The growth curve of TX01, TX01Δ*yeoB*, and TX01Δ*yefMyeoB* in LB medium under normal condition. **(B)** The growth curve of TX01, TX01Δ*yeoB*, and TX01Δ*yefMyeoB* in LB medium under high temperature (40°C). **(C)** The survival rate of TX01, TX01Δ*yeoB*, TX01Δ*yefMyeoB*, and TX01Δ*yefMyeoB*C under oxidation stress. Strains were cultured to logarithmic phase in normal LB medium, then bacteria were incubated with H_2O_2 (3.2 mM) or PBS for 1 h. The number of the viable bacteria was determined by plate counting. **(D)** The survival rate of TX01, TX01Δ*yeoB*, TX01Δ*yefMyeoB*, and TX01Δ*yefMyeoB*C against non-immune fish serum. Strains in the early logarithmic phase were incubated with non-immune tilapia serum or PBS (control) for 1 h. The number of the viable bacteria was determined by plate counting. Data are the means of three independent experiments and presented as means of three independent experiments and presented as means ± SEM ($N = 3$). N, the number of times the experiments was performed. *$P < 0.05$; **$P < 0.01$.

and TX01Δ*yefM-yoeB* at logarithmic phase were transferred to new LB medium with or without oxidative stress (H_2O_2) and cultured for another 1 h, then the number of the viable bacteria was determined by plate counting. The result showed that under the condition of oxidative pressure, the survival amount of TX01Δ*yoeB* was comparative to that of TX01, but the survival amount of TX01Δ*yefM-yoeB* was significantly lower than that of TX01 (**Figure 3C**). The result indicates that the deletion of the whole TA system *yefM-yoeB* impairs the ability of *E. piscicida* to resist oxidative stress, but only the deficiency of *yoeB* had no effect on bacterial resistance against oxidative stress. To examine the role of the TA system in acid pressure, strains at logarithmic phase was transferred to new normal LB medium (pH = 7.0) or acidic LB medium (pH = 4) and cultured for another 1 h, then the number of the viable bacteria was determined. The result showed that survival rate of three strains (TX01, TX01*yoeB*, and TX01Δ*yefM-yoeB*) did not displayed significantly difference (data not shown), which indicates YefM-YoeB TA system is not related to acid tolerance.

Effects of *yoeB* and *yefM-yoeB* Mutants on Bacterial Resistance Against Non-immune Fish Serum

Host serum bactericidal activity is a vital immune weapon for eliminating pathogens. Resistance against host serum killing is an important characteristic of *E. piscicida* (Li et al., 2015). To examine whether *yoeB* and *yefM-yoeB* mutation affect the ability of *E. piscicida* to tolerate host serum stress, TX01, TX01Δ*yoeB*, and TX01Δ*yefM-yoeB* were mixed with tilapia serum, and viable bacteria was detected by plat counting. As shown in **Figure 3D**, TX01 and TX01Δ*yoeB* exhibited similar capability of serum resistance, as 79 and 77% of bacteria survived after treatment with tilapia serum, respectively. In contrast, compared to TX01

and TX01Δ*yoeB*, TX01Δ*yefM-yoeB* demonstrated significantly stronger resistance ability to host serum, as 120% of cells survived. The result showed TA system YefM-YoeB of *E. piscicida* participated in the host serum resistance, indicating the probable involvement of YefM-YoeB in pathogenicity of *E. piscicida*. As far as we known, this is the first study about the relationship between type II TA system and serum resistance.

Effects of *yoeB* and *yefM-yoeB* Mutants on Bacterial Biofilm Formation

Bacterial biofilm formation is also closely related with pathogenicity. Since type II TA systems contribute extensively to bacterial biofilm (Fraikin et al., 2019), we investigated the relationship between YefM-YoeB and biofilm growth of *E. piscicida*. For this purpose, TX01, TX01Δ*yoeB*, and TX01Δ*yefM-yoeB* were cultured in polystyrene plate. The biofilm formed around the plate was fixed with Bouin and dyed with crystal violet. The subsequent result indicated that the biofilm formation of TX01Δ*yefM-yoeB* was remarkably higher than those of TX01 and TX01Δ*yoeB*, the latter two exhibited similar biofilm forming ability (**Figure 4A**). To confirm the result, we acquired images of the biofilms using CLSM. The result displayed that compared to wild type TX01, TX01Δ*yefM-yoeB* exhibited a substantial increase in the thickness and density of the biofilm, and TX01Δ*yoeB* presented a similar level to TX01 (**Figure 4B**). These results suggest that the deletion of TA system YefM-YoeB increases the ability of *E. piscicida* to form biofilm, indicating the probable involvement of YefM-YoeB in pathogenicity of *E. piscicida*.

Effects of *yoeB* and *yefM-yoeB* Mutants on Cell Invasion and Intracellular Survival

Since the deletion of *yefM-yoeB* has significant impact on serum resistance and biofilm information, we infer that TA system YefM-YoeB is involved in the virulence of *E. piscicida*. To examine the role of YefM-YoeB in the infectivity of *E. piscicida*, cultured FG cells were infected with the same number of TX01, TX01Δ*yoeB*, and TX01Δ*yefM-yoeB* for 1 and 2 h. After washing with PBS, the bacterial that were adhered with and invaded into the host cells were detected. As shown in **Figure 5A**, the amount of TX01Δ*yefM-yoeB* obtained from FG cells was markedly higher than that of wild strain at 1 h and 2 hpi, however, as we expected, the amount of TX01Δ*yoeB* was comparative to that of TX01 (**Figure 5A**). The result shows that the deficiency of *yefM-yoeB*, but not *YoeB*, significantly enhanced the invasion of *E. piscicida* to host cells, which is consistent with results of serum resistance and biofilm information.

Survival and replication in host macrophages is a typical characteristic of *E. piscicida* (Sui et al., 2017). We want to examined the participation of YefM-YoeB in intracellular survival of phagocyte. For this purpose, RAW264.7 cells were infected with the same number of three *E. piscicida* strains. After killing the extracellular bacteria, the cells were cultured further in normal medium for different time, then the amount of intracellular bacteria was detected. Unexpectedly, the results displayed that the bacterial number of TX01Δ*yefM-yoeB* from the intracellular RAW264.7 cells was comparative to those of TX01 and TX01Δ*yoeB* (**Figure 5B**), which indicates that type

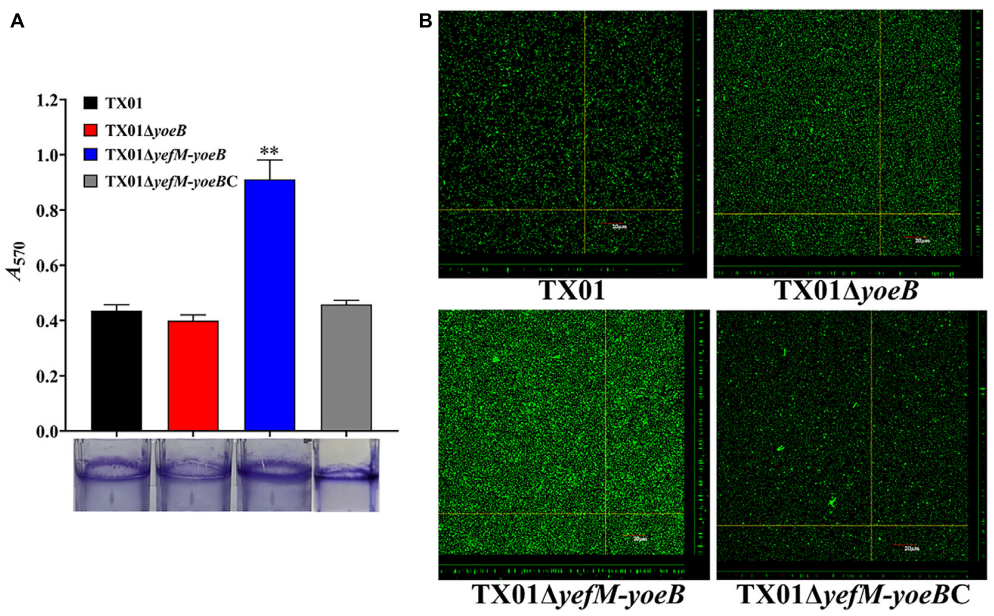

FIGURE 4 | Effects of *yeoB* and *yefMyeoB* mutation on bacteria biofilm growth. **(A)** Biofilm-forming capacity of *E. piscicida*. TX01, TX01Δ*yeoB*, TX01Δ*yefMyeoB*, and TX01Δ*yefMyeoB*C were incubated in polystyrene plates, and biofilm formation was determined by measuring the A_{570} of the final eluates of crystal violet staining. Data are presented as the means ± SEMs ($N = 3$). N, the number of times the experiment was performed. $^{**}P < 0.01$. **(B)** The viability of biofilm growth of *E. piscicida* as determined by confocal laser scanning microscopy (CLSM). Cells in the biofilms were stained with a BacLight LIVE/DEAD kit to reveal viable (green fluorescence) and non-viable (red fluorescence) bacteria.

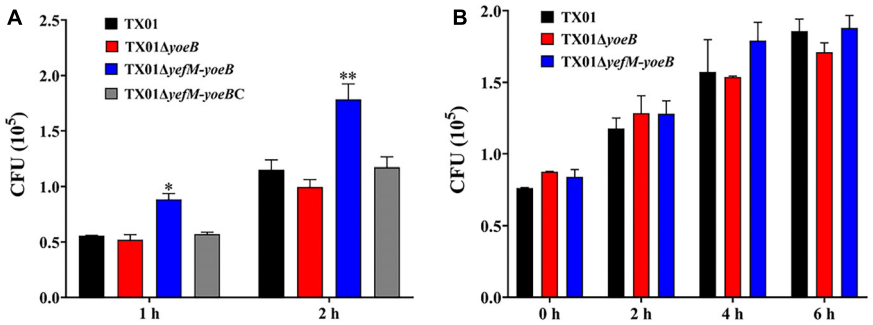

FIGURE 5 | Effects of *yeoB* and *yefMyeoB* mutation on cellular infection and replication. **(A)** The association and invasion of *E. piscicida* to flounder gill cells (FG cells). FG cells were infected with the same dose of TX01, TX01Δ*yeoB*, TX01Δ*yefMyeoB*, and TX01Δ*yefMyeoB*C for various time and washed with PBS. Then the FG cells were lysed, the bacteria associated with and invaded into the host cells were determined by plate counting. **(B)** Survival and replication of *E. piscicida* in mouse macrophage cell RAW264.7. RAW264.7 cells were hatched with TX01, TX01Δ*yeoB*, TX01Δ*yefMyeoB* for 2 h, then the mouse macrophages were treated with gentamicin for 2 h. After the cells were incubated with bacterial for various hours, the number of intracellular bacteria was determined by plate counting. Data are presented as the means ± SEMs ($N = 3$). N, the number of times the experiment was performed. $^{*}P < 0.05$; $^{**}P < 0.01$.

II TA system YefM-YoeB is not involved in the intracellular survival of macrophage.

Effects of *yoeB* and *yefM-yoeB* Mutants on Bacterial Dissemination in Tissues and General Virulence

To further clarify the participation of the TA system in the virulence of *E. piscicida*, *in vivo* experiment of tissue infectivity was performed. The same dose of TX01, TX01Δ*yoeB*, and TX01Δ*yefM-yoeB* were used to infect Tilapia and viable bacteria from spleen were determined after infection 24 and 48 h. As shown in **Figure 6A**, bacteria amount from TX01Δ*yefM-yoeB*-infected fish was significantly higher than that of TX01-infected fish, but TX01Δ*yoeB*-infected fish was comparative to that of TX01-infected fish, which is consistent with the result of invading FG cells.

To detect the effect of *yefM-yoeB* mutation on bacterial virulence, fish were infected with TX01, TX01Δ*yoeB*, and TX01Δ*yefM-yoeB* and the mortality of fish was monitored. The results displayed that at the end of the monitored period (25 days), the survival rate of TX01- and TX01Δ*yoeB*-infected fish was 29 and 20%, respectively, which was significantly higher than that of TX01Δ*yefM-yoeB*-infected fish (0%) (**Figure 6B**). These findings indicate the deletion of the whole TA system enhances the pathogenicity of *E. piscicida*.

Genetic Complementation of the *yefM-yoeB* Deletion and Its Effect on Stress Resistance and Virulence

To further clarify the function of *yefM-yoeB*, the complementary strain of *yefM-yoeB* mutant TX01Δ*yefM-yoeB*, TX01Δ*yefM-yoeB*C, was constructed. In contrast to TX01Δ*yefM-yoeB*, TX01Δ*yefM-yoeB*C exhibited a comparative resistance against oxidative stress and host serum killing and a comparative capacity of biofilm growth to those of TX01 (**Figures 3**, **4**). Likewise, the bacterial infective and dissemination capacities of TX01Δ*yefM-yoeB*C in host cells and tissues were comparable to those of TX01 (**Figures 5**, **6**).

The Expression of *yefM-yoeB* Was Regulated by YefM and YoeB

In most type II TA systems, the antitoxin and toxin proteins participate in transcriptional autoregulation under stress conditions (Kedzierska et al., 2007; Overgaard et al., 2008). In the 5′-UTR of *yefM-yoeB*, a promoter region was predicted and two mirror repeat sequences were found (**Figure 1A**). To survey the regulatory effect of YefM-YoeB on its own expression, the speculative promoter of *yefM-yoeB*, P345, was inserted into pSC11, the recombinant strain was named DH5α/pSCP345. When DH5α/pSCP345 was grew on LB agar plates including X-gal, the bacterial colonies were blue, which indicates that P345 possesses promoter activity. Then pTYefM (expressing YefM), pTYefM-YoeB (expressing YefM-YoeB) and control plasmid pT were transformed into DH5α/pSCP345, respectively. On the same X-gal plate, the blue of DH5α/pSCP345/pTYefM was slightly weaker than that of DH5α/pSCP345/pT, and DH5α/pSCP345/pTYefM-YoeB was obviously weaker than that of DH5α/pSCP345/pTYefM (**Figure 7A**). β-galactosidase assay displayed that the Miller units produced by DH5α/pSCP345/pTYefM were moderately lower than that produced by DH5α/pSCP345/pT, and the Miller units produced by DH5α/pSCP345/pTYefM-YoeB was significantly lower than that produced by DH5α/pSCP345/pT (**Figure 7B**). These results suggested that YefM-YoeB negatively regulated the expression of *yefM-yoeB* transcription. Next, we wanted to explore the interaction between YefM-YoeB and the promoter of *yefM-yoeB*. We did not obtain the complex of rYefM and rYoeB, but rYefM was successfully expressed and purified from *E. coli* (**Figure 7C**). EMSA was performed and the result showed that purified rYefM could bind the P345 (**Figure 7D**), which suggests that YefM-YoeB could regulate directly the expression of operon *yefM-yoeB*.

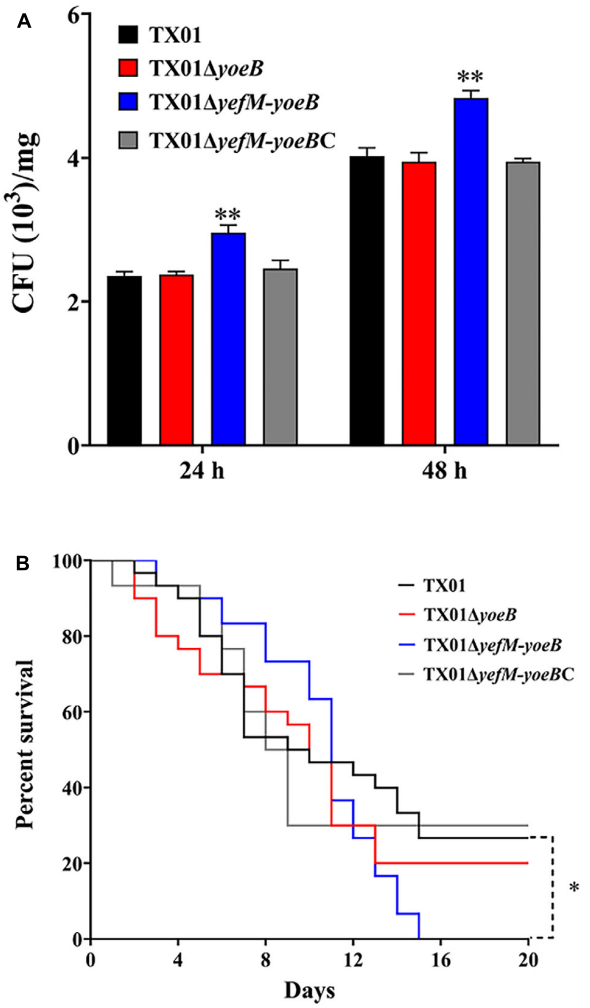

FIGURE 6 | Effects of *yeoB* and *yefMyeoB* mutation on bacterial dissemination of fish tissues and general virulence. **(A)** Bacterial dissemination in the fish tissues. Tilapia were infected with the same dose of TX01, TX01Δ*yeoB*, TX01Δ*yefMyeoB*, and TX01Δ*yefMyeoB*C, and bacterial recovery from the spleen was determined by plate counting at 48 and 72 h post-infection. **(B)** Host mortality induced by *E. piscicida*. Tilapia were infected with equivalent doses of TX01, TX01Δ*yeoB*, TX01Δ*yefMyeoB*, and TX01Δ*yefMyeoB*C, and accumulated mortality were monitored for a period of 25 days (only 20 days are shown since no more deaths occurred after 20 days). Significance between the survivals of wild type and mutant infected fish was determined with logrank test. Data are presented as the means ± SEMs ($N = 3$). N, the number of times the experiment was performed. *$P < 0.05$; **$P < 0.01$.

DISCUSSION

In the course of evolution, pathogens usually assimilate and integrated exogenous genetic materials into its genome to develop quick adaptive advantages in intricate habitat. As a product of evolution, type II TA system are often found in chromosomes and some mobile components such as plasmids and prophages (Harms et al., 2018). Recently, type II TA system has attracted increasing attention since its important roles in physiology, stress, and pathogenicity (Wang and Wood, 2011; Bukowski et al., 2013; Harms et al., 2018; Równicki et al., 2020). As a leading pathogen threatening worldwide aquaculture industries, *E. piscicida* has received more and more attention and has been considered as a model organism for studying intracellular and systemic infections (Leung et al., 2019). However, for all we know, TA systems are totally unknown in *E. piscicida* so fa. By means of TADB 2.0 (Xie et al., 2018), we performed a scan for whole genome of *E. piscicida* TX01 and found the YefM and YoeB. Bioinformatics analysis showed that YefM and YoeB share high homology with type II toxin-antitoxin system Phd/YefM family antitoxin and toxin YoeB, respectively. *yefM* and *yoeB* are transcriptionally organized in a bicistronic operon, and *yefM* locates upstream of the *yoeB*, which is one of typical characteristic of most of type II TA system (Yamaguchi et al., 2011). We name the bicistronic operon as type II TA system YefM-YoeB. It has been reported that the function of the toxin molecule is often associated with the inhibition of DNA replication or protein translation, resulting in cell growth arrest, which was neutralized by its cognate antitoxin protein (Page and Peti, 2016; Chan et al., 2018; Równicki et al., 2020). Consistently with other type II TA system, we found when YoeB of *E. piscicida* expressed in *E. coli*, the growth of strain delayed obviously, and the toxic effect of YoeB was relieved by YefM. These results indicate that YefM-YoeB is a functional type II TA system of *E. piscicida*.

The emergence of antibiotic-resistant bacteria is a tricky and confronted issue in modern medicine, and one of important reasons is the widespread of toxin-antitoxin (TA) systems in pathogenic bacteria (Równicki et al., 2020). The TA system usually induces cells to enter a dormant state so that the cells can escape the effects of antibiotics (Wang et al., 2011). As reported in *E. coli*, the number of persistent cells of *E. coli* lacking *mqsRA* is significantly reduced under high concentration of antibiotics (Kim and Wood, 2010). Compared with the wild type, the cell survival rate of *E. coli* lacking *yafQ* under the bactericidal concentration of antibiotics decreased by 2,400-folds (Harrison et al., 2009). Studies have shown that in *E. coli*, the MazEF plays an important role in the formation of persistent bacteria and the MazF-mediated persistence phenotype was found to dependent on the presence of the ClpP and Lon proteases (Tripathi et al., 2014). In this study, we found the persister forming ability of TX01Δ*yoeB* and TX01Δ*yefM-yoeB* was significantly reduced compared to that of TX01, which indicates the involvement of YefM-YoeB in bacterial persister formation, but its mechanism needs further study.

Response to environmental stress is one of prominent functions of TA systems. Under pressure, the labile antitoxins are proteolytically degraded, which releases toxins. Exposed toxins inhibit bacterial growth and help bacteria survival in adversity (Christensen-Dalsgaard et al., 2010; Bukowski et al., 2013). For survival in host, pathogen must overcome the oxidative stress (Forman and Torres, 2002). It is reported that multiple type II TA system genes in *Klebsiella pneumoniae* were involved in response to oxidative stress (Narimisa et al., 2020). In *E. coli*, upon oxidative stress, antitoxin MqsA is degraded and toxin MqsR was liberated, which enriched ghoT mRNAs as well as

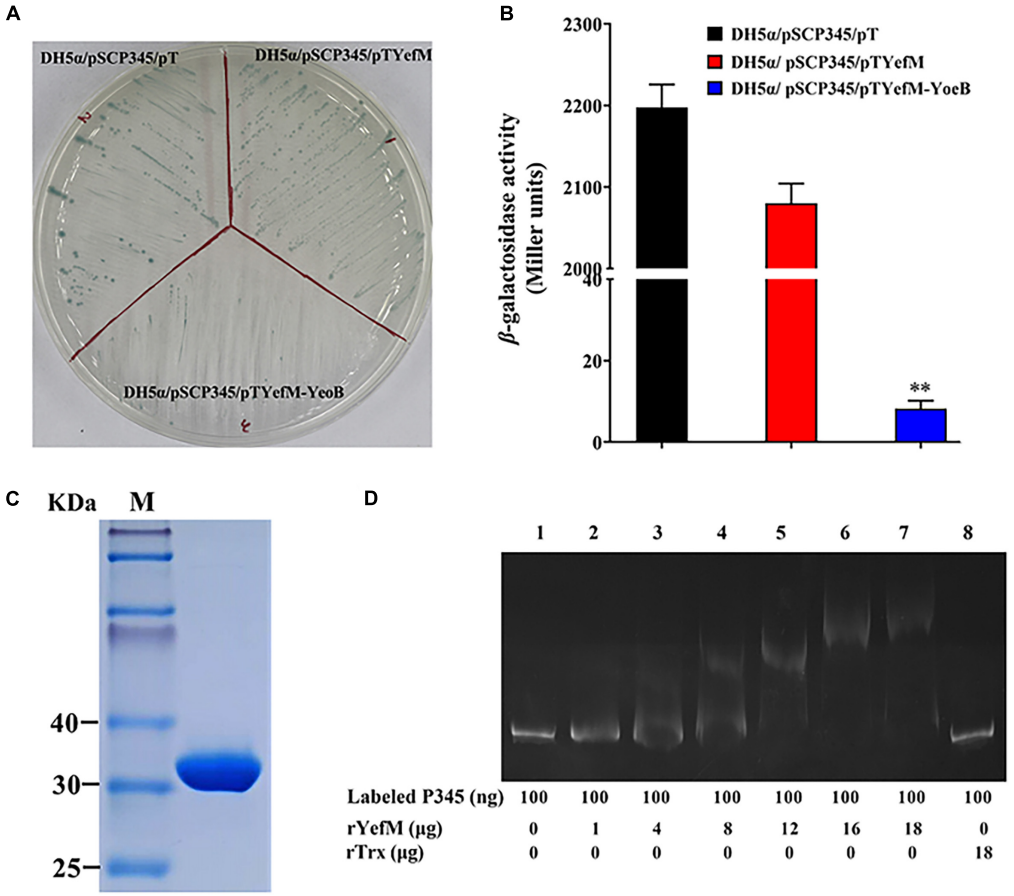

FIGURE 7 | Expression of *yefMyeoB* was regulated by YefM and YefM/YeoB. **(A)** DH5α/pSCP345/pT, DH5α/pSCP345/pTYefM, and DH5α/pSCP345/pTYefM-YeoB were streaked and cultured on LB plates with X-gal, kanamycin, and ampicillin. **(B)** The β-galactosidase activities of DH5α/pSCP345/pT, DH5α/pSCP345/pTYefM, and DH5α/pSCP345/pTYefM-YeoB was determined and shown by Miller units. Data are presented as the means ± SEMs ($N = 3$). N, the number of times the experiment was performed. $^{**}P < 0.01$. **(C)** Purified rYefM was analyzed by SDS-PAGE. **(D)** Interaction between YefM and the speculative promoter regions of *yefMyeoB*. An electrophoresis mobility shift assay (EMSA) was performed in binding buffer containing rYefM, rTrx (control), carboxyfuorescein-labeled P345, and the speculative promoter regions (P345) of *yefMyeoB*. The negative control DNA.

other stress-related transcripts and leaded to the formation of persister cells (Wang et al., 2013). However, the deletion of whole TA system MqsRA have no effect on oxidative stress resistance (Fraikin et al., 2019). On the contrary, the deletion of whole TA system YefM-YoeB in *S. pneumoniae* leads to reduced resistance to oxidative stress (Chan et al., 2018). Consistently with the result in *S. pneumoniae*, we found the deficiency of the whole TA system *yefM-yoeB* impaired the ability of *E. piscicida* to resist oxidative stress, but only the inactivation of *yoeB* had no effect on resistance against oxidative stress, which indicates YefM perhaps plays an important role in oxidative pressure reaction, since deletion of *yoeB* releases YefM. In contrast to the result of oxidative stress, the deletion of whole TA system YefM-YoeB leads to enhance resistance of *E. piscicida* to high temperature stress and host serum stress. These observations in *E. coli* suggest that YefM-YoeB functions in adaptation to temperature stress (Janssen et al., 2015). As far as we known, there is no report of YefM-YoeB about serum resistance. All in all, these results suggest YefM-YoeB are extensively involved in response to stress and its functions in different pathogens are not in complete accord.

Accumulating reports have confirmed that TAs are involved in multiple important biological processes, such as biofilm formation (Eroshenko et al., 2020). For example, in the MazEF type II TA pair, overexpression of *mazF* toxin drives to the inhibition of biofilm formation (Ma et al., 2019). In HigBA pair, *higA* mutant and *higB* overexpression strain reduced the biofilm formation, which indicates HigB represses biofilm formation of *P. aeruginosa* (Wood and Wood, 2016). In the MqsR-MqsA pair, MqsA decreases the production of CsgD, the master regulator for biofilm formation (Soo and Wood, 2013). The deficiency of *yefM-yoeB* operon in *S. pneumoniae* bring about a considerable decrease in the thickness of the biofilm (Chan et al., 2018). However, in this study, deletion of *YoeB* did not affect the biofilm growth, but deletion of *yefM-yoeB* operon exhibited an increase of biofilm formation, which indicated the participation of YefM-YoeB TA system in the biofilm of *E. piscicida*. However, the role of YefM-YoeB in biofilm formation in *E. piscicida* are

contrary to the role in *S. pneumoniae* (Chan et al., 2018), which suggests the function and mechanism of YefM-YoeB in different pathogen are different, and also urges us to study and reveal these TA systems.

Increasing evidences confirm that TA systems have emerged as important elements that affect the pathogenicity of many bacteria (Wang and Wood, 2011; Harms et al., 2018; Równicki et al., 2020). For example, antitoxin HigA inhibits virulence gene *mvfR* expression in *P. aeruginosa* (Guo et al., 2019). The TA system SehA/SehB in *Salmonella* promotes bacterial infection in mice (De la Cruz et al., 2013). Since the inactivation of *yefM-yoeB* affects the resistance against adversity stress, biofilm growth, and host serum killing, which are related to the virulence (Shi et al., 2019; Wang et al., 2019; Jiang et al., 2020), so we examined role of YefM-YoeB in pathogenicity of *E. piscicida*. As we expected, *in vitro* experiment demonstrated that the deficiency of *yefM-yoeB* significantly increased the capacity of *E. piscicida* to adhere and invade to host cells. Consistently, *in vivo* experiment showed that the deletion of *yefM-yoeB* significantly enhanced the ability of to disseminate in the fish tissues and elevated general virulence. Introduction of an in trans-expressed *yefM-yoeB* restored the virulence of TX01Δ*yefM-yoeB*. In contrast to our results, deletion of the *yefM-yoeB* locus had no effect on the virulence of *Streptococcus suis* (Zheng et al., 2015). However, we found that only deletion of the *yoeB* also had no effect on the virulence of *E. piscicida*. Moreover, TX01Δ*yefM-yoeB* and TX01 exhibited the similar ability of survival and replication in macrophages. Taking all the above results together, we believe that YefM-YoeB participates the virulence of *E. piscicida*, but its mechanism is complex and different from other pathogens. In *E. piscicida*, we found *TX01*Δ*yefM-yoeB* displayed obvious difference with *TX01*Δ*yoeB* in stress resistance and pathogenicity. We speculate when *yoeB* is deleted, another toxin protein that is functionally and structurally similar to YeoB could bind with YefM, just as the finding that YeeU is structurally similar to toxins YoeB in *E. coli* (Arbing et al., 2010). Therefor the phenotype of *TX01*Δ*yoeB* was similar to that of *TX01* but different from that of *TX01*Δ*yefM-yoeB*, which is totally missing the TA system.

In typical type II TA systems, the antitoxin alone or the TA complex binds to the promoter and regulates self the transcription of the TA operon (Page and Peti, 2016). In type II TA systems of *S. suis*, RelB1, RelB2, ParD, and ParDE negatively autoregulated the transcriptions of their respective TA operons, while RelBE2 positively autoregulated its TA operon transcription (Xu et al., 2018). In *Streptomyces lividans*, YefM-YoeB complex purified from *E. coli* could bind with high affinity to its own promoter region (Sevillano et al., 2012). Similarly, in *E. piscicida*, we also found YefM-YoeB dramatically inhibited the activity of the promoter of *yefM-yoeB*. Moreover, we found YefM directly bound with its own promoter. These results indicate that YefM-YoeB functions as transcriptional regulator and negatively autoregulate the its own expression.

In conclusion, we identified type II TA system YefM-YoeB in *E. piscicida*, an important pathogen threatening worldwide aquaculture industries. Our results show that the deletion of *yefM-yoeB* impaired the ability of *E. piscicida* to oxidative resistance and reduced the persistence bacteria formation ability, but enhanced the ability of biofilm formation, serum resistance, and host infection. The inactivation of yoeB has no effects on resistance to stress and virulence. YefM-YoeB negatively autoregulated its own expression and YefM can directly bind to the promoter of *yefM-yoeB*. This study provides new insights into the biological activity of type II TA system YefM-YoeB in aquatic pathogenic bacteria.

DATA AVAILABILITY STATEMENT

The original contributions presented in the study are included in the article/supplementary material, further inquiries can be directed to the corresponding author/s.

ETHICS STATEMENT

The animal study was reviewed and approved by the ethics committee of Institute of Tropical Bioscience and Biotechnology, Chinese Academy of Tropical Agricultural Sciences. Efforts were taken to ensure that all research animals received good care and humane treatment.

AUTHOR CONTRIBUTIONS

DMM carried out the experiments. HJG analyzed the data and revised the manuscript. YJS participated in gene knock-out experiments. HQH participated in the infection experiments. DMS participated in the experiment design and drafted the manuscript. HYH designed the experiments, interpreted results, and wrote the manuscript. All authors contributed to the article and approved the submitted version.

FUNDING

This work was supported by the Hainan Provincial Natural Science Foundation of China (2019CXTD413), the Central Public-interest Scientific Institution Basal Research Fund for Chinese Academy of Tropical Agricultural Sciences (19CXTD-32 and 1630052020011), and the Financial Fund of the Ministry of Agriculture and Rural Affairs, China (NFZX2018).

REFERENCES

Abayneh, T., Colquhoun, D. J., and Sørum, H. (2013). *Edwardsiella piscicida* sp. nov., a novel species pathogenic to fish. *J. Appl. Microbiol.* 114, 644–654.

Amraei, F., Narimisa, N., Sadeghi, K. B., Lohrasbi, V., and Masjedian, J. F. (2020). *Brucella melitensis* Persister cells formation and expression of type II Toxin-Antitoxin system genes in (16M) (B19). *Iran. J. Pathol.* 15, 127–133. doi: 10.30699/ijp.2020.118902.2294

Arbing, M. A., Handelman, S. K., Kuzin, A. P., Verdon, G., Wang, C., Su, M., et al. (2010). Crystal structures of Phd-Doc, HigA, and YeeU establish multiple evolutionary links between microbial growth-regulating toxin-antitoxin systems. *Structure* 18, 996–1010. doi: 10.1016/j.str.2010.04.018

Bernier, S. P., Lebeaux, D., DeFrancesco, A. S., Valomon, A., Soubigou, G., Coppée, J. Y., et al. (2013). Starvation, together with the SOS response, mediates high biofilm-specific tolerance to the fluoroquinolone ofloxacin. *PLoS Genet*. 9:e1003144. doi: 10.1371/journal.pgen.1003144

Brzozowska, I., and Zielenkiewicz, U. (2013). Regulation of toxin-antitoxin systems by proteolysis. *Plasmid* 70, 33–41. doi: 10.1016/j.plasmid.2013.01.007

Bukowski, M., Lyzen, R., Helbin, W. M., Bonar, E., Szalewska-Palasz, A., Wegrzyn, G., et al. (2013). A regulatory role for *Staphylococcus aureus* toxin-antitoxin system PemIKSa. *Nat. Commun*. 4:2012. doi: 10.1038/ncomms3012

Chan, W. T., Domenech, M., Moreno-Córdoba, I., Navarro-Martínez, V., Nieto, C., Moscoso, M., et al. (2018). The *Streptococcus pneumoniae* yefM-yoeB and relBE Toxin-Antitoxin Operons Participate in Oxidative Stress and Biofilm Formation. *Toxins* 10:378. doi: 10.3390/toxins10090378

Chan, W. T., Moreno-Córdoba, I., Yeo, C. C., and Espinosa, M. (2012). Toxin-antitoxin genes of the Gram-positive pathogen *Streptococcus pneumoniae*: so few and yet so many. *Microbiol. Mol. Biol. Rev*. 76, 773–791. doi: 10.1128/MMBR.00030-12

Christensen-Dalsgaard, M., Jorgensen, M. G., and Gerdes, K. (2010). Three new RelE-homologous mRNA interferases of *Escherichia coli* differentially induced by environmental stresses. *Mol. Microbiol*. 75, 333–348. doi: 10.1111/j.1365-2958.2009.06969.x

De la Cruz, M. A., Zhao, W., Farenc, C., Gimenez, G., Raoult, D., Cambillau, C., et al. (2013). A toxin-antitoxin module of *Salmonella* promotes virulence in mice. *PLoS Pathog*. 9:e1003827. doi: 10.1371/journal.ppat.1003827

Eroshenko, D. V., Polyudova, T. V., and Pyankova, A. A. (2020). VapBC and MazEF toxin/antitoxin systems in the regulation of biofilm formation and antibiotic tolerance in nontuberculous mycobacteria. *Int. J. Mycobacteriol*. 9, 156–166. doi: 10.4103/ijmy.ijmy_61_20

Ewing, W. H., Mcwhorter, A. C., Escobar, M. R., and Lubin, A. H. (1965). *Edwardsiella*, a new genus of *Enterobacteriaceae* based on a new species. *E. tarda*. *Int. J. Syst. Evol. Microbiol*. 15, 33–38.

Fang, Q. J., Han, Y. X., Shi, Y. J., Huang, H. Q., Fang, Z. G., and Hu, Y. H. (2019). Universal stress proteins contribute *Edwardsiella piscicida* adversity resistance and pathogenicity and promote blocking host immune response. *Fish Shellfish. Immunol*. 95, 248–258. doi: 10.1016/j.fsi.2019.10.035

Forman, H. J., and Torres, M. (2002). Reactive oxygen species and cell signaling: respiratory burst in macrophage signaling. *Am. J. Respir. Crit. Care Med*. 166, S4–S8. doi: 10.1164/rccm.2206007

Fraikin, N., Rousseau, C. J., Goeders, N., and Van Melderen, L. (2019). Reassessing the Role of the Type II MqsRA Toxin-Antitoxin System in Stress Response and Biofilm Formation: mqsA Is Transcriptionally Uncoupled from mqsR. *mBio* 10, e2678–e2619. doi: 10.1128/mBio.02678-19

Gerdes, K., and Maisonneuve, E. (2012). Bacterial persistence and toxin-antitoxin loci. *Annu. Rev. Microbiol*. 66, 103–123. doi: 10.1146/annurev-micro-092611-150159

Gu, H. J., Wang, B., He, J. J., and Hu, Y. H. (2021). Macrophage colony stimulating factor (MCSF) of Japanese flounder (*Paralichthys olivaceus*): Immunoregulatory property, anti-infectious function, and interaction with MCSF receptor. *Dev. Comp. Immunol*. 116:103920. doi: 10.1016/j.dci.2020.103920

Guo, Y., Sun, C., Li, Y., Tang, K., Ni, S., and Wang, X. (2019). Antitoxin HigA inhibits virulence gene mvfR expression in *Pseudomonas aeruginosa*. *Environ. Microbiol*. 21, 2707–2723. doi: 10.1111/1462-2920.14595

Harms, A., Brodersen, D. E., Mitarai, N., and Gerdes, K. (2018). Toxins, Targets, and Triggers: An Overview of Toxin-Antitoxin Biology. *Mol. Cell*. 70, 768–784. doi: 10.1016/j.molcel.2018.01.003

Harms, A., Maisonneuve, E., and Gerdes, K. (2016). Mechanisms of bacterial persistence during stress and antibiotic exposure. *Science* 354:aaf4268. doi: 10.1126/science.aaf4268

Harrison, J. J., Wade, W. D., Akierman, S., Vacchi-Suzzi, C., Stremick, C. A., Turner, R. J., et al. (2009). The chromosomal toxin gene yafQ is a determinant of multidrug tolerance for *Escherichia coli* growing in a biofilm. *Antimicrob. Agents Chemother*. 53, 2253–2258. doi: 10.1128/AAC.00043-09

He, T. T., Zhou, Y., Liu, Y. L., Li, D. Y., Nie, P., Li, A. H., et al. (2020). *Edwardsiella piscicida* type III protein EseJ suppresses apoptosis through down regulating type 1 fimbriae, which stimulate the cleavage of caspase-8. *Cell Microbiol*. 22:e13193. doi: 10.1111/cmi.13193

Helaine, S., Cheverton, A. M., Watson, K. G., Faure, L. M., Matthews, S. A., and Holden, D. W. (2014). Internalization of *Salmonella* by macrophages induces formation of nonreplicating persisters. *Science* 343, 204–208. doi: 10.1126/science.1244705

Hu, Y. H., Li, Y. X., and Sun, L. (2014). *Edwardsiella tarda* Hfq: impact on host infection and global protein expression. *Vet. Res*. 45:23. doi: 10.1186/1297-9716-45-23

Hu, Y. H., Liu, C. S., Hou, J. H., and Sun, L. (2009a). Identification, characterization, and molecular application of a virulence-associated autotransporter from a pathogenic *Pseudomonas fluorescens* strain. *Appl. Environ. Microbiol*. 75, 4333–4340. doi: 10.1128/AEM.00159-09

Hu, Y. H., Wang, H. L., Zhang, M., and Sun, L. (2009b). Molecular analysis of the copper-responsive CopRSCD of a pathogenic *Pseudomonas fluorescens* strain. *J. Microbiol*. 47, 277–286. doi: 10.1007/s12275-008-0278-9

Janda, J. M., and Abbott, S. L. (1993). Infections associated with the genus *Edwardsiella*: the role of Edwardsiella tarda in human disease. *Clin. Infect. Dis*. 17, 742–748. doi: 10.1093/clinids/17.4.742

Janssen, B. D., Garza-Sánchez, F., and Hayes, C. S. (2015). YoeB toxin is activated during thermal stress. *MicrobiologyOpen* 4, 682–697. doi: 10.1002/mbo3.272

Jiang, C., Cheng, Y., Cao, H., Zhang, B., Li, J., Zhu, L., et al. (2020). Effect of cAMP Receptor Protein Gene on Growth Characteristics and Stress Resistance of *Haemophilus parasuis* Serovar 5. *Front. Cell. Infect. Microbiol*. 10:19. doi: 10.3389/fcimb.2020.00019

Kedzierska, B., Lian, L. Y., and Hayes, F. (2007). Toxin-antitoxin regulation: bimodal interaction of YefM-YoeB with paired DNA palindromes exerts transcriptional autorepression. *Nucleic Acids Res*. 35, 325–339. doi: 10.1093/nar/gkl1028

Kim, Y., and Wood, T. K. (2010). Toxins Hha and CspD and small RNA regulator Hfq are involved in persister cell formation through MqsR in *Escherichia coli*. *Biochem. Biophys. Res. Commun*. 391, 209–213. doi: 10.1016/j.bbrc.2009.11.033

Leung, K. Y., Siame, B. A., Tenkink, B. J., Noort, R. J., and Mok, Y. K. (2012). *Edwardsiella tarda* - virulence mechanisms of an emerging gastroenteritis pathogen. *Microbes Infect*. 14, 26–34. doi: 10.1016/j.micinf.2011.08.005

Leung, K. Y., Wang, Q., Yang, Z., and Siame, B. A. (2019). *Edwardsiella piscicida*: A versatile emerging pathogen of fish. *Virulence* 10, 555–567. doi: 10.1080/21505594.2019.1621648

Li, M. F., Jia, B. B., Sun, Y. Y., and Sun, L. (2020). The Translocation and Assembly Module (TAM) of *Edwardsiella tarda* Is Essential for Stress Resistance and Host Infection. *Front. Microbiol*. 11:1743. doi: 10.3389/fmicb.2020.01743

Li, M. F., Sun, L., and Li, J. (2015). *Edwardsiella tarda* evades serum killing by preventing complement activation via the alternative pathway. *Fish Shellf. Immunol*. 43, 325–329. doi: 10.1016/j.fsi.2014.12.037

Lobato-Márquez, D., Díaz-Orejas, R., and García-Del Portillo, F. (2016). Toxin-antitoxins and bacterial virulence. *FEMS Microbiol. Rev*. 40, 592–609. doi: 10.1093/femsre/fuw022

Ma, D., Mandell, J. B., Donegan, N. P., Cheung, A. L., Ma, W., Rothenberger, S., et al. (2019). The Toxin-Antitoxin MazEF Drives Staphylococcus aureus Biofilm Formation. *Antib. Toleran. Chronic Infect. mBio*. 10, e1658–e1619. doi: 10.1128/mBio.01658-19

Mohanty, B. R., and Sahoo, P. K. (2007). Edwardsiellosis in fifish: a brief review. *J. Biosci*. 32, 1331–1344. doi: 10.1007/s12038-007-0143-8

Narimisa, N., Amraei, F., Kalani, B. S., Mohammadzadeh, R., and Jazi, F. M. (2020). Effects of sub-inhibitory concentrations of antibiotics and oxidative stress on the expression of type II toxin-antitoxin system genes in *Klebsiella pneumoniae*. *J. Glob. Antimicrob. Resist*. 21, 51–56. doi: 10.1016/j.jgar.2019.09.005

Norton, J. P., and Mulvey, M. A. (2012). Toxin-antitoxin systems are important for niche-specific colonization and stress resistance of uropathogenic *Escherichia coli*. *PLoS Pathog*. 8:e1002954. doi: 10.1371/journal.ppat.1002954

Ogura, T., and Hiraga, S. (1983). Mini-F plasmid genes that couple host cell division to plasmid proliferation. *Proc. Natl. Acad. Sci. U. S. A*. 80, 4784–4788. doi: 10.1073/pnas.80.15.4784

Oron-Gottesman, A., Sauert, M., Moll, I., and Engelberg-Kulka, H. (2016). A Stress-Induced Bias in the Reading of the Genetic Code in *Escherichia coli*. *MBio* 7, e1855–e1816. doi: 10.1128/mBio.01855-16

Overgaard, M., Borch, J., Jørgensen, M. G., and Gerdes, K. (2008). Messenger RNA interferase RelE controls relBE transcription by conditional cooperativity. *Mol. Microbiol.* 69, 841–857. doi: 10.1111/j.1365-2958.2008.06313.x

Page, R., and Peti, W. (2016). Toxin-antitoxin systems in bacterial growth arrest and persistence. *Nat. Chem. Biol.* 12, 208–214. doi: 10.1038/nchembio.2044

Park, S. B., Aoki, T., and Jung, T. S. (2012). Pathogenesis of and strategies for preventing *Edwardsiella tarda* infection in fish. *Vet. Res.* 43:67. doi: 10.1186/1297-9716-43-67

Równicki, M., Lasek, R., Trylska, J., and Bartosik, D. (2020). Targeting Type II Toxin-Antitoxin Systems as Antibacterial Strategies. *Toxins* 12:568. doi: 10.3390/toxins12090568

Schuster, C. F., and Bertram, R. (2013). Toxin-antitoxin systems are ubiquitous and versatile modulators of prokaryotic cell fate. *FEMS Microbiol. Lett.* 340, 73–85. doi: 10.1111/1574-6968.12074

Sevillano, L., Díaz, M., Yamaguchi, Y., Inouye, M., and Santamaría, R. I. (2012). Identification of the first functional toxin-antitoxin system in *Streptomyces*. *PLoS One*. 7:e32977. doi: 10.1371/journal.pone.0032977

Shi, Y. J., Fang, Q. J., Huang, H. Q., Gong, C. G., and Hu, Y. H. (2019). HutZ is required for biofilm formation and contributes to the pathogenicity of *Edwardsiella piscicida*. *Vet Res.* 50:76. doi: 10.1186/s13567-019-0693-4

Soo, V. W., and Wood, T. K. (2013). Antitoxin MqsA represses curli formation through the master biofilm regulator CsgD. *Sci. Rep.* 3:3186. doi: 10.1038/srep03186

Sui, Z. H., Xu, H., Wang, H., Jiang, S., Chi, H., and Sun, L. (2017). Intracellular Trafficking Pathways of *Edwardsiella tarda*: From Clathrin- and Caveolin-Mediated Endocytosis to Endosome and Lysosome. *Front. Cell. Infect. Microbiol.* 7:400. doi: 10.3389/fcimb.2017.00400

Sun, C., Guo, Y., Tang, K., Wen, Z., Li, B., Zeng, Z., et al. (2017). MqsR/MqsA Toxin/Antitoxin System Regulates Persistence and Biofilm Formation in *Pseudomonas putida* KT2440. *Front. Microbiol.* 8:840. doi: 10.3389/fmicb.2017.00840

Tripathi, A., Dewan, P. C., Siddique, S. A., and Varadarajan, R. (2014). MazF-induced growth inhibition and persister generation in *Escherichia coli*. *J. Biol. Chem.* 289, 4191–4205. doi: 10.1074/jbc.M113.510511

Verstraeten, N., Knapen, W. J., Kint, C. I., Liebens, V., Van den Bergh, B., Dewachter, L., et al. (2015). Obg and Membrane Depolarization Are Part of a Microbial Bet-Hedging Strategy that Leads to Antibiotic Tolerance. *Mol. Cell.* 59, 9–21. doi: 10.1016/j.molcel.2015.05.011

Wang, B. Y., Huang, H. Q., Li, S., Tang, P., Dai, H. F., Xian, J. A., et al. (2019). Thioredoxin H (TrxH) contributes to adversity adaptation and pathogenicity of *Edwardsiella piscicida*. *Vet. Res.* 50:26. doi: 10.1186/s13567-019-0645-z

Wang, X., Kim, Y., Hong, S. H., Ma, Q., Brown, B. L., Pu, M., et al. (2011). Antitoxin MqsA helps mediate the bacterial general stress response. *Nat. Chem. Biol.* 7, 359–366. doi: 10.1038/nchembio.560

Wang, X., Lord, D. M., Hong, S. H., Peti, W., Benedik, M. J., Page, R., et al. (2013). Type II toxin/antitoxin MqsR/MqsA controls type V toxin/antitoxin GhoT/GhoS. *Environ. Microbiol.* 15, 1734–1744. doi: 10.1111/1462-2920.12063

Wang, X., and Wood, T. K. (2011). Toxin-antitoxin systems influence biofilm and persister cell formation and the general stress response. *Appl. Environ. Microbiol.* 77, 5577–5583. doi: 10.1128/AEM.05068-11

Wen, W., Liu, B., Xue, L., Zhu, Z., Niu, L., and Sun, B. (2018). Autoregulation and Virulence Control by the Toxin-Antitoxin System SavRS in *Staphylococcus aureus*. *Infect. Immun.* 86, e32–e18. doi: 10.1128/IAI.00032-18

Wood, T. L., and Wood, T. K. (2016). The HigB/HigA toxin/antitoxin system of *Pseudomonas aeruginosa* influences the virulence factors pyochelin, pyocyanin, and biofilm formation. *MicrobiologyOpen* 5, 499–511. doi: 10.1002/mbo3.346

Xie, Y., Wei, Y., Shen, Y., Li, X., Zhou, H., Tai, C., et al. (2018). TADB 2.0: an updated database of bacterial type II toxin-antitoxin loci. *Nucleic Acids Res.* 46, D749–D753. doi: 10.1093/nar/gkx1033

Xu, J., Zhang, N., Cao, M., Ren, S., Zeng, T., Qin, M., et al. (2018). Identification of Three Type II Toxin-Antitoxin Systems in *Streptococcus suis* Serotype 2. *Toxins* 10:467. doi: 10.3390/toxins10110467

Xue, L., Yue, J., Ke, J., Khan, M. H., Wen, W., Sun, B., et al. (2020). Distinct oligomeric structures of the YoeB-YefM complex provide insights into the conditional cooperativity of type II toxin-antitoxin system. *Nucleic Acids Res.* 48, 10527–10541. doi: 10.1093/nar/gkaa706

Yamaguchi, Y., Park, J. H., and Inouye, M. (2011). Toxin-antitoxin systems in bacteria and archaea. *Annu Rev Genet.* 45, 61–79. doi: 10.1146/annurev-genet-110410-132412

Yin, K., Guan, Y., Ma, R., Wei, L., Liu, B., Liu, X., et al. (2018). Critical role for a promoter discriminator in RpoS control of virulence in *Edwardsiella piscicida*. *PLoS Pathog.* 14:e1007272. doi: 10.1371/journal.ppat.1007272

Yoon, J. B., Hwang, S., Baek, S. W., Lee, S., Bang, W. Y., and Moon, K. H. (2020). In vitro *Edwardsiella piscicida* CK108 Transcriptome Profiles with Subinhibitory Concentrations of Phenol and Formalin Reveal New Insights into Bacterial Pathogenesis Mechanisms. *Microorganisms* 8:1068. doi: 10.3390/microorganisms8071068

Yoshizumi, S., Zhang, Y., Yamaguchi, Y., Chen, L., Kreiswirth, B. N., and Inouye, M. (2009). *Staphylococcus aureus* YoeB homologues inhibit translation initiation. *J. Bacteriol.* 191, 5868–5872. doi: 10.1128/JB.00623-09

Zander, I., Shmidov, E., Roth, S., Ben-David, Y., Shoval, I., Shoshani, S., et al. (2020). Characterization of PfiT/PfiA toxin-antitoxin system of *Pseudomonas aeruginosa* that affects cell elongation and prophage induction. *Environ. Microbiol.* 22, 5048–5057. doi: 10.1111/1462-2920.15102

Zhang, W. W., Sun, K., Cheng, S., and Sun, L. (2008). Characterization of DegQVh, a serine protease and a protective immunogen from a pathogenic Vibrio harveyi strain. *Appl. Environ. Microbiol.* 74, 6254–6262. doi: 10.1128/AEM.00109-08

Zheng, C., Xu, J., Ren, S., Li, J., Xia, M., Chen, H., et al. (2015). Identification and characterization of the chromosomal yefM-yoeB toxin-antitoxin system of *Streptococcus suis*. *Sci. Rep.* 5:13125. doi: 10.1038/srep13125

Conflict of Interest: The authors declare that the research was conducted in the absence of any commercial or financial relationships that could be construed as a potential conflict of interest.

frontiers in Microbiology

ORIGINAL RESEARCH
published: 11 March 2021
doi: 10.3389/fmicb.2021.643498

Identification and Characterization of EvpQ, a Novel T6SS Effector Encoded on a Mobile Genetic Element in *Edwardsiella piscicida*

*Duan You Li[1,2], Ying Li Liu[1], Xiao Jian Liao[1,2], Tian Tian He[1], Shan Shan Sun[1,2], Pin Nie[1,3,4] and Hai Xia Xie[1]**

[1] State Key Laboratory of Freshwater Ecology and Biotechnology, Key Laboratory of Aquaculture Disease Control, Ministry of Agriculture, Institute of Hydrobiology, Chinese Academy of Sciences, Wuhan, China, [2] College of Advanced Agricultural Sciences, University of Chinese Academy of Sciences, Beijing, China, [3] Laboratory for Marine Biology and Biotechnology, Pilot National Laboratory for Marine Science and Technology, Qingdao, China, [4] School of Marine Science and Engineering, Qingdao Agricultural University, Qingdao, China

OPEN ACCESS

Edited by:
Bo Peng,
Sun Yat-sen University, China

Reviewed by:
Ka Yin Leung,
Guangdong Technion-Israel Institute of Technology, China
Qi Yao Wang,
East China University of Science and Technology, China

***Correspondence:**
Hai Xia Xie
xieh@ihb.ac.cn

Specialty section:
This article was submitted to Antimicrobials, Resistance and Chemotherapy, a section of the journal Frontiers in Microbiology

Received: 18 December 2020
Accepted: 05 February 2021
Published: 11 March 2021

Citation:
Li DY, Liu YL, Liao XJ, He TT, Sun SS, Nie P and Xie HX (2021) Identification and Characterization of EvpQ, a Novel T6SS Effector Encoded on a Mobile Genetic Element in Edwardsiella piscicida. Front. Microbiol. 12:643498. doi: 10.3389/fmicb.2021.643498

In this study, a hypothetical protein (ORF02740) secreted by *Edwardsiella piscicida* was identified. We renamed the ORF02740 protein as EvpQ, which is encoded by a mobile genetic element (MGE) in *E. piscicida* genome. The *evpQ* gene is spaced by 513 genes from type VI secretion system (T6SS) gene cluster. Low GC content, three tRNA, and three transposase genes nearby *evpQ* define this MGE that *evpQ* localizes as a genomic island. Sequence analysis reveals that EvpQ shares a conserved domain of C70 family cysteine protease and shares 23.91% identity with T3SS effector AvrRpt2 of phytopathogenic *Erwinia amylovora.* Instead, EvpQ of *E. piscicida* is proved to be secreted at a T6SS-dependent manner, and it can be translocated into host cells. EvpQ is thereof a novel T6SS effector. Significantly decreased competitive index of Δ*evpQ* strain in blue gourami fish (0.53 ± 0.27 in head kidney and 0.44 ± 0.19 in spleen) indicates that EvpQ contributes to the pathogenesis of *E. piscicida*. At 8-, 18-, and 24-h post-subculture into DMEM, the transcription of *evpQ* was found to be negatively regulated by Fur and positively regulated by EsrC, and the steady-state protein levels of EvpQ are negatively controlled by RpoS. Our study lays a foundation for further understanding the pathogenic role of T6SS in edwardsiellosis.

Keywords: type VI secretion system, effector, EvpQ, regulation, mobile genetic element, *Edwardsiella piscicida*

INTRODUCTION

Edwardsiella piscicida, previously known as *Edwardsiella tarda*, is a Gram-negative intracellular pathogen (Abayneh et al., 2013; Shao et al., 2015). It causes edwardsiellosis in more than 20 important species of farmed fish, especially flounder (*Paralichthys olivaceus*) and turbot (*Scophthalmus maximus*) (Matsuyama et al., 2005; Padrós et al., 2006; Mohanty and Sahoo, 2007). The survival and replication of *E. piscicida* in its hosts depends on its type

VI secretion system (T6SS) and type III secretion system (T3SS) (Tan et al., 2005; Okuda et al., 2006; Zheng and Leung, 2007).

Srinivasa Rao et al. (2004) identified the *Edwardsiella* virulent proteins (EVPs) from *E. piscicida* PPD130/91 in a mass spectrometric screen for secreted virulence factors. These EVPs were analogous to the T6SS proteins named first by Pukatzki et al. (2006). *E. piscicida* T6SS are encoded in a gene cluster which contains 13 conserved core genes encoding proteins necessary to assemble the basic secretion apparatus (Zheng and Leung, 2007). Besides the core apparatus protein, EvpP (T6SS effector protein), EvpC (a homolog of Hcp), and EvpI (a homolog of VgrG) are three secreted proteins encoded inside the T6SS gene cluster (Zheng and Leung, 2007). T6SS is a contractile injection apparatus that translocates a tail tube and a spike loaded with various effectors directly into eukaryotic or prokaryotic target cells (Silverman et al., 2013; Flaugnatti et al., 2016; Hernandez et al., 2020; Wettstadt and Filloux, 2020). The T6SS spike punctures the bacterial cell envelope allowing the transport of effectors, and it consists of a torch-like VgrG trimer (encoded by *evpI* in *E. piscicida*) on which sits a PAAR protein sharpening the VgrG tip (encoded by *evpJ* in *E. piscicida*), and VgrG itself sits on the Hcp tube (encoded by *evpC* in *E. piscicida*). All these elements are packed into a T6SS sheath and are propelled out of the bacterial cell and into target cells. *Vibrio cholerae* VgrG-1 is the first identified T6SS effector, which is secreted by T6SS and displays a C-terminal actin cross-linking domain upon its translocation into phagocytic target cells (Pukatzki et al., 2007; Ma et al., 2009). EvpP is the first T6SS effector identified in *Edwardsiella* spp., and it can target intracellular Ca^{2+} signaling to impair Jnk activation and ASC oligomerization, therefore promoting bacterial colonization (Chen et al., 2017).

Edwardsiella piscicida T6SS plays a pivotal role at the early infection stage *in vivo* when T3SS expression is repressed by alternative sigma factor RpoS (Yang et al., 2017; Yin et al., 2018). The two-component system sensor PhoQ detects changes of environmental temperature as well as Mg^{2+} concentration, and the response regulator PhoP regulates the T6SS through direct activation of *esrB* in *E. piscicida* (Chakraborty et al., 2010). PhoR-PhoB two-component system senses changes in Pi concentration, and the ferric uptake regulator (Fur) senses changes in iron concentration to regulate the expression of T6SS (Chakraborty et al., 2011). PhoB and EsrC bind simultaneously on DNA upstream of *evpA*, tightly regulating the transcription of whole T6SS cluster, except the T6SS effector gene *evpP*. Fur senses high iron concentration and binds directly to the Fur box in the promoter of *evpP* to inhibit the binding of EsrC to the same region (Chakraborty et al., 2011). The elegantly regulated T6SS contributes to the LD_{50} of *E. piscicida* by ∼100 times (Zheng and Leung, 2007).

In this study, the novel T6SS effector, EvpQ, was identified in *E. piscicida*. EvpQ was revealed to be encoded on a genomic island, and its regulation network and contribution to virulence was characterized.

MATERIALS AND METHODS

Bacterial Strains

Edwardsiella tarda PPD130/91 was recognized as *Edwardsiella piscicida* PPD130/91 ever since 2015 (Ling et al., 2000; Shao et al., 2015). The *E. piscicida* strains and plasmids used in this study are described in **Table 1**. *E. piscicida* strains were grown in TSB medium static. To activate T6SS and T3SS, *E. piscicida* and its derived strains were grown in Dulbecco's modified Eagle's medium (DMEM, Invitrogen) at 25°C under 5% (*v*/*v*) CO_2 atmosphere. When required, appropriate antibiotics were supplemented at the concentrations of 100 μg/ml ampicillin (Amp; Sigma), 12.5 μg/ml colistin (Col; Sigma), 34 μg/ml chloramphenicol (Cm; Amresco), 15 μg/ml tetracycline (Tet; Amresco), and 50 μg/ml kanamycin (Km; BioFroxx).

Cell Line and Cultivation

Epithelioma papillosum of carp (*Cyprinus carpio*) (EPC) cells (Wolf and Mann, 1980) were grown in M199 medium (HyClone), supplemented with 10% fetal bovine serum (FBS, Gibco). EPC cells were maintained in a 5% CO_2 atmosphere at 25°C.

Mutant Strain Construction

Using the λ Red recombination system as described previously (Datsenko and Wanner, 2000), the chromosomal copy of *evpQ* gene was replaced with kanamycin gene, obtaining the strain Δ*evpQ*::km. The scarless mutant strains Δ*evpQ* and Δ*rpoS* were obtained by *sacB*-based allelic exchange using a method as previously described (Edwards et al., 1998; Zheng et al., 2005). All mutants obtained were verified by DNA sequencing. All primers used are listed in **Table 2**.

Plasmid Construction

The pACYC-*evpQ*-HA is derived from pACYC-184 (Amersham), which carries the *evpQ*-HA gene under the control of tetracyclin resistance gene promoter. To construct, DNA fragment including the ribosome-binding site and complete ORF of *evpQ* were amplified by PCR from *E. piscicida* PPD130/91 genomic DNA using primer pair *evpQ*-com-for and *evpQ*-com-rev (**Table 2**). The PCR products, containing *Eco*RI and *Sca*I sites, were digested and ligated into pACYC-184 to generate pACYC-*evpQ*-HA. The *evpQ* gene together with its ribosome-binding site digested with *Bam*HI and *Bgl*II was inserted into pACYC-*escE-cyaA* (Lu et al., 2016), which was also digested with the same two restriction enzymes, acquiring pACYC-*evpQ-cyaA*. All the plasmids constructed were verified by DNA sequencing before being introduced into *E. piscicida* strains by electroporation. The strains obtained were verified by immunoblotting.

Epitope Tagging of the Chromosomal Copy of *evpQ* With a 2HA Tag

To tag the chromosomal copy of *evpQ* with DNA encoding a double HA epitope, the λ Red recombination system was used

as described (Datsenko and Wanner, 2000; Uzzau et al., 2001). Briefly, the forward primer (*evpQ*-2HA-for) containing the 3'-terminal sequence (without the stop codon) of *evpQ* followed by a sequence encoding a 2HA epitope and the reverse primer (*evpQ*-2HA-rev) corresponding to a chromosomal region downstream from *evpQ* were used to amplify the kanamycin (Km) resistance gene from pSU315. The PCR product was electroporated into competent cells of *E. piscicida* PPD130/91 wild-type strain, its isogenic mutant strain Δ*esrC*, Δ*rpoS*, or Δ*fur* strain, and each of which were transformed with pKD46 (Datsenko and Wanner, 2000). The colonies obtained were screened through probing with anti-HA antibody.

Immunoblotting Analysis

Secreted proteins [extracellular proteins (E)] and bacterial lysates [total bacterial proteins (TBPs)] were prepared as described by Zheng and Leung (2007). ECPs and TBPs were loaded onto a NuPAGE 12% gel for electrophoresis in MES SDS running buffer (Invitrogen). Proteins on sodium dodecyl sulfate polyacrylamide gel electrophoresis (SDS-PAGE) gel were transferred onto polyvinylidene fluoride (PVDF) membrane (Millipore), before being probed with rabbit antibodies against HA (1:2,000) (Sigma), DnaK (1:10,000) (Cusabio Technology LLC), EseG (1:1,000) (Xie et al., 2010), EseE (1:1,000) (Yi et al., 2016), and EvpC (1:5,000) (Zheng and Leung, 2007).

TABLE 1 | Strains and plasmids used in this study.

Strain or plasmid	Description and/or genotype	Reference or source
Bacteria		
Edwardsiella piscicida		
PPD130/91	Wild type, Km^s, Col^r, Amp^s, and $LD_{50} = 10^{5.0}$	Ling et al. (2000)
WT *evpQ*:2HA	PPD130/91with chromosomal expression of *evpQ*-2HA, Amp^r, and Km^r	This study
Δ*esaB*	PPD130/91, *esaB* in-frame deletion of aa 1 to 149	Liu et al. (2017)
Δ*esaB*Δ*esaN*	PPD130/91, in-frame deletion of *esaB* and *esaN*	This study
Δ*esaN*	PPD130/91 with in-frame deletion of *esaN*	Xie et al. (2010)
Δ*esaN evpQ*::2HA	Δ*esaN* with chromosomal expression of *evpQ*-2HA, Amp^r, and Km^r	This study
Δ*evpO*	PPD130/91, *evpO* in-frame deletion of aa 13 to 1257	Zheng and Leung (2007)
Δ*evpO evpQ*::2HA	Δ*evpO* with chromosomal expression of *evpQ*-2HA, Amp^r, Km^r	This study
Δ*esaB evpQ*::2HA	Δ*esaB* with chromosomal expression of *evpQ*-2HA, Amp^r, and Km^r	This study
Δ*evpQ*	PPD130/91, ETAE_2037 in-frame deletion of aa 1 to 173	This study
Δ*evpQ*::km	PPD130/91, ETAE_2037 replaced with Km^r	This study
Δ*rpoS*	PPD130/91, *rpoS* in-frame deletion of aa 1 to 490	This study
Δ*rpoS evpQ*::2HA	Δ*rpoS* with chromosomal expression of *evpQ*-2HA, Amp^r, and Km^r	This study
Δ*esrC*	PPD130/91, *esrC* in-frame deletion of aa 12 to 220	Zheng et al. (2005)
Δ*fur*	PPD130/91 with in-frame deletion of *fur* protein aa 1–112	Zhang et al. (2019)
Δ*fur evpQ*::2HA	Δ*fur* with chromosomal expression of *evpQ*-2HA, Amp^r, and Km^r	This study
WT/pACYC-*eseG*::*cyaA*	PPD130/91 with pACYC-*eseG*::*cyaA*	Lu et al. (2016)
Δ*esaN*/pACYC-*eseG*::*cyaA*	Δ*esaN* with pACYC-*eseG*::*cyaA*	Lu et al. (2016)
WT/pACYC-*evpQ*::*cyaA*	PPD130/91 with pACYC-*evpQ*::*cyaA*	This study
Δ*esaN*/pACYC-*evpQ*::*cyaA*	Δ*esaN* with pACYC-*evpQ*::*cyaA*	This study
Δ*evpO*/pACYC-*evpQ*::*cyaA*	Δ*evpO* with pACYC-*evpQ*::*cyaA*	This study
WTpFPV-P-$evpQ_{-594\ to\ -1}$	PPD130/91 with pFPV-P-$evpQ_{-594\ to\ -1}$	This study
Δ*esrC*/pFPV-P-$evpQ_{-594\ to\ -1}$	Δ*esrC* with pFPV-P-$evpQ_{-594\ to\ -1}$	This study
Δ*rpoS*/pFPV-P-$evpQ_{-594\ to\ -1}$	Δ*rpoS* with pFPV-P-$evpQ_{-594\ to\ -1}$	This study
Δ*fur*/pFPV-P-$evpQ_{-594\ to\ -1}$	Δ*fur* with pFPV-P-$evpQ_{-594\ to\ -1}$	This study
Escherichia coli		
DH5α	α Complementation	Stratagene
S17-1 λpir	RK2 *tra* regulon, λ*pir*	Simon et al. (1983)
Plasmids		
pMD18-T	Cloning vector, Amp^r	TaKaRa
pRE112	Suicide plasmid, *pir*dependent, Cm^r, *oriT*, *oriV*, and *sacB*	Edwards et al. (1998)
pACYC-184	Tet^r and Cm^r	Amersham
pACYC-*evpQ*-HA	Tet^r	This study
pKD46	Red helper plasmid, Amp^r	Datsenko and Wanner (2000)
pKD4	Template plasmid for PCR amplify FRT-flanked resistance gene, Km^r and Amp^r	Datsenko and Wanner (2000)
pSU315	Template plasmid with FLP recognition target site and 2HA tag sequence, Amp^r, and Km^r	Uzzau et al. (2001)
pFPV25	Plasmid with promoterless *gfp* gene	Valdivia and Falkow (1996)
pFPV-P-$evpQ_{-594\ to\ -1}$	-594 to -1 of *evpQ* inserted into upstream of *gfp* in pFPV25	This study

Col, colistin; Amp, ampicillin; Tet, tetracycline; Cm, chloramphenicol; Km, kanamycin; Superscripts: r, resistance; s, sensitivity.

CyaA-Based Translocation Assay

CyaA translocation assay was conducted on EPC cells as previously described (Xie et al., 2015), and cyclic AMP (cAMP) levels were assayed by using an enzyme-linked immunoassay (ELISA) according to the instruction of the manufacturer (ARBOR ASSAYS).

Mechanic Fractionation of EPC Cells

Infected EPC cells were fractionated as described by Coombes et al. (2007) with minor modifications. Briefly, EPC cells were seeded at 6×10^6 cells per 100 mm diameter tissue culture dish 1 day before infection. Before infection, the *E. piscicida* culture reaching 0.5 at OD_{540nm} were applied onto EPC cells, at an MOI of 15 in 3 ml M199 medium per dish. Dishes were maintained at 25°C in a 5% CO_2 incubator for 30 min before the medium was aspirated, and DMEM supplemented with 16 μg/ml gentamycin was added. Infections were allowed to proceed for another 2 h before the EPC cells were harvested and resuspended in 300 μl homogenization buffer (HB) [250 mM sucrose, 3 mM imidazole, 0.5 mM EDTA (pH 7.4)] supplemented with halt protease inhibitor cocktail (Thermo Fisher Scientific). The cells were homogenized on ice by mechanical lysis using a 1.0-ml syringe with a 22-gauge needle. The lysate was spun for 15 min at 3,000 × *g* at 4°C. The supernatants were precipitated by methanol and chloroform as described by Wang et al. (2017) and dissolved in 1 × sodium dodecyl sulfate (SDS) loading buffer.

TABLE 2 | Oligonucleotides used in this study.

Designation	Nucleotide sequence
evpQ-for	GCTCTAGAACCCAGCAGCCTGACATTG
evpQ-int-rev	TTTCGGCCTCACCTCTGATAGTTA
evpQ-int-for	ATCAGAGGTGAGGCCGAAAATG GCTATTTTTGCTCAGCTC
evpQ-rev	GCTCTAGA TCTTTAACGGTTGGGGATG
evpQ-com-for	GGAATTCATTGGGGAGGGGTAGAGTG
evpQ-com-rev	AAAAGTACTTTAAGCGTAATCT GGAACATCGTATGGGTAATT TGGCTCAAGCAATGGT
rpoS-for	ATGGTACCTACGCTGGTTACAATGTGGCT
rpoS-int-rev	AGCTGTACCCTACCCGTGATTTG
rpoS-int-for	CAAATCACGGGTAGGGTACAGC TGCGATGCGGTCAAAAAAAACGG
rpoS-rev	ATGGTACCGCTACGTCCGCCCACAGCTGA
pSU315-*evpQ*::2HA for	CATTGACATAAATGTGCTGACACGG AGCAAAGGGAGGCGGTCCATA TGAATATCCTCCTTAGT
pSU315-*evpQ*-rev	TATAGGCTATCGTTAACCAG GCAAGGATTCCATGTATCA TCACATATGAATATCCTCCTTAG
evpQ-cyaA-for	GC GGATCC ATAAAGATTGGGGAGGGGT
evpQ-cyaA-rev	GA AGATCT ATTTGGCTCAAGCAATGGT
evpQ-cyaA-check-rev	TTGCCGCAGATAGTCAAGCCGCT
P-*evpQ*$_{-594\ to\ -1}$ for	CGGAATTCGAGTTATTAAACCCGTCAAG
P-*evpQ*$_{-594\ to\ -1}$ rev	CGGGATCCTTTCGGCCTCACCTCTGATA
16S-qfor	ACTGAGACACGGTCCAGACTCCTAC
16S-qrev	TTAACGTTCACACCTTCCTCCCTA
evpQ-qfor	TGTGCTAATCGTCGGGGTTA
evpQ-qrev	TTCATTGCGCAGTTTACGGA

Competitive Index in Blue Gourami Fish

Mixed competitive infection in naïve blue gourami (*Trichogaster trichopterus* Pallas) (9.54 ± 1.52 g) was performed to determine the contribution of EvpQ to pathogenesis. Overnight-cultured *E. piscicida* wild-type and Δ*evpQ*::*km* strains were subcultured at 1:40, respectively, and cultured at 25°C in TSB for 2.5 h. The bacteria were washed three times in PBS, and the OD_{540} was adjusted to 0.5. Equal amounts of bacteria were mixed and injected intramuscularly (i.m.) at 1×10^5 CFU per fish. At 48 h post-inoculation, spleen and head kidney were dissected and homogenized, and a series dilution were spread onto TSA plates supplemented with colistin. The colonies obtained were patched onto TSA plate with colistin/kanamysin and TSA plate with colistin to determine the ratio of Δ*evpQ*::*km* strain to the wild-type strain. The competitive index (CI) value is the ratio of the Δ*evpQ*:*km* strain and wild-type strain within the output divided by their ratio within the input.

The experiments with fish were performed in strict accordance with the recommendations in the Guide for the Care and Use of Laboratory Animals of the Institute of Hydrobiology, Chinese Academy of Sciences.

Statistical Analysis

Probability (*P*) values were calculated by two-way analysis of variance and least-significant difference (LSD) or Student's *t*-test, as stated in the figure legends, and they were considered significantly different if the *P*-values were less than 0.05.

RESULTS

EvpQ Is a Novel Secreted Protein

To understand the strategies that *Edwardsiella* spp. use to combat host immune system, our previous study searched new proteins secreted by T3SS through comparative proteomics on the extracellular proteins of the Δ*esaB* and Δ*esaB*Δ*esaN* strains. This approach is based on the fact that the *spiC* mutant over-secretes the *Salmonella* pathogenesis island-2 (SPI-2) effector proteins (Yu et al., 2004). *E. piscicida* EsaB is homologous with *Salmonella* SpiC (Liu et al., 2017). EsaN is an ATPase that energizes the transportation of T3SS effectors (Xie et al., 2010). The protein encoded by ORF02740 was found to be slightly hyper-secreted by Δ*esaB*Δ*esaN* strain than by Δ*esaB* strain (data not shown). This suggests that ORF02740 is secreted, not depending on T3SS. We named this protein as EvpQ (*Edwardsiella* virulent protein Q).

To corroborate the secretion of EvpQ from the comparative proteomics, a 2HA tag was introduced at the C-terminal of *evpQ* on the genome of *E. piscicida* wild-type 130/91 and its isogenic Δ*esaB* strain. The secretion of EvpQ was probed with anti-HA

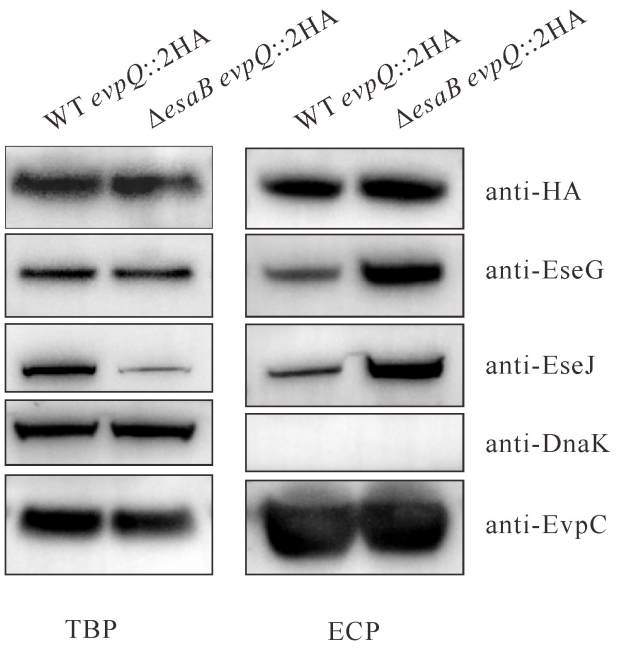

FIGURE 1 | EvpQ is secreted by *Edwardsiella piscicida* in a manner different from T3SS effectors. Five percent of bacterial pellets (TBPs) and 10% of culture supernatants (ECPs) from similar amounts of WT *evpQ*:2HA and Δ*esaB evpQ*:2HA strains grown in Dulbecco's modified Eagle's medium (DMEM) were separated using sodium dodecyl sulfate polyacrylamide gel electrophoresis (SDS-PAGE) and transferred onto polyvinylidene fluoride (PVDF) membranes for probing with anti-HA (EvpQ), anti-EseG, anti-EseJ, anti-DnaK, and anti-EvpC.

antibody. EvpC, a major protein secreted via T6SS was used as a loading control (Zheng and Leung, 2007). As shown in **Figure 1**, dramatically increased secretion of T3SS effectors EseG and EseJ was detected from the Δ*esaB* strain as compared with the wild-type strain; however, no secretion difference can be discerned for EvpQ. Chaperone protein DnaK was not detected from the ECPs, indicating that the detection of EvpQ from the ECPs is not due to leakage from bacterial pellets (**Figure 1**). These results indicate that EvpQ is secreted in a manner different from T3SS effectors.

The *evpQ* gene encodes a peptide of 173-amino acid residues with a predicted molecular mass of 20.1 kDa, and a predicated isoelectric (pI) point of 9.3. Homologs of EvpQ were not detected from the other species of *Edwardsiella*, such as *Edwardsiella ictaluri* 93–146, *Edwardsiella anguillarum* ET080813, *Edwardsiella hoshinae* ATCC 35051, or *Edwardsiella tarda* KC-Pc-HB1. Using InterPro[1] for informative analysis, the EvpQ protein was found to belong to peptidase_C70 super family. SWISS-MODEL analysis reveals that EvpQ shares 23.91% identity with type III effector protein AvrRpt2 from *Erwinia amylovora*. AvrRpt2 is a T3SS effector that manipulates the host to evade proteolysis (Mudgett and Staskawicz, 1999; Shindo and Van der Hoorn, 2008). The EvpQ protein was thereof speculated to be a novel virulence factor of *E. piscicida*.

[1]http://www.ebi.ac.uk/interpro/scan.html

EvpQ Is Secreted at a T6SS-Dependent Manner

T6SS plays a pivotal role in the pathogenesis of *E. piscicida* (Zheng and Leung, 2007). To investigate if EvpQ is secreted through T6SS, the pACYC-*evpQ*-HA was introduced into *E. piscicida* wild-type PPD130/91, T6SS-deficient Δ*evpO* strain, and T3SS-deficient Δ*esaN* strain. The expression of T3SS and T6SS was induced by culturing the aforementioned strains in DMEM. EvpO is an ATPase that energizes the transportation of T6SS substrates (Zheng and Leung, 2007). It was observed that the secretion of EvpQ was dependent totally on T6SS and not through T3SS (**Figure 2A**). The expression and secretion of T3SS effector EseG and T6SS substrate EvpC were examined as the control. As expected, EseG was not secreted from the Δ*esaN* strain and EvpC not from the Δ*evpO* strain, indicating that the strains are correct. EseG was not detected from the ECP of the Δ*esaN* strain, indicating that the detection of EvpQ from the Δ*esaN* strain is not due to its leakage from bacterial pellets (**Figure 2A**). Together, these results demonstrate that EvpQ depends on an active T6SS for its secretion.

Some regulators can also be secreted through bacterial secretion system, and deletion of regulator gene changes the extracellular protein profile (Rietsch et al., 2005). To learn whether EvpQ could be a secreted regulator, we examined the extracellular and intracellular protein profiles (ECPs and TBPs) of *E. piscicida* wild-type strain, Δ*evpQ* strain, and Δ*evpQ*/pACYC-*evpQ*-HA strain. As shown in **Figure 2B**, depletion or overexpression of EvpQ did not change the extracellular or intracellular protein profile of the *E. piscicida* strains. This result suggests that EvpQ is not a secreted regulator, and it could be a T6SS effector.

EvpQ Is Translocated Into Host Cells

Will EvpQ be translocated into host cells? To answer this question, we constructed a reporter plasmid pACYC-*evpQ*::*cyaA*, expressing a chimeric protein EvpQ::CyaA, as described by Lu et al. (2016). When the CyaA fusion is translocated into the host cell cytoplasm, CyaA will convert ATP into cAMP in the presence of the eukaryotic-cell cytoplasmic protein calmodulin. The increase of cAMP is taken as the translocation of EvpQ protein. This method has been used in many pathogenic bacteria, including *E. piscicida*, to successfully monitor the translocation of bacterial T3SS effectors (Sory and Cornelis, 1994; Casper-Lindley et al., 2002; Xie et al., 2015). The pACYC-*evpQ*::*cyaA* was introduced into *E. piscicida* strains to infect EPC cells. At 2 h post-infection (hpi), the cAMP levels inside EPC cells were measured as a readout of translocation of EvpQ::*CyaA*. As shown in **Figure 2C**, the cAMP level in WT/pACYC-*eseG*::*cyaA*-infected cells was examined as the positive control (423.46 ± 70.12 fmol/μg protein), and in Δ*esaN*/pACYC-*eseG*::*cyaA*-infected cells as the negative control (18.86 ± 8.75 fmol/μg protein). It was found that the cAMP level in WT/pACYC-*evpQ*::*cyaA*-infected cells was 7.97 ± 3.59 fmol/μg protein, in Δ*esaN*/pACYC-*evpQ*::*cyaA*-infected cells was 17.65 ± 7.27 fmol/μg protein, and in Δ*evpO*/pACYC-*evpQ*::*cyaA*-infected cells was

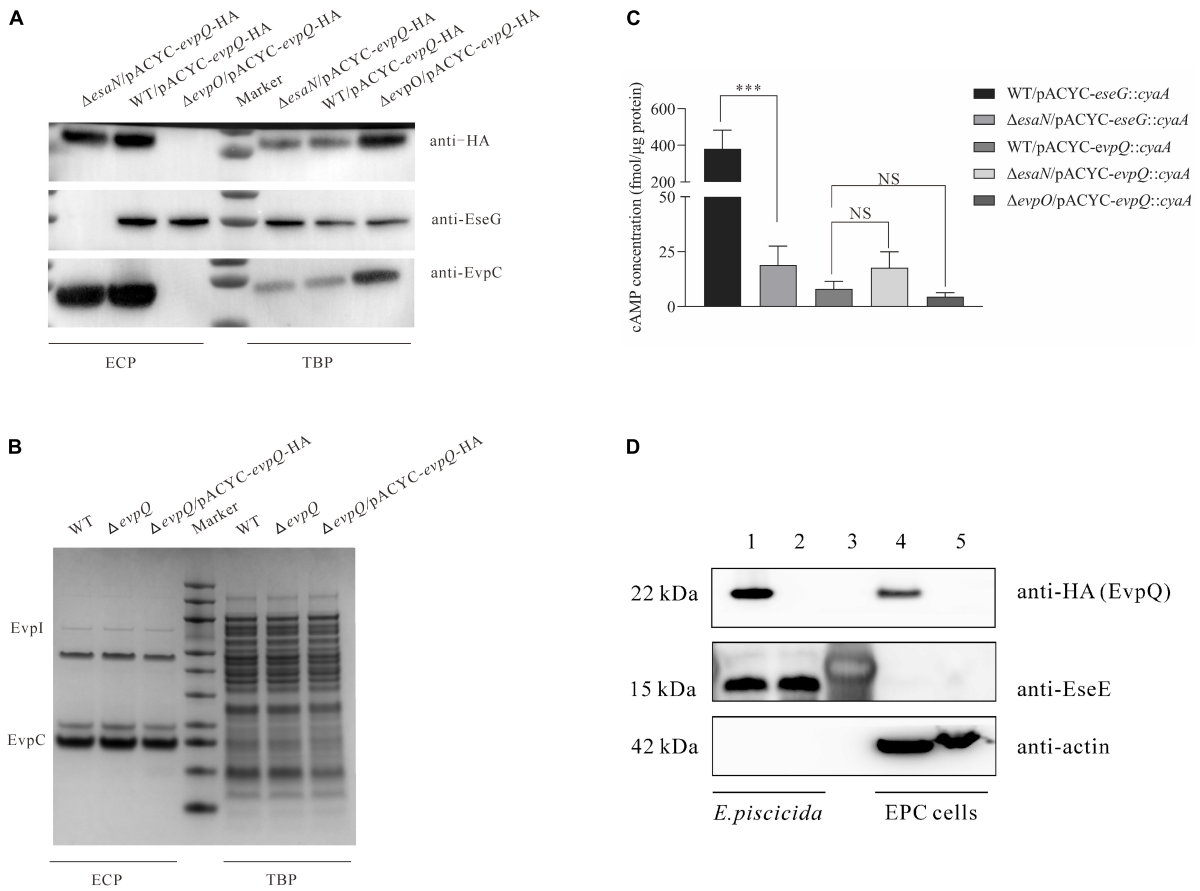

FIGURE 2 | EvpQ is secreted at a T6SS-dependent manner and is translocated into eukayotic host. **(A)** EvpQ is secreted at a T6SS-dependent manner. TBPs and ECPs from each strain grown in DMEM were harvested at stationary phase, and equal amount of TBPs and ECPs were loaded for separating by SDS-PAGE and transferred onto PVDF membranes for immunoblotting. **(B)** Extracellular and intracellular profiles of *E. piscicida* strains. ECPs from similar amounts of *E. piscicida* strains grown in DMEM were separated using SDS-PAGE and stained with Coomassie blue. EvpI, EvpP, and EvpC are T6SS proteins secreted. **(C)** EvpQ does not depend on T3SS for its translocation. The EPC cells were infected with *E. piscicida* strains transformed with pACYC-*evpQ*::*cyaA*. At 2 h post-infection, the EPC monolayers were processed to examine the intracellular cAMP level as described in section "Materials and Methods." Means ± SD from one representative experiment was shown. ***$P < 0.001$; NS, not significant. **(D)** EvpQ is translocated into host cells. EPC cells were infected, respectively, with WT *evpQ*::2HA strain and Δ*evpQ* strain before fractionation by mechanical disruption. Cell lysates of EPC cells and bacteria were analyzed by immunoblotting using anti-HA, anti-EseE, and anti-actin antibodies. Lanes 1–2, *E. piscicida* cell lysates of WT *evpQ*::2HA strain and Δ*evpQ* strain, respectively; lane 3, protein marker; lanes 4–5, cell lysates of EPC cells infected, respectively, with WT *evpQ*::2HA strain and Δ*evpQ* strain.

4.45 ± 1.89 fmol/μg protein. No significant difference of cAMP levels was detected from the three strains examined. These data demonstrate that EvpQ is not translocated into host cells in a T3SS-dependent manner. However, we could not draw a conclusion that EvpQ cannot be translocated into host cells through T6SS. Considering that the cAMP system was primarily set up for T3SS effector identification (Sory and Cornelis, 1994), moreover, EvpQ is fused at the N-termini of CyaA (501 aa), this results in a large fusion protein, which could have blocked its translocation through T6SS tail tube.

Next, we labeled *evpQ* on the genome with 2HA tag (18 aa) using the λ Red recombinase method (Datsenko and Wanner, 2000). To localize EvpQ in infected host cells, EPC cells infected with the *E. piscicida* WT *evpQ*::2HA and Δ*evpQ* strains were subjected to mechanic fractionation. Actin was used as marker of host cell component in EPC cells. EseE, a T3SS chaperone of EseC (Yi et al., 2016), was used as a marker of bacterial components. EvpQ-2HA, but not EseE, was detected from the supernatants of the infected EPC cell lysates (cytosol and membrane) (**Figure 2D**). This indicates that this fraction was not contaminated by the bacteria. This data provide evidence on the translocation of EvpQ into EPC cells. Taken together, we have demonstrated that EvpQ is a T6SS effector that is translocated into eukaryotic host cells.

EvpQ Facilitates the Replication of *E. piscicida* in Blue Gourami Infection Model

The role of EvpQ in the pathogenesis of *E. piscicida* was investigated in blue gourami infection model by using CI assay. The equal number of the Δ*evpQ*:*km* strain and wild-type strain

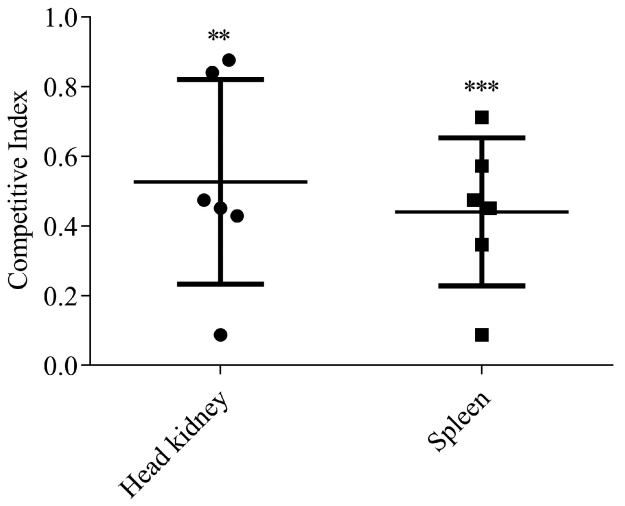

FIGURE 3 | The Δ*evpQ* strain is less competitive than wild-type *E. piscicida*. Six naïve blue gourami fish were injected intramuscularly with a mixture of equal numbers of wild-type and Δ*evpQ*::*km* strains and killed 48 h post-injection. CIs from spleen and head kidney were given for individual fish, and means ± SD were shown by the horizontal lines. Student's *t* test was used to calculate the *P*-value with the hypothetical mean of 1.0. ***$P < 0.001$; **$P < 0.01$.

were mixed to inject blue gourami fish i.m. at 1×10^5 CFU per fish. At 48 h post-inoculation, spleen and head kidney were dissected to determine the amount of Δ*evpQ*:*km* and wild-type strains. The CIs from head kidney were 0.53 ± 0.27, and the CIs from spleen were 0.44 ± 0.19 (**Figure 3**). As the CIs were significantly less than 1.0, we conclude that the deletion of *evpQ* significantly attenuates the virulence of *E. piscicida* PPD130/91.

EvpQ Is Encoded by a Genomic Island, a Mobile Genetic Element

With the help of MGE, many bacteria have accessorized their genomes with DNA from bacteria outside of their species or genus. The most common MGEs of horizontal transfer are genomic islands (GIs), plasmids, and bacteriophages. GIs are areas of the genome that are flanked by specific DNA sequences, which contain direct repeats and are often inserted in highly conserved genes, e.g., tRNA genes. The specific DNA sequences also carry genes coding for genetic mobility such as transposases (Jackson et al., 2011). The *evpQ* gene (*orf* 02740) is spaced by 513 genes from *evpP* (*orf* 03254), the first gene of the T6SS gene cluster. Three consecutive tRNA genes and three IS903 transposase genes were found upstream of *evpQ* (**Figure 4**). Moreover, by the DNAstar analysis, the mean GC content of this MGE that *evpQ* localizes is 49.0%, which is much lower than that of the genome of *E. piscicida* PPD130/91 (59.8%). This indicates that EvpQ is encoded by horizontal transferred genomic island. Besides, TssA was also encoded by the same the GI. TssA protein is reported to play a role in coordinating T6SS inner tube/sheath assembly (Dix et al., 2018). This indicates that the genomic island is probably a pathogenicity island.

Transcription of *evpQ* Is Positively Regulated by EsrC and Negatively by Fur

RpoS inhibits *E. piscicida* T6SS by blocking RpoD-mediated transcription of *esrB* (Yin et al., 2018). EsrB positively regulates T6SS through EsrC (Tan et al., 2005; Zheng et al., 2005; Chakraborty et al., 2011). EsrC and Fur compete to bind directly to the Fur box in the promoter of *evpP* (Chakraborty et al., 2011). To learn whether these proteins also regulate the transcription of the novel T6SS effector EvpQ, a DNA fragment (bp -594 to -1) upstream of *evpQ* was inserted into the promoterless *gfp* shuttle vector pFPV25 to create pFPV-594 to -1. The resulting construct (pFPV-594 to -1) was introduced into *E. piscicida* WT, Δ*rpoS*, Δ*fur*, Δ*esrB*, and Δ*esrC* strain, respectively. At 8-, 18-, and 24-h post-subculture (hps) in DMEM, the activity of this putative promoter in the aforementioned strains were tested with a microplate reader (Synergy neo2, Biotek, United States). As seen in **Figure 5A**, similar levels of fluorescent intensity were detected from the Δ*rpoS* strain and wild-type strain, whereas dramatically elevated fluorescence intensity was detected from the Δ*fur* strain, and sharply decreased levels of fluorescence intensity were detected in the Δ*esrC* strain at each time point examined (8, 18, and 24 hps). These data indicate that when culturing in DMEM, *evpQ* is negatively regulated by Fur and positively regulated by EsrC; however, RpoS seems not to be involved in the transcription of *evpQ*.

The Steady-State Protein Level of EvpQ Is Negatively Controlled by RpoS

The steady-state protein level of EvpQ in the aforementioned strains was examined. As shown in **Figure 5B**, similar levels of steady-state EvpQ were detected from WT, Δ*rpoS*, and Δ*fur* strain at 8 hps. At 18 or 24 hps, the steady-state protein level of EvpQ increased slightly in WT or Δ*fur* strain, meanwhile it increased starkly in Δ*rpoS* strain and reached maximum at 24 hps. As a control, protein level of type III effector EseG was examined. It was found that EseG was also negatively controlled by RpoS. The highest protein level of EseG was detected in Δ*rpoS* strain at 8 hps, and it deceases with its growth. Equal amounts of proteins were loaded per lane as indicated by the DnaK protein level. These data indicate that both EvpQ and EseG are negatively controlled by RpoS, and intracellular EvpQ increases while EseG decreases with its growth.

The Expression and Secretion of EvpQ Are Influenced by Temperature

Edwardsiella piscicida PhoQ sensor domain detects temperatures through a conformational change of its secondary structure, and it regulates the types III and VI secretion systems through direct activation of *esrB* (Chakraborty et al., 2010). *E. piscicida* types III and VI secretion systems are activated from 23 to 35°C, but they are suppressed at or below 20°C, at or above 37°C. Will the protein level of EvpQ be subject to temperature? To answer this question, we compared the intracellular and extracellular protein levels of EvpQ at 25, 35, and 37°C from the WT *evpQ*::2HA strain cultured in DMEM. As shown in **Figure 5C**, the expression and secretion of EvpQ decreased sharply at 35°C as compared

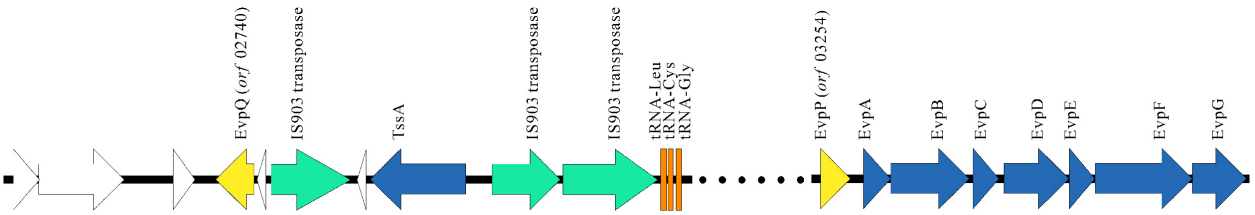

FIGURE 4 | EvpQ is encoded by a genomic island far outsides T6SS gene cluster. Gene organization of T6SS gene cluster and the GI that encodes EvpQ. Data were from reference (Zheng and Leung, 2007) and our laboratory. Open reading frames with identifiable orthologs in the horizontal transferred fragment are labeled. Yellow arrows, T6SS effector genes; azure arrows, T6SS apparatus genes; green arrows, transposase genes; orange arrows, tRNA genes; white arrows, hypothetical genes.

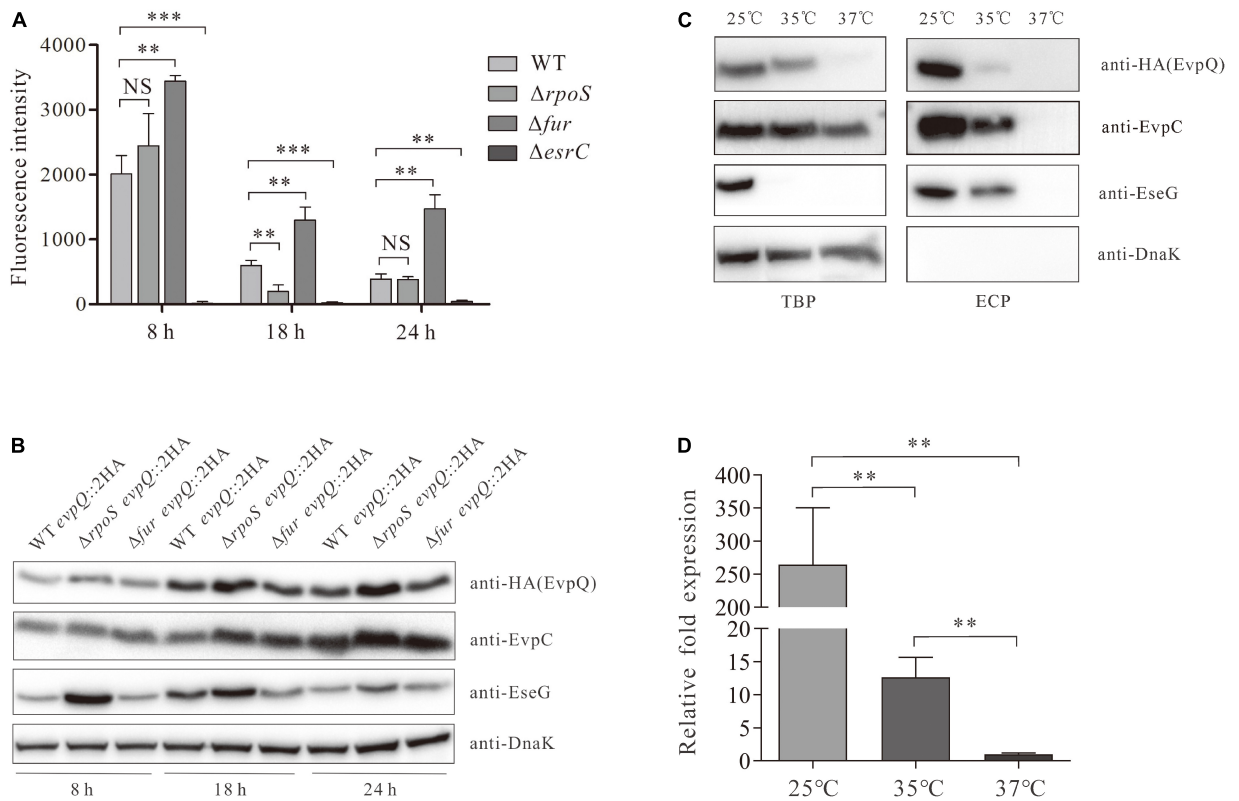

FIGURE 5 | EvpQ is under the control of EsrC, RpoS, Fur, and temperature. **(A)** Comparison of the transcriptional level of *evpQ* in WT, Δ*esrC*, Δ*rpoS*, and Δ*fur* strains. The DNA fragment (bp -594 to -1) upstream of *evpQ* was inserted into the promoterless *gfp* shuttle vector pFPV25 to create pFPV-*evpQ*$_{-594to\ -1}$. This plasmid was then introduced into *E. piscicida* strains. At 8, 18, and 24 hps in DMEM, the fluorescence intensity of those *E. piscicida* strains were evaluated by using a microplate reader. Means ± SD from one representative experiment was shown. ***$P < 0.001$; **$P < 0.01$; NS, not significant. **(B)** Examination on the steady-state protein level of EvpQ in different *E. piscicida* strains at 8-, 18-, and 24-h post-subculture in DMEM. This experiment was repeated separately for at least three times, and one representative blot was shown. **(C)** The expression and secretion of EvpQ from *E. piscicida* wild type cultured in DMEM at different temperatures. ECPs and TCPs from similar amounts of the WT *evpQ*:2HA cultured at 25, 35, or 37°C were probed with anti-HA, anti-EvpC, anti-EseG, and anti-DanK antibodies. **(D)** The transcription levels of *evpQ* from *E. piscicida* wild type cultured in DMEM at different temperatures. The mRNA levels of *evpQ* from the wild-type strain cultured at 25, 35, or 37°C were examined by qRT-PCR. 16S rRNA was used as the reference gene. Transcription levels of *evpQ* relative to that of 16S rRNA are presented (i.e., relative fold changes in gene expression). Data are presented as means ± SD. **$P < 0.01$.

with that at 25°C, and EvpQ almost failed to be detected from TBP and ECP when WT *evpQ*::2HA strain was cultured at 37°C. Meanwhile, the secretion level of T3SS effector EseG mildly decreased at 35°C as compared with that at 25°C. This indicates that T6SS effector EvpQ is more susceptible to temperature change than T3SS effector EseG.

To investigate whether the decreased steady-state protein level of EvpQ resides in the decreased transcription level of *evpQ* when the culture temperature increases. We compared the transcript levels of *evpQ* gene from the wild-type strain cultured at 25, 35, and 37°C, respectively. 16S rRNA was used as the reference gene. The transcript levels of *evpQ* were

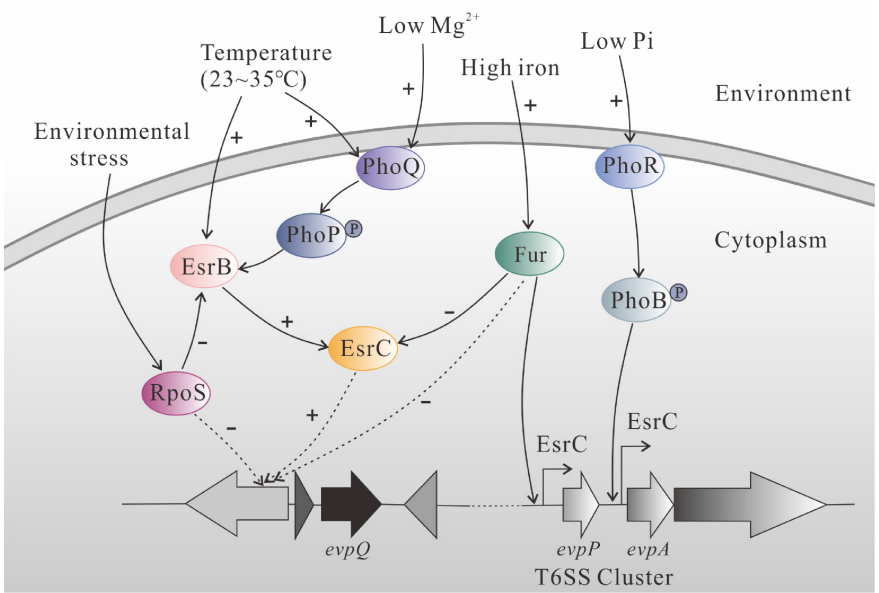

FIGURE 6 | Schematic diagram of regulatory network of EsrC, RpoS, and Fur on EvpQ and T6SS gene cluster in *E. piscicida* PPD130/91, based on reference papers and our results from the current study. PhoQ senses the change of ambient temperature (23~35°C) and transmits the signal to PhoP, and the phosphorylated PhoP binds directly to the PhoP box within the promoter region of *esrB* to activate its transcription (Chakraborty et al., 2010). The activated EsrB protein upregulates the transcription of T6SS through EsrC (Zheng et al., 2005; Chakraborty et al., 2010). High concentration of iron activates the Fur protein, and activated Fur binds directly to the Fur box in the promoter of T6SS effector gene *evpP*. The binding of Fur inhibits the binding of EsrC to the same region (Chakraborty et al., 2011). The EvpQ encoded by the genomic island is also negatively regulated by Fur and positively regulated by EsrC, while it remains to be resolved whether EsrC and Fur directly bind the promoter of *evpQ*. The sigma factor RpoS, antagonizing the expression of *esrB* (Yin et al., 2018), negatively controls the expression of EvpQ.

significantly ($P < 0.01$) downregulated by 265- and 21-fold, respectively, at 37 and 35°C when comparing with that at 25°C, and downregulated by 13-fold when comparing between 37 and 35°C (**Figure 5D**). Thus, the deceased expression level of EvpQ is due to the decreased transcription of *evpQ* with the elevation of culture temperature.

DISCUSSION

T6SS is a versatile machinery playing roles in both pathogenesis and interbacterial competition by translocating T6SS effectors. T6SS effectors are loaded into the inner tube or associate with the spike trimer during T6SS assembly (Silverman et al., 2013; Flaugnatti et al., 2016; Hernandez et al., 2020). Contraction of the sheath propels the inner tube/spike, which allows perforation of the target cell membrane, delivering effectors into the cytosol of target cells (Journet and Cascales, 2016). Sory and Cornelis (1994) set up a system to examine the translocation of T3SS effector. By this method, effector candidate was fused at the N-terminal of CyaA, and CyaA converts ATP into cAMP in the presence of calmodulin when the fusion protein is translocated into host cell cytoplasm. The increase in cAMP of taken as the translocation of T3SS effector candidate. In this study, EvpQ was fused at the N-terminal of CyaA (501 aa), while we failed to detect the translocation of EvpQ::CyaA into EPC cells. It is speculated that this method may not be applicable to indicate the translocation of T6SS effector. On one aspect, the large size of the fusion protein may block its translocation through T6SS inner tube; on the other aspect, the fusion of CyaA to EvpQ could have changed the ability of EvpQ to attach to spike trimer, thereof disabling its translocation. When 2HA tag (18 aa) was fused at the C-terminal of *evpQ* on the genome, the translocation of EvpQ::2HA (191 aa) was successfully detected by mechanic fractionation of EPC cells infected. EvpQ::2HA could have been translocated through the T6SS tail tube.

EsrB elaborately controls T6SS expression through EsrC (Zheng et al., 2005). Fur requires iron binding for its activity, and the activated Fur binds to promoters of iron-responsive genes to repress their transcription under iron replete conditions (Escolar et al., 1999). Fur was reported to represses *Salmonella* SPI-2 expression that is activated inside macrophages and under acidic conditions (Choi et al., 2014). In *E. piscicida*, Fur senses high iron concentration and binds directly to the Fur box in the promoter of *evpP* to inhibit EsrC's binding to the same region (Chakraborty et al., 2011). EvpQ was negatively regulated by Fur and positively regulated by EsrC. Whether Fur and EsrC compete in binding with the promoter of EvpQ awaits further study. Moreover, we revealed in this study that the steady-state protein level of EvpQ was negatively controlled by RpoS when *E. piscicida* was cultured in DMEM. Accordingly, Yin et al. (2018) revealed that ETAE_2037 of *E. piscicida* EIB202 (renamed as EvpQ in the current study) was negatively regulated by the sigma factor RpoS when cultured in DMEM, as revealed by RNAseq. Our study failed to detect the difference in the transcription of *evpQ* between wild-type and Δ*rpoS* strains at 8 and 24 hps. This is probably

due to the low sensibility of fluorescence detection system, when comparing with the RNAseq assay.

Based on references and our results, we drew a schematic diagram to summarize regulatory role of EsrC, RpoS, and Fur on EvpQ and T6SS gene cluster (**Figure 6**). PhoQ senses the change of the ambient temperature (23∼35°C) and transmits the signal to PhoP, and the phosphorylated PhoP binds directly to the PhoP box within the promoter region of *esrB* to activate its transcription (Chakraborty et al., 2010). The activated EsrB protein upregulates the transcription of T6SS through EsrC (Zheng et al., 2005: Chakraborty et al., 2010). High concentration of iron activates the Fur protein, the activated Fur binds directly to the Fur box in the promoter of T6SS effector gene *evpP*, and the binding of Fur inhibits the binding of EsrC to the same region (Chakraborty et al., 2011). The novel T6SS effector *evpQ* that is localized on the genomic island is also negatively regulated by Fur and positively regulated by EsrC; it remains to be resolved in the near future whether or not EsrC and Fur binds the promoter of *evpQ* directly. RpoS can block RpoD-mediated transcription of *esrB*, antagonizing the expression of *esrB*, thereof inhibiting the expression of *E. piscicida* T6SS proteins (Yin et al., 2018). RpoS negatively controls the expression of EvpQ. RpoS represses promoters containing a -6G in their respective discriminator sequences (Yin et al., 2018). Whether or not RpoS represses EvpQ through binding to a -6G in the promoter of *evpQ* awaits further study.

EvpQ is encoded by a genomic island, and it exists only in *E. piscicida* but not in any other species of the genus *Edwardsiella*, such as *E. ictaluri*, *E. anguillarum*, *E. hoshinae*, or *E. tarda*. Alike EvpQ, GtgE localizes on the Gifsy-2 prophage of *Salmonella* Typhimurium (Ho et al., 2002). *S.* Typhimurium can infect a broad range of vertebrate species, whereas *Salmonella* Typhi only infects humans. GtgE is not encoded by *S.* Typhi, and introducing GtgE into *S.* Typhi enables this human-adapted serovar to survive within non-permissive host cells (Spanò and Galán, 2012). *E. ictaluri* only infects fish in the *siluriformes*, while *E. piscicida* infects fish from wide orders. It is interesting to investigate in the future whether introducing EvpQ into *E. ictaluri* extends its hosts or not.

EvpQ shares similarity with papain-like cysteine protease AvrRpt2, which suppresses plant immunity by modulating auxin signaling and cleavage of the membrane localized defense regulator RIN4 (Axtell et al., 2003; Mackey et al., 2003; Cui et al., 2013). AvrRpt2 also specifically suppresses pathogen-associated molecular pattern (PAMP)-induced activation of MPK4 and MPK11 but not of MPK3 and MPK6 (Eschen-Lippold et al., 2016). Whether EvpQ manipulate and fine-tune MPK signaling pathway upon its translocation into fish hosts awaits further investigation.

DATA AVAILABILITY STATEMENT

The original contributions presented in the study are included in the article/supplementary material, further inquiries can be directed to the corresponding author.

ETHICS STATEMENT

The animal study was reviewed and approved by the Animal Ethical and Welfare Committee, Institute of Hydrobiology, Chinese Academy of Sciences.

AUTHOR CONTRIBUTIONS

DL, YL, XL, TH, and SS performed the experiments and prepared materials for the manuscript. HX and PN designed and supervised the experiments, and interpreted the data. DL, YL, and HX wrote the manuscript. All authors contributed to the article and approved the submitted version.

FUNDING

This work was funded by the National Key Research and Development Program of China (No. 2018YFD0900504) and National Natural Science Foundation of China (No. U1706205).

REFERENCES

Abayneh, T., Colquhoun, D. J., and Sørum, H. (2013). *Edwardsiella piscicida* sp. nov., a novel species pathogenic to fish. *J. Appl. Microbiol.* 114, 644–654. doi: 10.1111/jam.12080

Axtell, M. J., Chisholm, S. T., Dahlbeck, D., and Staskawicz, B. J. (2003). Genetic and molecular evidence that the *Pseudomonas syringae* type III effector protein AvrRpt2 is a cysteine protease. *Mol. Microbiol.* 49, 1537–1546. doi: 10.1046/j.1365-2958.2003.03666.x

Casper-Lindley, C., Dahlbeck, D., Clark, E. T., and Staskawicz, B. J. (2002). Direct biochemical evidence for type III secretion-dependent translocation of the AvrBs2 effector protein into plant cells. *Proc. Natl. Acad. Sci. U.S.A.* 99, 8336–8341. doi: 10.1073/pnas.122220299

Chakraborty, S., Li, M., Chatterjee, C., Sivaraman, J., Leung, K. Y., and Mok, Y.-K. (2010). Temperature and Mg^{2+} sensing by a novel PhoP-PhoQ two-component system for regulation of virulence in *Edwardsiella tarda*. *J. Biol. Chem.* 285, 38876–38888. doi: 10.1074/jbc.m110.179150

Chakraborty, S., Sivaraman, J., Leung, K. Y., and Mok, Y. K. (2011). Two-component PhoB-PhoR regulatory system and ferric uptake regulator sense phosphate and iron to control virulence genes in type III and VI secretion systems of *Edwardsiella tarda*. *J. Biol. Chem.* 286, 39417–39430. doi: 10.1074/jbc.m111.295188

Chen, H., Yang, D., Han, F., Tan, J., Zhang, L., Xiao, J., et al. (2017). The Bacterial T6SS effector EvpP prevents NLRP3 inflammasome activation by inhibiting the Ca^{2+}-dependent MAPK-Jnk pathway. *Cell Host Microbe* 21, 47–58. doi: 10.1016/j.chom.2016.12.004

Choi, E., Kim, H., Lee, H., Nam, D., Choi, J., and Shin, D. (2014). The iron-sensing *fur* regulator controls expression timing and levels of *Salmonella* pathogenicity island 2 genes in the course of environmental acidification. *Infect. Immun.* 82, 2203–2210.

Coombes, B. K., Lowden, M. J., Bishop, J. L., Wickham, M. E., Brown, N. F., Duong, N., et al. (2007). SseL is a *Salmonella*-specific translocated effector integrated into the SsrB-controlled *Salmonella* pathogenicity island 2 type III secretion system. *Infect. Immun.* 75, 574–580.

Cui, F., Wu, S., Sun, W., Coaker, G., Kunkel, B., He, P., et al. (2013). The *Pseudomonas syringae* type III effector AvrRpt2 promotes pathogen virulence via stimulating *Arabidopsis* auxin/indole acetic acid protein turnover. *Plant Physiol.* 162, 1018–1029. doi: 10.1104/pp.113.219659

Datsenko, K. A., and Wanner, B. L. (2000). One-step inactivation of chromosomal genes in *Escherichia coli* K-12 using PCR products. *Proc. Natl. Acad. Sci. U.S.A.* 97, 6640–6645. doi: 10.1073/pnas.120163297

Dix, S. R., Owen, H. J., Sun, R., Ahmad, A., Shastri, S., Spiewak, H. L., et al. (2018). Structural insights into the function of type VI secretion system TssA subunits. *Nat. Commun.* 9:4765. doi: 10.1038/s41467-018-07247-1

Edwards, R. A., Keller, L. H., and Schifferli, D. M. (1998). Improved allelic exchange vectors and their use to analyze 987P fimbria gene expression. *Gene* 207, 149–157. doi: 10.1016/S0378-1119(97)00619-7

Eschen-Lippold, L., Jiang, X., Elmore, J. M., Mackey, D., Shan, L., Coaker, G., et al. (2016). Bacterial AvrRpt2-like cysteine proteases block activation of the *Arabidopsis* mitogen-activated protein kinases, MPK4 and MPK11. *Plant Physiol.* 171, 2223–2238. doi: 10.1104/pp.16.00336

Escolar, L., Perez-Martin, J., and de Lorenzo, V. (1999). Opening the iron box: transcriptional metalloregulation by the Fur protein. *J. Bacteriol.* 181, 6223–6229. doi: 10.1128/jb.181.20.6223-6229.1999

Flaugnatti, N., Le, T. T., Canaan, S., Aschtgen, M. S., Nguyen, V. S., Blangy, S., et al. (2016). A phospholipase A1 antibacterial type VI secretion effector interacts directly with the C-terminal domain of the VgrG spike protein for delivery. *Mol. Microbiol.* 99, 1099–1118. doi: 10.1111/mmi.13292

Hernandez, R. E., Gallegos-Monterrosa, R., and Coulthurst, S. J. (2020). Type VI secretion system effector proteins: effective weapons for bacterial competitiveness. *Cell. Microbiol.* 22:e13241. doi: 10.1111/cmi.13241

Ho, T. D., Figueroa-Bossi, N., Wang, M., Uzzau, S., Bossi, L., and Slauch, J. M. (2002). Identification of GtgE, a novel virulence factor encoded on the Gifsy-2 bacteriophage of *Salmonella enterica* serovar Typhimurium. *J. Bacteriol.* 184, 5234–5239. doi: 10.1128/jb.184.19.5234-5239.2002

Jackson, R. W., Vinatzer, B., Arnold, D. L., Dorus, S., and Murillo, J. (2011). The influence of the accessory genome on bacterial pathogen evolution. *Mob. Genet. Elements* 1, 55–65. doi: 10.4161/mge.1.1.16432

Journet, L., and Cascales, E. (2016). The type VI secretion system in *Escherichia coli* and related species. *EcoSal Plus.* 7. doi: 10.1128/ecosalplus.esp-0009-2015

Ling, S. H. M., Wang, X. H., Xie, L., Lim, T. M., and Leung, K. Y. (2000). Use of green fluorescent protein (GFP) to track the invasive pathways of *Edwardsiella tarda* in the *in vivo* and *in vitro* fifish models. *Microbiology* 146, 7–19. doi: 10.1099/00221287-146-1-7

Liu, L. Y., Nie, P., Yu, H. B., and Xie, H. X. (2017). Regulation of type III secretion of translocon and effector proteins by the EsaB/EsaL/EsaM complex in *Edwardsiella tarda*. *Infect. Immun.* 85:e00322-17. doi: 10.1128/iai.00322-17

Lu, J. F., Wang, W. N., Wang, G. L., Zhang, H., Zhou, Y., Gao, Z. P., et al. (2016). *Edwardsiella tarda* EscE (Orf13 protein) is a type III secretion system-secreted protein that is required for the injection of effectors, secretion of translocators, and pathogenesis in fish. *Infect. Immun.* 84, 2–10. doi: 10.1128/iai.00986-15

Ma, A. T., McAuley, S., Pukatzki, S., and Mekalanos, J. J. (2009). Translocation of a *Vibrio cholerae* type VI secretion effector requires bacterial endocytosis by host cells. *Cell Host Microbe* 5, 234–243. doi: 10.1016/j.chom.2009.02.005

Mackey, D., Belkhadir, Y., Alonso, J. M., Ecker, J. R., and Dangl, J. L. (2003). Arabidopsis RIN4 is a target of the type III virulence effector AvrRpt2 and modulates RPS2-mediated resistance. *Cell* 112, 379–389. doi: 10.1016/S0092-8674(03)00040-0

Matsuyama, T., Kamaishi, T., Ooseko, N., Kurohara, K., and Iida, T. (2005). Pathogenicity of motile and non-motile *Edwardsiella tarda* to some marine fish. *Fish Pathol.* 40, 133–135.

Mohanty, B. R., and Sahoo, P. K. (2007). Edwardsiellosis in fish: a brief review. *J. Biosci.* 32, 1331–1344.

Mudgett, M. B., and Staskawicz, B. J. (1999). Characterization of the *Pseudomonas syringae* pv. tomato AvrRpt2 protein: demonstration of secretion and processing during bacterial pathogenesis. *Mol. Microbiol.* 32, 927–941. doi: 10.1046/j.1365-2958.1999.01403.x

Okuda, J., Arikawa, Y., Takeuchi, Y., Mahmoud, M. M., Suzaki, E., Kataoka, K., et al. (2006). Intracellular replication of *Edwardsiella tarda* in murine macrophage is dependent on the type III secretion system and induces an up-regulation of anti-apoptotic NF-kappaB target genes protecting the macrophage from staurosporine-induced apoptosis. *Microb. Pathog.* 41, 226–240. doi: 10.1016/j.micpath.2006.08.002

Padrós, F., Zarza, C., Dopazo, L., Cuadrado, M., and Crespo, S. (2006). Pathology of *Edwardsiella tarda* infection in turbot, *Scophthalmus maximus* (L.). *J. Fish Dis.* 29, 87–94.

Pukatzki, S., Ma, A. T., Revel, A. T., Sturtevant, D., and Mekalanos, J. J. (2007). Type VI secretion system translocates a phage tail spike-like protein into target cells where it cross-links actin. *Proc. Natl. Acad. Sci. U.S.A.* 104, 15508–15513. doi: 10.1073/pnas.0706532104

Pukatzki, S., Ma, A. T., Sturtevant, D., Krastins, B., Sarracino, D., Nelson, W. C., et al. (2006). Identification of a conserved bacterial protein secretion system in *Vibrio cholerae* using the *Dictyostelium* host model system. *Proc. Natl. Acad. Sci. U.S.A.* 103, 1528–1533. doi: 10.1073/pnas.0510322103

Rietsch, A., Vallet-Gely, I., Dove, S. L., and Mekalanos, J. J. (2005). ExsE, a secreted regulator of type III secretion genes in *Pseudomonas aeruginosa*. *Proc. Natl. Acad. Sci. U.S.A.* 102, 8006–8011. doi: 10.1073/pnas.0503005102

Shao, S., Lai, Q. L., Liu, Q., Wu, H. Z., Xiao, J. F., Shao, Z. Z., et al. (2015). Phylogenomics characterization of a highly virulent *Edwardsiella* strain ET080813T encoding two distinct T3SS and three T6SS gene clusters: propose a novel species as *Edwardsiella anguillarum* sp. nov. *Syst. Appl. Microbiol.* 38, 36–47. doi: 10.1016/j.syapm.2014.10.008

Shindo, T., and Van der Hoorn, R. A. (2008). Papain-like cysteine proteases: key players at molecular battlefields employed by both plants and their invaders. *Mol. Plant Pathol.* 9, 119–125. doi: 10.1111/j.1364-3703.2007.00439.x

Silverman, J. M., Agnello, D. M., Zheng, H., Andrews, B. T., Li, M., Catalano, C. E., et al. (2013). Haemolysin coregulated protein is an exported receptor and chaperone of type VI secretion substrates. *Mol. Cell* 51, 584–593.

Simon, R., Priefer, U., and Pühler, A. (1983). A broad host range mobilization system for *in vivo* genetic engineering: transposon mutagenesis in gram negative bacteria. *Nat. Biotechnol.* 1, 784–791.

Sory, M. P., and Cornelis, G. R. (1994). Translocation of a hybrid YopE adenylate-cyclase from *Yersinia enterocolitica* into HeLa cells. *Mol. Microbiol.* 14, 583–594. doi: 10.1111/j.1365-2958.1994.tb02191.x

Spanò, S., and Galán, J. E. (2012). A Rab32-dependent pathway contributes to *Salmonella* Typhi host restriction. *Science* 338, 960–963. doi: 10.1126/science.1229224

Srinivasa Rao, P. S., Yamada, Y., Yan, Y. P., and Leung, K. Y. (2004). Use of proteomics to identify novel virulence determinants that are required for *Edwardsiella tarda* pathogenesis. *Mol. Microbiol.* 53, 573–586. doi: 10.1111/j.1365-2958.2004.04123.x

Tan, Y. P., Zheng, J., Tung, S. L., Rosenshine, I., and Leung, K. Y. (2005). Role of type III secretion in *Edwardsiella tarda* virulence. *Microbiology* 151, 2301–2313. doi: 10.1099/mic.0.28005-0

Uzzau, S., Figueroa-Bossi, N., Rubino, S., and Bossi, L. (2001). Epitope tagging of chromosomal genes in *Salmonella*. *Proc. Natl. Acad. Sci. U.S.A.* 98, 15264–15269. doi: 10.1073/pnas.261348198

Valdivia, R. H., and Falkow, S. (1996). Bacterial genetics by flow cytometry: rapid versatile emerging pathogen of fish. *Virulence* 10, 555–567. doi: 10.1080/21505594.2019.1621648

Wang, X., Gong, P., Zhang, X., Wang, J., Tai, L., Wang, X., et al. (2017). NLRP3 inflammasome activation in murine macrophages caused by *Neospora caninum* infection. *Parasit. Vectors* 10:266. doi: 10.1186/s13071-017-2197-2

Wettstadt, S., and Filloux, A. (2020). Manipulating the type VI secretion system spike to shuttle passenger proteins. *PLoS One* 15:e0228941. doi: 10.1371/journal.pone.0228941

Wolf, K., and Mann, J. A. (1980). Poikilotherm vertebrate cell lines and viruses, a current listing for fishes. *In Vitro* 16, 168–179. doi: 10.1007/bf02831507

Xie, H. X., Lu, J. F., Zhou, Y., Yi, J., Yu, X. J., Leung, K. Y., et al. (2015). Identification and functional characterization of a novel *Edwardsiella tarda* effector EseJ. *Infect. Immun.* 83, 1650–1660. doi: 10.1128/IAI.02566-14

Xie, H. X., Yu, H. B., Zheng, J., Nie, P., Foster, L. J., Mok, Y. K., et al. (2010). EseG, an effector of the type III secretion system of *Edwardsiella tarda*, triggers microtubule destabilization. *Infect. Immun.* 78, 5011–5021. doi: 10.1128/iai.00152-10

Yang, G. H., Billings, G., Hubbard, T. P., Park, J. S., Leung, K. Y., Liu, Q., et al. (2017). Time-resolved transposon insertion sequencing reveals genome-wide fitness dynamics during infection. *mBio* 8:e01581-17. doi: 10.1128/mbio.01581-17

Yi, J., Xiao, S. B., Zeng, Z. X., Lu, J. F., Liu, L. Y., Laghari, Z. A., et al. (2016). EseE of *Edwardsiella tarda* augments secretion of translocon protein EseC and expression of the *escC-eseE* operon. *Infect. Immun.* 84, 2336–2344. doi: 10.1128/iai.00106-16

Yin, K., Guan, Y., Ma, R., Wei, L., Liu, B., Liu, X., et al. (2018). Critical role for a promoter discriminator in RpoS control of virulence in *Edwardsiella piscicida*. *PLoS Pathog.* 14:e1007272. doi: 10.1371/journal.ppat.1007272

Yu, X. J., Liu, M., and Holden, D. W. (2004). SsaM and SpiC interact and regulate secretion of *Salmonella* pathogenicity island 2 type III secretion system effectors and translocators. *Mol. Microbiol.* 54, 604–619. doi: 10.1111/j.1365-2958.2004.04297.x

Zhang, Q., He, T. T., Li, D. Y., Liu, L. Y., Nie, P., and Xie, H. X. (2019). The *Edwardsiella piscicida* type III effector EseJ suppresses expression of type 1 fimbriae, leading to decreased bacterial adherence to host cells. *Infect. Immun.* 87:e00187-19. doi: 10.1128/iai.00187-19

Zheng, J., and Leung, K. Y. (2007). Dissection of a type VI secretion system in *Edwardsiella tarda*. *Mol. Microbiol.* 66, 1192–1206. doi: 10.1111/j.1365-2958.2007.05993.x

Zheng, J., Tung, S. L., and Leung, K. Y. (2005). Regulation of a type III and a putative secretion system in *Edwardsiella tarda* by EsrC is under the control of a two-component system. *EsrA-EsrB*. *Infect. Immun.* 73, 4127–4137. doi: 10.1128/iai.73.7.4127-4137.2005

Conflict of Interest: The authors declare that the research was conducted in the absence of any commercial or financial relationships that could be construed as a potential conflict of interest.

frontiers in Microbiology

ORIGINAL RESEARCH
published: 06 April 2021
doi: 10.3389/fmicb.2021.641846

Gentamicin Combined With Hypoionic Shock Rapidly Eradicates Aquaculture Bacteria *in vitro* and *in vivo*

Yuanyuan Gao[1,2†], Zhongyu Chen[1†], Wei Yao[1], Daliang Li[3,4] and Xinmiao Fu[1,2*]*

[1] Provincial University Key Laboratory of Cellular Stress Response and Metabolic Regulation, Key Laboratory of Optoelectronic Science and Technology for Medicine of Ministry of Education, College of Life Sciences, Fujian Normal University, Fuzhou, China, [2] Engineering Research Center of Industrial Microbiology of Ministry of Education, Fujian Normal University, Fuzhou, China, [3] Fujian Key Laboratory of Innate Immune Biology, Biomedical Research Center of South China, Fuzhou, China, [4] College of Life Science, Fujian Normal University, Fuzhou, China

OPEN ACCESS

Edited by:
Bo Peng,
Sun Yat-sen University, China

Reviewed by:
Hetron Mweemba Munang'andu,
Norwegian University of Life Sciences, Norway
Xiangmin Lin,
Fujian Agriculture and Forestry University, China

***Correspondence:**
Yuanyuan Gao
gaoy@fjnu.edu.cn
Xinmiao Fu
xmfu@fjnu.edu.cn

[†] These authors have contributed equally to this work

Specialty section:
This article was submitted to Antimicrobials, Resistance and Chemotherapy, a section of the journal Frontiers in Microbiology

Received: 15 December 2020
Accepted: 01 March 2021
Published: 06 April 2021

Citation:
Gao Y, Chen Z, Yao W, Li D and Fu X (2021) Gentamicin Combined With Hypoionic Shock Rapidly Eradicates Aquaculture Bacteria in vitro and in vivo. Front. Microbiol. 12:641846. doi: 10.3389/fmicb.2021.641846

Bacterial pathogens are a major cause of infectious diseases in aquatic animals. The abuse of antibiotics in the aquatic industry has led to the proliferation of antibiotic resistance. It is therefore essential to develop more effective and safer strategies to increase the efficacy and extend the life span of the antibiotics used in aquaculture. In this study, we show that six aquaculture bacterial pathogens (i.e., *Aeromonas hydrophila*, *Vibrio alginolyticus*, *Edwardsiella tarda*, *Streptococcus iniae*, *Vibrio harveyi*, and *Vibrio fluvialis*) in the stationary phase can be rapidly killed after immersion in gentamicin- or neomycin-containing, ion-free solutions for a few minutes. Such hypoionic shock treatment enhances the bacterial uptake of gentamicin in an ATP-dependent manner. Importantly, we demonstrate, as a proof of concept, that gentamicin under hypoionic shock conditions can effectively kill *A. hydrophila in vivo* in a skin infection model of zebrafish (*Danio rerio*), completely curing the infected fish. Given that pathogenic bacteria generally adhere to the skin surface and gills of aquatic animals, our strategy is of potential significance for bacterial infection control, especially for small-scale economic fish farming and ornamental fish farming. Further, the combined treatment can be completed within 5 min with a relatively small volume of solution, thus minimizing the amount of residual antibiotics in both animals and the environment.

Keywords: aquaculture bacteria, persister, antibiotic tolerance, aminoglycoside, gentamicin, neomycin, hypoionic shock, zebrafish

INTRODUCTION

Aquaculture is the fastest-growing animal food industry at present and provides human society with one of the most sustainable forms of edible protein and nutrient production, making it a fundamental part of future food production (Froehlich et al., 2018). Similar to other animal production sectors, fish production relies on intensive and semi-intensive cultivations, which result in increased disease outbreaks (Little et al., 2016; Kotob et al., 2017). Fish diseases are often caused by bacteria, viruses, fungi, parasites, or a combination of these pathogens, with bacterial pathogens

being the most common etiology (Dhar et al., 2014; Lafferty et al., 2015). Given that bacteria can survive well in aquatic environments independent of a host, bacterial diseases have become major impediments to aquaculture (Haenen et al., 2013). Various effective vaccines have been developed against many fish bacterial pathogens. Nevertheless, some infectious bacterial diseases that cannot be controlled using conventional inactivated vaccines are threatening aquaculture (Tafalla et al., 2013). In addition, attenuated bacterial vaccines can potentially revert to a pathogenic form, which poses a tremendous risk to the whole environment (Matsuura et al., 2019). Furthermore, some bacterial pathogens are difficult to culture or completely unculturable, making them unsuitable for vaccine development (Takano et al., 2016).

Antibiotics are widely used to prevent and control bacterial diseases in aquaculture (Cabello et al., 2016; Santos and Ramos, 2018). Nevertheless, long-term antibiotic usage, particular overuse and misuse, has led to the emergence and proliferation of antibiotic resistance (Baym et al., 2016; Du et al., 2019). Improving the efficacy of antibiotics is a promising strategy for extending the life span of current antibiotic drugs (Levy and Marshall, 2004; Nambiar et al., 2014). Previously, we found that treatment in non-electrolyte (e.g., glycerol) solutions or in ultrapure water exhibits a potentiation effect on the killing of bacteria by aminoglycosides, while treatment in strong electrolyte (e.g., NaCl) solutions barely exhibits any potentiation effects (Jiafeng et al., 2015). In particular, stationary-phase *Escherichia coli* cells can be killed after treatment in aminoglycoside-containing ultrapure water for only 1–2 min (Jiafeng et al., 2015). It should be noted that bacteria enter a non-growth state defined as a stationary phase when nutrients are insufficient in their living surroundings (Navarro Llorens et al., 2010), and stationary-phase bacteria are much more resistant than exponential-phase cells to destruction by antibiotics (Levin and Rozen, 2006; McCall et al., 2019). Furthermore, we showed that such hypoionic shock (i.e., the absence of ions) could dramatically potentiate the killing of nutrient shift- or starvation-induced *E. coli* persister cells by aminoglycosides in 3 min (Chen et al., 2019).

Here, we investigated whether this unique approach can kill aquaculture bacterial pathogens, given that bacterial pathogens usually infect fish by attaching to their skin surface, gills, and gut lining, which are always in intimate contact with the surrounding water (Benhamed et al., 2014). We show that six aquaculture bacterial pathogens (i.e., *Aeromonas hydrophila*, *Vibrio alginolyticus*, *Edwardsiella tarda*, *Streptococcus iniae*, *Vibrio harveyi*, and *Vibrio fluvialis*) in the stationary phase are killed rapidly *in vitro* by gentamicin and neomycin under hypoionic shock conditions. Importantly, we demonstrate the *in vivo* efficacy of the new approach against *A. hydrophila* infections in a zebrafish model.

MATERIALS AND METHODS

Strains, Media, and Reagents

The aquatic bacterial strains used in this study consisted of five Gram-negative bacteria (i.e., *Aeromonas hydrophila*, *Vibrio alginolyticus*, *Edwardsiella tarda*, *Vibrio harveyi*, and *Vibrio fluvialis*) and one Gram-positive strain (i.e., *Streptococcus iniae*). The sources of all aquatic bacterial strains and their relevant characteristics are listed in **Supplementary Table S1**. Bacteria were cultured in Lysogeny broth (LB) medium at 37°C (*V. alginolyticus*, *E. tarda*, *V. harveyi*, and *V. fluvialis*) or 30°C (*A. hydrophila* and *S. iniae*) in a shaker (220 rpm). The antibiotics used in this study were gentamicin and neomycin. Other chemicals used included carbonyl cyanide *m*-chlorophenyl hydrazone (CCCP) and its analog carbonyl cyanide-trifluoromethoxyphenyl hydrazone (FCCP), as well as eugenol (an anesthetic for zebrafish). The information for the antibiotics and chemicals used in the study is presented in **Supplementary Table S2**. All chemical reagents were of analytical purity.

Antibiotic Tolerance Test for Six Aquatic Bacterial Cells in Stationary Phase

In brief, the aquatic bacterial strains from frozen stock listed in **Supplementary Table S1** were seeded in LB medium at a ratio of 1:1,000 and cultured at 37°C (*V. alginolyticus*, *E. tarda*, *V. harveyi*, and *V. fluvialis*) or 30°C (*A. hydrophila* and *S. iniae*) in a shaker (220 rpm) for 24 h to prepare stationary-phase cells, as previously described (Yao et al., 2016; Chen et al., 2019). Each antibiotic was added to the cultured cells at varying concentrations (refer to **Supplementary Table S2**), and the mixture was further agitated for 5 min or 3 h. Hundred microliters of the treated cells was washed twice using phosphate-buffered saline (PBS; 0.27 g/L of KH_2PO_4, 1.42 g/L of Na_2HPO_4, 8 g/L of NaCl, and 0.2 g/L of KCl, pH = 7.4) with centrifugation (13,000 *g*, 30 s) and spot-plated onto LB agar dishes at a 10-fold serial dilution in PBS. After incubation at 37°C for at least 12 h, the colony-forming units (CFU) on the dishes were counted after taking a picture of each dish.

Eradication of Aquatic Bacteria by Aminoglycosides Under Hypoionic Shock Conditions

Treatment with aminoglycosides combined with hypoionic shock was performed as previously described (Jiafeng et al., 2015; Chen et al., 2019). In brief, 100 μl of stationary-phase cells was centrifuged (12,000 *g*, 1 min) in an Eppendorf tube, and the medium was completely removed. Cell pellets were re-suspended in ultrapure water (i.e., without the presence of ions; 0.9% NaCl solution was used as the negative control) containing gentamicin or neomycin at the concentrations listed in **Supplementary Table S2**. Ultrapure water was prepared by Milli-Q® Advantage A10 (Millipore). The cell suspension was kept at room temperature (i.e., 25°C) for 5 min, and the cells were washed twice with PBS before spot-plating on LB agar dishes for cell survival assays as described above. Similarly, the effect of ATP was evaluated by agitating the cell culture in the presence of 20 μM of protonophore CCCP or FCCP for 1 h before the combined treatment.

Intracellular ATP Level Assay

A luciferase-based kit (BacTiter-Glo^{TM}, Promega, G8231) was used to measure ATP levels according to the manufacturer's instructions. Briefly, stationary-phase cells, with or without 20 μM of protonophore CCCP or FCCP pretreatment for 1 h, were quickly mixed with the working solution at equal volumes and then transferred to a 96-well plate before light recording on a FLUOstar Omega Microplate Reader using a Luminometer.

Assay for the Uptake of Fluorescent-Labeled Gentamicin

A fluorescent probe ($Ex_{580\ nm}$, $Em_{600-700\ nm}$) was attached to gentamicin as we recently reported (Wu et al., 2020). After salts were removed through dialysis, the fluorescent-labeled gentamicin was dissolved in ultrapure water at 100 μg/ml for the treatment of *A. hydrophila* or *V. alginolyticus* cells as described above. The cells were then washed twice with PBS and re-suspended in 500 μl of cell wall-digestion buffer (30 mM of Tris–HCl, pH 8.0, 1 mM of EDTA, 1 mg/ml of lysozyme) for further incubation at room temperature for 5 h. The cells were subjected to three cycles of freezing treatment at −80°C, followed by thermal denaturation at 90°C for 10 min (note: we confirmed that gentamicin had high thermal stability; Chen et al., 2019), and then centrifuged to remove the cell debris and denatured proteins. Afterward, an equal volume of supernatant containing fluorescent-labeled gentamicin was placed in a quartz cuvette, and the fluorescence intensity in the supernatant was determined with a fluorescence spectrometer (Spectrofluorometer FS5, EDINBURGH). In addition, the amount of fluorescent-labeled gentamicin uptaken by CCCP or FCCP-pretreated cells was measured. A standard curve was prepared by directly adding fluorescent-labeled gentamicin at different concentrations (0, 25, 50, and 100 μg/ml) to persister cells suspended in cell wall digestion buffer. All procedures described above were performed under dim lighting to prevent fluorescence quenching.

Animal Experiments

Zebrafish were purchased from Fuzhou aquarium market and acclimated for 2 weeks before infection. The zebrafish were handled according to the procedures defined by the Animal Ethical and Welfare Committee of Fujian Normal University (approval no. IACUC 20190006, Fuzhou, China). The zebrafish were anesthetized after being immersed in 45 mg/L of eugenol for about 8 min (Sánchez-Vázquez et al., 2011). After anesthesia, the fish were lightly scraped along the lateral surface behind the pectoral fins with a sterile scalpel to remove several scales (Neely et al., 2002; Zhang et al., 2016). When the scraped fish recovered from anesthesia, they were infected by swimming in water containing 5.0×10^7 CFU/ml of *A. hydrophila* at 30°C for 3 h. Zebrafish infected by *A. hydrophila* were rinsed with deionized water for a few seconds and then were randomly divided into three groups (A: mock group without treatment; B: treated with gentamicin-containing ultrapure water; and C: treated with gentamicin-containing 0.9% NaCl solution). The concentration of gentamicin in animal experiments is 25 μg/ml. After treatment for 5 min, three fish from each group were selected randomly, and two-fifths of each fish's body was cut, weighed, and homogenized in saline at a ratio of 100 mg/ml (w/v). The lysates were spot-plated on LB agar dishes for bacterial survival assays. For quantification, each sample was spot-plated in triplicate. The injury and survival rates of the zebrafish were observed 48 h after antibiotics treatment. All experiments were performed three times. In addition, three fish scraped without infection were homogenized to count the basal number of bacteria in the fish themselves.

RESULTS

Five-Minute Hypoionic Shock Treatment Enables Gentamicin and Neomycin to Kill Stationary-Phase Aquaculture Bacteria

Bacteria in the stationary phase are highly tolerant to antibiotics under conventional treatment conditions, presumably due to stress- or starvation-induced growth arrest (Rittershaus et al., 2013; Martins et al., 2018). Here, we examined the antibiotic tolerance of six aquaculture bacteria, specifically *Aeromonas hydrophila*, *Vibrio alginolyticus*, *Vibrio fluvialis*, *Vibrio harveyi*, *Edwardsiella tarda*, and *Streptococcus iniae* (with the concentrations of these cells being 8.6×10^9, 3×10^9, 3.6×10^9, 3.9×10^9, 5.5×10^8, and 3.4×10^8, respectively), by treating the stationary-phase cells with aminoglycoside antibiotics dissolved in 0.9% NaCl solution (**Figure 1** and **Supplementary Figure S1**). In China, gentamicin is widely used, and neomycin is the only aminoglycoside currently certified for aquaculture applications (Liu et al., 2017). Therefore, these two aminoglycosides were evaluated. We found that neither gentamicin nor neomycin could kill the above bacteria after incubation for 5 min when dissolved in 0.9% NaCl solution. When the cells were treated with the antibiotics in 0.9% NaCl solution for 3 h, the bacteria exhibited different degrees of antibiotic susceptibility: 3.4 and 31.3% of *A. hydrophila* were killed by gentamicin and neomycin, respectively; *V. alginolyticus*, *V. fluvialis*, and *V. harveyi* were eliminated by 1∼2 orders of magnitude; *E. tarda* and *S. iniae* were killed by gentamycin by about 4 orders of magnitude.

Bacterial cells in the stationary phase were next treated with gentamicin- or neomycin-containing ultrapure water for 5 min for comparison with the antibiotic treatment in 0.9% NaCl solution (**Figure 2** and **Supplementary Figure S2**). Substantial amounts of all aquaculture bacteria were killed by neomycin-containing ultrapure water. Similarly, *S. iniae* colonies were undetectable on LB agar dishes after 5 min treatment with neomycin-containing ultrapure water (as indicated by the asterisks in **Figure 2E**), indicating a reduction in the surviving cells by more than 6 orders or magnitude. Notably, *A. hydrophila*, *V. alginolyticus*, *E. tarda*, and *S. iniae* were killed by gentamicin-containing ultrapure water by 3∼4 orders of magnitude, but only a very limited potentiation effect was observed on gentamicin with *V. fluvialis* and *V. harveyi* (**Supplementary Figure S2B**). In contrast, neither gentamicin nor neomycin had a killing effect when dissolved in the NaCl solution. These results indicate that

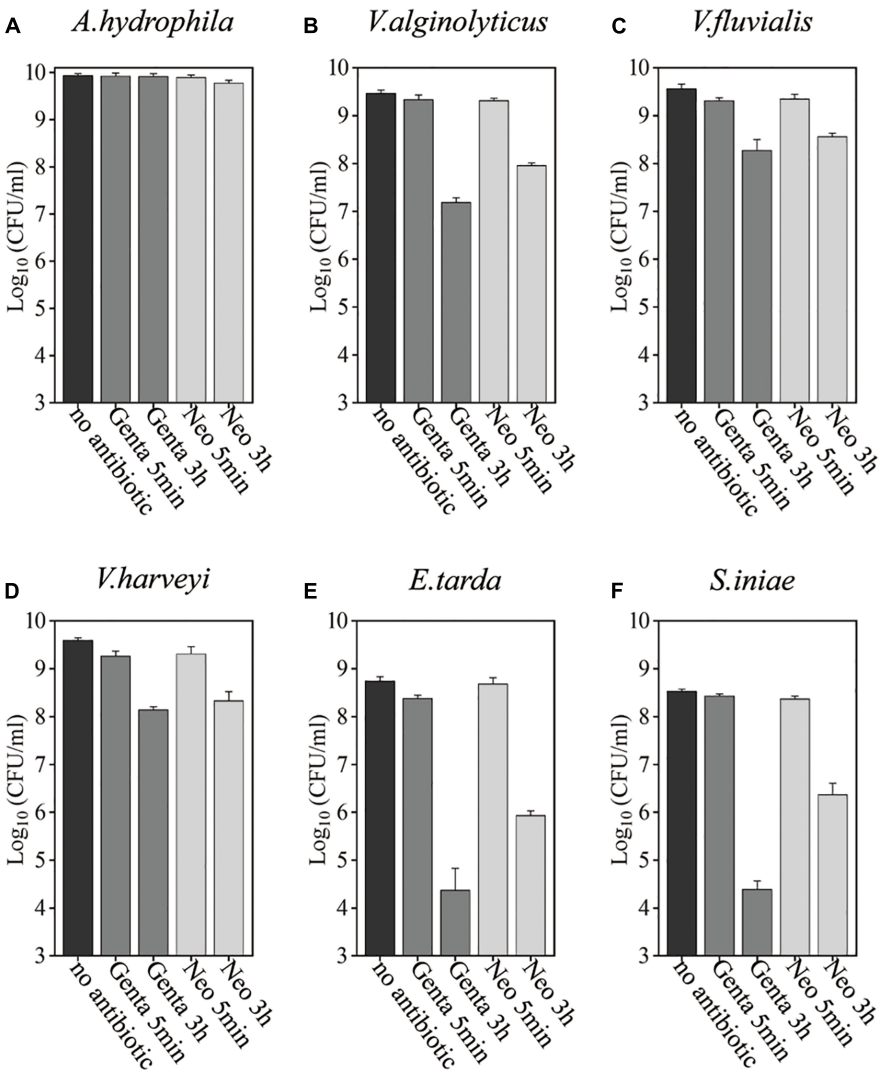

FIGURE 1 | Antibiotic tolerance of six aquaculture bacteria under conventional treatment conditions. **(A–F)** Stationary-phase cells of the indicated bacteria [*Aeromonas hydrophila*, *Vibrio alginolyticus*, *Vibrio fluvialis*, *Vibrio harveyi*, *Edwardsiella tarda*, and *Streptococcus iniae*, **(A–F)**, respectively], which were treated with gentamicin (Genta) or neomycin (Neo) dissolved in 0.9% NaCl solution for 5 min or 3 h and then spot-plated on Lysogeny broth (LB) agar dishes for cell survival assays. The concentrations of antibiotics used were as follows: 25 μg/ml of Genta and 50 μg/ml f Neo for S. iniae; 100 μg/ml f Genta and 200 μg/ml f Neo for the other five bacteria.

hypoionic shock treatment enables aminoglycoside antibiotics to rapidly reduce stationary-phase aquaculture bacteria.

Hypoionic Shock-Induced Gentamicin Potentiation Against Aquaculture Bacteria Is Partially Dependent on ATP

The tolerance of bacteria to antibiotics is closely related to intracellular ATP levels (Meylan et al., 2017; Shan et al., 2017; Pu et al., 2019). We next sought to determine whether hypoionic shock-induced aminoglycoside potentiation against aquaculture bacteria is affected by the ATP level in the bacterial cells. CCCP and FCCP are uncouplers of the proton motive force (PMF) that drives ATP synthesis and thus are able to reduce intracellular ATP levels (Kinoshita et al., 1984; Tapia et al., 2006). To this end, we treated aquaculture bacteria (*A. hydrophila*, *V. alginolyticus*, *E. tarda*, and *S. iniae*) with CCCP and FCCP for 1 h and then subjected them to gentamicin treatment under hypoionic shock conditions (note: *V. fluvialis* and *V. harveyi* were not analyzed here due to a very limited potentiation effect of hypoionic shock on gentamicin).

Cell survival assays revealed that CCCP, as well as its functional analog FCCP, efficiently suppressed the hypoionic shock-induced gentamicin potentiation that kills stationary-phase aquaculture bacteria in 5 min (**Figure 3** and **Supplementary Figure S3**). An intracellular ATP assay also confirmed that pretreatment with CCCP or FCCP significantly reduced the intracellular ATP levels in all of the bacteria

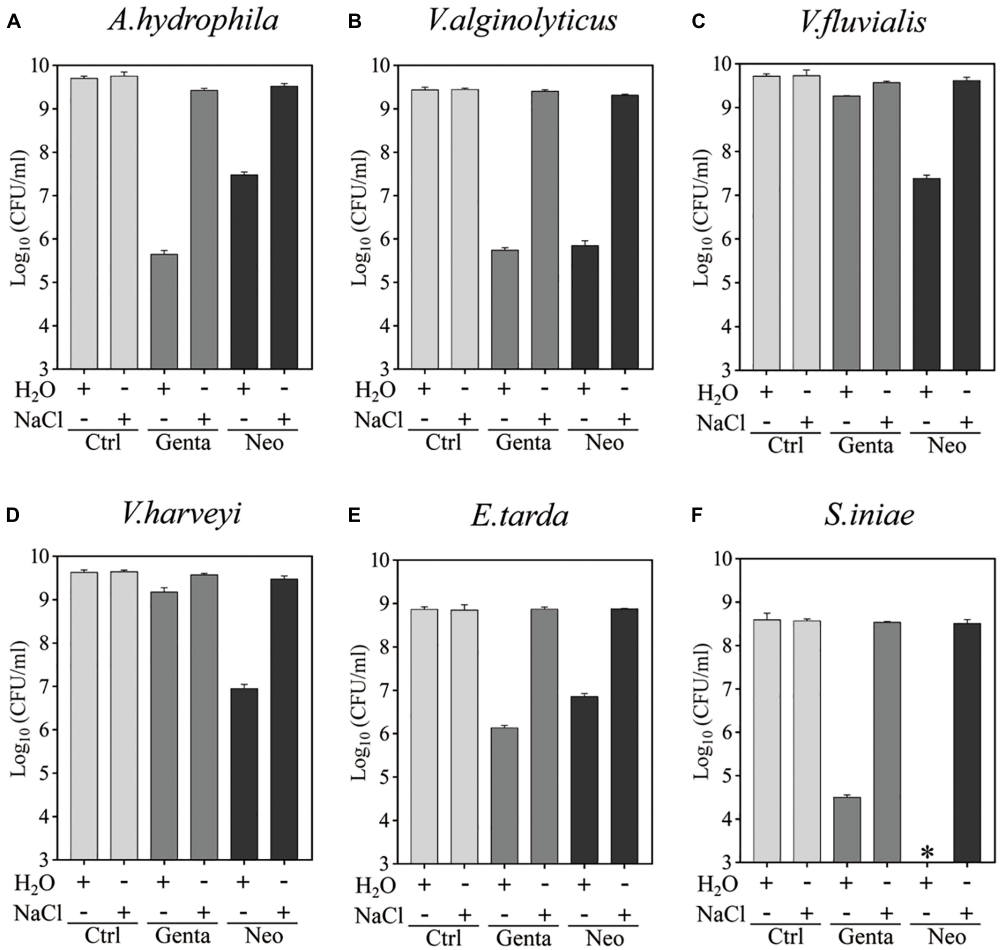

FIGURE 2 | Hypoionic shock-induced potentiation of gentamicin and neomycin effects against the six aquaculture bacteria. **(A–F)** Survival of stationary-phase cells of *Aeromonas hydrophila* **(A)** *Vibrio alginolyticus* **(B)**, *Vibrio fluvialis* **(C)**, *Vibrio harveyi* **(D)**, *Edwardsiella tarda* **(E)**, and *Streptococcus iniae* **(F)** following 5 min treatment with Genta or Neo dissolved in ultrapure water or 0.9% NaCl. The concentrations of antibiotics used were as follows: 25 μg/ml of Genta and 50 μg/ml of Neo for S. iniae; 100 μg/ml of Genta and 200 μg/ml of Neo for the other five bacteria. *in Panel F indicates that No CFU detected during cell survival assay by 100000-fold dilution.

evaluated (**Figure 3**). These results suggest that hypoionic shock-induced potentiation of gentamicin's effect against aquaculture bacteria is, at least, partially dependent on intracellular ATP.

Hypoionic Shock Enhances the Bacterial Uptake of Gentamicin

Aminoglycoside antibiotics such as gentamicin and tobramycin must traverse the bacterial cytoplasmic membrane prior to initiating their lethal effects, and the uptake of aminoglycosides is facilitated by the PMF or ATP (Taber et al., 1987; Fraimow et al., 1991; Allison et al., 2011). Therefore, we further explored whether hypoionic shock treatment affects the bacterial uptake of gentamicin antibiotics. For this purpose, fluorescent gentamicin was synthesized by conjugating coumarin–hemicyanine scaffolds to gentamicin (Wu et al., 2020). The conjugation did not affect the bactericidal efficacy of gentamicin (**Supplementary Figure S4A**). The fluorescent gentamicin taken up by *A. hydrophila* or *V. alginolyticus* was extracted through cell wall digestion coupled with cycled freezing/thawing and thermal denaturation and then subjected to a fluorescence assay. Fluorescent gentamicin at standard concentrations was directly incubated with bacterial lysates before a fluorescence assay. The maximal fluorescent intensity of fluorescent gentamicin was approximately 640 nm (**Figure 4A**).

A regression analysis (**Supplementary Figure S4B**) based on the standards (**Figure 4A**) showed that the concentration of gentamicin extracted from *A. hydrophila* upon hypoionic shock was approximately 69.58 μg/ml, while that extracted from the cells treated with 0.9% NaCl solution was only 37.96 μg/ml. Notably, we found that the amount of gentamicin taken up by the cells pretreated with CCCP or FCCP was reduced to 60–70%. Similarly, the concentration of gentamicin extracted from *V. alginolyticus* upon hypoionic shock was about 64.45 μg/ml, which was significantly reduced in NaCl solution or upon pretreatment with CCCP or FCCP (**Figure 4B**).

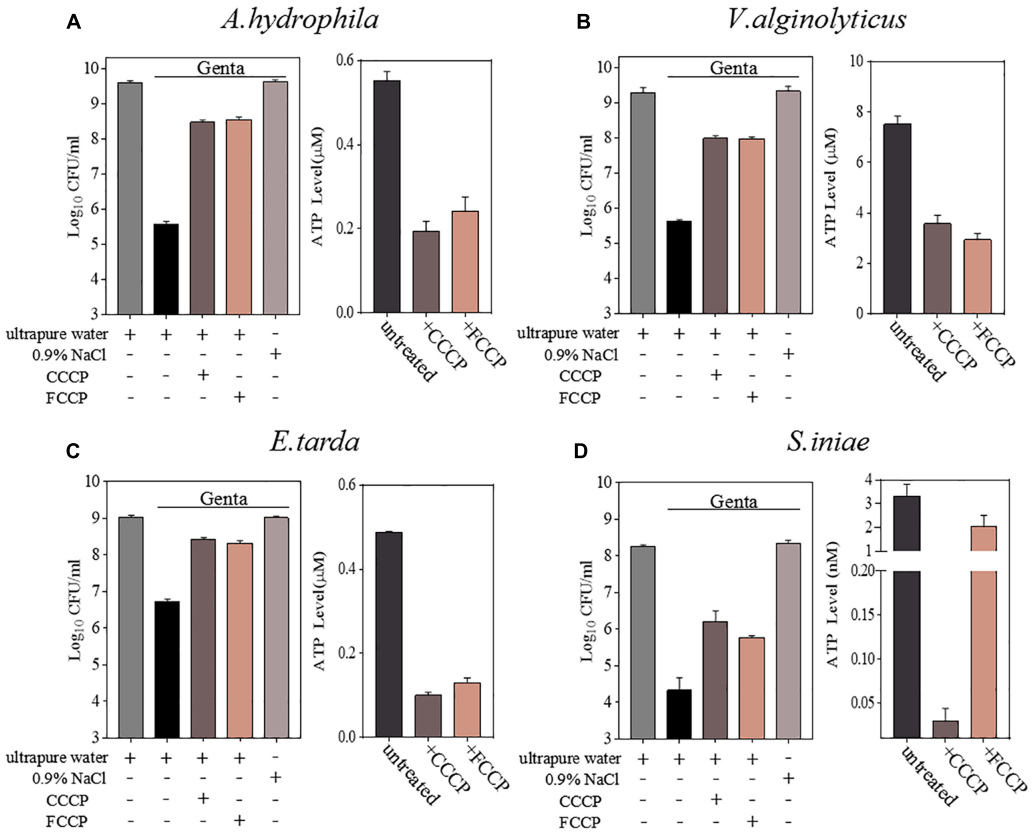

FIGURE 3 | Hypoionic shock-induced potentiation of gentamicin effects against aquatic pathogenic bacteria is partially dependent on ATP. **(A–D)** Left parts in each panel: survival of stationary-phase cells of *Aeromonas hydrophila*, *Vibrio alginolyticus*, *Edwardsiella tarda*, and *Streptococcus iniae*. Cells were pretreated with CCCP or FCCP for 1 h and then subjected to 5-min treatment with gentamicin dissolved in ultrapure water. Right parts in each panel: ATP levels in CCCP- or FCCP-pretreated cells.

Gentamicin Under Hypoionic Shock Conditions Significantly Improved the Survival of Zebrafish Infected by *Aeromonas hydrophila*

In recent years, zebrafish (*Danio rerio*) has been used as an important alternative to mammalian models in the study of human infectious disease (Allen and Neely, 2010; Meijer and Spaink, 2011; Sullivan et al., 2017). In order to explore the *in vivo* efficacy of combined treatment with hypoionic shock and also probe the potential application of the combined treatment against aquaculture bacterial pathogens, a zebrafish infection model was used in this study. After infection by *A. hydrophila* (for details, refer to the "Materials and Methods" section), the zebrafish were rinsed with deionized water for a few seconds and randomly divided into three groups before being subjected to different treatments for 5 min: mock treatment, gentamicin dissolved in ultrapure water (Genta + H_2O), and gentamicin dissolved in NaCl solution (Genta + NaCl).

Bacterial cell survival assays revealed that 3.75×10^6 CFU/ml of *A. hydrophila* cells from the homogenate of wound tissues from zebrafish were viable without treatment (mock). Treatment with Genta + NaCl reduced the number of viable cells to 3.3×10^5 CFU/ml. Strikingly, viable *A. hydrophila* cells were almost undetectable when the zebrafish were treated with Genta + H_2O (**Figure 5A**). These results indicated that short-term exposure to gentamicin-containing ultrapure water is more effective at killing bacteria in infected fish than exposure to gentamicin-containing NaCl solution.

Consistently, we observed that the infection sites in some fish in the mock group and Genta + NaCl group became red and swollen 12 h after infection (**Figure 5B**). Animal survival assays revealed that approximately 20% of zebrafish in the control (mock) group began to die 12 h post-infection, and only about 60% of this group survived 48 h post-infection. In the Genta + NaCl group, 70% of zebrafish survived 48 h post-infection. Surprisingly, none of the zebrafish in the Genta + H_2O group died or exhibited swelling (**Figure 5C**).

DISCUSSION

Outbreaks of infectious disease are considered a significant constraint in the aquaculture industry, causing more than 10 billion USD worth of losses annually on a global scale (Evensen, 2016). The currently available commercial vaccines are aimed at

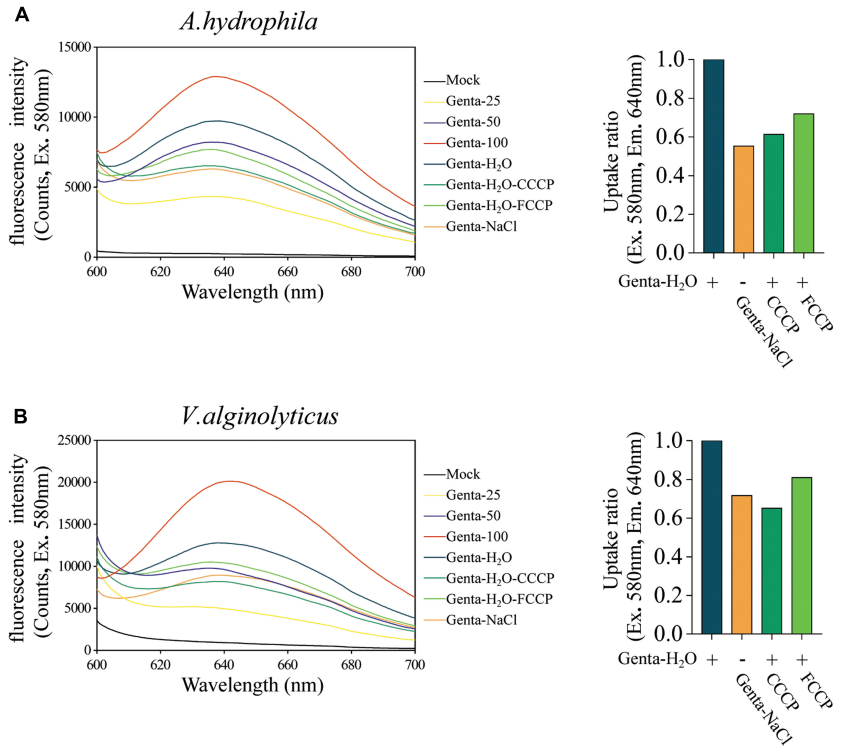

FIGURE 4 | Hypoionic shock enhances the bacterial uptake of fluorescent-labeled gentamicin. **(A,B)** Left parts: the fluorescence spectra for fluorescent gentamicin taken up by *Aeromonas hydrophila* **(A)** or *Vibrio alginolyticus* **(B)** were monitored with a spectrofluorometer. Mock, bacteria lysate without antibiotic treatment. Genta 25–100, standard concentration fluorescence labeled antibiotic (25, 50, and 100 μg/ml) mixed with bacteria lysate. In the Genta-H_2O (Genta dissolved in ultrapure water), Genta-NaCl (Genta dissolved in saline), Genta-H_2O-CCCP (CCCP-pretreated and Genta dissolved in ultrapure water), and Genta-H_2O-FCCP (FCCP-pretreated and Genta dissolved in ultrapure water) groups, the fluorescent gentamicin taken up by bacterial cells was monitored with a spectrofluorometer. **(A,B)** Right parts: ratios for fluorescent gentamicin uptake in different experimental groups compared with those in the hypoionic shock-treated group (Genta-H_2O).

specific animals, for example, some fish and lobsters (Assefa and Abunna, 2018; Adams, 2019), and cannot be widely administered to other aquatic animals, especially invertebrates lacking acquired immunity. Most of the novel alternative biocontrol strategies for fish bacterial diseases, such as probiotics, bio-encapsulated vaccines, and phage therapy, are still in the research phase (Pérez-Sánchez et al., 2018; Soliman et al., 2019). On the contrary, the activity spectrum, mode of action, resistance mechanisms, and current applications of most important antibiotic classes have been well investigated (Mohr, 2016). It is highly desirable to develop more effective and safer approaches for current antibiotics. For example, Peng et al. (2015) found that exogenous glucose or alanine plus kanamycin can kill multidrug-resistant *Edwardsiella tarda* both *in vitro* and in a mouse model for urinary tract infection. Glycerol monolaurate, lauric acid, 5-methylindole, and even the commonly used diabetic drug metformin were found to act synergistically with aminoglycoside to eliminate *Staphylococcus aureus* persisters (Hess et al., 2014; Liu et al., 2020; Sun et al., 2020). Various adjuvants, including metabolites (Allison et al., 2011; Peng et al., 2015), for antibiotic potentiation have been well documented (Liu et al., 2019).

Here, we show that hypoionic shock enables gentamicin and/or neomycin antibiotics to reduce six stationary-phase aquaculture pathogenic bacteria, consistent with our previous studies (Jiafeng et al., 2015; Chen et al., 2019). Furthermore, this hypoionic shock-induced potentiation of gentamicin was also observed in zebrafish infected with *Aeromonas hydrophila*. Mechanistically, the potentiation seems to be achieved by enhancing the bacterial uptake of gentamicin under hypoionic shock conditions. Given pathogenic bacteria generally infect fish on the surface of the skin (Benhamed et al., 2014), our approach may represent a promising strategy for bacterial infection control in aquaculture. This approach is eco-friendly, non-toxic, and non-immunogenic, with the exception of the required operation to transfer the fish into aminoglycoside-containing ultrapure water. Currently, a small-scale application of this approach is being performed in our laboratory.

Our approach is also advantageous with respect to food safety and environmental health, given that it takes only a few minutes to complete the treatment; therefore, a smaller amount of antibiotics and less time for antibiotic exposure are required. As such, contamination of the environment by residual antibiotics and/or retention of the antibiotics within animal bodies can be minimized. Currently, the use of antibiotics in aquaculture leads to the accumulation of residual antibiotics in sea and freshwater foods (Song et al., 2017; Chen et al., 2018), which may have adverse effects on humans (Cabello, 2006). Similarly, residual antibiotics in water or aquatic sediments may facilitate the spread

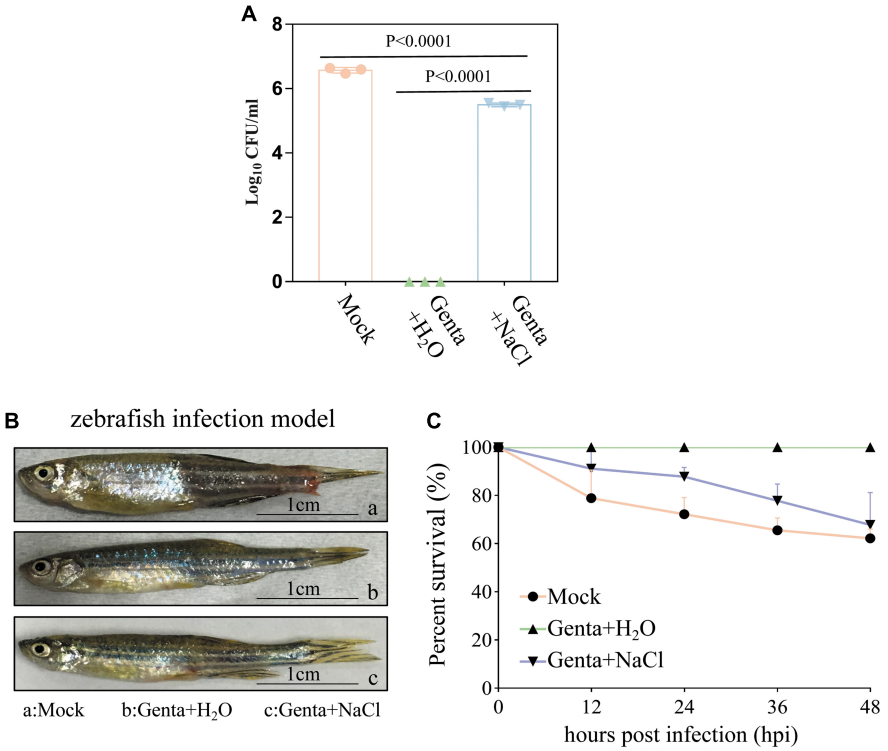

FIGURE 5 | Hypoionic shock facilitates gentamicin killing of *Aeromonas hydrophila* in a zebrafish model. **(A)** The survival percentage of the pathogenic bacteria on/in the zebrafish treated with gentamicin dissolved in ultrapure water (Genta + H_2O) or in 0.9% NaCl solution (Genta + NaCl) for only 5 min. The mock groups were not treated with antibiotics. The number of bacteria on/in the zebrafish before infection was subtracted (**Supplementary Figure S5C**) from the results for each group. **(B)** The gross pathology of zebrafish infected by *A. hydrophila* at 12 h. The infection site of some fish in the mock groups and salt treatment groups became red and swollen. **(C)** The survival percentage of zebrafish infected by *A. hydrophila* after 48 h.

of antibiotic resistance in environmental bacteria (Gullberg et al., 2011; Cabello et al., 2016). In addition, compared with the stimulation of aminoglycoside potentiation by metabolites, which takes a few hours to manifest (Allison et al., 2011; Peng et al., 2015), our approach, which does not consume metabolites and requires only a few minutes, may have certain advantages.

DATA AVAILABILITY STATEMENT

The original contributions presented in the study are included in the article/**Supplementary Material**, further inquiries can be directed to the corresponding author/s.

ETHICS STATEMENT

The animal study was reviewed and approved by the Animal Ethical and Welfare Committee of Fujian Normal University (approval no. IACUC 20190006, Fuzhou, China).

AUTHOR CONTRIBUTIONS

XF and YG designed the study. ZC and WY performed the experiments. DL synthesized the fluorescent gentamicin. YG and XF analyzed the data and wrote the manuscript. All authors contributed to the article and approved the submitted version.

FUNDING

This work was supported by the research grants from the National Natural Science Foundation of China (Nos. 31972918 and 31770830 to XF) and Natural Science Foundation of Fujian Province (No. 2020J01175 to YG).

ACKNOWLEDGMENTS

We thank Prof. Yueling Zhang at Shantou University and Dr. Chao Wang at Shandong Freshwater Fisheries Research Institute for their kindness in providing bacterial strains as described in **Supplementary Table S1**.

SUPPLEMENTARY MATERIAL

The Supplementary Material for this article can be found online at: https://www.frontiersin.org/articles/10.3389/fmicb.2021.641846/full#supplementary-material

REFERENCES

Adams, A. (2019). Progress, challenges and opportunities in fish vaccine development. *Fish Shellfish Immunol.* 90, 210–214. doi: 10.1016/j.fsi.2019.04.066

Allen, J. P., and Neely, M. N. (2010). Trolling for the ideal model host: zebrafish take the bait. *Future Microbiol.* 5, 563–569. doi: 10.2217/fmb.10.24

Allison, K. R., Brynildsen, M. P., and Collins, J. J. (2011). Metabolite-enabled eradication of bacterial persisters by aminoglycosides. *Nature* 473, 216–220. doi: 10.1038/nature10069

Assefa, A., and Abunna, F. (2018). Maintenance of fish health in aquaculture: review of epidemiological approaches for prevention and control of infectious disease of fish. *Vet. Med. Int.* 2018:5432497. doi: 10.1155/2018/5432497

Baym, M., Stone, L. K., and Kishony, R. (2016). Multidrug evolutionary strategies to reverse antibiotic resistance. *Science (New York, N.Y.)* 351:aad3292. doi: 10.1126/science.aad3292

Benhamed, S., Guardiola, F. A., Mars, M., and Esteban, M. (2014). Pathogen bacteria adhesion to skin mucus of fishes. *Vet. Microbiol.* 171, 1–12. doi: 10.1016/j.vetmic.2014.03.008

Cabello, F. C. (2006). Heavy use of prophylactic antibiotics in aquaculture: a growing problem for human and animal health and for the environment. *Environ. Microbiol.* 8, 1137–1144. doi: 10.1111/j.1462-2920.2006.01054.x

Cabello, F. C., Godfrey, H. P., Buschmann, A. H., and Dölz, H. J. (2016). Aquaculture as yet another environmental gateway to the development and globalisation of antimicrobial resistance. *Lancet Infect. Dis.* 16, e127–e133. doi: 10.1016/s1473-3099(16)00100-6

Chen, H., Liu, S., Xu, X. R., Diao, Z. H., Sun, K. F., Hao, Q. W., et al. (2018). Tissue distribution, bioaccumulation characteristics and health risk of antibiotics in cultured fish from a typical aquaculture area. *J. Hazard. Mater.* 343, 140–148. doi: 10.1016/j.jhazmat.2017.09.017

Chen, Z., Gao, Y., Lv, B., Sun, F., Yao, W., Wang, Y., et al. (2019). Hypoionic shock facilitates aminoglycoside killing of both nutrient shift- and starvation-induced bacterial persister cells by rapidly enhancing aminoglycoside uptake. *Front. Microbiol.* 10:2028. doi: 10.3389/fmicb.2019.02028

Dhar, A. K., Manna, S. K., and Thomas Allnutt, F. C. (2014). Viral vaccines for farmed finfish. *Virusdisease* 25, 1–17. doi: 10.1007/s13337-013-0186-4

Du, B., Yang, Q., Wang, R., Wang, R., Wang, Q., and Xin, Y. (2019). Evolution of antibiotic resistance and the relationship between the antibiotic resistance genes and microbial compositions under long-term exposure to tetracycline and sulfamethoxazole. *Int. J. Environ. Res. Public Health* 16:4681. doi: 10.3390/ijerph16234681

Evensen, Ø (2016). "Development of fish vaccines: focusing on methods," in *Fish Vaccines, Birkhäuser Advances in Infectious Diseases*, ed. A. Adams (Basel: Springer Basel), 53–74. doi: 10.1007/978-3-0348-0980-1_3

Fraimow, H. S., Greenman, J. B., Leviton, I. M., Dougherty, T. J., and Miller, M. H. (1991). Tobramycin uptake in *Escherichia coli* is driven by either electrical potential or ATP. *J. Bacteriol.* 173, 2800–2808. doi: 10.1128/jb.173.9.2800-2808.1991

Froehlich, H. E., Runge, C. A., Gentry, R. R., Gaines, S. D., and Halpern, B. S. (2018). Comparative terrestrial feed and land use of an aquaculture-dominant world. *Proc. Natl. Acad. Sci. U.S.A.* 115, 5295–5300. doi: 10.1073/pnas.1801692115

Gullberg, E., Cao, S., Berg, O. G., Ilbäck, C., Sandegren, L., Hughes, D., et al. (2011). Selection of resistant bacteria at very low antibiotic concentrations. *PLoS Pathog.* 7:e1002158. doi: 10.1371/journal.ppat.1002158

Haenen, O. L., Evans, J. J., and Berthe, F. (2013). Bacterial infections from aquatic species: potential for and prevention of contact zoonoses. *Rev. Sci. Tech.* 32, 497–507. doi: 10.20506/rst.32.2.2245

Hess, D. J., Henry-Stanley, M. J., and Wells, C. L. (2014). Antibacterial synergy of glycerol monolaurate and aminoglycosides in *Staphylococcus aureus* biofilms. *Antimicrob. Agents Chemother.* 58, 6970–6973. doi: 10.1128/aac.03672-14

Jiafeng, L., Fu, X., and Chang, Z. (2015). Hypoionic shock treatment enables aminoglycosides antibiotics to eradicate bacterial persisters. *Sci. Rep.* 5:14247. doi: 10.1038/srep14247

Kinoshita, N., Unemoto, T., and Kobayashi, H. (1984). Proton motive force is not obligatory for growth of *Escherichia coli*. *J. Bacteriol.* 160, 1074–1077. doi: 10.1128/jb.160.3.1074-1077.1984

Kotob, M. H., Menanteau-Ledouble, S., Kumar, G., Abdelzaher, M., and El-Matbouli, M. (2017). Erratum to: the impact of co-infections on fish: a review. *Vet. Res.* 48:26. doi: 10.1186/s13567-017-0432-7

Lafferty, K. D., Harvell, C. D., Conrad, J. M., Friedman, C. S., Kent, M. L., Kuris, A. M., et al. (2015). Infectious diseases affect marine fisheries and aquaculture economics. *Annu. Rev. Mar. Sci.* 7, 471–496. doi: 10.1146/annurev-marine-010814-015646

Levin, B. R., and Rozen, D. E. (2006). Non-inherited antibiotic resistance. *Nat. Rev. Microbiol.* 4, 556–562. doi: 10.1038/nrmicro1445

Levy, S. B., and Marshall, B. (2004). Antibacterial resistance worldwide: causes, challenges and responses. *Nat. Med.* 10, S122–S129. doi: 10.1038/nm1145

Little, D. C., Newton, R. W., and Beveridge, M. C. (2016). Aquaculture: a rapidly growing and significant source of sustainable food? Status, transitions and potential. *Proc. Nutr. Soc.* 75, 274–286. doi: 10.1017/s0029665116000665

Liu, X., Steele, J. C., and Meng, X. Z. (2017). Usage, residue, and human health risk of antibiotics in Chinese aquaculture: a review. *Environ. Pollut. (Barking, Essex 1987)* 223, 161–169. doi: 10.1016/j.envpol.2017.01.003

Liu, Y., Jia, Y., Yang, K., Li, R., Xiao, X., Zhu, K., et al. (2020). Metformin restores tetracyclines susceptibility against multidrug resistant bacteria. *Adv. Sci. (Weinheim Baden Wurttemberg Germany)* 7:1902227. doi: 10.1002/advs.201902227

Liu, Y., Li, R., Xiao, X., and Wang, Z. (2019). Antibiotic adjuvants: an alternative approach to overcome multi-drug resistant Gram-negative bacteria. *Crit. Rev. Microbiol.* 45, 301–314. doi: 10.1080/1040841X.2019.1599813

Martins, D., Mckay, G., Sampathkumar, G., Khakimova, M., and Nguyen, D. (2018). Superoxide dismutase activity confers (p)ppGpp-mediated antibiotic tolerance to stationary-phase *Pseudomonas aeruginosa*. *Proc. Natl. Acad. Sci. U.S.A.* 115:201804525. doi: 10.1073/pnas.1804525115

Matsuura, Y., Terashima, S., Takano, T., and Matsuyama, T. (2019). Current status of fish vaccines in Japan. *Fish Shellfish Immunol.* 95, 236–247. doi: 10.1016/j.fsi.2019.09.031

McCall, I. C., Shah, N., Govindan, A., Baquero, F., and Levin, B. R. (2019). Antibiotic killing of diversely generated populations of nonreplicating bacteria. *Antimicrob. Agents Chemother.* 63:e02360-18. doi: 10.1128/AAC.02360-18

Meijer, A. H., and Spaink, H. P. (2011). Host-pathogen interactions made transparent with the zebrafish model. *Curr. Drug Targets* 12, 1000–1017. doi: 10.2174/138945011795677809

Meylan, S., Porter, C. B. M., Yang, J. H., Belenky, P., Gutierrez, A., Lobritz, M. A., et al. (2017). Carbon sources tune antibiotic susceptibility in *Pseudomonas aeruginosa* via tricarboxylic acid cycle control. *Cell Chem. Biol.* 24, 195–206. doi: 10.1016/j.chembiol.2016.12.015

Mohr, K. I. (2016). History of antibiotics research. *Curr. Top. Microbiol. Immunol.* 398, 237–272. doi: 10.1007/82_2016_499

Nambiar, S., Laessig, K., Toerner, J., Farley, J., and Cox, E. (2014). Antibacterial drug development: challenges, recent developments, and future considerations. *Clin. Pharmacol. Ther.* 96, 147–149. doi: 10.1038/clpt.2014.116

Navarro Llorens, J. M., Tormo, A., and Martínez-García, E. (2010). Stationary phase in gram-negative bacteria. *FEMS Microbiol. Rev.* 34, 476–495. doi: 10.1111/j.1574-6976.2010.00213.x

Neely, M. N., Pfeifer, J. D., and Caparon, M. (2002). Streptococcus-zebrafish model of bacterial pathogenesis. *Infect. Immun.* 70, 3904–3914. doi: 10.1128/iai.70.7.3904-3914.2002

Peng, B., Su, Y. B., Li, H., Han, Y., Guo, C., Tian, Y. M., et al. (2015). Exogenous alanine and/or glucose plus kanamycin kills antibiotic-resistant bacteria. *Cell Metab.* 21, 249–262. doi: 10.1016/j.cmet.2015.01.008

Pérez-Sánchez, T., Mora-Sánchez, B., and Balcázar, J. L. (2018). Biological approaches for disease control in aquaculture: advantages, limitations and challenges. *Trends Microbiol.* 26, 896–903. doi: 10.1016/j.tim.2018.05.002

Pu, Y., Li, Y., Jin, X., Tian, T., Ma, Q., Zhao, Z., et al. (2019). ATP-dependent dynamic protein aggregation regulates bacterial dormancy depth critical for antibiotic tolerance. *Mol. Cell* 73, 143–156.e144. doi: 10.1016/j.molcel.2018.10.022

Rittershaus, E. S., Baek, S. H., and Sassetti, C. M. (2013). The normalcy of dormancy: common themes in microbial quiescence. *Cell Host Microbe* 13, 643–651. doi: 10.1016/j.chom.2013.05.012

Sánchez-Vázquez, F. J., Terry, M. I., Felizardo, V. O., and Vera, L. M. (2011). Daily rhythms of toxicity and effectiveness of anesthetics (MS222 and eugenol) in

zebrafish (*Danio rerio*). *Chronobiol. Int.* 28, 109–117. doi: 10.3109/07420528.2010.538105

Santos, L., and Ramos, F. (2018). Antimicrobial resistance in aquaculture: current knowledge and alternatives to tackle the problem. *Int. J. Antimicrob. Agents* 52, 135–143. doi: 10.1016/j.ijantimicag.2018.03.010

Shan, Y., Brown Gandt, A., Rowe, S. E., Deisinger, J. P., Conlon, B. P., and Lewis, K. (2017). ATP-dependent persister formation in *Escherichia coli*. *mBio* 8:e02267-16. doi: 10.1128/mBio.02267-16

Soliman, W. S., Shaapan, R. M., Mohamed, L. A., and Gayed, S. S. R. (2019). Recent biocontrol measures for fish bacterial diseases, in particular to probiotics, bio-encapsulated vaccines, and phage therapy. *Open Vet. J.* 9, 190–195. doi: 10.4314/ovj.v9i3.2

Song, C., Li, L., Zhang, C., Qiu, L., Fan, L., Wu, W., et al. (2017). Dietary risk ranking for residual antibiotics in cultured aquatic products around Tai Lake, China. *Ecotoxicol. Environ. Saf.* 144, 252–257. doi: 10.1016/j.ecoenv.2017.06.036

Sullivan, C., Matty, M. A., Jurczyszak, D., Gabor, K. A., Millard, P. J., Tobin, D. M., et al. (2017). Infectious disease models in zebrafish. *Methods Cell Biol.* 138, 101–136. doi: 10.1016/bs.mcb.2016.10.005

Sun, F., Bian, M., Li, Z., Lv, B., Gao, Y., Wang, Y., et al. (2020). 5-Methylindole potentiates aminoglycoside against gram-positive bacteria including *Staphylococcus aureus* persisters under hypoionic conditions. *Front. Cell. Infect. Microbiol.* 10:84. doi: 10.3389/fcimb.2020.00084

Taber, H. W., Mueller, J. P., Miller, P. F., and Arrow, A. S. (1987). Bacterial uptake of aminoglycoside antibiotics. *Microbiol. Rev.* 51, 439–457. doi: 10.1128/MMBR.51.4.439-457.1987

Tafalla, C., Bøgwald, J., and Dalmo, R. A. (2013). Adjuvants and immunostimulants in fish vaccines: current knowledge and future perspectives. *Fish Shellfish Immunol.* 35, 1740–1750. doi: 10.1016/j.fsi.2013.02.029

Takano, T., Matsuyama, T., Sakai, T., Nakamura, Y., Kamaishi, T., Nakayasu, C., et al. (2016). *Ichthyobacterium seriolicida* gen. nov., sp. nov., a member of the phylum 'Bacteroidetes', isolated from yellowtail fish (*Seriola quinqueradiata*) affected by bacterial haemolytic jaundice, and proposal of a new family, Ichthyobacteriaceae fam. nov. *Int. J. Syst. Evol. Microbiol.* 66, 580–586. doi: 10.1099/ijsem.0.000757

Tapia, J. A., Jensen, R. T., and García-Marín, L. J. (2006). Rottlerin inhibits stimulated enzymatic secretion and several intracellular signaling transduction pathways in pancreatic acinar cells by a non-PKC-delta-dependent mechanism. *Biochim. Biophys. Acta.* 1763, 25–38. doi: 10.1016/j.bbamcr.2005.10.007

Wu, L., Chen, L., Kou, M., Dong, Y., Deng, W., Ge, L., et al. (2020). The ratiometric fluorescent probes for monitoring the reactive inorganic sulfur species (RISS) signal in the living cell. *Spectrochim. Acta A Mol. Biomol. Spectrosc.* 231:118141. doi: 10.1016/j.saa.2020.118141

Yao, Z., Wang, Z., Sun, L., Li, W., Shi, Y., Lin, L., et al. (2016). Quantitative proteomic analysis of cell envelope preparations under iron starvation stress in *Aeromonas hydrophila*. *BMC Microbiol.* 16:161. doi: 10.1186/s12866-016-0769-5

Zhang, Q., Dong, X., Chen, B., Zhang, Y., Zu, Y., and Li, W. (2016). Zebrafish as a useful model for zoonotic *Vibrio parahaemolyticus* pathogenicity in fish and human. *Dev. Comp. Immunol.* 55, 159–168. doi: 10.1016/j.dci.2015.10.021

Conflict of Interest: The authors declare that the research was conducted in the absence of any commercial or financial relationships that could be construed as a potential conflict of interest.

frontiers in Microbiology

ORIGINAL RESEARCH
published: 08 June 2021
doi: 10.3389/fmicb.2021.699415

Proteomics Analysis Reveals Bacterial Antibiotics Resistance Mechanism Mediated by *ahslyA* Against Enoxacin in *Aeromonas hydrophila*

*Zhen Li[1,2,3,4], Lishan Zhang[1,3], Qingli Song[1,3], Guibin Wang[1,5], Wenxiao Yang[1,3], Huamei Tang[1,3], Ramanathan Srinivasan[1,3], Ling Lin[1,3] and Xiangmin Lin[1,3,4]**

[1] Fujian Provincial Key Laboratory of Agroecological Processing and Safety Monitoring, School of Life Sciences, Fujian Agriculture and Forestry University, Fuzhou, China, [2] Zhangzhou Health Vocational College, Zhangzhou, China, [3] Key Laboratory of Crop Ecology and Molecular Physiology, Fujian Agriculture and Forestry University, Fujian Province University, Fuzhou, China, [4] Key Laboratory of Marine Biotechnology of Fujian Province, Institute of Oceanology, Fujian Agriculture and Forestry University, Fuzhou, China, [5] State Key Laboratory of Proteomics, Beijing Proteome Research Center, National Center for Protein Sciences, Beijing Institute of Lifeomics, Beijing, China

OPEN ACCESS

Edited by:
Bo Peng,
Sun Yat-sen University, China

Reviewed by:
Lixing Huang,
Jimei University, China
Lewis Oscar Felix Raj Lucas,
Rhode Island Hospital, United States

***Correspondence:**
Xiangmin Lin
xiangmin@fafu.edu.cn

Specialty section:
This article was submitted to Antimicrobials, Resistance and Chemotherapy, a section of the journal Frontiers in Microbiology

Received: 23 April 2021
Accepted: 17 May 2021
Published: 08 June 2021

Citation:
Li Z, Zhang L, Song Q, Wang G, Yang W, Tang H, Srinivasan R, Lin L and Lin X (2021) Proteomics Analysis Reveals Bacterial Antibiotics Resistance Mechanism Mediated by ahslyA Against Enoxacin in Aeromonas hydrophila. Front. Microbiol. 12:699415. doi: 10.3389/fmicb.2021.699415

Bacterial antibiotic resistance is a serious global problem; the underlying regulatory mechanisms are largely elusive. The earlier reports states that the vital role of transcriptional regulators (TRs) in bacterial antibiotic resistance. Therefore, we have investigated the role of TRs on enoxacin (ENX) resistance in *Aeromonas hydrophila* in this study. A label-free quantitative proteomics method was utilized to compare the protein profiles of the *ahslyA* knockout and wild-type *A. hydrophila* strains under ENX stress. Bioinformatics analysis showed that the deletion of *ahslyA* triggers the up-regulated expression of some vital antibiotic resistance proteins in *A. hydrophila* upon ENX stress and thereby reduce the pressure by preventing the activation of SOS repair system. Moreover, *ahslyA* directly or indirectly induced at least 11 TRs, which indicates a complicated regulatory network under ENX stress. We also deleted six selected genes in *A. hydrophila* that altered in proteomics data in order to evaluate their roles in ENX stress. Our results showed that genes such as *AHA_0655*, *narQ*, *AHA_3721*, *AHA_2114,* and *AHA_1239* are regulated by *ahslyA* and may be involved in ENX resistance. Overall, our data demonstrated the important role of *ahslyA* in ENX resistance and provided novel insights into the effects of transcriptional regulation on antibiotic resistance in bacteria.

Keywords: antibiotics resistance, AhSlyA, enoxacin, quantitative proteomics, *Aeromonas hydrophila*

INTRODUCTION

Antibiotic-resistant bacterial strains were discovered over 90 years ago. Since then, antibiotic-resistant bacterial strains have been found to be widely distributed in various environments, such as in hospitals, seafood, and aquaculture farms, and as a result, they pose a serious public health problem worldwide (Fritsche et al., 2009; Peng et al., 2015). Although, several mechanisms of antibiotic resistance such as membrane permeability, plasmid transfer, antibiotic modification or

degradation, efflux, and biofilm formation have been described in recent years, the underlying mechanism of acquire antibiotic resistance in bacteria is still largely unknown (Peterson and Kaur, 2018). The emergences of drugs resistant bacterial strains have been caused by many complicated characteristics, one of which is the antimicrobial resistance genes (ARGs) transcriptional regulators (TRs). Bacterial TRs play an important role in the transcriptional regulation of functional genes needed to survive environmental stresses, including antibiotic resistance (Zhou and Yang, 2006; Tang et al., 2019a). For example, a mutation in the multiple antibiotic resistance (MarR) TRs in *Escherichia coli* has been shown to lead to the expression of the *marRAB* operon. Therefore, it promotes the expression of the transcription factor MarA and activation of the *acrAB* and *tolC* efflux pump genes, resulting in multi-drug resistance to tetracycline, quinolones, β-lactams, and phenolic compounds (Pourahmad Jaktaji and Ebadi, 2013; Lankester et al., 2019). Additionally, the TR EmrR is an inhibitor of efflux pump EmrCAB in *Chromobacterium violaceum* and the mutation of $emrR_{R92H}$ increases the resistance of *C. violaceum* to nalidixic acid (Barroso et al., 2018). Nonetheless, there are hundreds of bacterial TRs with biological functions that are poorly characterized and most of the direct and indirect effects of TRs on bacterial antibiotic resistance are largely unknown.

Aeromonas hydrophila is a widely distributed environmental bacterium and a well-known fish pathogen. The use of antibiotics in aquaculture industries has resulted in the emergence of multi-drug resistant *A. hydrophila* strains in aquaculture and even in hospital settings (Li et al., 2020; Zhu et al., 2020). In recent years, many research, including our previous study, have been found that the several metabolic pathways related genes were involved in the drug-resistance on this pathogen by multi omics technologies (Hossain et al., 2018; Sun et al., 2019; Li et al., 2021). In our previous study, we reported that the LysR-type TR YeeY in *A. hydrophila* plays an important role in the regulation of furazolidone resistance by directly regulating ARGs, including *AHA_3222* and *AHA_4275*. It indicates the crucial role of TRs in the antibiotic resistance of this pathogen. However, the underlying mechanisms of antibiotic resistance regulated by TRs in *A. hydrophila* are needed to be further investigated.

To better understanding the role and regulatory mechanism of TR on the bacterial physiological function. In this study, we reported on a MarR family TR in *A. hydrophila,* AhSlyA (gene name *ahslyA* or *AHA_1240*). AhSlyA is a winged helix-turn-helix (wHTH) DNA-binding TR. Previous research reported the homologous proteins of this TR in other bacterial species play diverse biological functions such as cell metabolism and virulence, while its biological effect and molecular mechanism are still largely unknown, especially for the bacterial antibiotics resistance in *A. hydrophila* (Banda et al., 2019; Tian et al., 2021). In this study, we constructed an *ahslyA* deletion mutant (Δ*ahslyA*) in *A. hydrophila* and found that it displayed significantly decreased resistance to the quinolone antibiotic, enoxacin (ENX), as compared to the wild-type (WT) parent strain. To further investigate the direct or indirect effect of this TR on the antibiotic resistance of *A. hydrophila*, a label-free quantitative proteomics method was used to compare the differentially expressed proteins between the Δ*ahslyA* and WT strains under ENX stress. Moreover, a several differentially expressed genes were deleted and their antibiotic susceptibility to ENX was validated. This study will conduce to further understand the complicated antibiotic resistance mechanisms mediated by bacterial TRs.

MATERIALS AND METHODS

Bacterial Strains and Culture Conditions

The strains used in this study are *A. hydrophila* ATCC 7966, Δ*ahslyA,* and the *ahslyA* complemented strain. *E. coli* MC1061 and S17 were stored in our laboratory previously. The culture temperature of *A. hydrophila* and *E. coli* were 30 and 37°C, respectively. Both bacterial strains were cultured in Luria–Bertani (LB) medium with appropriate antibiotics.

Construction of the Gene Deletion Strain

The deletion strain was constructed based on the principle of two-step homologous recombination using the suicide vector pRE112, as previously described (Yu et al., 2005). Briefly, the pRE112 plasmid fused with about 500-bp of the upstream and downstream flanking regions of the target gene was constructed using *A. hydrophila* ATCC 7966 genomic DNA as template and then transferred into competent *E. coli* MC1061 cells. Then, the plasmid of a positive clone was extracted and transferred into *E. coli* S17 competent cells. After verifying by PCR amplification, the *E. coli* S17 carrying the pRE112 recombined vector was then conjugated with *A. hydrophila* in a 4:1 ratio to the first step of homologous recombination. Positive *A. hydrophila* clones were selected on LB agar plates with ampicillin and chloramphenicol (Yeasen Inc., Shanghai, China). The second step of homologous recombination was carried out in LB medium containing 20% sucrose. The Δ*ahslyA* in *A. hydrophila* was confirmed by plating chloramphenicol, followed by PCR and DNA sequencing. Finally, after about 20 generations of stable inheritance and correct DNA sequencing, the Δ*ahslyA* mutant was stocked and stored in the freezer at −80°C.

Protein Sample Preparation

Bacterial strains were inoculated in 5 mL LB medium, cultured for 16 h and then transferred at the ratio of 1:100 into 100 mL of LB medium containing ENX at a final concentration of 0.0078 μg/mL. After culturing for about 3 h (until the culture reached an OD_{600} of approximately 1.0), the cells were collected by centrifugation at 8,000 × *g* at 4°C for 20 min and washed twice with PBS. The bacterial samples were then resuspended in 5 mL of PBS buffer containing 1 mM phenylmethanesulfonyl fluoride (PMSF) and then lysed by ultra-sonication. The supernatant was collected by centrifugation at 8,000 × *g* for 20 min and the total protein concentration was detected *via* the Bradford method. About 50 μg of each protein sample was reduced with 50 mM dithiothreitol at 56°C, alkylated with 25 mM iodoacetamide in dark and then digested to peptides with a 1:20 ratio of trypsin (Promega Inc., Shanghai, China). The enzymatic peptides were desalted with a C18 column (Waters Inc., Milford, MA,

United States) and dried with a centrivap concentrator (Labconco Inc., Kansas City, MO, United States). Each group sample was performed three independent repeats for biological replicates.

Label-Free LC-MS/MS

The desalted peptides were dissolved in liquid chromatography mobile phase buffer A [containing 2% acetonitrile, 0.1% formic acid (FA)], loaded onto the pre-column at a flow rate of 4.5 μL/min on the chromatographic system and then injected into the column at a flow rate of 300 nL/min by an easy-nlc1200 system (Thermo Scientific Inc., Waltham, MA, United States). The liquid gradient setting was as follows: 0–3 min, buffer B (containing 80% acetonitrile, 0.1% FA) increased linearly from 2 to 5%; 3–103 min, solution B increased linearly from 5 to 28%; 103–108 min, solution B increased linearly from 35 to 90%; 110–120 min, the solubility of solution B was maintained at 90%. Mass spectrometry was performed with an Orbitrap Fusion Lumos system (Thermo Scientific Inc., Waltham, MA, United States) nanospray ion source. The spray voltage was 2.0 KV and the ion transfer tube temperature was 300°C. We used the data-dependent acquisition mode to the collect data. The parameters were as follows: the precursors from 350 to 1,600 m/z were scanned at a resolution of 60,000, and the AGC target was set at 4e5. For MS/MS, the HCD collision energy was 30% with a resolution of 15,000. The AGC target was set to 5e4. The cycle time was 3 s. All raw data were searched by Maxquant software v.1.6.3.4 against Uniprot *A. hydrophila* ATCC7966 database. Proteins with the number of peptides greater than 2, *p*-value less than 0.05, and protein ratio difference greater than 1.5 times were selected as differential proteins for bioinformatics analysis. The raw MS files were submitted to the iProx (Integrated Proteome resources) database under the accession number IPX0002908000 (Ma et al., 2019).

Bioinformatics Analysis

The GO (gene ontology) analysis of altered proteins were performed using the online software DAVID[1] and visualized with GOplot package in R language software (Walter et al., 2015; Zhang L.S. et al., 2020). The protein-protein interaction (PPI) network was predicted using the String[2] online database with a confidence score ≥ 0.7 and the network was clustered using the "Markov Cluster Algorithm (MCL)" and the inflation parameter was set as 4 (Szklarczyk et al., 2017). Finally, the visualized network diagram of PPI was drawn using Cytoscape 3.8.0[3] (Shannon et al., 2003).

Determination of Minimal Bactericidal Concentrations

The minimal bactericidal concentration (MBC) assay was performed by the agar dilution method, as previously described (Jiang et al., 2020). Briefly, an overnight bacterial culture was passaged into fresh LB medium, incubated at 30°C with shaking until the OD_{600} reached about 1.0 and then diluted 100 times. Then, 2 μL of each dilution was spotted onto an LB agar plates with twofold dilution gradient concentration of antibiotics (ciprofloxacin, levofloxacin, enoxacin, and enrofloxacin purchased from Yeasen biotech, Ltd., Shanghai, China), respectively, and incubated at 30°C for 16 h. Each experiment was performed at least three times with biological duplicates.

[1]https://david.ncifcrf.gov/

[2]https://string-db.org

[3]http://www.cytoscape.org

RESULTS

ahslyA Mutant Affects Antibiotic Susceptibility in *Aeromonas hydrophila*

In order to better understand the characteristics of the TR AhslyA on bacterial antibiotic resistance, we first constructed Δ*ahslyA* mutant strain and then tested its antibiotic susceptibilities against various antibiotics, including several quinolone antibiotics. As shown in **Figure 1**, loss of *ahslyA* caused a twofold increase in the MBC to ciprofloxacin (CIP) and levofloxacin (LVX), and increased the MBC of ENX by four times; however, it did not affect the susceptibility to enrofloxacin (ENR). Moreover, complementation of the Δ*ahslyA* strain restored the antibiotic susceptibilities similar level to the WT strain, which is suggesting that the *ahslyA* gene in *A. hydrophila is* involved in the regulation of several antibiotic resistances, especially ENX.

Quantitative Proteomics Comparison Between WT and Δ*ahslyA* Strains Under ENX Stress

In order to further investigate the regulatory mechanism of *ahslyA* on ENX antibiotic resistance, we isolated whole protein samples from WT and Δ*ahslyA* strains with or without exposure to 0.0078 μg/mL ENX treatments. After trypsin digestion, each sample was quantified by a label-free quantitative proteomics method to compare the differentially expressed proteins between both groups. As shown in **Figure 2A**, positive correlations greater than 0.98 were found between the intensities of the MS of each sample with the regression coefficients, which indicated that the quantitative analysis results of MS in this study were stable and reliable. A principal component analysis (PCA) scatter diagram was drawn to cluster the samples. The dots of different colors in **Figure 2B** represent three groups of repeats of the same sample. It can be seen from the diagram that the three dots of the same color are relatively close; indicating that the gene expression pattern of the three repeats of the same sample had a small difference and suitable data repeatability. The proteomic analysis of the Δ*ahslyA* + ENX group was significantly separated from the WT + ENX group in the direction of PC1, indicating that there may be significant differences between them. These results indicate that the effect of the deletion of *ahslyA* on bacterial proteome is more than the effect of ENX stress.

The Differential Protein Abundances of WT and Δ*ahslyA* in Response to ENX Stress

In this study, a total of 2,534 proteins were identified by mass spectrometry (unique peptide number ≥ 2 and false

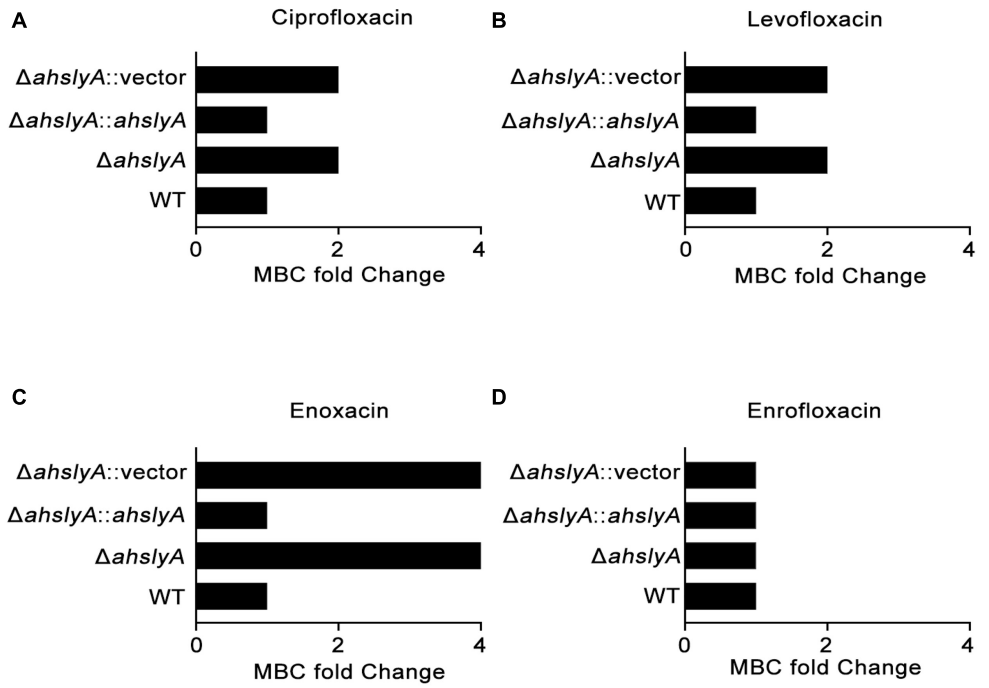

FIGURE 1 | Measurement of the MBCs of *ahslyA* derivatives in *A. hydrophila* to four quinolone antibiotics. **(A)** The MBCs of Δ*ahslyA* and complemented Δ*ahslyA* strains, in addition to WT and Δ*ahslyA* carrying an empty vector as negative controls, were tested for their sensitivity to **(A)** ciprofloxacin, **(B)** levofloxacin, **(C)** enoxacin, and **(D)** enrofloxacin. The MBCs of each strain to antibiotics were compared with WT as MBC fold change.

discovery rate (FDR) < 1%). The protein abundance ratio that was ≥ 1.5 (upregulated expression) and ≤0.667 (downregulated expression) with a *p*-value < 0.05 of each compared group was regarded as differentially expressed proteins. We analyzed the data by two comparisons, Δ*ahslyA* + ENX vs. Δ*ahslyA* and Δ*ahslyA* + ENX vs. WT + ENX, in order to interpret the *ahslyA* mediated ENX resistance in this study. When compared with Δ*ahslyA* without antibiotic treatment, there was 49 differentially expressed proteins were found, which accounted for 1.77% of the total identified proteins, including 35 increasing and 14 decreasing in abundance in the Δ*ahslyA* + ENX treatment group (**Figure 2C**). When compared with WT + ENX, a total of 172 proteins, including 101 increasing and 71 decreasing in abundance, were altered in the Δ*ahslyA* + ENX treatment group (**Figure 2D**). The following overlap analysis between both group comparisons showed that Δ*ahslyA* + ENX vs. Δ*ahslyA* and Δ*ahslyA* + ENX vs. WT + ENX have 14 common altered proteins, of which seven have the same protein expression trend and another seven have the opposite expression (**Supplementary Table 1** and **Figure 2E**).

Bioinformatics Analysis of Altered Proteins in Δ*ahslyA* + ENX/Δ*ahslyA* and Δ*ahslyA* + ENX/WT + ENX Comparisons

We then used GO terms enrichment to analyze altered proteins in both comparisons. In the biological process (BP) enrichment, the DNA metabolic process, cellular response to stimulus, SOS response, and cell communication were the most enriched terms in the Δ*ahslyA* + ENX vs. Δ*ahslyA* comparison. Additionally, the response to stress, the response to stimulus, the DNA metabolic process, and the cellular response to external stimulus were the most enriched terms in the Δ*ahslyA* + ENX vs. WT + ENX comparison. When comparing both group, the response to stress and the cellular response to stress in the Δ*ahslyA* + ENX vs. WT + ENX comparison changed significantly, while no change were observed in the Δ*ahslyA* + ENX vs. Δ*ahslyA* comparison (**Figures 3A,B**).

We further analyzed the predicted PPI network of altered proteins in both comparisons using STRING software and then clustered them using the MCL algorithm. In the Δ*ahslyA* + ENX vs. Δ*ahslyA* comparison, there were five clusters that were enriched (**Figure 4**). Eight increasing proteins were clustered in cluster 1, and most of them were SOS or DNA repair-related proteins. There were six metabolic pathway-related proteins clustered in cluster 2, including three proteins that might be involved in acyl-CoA metabolism, namely, acyl-CoA thioester hydrolase YciA (gene name *AHA_1563*), acyl-CoA thioesterase I (*AHA_3489*), and acyl carrier protein (*acpP*). Both *AHA_3297* and *AHA_0044* are a sensor histidine kinase and sensory box/GGDEF family gene, respectively, which were present in clusters 3–5. It indicates that *ahslyA* may affect a bacterial two-component or cyclic di-GMP signaling system. The top 14 clusters of the Δ*ahslyA* + ENX vs. WT + ENX

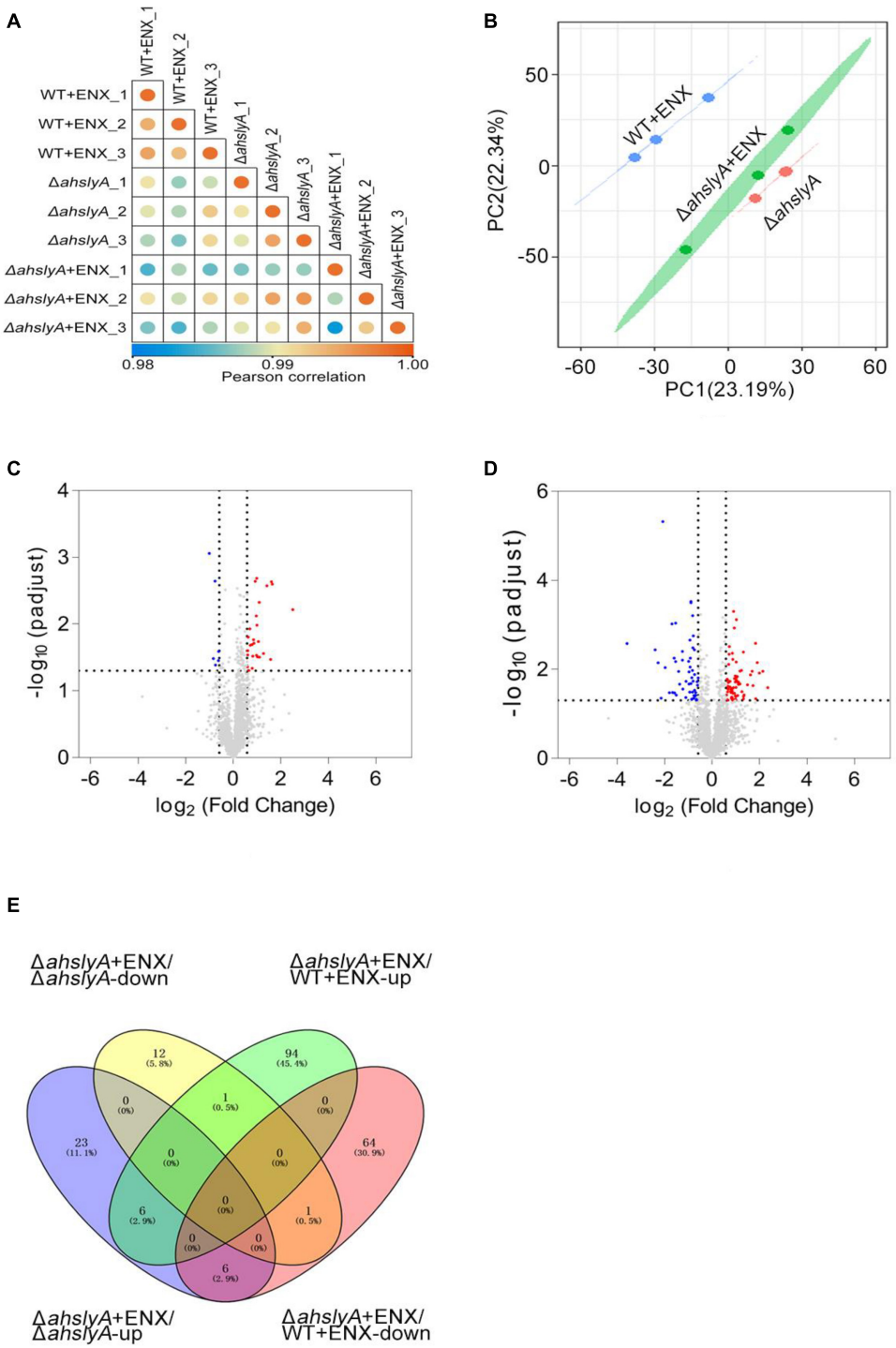

FIGURE 2 | Label-free quantitative proteomics data analysis. **(A)** Correlation coefficient analysis of protein MS intensity in three biological replications. **(B)** PCA of WT + ENX, Δ*ahslyA* + ENX, and Δ*ahslyA*. **(C,D)** Volcano maps comparing the abundance ratios of proteins with significant differences in expression between Δ*ahslyA* + ENX vs. Δ*ahslyA* and Δ*ahslyA* + ENX vs. WT + ENX, respectively. The blue dots represent downregulated proteins, red dots represent upregulated proteins, and the gray color represents non-differentially expressed proteins. **(E)** Venn-diagram of differentially expressed proteins between two comparisons.

comparison are shown in **Figure 3B**. In cluster 1, at least seven proteins, including RecA, UvrA, UvrD, LexA, DinB, RecN, and RecG are involved in DNA repair processes and all seven were decreasing in abundance. *AHA_3525* is a response regulator, which was the network hub in cluster 2. Moreover, *AHA_3525* interacted with three TRs, namely, *AHA_0137* (response

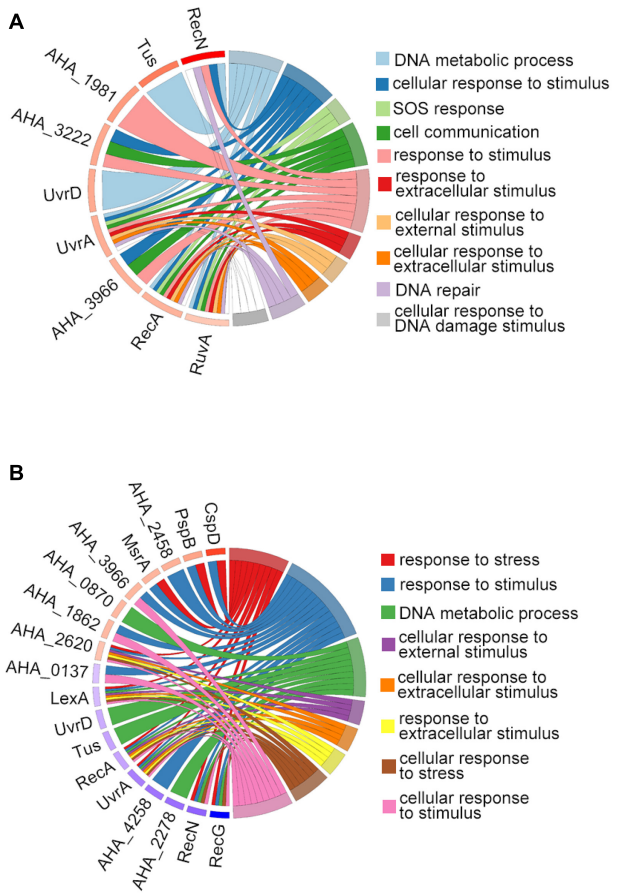

FIGURE 3 | Chord plot showing GO terms BP analysis of differentially expressed proteins in the two comparisons. **(A)** Δ*ahslyA* + ENX vs. WT + ENX, and **(B)** Δ*ahslyA* + ENX vs. Δ*ahslyA*.

regulator, GltR), *AHA_1862* (response regulator protein), and *AHA_3966* (DNA-binding response regulator), in addition to *AHA_3297* (diguanylate cyclase DosC), and most of these genes were increasing in abundance. In cluster 3, most of altered proteins were metal ion-related proteins. For example, SelA, SelD, and the SelT/SelW/SelH domain (*AHA_1610*) were involved in selenium metabolism in prokaryotes. Additionally, clusters 4–6 were mostly clustered in oxidative respiration, uncharacterized protein and sulfate metabolism.

The ENX-Resistance Capabilities of Proteins Regulated by *ahslyA*

In order to better understand the ENX resistance mechanism mediated by the TR *ahslyA*, we further assessed the effect of several gene mutants on the resistance to ENX, which were shown to be regulated directly or indirectly by *ahslyA* in our proteomics results. Selected gene deletion strains, including three genes related to decreasing in protein abundance (*AHA_0655*, *AHA_1195*, and *AHA_3721*) and three genes related to increasing in protein abundance (*AHA_1239*, *AHA_2114*, and *narQ*) in the Δ*ahslyA* + ENX vs. WT + ENX proteomic comparison, were successfully constructed *via* a two-step homologous recombination method using the primer pairs listed in **Supplementary Table 2**. Each mutant was assessed for sensitivity to ENX using an antibiotic susceptibility assay. As showed in **Figure 5**, the Δ*AHA_0655* exhibited a slightly decreased resistance while other mutants showed no significant difference to 0.0078 μg/mL of ENX. The Δ*AHA_2114* and Δ*narQ* showed a slight decrease in resistance to 0.01 μg/mL of ENX, and the Δ*AHA_1239* and Δ*AHA_3721* demonstrated significantly increased resistance to 0.01 μg/mL of ENX. These results suggested that *ahslyA* may regulate the transcription of *AHA_0655*, *narQ*, *AHA_3721*, *AHA_2114*, or *AHA_1239* to against ENX stress.

DISCUSSION

It is well known that bacterial TRs play a crucial regulatory role in diverse physiological and pathological functions. However, as there are hundreds of TRs are identified in prokaryotes and only a few of them have been well described, the intrinsic regulatory mechanisms of prokaryotic TRs are largely unknown (Brown et al., 2003). SlyA belongs to the TR MarR family that possesses a winged-helix DNA binding domain (Wilkinson and Grove, 2006). It was first reported to regulate virulence in many pathogens, such as *Salmonella typhimurium*, *Enterococcus faecalis*, and *Dickeya dadantii* (Libby et al., 1994; Haque et al., 2009; Michaux et al., 2011b). It has also been shown to play important roles in oxidative stress, bile salt stress, antimicrobial peptide resistance, heat, and acid stress (Buchmeier et al., 1997; Spory et al., 2002; Shi et al., 2004; Michaux et al., 2011a). Therefore, it suggests that this TR plays an important role in numerous physiological functions. However, the mechanism underlying these biological functions remains elusive.

Since SlyA plays an important role in the resistance to environmental stresses, we speculated that it may contribute to bacterial antibiotic resistance, because antibiotics are toxic small molecules like bile salts. To test our hypothesis, the antibiotic susceptibilities of the *slyA* gene deletion mutant and its complemented strains were analyzed in this study. We found that the Δ*ahslyA* had increased resistance against several quinolone antibiotics, suggesting that this TR may negatively regulate resistance to certain antibiotics, especially ENX. We then performed label-free quantitative MS to characterize the effect of *ahslyA* gene deletion on the proteome of *A. hydrophila* cells with or without ENX treatment. Here, we analyzed two group comparisons in order to understand the ENX resistance mediated by *ahslyA*. In the Δ*ahslyA* + ENX vs. Δ*ahslyA*, we identified 49 altered proteins, and when Δ*ahslyA* + ENX was compared to WT + ENX, there were 172 differentially expressed proteins. GO bioinformatics analysis showed that both comparisons were related to a stress response or stimulus, which indicated that *ahslyA* may play an important role in stress resistance to environmental factors, including antibiotics. Although, we have not obtained a significant KEGG (Kyoto Encyclopedia of genes and genes) pathway enriched altered proteins in either of the comparisons in this study. The PPI prediction plus the MCL

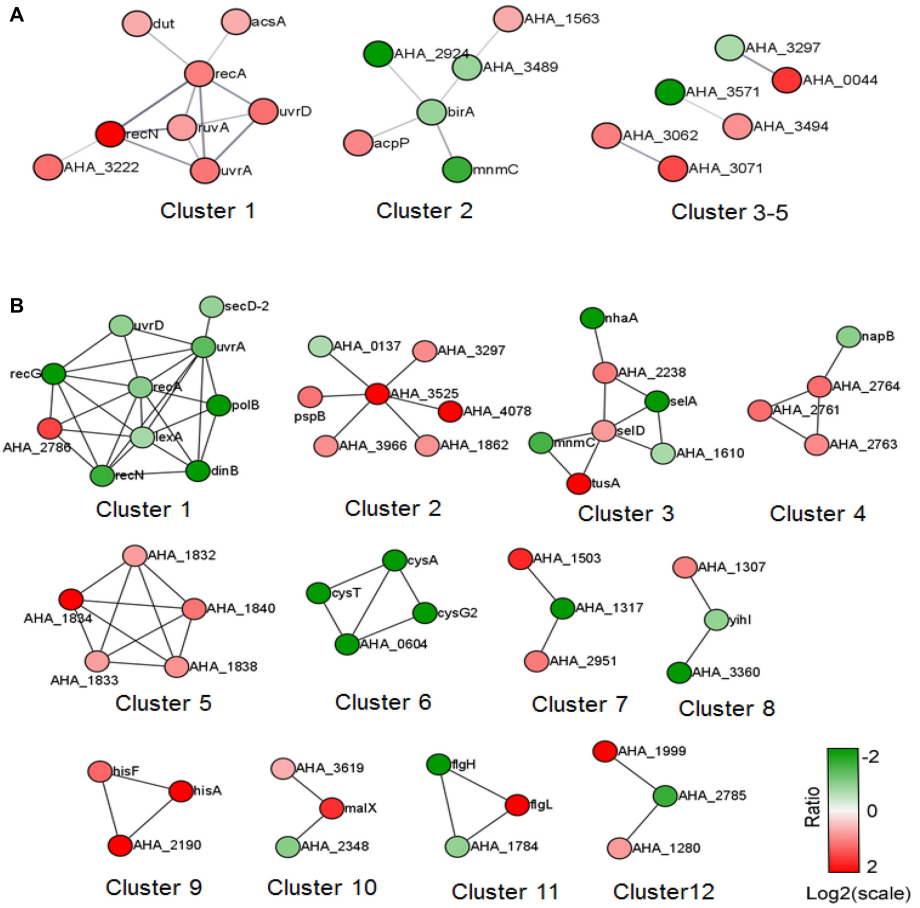

FIGURE 4 | The PPI prediction network of altered proteins in the two comparisons. **(A)** Δ*ahslyA* + ENX vs. WT + ENX, and **(B)** Δ*ahslyA* + ENX vs. Δ*ahslyA*. The green dots represent downregulated proteins and red dots represent upregulated proteins.

algorithm showed that these altered proteins can be classified into several clusters. In the Δ*ahslyA* + ENX vs. Δ*ahslyA* comparison, five DNA repair-related proteins (RecA, RecN, RuvA, UvrA, and UrvD) were significantly increased in abundance. It is well known that quinolone antibiotics inhibit DNA synthesis and cause DNA strand cleavage or cell death. The underlying mechanism of quinolone antibiotic resistance in bacteria is due to the upregulation of DNA repair related proteins. In our previous study, 11 SOS responses or DNA repair-related proteins of *A. hydrophila* were reported to be increased under ENX stress (Zhang L.S. et al., 2020). Moreover, the deletion of *uvrA* decreased the ENX tolerance in *A. hydrophila*, which suggests the important role of the DNA repair process in protecting the DNA from quinolone-induced damage. Interestingly, we found that many of the DNA repair-related proteins decreased in abundance in the Δ*ahslyA* + ENX vs. WT + ENX comparison. This could have happened for a few reasons. First, the loss of *ahslyA* likely slowed down the toxic effect of ENX, so that bacteria did not trigger the DNA repair system. Second, the DNA repair response should be a last resort against ENX, as it may cause genetic mutations that influence bacterial survival. Third, *ahslyA* may regulate other drug resistance genes, aside from just DNA repair processes.

In both proteomic comparisons, the Δ*ahslyA* + ENX vs. WT + ENX comparison may be better than the Δ*ahslyA* + ENX vs. Δ*ahslyA* comparison to interpret *ahslyA*-mediated ENX resistance, because the first comparison is on the same ENX background. Therefore, we focused more on the properties of altered proteins between Δ*ahslyA* + ENX compared to Δ*ahslyA*. Of these altered proteins, we found *ahslyA* could directly or indirectly regulate at least 11 TRs (*gltR*, *yidZ*, *ycaN*, *citA*, *AHA_3297*, *AHA_0117*, *AHA_3721*, *AHA_1240*, *AHA_4233*, *AHA_1862,* and *AHA_3966*), which indicating that these TRs may construct a complicated gene regulatory network to maintain the intracellular homeostasis during ENX stress. Of these TRs, *AHA_3966* is homologous with *E. coli ompR,* with an identity of 49%. The *ompR* gene belongs to a well-known two-component regulatory system and plays important roles in multiple physiological functions, including antibiotic resistance (Lin et al., 2012; Zhang M.M. et al., 2020). Moreover, both *AHA_1862* and *AHA_3297* coded diguanylate cyclase and *AHA_3525* coded phosphodiesterase that govern the cellular level of c-di-GMP, which acts as a unique bacterial second messenger to trigger various cellular responses, such as in motility, biofilm formation, and antibiotics resistance (De et al., 2008;

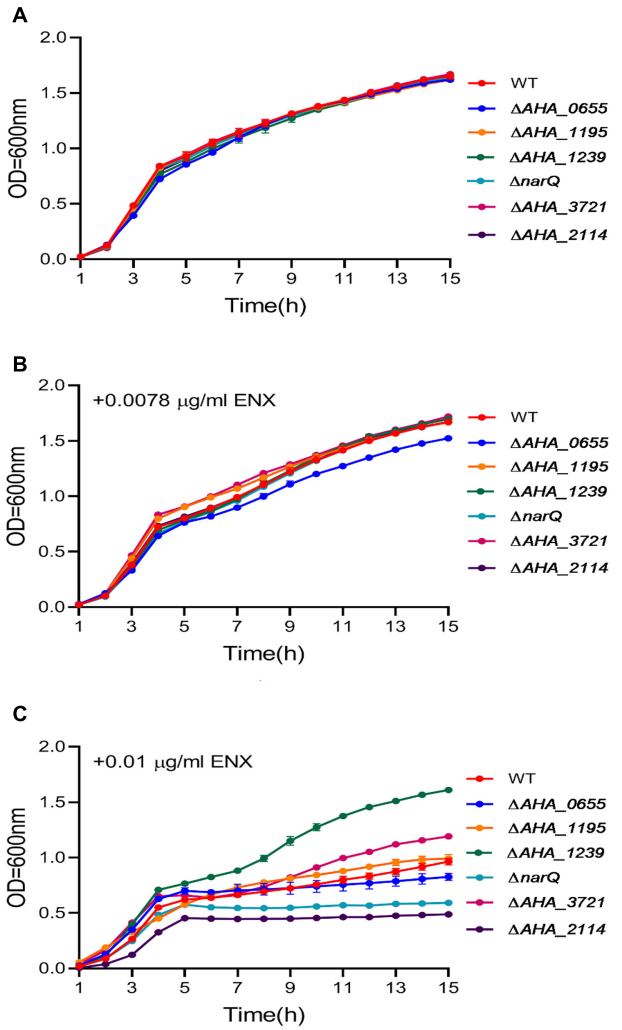

FIGURE 5 | The Growth curves of *A. hydrophila* WT and a total six gene deletion strains with or without ENX treatment. **(A)** LB medium alone; **(B)** LB medium + 0.0078 μg/mL ENX; **(C)** LB medium + 0.01 μg/mL ENX.

Gupta et al., 2014). However, the relationship between *ahslyA* and c-di-GMP is not clear.

To further understand the effect of *ahslyA* on the regulation of ENX resistance-related proteins, six target genes (*AHA_0655*, *AHA_1195*, *AHA_3721*, *AHA_1239*, *AHA_2114,* and *narQ*) that encode altered proteins in the proteomics data were selected to construct targeted gene deletion strains to determine their roles in susceptibility against ENX. Among these selected genes or proteins, *AHA_0655* (A0KG12) encodes an ATP-binding cassette transporter that belongs to a multi-drug efflux transporter family and plays a crucial role in the uptake of nutritional or toxic substrates from the environment, including antibiotics (Pletzer et al., 2015; Tang et al., 2019b). The decreased expression of A0KG12 in this study suggests that *ahslyA* may negatively regulate this protein to uptake ENX into cells. *AHA_1239* encodes a HlyD family secretion protein, was the protein that increased most in abundance in our MS data. *AHA_1239* increased 3,899 folds in the Δ*ahslyA* + ENX vs. WT + ENX comparison. Interestingly, *AHA_1239* is the downstream gene of *ahslyA* (*AHA_1240*), and its amino acid sequence has 30% identity to multi-drug resistance protein MdtN in *E. coli*. Moreover, the deletion of *ahslyA* and exposure to ENX stress also caused an upregulation of A0KK37 (*AHA_2114*), which is the multi-drug resistance protein MdtK. Since both proteins are members of the MATE (multi-drug and toxic compound extrusion) protein family. Further, the overexpression of MdtK increases resistance to norfloxacin, doxorubicin, and acriflavine in *Salmonella enterica* serovar Typhimurium. More, the *ahslyA* may negatively regulate both MdtN and MdtK to obtain ENX resistance in this study (Nishino et al., 2006). Additionally, the TRs A0KHI5 (*AHA_1195, YcaN*) and A0KPG8 (*AHA_3721*), nitrate sensor protein, A0KIL7 (*narQ*), belong to a two-component regulatory system play important roles on diverse biological functions in other bacterial species (Oshima et al., 2002). In this study, A0KHI5 and A0KPG8 were down-regulated, while NarQ increased in the Δ*ahslyA* + ENX vs. WT + ENX proteomics data, suggesting that they may affect ENX resistance regulated by *ahslyA*.

To test our hypothesis, the antibiotic susceptibilities of these six gene deletion mutants were determined. Our results showed that the deletion of *AHA_0655* slightly decreased the growth of *A. hydrophila* under low dose of ENX stress. Further the deletion of *AHA_2114* and *narQ* significantly decreased bacterial growth under high dose of ENX stress, while the deletion of *AHA_3721* increased antibiotic susceptibility in *A. hydrophila*. Which suggested that *ahslyA* may regulate *AHA_0655*, *narQ*, *AHA_3721*, and *AHA_2114* for ENX resistance. Although *AHA_1239* may act as a multi-drug resistance protein, the deletion of *AHA_1239* caused significant resistance to ENX in this study. The inherent reason is unknown, but based on the fact that *AHA_1239* is the downstream neighbor of *ahslyA*, the deletion of *AHA_1239* may affect the expression of *ahslyA* and then trigger other ARGs or systems against ENX stress. Overall, our data demonstrated the important role of *ahslyA* in the multiple ARGs regulation during ENX resistance and provided novel insights into the effects of TRs on the antibiotic resistance of bacteria.

DATA AVAILABILITY STATEMENT

The datasets presented in this study can be found in online repositories. The names of the repository/repositories and accession number(s) can be found below: http://www.proteomexchange.org/, PXD024843.

AUTHOR CONTRIBUTIONS

XL and LZ conceptualized and validated the study. ZL, LL, and LZ performed the methodology and the data curation and wrote the manuscript for the final draft. ZL, GW, and QS performed the formal analysis. XL was responsible for the resources, supervised

the study, and performed the funding acquisition. RS, WY, HT, and XL wrote, reviewed, and edited the manuscript. All authors contributed to the article and approved the submitted version.

FUNDING

This work was sponsored by grants from Key projects of Natural Science Foundation of Fujian Province (No. 2020J02023), NSFC projects (Nos. 31670129 and 31802343), China Post-doctoral Science Foundation (Grant No. 2019M662214), and Program for Innovative Research Team in Fujian Agricultural and Forestry University (No. 712018009).

ACKNOWLEDGMENTS

We acknowledge the support of the program for Key Laboratory of Marine Biotechnology of Fujian Province (2020MB04) and the Fujian-Taiwan Joint Innovative Center for Germplasm Resources and Cultivation of Crop (FJ 2011 Program, No. 2015-75, China). We would also like to thank the help from Central Laboratory, Fujian Medical University Union Hospital, China.

SUPPLEMENTARY MATERIAL

The Supplementary Material for this article can be found online at: https://www.frontiersin.org/articles/10.3389/fmicb.2021.699415/full#supplementary-material

Supplementary Figure 1 | Construction and confirmation of the six gene deletion strains.

Supplementary Table 1 | The identification of 14 common altered proteins between both group comparisons using label-free analysis.

Supplementary Table 2 | The primer pairs used in this study.

REFERENCES

Banda, M. M., Zavala-Alvarado, C., Perez-Morales, D., and Bustamante, V. H. (2019). SlyA and HilD counteract H-NS-mediated repression on the ssrAB virulence operon of *Salmonella enterica Serovar typhimurium* and thus promote its activation by OmpR. *J. Bacteriol.* 201:e00530-18.

Barroso, K. C. M., Previato-Mello, M., Batista, B. B., Batista, J. H., da Silva, and Neto, J. F. (2018). EmrR-dependent upregulation of the efflux pump EmrCAB contributes to antibiotic resistance in *Chromobacterium violaceum*. *Front. Microbiol.* 9:2756.

Brown, N. L., Stoyanov, J. V., Kidd, S. P., and Hobman, J. L. (2003). The MerR family of transcriptional regulators. *FEMS Microbiol. Rev.* 27, 145–163. doi: 10.1016/s0168-6445(03)00051-2

Buchmeier, N., Bossie, S., Chen, C. Y., Fang, F. C., Guiney, D. G., and Libby, S. J. (1997). SlyA, a transcriptional regulator of *Salmonella typhimurium*, is required for resistance to oxidative stress and is expressed in the intracellular environment of macrophages. *Infect. Immun.* 65, 3725–3730. doi: 10.1128/iai.65.9.3725-3730.1997

De, N., Pirruccello, M., Krasteva, P. V., Bae, N., Raghavan, R. V., and Sondermann, H. (2008). Phosphorylation-independent regulation of the diguanylate cyclase WspR. *PLoS Biol.* 6:e67. doi: 10.1371/journal.pbio.0060067

Fritsche, T. R., Biedenbach, D. J., and Jones, R. N. (2009). Antimicrobial activity of prulifloxacin tested against a worldwide collection of gastroenteritis-producing pathogens, including those causing traveler's diarrhea. *Antimicrob. Agents Chemother.* 53, 1221–1224. doi: 10.1128/aac.01260-08

Gupta, K., Liao, J., Petrova, O. E., Cherny, K. E., and Sauer, K. (2014). Elevated levels of the second messenger c-di-GMP contribute to antimicrobial resistance of *Pseudomonas aeruginosa*. *Mol. Microbiol.* 92, 488–506. doi: 10.1111/mmi.12587

Haque, M. M., Kabir, M. S., Aini, L. Q., Hirata, H., and Tsuyumu, S. (2009). SlyA, a MarR family transcriptional regulator, is essential for virulence in *Dickeya dadantii* 3937. *J. Bacteriol.* 191, 5409–5418. doi: 10.1128/jb.00240-09

Hossain, S., De Silva, B. C. J., Wimalasena, S., Pathirana, H., Dahanayake, P. S., and Heo, G. J. (2018). Distribution of antimicrobial resistance genes and class 1 integron gene cassette arrays in motile Aeromonas spp. isolated from goldfish (*Carassius auratus*). *Microb. Drug Resist.* 24, 1217–1225. doi: 10.1089/mdr.2017.0388

Jiang, M., Kuang, S. F., Lai, S. S., Zhang, S., Yang, J., Peng, B., et al. (2020). Na+-NQR confers aminoglycoside resistance via the regulation of l-alanine metabolism. *mBio* 11:e002086-20.

Lankester, A., Ahmed, S., Lamberte, L. E., Kettles, R. A., and Grainger, D. C. (2019). The *Escherichia coli* multiple antibiotic resistance activator protein represses transcription of the lac operon. *Biochem. Soc. Trans.* 47, 671–677. doi: 10.1042/bst20180498

Li, L., Peng, B., Peng, X. X., and Li, H. (2020). Reprogramming metabolomics reveals membrane potential-dependent colistin resistance in *Vibrio alginolyticus*. *Environ. Microbiol.* 22, 4295–4313. doi: 10.1111/1462-2920.15021

Li, W. X., Zhao, Y. Y., Yu, J., Lin, L., Ramanathan, S., Wang, G. B., et al. (2021). TonB-dependent receptors affect the spontaneous oxytetracycline resistance evolution in *Aeromonas hydrophila*. *J. Proteome Res.* 20, 154–163. doi: 10.1021/acs.jproteome.9b00708

Libby, S. J., Goebel, W., Ludwig, A., Buchmeier, N., Bowe, F., Fang, F. C., et al. (1994). A cytolysin encoded by Salmonella is required for survival within macrophages. *Proc. Natl. Acad. Sci. USA* 91, 489–493. doi: 10.1073/pnas.91.2.489

Lin, X. M., Wang, C., Guo, C., Tian, Y. M., Li, H., and Peng, X. X. (2012). Differential regulation of OmpC and OmpF by AtpB in *Escherichia coli* exposed to nalidixic acid and chlortetracycline. *J. Proteomics* 75, 5898–5910. doi: 10.1016/j.jprot.2012.08.016

Ma, J., Chen, T., Wu, S. F., Yang, C. Y., Bai, M. Z., Shu, K. X., et al. (2019). iProX: an integrated proteome resource. *Nucleic Acids Res.* 47, D1211–D1217. doi: 10.1093/nar/gky869

Michaux, C., Martini, C., Hanin, A., Auffray, Y., Hartke, A., and Giard, J.-C. (2011a). SlyA regulator is involved in bile salts stress response of *Enterococcus faecalis*. *FEMS Microbiol. Lett.* 324, 142–146. doi: 10.1111/j.1574-6968.2011.02390.x

Michaux, C., Sanguinetti, M., Reffuveille, F., Auffray, Y., Posteraro, B., Gilmore, M. S., et al. (2011b). SlyA is a transcriptional regulator involved in the virulence of *Enterococcus faecalis*. *Infect. Immun.* 79, 2638–2645. doi: 10.1128/iai.01132-10

Nishino, K., Latifi, T., and Groisman, E. A. (2006). Virulence and drug resistance roles of multidrug efflux systems of *Salmonella enterica Serovar Typhimurium*. *Mol. Microbiol.* 59, 126–141. doi: 10.1111/j.1365-2958.2005.04940.x

Oshima, T., Aiba, H., Masuda, Y., Kanaya, S., Sugiura, M., Wanner, B. L., et al. (2002). Transcriptome analysis of all two-component regulatory system mutants of *Escherichia coli* K-12. *Mol. Microbiol.* 46, 281–291. doi: 10.1046/j.1365-2958.2002.03170.x

Peng, B., Su, Y. B., Li, H., Han, Y., Guo, C., Tian, Y. M., et al. (2015). Exogenous Alanine and/or glucose plus kanamycin kills antibiotic-resistant bacteria. *Cell Metab.* 21, 249–261. doi: 10.1016/j.cmet.2015.01.008

Peterson, E., and Kaur, P. (2018). Antibiotic resistance mechanisms in bacteria: relationships between resistance determinants of antibiotic producers, environmental bacteria, and clinical pathogens. *Front. Microbiol.* 9:2928. doi: 10.3389/fmicb.2018.02928

Pletzer, D., Braun, Y., Dubiley, S., Lafon, C., Köhler, T., Page, M. G. P., et al. (2015). The *Pseudomonas aeruginosa* PA14 ABC transporter NppA1A2BCD is required for uptake of peptidyl nucleoside antibiotics. *J. Bacteriol.* 197, 2217–2228. doi: 10.1128/jb.00234-15

Pourahmad Jaktaji, R., and Ebadi, R. (2013). Study the expression of marA gene in ciprofloxacin and tetracycline resistant mutants of *Escherichia coli*. *Iran. J. Pharm. Res.* 12, 923–928.

Shannon, P., Markiel, A., Ozier, O., Baliga, N. S., Wang, J. T., Ramage, D., et al. (2003). Cytoscape: a software environment for integrated models of biomolecular interaction networks. *Genome Res.* 13, 2498–2504. doi: 10.1101/gr.1239303

Shi, Y., Latifi, T., Cromie, M. J., and Groisman, E. A. (2004). Transcriptional control of the antimicrobial peptide resistance ugtL gene by the Salmonella PhoP and SlyA regulatory proteins. *J. Biol. Chem.* 279, 38618–38625. doi: 10.1074/jbc.m406149200

Spory, A., Bosserhoff, A., von Rhein, C., Goebel, W., and Ludwig, A. (2002). Differential regulation of multiple proteins of *Escherichia coli* and *Salmonella enterica* serovar Typhimurium by the transcriptional regulator SlyA. *J. Bacteriol.* 184, 3549–3559. doi: 10.1128/jb.184.13.3549-3559.2002

Sun, L. N., Yao, Z. J., Guo, Z., Zhang, L. S., Wang, Y. Q., Mao, R. R., et al. (2019). Comprehensive analysis of the lysine acetylome in *Aeromonas hydrophila* reveals cross-talk between lysine acetylation and succinylation in LuxS. *Emerg. Microbes Infec.* 8, 1229–1239. doi: 10.1080/22221751.2019.1656549

Szklarczyk, D., Morris, J. H., Cook, H., Kuhn, M., Wyder, S., Simonovic, M., et al. (2017). The STRING database in 2017: quality-controlled protein-protein association networks, made broadly accessible. *Nucleic Acids Res.* 45, D362–D368.

Tang, R. Q., Luo, G., Zhao, L. M., Huang, L. X., Qin, Y. X., Xu, X. J., et al. (2019a). The effect of a LysR-type transcriptional regulator gene of *Pseudomonas* plecoglossicida on the immune responses of *Epinephelus coioides*. *Fish Shellfish Immunol.* 89, 420–427. doi: 10.1016/j.fsi.2019.03.051

Tang, R. Q., Zhao, L. M., Xu, X. J., Huang, L. X., Qin, Y. X., Su, Y. Q., et al. (2019b). Dual RNA-Seq uncovers the function of an ABC transporter gene in the host-pathogen interaction between *Epinephelus coioides* and *Pseudomonas plecoglossicida*. *Fish Shellfish Immunol.* 92, 45–53. doi: 10.1016/j.fsi.2019.05.046

Tian, S. C., Wang, C., Li, Y. Y., Bao, X. M., Zhang, Y. W., and Tang, T. (2021). The impact of SlyA on cell metabolism of *Salmonella typhimurium*: a joint study of transcriptomics and metabolomics. *J. Proteome Res.* 20, 184–190. doi: 10.1021/acs.jproteome.0c00281

Walter, W., Sanchez-Cabo, F., and Ricote, M. (2015). GOplot: an R package for visually combining expression data with functional analysis. *Bioinformatics* 31, 2912–2914. doi: 10.1093/bioinformatics/btv300

Wilkinson, S. P., and Grove, A. (2006). Ligand-responsive transcriptional regulation by members of the MarR family of winged helix proteins. *Curr. Issues Mol. Biol.* 8, 51–62.

Yu, H. B., Zhang, Y. L., Lau, Y. L., Yao, F., Vilches, S., Merino, S., et al. (2005). Identification and characterization of putative virulence genes and gene clusters in *Aeromonas hydrophila* PPD134/91. *Appl. Environ. Microbiol.* 71, 4469–4477. doi: 10.1128/aem.71.8.4469-4477.2005

Zhang, L. S., Li, W. X., Sun, L. N., Wang, Y. Q., Lin, Y. X., and Lin, X. M. (2020). Quantitative proteomics reveals the molecular mechanism of *Aeromonas hydrophila* in enoxacin stress. *J. Proteomics* 211:103561. doi: 10.1016/j.jprot.2019.103561

Zhang, M. M., Kang, J. P., Wu, B., Qin, Y. X., Huang, L. X., Zhao, L. M., et al. (2020). Comparative transcriptome and phenotype analysis revealed the role and mechanism of ompR in the virulence of fish pathogenic *Aeromonas hydrophila*. *Microbiologyopen* 9:e1041.

Zhou, D., and Yang, R. (2006). Global analysis of gene transcription regulation in prokaryotes. *Cell Mol. Life Sci.* 63, 2260–2290. doi: 10.1007/s00018-006-6184-6

Zhu, W., Zhou, S. X., and Chu, W. H. (2020). Comparative proteomic analysis of sensitive and multi-drug resistant *Aeromonas hydrophila* isolated from diseased fish. *Microb. Pathog.* 139:103930. doi: 10.1016/j.micpath.2019.103930

Conflict of Interest: The authors declare that the research was conducted in the absence of any commercial or financial relationships that could be construed as a potential conflict of interest.

frontiers in Microbiology

ORIGINAL RESEARCH
published: 16 August 2021
doi: 10.3389/fmicb.2021.720967

The Effect of *tonB* Gene on the Virulence of *Pseudomonas plecoglossicida* and the Immune Response of *Epinephelus coioides*

Lingfei Hu[1], Lingmin Zhao[1], Zhixia Zhuang[2], Xiaoru Wang[2], Qi Fu[2], Huabin Huang[2], Lili Lin[2], Lixing Huang[1], Yingxue Qin[1], Jiaonan Zhang[3] and Qingpi Yan[1,2,3]**

[1] Fisheries College, Jimei University, Xiamen, China, [2] College of Environment and Public Health, Xiamen Huaxia University, Xiamen, China, [3] Key Laboratory of Special Aquatic Feed for Fujian, Fujian Tianma Technology Company Limited, Fuzhou, China

OPEN ACCESS

Edited by:
Xinhua Chen,
Fujian Agriculture and Forestry University, China

Reviewed by:
Xiangmin Lin,
Fujian Agriculture and Forestry University, China
Minh-Thu Nguyen,
Institute of Medical Microbiology, University Hospital Münster, Germany

***Correspondence:**
Qingpi Yan
yanqp@jmu.edu.cn
Lili Lin
linll@hxxy.edu.cn

Specialty section:
This article was submitted to Antimicrobials, Resistance and Chemotherapy, a section of the journal Frontiers in Microbiology

Received: 05 June 2021
Accepted: 21 July 2021
Published: 16 August 2021

Citation:
Hu L, Zhao L, Zhuang Z, Wang X, Fu Q, Huang H, Lin L, Huang L, Qin Y, Zhang J and Yan Q (2021) The Effect of tonB Gene on the Virulence of Pseudomonas plecoglossicida and the Immune Response of Epinephelus coioides. Front. Microbiol. 12:720967. doi: 10.3389/fmicb.2021.720967

Pseudomonas plecoglossicida is the causative agent of "visceral white spot disease" in cultured fish and has resulted in serious economic losses. *tonB* gene plays a crucial role in the uptake of nutrients from the outer membranes in Gram-negative bacteria. The previous results of our lab showed that the expression of *tonB* gene of *P. plecoglossicida* was significantly upregulated in the spleens of infected *Epinephelus coioides*. To explore the effect of *tonB* gene on the virulence of *P. plecoglossicida* and the immune response of *E. coioides*, *tonB* gene of *P. plecoglossicida* was knocked down by RNAi; and the differences between the wild-type strain and the *tonB*-RNAi strain of *P. plecoglossicida* were investigated. The results showed that all of the four mutants of *P. plecoglossicida* exhibited significant decreases in mRNA of *tonB* gene, and the best knockdown efficiency was 94.0%; the survival rate of *E. coioides* infected with the *tonB*-RNAi strain was 20% higher than of the counterpart infected with the wild strain of *P. plecoglossicida*. Meanwhile, the *E. coioides* infected with the *tonB*-RNAi strain of *P. plecoglossicida* carried less pathogens in the spleen and less white spots on the surface of the spleen; compared with the wild-type strain, the motility, chemotaxis, adhesion, and biofilm formation of the *tonB*-RNAi strain were significantly attenuated; the transcriptome data of *E. coioides* infected with the *tonB*-RNAi strain were different from the counterpart infected with the wild strain of *P. plecoglossicida*; the antigen processing and presentation pathway and the complement and coagulation cascade pathway were the most enriched immune pathways. The results indicated that *tonB* was a virulence gene of *P. plecoglossicida*; *tonB* gene was involved in the regulation of motility, chemotaxis, adhesion, and biofilm formation; *tonB* gene affected the immune response of *E. coioides* to *P. plecoglossicida* infection.

Keywords: *Pseudomonas plecoglossicida*, *tonB*, pathogenicity, *Epinephelus coioides*, immune response

INTRODUCTION

Pseudomonas plecoglossicida is the causative agent of "visceral white spot disease" in *Epinephelus coioides* and *Larimichthys crocea* under the water temperatures of 15–20°C and has resulted in high mortality and heavy economic loss (Zhang et al., 2018; Huang et al., 2020). To alleviate the harm caused by *P. plecoglossicida*, its pathogenic mechanism has attracted much attention. The pathogenicity of pathogens was reported to be controlled by different genes. So far, many genes have been shown to have a strong relationship with the virulence regulation of aquatic pathogens, such as *sodA* and *sodB* to *Aeromonas hydrophila* (Zhang et al., 2019); *secA* and *cheB* to *Vibrio alginolyticus* (Guo et al., 2018); *ssaV* to *Edwardsiella piscicida* (Edrees et al., 2018); *toxA* and *toxB* to *Vibrio parahaemolyticus* (Singhapol and Tinrat, 2020); and *secY* and *tssD-1* to *P. plecoglossicida* (Luo et al., 2020; Ye et al., 2021). The previous transcriptome data (NCBI, SRP115064) of our lab showed that *tonB* gene of *P. plecoglossicida* was highly expressed in the spleen of *E. coioides*, which suggested that it might play a role in the virulence of *P. plecoglossicida*.

tonB gene encodes TonB, which is an element of the TonB system (TonB-ExbB-ExbD). The TonB system occupies a crucial position in the transport of nutrients, including iron, carbohydrates, hemin, transition metal elements, and vitamin B12 (Schauer et al., 2008; Huang and Wilks, 2017; Gomez-Santos et al., 2019). In Gram-negative bacteria, the TonB system and *tonB*-dependent transporter (TBDT) accomplish jointly transport of nutrients. TBDT can acquire energy to transport nutrients from the outer membrane with the help of the TonB system (Oeemig et al., 2018; Kopp and Postle, 2020; Samantarrai et al., 2020). Dong et al. (2019) found that the pathogenicity of *A. hydrophila* was attenuated due to the deletion of *tonB* gene. However, there have been no reports about *P. plecoglossicida tonB* gene.

Considering the great harms of *P. plecoglossicida* to aquaculture and the potentially important role of *tonB* in the pathogenicity of *P. plecoglossicida*, this article is devoted to exploring the contribution of *tonB* in the virulence of *P. plecoglossicida* and the immune response of *E. coioides* to *P. plecoglossicida* infection. *tonB* gene of *P. plecoglossicida* was stably knocked down by RNAi; the spleens at 3 and 5 day post injection (dpi) infected with the wild-type strain or the *tonB*-RNAi strain were sampled and subjected to RNA-seq to monitor the transcriptomes of *E. coioides*, and the transcriptome data were compared and analyzed.

MATERIALS AND METHODS

Bacterial Strains and Culture Conditions

The virulent wild-type strain of *P. plecoglossicida* (NZBD9) was isolated from the spleen of large yellow croaker suffered from "visceral white spot disease" and was stored at −80°C (Huang et al., 2019). The *tonB*-RNAi strain of *P. plecoglossicida* was constructed from the wild-type strain of *P. plecoglossicida*. *P. plecoglossicida* was routinely grown in Luria Bertani (LB) broth under 18 or 28°C with shaking at 220 rpm. *Escherichia coli* DH5α was obtained from TransGen Biotech (Beijing, China) and grown in LB broth at 37°C with shaking at 220 rpm.

RNAi-Induced Knockdown of *Pseudomonas plecoglossicida tonB* Gene

Pseudomonas plecoglossicida tonB gene was knocked down according to the methods described by Choi and Schweizer (2006) and Darsigny et al. (2010), with minor modifications. Four oligonucleotides complementary to short hairpin RNA (shRNA) sequences targeting *tonB* gene (**Supplementary Table 1**) were designed by BLOCK-iT^{TM}RNAi Designer[1] and synthesized by Shanghai Generay Biotech Co., Ltd. (Shanghai, China). The oligonucleotides were ligated to pCM130/tac vector using T4 DNA ligase (Takara Biomedical Technology, Beijing, China), according to the manufacturer's recommendations. The recombinant plasmids were transformed into competent *E. coli* DH5α cells by heat shock and electroporated into *P. plecoglossicida* NZBD9 as described by Luo et al. (2019). The mRNA level of *tonB* gene in four mutants was determined by quantitative real-time polymerase chain reaction (qRT-PCR).

Growth Rate Assay

The bacterial suspension were adjusted to optical density at a wavelength of 600 nm (OD_{600}) = 0.3 and diluted 1,000-fold with LB broth. Aliquot of 200 μl of the bacterial diluent was added into per well of 96-well plate and incubated at 28°C. The OD_{600} values of bacterial culture were measured hourly for 48 h (Zuo et al., 2019). Ten replicates were carried out for each group.

Bacterial Chemotaxis Assay

The bacterial chemotaxis assay for *P. plecoglossicida* was performed with fine-tuning as described by Zhang et al. (2020). The overnight culture of *P. plecoglossicida* was adjusted to OD_{600} nm ≈ 1.0 with sterile phosphate-buffered saline (PBS), and 0.25 ml of bacterial suspension was aspirated into a 1-ml syringe. Then, a capillary tube (inner diameter of 0.1 mm, one end sealed) filled with mucus was dipped into the bacterial suspension and incubated at 28°C for 1 h. Finally, the mucus in the capillary was blown out, and the colony-forming unit (cfu) number of *P. plecoglossicida* in the mucus was determined by dilution method of plate counting. Three replicates were performed.

Biofilm Formation Assay

Biofilm formation assay of *P. plecoglossicida* was performed according to the method described by Mao et al. (2020), with some modifications. *P. plecoglossicida* at exponential growth period was adjusted to OD_{600} = 0.2 by fresh LB broth. Then, 100 μl of diluted bacterial suspension was added into per

[1]http://rnaidesigner.thermofisher.com/rnaiexpress/setOption.do?designOption=shrna&pid=708587103220684543

well of microtiter plate and incubated at 28°C for 24 h. After that, each well was washed twice with sterile PBS, dyed with 175 μl of crystal violet (0.1%) for 15 min, washed twice with sterile PBS, and air-dried. Finally, the stained biofilm was solubilized into 200 μl of 33% acetic acid, and the OD values of each well were measured at 590 nm. Eight independent replicates were performed.

Motility Assay

The soft agar plate motility assay for *P. plecoglossicida* was performed as described by Zhang et al. (2019), with minor modifications. The overnight culture in LB was diluted with PBS and adjusted to OD_{600} = 0.3. Bacterial suspension of 1 μl was inoculated on LB semisolid agar plates supplemented with 0.4% agar and incubated at 28°C for 16–20 h. The diameters of bacterial colonies were measured. Biological replicates were carried out in triplicate for each group.

Adhesion Assay

The bacterial adhesion assay was conducted according to the method depicted by Guo et al. (2018), with some modifications. Aliquot of 20 μl of sterile mucus was spread uniformly over the 22 × 22 mm glass slide area. After the mucus was air-dried, 4% methanol was used to fix mucus for 30 min. Bacterial suspension of 200 μl (OD_{600} = 0.3) was spread equably on the region of mucus on glass slides. Sterile PBS of 200 μl instead of bacterial suspension was used as the negative control. After incubation at 28°C for 2 h in a damp chamber, the slides were washed three times with PBS to remove the un-adhered bacterial cells. The adhering bacterial cells on the slide were fixed by 200 μl of 4% methanol for 30 min and dyed with 0.1% crystal violet for 3 min. After the unstained crystal violet were washed with PBS, the adhering bacterial cells in 10 randomly selected fields were counted under a microscope (×1,000). Five replicates were performed.

Epinephelus coioides Infection and Sampling

All *E. coioides* infection experiments were executed completely following the proposals in the "Guide for the Care and Use of Laboratory Animals" set by the National Research Council (Copyright 1996 by the National Academy of Sciences). The animal protocols were officially ratified by the Animal Ethics Committee of Jimei University (Acceptance No. JMULAC201159).

Healthy weight-matched *E. coioides* were obtained from Zhangzhou (Fujian, China) and were acclimatized at 18 ± 1°C for 10 days in recirculating aquaculture systems.

For survival assay, size-matched *E. coioides* (60 fish per group) were intraperitoneally injected with the wild-type strain or *tonB*-RNAi strain of *P. plecoglossicida* at a dose of 5×10^4 cfu/fish. In addition, 60 *E. coioides* intraperitoneally injected with PBS were used as the negative control. The daily mortality of experimental fish was observed and recorded until 10 dpi.

For RNA-seq, six spleens of three different groups (wild-type strain group, *tonB*-RNAi strain group, and PBS group) were sampled at 3 and 5 dpi, and two spleens were mixed into one sample. All of the samples were sent to Shanghai Majorbio Biopharm Technology Co., Ltd. (Shanghai, China) for sequencing.

For the pathogen load assay and *tonB* expression assay, six spleens of *E. coioides* intraperitoneally infected with the wild-type strain or *tonB*-RNAi strain of *P. plecoglossicida* were randomly sampled at 1, 2, 3, 4, 5, and 6 dpi. *P. plecoglossicida* cultured at 18°C *in vitro* was considered as the control.

Quantitative Real-Time Polymerase Chain Reaction

Quantitative real-time polymerase chain reaction was performed by a QuantStudio 6 Flex real-time PCR system (Life Technologies, Carlsbad, CA, United States). Primers are synthesized by Xiamen Borui Biotechnology, and primer sequences are provided in **Supplementary Table 2**. The 16S rDNA (Sun et al., 2019) was applied to normalize *tonB* gene

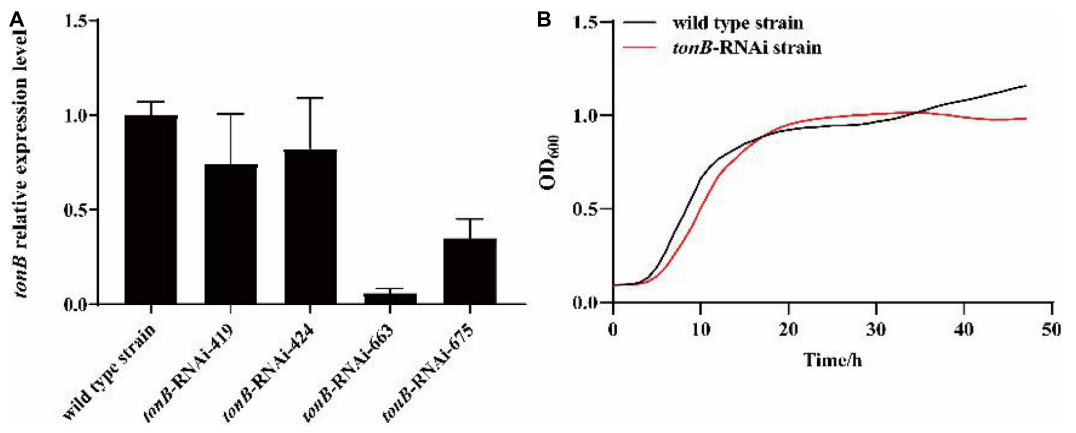

FIGURE 1 | Construction and growth curve of the *tonB*-RNAi strain of *Pseudomonas plecoglossicida*. **(A)** The *tonB* mRNA levels of four mutant strains. **(B)** Growth curve of the wild-type strain and *tonB*-RNAi strain.

expression levels of *P. plecoglossicida*. The pathogen load of *P. plecoglossicida* in the infected spleens was assessed by the copy number of housekeeping gene *gyrB* (Xin et al., 2020). The relative expression of gene in different groups was calculated using $2^{-\Delta\Delta CT}$ method (Luo et al., 2020).

Transcriptomic Analysis

A TruSeq™ RNA sample preparation Kit (Illumina, San Diego, CA, United States) was used to prepare the RNA-seq libraries under protocols of the Kit. The RNA quality was detected and quantified by the Agilent 2100 Bioanalyzer system (Agilent Technologies, Santa Clara, CA, United States) and the ND-2000 instrument (NanoDrop Technologies, Thermo Fisher Scientific, Waltham, MA, United States) separately. The high-quality RNA samples [OD260/280 = 2.03–2.09, RNA integrity number (RIN) ≥ 9.0, 28S:18S ≥ 1.0, ≥1.6 μg) met the construction of individual sequencing libraries. The rRNA-depleted RNA samples were fragmented in fragmentation buffer, and cDNA synthesis was carried out with protocols supplied with the SuperScript double-stranded cDNA synthesis kit (Invitrogen, Carlsbad, CA, United States). The cDNA libraries were amplified by Phusion DNA polymerase (NEB) after end repair, phosphorylation, and poly(A) addition. Sequencing was performed on the Illumina HiSeq4000 sequencing platform at Majorbio Biotech Co., Ltd. (Shanghai, China). The trimming and quality control of the raw Illumina reads were performed using SeqPrep[2] and Sickle[3] with the default settings. The mapped

[2]https://github.com/jstjohn/SeqPrep

[3]https://github.com/najoshi/sickle

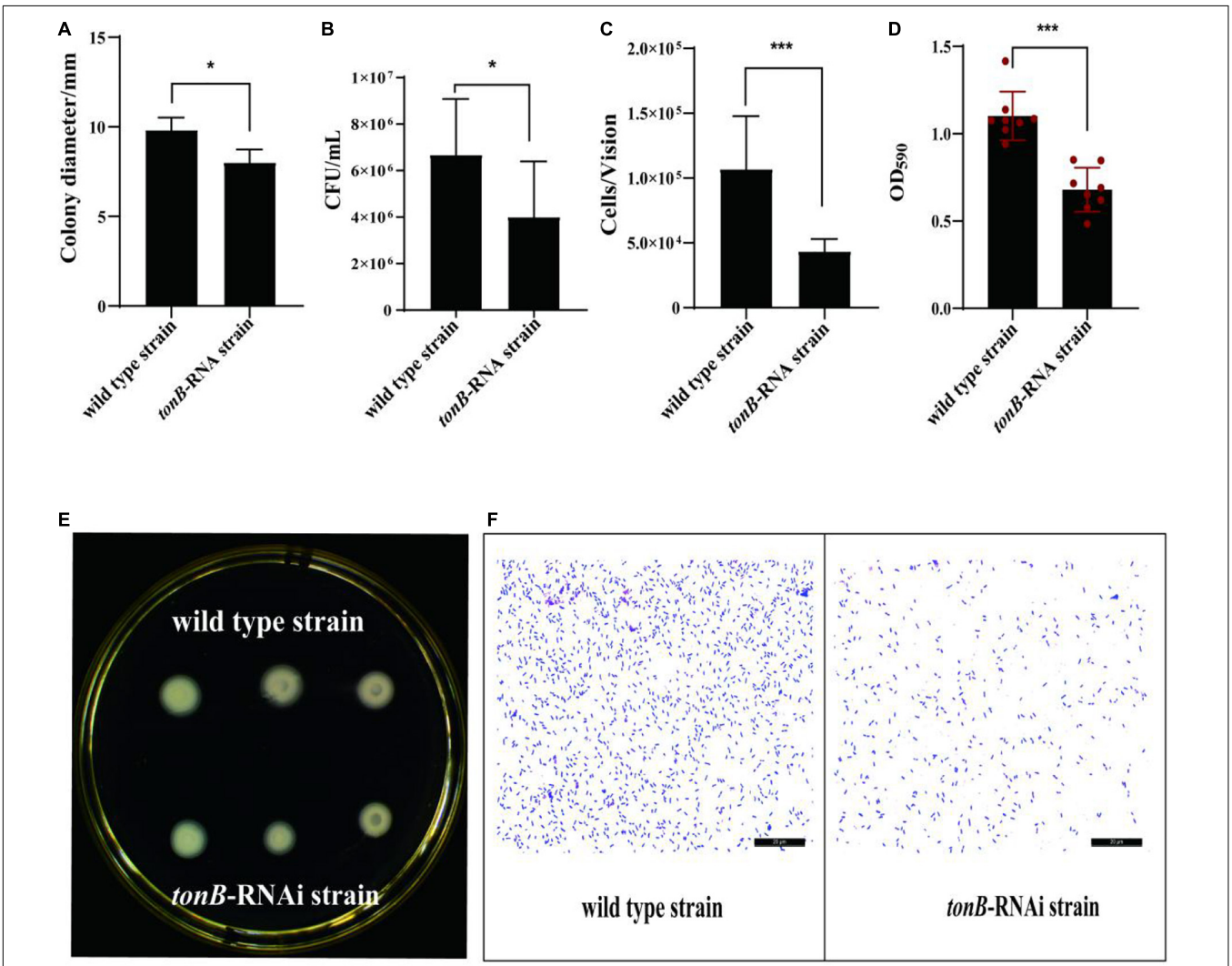

FIGURE 2 | The characteristics of two strains of *Pseudomonas plecoglossicida*. **(A)** Colony diameters of wild-type strain and *tonB*-RNAi strain. **(B)** Chemotaxis capacity of wild-type strain and *tonB*-RNAi strain. **(C)** Adhesion ability of wild-type strain and *tonB*-RNAi strain. **(D)** Biofilm formation ability of wild-type strain and *tonB*-RNAi strain. **(E)** Colonies of wild-type strain and *tonB*-RNAi strain on a plate. **(F)** Adhering bacteria under the microscope. Data are presented as mean ± SD. $^{*}p < 0.05$, $^{**}p < 0.01$, $^{***}p < 0.001$.

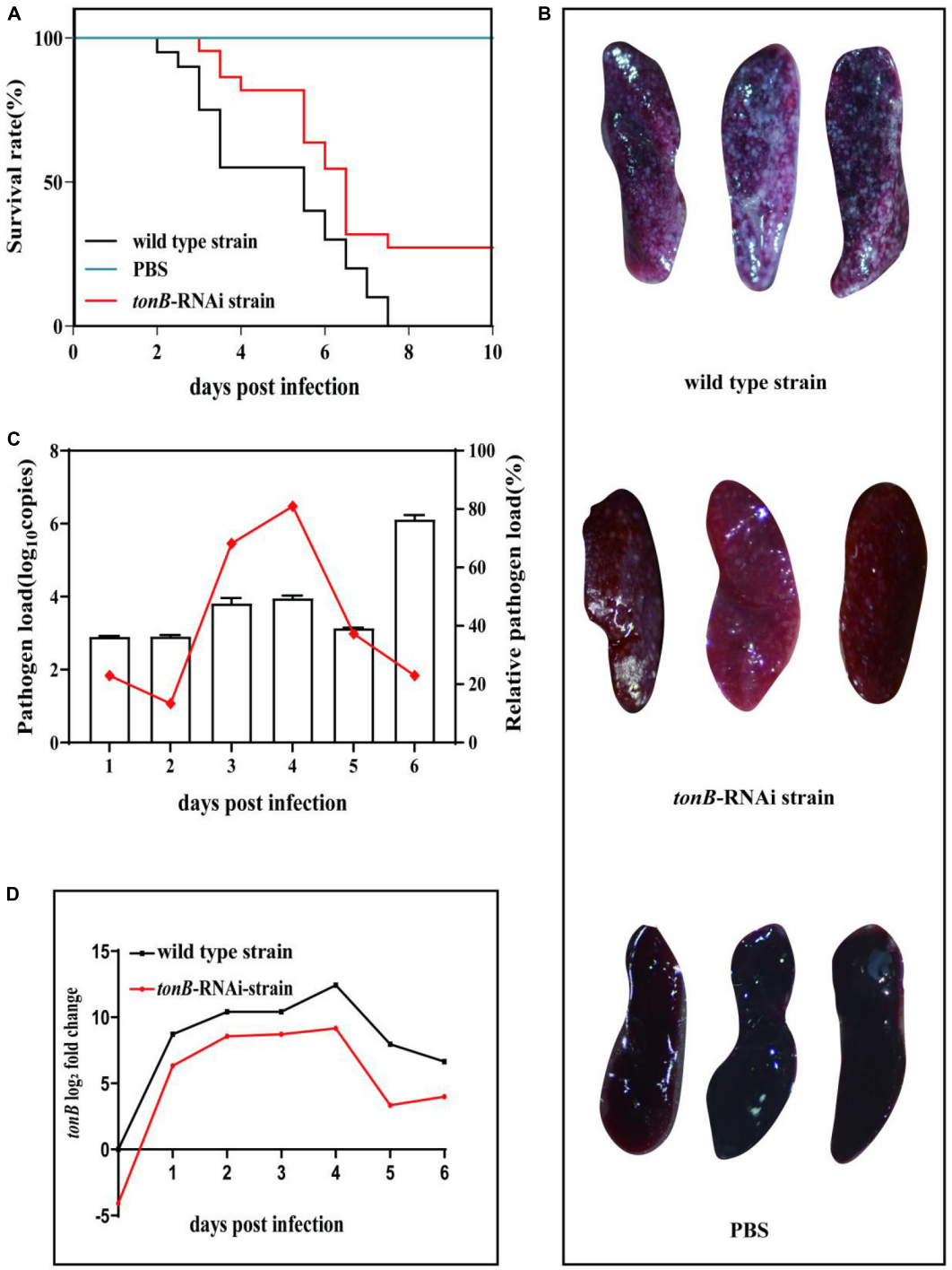

FIGURE 3 | Pathogenicity of two strains of *Pseudomonas plecoglossicida* to *Epinephelus coioides*. **(A)** Survival rate of *E. coioides* infected with wild-type strain or *tonB*-RNAi strain. **(B)** Symptoms of *E. coioides* spleen after infection of wild-type strain or *tonB*-RNAi strain. **(C)** Pathogen load of *tonB*-RNAi strain of *P. plecoglossicida* in the spleens of *E. coioides* during infection. The bar graph represents the pathogen load and is represented by the copy number of *gyrB* gene; the line graph represents the relative pathogen load, which is represented by (copy number of *gyrB* gene of *tonB*-RNAi strain/copy number of *gyrB* gene of wild-type strain). **(D)** mRNA level of *tonB* gene of *P. plecoglossicida* in *E. coioides* spleen during infection.

reads were used for *de novo* assembly as the unigenes of *E. coioides*.

To investigate the biological processes, the BLAST2GO software[4] was used for the Gene Ontology (GO) annotation (Conesa et al., 2005), which accomplished the molecular annotation of differentially expressed transcripts of *E. coioides*. The differentially expressed mRNAs (DEMs) met the standards [| log2FC| $\geq$ 1 and false discovery rate (FDR) $<$ 0.05] was deemed as significant. The GO enrichment analysis visualization of *E. coioides* transcriptome data was performed by the clusterProfiler R package (Yu et al., 2012). Finally, metabolic pathways were analyzed with Kyoto Encyclopedia of Genes and Genomes (KEGG) (Okuda et al., 2008). Furthermore, 10 genes were randomly selected from *E. coioides* to verify the reliability of RNA-seq by qRT-PCR (**Supplementary Figure 1**).

Statistical Analyses

The experimental data are showed as means ± SD and dissected with one-way ANOVA followed by Dunnett's test using IBM SPSS Statistics 26.0 (Armonk, NY, United States). $p < 0.05$ was considered as statistically significant.

[4]https://www.blast2go.com/

Data Access

The RNA sequencing results were put aside in the GenBank SRA database under accession number SRP315640.

RESULTS

Effect of RNAi on *tonB* mRNA Level of *Pseudomonas plecoglossicida*

After shRNA sequence design and synthesis, recombinant plasmid construction, and electrical transfer, four RNAi mutant strains (*tonB*-RNAi-419, *tonB*-RNAi-424, *tonB*-RNAi-663, and *tonB*-RNAi-675) were successfully constructed. The results of qRT-PCR showed that *tonB* gene mRNA levels of four mutants were lower than those of the wild-type strain of *P. plecoglossicida* (**Figure 1A**). The mutant named *tonB*-RNAi-663 (hereafter called the *tonB*-RNAi strain) exhibited the best silencing efficiency (94.0%) and was chosen for further research.

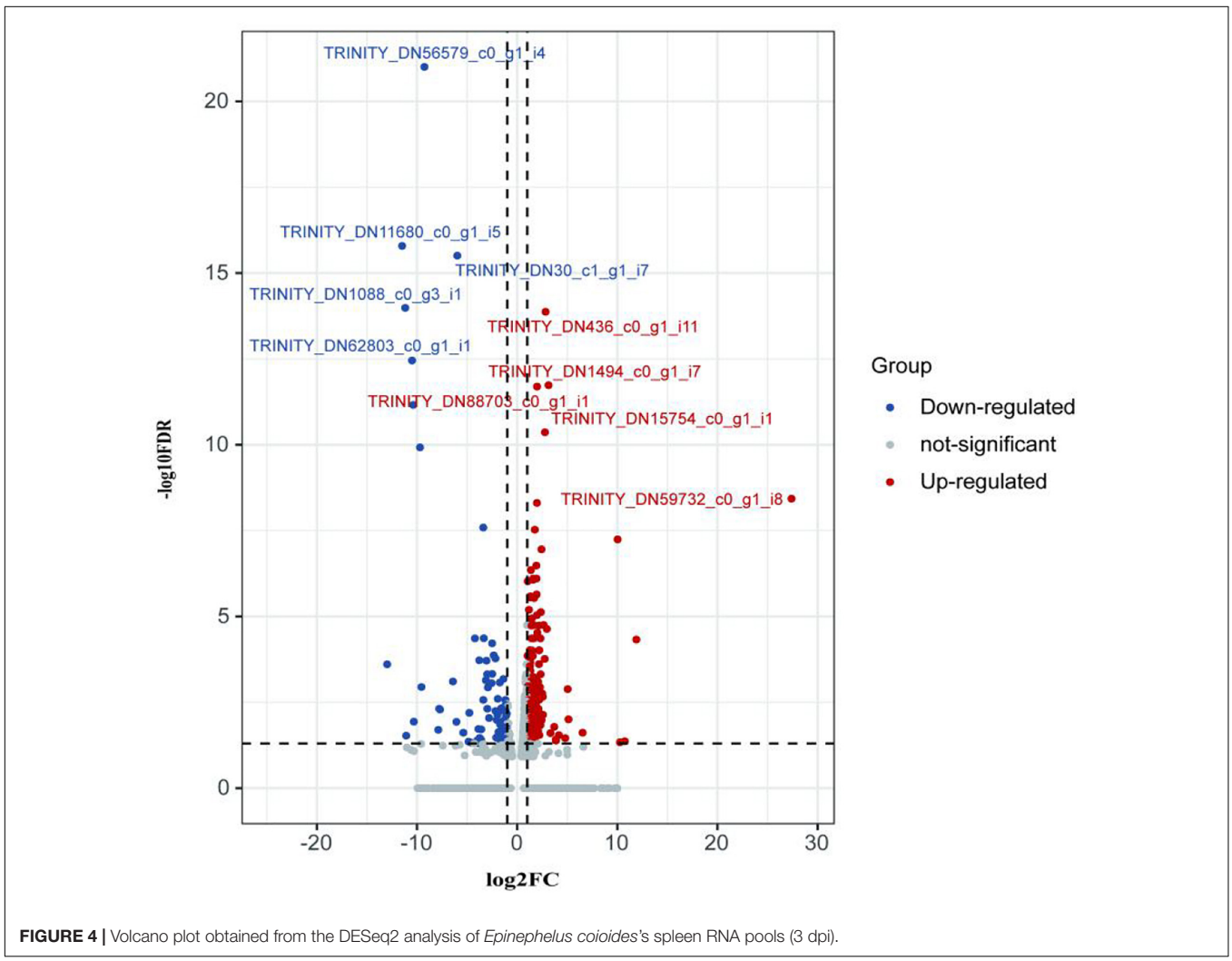

FIGURE 4 | Volcano plot obtained from the DESeq2 analysis of *Epinephelus coioides*'s spleen RNA pools (3 dpi).

Effects of *tonB* Gene Silencing on the Growth of *Pseudomonas plecoglossicida*

The growth curve of the *tonB*-RNAi strain and wild-type strain of *P. plecoglossicida* under the same culture conditions was determined. The results illustrated that there was no significant difference between the growth rate of the *tonB*-RNAi strain and wild-type strain of *P. plecoglossicida* (**Figure 1B**).

Effects of *tonB* Gene Silencing on the Characteristics of *Pseudomonas plecoglossicida*

The motility, chemotaxis, and adhesion of the *tonB*-RNAi strain of *P. plecoglossicida* were enervated compared with the wild-type strain; and the motility, chemotaxis, and adhesion of *tonB* have weakened by 18.17% (**Figures 2A,E**), 39.99% (**Figure 2B**), and 59.34% (**Figures 2C,F**), respectively, at corresponding periods. Meanwhile, the *tonB*-RNAi strain of *P. plecoglossicida* showed an extremely significant difference ($p < 0.001$) in biofilm formation as compared with the wild-type strain. When the expression of *tonB* was inhibited, the biofilm formation ability of *P. plecoglossicida* decreased at 38.35% (**Figure 2D**).

Effects of *tonB* Gene Silencing on the Virulence of *Pseudomonas plecoglossicida*

Infection of the wild-type strain of *P. plecoglossicida* caused the death of *E. coioides*. The first death was recorded at 2 dpi, and the mortality reached 100% at 7.5 dpi. Infection of same dose of the *tonB*-RNAi strain of *P. plecoglossicida* resulted in 1 day delay in the time of first death and 20% decrease in

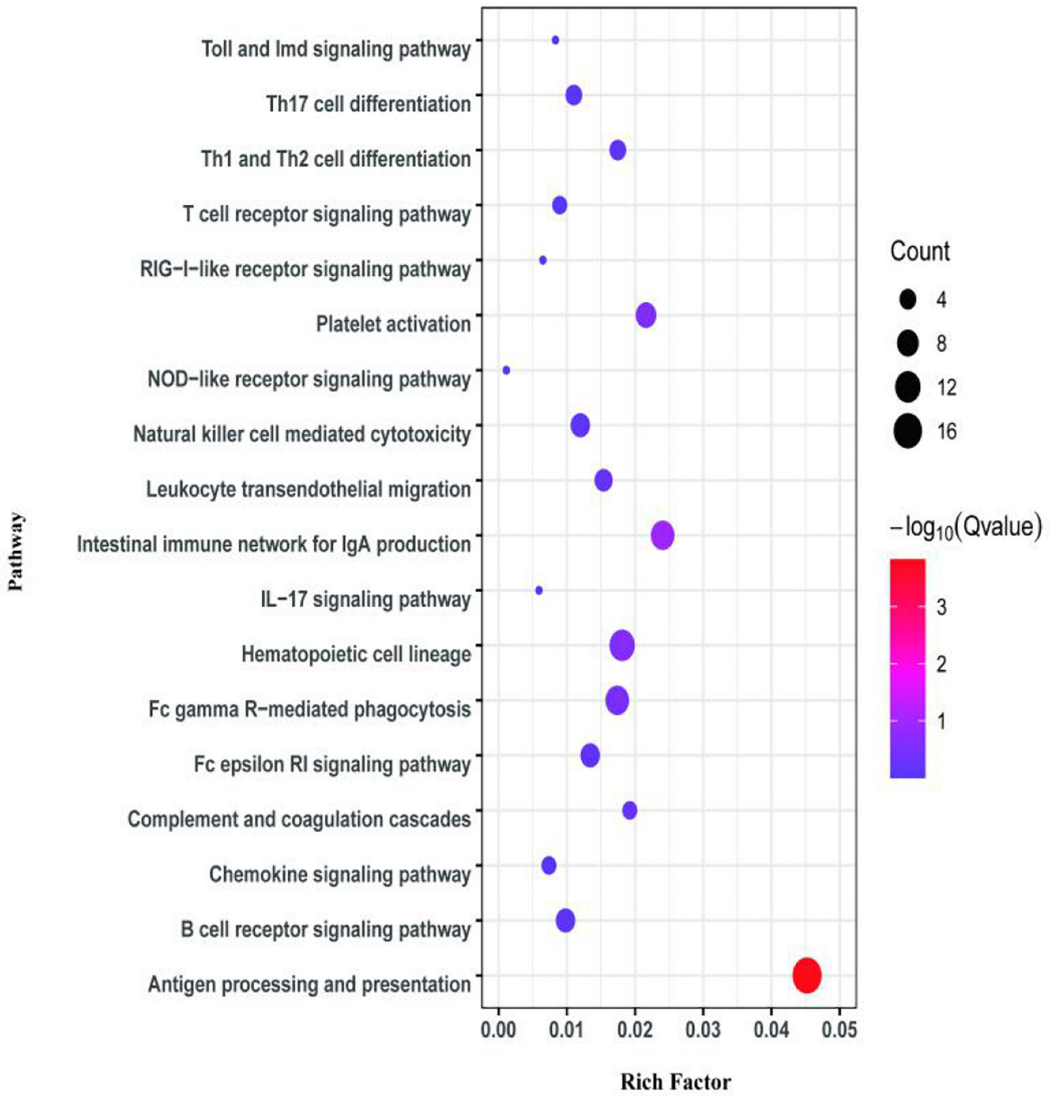

FIGURE 5 | Kyoto Encyclopedia of Genes and Genomes (KEGG) pathway enrichment analysis for differentially expressed mRNAs (DEMs) of transcriptome at 3 dpi.

cumulative mortality. No death of *E. coioides* injected with PBS was recorded (**Figure 3A**).

The surface of *E. coioides* spleens injected with the wild-type strain of *P. plecoglossicida* was covered with numerous white nodules, while much fewer white nodules were found on the surface of counterpart spleens infected with the *tonB*-RNAi strain, and no white nodule was found on the surface of counterpart spleens injected with PBS (**Figure 3B**).

The pathogen loads of the *tonB*-RNAi strain of *P. plecoglossicida* were always lower than those of the wild-type strain during the whole infection. The relative pathogen load (pathogen load of the *tonB*-RNAi strain/pathogen load of the wild-type strain) of *P. plecoglossicida* peaked at 4 dpi. Although the *tonB*-RNAi strain had a higher pathogen load at 6 dpi than on other times, the relative pathogen load at 6 dpi was lower than that on other times except that at 2 dpi (**Figure 3C**). The mRNA level of *tonB* gene of *P. plecoglossicida* in the spleen of *E. coioides* was always higher than that *in vitro*, and the highest values were recorded at 4 dpi. Simultaneously, the expression levels of *tonB* in the *tonB*-RNAi strain were always lower than those in the wild-type strain (**Figure 3D**).

The Effects of *tonB* Gene on the Immune Response of *Epinephelus coioides* to *Pseudomonas plecoglossicida* Infection

Quality Control of RNA-Seq Data

The *E. coioides*'s spleens were subjected to RNA-seq after being infected with the *tonB*-RNAi strain or wild-type strain of *P. plecoglossicida*. The A/T/G/C base content distribution was

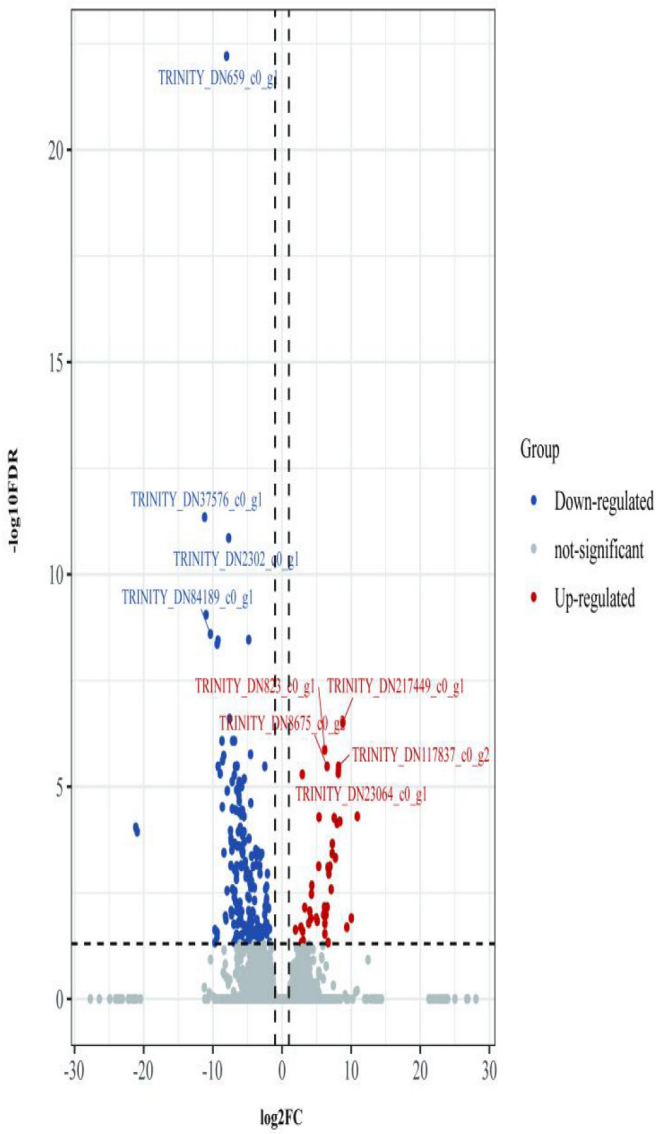

FIGURE 6 | Volcano plot obtained from the DESeq2 analysis of *Epinephelus coioides*'s spleen RNA pools (5 dpi).

balanced, and N% met the normative range (**Supplementary Figure 2**). The main criterion of evaluating the quality of reads was Q20, which fulfilled the requirement of sequencing data of each sample (Q20 > 98%) (**Supplementary Figure 3**). The base error rate of the sequencing data was <0.1%. Pearson's correlation coefficients (r) showed that three biological replicate samples were closely correlated ($r > 0.9$) (**Supplementary Figure 4**). The quality of sequence data satisfied the requirements for the subsequent data process and analysis steps.

Analysis of Differentially Expressed mRNAs

DESeq2 was used for the analysis of significantly differentially expressed transcripts of *E. coioides*. The criteria of the statistically significant of mRNA expression level changes in the transcriptome data were FDR < 0.05 and $|\log2FC| \geq 1$. GO and KEGG pathway enrichment analyses were performed for DEMs.

The first analyzed transcriptome data from the *E. coioides*'s spleens were sampled at 3 dpi. There exist 375 DEMs between the spleen infected with *tonB*-RNAi strains and wild-type strains of *P. plecoglossicida*, which included 291 upregulated mRNAs and 84 downregulated mRNAs (**Figure 4**). Further KEGG analysis showed that 20 KEGG pathways involved in immune response were enriched (**Figure 5**). Of the total DEMs, 26.67% were enriched in immune system pathways, including Toll and Imd signaling pathway, Intestinal immune network for IgA production, B-cell receptor signaling pathway, and antigen processing and presentation. The antigen processing and presentation pathway (KO ID: ko04612) was significantly enriched based on the p-value of Fisher's exact test.

The second analyzed transcriptome data from the *E. coioides*'s spleens were sampled at 5 dpi. A total of 218 mRNAs collected from the spleen infected with the *tonB*-RNAi strain of *P. plecoglossicida* were identified as significant differences in expression compared with the spleen infected with the wild-type strain, which included 43 upregulated mRNAs and 175 downregulated mRNAs (**Figure 6**). According to the GO annotation conventions, DEMs fall into three categories: biological processes, cellular components, and molecular functions. A total of 117 GO terms were enriched, including 29 significantly enriched GO terms. The 29 notably enriched GO terms of the three categories were selected for statistical analysis. The GO analysis results showed that *tonB* gene had a great influence on the immune system, because more than half of the immune GO terms were enriched in biological processes (**Figure 7**). Of the DEMs, 19.3% were enriched in immune GO terms. According to the KEGG database, 145 KEGG pathways were enriched, including 14 immune-related KEGG pathways. Of the total DEMs, 35.78% were enriched in immune system pathways (**Figure 8**). Complement and coagulation cascade pathway (ko04610), which included the greatest number of DEMs, was significantly enriched according to the p-value of Fisher's exact test.

The most significant enrichment pathways were complement and coagulation cascades pathway and antigen processing and presentation pathway according to the KEGG enrichment analysis of the transcriptome data that from the *E. coioides*'s spleens were sampled at 3 and 5 dpi, respectively. Antigen processing and presentation pathway enriched 17 DEMs significantly, which including six downregulated DEMs (such as MHCII and TAP1/2) and 11 upregulated DEMs (such as MHCI, AEP, CTSB/L/S, TCR, TAPBP, and HSP70) (**Figure 9A**). Complement and coagulation cascades pathway enriched 21 downregulated DEMs significantly (such as FI, C3, C5, C6, C7, C8, and C9) (**Figure 9B**).

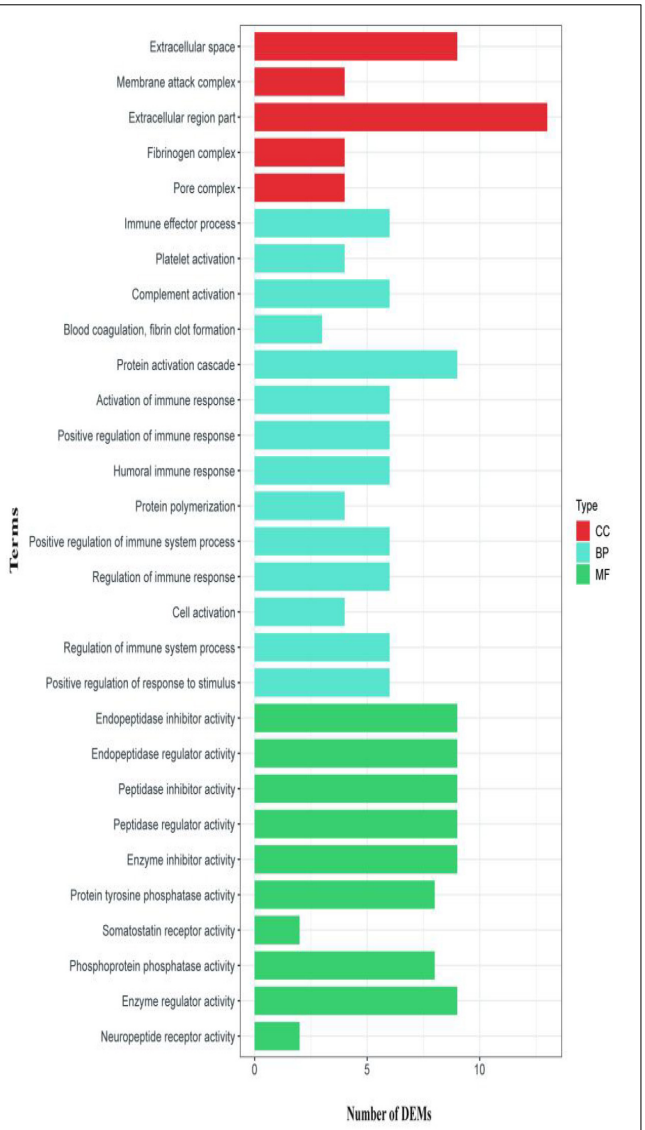

FIGURE 7 | Gene Ontology (GO) enrichment analysis for differentially expressed mRNAs (DEMs) of transcriptome at 5 dpi.

DISCUSSION

RNA interference has been used for many fields to explore the functions of genes (Belles, 2010; Cooper et al., 2021). In this study, four shRNAs exhibited different silence efficiencies to *tonB* gene,

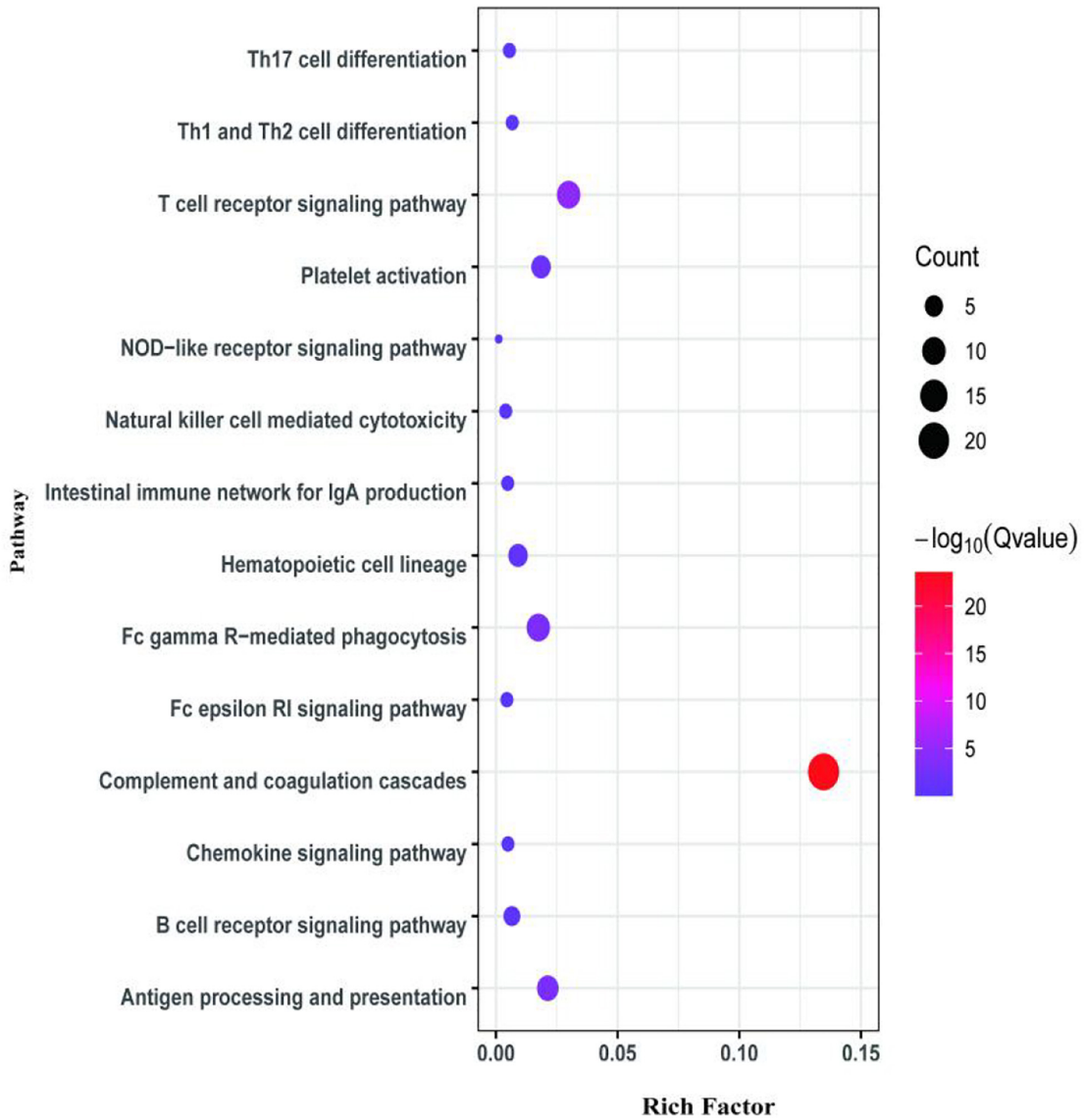

FIGURE 8 | Kyoto Encyclopedia of Genes and Genomes (KEGG) pathway enrichment analysis for differentially expressed mRNAs (DEMs) of the second transcriptome (5 dpi).

which were consistent with the previous RNAi results (Liu et al., 2020; Xin et al., 2020). The best silence efficiency of four shRNAs to *tonB* gene was 94%, which was higher than that of *pvdE* gene (Xin et al., 2020) but lower than that of *impB* gene (Liu et al., 2020). The stability of gene silencing is crucial to the study of gene function. In the present study, *tonB* gene in the *tonB*-RNAi strain of *P. plecoglossicida* was persistently silenced during the infection process, and the relative expressions of *tonB* gene in the *tonB*-RNAi strain were always lower than those of the wild-type strain. These results indicated that RNAi of *tonB* gene was reliable and laid the foundation for subsequent research.

The TonB protein, encoded by *tonB* gene, has amalgamated to form the TonB system with ExbB and ExbD proteins (Liao et al., 2015). Abdelhamed et al. (2017) investigated the virulence of *tonB* gene of *Edwardsiella ictaluri*, and their findings show that the *E. ictaluri* mutant defective in *tonB* has a 2.16-fold reduction in virulence as compared with the wild-type of *E. ictaluri*. Wang et al. (2008) found that the LD_{50} value of three *tonB* mutant strains of *V. alginolyticus* was increased by 11-fold, 14-fold, and 25-fold, respectively. RNAi of *tonB* gene caused a 20% increase in the survival rate of *E. coioides* to *P. plecoglossicida* infection and had no significant effect on the growth rate of *P. plecoglossicida*, which suggested that the decline in mortality of *E. coioides* was due to the decrease of *P. plecoglossicida* virulence, not due to the decrease of bacterial growth rate. These results suggested that *tonB* gene contributed to the pathogenicity of *P. plecoglossicida*. These results agreed with previous studies of *tonB* gene contribution to the virulence

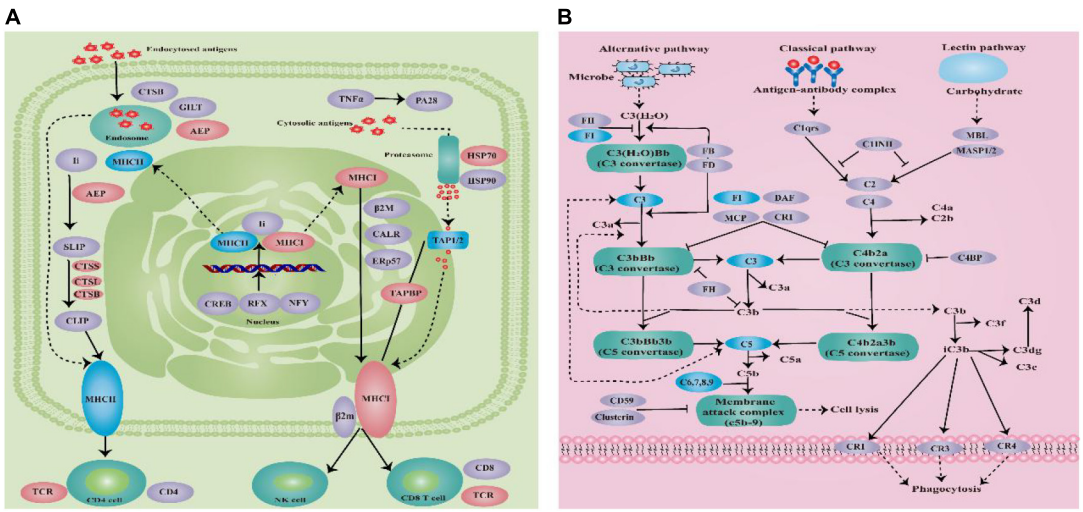

FIGURE 9 | (A) Schematic diagram of antigen processing and presentation pathway. **(B)** Schematic diagram of complement and coagulation cascades pathway (blue indicates downregulation, red indicates upregulation, and purple indicates no significant change).

in other bacterial strains. The different influence degrees of *tonB* gene on the pathogenic of different bacteria might be due to the bacterial species, the host species, and the conditions of infection. The results of pathogen load and symptoms agreed with the mortality result. Several genes have been verified to associate with the virulence of *P. plecoglossicida* (Luo et al., 2019). The silencing of some of these genes in *P. plecoglossicida* resulted in lower mortality in experimental fish infected with the mutants (Tang et al., 2019; Wang et al., 2019), and silencing of other virulence genes did not result in the death of *E. coioides* infected with the mutants of *P. plecoglossicida* (Liu et al., 2020; Xin et al., 2020).

RNAi of *tonB* gene attenuated bacterial motility, chemotaxis, adhesion, and biofilm formation of *P. plecoglossicida*. Bacterial motility (Luo et al., 2016), chemotaxis (Zhang et al., 2020), adhesion (Guo et al., 2018), and biofilm formation (Zhang et al., 2019) have been demonstrated to be related to the pathogenic of pathogen. Some studies showed that *tonB* mutant had great influences on motility, adhesion, and *in vivo* virulence due to its ability of helping the formation of type IV pili (Huang et al., 2004; Duong-Nu et al., 2016).

Nowadays, transcriptome analysis is an important way to reveal the mechanisms of host immune response to infection (Wu and Chen, 2016; Song et al., 2017; Li et al., 2021). In this study, compared with the transcriptome data from *E. coioides* infected with the wild strain of *P. plecoglossicida*, significant changes of transcriptome were observed in the spleen of *E. coioides* infected with the *tonB*-RNAi strain. The GO analysis results showed that the *tonB*-RNAi strain had a great influence on the immune system, and more than half of the immune pathways were enriched in biological processes. The KEGG pathway analysis results showed that the most significant pathways for enrichment were complement and coagulation cascades pathway and antigen processing and presentation pathway.

Complement and coagulation cascades pathway is an immune defense mechanism of the host, and the complement cascades are closely associated with coagulation cascades to jointly achieve effective protection of the host (Lupu et al., 2014; Wiegner et al., 2016). It is widely known that the activation and generation of C3a and C5a have serious proinflammatory effects (Pontrelli et al., 2020). Compared with the transcriptome data from *E. coioides* infected with the wild-type strain of *P. plecoglossicida*, all of the DEMs in transcriptome data from *E. coioides* infected with the *tonB*-RNAi strain were significantly downregulated in the complement and coagulation cascades pathway, which indicated that the inflammatory reaction significantly declined in *E. coioides* infected with the *tonB*-RNAi strain of *P. plecoglossicida*.

The antigen processing and presentation pathway plays a crucial role in immunological process, which is presented by major histocompatibility complexes (MHCs) (Park and Jae-Hwan, 2011; Wieczorek et al., 2017). MHCI relies on proteasomal proteolysis to present foreign peptides that come from degradation of endocellular microbial pathogens; MHCII depends upon lysosomal degradation to accomplish the presentation and processing of extracellular antigens (Wilson, 2017). Therefore, the determining factor of the successful pathogen elimination obviously depends on the recognition of MHCs in the immune system (Unanue, 2002). Compared with the transcriptome data from *E. coioides* infected with the wild-type strain of *P. plecoglossicida*, most of the DEMs in transcriptome data from *E. coioides* infected with the *tonB*-RNAi strain related with MHCI and MHCII were significantly upregulated in the antigen processing and presentation pathway. These results indicated that *E. coioides*'s immune system could more efficiently identify the *tonB*-RNAi strain of *P. plecoglossicida*, which might cause the immune system to remove the mutant strain more efficiently.

CONCLUSION

In conclusion, *tonB* is a virulence gene of *P. plecoglossicida*; *tonB* gene is involved in the regulation of bacterial motility, chemotaxis, adhesion, and biofilm formation of *P. plecoglossicida*; RNAi of *tonB* gene significantly affected the immune response of *E. coioides* to *P. plecoglossicida* infection; complement and coagulation cascades pathway and antigen processing and presentation pathway are the most affected immune pathways.

DATA AVAILABILITY STATEMENT

The datasets presented in this study can be found in online repositories. The names of the repository/repositories and accession number(s) can be found in the article/**Supplementary Material**.

ETHICS STATEMENT

The animal study was reviewed and approved by the Animal Ethics Committee of Jimei University (Acceptance No. JMULAC201159).

AUTHOR CONTRIBUTIONS

All authors contributed to the article. QY, LL, ZZ, and XW conceived the experiments. LFH, LL, and LZ conducted the experiments. All authors assisted in the collection and interpretation of data. LFH, ZZ, and QY wrote the manuscript.

FUNDING

This work was supported by the National Natural Science Foundation of China under contract No. 31972836, open fund of Fujian Province Key Laboratory of Special Aquatic Formula Feed under contract No. TMKJZ2002, and the Fund of Fujian Key Laboratory of Functional Aquafeed and Culture Environment Control (FACE20200007).

SUPPLEMENTARY MATERIAL

The Supplementary Material for this article can be found online at: https://www.frontiersin.org/articles/10.3389/fmicb.2021.720967/full#supplementary-material

Supplementary Figure 1 | Verification of transcriptome data with qRT-PCR.

Supplementary Figure 2 | Bases content along raw reads.

Supplementary Figure 3 | Mean errors distribution along raw reads.

Supplementary Figure 4 | Correlation of transcriptional data.

Supplementary Table 1 | The sequences of four shRNAs for *tonB* gene.

Supplementary Table 2 | The sequence of Primers for PCR and qRT-PCR.

REFERENCES

Abdelhamed, H., Lawrence, M. L., and Karsi, A. (2017). The role of *Edwardsiella ictaluri* TonB mutant in *Edwardsiella ictaluri* virulence. *Front. Physiol.* 8:1066. doi: 10.3389/fphys.2017.01066

Belles, X. (2010). Beyond *Drosophila*: RNAi in vivo and functional genomics in insects. *Annu. Rev. Entomol.* 55, 111–128. doi: 10.1093/bfgp/elp052

Choi, K.-H., and Schweizer, H. P. (2006). mini-Tn7 insertion in bacteria with single attTn7 sites: example *Pseudomonas aeruginosa*. *Nat. Protoc.* 1, 153–161. doi: 10.1038/nprot.2006.24

Conesa, A., Gotz, S., Garcia-Gomez, J. M., Terol, J., Talon, M., and Robles, M. (2005). Blast2GO: a universal tool for annotation, visualization and analysis in functional genomics research. *Bioinformatics* 21, 3674–3676. doi: 10.1093/bioinformatics/bti610

Cooper, A. M. W., Song, H., Shi, X., Yu, Z., Lorenzen, M., Silver, K., et al. (2021). Characterization, expression patterns, and transcriptional responses of three core RNA interference pathway genes from *Ostrinia nubilalis*. *J. Insect Physiol.* 129, 104181–104181. doi: 10.1016/j.jinsphys.2020.104181

Darsigny, M., Babeu, J.-P., Seidman, E. G., Gendron, F.-P., Levy, E., Carrier, J., et al. (2010). Hepatocyte nuclear factor-4α promotes gut neoplasia in mice and protects against the production of reactive oxygen species. *Cancer Res.* 70, 9423–9433. doi: 10.1158/0008-5472.CAN-10-1697

Dong, Y., Geng, J., Liu, J., Pang, M., Awan, F., Lu, C., et al. (2019). Roles of three TonB systems in the iron utilization and virulence of the *Aeromonas hydrophila* Chinese epidemic strain NJ-35. *Appl. Microbiol. Biotechnol.* 103, 4203–4215. doi: 10.1007/s00253-019-09757-4

Duong-Nu, T.-M., Jeong, K., Hong, S. H., Hong-Vu, N., Van-Hoan, N., Min, J.-J., et al. (2016). All three TonB systems are required for *Vibrio vulnificus* CMCP6 tissue invasiveness by controlling flagellum expression. *Infect. Immun.* 84, 254–265. doi: 10.1128/iai.00821-15

Edrees, A., Abdelhamed, H., Nho, S. W., Park, S. B., Karsi, A., Austin, F. W., et al. (2018). Construction and evaluation of type III secretion system mutants of the catfish pathogen *Edwardsiella piscicida*. *J. Fish Dis.* 41, 805–816. doi: 10.1111/jfd.12784

Gomez-Santos, N., Glatter, T., Koebnik, R., Swiatek-Polatynska, M. A., and Sogaard-Andersen, L. (2019). A TonB-dependent transporter is required for secretion of protease PopC across the bacterial outer membrane. *Nat. Commun.* 10:1360.

Guo, L., Huang, L., Su, Y., Qin, Y., Zhao, L., and Yan, Q. (2018). secA, secD, secF, yajC, and yidC contribute to the adhesion regulation of *Vibrio alginolyticus*. *Microbiologyopen* 7:e00551. doi: 10.1002/mbo3.551

Huang, B. X., Ru, K., Yuan, Z., Whitchurch, C. B., and Mattick, J. S. (2004). tonB3 is required for normal twitching motility and extracellular assembly of type IV pili. *J. Bacteriol.* 186, 4387–4389. doi: 10.1128/jb.186.13.4387-4389.2004

Huang, L., Zhao, L., Qi, W., Xu, X., Zhang, J., Zhang, J., et al. (2020). Temperature-specific expression of cspA1 contributes to activation of sigX during pathogenesis and intracellular survival in *Pseudomonas plecoglossicida*. *Aquaculture* 518:734861. doi: 10.1016/j.aquaculture.2019.734861

Huang, L., Zuo, Y., Jiang, Q., Su, Y., Qin, Y., Xu, X., et al. (2019). A metabolomic investigation into the temperature-dependent virulence of *Pseudomonas plecoglossicida* from large yellow croaker (*Pseudosciaena crocea*). *J. Fish Dis.* 42, 431–446. doi: 10.1111/jfd.12957

Huang, W., and Wilks, A. (2017). Extracellular heme uptake and the challenge of bacterial cell membranes. *Annu. Rev. Biochem.* 86, 799–823. doi: 10.1146/annurev-biochem-060815-014214

Kopp, D. R., and Postle, K. (2020). The intrinsically disordered region of ExbD is required for signal transduction. *J. Bacteriol.* 202:e00687–19.

Li, C., Jiang, J., Xie, J., Yang, W., and Wang, Y. (2021). Transcriptome profiling and differential expression analysis of the immune-related genes during the acute phase of infection with *Mycobacterium marinum* in the goldfish (Carassius auratus L.). *Aquaculture* 533:736198. doi: 10.1016/j.aquaculture.2020.736198

Liao, H., Liu, M., and Cheng, A. (2015). Structural features and functional mechanism of TonB in some Gram-negative bacteria-A review. *Wei Sheng Wu Xue Bao* 55, 529–536.

Liu, Z., Zhao, L., Huang, L., Qin, Y., Zhang, J., Zhang, J., et al. (2020). Integration of RNA-seq and RNAi provides a novel insight into the immune responses of *Epinephelus coioides* to the impB gene of *Pseudomonas plecoglossicida*. *Fish Shellfish Immunol.* 105, 135–143. doi: 10.1016/j.fsi.2020.06.023

Luo, G., Huang, L., Su, Y., Qin, Y., Xu, X., Zhao, L., et al. (2016). *flrA*, *flrB*, and *flrC* regulate adhesion by controlling the expression of critical virulence genes in *Vibrio alginolyticus*. *Emerg. Microbes and Infect.* 5, e85. doi: 10.1038/emi.2016.82

Luo, G., Sun, Y., Huang, L., Su, Y., Zhao, L., Qin, Y., et al. (2020). Time-resolved dual RNA-seq of tissue uncovers *Pseudomonas plecoglossicida* key virulence genes in host-pathogen interaction with *Epinephelus coioides*. *Environ. Microbiol.* 22, 677–693. doi: 10.1111/1462-2920.14884

Luo, G., Zhao, L., Xu, X., Qin, Y., Huang, L., Su, Y., et al. (2019). Integrated dual RNA-seq and dual iTRAQ of infected tissue reveals the functions of a diguanylate cyclase gene of *Pseudomonas plecoglossicida* in host-pathogen interactions with *Epinephelus coioides*. *Fish Shellf. Immunol.* 95, 481–490. doi: 10.1016/j.fsi.2019.11.008

Lupu, F., Keshari, R. S., Lambris, J. D., and Coggeshall, K. M. (2014). Crosstalk between the coagulation and complement systems in sepsis. *Thromb. Res.* 133, S28–S31.

Mao, L., Qin, Y., Kang, J., Wu, B., Huang, L., Wang, S., et al. (2020). Role of LuxR-type regulators in fish pathogenic *Aeromonas hydrophila*. *J. Fish Dis.* 43, 215–225. doi: 10.1111/jfd.13114

Oeemig, J. S., Ollila, O. H. S., and Iwai, H. (2018). NMR structure of the C-terminal domain of TonB protein from *Pseudomonas aeruginosa*. *PeerJ* 6:e5412. doi: 10.7717/peerj.5412

Okuda, S., Yamada, T., Hamajima, M., Itoh, M., Katayama, T., Bork, P., et al. (2008). KEGG atlas mapping for global analysis of metabolic pathways. *Nucleic Acids Res.* 36, W423–W426.

Park, H.-L., and Jae-Hwan, N. (2011). Regulation of innate immunity via MHC class II-mediated signaling; non-classical role of MHC class II in innate immunity. *J. Bacteriol. Virol.* 41, 205–207. doi: 10.4167/jbv.2011.41.3.205

Pontrelli, P., Grandaliano, G., and Van Kooten, C. (2020). Editorial: kidney transplantation and innate immunity. *Front. Immunol.* 11:603982. doi: 10.3389/fimmu.2020.603982

Samantarrai, D., Sagar, A. L., Gudla, R., and Siddavattam, D. (2020). TonB-dependent transporters in sphingomonads: unraveling their distribution and function in environmental adaptation. *Microorganisms* 8:359. doi: 10.3390/microorganisms8030359

Schauer, K., Rodionov, D. A., and de Reuse, H. (2008). New substrates for TonB-dependent transport: do we only see the 'tip of the iceberg'? *Trends Biochem. Sci.* 33, 330–338. doi: 10.1016/j.tibs.2008.04.012

Singhapol, C., and Tinrat, S. (2020). Virulence genes analysis of *Vibrio parahaemolyticus* and anti-vibrio activity of the citrus extracts. *Curr. Microbiol.* 77, 1390–1398. doi: 10.1007/s00284-020-01941-4

Song, X., Hu, X., Sun, B., Bo, Y., Wu, K., Xiao, L., et al. (2017). A transcriptome analysis focusing on inflammation-related genes of grass carp intestines following infection with *Aeromonas hydrophila*. *Sci. Rep.* 7:40777.

Sun, Y., Zhuang, Z., Wang, X., Huang, H., Fu, Q., and Yan, Q. (2019). Dual RNA-seq reveals the effect of the flgM gene of *Pseudomonas plecoglossicida* on the immune response of *Epinephelus coioides*. *Fish Shellfish Immunol.* 87, 515–523. doi: 10.1016/j.fsi.2019.01.041

Tang, Y., Sun, Y., Zhao, L., Xu, X., Huang, L., Qin, Y., et al. (2019). Mechanistic insight into the roles of *Pseudomonas plecoglossicida clpV* gene in host-pathogen interactions with *Larimichthys crocea* by dual RNA-seq. *Fish Shellf. Immunol.* 93, 344–353. doi: 10.1016/j.fsi.2019.07.066

Unanue, E. R. (2002). Perspective on antigen processing and presentation. *Immunol. Rev.* 185, 86–102. doi: 10.1034/j.1600-065x.2002.18510.x

Wang, L., Sun, Y., Zhao, L., Xu, X., Huang, L., Qin, Y., et al. (2019). Dual RNA-seq uncovers the immune response of *Larimichthys crocea* to the *secY* gene of *Pseudomonas plecoglossicida* from the perspective of host-pathogen interactions. *Fish Shellf. Immunol.* 93, 949–957. doi: 10.1016/j.fsi.2019.08.040

Wang, Q., Liu, Q., Cao, X., Yang, M., and Zhang, Y. (2008). Characterization of two TonB systems in marine fish pathogen *Vibrio alginolyticus*: their roles in iron utilization and virulence. *Arch. Microbiol.* 190, 595–603. doi: 10.1007/s00203-008-0407-1

Wieczorek, M., Abualrous, E. T., Sticht, J., Alvaro-Benito, M., Stolzenberg, S., Noe, F., et al. (2017). Major histocompatibility complex (MHC) class I and MHC class II proteins: conformational plasticity in antigen presentation. *Front. Immunol.* 8:292. doi: 10.3389/fimmu.2017.00292

Wiegner, R., Chakraborty, S., and Huber-Lang, M. (2016). Complement-coagulation crosstalk on cellular and artificial surfaces. *Immunobiology* 221, 1073–1079. doi: 10.1016/j.imbio.2016.06.005

Wilson, A. B. (2017). MHC and adaptive immunity in teleost fishes. *Immunogenetics* 69, 521–528. doi: 10.1007/s00251-017-1009-3

Wu, C.-C., and Chen, B.-S. (2016). A systems biology approach to the coordination of defensive and offensive molecular mechanisms in the innate and adaptive host-pathogen interaction networks. *PLoS One* 11:e0149303. doi: 10.1371/journal.pone.0149303

Xin, G., Wang, F., Zhao, L., Qin, Y., Huang, L., and Yan, Q. (2020). Integration of RNA-seq and RNAi provides a novel insight into the effect of pvdE gene to the pathogenic of *Pseudomonas plecoglossicida* and on the immune responses of orange-spotted grouper (*Epinephelus coioides*). *Aquaculture* 529:735695. doi: 10.1016/j.aquaculture.2020.735695

Ye, H., Xu, Z., Tao, Z., Li, W., Li, Y., Yang, A., et al. (2021). Efficacy and safety of *Pseudomonas plecoglossicida* mutant Delta tssD-1 as a live attenuated vaccine for the large yellow croaker (*Larimichthys crocea*). *Aquaculture* 531, 1–7.

Yu, G., Wang, L.-G., Han, Y., and He, Q.-Y. (2012). clusterProfiler: an R package for comparing biological themes among gene clusters. *OMICS* 16, 284–287. doi: 10.1089/omi.2011.0118

Zhang, B., Luo, G., Zhao, L., Huang, L., Qin, Y., Su, Y., et al. (2018). Integration of RNAi and RNA-seq uncovers the immune responses of *Epinephelus coioides* to L321_RS19110 gene of *Pseudomonas plecoglossicida*. *Fish Shellfish Immunol.* 81, 121–129. doi: 10.1016/j.fsi.2018.06.051

Zhang, M., Kang, J., Wu, B., Qin, Y., Huang, L., Zhao, L., et al. (2020). Comparative transcriptome and phenotype analysis revealed the role and mechanism of ompR in the virulence of fish pathogenic *Aeromonas hydrophila*. *Microbiologyopen* 9:e1041.

Zhang, M., Qin, Y., Huang, L., Yan, Q., Mao, L., Xu, X., et al. (2019). The role of sodA and sodB in *Aeromonas hydrophila* resisting oxidative damage to survive in fish macrophages and escape for further infection. *Fish Shellfish Immunol.* 88, 489–495. doi: 10.1016/j.fsi.2019.03.021

Zuo, Y., Zhao, L., Xu, X., Zhang, J., Zhang, J., Yan, Q., et al. (2019). Mechanisms underlying the virulence regulation of new *Vibrio alginolyticus* ncRNA Vvrr1 with a comparative proteomic analysis. *Emerg. Microbes Infect.* 8, 1604–1618. doi: 10.1080/22221751.2019.1687261

Conflict of Interest: JZ and QY were employed by company Fujian Tianma Technology Company Limited.

The remaining authors declare that the research was conducted in the absence of any commercial or financial relationships that could be construed as a potential conflict of interest.

Publisher's Note: All claims expressed in this article are solely those of the authors and do not necessarily represent those of their affiliated organizations, or those of the publisher, the editors and the reviewers. Any product that may be evaluated in this article, or claim that may be made by its manufacturer, is not guaranteed or endorsed by the publisher.

frontiers in Microbiology

ORIGINAL RESEARCH
published: 17 September 2021
doi: 10.3389/fmicb.2021.733668

Insight Into Whole Genome of *Aeromonas veronii* Isolated From Freshwater Fish by Resistome Analysis Reveal Extensively Antibiotic Resistant Traits

Rungnapa Sakulworakan[1,2], Putita Chokmangmeepisarn[1,2], Nguyen Dinh-Hung[1], Elayaraja Sivaramasamy[2], Ikuo Hirono[3], Rungthip Chuanchuen[4], Pattanapon Kayansamruaj[5] and Channarong Rodkhum[2]**

[1] The International Graduate Program of Veterinary Science and Technology (VST), Faculty of Veterinary Science, Chulalongkorn University, Bangkok, Thailand, [2] Center of Excellent in Fish Infectious Diseases (CE FID), Department of Veterinary Microbiology, Faculty of Veterinary Science, Chulalongkorn University, Bangkok, Thailand, [3] Tokyo University of Marine Science and Technology, Minato-ku, Japan, [4] Department of Veterinary Public Health, Faculty of Veterinary Science, Chulalongkorn University, Bangkok, Thailand, [5] Department of Aquaculture, Faculty of Fisheries, Kasetsart University, Bangkok, Thailand

OPEN ACCESS

Edited by:
Bo Peng,
Sun Yat-sen University, China

Reviewed by:
Guilherme Campos Tavares,
Federal University of Minas Gerais, Brazil
Soojin Jang,
Korea Pasteur Institute, South Korea

***Correspondence:**
Pattanapon Kayansamruaj
pattanapon.k@ku.th
Channarong Rodkhum
channarong.R@chula.ac.th

Specialty section:
This article was submitted to Antimicrobials, Resistance and Chemotherapy, a section of the journal Frontiers in Microbiology

Received: 30 June 2021
Accepted: 19 August 2021
Published: 17 September 2021

Citation:
Sakulworakan R, Chokmangmeepisarn P, Dinh-Hung N, Sivaramasamy E, Hirono I, Chuanchuen R, Kayansamruaj P and Rodkhum C (2021) Insight Into Whole Genome of Aeromonas veronii Isolated From Freshwater Fish by Resistome Analysis Reveal Extensively Antibiotic Resistant Traits. Front. Microbiol. 12:733668. doi: 10.3389/fmicb.2021.733668

Aeromonas veronii outbreaks in tilapia farming caused relatively high mortalities, and the bacteria was resistant to many kinds of antimicrobials used in Thailand aquaculture. According to the CLSI standard, the determination of antimicrobials efficacy has been limited to phenotypic analyses, and a genomics study is required. This research aimed to analyze the resistome of *A. veronii* isolated from diseased tilapia in Chainat, Nong Khai, and Uttaradit provinces in Thailand. A total of 12 isolates of *A. veronii* were identified based on the *gyrB* sequencing and then, the MIC values to eight antimicrobials (AMP, AML, GEN, ENR, OXO, OTC, SXT, and FFC) were determined. According to the MIC patterns, whole genome sequencing (WGS) of five representatives and resistome analysis were performed, including 15 genomes of *A. veronii* isolated from freshwater fish available in the NCBI. All tilapia isolates were susceptible to FFC but resistant to AML and AMP while OTC resistance was the most dominant. In addition to the WGS analysis, 4.5 Mbp of *A. veronii* was characterized. A total of 20 ARGs were detected by resistome analysis and 16 genes were shared among the *A. veronii* population. In conclusion, *A. veronii* strains isolated from tilapia exhibited a resistance to several antimicrobials and multidrug resistance (MDR) which was related to the presence of multiple ARGs. *Aeromonas veronii* shared the ARGs in their population worldwide with a possibility of a plasmid-mediated acquisition due to the presence of resistance islands.

Keywords: *Aeromonas veronii*, antimicrobial resistance, genomic islands, resistome analysis, tilapia, whole genome sequencing

INTRODUCTION

Thailand is an important aquaculture producer and one of the top world fish exporting countries (Food and Agriculture Organization (FAO), 2018). The total production of Nile tilapia (*Oreochromis niloticus*) reached 217.9 metric tons in 2017 and was regarded the highest among other economically important freshwater aquaculture (52.7% of the total production yield)

(Department of Fisheries (DOF), 2019). Nowadays, inland intensive farming system has become the standard practice for Nile tilapia production which corresponds to the continual increase of consumer demand. However, the intensive farming can lead to more stressful conditions and eventually bring the risk of infectious diseases which threatens the tilapia industry as a whole (Dong et al., 2015). *Aeromonas veronii*, an etiological organism of Motile Aeromonas Septicemia (MAS), contributed to major losses all-year-round with the cumulative mortality varying from 10 to 100% (Dong et al., 2017). More importantly, these bacteria can also cause disease in a wide range of hosts such as human, amphibian, and other aquatic animals (Martino et al., 2016). Antimicrobial therapy is a standard practice for controlling bacterial diseases occurring in tilapia farms. However, several antimicrobial groups that are allowed for use in Thailand aquaculture have also been widely used in human medication such as Beta-lactam, Quinolone, Tetracycline, or Sulfonamides (FCSTD, 2012). The situation of antimicrobial resistance (AMR) and multi drug resistance (MDR; resistant to at least one drug in three or more group of antimicrobials) (Magiorakos et al., 2012) has not only been found in human medicine but also in aquaculture as well, with the report of resistant isolates from different countries (Caruso, 2016; Deng et al., 2016; Baron et al., 2017; Yang et al., 2017; Roh et al., 2019). Wastewater from aquaculture may contain drug residues and resistant bacteria which subsequently pass on to the environment and, ultimately, the consumers. The AMR property can be transferred horizontally to other terrestrial bacteria through the mobile genetic elements (MGEs) (Subramani and Michael, 2017). *Aeromonas* spp. has been well-known as potential bacteria harboring several AMR determinants including plasmid, integron, and genomic island (Piotrowska and Popowska, 2015). However, concerning the current situation of *A. veronii* outbreaks in Thailand, antimicrobial susceptibility is very limited with little available AMR information. Therefore, this research aimed to gain the comprehensive understanding of AMR, as well as the potentially correlated genetic determinants in the recent isolates of *A. veronii* isolated from tilapia using a genome-wide investigation of the AMR genetic determinants (resistome analysis). Due to the potency of whole genome sequencing, WGS can simultaneously investigate the collection of resistance-associated genes which can lead to the *in silico* prediction of AMR traits (Zankari et al., 2012). Nevertheless, the information of intrinsic and acquired resistance genes can be beneficial to the public health concern by revealing the potential transferable AMR determinants in *A. veronii* and increases the awareness of the possible distribution of AMR traits in the future.

MATERIALS AND METHODS

Bacterial Isolates

A total of 12 isolates of *Aeromonas veronii* were obtained from the bacterial collection of FID-RU (Fish Infectious Disease Research Unit, Chulalongkorn University, Thailand), which were isolated from Nile tilapia (*Oreochromis niloticus*) and hybrid red tilapia (*O. mossambicus* × *O. niloticus*) during the disease outbreaks from 2015 and 2018 in Thailand. The details of each isolate are presented in **Table 1**. The bacterial isolation method and biosecurity were approved by Chulalongkorn University, Faculty of Veterinary Science Institutional Biosafety Committee (CU-VET-IBC) under the permit ID: IBC 183104.

Taxonomic Identification

Aeromonas veronii stocks (TSB with 20% of glycerol) were recovered by streaking on a tryptic soy agar (TSA; Difco, United States) with an overnight incubation at 28°C. A single colony was then inoculated into 3 mL of tryptic soy broth (TSB; Bacto, United States) and incubated at 28°C for 24 h with shaking at 160 rpm. Bacterial suspension was used for DNA extraction using the Wizard Genomic DNA purification kit (Promega Corporation, United States) following the instructions of the manufacturer. To confirm the bacterial taxonomy, partial *gyrB* (∼1.4-kb-long) was amplified using the universal primers (*gyrB*3F: TCC GGC GGT CTG CAC GGC GT and *gyrB*14R: TTG TCC GGG TTG TAC TCG TC) with PCR conditions described in the original publication (Hoel et al., 2017). PCR product was separated on 1% agarose Tris-borate-EDTA gel using NucleoSpin® Gel and PCR cleanup (Macherey-Nagel, United States). The purified amplicon was submitted to FirstBASE laboratory service (Malaysia) for Sanger sequencing. The reads were assembled into a contiguous sequence using the ContigExpress software. The identity of the contig was searched against the NCBI nucleotide database using Megablast. Species level demarcation cut-off was set to a sequence coverage of ≥99% (Hoel et al., 2017).

Determination of the Minimum Inhibitory Concentration

A total of 12 isolates from the glycerol stock were recovered on the TSA supplemented with 5% sheep blood and incubated at 28°C for 24 h (Hassan et al., 2017). Each single colony was sub-cultured on the Mueller-Hinton agar (MHA) for the MIC determination by broth microdilution assay with eight antimicrobials including Amoxicillin, AMC [256–0.5 mg/L]; Ampicillin, AMP [256–0.5 mg/L]; Enrofloxacin, ENR [16–0.03 mg/L]; Florfenicol, FFC [64–0.125 mg/L]; Gentamicin, GEN [256–0.5 mg/L]; Oxolinic acid, OXO [64–0.125 mg/L]; Oxytetracycline, OTC [256–0.5 mg/L]; and Sulfamethoxazole + trimethoprim, SXT [256–0.5 mg/L] (Oxoid, United Kingdom) according to the CLSI guideline VET04 (Clinical and Laboratory Standards Institute (CLSI), 2014). The concentration of the bacterial suspension was adjusted by aliquoting 0.85% normal saline to obtain 0.5 McFarland turbidity. Subsequently, the adjusted bacterial suspension was mixed with the cation-adjusted Mueller-Hinton broth (CAMHB) containing an antimicrobial agent at a ratio of 1:1 (V/V) (Baron et al., 2017). Incubation was carried out at 28°C for 24 h. The MIC value was interpreted from a visible growth of bacteria in the medium solution. The resistance trait of each bacterial isolate was categorized into either resistant, sensitive, or multidrug resistant (at least one drug from three or more antimicrobial class) based on the epidemiological cut-off value of the *Aeromonas* species

TABLE 1 | Details of *Aeromonas veronii* isolates used in this study.

Year	Location	Host	Clinical manifestation	Chemical usage	Isolate	Reference
2015	Nong Khai, Thailand	Nile tilapia	NA	NA	NK01	Dong et al., 2015
					NK02	
					NK03	
					NK04	
					NK05	
					NK06	
					NK07	
2018	Uttaradit, Thailand	Hybrid red tilapia	Hemorrhage on skin kidney and fin	OTC and Vitamin C	UDRT09	This study
2018	Chainat, Thailand	Hybrid red tilapia	Hemorrhage on skin and kidney enlargement with fin rot	OTC	CNRT07	This study
					CNRT11	
					CNRT12	
					CNRT13	

NA, not applicable; OTC, oxytetracycline.

published previously (Baron et al., 2017). Herein, *Escherichia coli* ATCC 25922 was used as an internal control of this MIC assay.

Whole Genome Sequencing

Five representative *A. veronii* isolates, namely NK01 (resistant to three antimicrobial classes, 3MDR), NK02 (gentamicin resistant), NK07 (5MDR), UDRT09 (4MDR), and CNRT12 (sensitive to all tested drugs except beta-lactam antibiotics), were subjected to genome sequencing. Genomic DNA of these isolates was extracted by the Wizard Genomic DNA purification kit prior to RNaseA treatment to minimize RNA contamination (Promega Corporation, Madison, WI, United States). The integrity of the genomic DNA was determined by 1% agarose gel electrophoresis, whereas DNA purity and concentration were evaluated by the $OD_{260/280}$ spectrophotometer and Qubit dsDNA BR Assay Kit Fluorometric Quantitation (Invitrogen, Carlsbad, CA, United States), respectively. Paired-end libraries were prepared using the NEBNext® Ultra™ DNA Library Prep Kit for Illumina® and genome sequencing was performed using an Illumina HiSeq instrument with the read length of 150 bp.

Genome Assembly and Annotation

Adaptor sequences and low-quality bases (Q score < 25) were trimmed from raw reads using the Trimmomatic ver. 0.32 (Bolger et al., 2014). The improvement of the read quality was determined using the FastQC ver. 0.11.8.[1] Trimmed reads were assembled into contigs by the SPAdes ver. 3.13.0 software and assembly quality was verified by the QUAST web service[2] (Bankevich et al., 2012). To construct the scaffold, contigs were aligned to the reference genome (*A. veronii* B565, GCA_000204115.1) using the Medusa server.[3] To improve the genome assembly quality, trimmed reads were mapped to the obtained scaffolds by the BWA software[4] and gaps were filled using Pilon and GMcloser, sequentially (Li and Durbin, 2010; Walker et al., 2014; Kosugi et al., 2015). The assembled genomes were annotated automatically by the NCBI Prokaryotic Genome Annotation Pipeline (PGAP) when the assembled genomes were submitted to the NCBI whole genome shotgun (WGS) web portal (Tatusova et al., 2016). The genomes were assigned the accession numbers GCA_012029595.1 (UDRT09), GCA_012029535.1 (CNRT12), GCA_012029545.1 (NK01), GCA_012029575.1 (NK02), and GCA_012029585.1 (NK07).

Genome-Based Phylogenetic Analysis

The genome-level taxonomic identification was conducted by submitting the assembled genomes to the Type Strain Genome Server[5] in which the closest species was determined via the MASH algorithm (Meier-Kolthoff and Goker, 2019). Additionally, the average nucleotide identity (ANI) of the newly assembled genomes in comparison with *A. veronii* biovar sobria [strain 312M (GCA_003859745.1) and LMG13067 (GCA_000820385.1)] and biovar veronii [strain CECT4257 (GCA_000820225.1), CCM4359 (GCA_001908535.1), and C198 (GCA_013697145.1)] was calculated using the ANI calculator[6] with the ANI cut-off value $\geq$ 95% (Jain et al., 2018).

Phylogenetic analysis of the newly assembled genomes and other reference strains (n = 15, **Table 2**) was carried out. The sequence type (ST) of the *A. veronii* genomes was classified in comparison with the PubMLST database using the Sequence Query tool provided in the PubMLST website (Jolley et al., 2018). The MLST scheme for *Aeromonas* spp. included the *gltA*, *groL*, *gyrB*, *metG*, *ppsA*, and *redA* genes. The DNA sequence of each locus was exported from the PubMLST: Sequence Query output page. Multilocus sequence analysis (MLSA) was conducted in the PhyloSuite v1.2.1 program based on the DNA sequence variation among these loci (Zhang et al., 2020). Briefly, a multiple sequence alignment of each locus was performed using MAFFT (Katoh and Standley, 2013). All aligned sequences were then concatenated into a contig, and the maximum likelihood tree was constructed using IQ-tree (Nguyen et al., 2015) under the TIM2 + R3 + F

[1]http://www.bioinformatics.babraham.ac.uk/projects/fastqc/

[2]http://quast.bioinf.spbau.ru/

[3]http://combo.dbe.unifi.it/medusa

[4]http://bio-bwa.sourceforge.net/

[5]https://tygs.dsmz.de/

[6]https://www.ezbiocloud.net/tools/ani

model for 5,000 ultrafast bootstraps (Minh et al., 2013). Herein, *Aeromonas schubertii* WL1483 (accession no. NZ_CP013067) was used as the outgroup for MLSA. The consensus tree was visualized using the MEGA X software (Kumar et al., 2018). A total of 14 *gyrB* sequences were retrieved from the *A. veronii* genomes and were used to generate the phylogenetic tree separately from the MLST tree. *Aeromonas schubertii* was used as an outgroup. Phylogenetic analysis was performed using the Molecular Evolutionary Genetic Analysis X (MEGA X) software (Kumar et al., 2018). The Maximum likelihood tree was constructed under the Tamura 3-parameter + GI model with 1,000 replicates. Moreover, a genome-level phylogenetic analysis was also performed based on the sequence variation in the core genome, also called genome-wide SNPs. Core genome among the distinct *A. veronii* genomes was detected and SNPs were called/concatenated/aligned using the automated web-tool CSI Phylogeny v1.4 using the default setting (Kaas et al., 2014). Aligned SNP sequence was used for the maximum likelihood tree reconstruction via the PhyloSuite program as described previously.

Resistome Analysis

The *A. veronii* genomes listed in **Table 2** were also used for the resistome analysis. The genomes were queried against the Comprehensive Antibiotic Resistance Database (CARD[7]) (Alcock et al., 2019) for the *in silico* prediction of the possible antimicrobial resistance gene (ARGs) contained in the genome. Resistance Gene Identifier (RGI) automate tool was used for the gene analysis in CARD. The search criteria were set as "perfect and strict hits only" with a "high quality/coverage" sequence quality. Nucleotide identity to query sequences lower than 96% were excluded (Lomonaco et al., 2018). In addition, the presence of acquired antimicrobial resistance genes in the *A. veronii* genomes were also analyzed through ResFinder V3.1[8] (Bortolaia et al., 2020). Genome (fasta file) was uploaded to the web resource with a 95% identity of sequence threshold and 80% minimum length of alignment setting (Lomonaco et al., 2018). The amino acid sequences of the predicted ARGs were downloaded from CARD and ResFinder and were used to construct the local blast database on the Blast2GO software in order to perform a reciprocal BLAST. The deduced amino acid sequences (proteome) from each *A. veronii* isolate of this study were queried against the local blast database using blastp implemented in the Blast2GO program (Conesa et al., 2005).

Genomic Islands Analysis

The presence of genomic island (GI) and resistance island (RI) within the newly sequenced *A. veronii* genomes (NK01, NK02, NK07, CNRT12, and UDRT09) were predicted using IslandViewer4[9] (Bertelli et al., 2017). The GenBank file was uploaded to the IslandViewer4 web interface in which *A. veronii* 17ISAe was selected as a reference genome for the alignment. GI was predicted using the IslandPick, SIGI-HMM, and IslandPath-DIMOB methods (Bertelli et al., 2017) implemented in IslandViewer. The output was manually compared to the complete *A. veronii* genomes (strain CB51, TH0426, X11, X12, MS1837, and 17ISAe).

[7]http://arpcard.mcmaster.ca/

[8]http://cge.cbs.dtu.dk/services/ResFinder

[9]https://www.pathogenomics.sfu.ca/islandviewer

RESULTS

Taxonomic Identification

According to the partial *gyrB* sequence (1.4-kb-long), all bacterial isolates were mostly similar to *A. veronii* with a 98%–99% sequence identity (100% query coverage). Likewise, the TYGS web tool also indicated that the representative genomes of this study (NK01, NK02, NK07, CNRT12, and UDRT09) are genotypically closest to *A. veronii* CECT 4257. The digital DNA-DNA hybridization (dDDH) value of the current genomes in comparison with *A. veronii* CECT 4257 is 69.18% (d_4 formula) and the GC% difference is 0.28. The dDDH cut-off for the bacterial species demarcation is $\geq$70%. Thus, the Aeromonad isolates used in this study should be classified as *A. veronii*. Herein, the type strain *A. veronii* CECT 4257 belongs to biovar veronii. This study also attempted to identify the biovar of the current isolates based on a pairwise genome comparison against both biovars of *A. veronii*, namely biovar sobria and biovar veronii. The ANI calculator revealed that the genomes of this study were similar to both biovar sobria (ANI = 96.05%–96.45%) and biovar veronii (ANI = 96.16%–96.48%). The ANI values in comparison with both biovars are demonstrated in the supplementary information (**Supplementary Table 1**). Since the ANI cut-off for species demarcation is $\geq$95%, we cannot differentiate the biovar of the current *A. veronii* isolates based on their genomes alone. However, there was evidence that biovar veronii could be differentiated from biovar sobria by the exhibition of ornithine decarboxylase negative and arginine dihydrolase positive activities (Abbott et al., 2003). According to the biochemical profiles shown in **Supplementary Table 2**, the recent isolates shared a similar characteristic with the isolates determined in our previous study (Dong et al., 2015). Thus, with reference to the biochemical profile, *A. veronii* in the present study can be distinguished as biovar veronii.

Determination of the Minimum Inhibitory Concentration

The broth microdilution method was used to evaluate the MIC and the results are demonstrated in **Table 3**. The results suggested that the isolates of this study were completely resistant to beta-lactams (ampicillin and amoxicillin; MIC > 256 mg/L). On contrary, all isolates were susceptible to florfenicol with the MIC lower than 1 mg/L. The percentage of resistance to other antimicrobials ranged from oxytetracycline (67%) to oxolinic acid (33%) and enrofloxacin (17%). More importantly, this research found the first resistance of *A. veronii* isolated from freshwater fish to gentamicin and Trimethoprim/sulfamethoxazole (MIC > 256 mg/L) in the NK02 and NK07 isolates, respectively. Furthermore, the isolates with a diverse degree of multidrug resistance

TABLE 2 | List of *Aeromonas veronii* genome included in the resistome analysis.

Genome completeness	Accession no.	Strain	Host	Country	Genome size (Mb)	Year
Complete	GCA_001634345.1	CB51	Grass carp, *Ctenopharyngodon idella*	China	4.58	2016
	GCA_001593245.1	TH0426	Yellowhead catfish, *Tachysurus fulvidraco*	China	4.92	2016
	GCA_002803925.1	X11	Wuchang bream, *Megalobrama amblycephala*	China	4.28	2017
	GCA_002803945.1	X12		China	4.77	2017
	GCA_003722175.1	MS1837	Catfish, *Siluriformes sp.*	United States	4.68	2018
	GCA_003491365.1	17ISAe	Discus, *Symphysodon discus*	Korea	4.66	2018
Scaffold	GCA_002339005.1	UBA1835	European eel, *Anguilla Anguilla*	Spain	4.11	2017
	GCA_003345755.1	XHVA2	Channel catfish, *Ictalurus punctatus*	China	4.91	2018
Contig	GCA_000409545.1	PhIn2	Unknown	India	4.30	2013
	GCA_001748325.1	Ae52	Goldfish, *Carassius auratus*	Sri Lanka	4.56	2016
	GCA_002906945.1	ML09123	Catfish, *Siluriformes sp.*	United States	4.75	2018
	GCA_003611985.1	MS1788	Catfish, *Siluriformes sp.*	United States	5.18	2018
	GCA_003367145.1	NS	European bass, *Dicentrarchus labrax*	Greece	4.71	2018
	GCA_003367095.1	VCK	Unpublished	Greece	4.63	2018
	GCA_003036425.1	XHVA1	Channel catfish, *Ictalurus punctatus*	China	5.36	2018
	GCA_012029595.1	**UDRT09**	**Hybrid red tilapia, *Oreochromis mossambicus* × *Oreochromis niloticus***	**Thailand**	**4.61**	**2018**
	GCA_012029535.1	**CNRT12**		**Thailand**	**4.90**	**2018**
	GCA_012029545.1	**NK01**	**Nile tilapia, *Oreochromis niloticus***	**Thailand**	**4.56**	**2015**
	GCA_012029575.1	**NK02**	**Nile tilapia, *Oreochromis niloticus***	**Thailand**	**4.80**	**2015**
	GCA_012029585.1	**NK07**	**Nile tilapia, *Oreochromis niloticus*)**	**Thailand**	**4.78**	**2015**

Bold represents the newly sequenced genomes used in this study, while the other genomes were obtained from the GenBank database.

(MDR), namely NK07 (six drugs from five antimicrobial classes, 5MDR), UDRT09 (four antimicrobial classes, 4MDR), NK01 (three antimicrobial classes, 3MDR), NK02 (gentamicin resistant), and CNRT12 (resistant to only beta-lactam, Sense), were included in the subsequent genome investigation.

Phylogenetic Analysis

Among the 20 *A. veronii* genomes used for the genome analysis, ST could be assigned to only 4 genomes, i.e., MS1837 (ST 254), 17ISAe (ST485), NS, and VCK (ST 23). On the other hand, the other isolates were defined as an unknown ST due to the presence of new allele variants (**Supplementary Table 2**).

TABLE 3 | MIC values *Aeromonas veronii* of this study.

Antimicrobial		Cut-off value*	MIC (mg/L)									
Class	**Drug**		**NK01**	**NK02**	**NK03**	**NK04**	**NK05**	**NK06**	**NK07**	**CNRT07**	**CNRT11**	**CNRT12**	**CNRT13**	**UDRT09**
Beta-lactam	Amoxicillin	NA	> 256^{R}	> 256^{R}	> 256^{R}	> 256^{R}	> 256^{R}	> 256^{R}	> 256^{R}	> 256^{R}	> 256^{R}	> 256^{R}	> 256^{R}	> 256^{R}
	Ampicillin	NA	> 256^{R}	> 256^{R}	> 256^{R}	> 256^{R}	> 256^{R}	> 256^{R}	> 256^{R}	> 256^{R}	> 256^{R}	> 256^{R}	> 256^{R}	> 256^{R}
Aminoglycoside	Gentamicin	4	2	> 256^{R}	2	8	4	2	4	2	4	2	2	4
Fluoroquinolone	Enrofloxacin	0.125	2	0.5	2	1	< 0.03	1	4^{R}	0.5	0.5	< 0.03	0.5	> 16^{R}
Quinolone	Oxolinic acid	0.03	64^{R}	1	32^{R}	1	< 0.25	8	32^{R}	2	8	< 0.25	4	64^{R}
Tetracycline	Oxytetracycline	0.25	> 256^{R}	1	> 256^{R}	> 256^{R}	1	128^{R}	> 256^{R}	1	128^{R}	1	128^{R}	> 256^{R}
Sulfonamide	Sulfamethoxazole/ Trimethoprim	0.25	4	2	2	2	2	2	> 256^{R}	2	2	2	2	2
Phenicol	Florfenicol	2	1	1	1	1	1	1	1	1	1	1	1	1
Interpretation			3MDR		3MDR		Sense		5MDR			Sense		4MDR

**The cut-off referred to the generic epidemiological cut-off values of Aeromonas sp. in freshwater Baron et al., 2017.*
Bold represents the isolates used for whole-genome sequencing. Superscripts R indicated a resistance. NA, not applicable.

In this study, only four MLST loci (*gltA*, *groA*, *metG*, and *recA*), with a total length of 2,070 bp, were included for the phylogenetic tree reconstruction since *gyrB* and *ppsA* were absent in some isolates due to the incompleteness of the genomes. However, since *gyrB* is a key genetic marker for *Aeromonas* species identification, a phylogenetic analysis of *gyrB* was separately performed to compare with the MLST loci. The results from both the *gyrB*-based tree and MLSA-based tree suggested a high genetic diversity among the *A. veronii* isolates (**Figure 1A** and **Supplementary Figure 2**). The observed phylogeny was likely unrelated to the geographical origin, host species, and resistance phenotype of the analyzed taxa. For instance, the isolates from Thailand are clustered in distinct clade disperse, whereas the isolates NK02 and CNRT12 were grouped into the same subclade regardless of the difference in the resistance phenotype (aminoglycoside resistant vs. sensitive). Similarly, the phylogenetic tree based on the genome-wide SNPs also suggested a high genetic variability (**Figure 1B**). The numbers of core genome SNPs (shown in the **Supplementary Figure 1**) of the pairwise comparison across the *A. veronii* genomes were diverse with between 11 and 45,536 SNPs. It is worth mentioning that two out of five newly assembled genomes (NK01 and UDRT09) were almost genetically identical (only 27 SNPs) and have similar resistance phenotypes (resistant to quinolone, tetracycline, and beta-lactam). This indicated that NK01 and UDRT09 were derived from the same clone.

Resistome Analysis

Aeromonas veronii genomes were queried against two AMR databases, namely CARD and ResFinder, to identify the ARG repertoire, also known as resistome. The bacteria used in this analysis comprised of (i) the strains isolated from tilapia and (ii) other freshwater fishes whose genomes were retrieved from the NCBI (**Table 2**). The potential ARGs observed in each group of *A. veronii* strains were described as follows:

Resistome of *Aeromonas veronii* Isolated From Tilapia

There were 17 ARGs identified from the newly assembled genomes derived from tilapia (n = 5; NK01, NK02, NK07, UDRT09, and CNRT12). These ARGs can be categorized into nine groups according to the antimicrobial classes, i.e., aminoglycoside, beta-lactam, chloramphenicol, macrolide, organic compound, quinolone, sulfonamide, tetracycline, and multidrug resistance-associated (**Figure 2**). Among the five isolates, UDRT09 and NK07 carried the greatest number of ARGs (14 genes), while NK02, NK01, and CNRT12 carried 13, 12, and 12 genes, respectively. Of these 17 ARGs, 11 genes [*ceph-A3*, *qnr32*, *dfrA12*, *mcr-3*, *sul1*, *tetA*, *tetC*, *tetD*, *tetE*, *aac(6')-Ib-cr*, and *ade-F*] were shared by all *A. veronii* tilapia isolates. Herein, two ARGs associated with macrolide resistant (*mphA*), aminoglycoside resistant (*aac(3)-IIb*), and chloramphenicol (*catA1*) were specifically found in NK07, NK02, and UDRT09, respectively.

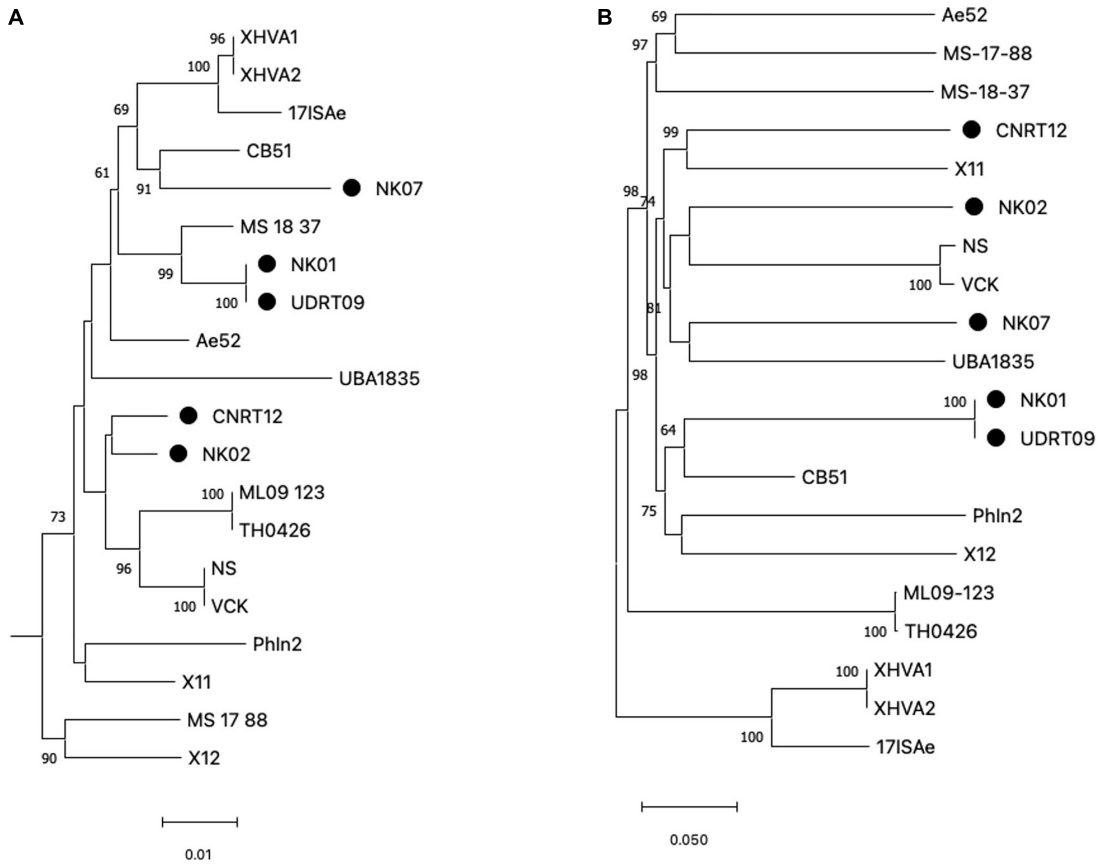

FIGURE 1 | Maximum likelihood tree generated from concatenated MLST loci **(A)** and genome-wide SNPs **(B)**. MLST loci included *gltA*, *groA*, *metG*, and *recA* with the total length of 2,070 bp and *Aeromonas schubertii* WL1483 as an outgroup (omitted from the tree). The genome-wide SNPs was concatenated into contig with a total length of 175,597 bp. Trees were constructed using IQ-tree with 5,000 ultrabootstrap. Numbers at the tree node represent the bootstrap value in percentage (only ≥ 60 value is shown). The newly assembled genomes (Thai isolates) are indicated by the filled circle adjacent to the taxa. Scale bar represents the nucleotide substitution per site.

Resistome of *Aeromonas veronii* Isolated From Other Freshwater Fishes

A total of 19 ARGs (ten drug classes) were identified from 15 genomes of *A. veronii* associated with an invasive disease in various freshwater fish species (**Figure 2**). The genomes from PhIn2 and Ae52 (isolated from India and Sri Lanka) harbored the highest number of ARGs (15 genes), followed by X11 (China), CB51 (China), 17ISAe (Korea), and MS1788 (United States) which carried 14, 13, 13, and 13 ARGs, respectively. The strains UBA1835 (Spain); ML09123 and MS1837 from United States; and TH0426, X12, XHVA1, and XHVA2 from China each carried 12 ARGs. Lastly, 11 ARGs were detected in VCK and NS from Greece. There was one strain, namely 17ISAe, that carried the rifamycin resistance gene (*arr*-3) which was absent in other *A. veronii* isolates, including the tilapia isolates.

Concerning the sharing of ARGs among the Aeromonad population, there were 16 ARGs detected in both tilapia and freshwater fish isolates (n = 20). The following genes: *aac* (6′)-*lb-cr*, *adeF*, *cphA3*, *qnrS2*, *drf A12*, *mcr*-3, *sul-1*, *tetA*, *tetC*, and *tetD* were detected in all isolates. The *OXA*-12 gene was observed in only two out of five tilapia isolates (NK02 and NK09), but abundant in the strains isolated from other fish species (14 out of 15). This was similar to the absence of *tetE* in only four isolates from freshwater fish. In addition, *catA1* and *mphA* were identified in one strain, i.e., Ae52, similar to the gene observed in UDRT09 and NK07 from the tilapia group.

Genomic Islands Analysis

Since the newly sequenced genomes used for GI detection are incomplete genomes, any predicted GI located near the boundary of contigs (< 1,000 bp from 5′ and 3′ termini) were omitted from this analysis to avoid a false positive detection. Herein, IslandViewer 4 predicted the presence of potential GIs in every tilapia *A. veronii* isolate genome. A manual investigation of the gene contents resided within these potential GIs showed that the NK07 isolate harbored a large resistance island (RI) with a size of 22,323 bp (**Figure 3**). This RI contained several AMRs and heavy metal resistance genes (MRGs) [mercury resistance (*mer*) operon and chromate (*chrA*) efflux pump]. There were at least six AMRs potentially associated with the resistant to diverse drug classes including sulfonamide (*sul1*), trimethoprim (*drfA12*), tetracycline (*tetR/acrR*), aminoglycoside

Country		USA			Greece		Spain	Korea	Sri lanka	India	China						Thailand				
Phenotypic resistance		Unpublished			AMP	Unpublished		MDR	MDR	Unpublished							OXO, OTC, AMP, AMC	GEN AMP, AMC	OTC, SXT ENR, OXO AMP, AMC	OTC ENR, OXO AMP, AMC	AMP, AMC
Genes \ Isolate		ML09123	MS1788	MS1837	NS	VCK	UBA1835	17ISAe	Ae52	Phin2	TH0426	CB51	X11	X12	XHVA1	XHVA2	NK01	NK02	NK07	UDRT09	CNRT12
Aminoglycoside	*aac(3)-Iib**							35.56	31.41				30.53					87.64			
Beta-lactam	*ampS**		98.48				98.86			98.98		98.3	98.48				97.92		98.48	97.92	98.3
	bla $_{TEM-116}$*																			99.73	
	ceph-A3	73.52	98.42	98.16	98.29	97.36	98.42	98.02	97.76	98.16	97.89	98.42	98.16	98.42	98.16	98.16	97.1	98.29	98.16	97.1	98.03
	OXA-12	98.86	48.55	98.86	98.86	98.86		98.48	98.67	48.55	98.86	48.55	48.55	98.48	98.3	98.3		98.48	48.55		
	TEM-1									99.91											
	TRU-1						87.74			60											
Chloramphenicol	*catA1**								68.75											99.31	
Quinolone	*qnrS2**	61.95	62.93	61.95	62.93	62.93	61.46	62.44	61.95	62.44	61.95	62.93	62.44	62.44	62.44	62.44	61.46	100	62.93	100	62.93
Macrolide	*mphA**								100										100		
Organic compounds	*dfrA12**	58.9	58.49	100	60.12	59.51	59.51	59.51	100	60.9	58.9	59.51	59.51	58.49	59.51	59.51	59.51	60.12	100	59.51	58.9
	*mcr-3**	74.72	74.16	74.16	74.34	74.34	73.7	98.14	97.84	74.34	74.72	74.53	74.34	74.72	74.53	74.53	74.34	74.34	74.72	74.34	74.34
Rifamycin	*arr-3**							100													
Sulfonamide	*sul1**	52.02	50.8	100	50.4	50.4	49.34	100	100	50.8	52.02	51.2	51.2	50.81	52.53	52.53	53.03	51.6	100	53.03	51.2
Tetracycline	*tetA**	49.34	49.45	49.34	49.34	58.86	47.61	90.85	91.33	59.01	48.19	48.21	49.45	48.64	49.45	49.45	49.34	49.34	91.33	49.34	49.45
	*tetC**	58.34	47.36	47.36	47.36	46.25	68	48.92	47.05	82.54	47.65	47.36	48.08	46.56	47.65	47.65	48.73	48.73	46.56	48.73	47.94
	*tetD**	68	56.4	68	68	68	41.67	68	68	68	68	68	68	68	68	68	68	68	68	68	68
	*tetE**	41.89	74.08	74.34					74.34	47.13	41.89	41.67	41.67	47.85	47.94	47.94	74.28	47.39	46.77	74.28	46.76
Multidrug	*aac(6')-Ib-cr**	61.22	61.22	61.22	61.22	61.22	61.22	100	59.18	61.22	61.22	61.22	61.22	61.22	61.22	61.22	61.22	100	61.22	61.22	61.22
	adeF	65.96	65.96	65.96	66.06	66.06	70.88	66.01	74.32	67.92	65.96	71	65.96	66.16	65.96	65.96	65.96	65.96	65.96	65.96	65.96

The best hit (90 - 100%) of the gene which may directly affect the phenotypic resistance

The fair hit (70 - 89%) of the gene which may directly affect the phenotypic resistance

FIGURE 2 | The presence of ARGs within the genomes of *A. veronii* isolated from freshwater fishes (n = 20). The numbers represent the pairwise percent identity (obtained from protein BLAST) using the deduced amino acid sequence and its homolog as query and subject sequence, respectively. High percent identity is suggested by a darker color, whereas an empty box indicated that no homologous gene is observed in either the CARD or ResFinder database. Strains isolated from tilapia (newly sequenced genomes) are defined by an underlined name. Acquired antimicrobial resistant genes are labeled with an asterisk.

(*aadA2*), macrolide (*mphA*), and multidrug efflux pump (MFS transporter). Additionally, this NK07-derived RI contained one antiseptic resistance gene (*qacE*). Interestingly, some resistance elements, i.e., *sul1*, *qacE*, and trimethropim-resistant dihydrofolate reductase (*dfrA*), were also observed in an important 19-kb-long RI presented in the reference strain 17ISAe (**Figure 3**), although other genetic contents were dissimilar to the NK07-derived RI. Regarding the other *A. veronii* tilapia isolates, the 12-kb-long RI containing tetracycline resistance genes (*tetE* and *tetR*) was identified in the genome of the NK01 and UDRT09 isolates (**Supplementary Figure 3**), while no GI carrying AMRs was observed in the NK02 and CNRT12 isolates.

DISCUSSION

Aeromonad infection is one of the global concerns to the loss of aquaculture production. Due to the rise of antimicrobial resistance (AMR), the solution and choice of antimicrobial use is a challenge to the farmer and researcher. In this study, *Aeromonas* spp. were isolated from tilapia and according to our findings, these were classified as *A. veronii* biovar veronii based on their biochemical characterization (Abbott et al., 2003).

Resistome analysis is capable of investigating the comprehensive data of AMR to improve the efficacy of antimicrobial use (Zankari et al., 2012). As a result, in the MIC assay, florfenicol showed the best efficacy against *A. veronii*. However, the isolates in this study were altogether resistant to beta-lactams (amoxicillin and ampicillin) with a high MIC value, similar to that reported in the previous publication (Janda and Abbott, 2010; Yang et al., 2017). Referring to the epidemiological cut-off values from the study of *Aeromonas* diversity in France (Baron et al., 2017), the MIC values of *A. veronii* in this study were seriously higher than the previous publication. Likewise, this is the first discovery of gentamicin and sulfamethoxazole/trimethoprim resistant *A. veronii* isolated from tilapia. These rare resistances were reported previously in the clinical and environmental samples from Australia where *Aeromonas* spp. was susceptible to gentamicin and sulfamethoxazole/trimethoprim, with more than 98% and 99%, respectively (Aravena-Roman et al., 2012).

According to the licensed antimicrobials allowed for use in Thailand (FCSTD, 2012), oxytetracyclines are commonly used in tilapia farming which promotes a high resistance as evidenced by the MIC values that were higher than those in the previous report (Skwor et al., 2014). In addition, oxolinic acid and enrofloxacin were both less effective against *A. veronii*, in contrast to the study from China whereby *A. veronii* isolated from Chinese long-snout catfish was susceptible to these antimicrobials (Cai et al., 2012). Besides, *A. veronii* isolated from tilapia revealed a resistance to multiple antimicrobials similar to the study in channel catfish (Yang et al., 2017). MDR was observed mainly in NK07 (5MDR) followed by UDRT09 and NK01, which are 4MDR and 3MDR, respectively.

Regarding the ARGs, their presence and transmission were implicated in the efficacy of human and animal diseases treatment caused by the resistant *A. veronii* (Yang et al., 2017). The resistome analysis of the recent *A. veronii* isolates from tilapia and other freshwater fish isolates was performed by the consideration of the ARGs associated with a phenotypic

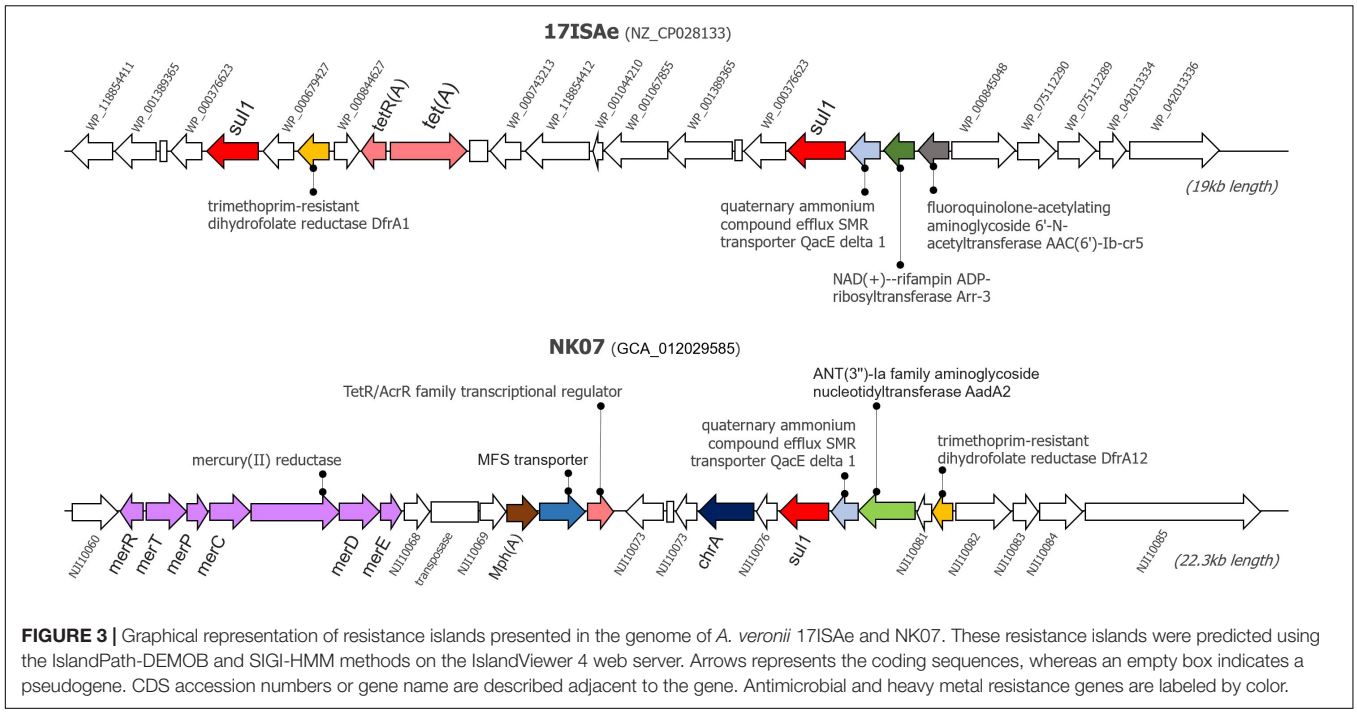

FIGURE 3 | Graphical representation of resistance islands presented in the genome of *A. veronii* 17ISAe and NK07. These resistance islands were predicted using the IslandPath-DEMOB and SIGI-HMM methods on the IslandViewer 4 web server. Arrows represents the coding sequences, whereas an empty box indicates a pseudogene. CDS accession numbers or gene name are described adjacent to the gene. Antimicrobial and heavy metal resistance genes are labeled by color.

resistance expression. It revealed 20 ARGs, which belong to nine groups of antimicrobial classes as shown in **Figure 2**. Overall, the ARGs were shared among the isolates from both tilapia and other fish species. The reciprocal protein BLAST against CARD-derived ARGs sequences indicated a relatively high percent identity (over 80%) suggesting a potentially complete or functional genes in this study.

Aminoglycoside Resistome

The resistant phenotype observed in NK02 was also in accordance with the presence of the potentially completed aminoglycoside resistance genes [*aac* (3)-*IIb* and *aac* (6′)-*Ib-cr*] exclusively found in its genome. Notably, there were few reports of aminoglycoside resistance in *Aeromonas* sp. from channel catfish and discus (Yang et al., 2017; Roh et al., 2019). In any case without evidence of drug use before, ARGs may then be acquired from the other pathogens or surrounding the environment (Heuer et al., 2002).

Beta-Lactam Resistome

Beta-lactams are broadly used worldwide; however, the recent *A. veronii* isolates were resistant to both amoxicillin and ampicillin categorized as broad-spectrum beta-lactams. The set of beta-lactam resistance genes were detected in all isolates which are typically found in the *Aeromonas* species (Chen et al., 2019). Previously, *A. hydrophila* and other species of *Aeromonas* have been reported as intrinsically ampicillin-resistant (Joseph et al., 1979; Yucel and Aslim, 2005). However, there is no official report of intrinsic resistance in *A. veronii*. Referring to the MIC values that were supported by the presence of beta-lactams resistance-associated genes (*ampS, ceph-A3* and *OXA-12*) with over a 97% sequence identity, *A. veronii* should be noted as an intrinsically broad-spectrum beta-lactam resistant as mentioned in the previous publications (Baron et al., 2017). Extended spectrum beta-lactamases (ESBLs) are enzymes which enable bacteria to hydrolyze an extended spectrum cephalosporin (Ghafourian et al., 2015). So far, there are no reports about ESBL drug group use in Thai aquaculture. However, the ESBL-related gene detected in this study was probably acquired from agricultural, human medication, or other sources as reported from a previous publication (Piotrowska et al., 2017). Further investigation of the phenotypic susceptibility to ESBL is needed.

Quinolone and Fluoroquinolone Resistome

The presence of the *qnrS2* gene refers to the plasmid-mediated quinolone resistance protein which was originally found in *Salmonella enterica* and plays a role on horizontal gene transfer (Jia et al., 2017). This gene was detected in all isolates but only showed a perfect identity in NK02 and UDRT09. However, there were few publications which reported that *A. veronii* encoded the *qnrS2* gene on a plasmid since the first report in 2008 (Sanchez-Cespedes et al., 2008). Generally, missense mutations in DNA gyrase (*gyrA* or *gyrB*) and topisomerase IV (*parC* or *parE*) encoded genes are common mechanisms that confer a resistance to fluoroquinolones while *qnrS2* plays a role as a supportive resistance gene (Sanchez-Cespedes et al., 2008; Redgrave et al., 2014).

Tetracycline Resistome

Five ARGs were blasted against the *A. veronii* isolates, and these included the *tetA*, *tetC*, *tetD*, *tetE*, and *adeF* genes. The *adeF* works as a secondary resistance gene and enhances tetracycline and fluoroquinolone resistance (Mobasseri et al., 2018). In

addition, a set of *tet* genes are located on a plasmid and functionally work for tetracycline resistance (Jia et al., 2017). Similar to the previous study, *A. veronii* resistance to tetracycline and their associated genes have been reported worldwide (Skwor et al., 2014; Baron et al., 2017; Yang et al., 2017). The set of *tetA*, *tetC*, *tetD*, *tetE*, and *adeF* genes were found in most of the isolates. As seen in the NK01, NK07, and UDRT09 isolates, the involvement of *tet* genes (high percent identity) coincide with higher MIC values as mentioned in the previous publication (Balassiano et al., 2007).

Sulfonamide Resistome

A sulfonamide resistance gene (*sul1*) is a gene encoding dihydropteroate synthase and it was reported as multidrug resistance mediated by class 1 integrons in *Aeromonas* (Deng et al., 2016). The gene was presented in all strains used in this analysis, although only four strains (MS1788, 17ISAe, Ae52, and NK07) presented a 100% sequence identity. Interestingly, the presence of a complete *sul1* in NK07 consistent to its Sulfamethoxazole/Trimethoprim resistance phenotype was indicated by the MIC assay.

Other Resistance Genes

The group of class 1 integron resistance association consists of genes *catA1* and *dfrA12*. These genes are acquired differently from other pathogens. Generally, *catA1* is a gene encoding chloramphenicol acetyltransferase from *Shigella flexneri* 2a and *dfrA12* is a gene encoding dihydrofolate reductase from *Vibrio cholera* (Jia et al., 2017). Similar to this study, *catA1* was detected in *A. salmonicida* and recently in *A. veronii* (Tanaka et al., 2016; Syrova et al., 2018). In addition, *dfrA12* was reported as MDR mediated by class 1 integrons in *Aeromonas* isolates (Deng et al., 2016). However, the effect of the high identity of *catA1* and *dfrA12* gene to the phenotypic resistance was not evaluated in UDRT09 and NK07. Lastly, *mcr-3*, a transferable colistin resistance gene which was firstly isolated from the pWJ1 plasmid of *E. coli*, showed a high amino acid identity to the *Aeromonas* species in this study (Yin et al., 2017). However, an evaluation of the colistin MIC value to confirm the potential contribution of the gene to phenotypic resistance was not performed in the current study.

Genomic Islands Analysis

Genomic Islands analysis enables the prediction of the potential resistance elements known as the Horizontal Gene Transfer (HGT) foundation (Soares et al., 2016). This study analyzed the potential of resistance and GIs association as clearly seen on the NK07 resistance island (NK07-RI). First of all, NK07-GIs are larger than 17ISAe (MDR isolate from discus) and much larger when compared to the less resistant isolates (NK01 and UDRT09). ARGs (*sul1*, *drfA12*, *tetR*/*acrR*, *aadA2*, and *mphA*) of NK07-RI had perfect sequence identity hits which are related to high MIC values. These genes have been reported as a mobile genetic element associated, as described before. Multidrug efflux pump (MFS transporter) plays an important role together with the mobile element protein to promote the MDR isolate (Pasqua et al., 2019). Moreover, antiseptic resistance gene (*qacE*) detected in NK07-RI has been studied in many pathogens with the effect of reducing the susceptibility of biocide (antiseptics and disinfectants) and antimicrobials (Vijayakumar and Sandle, 2019). Although, there is no study about this effect in *A. veronii*, the presence of *qacE* and resistance potential should be of concern. As seen in **Figure 3**, several MRGs were detected in NK07-RI. The chromate efflux pump associated gene (*chrA*) and mercury resistance (*mer*) operon are both generally encoded on a plasmid which mainly works on cell detoxify mechanism (Boyd and Barkay, 2012; Baaziz et al., 2017). Previously, *Mer* operon was detected in MDR *A. veronii* strain MS-18-37 isolated from United States catfish but no study about its function was demonstrated (Abdelhamed et al., 2019). Due to the ability of heavy metal uptake mechanism, *Aeromonas* spp. was tested as a bioremediation property for wastewater treatment (Ogugbue and Sawidis, 2011). This finding represents an adaptation ability to selective pressure in a microorganism induced by heavy metal residues contaminated in a water source. Although, there are several studies of MRGs with ARGs, their functions remain unclear (Chen et al., 2019).

CONCLUSION

Resistome analysis of *A. veronii* isolated from tilapia in Thailand provided evidence that conventional antimicrobials used in aquaculture are going to lose their effectiveness. According to the licensed antimicrobials allowed for use in Thailand, amoxicillin, oxytetracycline, and oxolinic acid may not be recommended for a longer use, likewise, enrofloxacin requires a high dosage for its usage (more than 16 mg/L) but there should be concern about the effect of resistant *A. veronii* in human medication. The last choice of the recommended antimicrobial use is sulfamethoxazole/trimethoprim and florfenicol (after license announcement by the FDA). In this study, *A. veronii* isolates were adapted into a multidrug-resistance related to the presence of multiple ARGs, and several genes were shared in the aquatic system among the *A. veronii* population worldwide. The prevalence of resistance against ESBL, beta-lactam, and colistin in *A. veronii* is highlighted and requires more insight study. Moreover, the possibility of plasmid-mediated resistance gene acquisition especially in gentamicin and sulfamethoxacin should be of concern as these can affect human and other animal health care. It should be noted that *A. veronii* has a broad-spectrum beta-lactam intrinsic resistance as revealed by the current and previous studies. At last, the outcomes of this study can be applied for AMR prediction and further treatment plans for effective antimicrobial use.

DATA AVAILABILITY STATEMENT

The datasets presented in this study can be found in online repositories. The names of the repository/repositories and accession number(s) can be found below: https://www.ncbi.nlm.nih.gov/bioproject/PRJNA612772.

AUTHOR CONTRIBUTIONS

RS, PC, ND-H, and PK: data curation. RS and PK: investigation and writing of the original draft. IH and CR: resources. PK and CR: supervision and validation. RS, PC, ND-H, ES, PK, RC, and CR: writing—review and editing. CR: funding acquisition. All authors contributed to the article and approved the submitted version.

FUNDING

This study was financially supported by the Oversea Research Experience Scholarship for Graduate Student, Chulalongkorn University, the 90th year Anniversary of Chulalongkorn University Scholarship (Ratchadaphiseksomphot Endowment Fund), and the Thailand Science Research and Innovation (TSRI) Fund [Grant number Chulalongkorn University_FRB64001_01_31_6].

ACKNOWLEDGMENTS

We would like to thank the Laboratory of Genome Science and Technology, Graduate School of Marine Science and Technology, Tokyo University of Marine Science and Technology for providing the whole genome sequence facilities.

SUPPLEMENTARY MATERIAL

The Supplementary Material for this article can be found online at: https://www.frontiersin.org/articles/10.3389/fmicb.2021.733668/full#supplementary-material

REFERENCES

Abbott, S. L., Cheung, W. K., and Janda, J. M. (2003). The genus Aeromonas: biochemical characteristics, atypical reactions, and phenotypic identification schemes. *J. Clin. Microbiol.* 41, 2348–2357. doi: 10.1128/jcm.41.6.2348-2357.2003

Abdelhamed, H., Lawrence, M. L., and Waldbieser, G. (2019). Complete genome sequence data of multidrug-resistant *Aeromonas veronii* strain MS-18-37. *Data Brief* 23:103689. doi: 10.1016/j.dib.2019.01.037

Alcock, B. P., Raphenya, A. R., Lau, T. T. Y., Tsang, K. K., Bouchard, M., Edalatmand, A., et al. (2019). CARD 2020: antibiotic resistome surveillance with the comprehensive antibiotic resistance database. *Nucleic Acids Res.* 48, D517–D525. doi: 10.1093/nar/gkz935

Aravena-Roman, M., Inglis, T. J., Henderson, B., Riley, T. V., and Chang, B. J. (2012). Antimicrobial susceptibilities of Aeromonas strains isolated from clinical and environmental sources to 26 antimicrobial agents. *Antimicrob. Agents Chemother.* 56, 1110–1112. doi: 10.1128/AAC.05387-11

Baaziz, H., Gambari, C., Boyeldieu, A., Ali Chaouche, A., Alatou, R., Méjean, V., et al. (2017). ChrASO, the chromate efflux pump of *Shewanella oneidensis*, improves chromate survival and reduction. *PLoS One* 12:e0188516. doi: 10.1371/journal.pone.0188516

Balassiano, I. T., Bastos, M. D. C. D. F., Madureira, D. J., Da Silva, I. G., De Freitas-Almeida, A. C., and De Oliveira, S. S. (2007). The involvement of *tetA* and *tetE* tetracycline resistance genes in plasmid and chromosomal resistance of *Aeromonas* in Brazilian strains. *Mem. Inst. Oswaldo Cruz* 102, 861–866. doi: 10.1590/s0074-02762007005000121

Bankevich, A., Nurk, S., Antipov, D., Gurevich, A. A., Dvorkin, M., Kulikov, A. S., et al. (2012). SPAdes: a new genome assembly algorithm and its applications to single-cell sequencing. *J. Comput. Biol.* 19, 455–477. doi: 10.1089/cmb.2012.0021

Baron, S., Granier, S. A., Larvor, E., Jouy, E., Cineux, M., Wilhelm, A., et al. (2017). Aeromonas Diversity and Antimicrobial Susceptibility in Freshwater-An Attempt to Set Generic Epidemiological Cut-Off Values. *Front. Microbiol.* 8:503. doi: 10.3389/fmicb.2017.00503

Bertelli, C., Laird, M. R., Williams, K. P., Simon Fraser University Research Computing, G, Lau, B. Y., Hoad, G., et al. (2017). IslandViewer 4: expanded prediction of genomic islands for larger-scale datasets. *Nucleic Acids Res.* 45, W30–W35. doi: 10.1093/nar/gkx343

Bolger, A. M., Lohse, M., and Usadel, B. (2014). Trimmomatic: a flexible trimmer for Illumina sequence data. *Bioinformatics* 30, 2114–2120. doi: 10.1093/bioinformatics/btu170

Bortolaia, V., Kaas, R. S., Ruppe, E., Roberts, M. C., Schwarz, S., Cattoir, V., et al. (2020). ResFinder 4.0 for predictions of phenotypes from genotypes. *J. Antimicrob. Chemother.* 75, 3491–3500. doi: 10.1093/jac/dkaa345

Boyd, E., and Barkay, T. (2012). The Mercury Resistance Operon: from an Origin in a Geothermal Environment to an Efficient Detoxification Machine. *Front. Microbiol.* 3:349. doi: 10.3389/fmicb.2012.00349

Cai, S. H., Wu, Z. H., Jian, J. C., Lu, Y. S., and Tang, J. F. (2012). Characterization of pathogenic *Aeromonas veronii* bv. veronii associated with ulcerative syndrome from chinese longsnout catfish (*Leiocassis longirostris günther*). *Br. J. Microbiol.* 43, 382–388. doi: 10.1590/s1517-83822012000100046

Caruso, G. (2016). Antibiotic Resistance in Fish Farming Environments: a Global Concern [Online]. *J. FisheriesSciences.com* 10, 9–13.

Chen, J., Li, J., Zhang, H., Shi, W., and Liu, Y. (2019). Bacterial Heavy-Metal and Antibiotic Resistance Genes in a Copper Tailing Dam Area in Northern China. *Front. Microbiol.* 10:1916. doi: 10.3389/fmicb.2019.01916

Clinical and Laboratory Standards Institute (CLSI) (2014). *Performance Standards For Antimicrobial Susceptibility Testing Of Bacteria Isoloated From Aquatic Animals; Second Information Supplement*. Annapolis Junction: Clinical and Laboratory Standards Institute.

Conesa, A., Gotz, S., Garcia-Gomez, J. M., Terol, J., Talon, M., and Robles, M. (2005). Blast2GO: a universal tool for annotation, visualization and analysis in functional genomics research. *Bioinformatics* 21, 3674–3676. doi: 10.1093/bioinformatics/bti610

Deng, Y., Wu, Y., Jiang, L., Tan, A., Zhang, R., and Luo, L. (2016). Multi-Drug Resistance Mediated by Class 1 Integrons in Aeromonas Isolated from Farmed Freshwater Animals. *Front. Microbiol.* 7:935. doi: 10.3389/fmicb.2016.00935

Department of Fisheries (DOF) (2019). *Fisheries Statistics of Thailand*. Bangkok: Department of Fisheries, Ministry of Agriculture.

Dong, H. T., Nguyen, V. V., Le, H. D., Sangsuriya, P., Jitrakorn, S., Saksmerprome, V., et al. (2015). Naturally concurrent infections of bacterial and viral pathogens in disease outbreaks in cultured Nile tilapia (*Oreochromis niloticus*) farms. *Aquaculture* 448, 427–435. doi: 10.1016/j.aquaculture.2015.06.027

Dong, H. T., Techatanakitarnan, C., Jindakittikul, P., Thaiprayoon, A., Taengphu, S., Charoensapsri, W., et al. (2017). *Aeromonas jandaei* and *Aeromonas veronii* caused disease and mortality in Nile *tilapia, Oreochromis niloticus* (L.). *J. Fish Dis.* 40, 1395–1403. doi: 10.1111/jfd.12617

Food and Agriculture Organization (FAO) (2018). *THE STATE OF THE WORLD series of the Food and Agriculture Organization of the United Nations*. Rome: Food and Agriculture Organization.

FCSTD (2012). *Veterinary Drugs, Chemicals And Hazardous Substances With Standard Aquaculture [Online]. Department of fisheries*. Available online at: https://www.fisheries.go.th/thacert/index.php/knowledge/76-drug-animal (Accessed September 1, 2018)

Ghafourian, S., Sadeghifard, N., Soheili, S., and Sekawi, Z. (2015). Extended Spectrum Beta-lactamases: definition, Classification and Epidemiology. *Curr. Issues Mol. Biol.* 17, 11–21.

Hassan, M. A., Noureldin, E. A., Mahmoud, M. A., and Fita, N. A. (2017). Molecular identification and epizootiology of *Aeromonas veronii* infection among farmed *Oreochromis niloticus* in Eastern Province, KSA. *Egypt. J. Aquat. Res.* 43, 161–167. doi: 10.1016/j.ejar.2017.06.001

Heuer, H., Krögerrecklenfort, E., Wellington, E. M., Egan, S., van Elsas, J. D., van Overbeek, L., et al. (2002). Gentamicin resistance genes in environmental bacteria: prevalence and transfer. *FEMS Microbiol. Ecol.* 42, 289–302. doi: 10.1111/j.1574-6941.2002.tb01019.x

Hoel, S., Vadstein, O., and Jakobsen, A. N. (2017). Species Distribution and Prevalence of Putative Virulence Factors in Mesophilic Aeromonas spp. Isolated from Fresh Retail Sushi. *Front. Microbiol.* 8:931. doi: 10.3389/fmicb.2017.00931

Jain, C., Rodriguez-R, L. M., Phillippy, A. M., Konstantinidis, K. T., and Aluru, S. (2018). High throughput ANI analysis of 90K prokaryotic genomes reveals clear species boundaries. *Nat. Commun.* 9:5114. doi: 10.1038/s41467-018-07641-9

Janda, J. M., and Abbott, S. L. (2010). The genus Aeromonas: taxonomy, pathogenicity, and infection. *Clin. Microbiol. Rev.* 23, 35–73. doi: 10.1128/CMR.00039-09

Jia, B., Raphenya, A. R., Alcock, B., Waglechner, N., Guo, P., Tsang, K. K., et al. (2017). CARD 2017: expansion and model-centric curation of the comprehensive antibiotic resistance database. *Nucleic Acids Res.* 45, D566–D573. doi: 10.1093/nar/gkw1004

Jolley, K. A., Bray, J. E., and Maiden, M. C. J. (2018). Open-access bacterial population genomics: BIGSdb software, the PubMLST.org website and their applications. *Wellcome Open Res.* 3:124. doi: 10.12688/wellcomeopenres.14826.1

Joseph, S. W., Daily, O. P., Hunt, W. S., Seidler, R. J., Allen, D. A., and Colwell, R. R. (1979). Aeromonas Primary Wound Infection of a Diver in Polluted Waters. *J. Clin. Microbiol.* 10, 46–49. doi: 10.1128/jcm.10.1.46-49.1979

Kaas, R. S., Leekitcharoenphon, P., Aarestrup, F. M., and Lund, O. (2014). Solving the problem of comparing whole bacterial genomes across different sequencing platforms. *PLoS One* 9:e104984. doi: 10.1371/journal.pone.0104984

Katoh, K., and Standley, D. M. (2013). MAFFT multiple sequence alignment software version 7: improvements in performance and usability. *Mol. Biol. Evol.* 30, 772–780. doi: 10.1093/molbev/mst010

Kosugi, S., Hirakawa, H., and Tabata, S. (2015). GMcloser: closing gaps in assemblies accurately with a likelihood-based selection of contig or long-read alignments. *Bioinformatics* 31, 3733–3741. doi: 10.1093/bioinformatics/btv465

Kumar, S., Stecher, G., Li, M., Knyaz, C., and Tamura, K. (2018). MEGA X: molecular Evolutionary Genetics Analysis across Computing Platforms. *Mol. Biol. Evol.* 35, 1547–1549. doi: 10.1093/molbev/msy096

Li, H., and Durbin, R. (2010). Fast and accurate long-read alignment with Burrows–Wheeler transform. *Bioinformatics* 26, 589–595. doi: 10.1093/bioinformatics/btp698

Lomonaco, S., Crawford, M. A., Lascols, C., Timme, R. E., Anderson, K., Hodge, D. R., et al. (2018). Resistome of carbapenem- and colistin-resistant *Klebsiella pneumoniae* clinical isolates. *PLoS One* 13:e0198526. doi: 10.1371/journal.pone.0198526

Magiorakos, A. P., Srinivasan, A., Carey, R. B., Carmeli, Y., Falagas, M. E., Giske, C. G., et al. (2012). Multidrug-resistant, extensively drug-resistant and pandrug-resistant bacteria: an international expert proposal for interim standard definitions for acquired resistance. *Clin. Microbiol. Infect.* 18, 268–281. doi: 10.1111/j.1469-0691.2011.03570.x

Martino, M. E., Fasolato, L., and Cardazzo, B. (2016). Aeromonas. *Encycl. Food Health* 2016, 61–67.

Meier-Kolthoff, J. P., and Goker, M. (2019). TYGS is an automated high-throughput platform for state-of-the-art genome-based taxonomy. *Nat. Commun.* 10:2182. doi: 10.1038/s41467-019-10210-3

Minh, B. Q., Nguyen, M. A., and von Haeseler, A. (2013). Ultrafast approximation for phylogenetic bootstrap. *Mol. Biol. Evol.* 30, 1188–1195. doi: 10.1093/molbev/mst024

Mobasseri, P., Azimi, L., Salehi, M., Hosseini, F., and Fallah, F. (2018). Distribution and Expression of Efflux Pump Gene and Antibiotic Resistance in *Acinetobacter baumannii*. *Arch. Clin. Infect. Dis.* 13:e67143. doi: 10.5812/archcid.67143

Nguyen, L. T., Schmidt, H. A., von Haeseler, A., and Minh, B. Q. (2015). IQ-TREE: a fast and effective stochastic algorithm for estimating maximum-likelihood phylogenies. *Mol. Biol. Evol.* 32, 268–274. doi: 10.1093/molbev/msu300

Ogugbue, C. J., and Sawidis, T. (2011). Bioremediation and Detoxification of Synthetic Wastewater Containing Triarylmethane Dyes by *Aeromonas hydrophila* Isolated from Industrial Effluent. *Biotech. Res. Int.* 2011:967925. doi: 10.4061/2011/967925

Pasqua, M., Grossi, M., Zennaro, A., Fanelli, G., Micheli, G., Barras, F., et al. (2019). The Varied Role of Efflux Pumps of the MFS Family in the Interplay of Bacteria with Animal and Plant Cells. *Microorgan* 7:285. doi: 10.3390/microorganisms7090285

Piotrowska, M., and Popowska, M. (2015). Insight into the mobilome of *Aeromonas* strains. *Front. Microbiol.* 6:494. doi: 10.3389/fmicb.2015.00494

Piotrowska, M., Przygodzinska, D., Matyjewicz, K., and Popowska, M. (2017). Occurrence and Variety of beta-Lactamase Genes among *Aeromonas* spp. Isolated from Urban Wastewater Treatment Plant. *Front. Microbiol.* 8:863. doi: 10.3389/fmicb.2017.00863

Redgrave, L. S., Sutton, S. B., Webber, M. A., and Piddock, L. J. (2014). Fluoroquinolone resistance: mechanisms, impact on bacteria, and role in evolutionary success. *Trends Microbiol.* 22, 438–445. doi: 10.1016/j.tim.2014.04.007

Roh, H. J., Kim, B. S., Kim, A., Kim, N. E., Lee, Y., Chun, W. K., et al. (2019). Whole-genome analysis of multi-drug-resistant *Aeromonas veronii* isolated from diseased discus (*Symphysodon discus*) imported to Korea. *J. Fish Dis.* 42, 147–153. doi: 10.1111/jfd.12908

Sanchez-Cespedes, J., Blasco, M. D., Marti, S., Alba, V., Alcalde, E., Esteve, C., et al. (2008). Plasmid-mediated QnrS2 determinant from a clinical Aeromonas veronii isolate. *Antimicrob. Agents Chemother.* 52, 2990–2991. doi: 10.1128/AAC.00287-08

Skwor, T., Shinko, J., Augustyniak, A., Gee, C., and Andrasoc, G. (2014). *Aeromonas hydrophila* and *Aeromonas veronii* Predominate among Potentially Pathogenic Ciprofloxacin- and Tetracycline-Resistant *Aeromonas* Isolates from Lake Erie. *Appl. Environ. Microbiol.* 80, 841–848. doi: 10.1128/AEM.03645-13

Soares, S. C., Geyik, H., Ramos, R. T., de Sa, P. H., Barbosa, E. G., Baumbach, J., et al. (2016). GIPSy: genomic island prediction software. *J. Biotechnol.* 232, 2–11. doi: 10.1016/j.jbiotec.2015.09.008

Subramani, P. A., and Michael, R. D. (2017). "Prophylactic and Prevention Methods Against Diseases in Aquaculture," in *Fish Diseases*, ed. G. Jeney (Amsterdam: Elsevier), 81–117. doi: 10.1016/b978-0-12-804564-0.00004-1

Syrova, E., Kohoutova, L., Dolejska, M., Papezikova, I., Kutilova, I., Cizek, A., et al. (2018). Antibiotic resistance and virulence factors in mesophilic *Aeromonas* spp. from Czech carp fisheries. *J. Appl. Microbiol.* doi: 10.1111/jam.14075 [Online ahead of print]

Tanaka, K. H., Vincent, A. T., Trudel, M. V., Paquet, V. E., Frenette, M., and Charette, S. J. (2016). The mosaic architecture of *Aeromonas salmonicida* subsp. salmonicida pAsa4 plasmid and its consequences on antibiotic resistance. *PeerJ.* 4:e2595. doi: 10.7717/peerj.2595

Tatusova, T., DiCuccio, M., Badretdin, A., Chetvernin, V., Nawrocki, E. P., Zaslavsky, L., et al. (2016). NCBI prokaryotic genome annotation pipeline. *Nucleic Acids Res.* 44, 6614–6624. doi: 10.1093/nar/gkw569

Vijayakumar, R., and Sandle, T. (2019). A review on biocide reduced susceptibility due to plasmid-borne antiseptic-resistant genes-special notes on pharmaceutical environmental isolates. *J. Appl. Microbiol.* 126, 1011–1022. doi: 10.1111/jam.14118

Walker, B. J., Abeel, T., Shea, T., Priest, M., Abouelliel, A., Sakthikumar, S., et al. (2014). Pilon: an Integrated Tool for Comprehensive Microbial Variant Detection and Genome Assembly Improvement. *PLoS One* 9:e112963. doi: 10.1371/journal.pone.0112963

Yang, Q., Zhao, M., Wang, K. Y., Wang, J., He, Y., Wang, E. L., et al. (2017). Multidrug-Resistant Aeromonas veronii Recovered from Channel Catfish

(*Ictalurus punctatus*) in China: prevalence and Mechanisms of Fluoroquinolone Resistance. *Microb. Drug Resist.* 23, 473–479. doi: 10.1089/mdr.2015.0296

Yin, H. L., Shen, Y., Liu, Z., Wang, S., Shen, Z., Zhang, R., et al. (2017). Novel Plasmid-Mediated Colistin Resistance Gene mcr-3 in *Escherichia coli*. *Am. Soc. Microbiol.* 8, e00543–17. doi: 10.1128/mBio

Yucel, N., and Aslim, B. (2005). Prevalence and resistance to antibiotics for aeromonas species isolated from retail fish in Turkey. *J. Food Qual.* 28, 313–324. doi: 10.1111/j.1745-4557.2005.00037.x

Zankari, E., Hasman, H., Cosentino, S., Vestergaard, M., Rasmussen, S., Lund, O., et al. (2012). Identification of acquired antimicrobial resistance genes. *J. Antimicrob. Chemother.* 67, 2640–2644. doi: 10.1093/jac/dks261

Zhang, D., Gao, F., Jakovlic, I., Zou, H., Zhang, J., Li, W. X., et al. (2020). PhyloSuite: an integrated and scalable desktop platform for streamlined molecular sequence data management and evolutionary phylogenetics studies. *Mol. Ecol. Resour.* 20, 348–355. doi: 10.1111/1755-0998.13096

Conflict of Interest: The authors declare that the research was conducted in the absence of any commercial or financial relationships that could be construed as a potential conflict of interest.

Publisher's Note: All claims expressed in this article are solely those of the authors and do not necessarily represent those of their affiliated organizations, or those of the publisher, the editors and the reviewers. Any product that may be evaluated in this article, or claim that may be made by its manufacturer, is not guaranteed or endorsed by the publisher.

frontiers in Microbiology

ORIGINAL RESEARCH
published: 11 October 2021
doi: 10.3389/fmicb.2021.734239

Nutrient Scarcity in a New Defined Medium Reveals Metabolic Resistance to Antibiotics in the Fish Pathogen *Piscirickettsia salmonis*

Javiera Ortiz-Severín[1,2], Camila J. Stuardo[1], Natalia E. Jiménez[2,3], Ricardo Palma[2,3], María P. Cortés[2,3], Jonathan Maldonado[1,2], Alejandro Maass[2,3] and Verónica Cambiazo[1,2]**

[1] Laboratorio de Bioinformática y Expresión Génica, Instituto de Nutrición y Tecnología de los Alimentos, Universidad de Chile, Santiago, Chile, [2] Fondap Center for Genome Regulation (Fondap 15200002), Universidad de Chile, Santiago, Chile, [3] Centro de Modelamiento Matemático (AFB170001), Departamento de Ingeniería Matemática, Facultad de Ciencias Físicas y Matemáticas, Universidad de Chile and UMI-CNRS 2807, Santiago, Chile

OPEN ACCESS

Edited by:
Hetron Mweemba Munang'andu, Norwegian University of Life Sciences, Norway

Reviewed by:
Javier Santander, Memorial University of Newfoundland, Canada
Simon Menanteau-Ledouble, Aalborg University, Denmark

***Correspondence:**
Javiera Ortiz-Severín
javiera.ortiz@inta.uchile.cl
Verónica Cambiazo
vcambiaz@inta.uchile.cl

Specialty section:
This article was submitted to Antimicrobials, Resistance and Chemotherapy, a section of the journal Frontiers in Microbiology

Received: 30 June 2021
Accepted: 14 September 2021
Published: 11 October 2021

Citation:
Ortiz-Severín J, Stuardo CJ, Jiménez NE, Palma R, Cortés MP, Maldonado J, Maass A and Cambiazo V (2021) Nutrient Scarcity in a New Defined Medium Reveals Metabolic Resistance to Antibiotics in the Fish Pathogen Piscirickettsia salmonis. Front. Microbiol. 12:734239. doi: 10.3389/fmicb.2021.734239

Extensive use of antibiotics has been the primary treatment for the Salmonid Rickettsial Septicemia, a salmonid disease caused by the bacterium *Piscirickettsia salmonis*. Occurrence of antibiotic resistance has been explored in various *P. salmonis* isolates using different assays; however, *P. salmonis* is a nutritionally demanding intracellular facultative pathogen; thus, assessing its antibiotic susceptibility with standardized and validated protocols is essential. In this work, we studied the pathogen response to antibiotics using a genomic, a transcriptomic, and a phenotypic approach. A new defined medium (CMMAB) was developed based on a metabolic model of *P. salmonis*. CMMAB was formulated to increase bacterial growth in nutrient-limited conditions and to be suitable for performing antibiotic susceptibility tests. Antibiotic resistance was evaluated based on a comprehensive search of antibiotic resistance genes (ARGs) from *P. salmonis* genomes. Minimum inhibitory concentration assays were conducted to test the pathogen susceptibility to antibiotics from drug categories with predicted ARGs. In all tested *P. salmonis* strains, resistance to erythromycin, ampicillin, penicillin G, streptomycin, spectinomycin, polymyxin B, ceftazidime, and trimethoprim was medium-dependent, showing resistance to higher antibiotic concentrations in the CMMAB medium. The mechanism for antibiotic resistance to ampicillin in the defined medium was further explored and was proven to be associated to a decrease in the bacterial central metabolism, including the TCA cycle, the pentose-phosphate pathway, energy production, and nucleotide metabolism, and it was not associated with decreased growth rate of the bacterium or with the expression of any predicted ARG. Our results suggest that nutrient scarcity plays a role in the bacterial antibiotic resistance, protecting against the detrimental effects of antibiotics, and thus, we propose that *P. salmonis* exhibits a metabolic resistance to ampicillin when growing in a nutrient-limited medium.

Keywords: *P. salmonis*, fish pathogen, defined medium, nutrient scarcity, antibiotic resistance, metabolic resistance

INTRODUCTION

Over the past few decades, the farmed salmon industry has grown substantially, becoming the largest single fish commodity by value and accounting for approximately 60% of the salmon produced worldwide (Food and Agriculture Organization of the United Nations FAO, 2018). However, the growth of salmon production has encountered important sanitary and environmental concerns, as the aquaculture sector is vulnerable to exotic, endemic, and emerging epizootics (Food and Agriculture Organization of the United Nations FAO, 2018; Jia et al., 2020). Salmonid Rickettsial Septicemia (SRS) is a bacterial disease first reported in 1980 in southern Chile (Bravo and Campos, 1989; Cvitanich et al., 1991); since then, it has been described in different salmonid and non-salmonid fish in other countries such as Australia and New Zealand, United Kingdom, Norway, and Canada (Rozas and Enriquez, 2014). In Chile, epizootics events of SRS have occurred in all farmed salmonid species, accounting for 50–97% of infectious disease mortality during the seawater growing phase (Mardones et al., 2018) and causing up to US$ 700 million in losses in the Chilean salmon industry every year (Avendaño-Herrera, 2018; Mardones et al., 2018).

The etiological agent of the SRS disease is the Gram-negative γ-Proteobacteria *Piscirickettsia salmonis* (Cvitanich et al., 1991; Fryer et al., 1992), a non-motile, aerobic, facultative intracellular pathogen that replicates inside cytoplasmic vacuoles, survives for long periods of time in seawater, and can be directly transmitted from the surrounding water to the fish (Lannan and Fryer, 1994; Smith et al., 1999; Jones et al., 2020). So far, vaccines have not proven to be effective toward SRS, thus forcing to rely on antimicrobials as treatment. In Chile, intensive usage of antimicrobials has taken place at least since 2007, with florfenicol and oxytetracycline being the most used antibiotics, which have proven to be effective against *P. salmonis* infections and accounted for nearly 98% of the antibiotics administered by this industry (SERNAPESCA, 2020). The excessive use of antibiotics in the Chilean salmon industry has led to several studies exploring the effects on the selection of resistant bacteria in the marine environment and in the farmed salmonids. Both antibiotic-resistant marine microorganisms and antibiotic resistance genes (ARGs) have been identified in water and sediments near salmon farms (Miranda and Rojas, 2007; Tamminen et al., 2011; Shah et al., 2014) and in salmon gut microbiota (Higuera-Llantén et al., 2018). Also, a higher proportion of quinolone-resistant *Escherichia coli* has been detected in the urinary tract of patients from a region with intensive aquaculture, suggesting that antibiotic resistance might have been transmitted from the farm environments to human pathogens (Tomova et al., 2015). Nevertheless, to this date, only one strain of *P. salmonis* has been described as resistant to the antibiotics used in aquaculture, a strain that harbors a multidrug resistance plasmid conferring resistance to oxytetracycline, chloramphenicol, streptomycin, and sulfamethoxazole/trimethoprim (Saavedra et al., 2018).

Although some reports have explored the potential antibiotic resistance of as much as 292 *P. salmonis* isolates (Yánez et al., 2013; Henríquez et al., 2016; Mancilla, 2018), all isolates were susceptible to the antibiotics administered for SRS treatment, at the recommended concentrations used in medicated feed (San Martín et al., 2019). Point mutations in *gyrA* (Henríquez et al., 2014), single-nucleotide polymorphisms in putative oxytetracycline and florfenicol resistance genes (Figueroa et al., 2019), the expression of tetracycline and florfenicol putative resistance genes along with multidrug pumps (Cartes et al., 2017), and an efflux pump modulated by florfenicol (Sandoval et al., 2016) have been described in different *P. salmonis* strains. However, all reports informed discrete minimum inhibitory concentration (MIC) values associated with the putative resistant phenotype. In accordance with the recommendations of the European Committee on Antimicrobial Susceptibility Testing (EUCAST), the definition of a "susceptible" or "resistant" microorganism should be related to the likelihood of therapeutic success or failure using a standard dosing regimen of the agent (EUCAST, 2019). Besides that, additional aspects need to be considered, among them, the inherent variability of MIC measurements that can be attributed to the difficulty of growing a particular fastidious organism (such as *P. salmonis*) or to unexpected effects of the combination of the organism, the culture media, and the antimicrobial agent (EUCAST, 2019).

According to recommendations of the Clinical Laboratory Standard Institute (CLSI), antimicrobial susceptibility testing to determine *P. salmonis* MIC values are performed in Austral-SRS (Miller et al., 2014), a nutrient-rich and undefined medium. However, several reports have brought into question the *in vivo* relevance of *in vitro* susceptibility testing in enriched culture media. Considering that the *in vivo* environment of bacterial pathogens is frequently regarded as nutrient-limited, nutrient-rich culture conditions may have a poor predictive value of antibiotics effectivity (Ersoy et al., 2017; Farha et al., 2018; Sanders et al., 2018). In addition, the inhibitory effects of antibiotics could be misleading as growth media composition can significantly alter bacterial metabolism (Pethe et al., 2010; Hicks et al., 2018). Thus, these studies highlight the need for a defined minimal medium that provides a more consistent nutritional setting for determining the susceptibility of *P. salmonis* to antibiotics. Furthermore, several reports have illustrated that the metabolic state of bacteria significantly affects their susceptibility to the antibiotics (Stokes et al., 2019). As described for *E. coli* (Lopatkin et al., 2019), in a metabolic coupled scenario, the bacterial growth rate positively correlates with its metabolism (i.e., an increase in metabolism generates energy that in turn increases bacterial growth), and both growth and metabolism are nutrient-limited. However, when growth is nutrient-limited in the presence of an excess of energy, nutrient availability is correlated with growth but not with the metabolism and metabolic uncoupling takes place (Erickson et al., 2017; Lopatkin et al., 2019). In a metabolic uncoupled scenario, the bacterial metabolic state more accurately predicts the antibiotic lethality. Similarly, increasing the basal respiration rate of *E. coli* by genetically uncoupling ATP synthesis from electron transport improves bactericidal antibiotic efficacy (Lobritz et al., 2015). The modulation of antibiotic resistance by bacterial metabolism is also supported by reports on phenotypic resistance, a transient and reversible state of reduced

susceptibility to antibiotics that is linked to the metabolic state of bacteria (Martínez and Rojo, 2011).

Since knowing the minimal metabolic requirements for *P. salmonis* growth is an important first step to decipher the mechanisms of *P. salmonis* susceptibility to antibiotics, here, we present a new culture medium with defined composition (CMMAB) with adjusted divalent cations, in compliance with CLSI standards (Miller et al., 2014; CLSI National Committee for Clinical Laboratory Standards, 2015) that supports growth of four *P. salmonis* strains. Both the CMMAB and the Austral-SRS media were utilized to conduct susceptibility testing of *P. salmonis* against a series of antibiotics for which a resistant phenotype was expected based on *in silico* prediction of *P. salmonis*-encoded ARGs. For macrolides, beta-lactams and aminoglycosides, an increase in bacterial resistance was detected in the CMMAB compared to the Austral-SRS medium. Ampicillin inhibited bacterial growth in Austral-SRS media, along with a decrease in doubling time, and an increase in carrying capacity. Phenotypic and transcriptomic data revealed that the bacterial metabolic state plays an important role in the resistance of *P. salmonis* to ampicillin, as bacterial energy production metabolism, TCA, pentose phosphate pathways, and nucleotide metabolism were downregulated in the CMMAB media, both with and without the antibiotic. Thus, the CMMAB medium can be a useful tool for identifying essential metabolic functions of *P. salmonis*, improving approaches for antimicrobial testing and drug design against this fish pathogen.

RESULTS

In silico analysis of *P. salmonis* LF-89 nutrient requirements by Cortés et al. (2017) suggested that there is a trade-off between the need for carbon and nitrogen sources for bacterial growth, and accordingly, the highest growth rate was obtained when a mixture of glucose and amino acids were used. Consequently, we sought to obtain the best combination of nutrients to increase bacterial growth. Based on the composition of the defined medium (called here as CMM1), different concentrations of vitamins, iron, glucose, NaCl, and amino acid mixtures were tested and their effect on *P. salmonis* growth was quantified and compared (**Figure 1**). For this, the area under the curve (auc) and the carrying capacity (k) parameters were selected. The first parameter represents the overall growth of the bacterium in a selected condition, including its replication rate, the highest growth achieved, and the time it took to achieve it; the second parameter represents a measure of bacterial load, which relates to the nutrient availability and the bacterial capacity to use it.

The defined media described in Cortés et al. (2017) allowed for sub-optimal growth in *P. salmonis*, as growth curve parameters such as generational time, carrying capacity, and overall growth curve dynamics (**Figures 1**, **2**) were significantly different from those obtained in the nutrient-rich media Austral-SRS. Therefore, the medium Austral-SRS was used as a positive control for growth. As shown in **Figure 1A**, *P. salmonis* growth was directly correlated to the glucose concentration in the media, as well as to NaCl concentration up to 10 g/L. Vitamin availability was not determinant in bacterial growth, even though it is reported that *P. salmonis* does not have complete biosynthesis pathways for them (Cortés et al., 2017). In addition, iron availability was important in bacterial growth, as a decrease in almost 20% in the k parameter was observed in the absence of an iron source in the defined medium. The iron oxidation state was also relevant, addition of Fe^{3+} caused the highest increase in growth, and a combination of Fe^{2+} and Fe^{3+} did result in further increasing the bacterial growth.

The CMM1 media contains a mixture of the 20 amino acids (aa), and 7 of them were predicted to be essential for *P. salmonis* because the bacteria does not possess the complete biosynthesis pathways (Cortés et al., 2017). Consequently, auxotrophy for the remaining 13 aa was tested, including a condition with excess of the aa (i.e., a higher concentration than the one used in CMM1). The excess aa condition was also tested for the essential aa arg, ile, leu, and met because *P. salmonis* is able to use them as a carbon source (Cortés et al., 2017). Comparison of bacterial growth curves showed an increased k parameter value in media without ala, asn, glu, trp, and tyr. As a result, a new minimal medium was created based on the minimal nutrient requirements for *P. salmonis* to reach k and auc values comparable to those attained in the nutrient Austral-SRS medium. This minimal medium contains no vitamins, 10 g/L NaCl, 400 μM Fe^{3+}, and a mixture of 14 aa. Since the objective of this work was to obtain a culture medium suitable for performing antibiotic susceptibility tests, some components were included in the minimal medium to (1) decrease the pH variability and (2) adjust divalent cations, in order to follow the CLSI standards. This was accomplished by changing the salts supply and including a buffer. For that, several media composition were tested based on other media described for bacterial cultures (Chamberlain, 1965; Cold Spring Harbor Protocols, 2006; Cortés et al., 2017). The buffer and salts composition that allowed better growth and less pH change over time was the CMM-KPh (**Figure 1B**), and therefore was incorporated in the minimal medium to create a new defined medium optimized for *P. salmonis* growth and suitable for antimicrobial susceptibility testing, named CMMAB. In addition, vitamins were included in this medium as the bacterium cannot synthesize them and other processes besides growth could be affected by their absence. The complete composition of each media and its reference (when corresponds) is listed in **Supplementary Table 1**.

The growth curves, doubling time (dt), and the k parameter were compared for *P. salmonis* LF-89 strain in the three media (**Figures 2A,B**). The dt for *P. salmonis* growing in CMMAB did not differ of the value reached by growing in nutrient-rich media, but it was significantly lower than the dt measured in CMM1, although the k parameter slightly decreased by 17.9%. When considering growth curve dynamics, especially dt and the time to reach the maximum growth, growth curves in CMMAB were more similar to Austral-SRS than to CMM1. Since the nutrient requirement prediction and culture media optimization were developed for LF-89 strain, we aim to evaluate the growth in CMMAB of different *P. salmonis* strains: EM-90 strain, and two strains isolated from more recent SRS outbreaks, CGR02 and Ps12201A. As observed in **Figures 2C,D**, the four strains

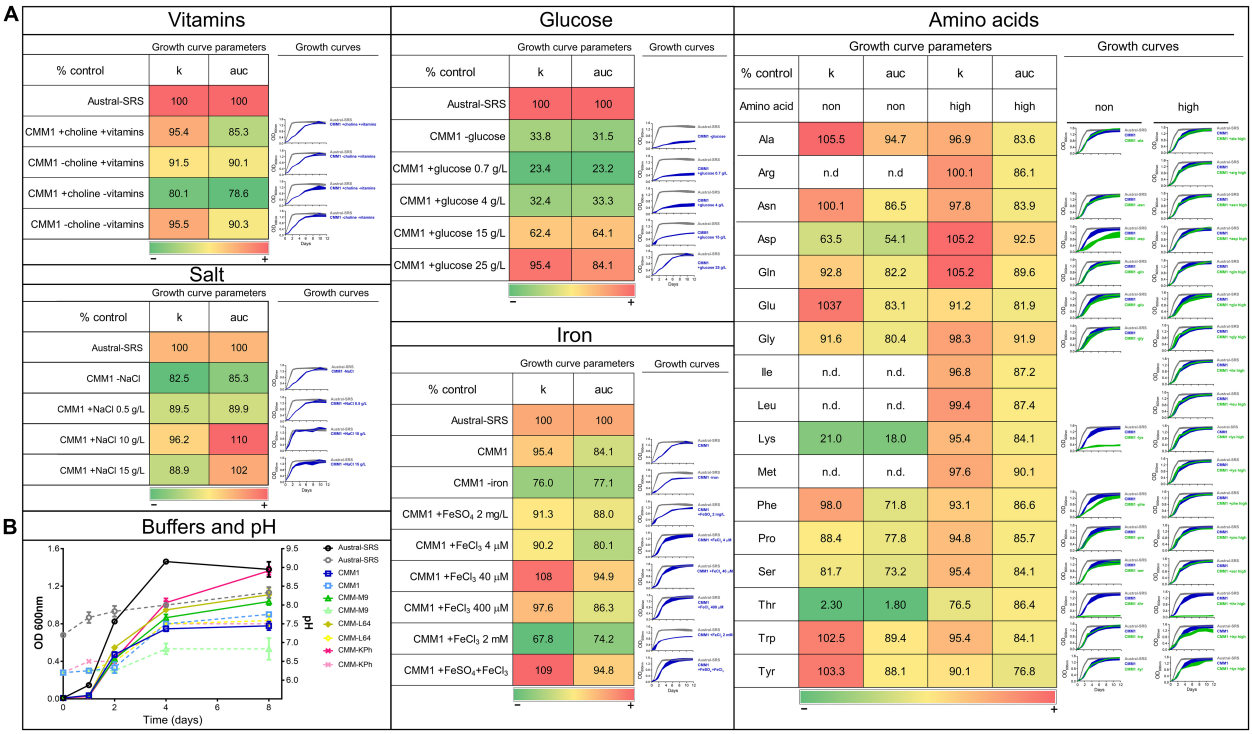

FIGURE 1 | Evaluation of nutrient composition and requirements for optimal growth of *P. salmonis* LF-89. Growth curves and growth curve parameters of *P. salmonis* LF-89 in the nutrient-rich medium Austral-SRS and the defined medium CMM1 with nutrient modifications. **(A)** The carrying capacity parameter (k) and the area under the curve of the fitted logistic equation for the OD_{600} measurements over time (auc), with its corresponding growth curve, for the bacterial growth in Austral-SRS medium as control, CMM1 defined medium or CMM1 with modifications in the vitamins, salt, glucose, iron, and amino acid constituents. In the growth curve graphs, the control media (Austral-SRS) is shown in gray, and CMM1 media and its modifications are in blue. Amino acid changes (in green) were set in two concentrations: 0 g/L (shown in the column "non") and at a higher concentration that the one used in CMM1 composition (column "high"). Essential amino acids required for bacterial growth were not tested (indicated with n.d.). Growth parameters are presented as percent of the control (Austral-SRS), higher values are shown in red, intermediate values are in yellow, and lower values are in green. **(B)** Growth curves of the bacterial growth (solid lines) and the culture media pH (dotted lines) using different buffers in the media. Specific composition of media is described in **Supplementary Table 1**.

showed optimal growth rate in CMMAB media. Moreover, bacterial infectivity was not affected by the medium, as observed by the similar decrease in CHSE-214 cell viability caused by the four bacterial strains grown in Austral-SRS or in CMMAB media (**Figure 2E**).

A Genomic Search for Antibiotic Resistance Genes in *Piscirickettsia salmonis*

As antimicrobial susceptibility testing has not been performed using CMMAB medium (or, to our knowledge, any other defined medium) we aim to test *P. salmonis* antibiotic resistance (AR) in a large-scale exploratory approach, without considering previous AR data. Thus, different computational approaches were used in the present study to detect potential ARGs in the genome of the four *P. salmonis* strains (**Table 1**) and afterward examine the resistance phenotype of the strains.

The SARGfam (Structured Antibiotic Resistance Genes v2.0 database with validated ARGs profile HMMs) search was set with strict parameters (e-value $< 10^{-5}$) as recommended. When using the RGI, the selection of "loose" hits allowed detecting new genes or distant ARG homologs. Thus, in this case, we used a cutoff value of 0.35 sequence identity with no query coverage requirements. The AMRFinder algorithm was able to detect only one to two ARGs per genome when the identity and sequence coverage cutoff were set within the recommended parameters. When no cutoff values were set, the number of detected ARGs was similar to that recovered with the other software. With these settings, each bioinformatic tool predicted approximately the same number of ARGs (between 47 and 69 ARGs for *P. salmonis* genome); however, few of them were detected by all three methods employed. As seen in **Supplementary Figure 1**, only three to seven common genes were predicted as ARGs by the three tools in the four *P. salmonis* strains. However, the SARGfam and AMRFinder tools, which use HMMs search method, predicted a higher number of common ARGs (20 to 22 genes, **Supplementary Figure 1**).

Putative *P. salmonis* ARGs were grouped by resistance mechanism (**Supplementary Table 2**) and by drug class (**Figure 3**), following CARD (Comprehensive Antibiotic Resistance Database) classification. Irrespectively of the strain and ARG prediction tool, most of the genes were categorized in antibiotic efflux and antibiotic target alteration resistance

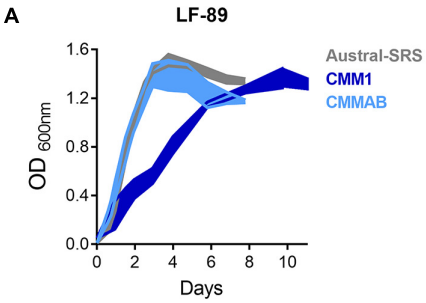

B

Culture media	dt	p-value	k	p-value
Austral-SRS	6.973 + 0.944	-	1.294 + 0.07	-
CMM1	17.59 + 1.34	<0.0001	1.250 + 0.101	0.0495
CMMAB	6.941 + 0.701	0.9473	1.062 + 0.0609	0.0001

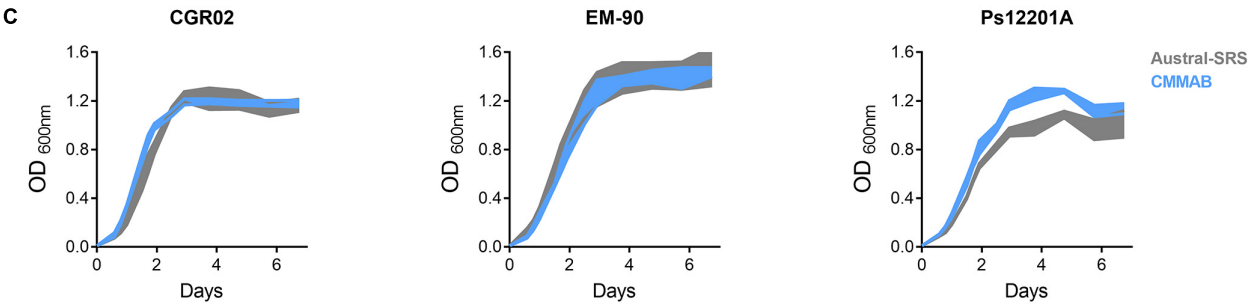

D

Strain	Culture media	dt	p-value	k	p-value
CGR02	Austral-SRS	7.432 + 0.268	-	1.122 + 0.0573	-
	CMMAB	6.766 + 0.938	0.1255	1.039 + 0.0545	0.0278
EM-90	Austral-SRS	7.537 + 0.484	-	1.325 + 0.0699	-
	CMMAB	7.234 + 0.825	0.4558	1.272 + 0.0646	0.1986
Ps12201A	Austral-SRS	10.38 + 0.33	-	0.9018 + 0.0813	-
	CMMAB	9.903 + 0.621	0.1267	1.153 + 0.0615	0.0001

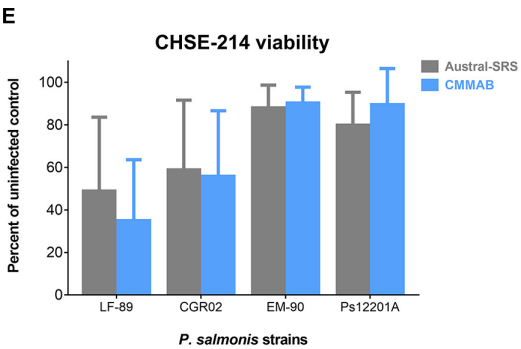

FIGURE 2 | Bacterial infection and growth comparison of different *P. salmonis* strains in nutrient-rich and in a defined culture media. **(A)** Growth curves of the reference strain LF-89 in Austral-SRS nutrient medium, CMM1 defined medium and the optimized defined medium CMMAB. **(B)** The carrying capacity parameter (k) and the maximum doubling time (dt) were obtained by assessing the unrestrained growth of *P. salmonis* LF-89 in the three media. A *t*-test was performed to compare the growth curve parameters between the bacteria grown in the CMM1 or in the CMMAB media with the control Austral-SRS medium. **(C)** Growth curves of *P. salmonis* strains CGR02, EM-90, and Ps12201A in the control nutrient media and the optimized defined media (Austral-SRS and CMMAB, respectively). **(D)** Growth curve parameters k and dt of CGR02, EM-90, and Ps12201A strains in Austral-SRS and CMMAB media. A *t*-test was performed to compare the growth curve parameters between the bacteria grown in CMMAB media and the control Austral-SRS medium. **(E)** Cell viability MTT assay after infection with *P. salmonis* strains grown in Austral-SRS (gray bars) or in CMMAB (light blue bars). A two-way ANOVA showed no significant differences between the effect on cell viability (presented as percent viability of uninfected controls) caused by bacteria grown in both media.

TABLE 1 | Summary of bioinformatics tools used for predicting ARGs in the genome of four *P. salmonis* strains.

AMR identifier	Reference database	Prediction method	Selection criteria	Number of ARGs			
				LF-89	CGR02	EM-90	Ps-12201A
SARGfam (Yin et al., 2018)	SARG database v2.0	HMM-based alignment	e-value $< 10^{-5}$	64	64	62	64
RGI (Alcock et al., 2020	Comprehensive Antibiotic Resistance Database CARD 2020	Nucleotide-based homology and SNP models	Loose hits; sequence identity > 0.35	51	47	47	49
AMRFinder (Feldgarden et al., 2019)	Bacterial Antimicrobial Resistance Reference Gene Database	Nucleotide-based homology and HMM-based alignment	All hits	66	67	69	67

Predicted ARGs are shown for each tool.

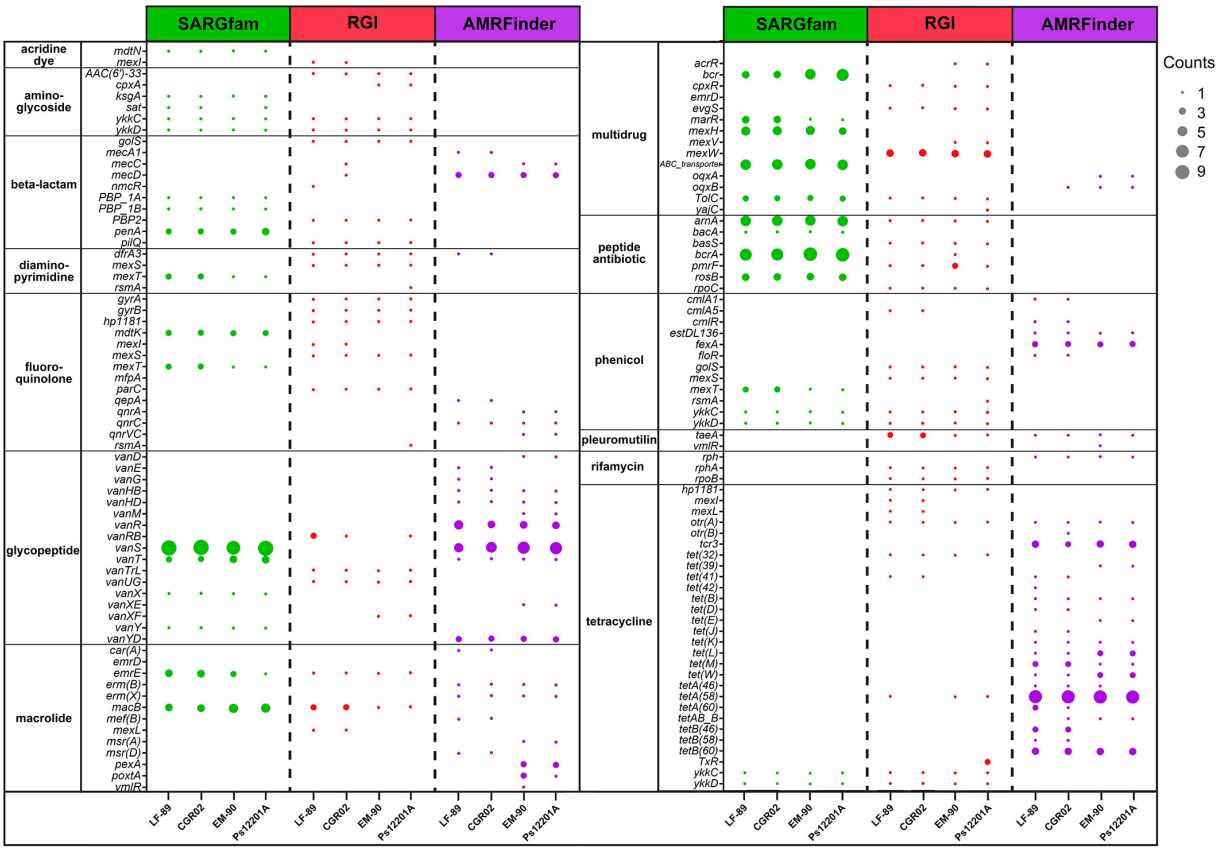

FIGURE 3 | Drug class of predicted ARGs. The number of identified genes for each drug class is shown for *P. salmonis* strains LF-89, CGR02, EM-90, and Ps12201A. The gene counts refer to the number of locus tag predicted with the same ARG name. Note that some ARGs were classified in more than one drug class.

mechanisms. Antibiotic target protection also grouped an important number of genes, but this category was tool-dependent, as more ARGs were identified with AMRFinder, followed by RGI, and no genes in this category were found using SARGfam. This search tool dependency also occurred with the antibiotic target replacement category. It is noteworthy that a small number of antibiotic inactivation genes were predicted, suggesting that enzymatic alteration of antibiotics might not be a significant resistance mechanism for *P. salmonis*.

Drug class categories of genes present in more than one strain and predicted with more than one tool are shown in **Figure 3**. As mentioned, depending on the bacterial strain, between two and seven genes were predicted as ARGs using the three tools (**Supplementary Figure 1**); however, when arranged in drug class categories as in **Figure 3**, no gene was observed to be predicted by the three tools. This difference was due to discrepancies in ARG name assignment. For example, the locus tag PSLF89_10 in *P. salmonis* LF-89 was identified as an ARG by SARGfam, RGI, and AMRFinder, but predicted as *penA*, *PBP2*, and *mecD*, respectively. Therefore, one locus tag could be identified as a different ARG by different tools, and several locus tags could have the same ARG name, as occurred with *bcrA*, *vanS*, *macB*, or *tetA(58)* (represented as a bigger dot in **Figure 3**). Overall, the same drug class ARGs were observed between the strains. The most representative drug class categories across *P. salmonis* strains were selected to conduct phenotypic assays, as we speculated that the higher number of ARGs predicted for a specific antibiotic could make a resistance phenotype more probably observed.

Antibiotic Susceptibility Phenotypes of *Piscirickettsia salmonis*

To validate the resistance phenotypes that were computationally predicted in the genome of the *P. salmonis* strains, a panel of antibiotics of the most represented drug classes were tested for antimicrobial susceptibility performing MIC tests, according to CLSI standards. For MIC testing, we used the optimized defined media broth CMMAB and the Austral-SRS medium which is the recommended medium by CLSI guidelines (Miller et al., 2014). Results are shown in **Table 2**. MIC data are displayed as range values to depict more accurately what was observed in the assay plates due to the variability of MIC values. For some antibiotics, such as tetracyclines, erythromycin, florfenicol, and ampicillin, MIC values were not always constant and could vary between one-fold and four-fold dilutions in a medium-independent fashion. The initial assumption was that CMMAB medium, by containing adjusted cations, will provide more stable

TABLE 2 | MIC values (μg/ml) observed for *P. salmonis* strains in nutrient broth (Austral-SRS) and the defined medium (CMMAB).

		LF-89				CGR02				EM-90				Ps12201A			
		MIC range		Phenotype		MIC range		Phenotype		MIC range		Phenotype		MIC range		Phenotype	
Drug family	**Antibiotic name**	**Austral-SRS**	**CMM-AB**	**Austral-SRS**	**CMM-AB**	**Austral-SRS**	**CMM-AB**	**Austral-SRS**	**CMM-AB**	**Austral-SRS**	**CMM-AB**	**Austral-SRS**	**CMM-AB**	**Austral-SRS**	**CMM-AB**	**Austral-SRS**	**CMM-AB**
Tetracyclines	Tetracycline	0.16–0.32	0.02–0.08	S	S	ND	ND	ND	ND	ND	ND	ND	ND	ND	ND	ND	ND
	Oxytetracycline[§]	0.16–0.32	0.02–0.08	S	S	0.08–0.32	0.02–0.08	S	S	0.08–0.16	0.02–0.16	S	S	0.08–0.16	0.02–0.08	S	S
Fluoroquinolone, quinolone antibiotic	Flumequine[§]	0.32–0.64	0.08–0.16	S	S	0.08–0.64	0.02–0.16	S	S	0.04–0.08	0.02–0.04	S	S	0.04–0.16	0.02	S	S
	Oxolinic acid	0.32	0.04–0.08	S	S	0.32–0.64	0.08–0.16	S	S	0.04–0.16	0.02–0.16	S	S	0.04–0.08	0.02	S	S
Macrolide antibiotic	Erythromycin	1.6–6.4	12.5–25	S	R	1.6–12.5	3.12–12.5	S	I	0.4–1.6	3.12–12.5	S	I	0.8–1.6	12.5–25	S	R
Phenicol antibiotic	Chloramphenicol	0.16–0.64	0.16–0.32	S	S	ND	ND	ND	ND	ND	ND	ND	ND	ND	ND	ND	ND
	Florfenicol[§]	0.08–0.32	0.32–0.64	S	S	0.04–0.64	0.08–1.28	S	S	0.08–0.32	0.312–1.25	S	S	0.08–0.32	0.32–1.28	S	S
Peptide antibiotic	Polymyxin B	6.25–12.5	12.5–25	I	R	12.5	6.25–12.5	R	I	12.5	25–125	R	R	12.5–25	12.5–50	R	R
Glycopeptide antibiotic	Vancomycin*	>1,000	>1,000	R	R	>1,000	>1,000	R	R	>1,000	>1,000	R	R	>1,000	>1,000	R	R
Beta-lactam, cephalosporin	Ampicillin	0.1–0.8**	200–400	S	R	0.1–0.4**	125–250	S	R	0.08–0.4**	31.2	S	R	0.08–0.4**	31.2–250	S	R
	Penicillin G	0.4–0.8**	25–200	S	R	ND	ND	ND	ND	ND	ND	ND	ND	ND	ND	ND	ND
	Ceftazidime	>1,000**	>1,000**	R	R	>1,000**	>1,000**	R	R	>1,000**	>1,000**	R	R	>1,000**	>1,000**	R	R
Aminoglycoside antibiotic	Streptomycin	6.25–12.5	50–100	I	R	3.12–6.25	100–400	S	R	6.25–12.5	400	I	R	6.25	100–400	S	R
	Spectinomycin	6.25–25	12.5–50	I	R	ND	ND	ND	ND	ND	ND	ND	ND	ND	ND	ND	ND
Diaminopyrimidine antibiotic	Trimethoprim	125	250	R	R	62.5–125	500	R	R	62.5–125	500	R	R	125	250–500	R	R
Rifamycin antibiotic	Rifampicin	1.6	0.8–1.56	S	S	1.6	0.8–1.6	S	S	0.8–1.6	0.8–1.6	S	S	0.8–1.6	0.8–1.6	S	S

Bacteria were considered resistant (R) to an antibiotic if MIC > 10 μg/ml; if not, they were labeled as susceptible (S). If MIC range was around the breakpoint of the resistant phenotype, then an intermediate range (I) of susceptibility was defined.

[§] *Antibiotics used in aquaculture.*

**Antibiotic for Gram-positive bacteria.*

***Suboptimal growth compared to the control.*

MIC values as they will not depend on membrane permeability (Nikaido, 2003; Hawke et al., 2005), but the results suggested that the variability was an intrinsic property of the bacteria. All tested *P. salmonis* strains were found to be resistant to polymyxin B, vancomycin, ceftazidime, and trimethoprim. Interestingly, the susceptibility to the antibiotics erythromycin, ampicillin, penicillin G, streptomycin, and spectinomycin was medium-dependent, showing higher MIC values in the CMMAB media. Of note, the four *P. salmonis* strains were found to be susceptible to the antibiotics of therapeutic significance, with MIC values for oxytetracycline ranging from 0.08 to 0.32 μg/ml in Austral-SRS and 0.02 to 0.32 μg/ml in CMMAB, and MIC values for florfenicol between 0.04 and 0.64 μg/ml in Austral-SRS and 0.08–1.28 μg/ml in CMMAB.

Vancomycin, an antibiotic for Gram-positive bacteria, was included in the MIC tests even though *P. salmonis* is Gram-negative, due to the high number of ARGs targeting vancomycin that were predicted with different tools. A total of 25 vancomycin resistance genes, corresponding to 18.2% of all ARGs, were identified in *P. salmonis* LF-89. As shown in **Table 2**, the level of resistance to vancomycin in *P. salmonis* was so high that it could be attributable to its Gram-negative nature, rather than the presence of these putative vancomycin-resistant genes. This supports the importance of manually curing the bioinformatics results and contrasting the bioinformatic predictions obtained by current available tools with phenotypic data.

According to **Table 2**, *P. salmonis* showed decreased susceptibility to ampicillin (amp) in the CMMAB medium compared to other tested antibiotics (resistant to >200 μg/ml of amp in MIC) and presented a higher difference in MIC values between both growth media (500- to 2000-fold). Thus, we sought to investigate the possible mechanism underlying the medium-dependent amp resistance in *P. salmonis*. As MIC tests are end-point experiments, we aimed to further evaluate the bacterial behavior by recording *P. salmonis* strain LF-89 growth curves (**Figure 4A**). Amp addition to the culture media impaired *P. salmonis* growth only in the nutrient media (Austral-SRS amp), as expected, whereas normal growth in CMMAB amp could be recorded.

Given that β-lactamase activity has been previously suggested for other *P. salmonis* strains (Mikalsen et al., 2007), and one ARG with antibiotic inactivation resistance mechanism was predicted in the LF-89 strain, we evaluated this possibility by performing clover-leaf tests. Agar Austral-SRS and CMMAB media allowed *P. salmonis* LF-89 growth, but no evidence of β-lactamase production was detected (**Figure 4B**).

To further investigate the resistance mechanism to amp, expression levels of selected ARGs were evaluated in *P. salmonis* strain LF-89 during exponential growth phase in both culture media, with or without the mentioned antibiotic (**Figure 5**). Since *P. salmonis* was not able to grow in the Austral-SRS medium with amp, the antibiotic was used only in the CMMAB medium and cultures with no antibiotic in both media were used as controls. The only gene predicted to inactivate amp, *nmcR*, was not overexpressed in the presence of amp, which correlated with the negative clover-leaf test. In addition, all antibiotic target alteration and antibiotic target replacement genes were not significantly overexpressed in the CMMAB amp or in the CMMAB media. Three antibiotic efflux genes were upregulated in the presence of the antibiotic, but only in the comparison between CMMAB amp and CMMAB media, whereas the expression levels were similar between bacteria grown in CMMAB amp and in Austral-SRS. The observed fold change in ARGs expression levels does not explain the radically different MIC values observed between both culture media. Thus, we speculated that media composition could be relevant for the resistant phenotype observed in *P. salmonis*, and the bacterial resistance to amp was not the result of overexpression of the predicted ARGs. To test that possibility, nutrient composition was changed in the culture media and growth parameters were compared. As shown in **Figure 6A**, neither glucose nor aa supplementation could recover *P. salmonis* growth in Austral-SRS medium, suggesting that addition of these nutrients is not sufficient to increase bacterial resistance. In contrast, the growth parameters of *P. salmonis* in CMMAB medium without glucose or with an excess of aa did not differ after exposing to ampicillin, indicating that *P. salmonis* remained resistant to amp in this defined medium (**Figure 6B**). This result also suggests that nutrient scarcity may play a role in the bacterial antibiotic resistance.

Evaluation of *Piscirickettsia salmonis* Transcriptome Changes by RNA-Sequencing

A transcriptomic analysis was performed to elucidate the molecular mechanisms of *P. salmonis* resistance to amp. *P. salmonis* transcriptomes were named as follows: sample S (*P. salmonis* grown in Austral-SRS), sample C (*P. salmonis* grown in CMMAB), and sample A (*P. salmonis* grown in CMMAB with amp), and three sets of biological replicates per sample were sequenced. We used an unsupervised classification method, principal component analysis (PCA), to characterize the differences between the gene expression profiles of the nine samples. **Figure 7A** shows that three of the biological replicates of sample A and two replicates of sample C grouped together and separated from the replicates of sample S, especially along the PC1 axis, which explains 54.36% of the variation. This result indicates that CMMAB and Austral-SRS media induced a gene expression response that differed over a wide range of genes, while the amp treatment did not produce additional changes in the gene expression levels. To assess these differences, we compared the transcriptome of *P. salmonis* growing in CMMAB (with or without amp) and in the Austral-SRS medium. A total of 1,545 genes were differentially expressed in the CMMAB medium with amp compared to the Austral-SRS medium (A/S), and 676 genes were differentially expressed in CMMAB without ampicillin compared to Austral-SRS (C/S), as shown in **Figures 7B,C**. In the CMMAB medium, most differentially expressed genes were upregulated in comparison to the Austral-SRS (60.8% of DEGs in C/S), whereas 51.2% of DEGs were upregulated in the A/S comparison (**Figure 7B**). However, only two genes were differentially expressed between *P. salmonis* growing in the CMMAB media with and without

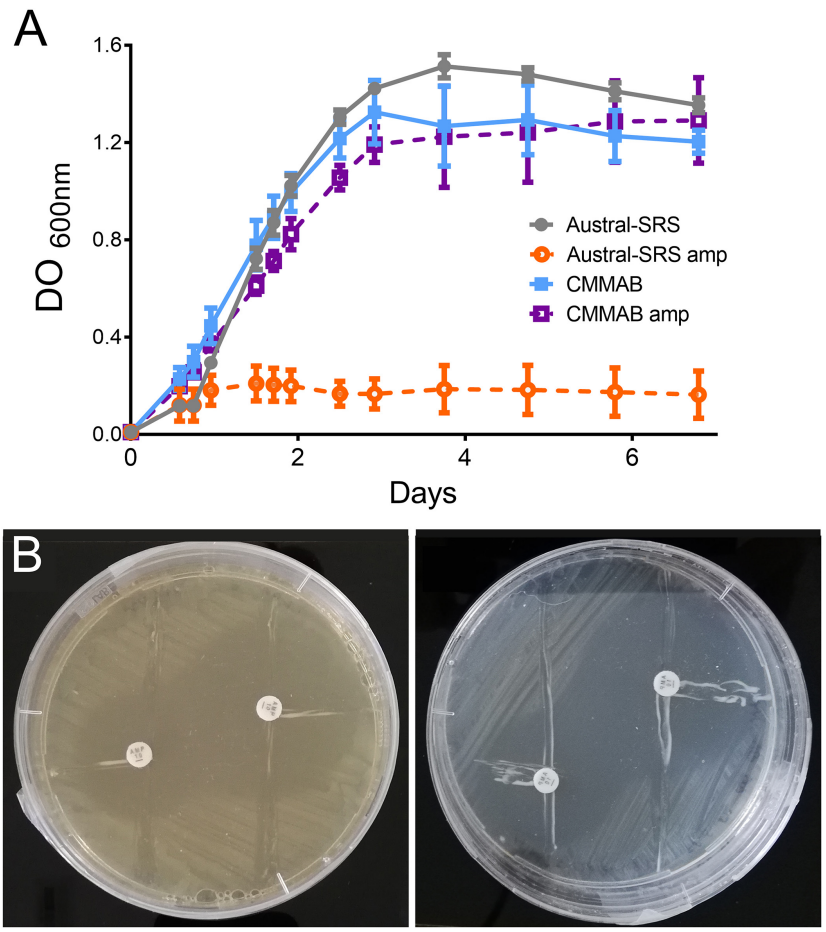

FIGURE 4 | *P. salmonis* LF-89 response to ampicillin. **(A)** *P. salmonis* growth curves in nutrient (Austral-SRS) and optimized defined (CMMAB) culture media with and without ampicillin (amp). **(B)** *P. salmonis* clover-leaf test for ampicillin. *E. coli* DH5α was used as the indicator strain. *E. coli* and *P. salmonis* were grown in Austral-SRS (left) and CMMAB (right) agar plates with disks containing 100 mg and 500 mg of amp (small and large inhibition zone, respectively).

ampicillin (A/C), and both genes (a hypothetical protein with CBS domain and a universal stress family protein) were downregulated in response to amp (**Supplementary Table 3**). Thus, the *P. salmonis* gene profile revealed that the presence of amp in the CMMAB medium had a marginal impact on gene expression; however, major expression changes took place when the bacteria were grown in CMMAB as compared to the nutrient-rich medium Austral-SRS (**Figure 7B**). As an independent measure of differential gene expression, we examined the relative expression of 14 genes derived from qPCR assays presented in **Figure 5** and compared them with the RNA-seq transcript levels (**Supplementary Figure 2**). Overall, a positive correlation between 0.58 and 0.87 (Pearson correlation) was determined between qPCR and RNA-seq for the combined data set ($p < 0.01$).

The differentially expressed genes were classified into biological and functional gene categories according to the Cluster of Orthologous Groups (COG) and Gene Ontology (GO) databases. COG categories assigned to A/S and C/S up- and downregulated genes are shown in **Figure 8A**. In general, most upregulated genes in A/S and C/S were classified in the categories mobilome, prophages, transposons, signal transduction mechanisms, and cell motility (X, T, and N, respectively). Downregulated genes, on the other hand, belonged to translation, and ribosomal structure and biogenesis categories for the A/S comparison, and to amino acid transport and metabolism, energy production and conversion, and cell wall/membrane/envelope biogenesis (E, C, and M, respectively) for both comparisons. Interestingly, most of the upregulated genes in A/S and C/S comparisons were unique to *P. salmonis* as they encoded hypothetical proteins with unknown orthologs (N.O.F. in the bar graphs, **Figure 8B**), suggesting that *P. salmonis* growth in the CMMAB medium triggers unknown adaptation mechanisms that are unique for this bacterium.

Enrichment analysis revealed significantly overrepresented biological processes in the dataset of differentially expressed genes (**Figure 8B** and **Supplementary Table 4**). Overrepresented GO terms in both comparisons were related to flagellum assembly and organization, chemotaxis, and response to external stimulus. In the A/S comparison, protein secretion, transport of peptides, amides, anions, nitrogen compounds, and organic substances

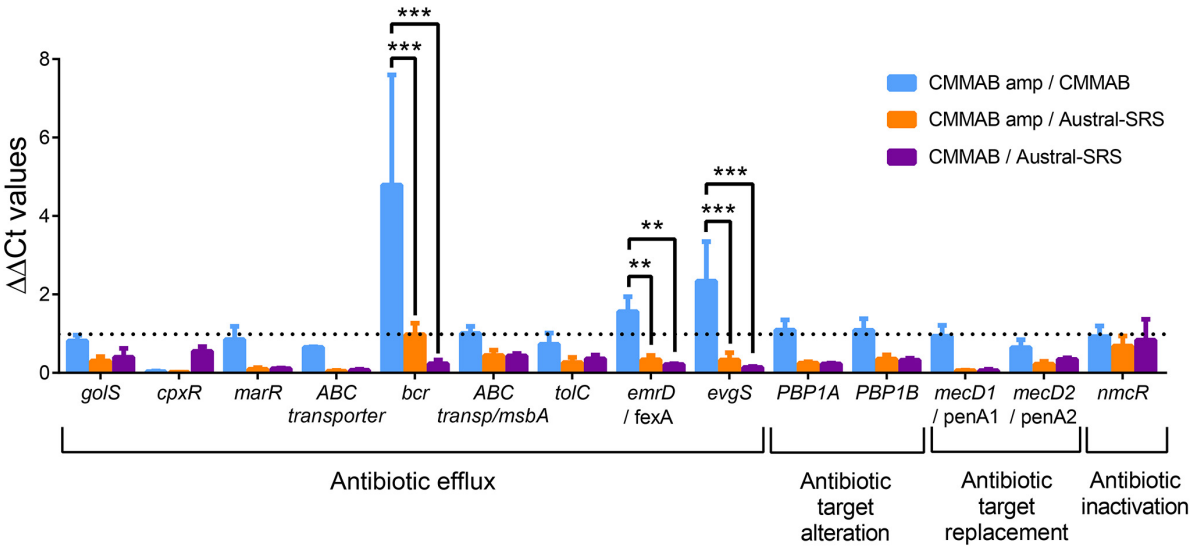

FIGURE 5 | Expression of putative amp resistance genes in *P. salmonis* grown in the different media. Relative transcript abundance of selected ARGs predicted to confer amp resistance in *P. salmonis* LF-89. Bar-graph showing transcript levels quantified by qPCR and expressed as ΔΔCt values normalized by the housekeeping genes *glyA* and *pykA*. The dotted line indicates the normalized control values (ΔΔCt = 1). A two-way ANOVA with Tukey's test for multiple comparisons was performed. Significantly different values are marked (***$p < 0.001$ and **$p < 0.01$).

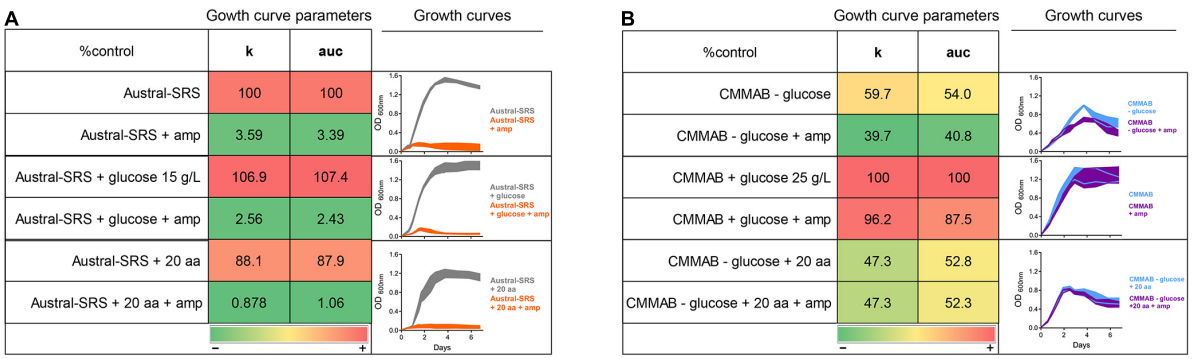

FIGURE 6 | Effect of glucose and amino acid supplements in amp resistance. *P. salmonis* LF-89 growth curves and curve parameters (carrying capacity k and area under the curve auc) in Austral-SRS nutrient medium **(A)** and the optimized defined medium CMMAB **(B)** with or without glucose and amino acid supplements and their effect in bacterial resistance to amp. Note that "20 aa" refers to the mixture of amino acids used in the CMM1 composition, and in the case of CMMAB, they were added in addition to the amino acids present in the medium.

were also overrepresented. It is worth noticing that genes belonging to these categories were also upregulated in the C/S comparison, although these GO terms did not achieve statistical significance after enrichment analysis. Some of the upregulated genes annotated to the term chemotaxis were related to flagellar- and/or cilium-dependent cell motility, whereas others were nutrient-sensing or nutrient transport mechanisms, such as the *phoQ* sensor histidine kinase (PSLF89_3272), sodium:proton exchanger family proteins (PSLF89_2485 and PSLF89_2203), and ABC-type amino acid transport signal transduction systems (PSLF89_1726 and PSLF89_1196). Although genes encoding the sensor proteins were upregulated, several sodium exchanger-type transporters and permeases were downregulated, such as a calcium:proton antiporter (PSLF89_2152), an acetylneuraminate ABC transporter (PSLF89_803), the proline:sodium symporter *putP* (PSLF89_1458), sodium:dicarboxylate symporter (DAACS) family protein (PSLF89_2288 and PSLF89_725), an aromatic amino acid transport family protein (PSLF89_3306), and various amino acid permeases (PSLF89_3168, PSLF89_2573, PSLF89_180 and PSLF89_817). This correlates with an underrepresentation of GO terms related to transmembrane transport (C/S comparison), and amino acid metabolic processes (C/S and A/S comparisons), which was indicative of a general metabolic downshift represented by a downregulation of the GO term generation of precursor metabolism and energy (C/S). In addition, numerous biosynthetic and metabolic processes were significantly downregulated in CMMAB and CMMAB amp media compared to Austral-SRS, especially those related

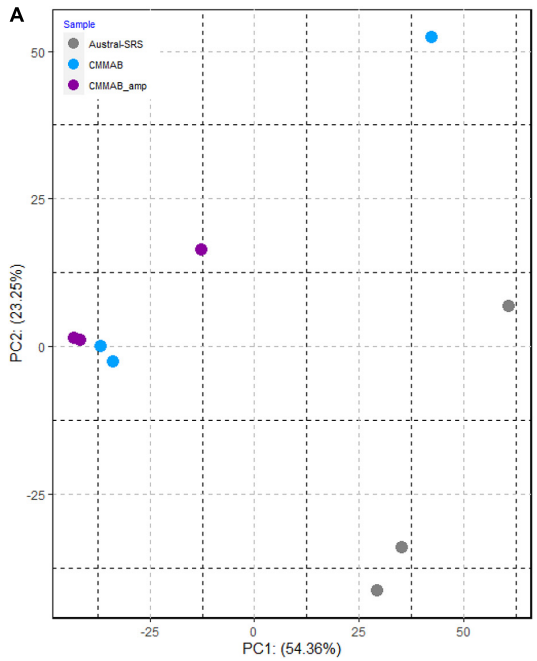

C

	A/S (CMMAB amp vs. Austral-SRS)	A/C (CMMAB amp vs. CMMAB)	C/S (CMMAB vs Austral-SRS)
Total number of genes	3265	3265	3265
Genes with expression levels ≠ 0	3188	3191	3189
DEGs (log_2FoldChange > |0.6|)	1934	865	2249
Genes with p < 0.05	1008	100	1710
Genes with adjp < 0.05	676	2	1560
DEGs with padj < 0.05	676	2	1545
Up-regulateds genes padj < 0.05	411	0	791
Down-regulateds genes padj < 0.05	265	2	769

FIGURE 7 | RNA sequence data for *P. salmonis* LF-89. **(A)** Principal component analysis (PCA) plot of gene expression profiles of bacteria grown in Austral-SRS, CMMAB, or CMMAB with amp. **(B)** Gene transcripts identified in the following comparisons: bacteria grown in CMMAB with amp vs. Austral-SRS (A/S, squares); bacteria grown in CMMAB with amp vs. CMMAB (A/C, inverted triangles); and bacteria grown in CMMAB vs. Austral-SRS (C/S, circles). Data between and below the dotted lines (marked in gray) were not statistically significant (adjusted *p*-value > 0.05, log_2 fold change < | 0.6|). **(C)** Table showing a summary of the number of genes identified after RNA sequencing and data processing.

to nucleotide, ribonucleotide, nucleoside, and ribonucleoside metabolic and biosynthetic processes (**Figure 8B**). Interestingly, A/S comparison differed from the C/S comparison in a downregulation of GO terms related to DNA metabolic process, gene expression, translation, and nucleobase metabolism and biosynthesis.

Based on these analysis, transcriptomic data were mapped to specific *P. salmonis* metabolic pathways using a genome-scale model previously reconstructed for this organism (Cortés et al., 2017). Particularly, metabolism of nucleotides, amino acids, glycolysis, and the TCA cycle were selected for analysis based on the categories associated to the differentially expressed genes (**Figure 8**). Metabolic pathway analysis revealed an overall downregulation of genes belonging to those processes, in the bacteria growing in the CMMAB medium with or without amp when compared to Austral-SRS medium (**Figures 9**, **10** and **Supplementary Table 4**), with fold changes being consistently smaller when the bacteria was exposed to the antibiotic. A selection of differentially expressed genes with significant fold-change values as shown in **Figures 9**, **10** were subjected to validation by comparing the normalized gene expressed levels (TMM+CPM) between the three samples (**Supplementary Figure 3**). Genes from relevant pathways in **Figures 9**, **10**, such as amino acid metabolism, nucleotide metabolism, TCA cycle, pentose phosphate pathways and glycolysis, were significantly downregulated in A and C samples (bacteria grown in CMMAB + amp and CMMAB, respectively) when compared to S samples (bacteria grown in Austral-SRS), with the exception of genes coding for PSP_L (amino acid metabolism), CS (TCA cycle), and PRFGS (nucleotide metabolism) enzymes, which were consistently found overexpressed in A and C when compared to S (red arrows).

Piscirickettsia salmonis exhibited lower expression of genes associated with glycolysis, even in reactions such as phosphofructokinase (PFK, PSLF89_1090) and fructose-bisphosphate aldolase (FBA, PSLF89_1028), which are associated with fructose 6 phosphate and fructose-1,6-bisphosphate, both of which are entry points of the pentose phosphate pathway (PPP). PPP provides precursors for the synthesis of nucleotides, which were also downregulated in *P. salmonis* growing on CMMAB with or without ampicillin (A/S and C/S). Downregulation of genes encoding components of the pyruvate node, a key point of regulation between glycolysis and the TCA cycle was also observed. Genes encoding pyruvate kinase (PYK, PSLF89_1027), pyruvate dehydrogenase (PDH, PSLF89_3190, PSLF89_3189, PSLF89_3188, PSLF89_2098, PSLF89_3189, and PSLF89_3190), and malic enzymes (ME1, PSLF89_3304, ME2, and PSLF89_234) showed lower expression levels in the CMMAB medium with or without amp compared to Austral-SRS medium. For the TCA cycle, a decrease in gene expression was observed for all the reactions in the CMMAB medium, with the exception of citrate synthase (CS, PSLF89_893). Genes encoding enzymes of the synthesis of glutamine, an amino acid that can also fuel the TCA cycle, were also downregulated [glutaminase

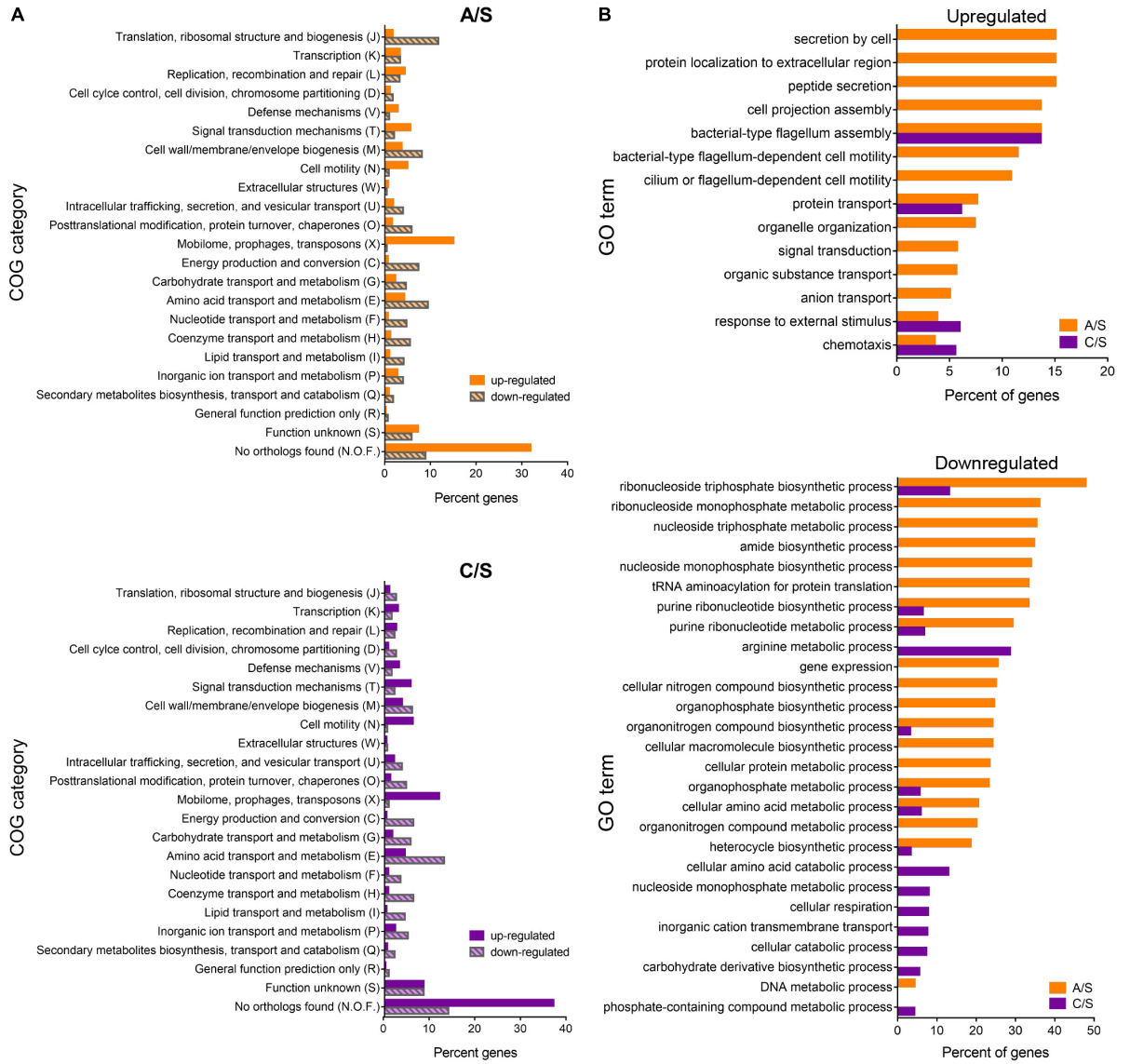

FIGURE 8 | Differentially expressed genes classified into biological and functional gene categories. **(A)** Functional categories of *P. salmonis* genes. Percent of differentially expressed genes in each COG (Cluster of Orthologous Groups) identified by total RNA sequencing for the exponentially growing bacteria in the comparisons CMMAB with ampicillin vs. Austral-SRS (A/S, orange), and CMMAB without ampicillin vs. Austral-SRS (C/S, purple). **(B)** Enrichment analysis of differentially expressed genes. Percent of genes categorized in significantly enriched GO terms are shown for up- and downregulated genes (top and bottom panels, respectively).

(GLUN, PSLF89_1767, and PSLF89_307), glutamine synthase (GLNS, PSLF89_179), and glutamate dehydrogenase (GLUDxi, PSLF89_2806)]; in this case, greater downregulation was observed in CMMAB medium supplemented with amp.

DISCUSSION

Piscirickettsia salmonis Nutrient Requirements

Two previous works have described *P. salmonis* nutritional requirements based on genomic reconstructions of the bacterial metabolism (Cortés et al., 2017; Fuentealba et al., 2017). Recently, Fuentealba et al. (2020) used these metabolic predictions to improve a defined medium intended to be used in vaccine development. In this wok, we created a new defined culture media that contains 14 essential amino acids for *P. salmonis* growth. As previous works stated, we observed the importance of glucose and amino acids as carbon sources in the media, although comparison of growth curve parameters revealed the importance of NaCl. The defined media described in Cortés et al. (2017) did not allow for *P. salmonis* growth without glucose as a carbon source; in contrast, Fuentealba et al. (2017) reported that a defined media with a mixture of 12 aa and no glucose or other

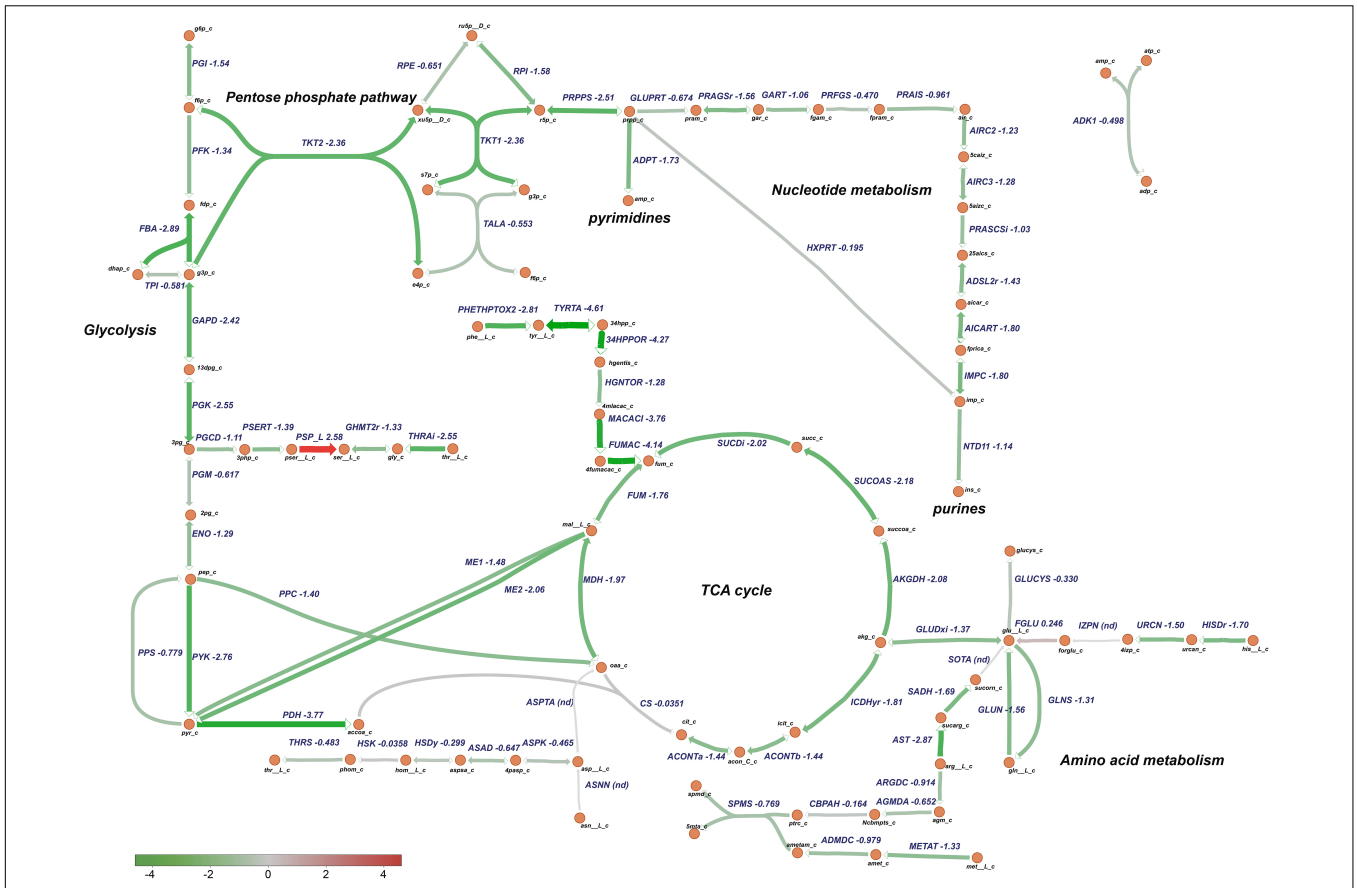

FIGURE 9 | Downregulation of central metabolic pathways in *P. salmonis* growing in CMMAB with amp. Genes differentially expressed between *P. salmonis* grown in the CMMAB amp medium and the Austral-SRS medium were mapped to glycolysis, the TCA cycle, pentose phosphate pathway, nucleotide, and amino acid metabolism using the genome-scale model iPS584 for this pathogen. Expression levels are shown as $\log_2$ fold-change values; downregulated genes are in green and upregulated genes are in red.

carbon sources allowed bacterial growth. Both defined media were composed of amino acids (20 aa in Cortés's defined media, and 12 aa in Fuentealba's media), vitamins, salts, and an iron source, but the main difference between them was the presence of NaCl and the absence of glucose in Fuentealba's media. Based on our results, the CMM1 media (similar to Cortés's defined media composition) without glucose allowed a 33.8% of the growth obtained in Austral-SRS, but by adding NaCl to the medium, the growth of *P. salmonis* increased to reach levels similar to those measured in the nutrient-rich medium (**Figure 1A**). Fuentealba's work described that 16% of *P. salmonis* transporters were specific for aa and peptides (Fuentealba et al., 2017), thus accounting for a greater capacity to assimilate amino acids from the surrounding environment. This observation, together with the presence of sodium/amino acid symporters in *P. salmonis* genome and our results on the effect of NaCl on *P. salmonis* growth, suggests that the capability of incorporating aa to the cell is related to the presence of NaCl in the medium.

The auxotrophy tests carried out in this work yielded similar results to those obtained by Fuentealba et al. (2020). Thus, arginine, isoleucine, leucine, lysine, methionine, proline, phenylalanine, threonine, and valine were needed for *P. salmonis* growth. Since *P. salmonis* is auxotrophic for the amino acids arginine, cysteine, histidine, isoleucine, leucine, methionine, and valine, and they are therefore strict nutritional requirements, the rest of the amino acids seem to be necessary to improve bacterial growth in the CMMAB medium. Improvement of growth allowed narrowing down the cultivation time, while still attaining growth levels similar to those observed in a nutrient-rich medium. Coincidences exists between the amino acid auxotrophies of *P. salmonis*, *L. pneumophila* (Tesh and Miller, 1981), and *C. burnetii* (Sandoz et al., 2016), two other intracellular bacteria often regarded as closely related to *P. salmonis*. Both *L. pneumophila* and *C. burnetii* exploit the amino acid pools of the host while replicating intracellularly and greatly rely on amino acids as a main source of carbon and energy (Price et al., 2014; Sandoz et al., 2016). Besides a previous work reporting the expression of a number of genes associated with the amino acid metabolism in *P. salmonis* and *S. salar* during infection (Valenzuela-Miranda and Gallardo-Escárate, 2018), the study of the metabolic connection between *P. salmonis* and its host remains poorly explored. Therefore, through the analysis

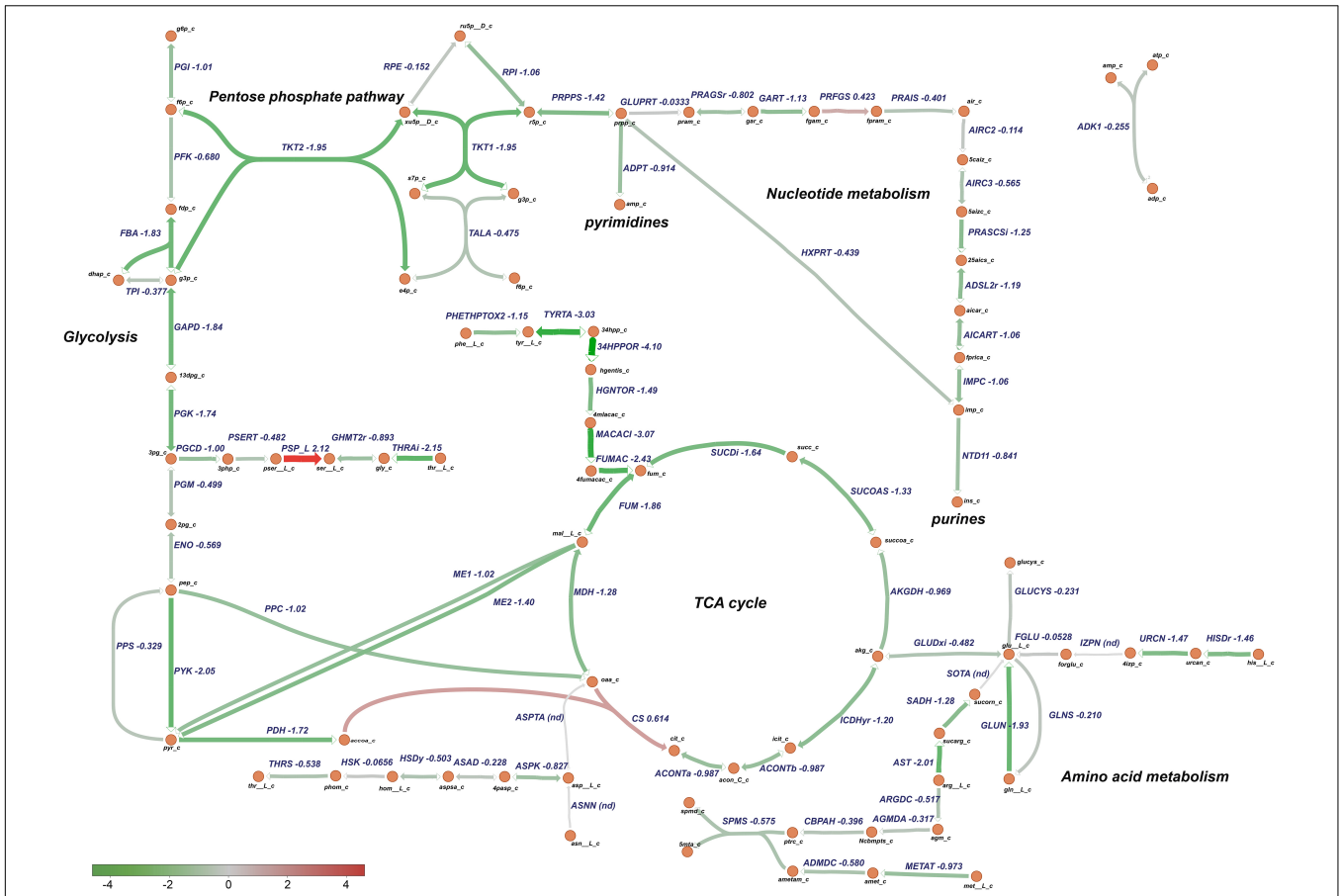

FIGURE 10 | Downregulation of central metabolic pathways in *P. salmonis* in CMMAB medium. Genes differentially expressed between *P. salmonis* grown in the CMMAB medium without amp and the Austral-SRS medium were mapped to the TCA cycle, pentose phosphate pathway, nucleotide, and amino acid metabolism using the genome-scale model iPS584. Expression levels are shown as $\log_2$ fold-change values; downregulated genes are in green and upregulated genes are in red.

of the nutritional requirements that promote the intracellular lifestyle of *P. salmonis*, it is expected that the CMMAB medium presented here could contribute to understand how *P. salmonis* exploits the host metabolism to replicate and survive in the intracellular milieu.

On the other hand, our results showed that *P. salmonis* growth was partially inhibited by supplementation with alanine, asparagine, glutamine, tryptophan, and tyrosine, an observation that was also in agreement with the work of Fuentealba et al. (2020). Inhibition of bacterial growth by amino acids seems to be caused by feedback inhibition of an early enzyme in the pathway of the amino acid synthesis; this inhibition in turn represses the production of other amino acids that use the common enzyme for their syntheses. The inhibitory effect of amino acids on bacterial growth has been known for many years, and growth inhibitions have been reported for *Streptococcus bovis* (Washburn and Niven, 1948), *E. coli* (Rowley, 1953), and *Chlamydia trachomatis* (Al-Younes et al., 2006), among other bacteria.

In our media composition, we included glucose as a carbon source additional to amino acids. In this condition, we observed that aspartic acid, glycine, and serine supplementation improved bacterial growth parameters, whereas glutamic acid decreased bacterial growth as opposed to what was described for the vaccine formulation in the absence of glucose (Fuentealba et al., 2020). In this context, our defined medium CMMAB improved bacterial growth to levels observed in the nutrient-rich medium (Austral-SRS), buffered the pH increasing over time, and sustained bacterial infectivity in the CHSE-214 cell line model; accordingly, cytopathic effects were indistinguishable from the ones observed when the bacterium was grown in Austral-SRS medium.

Piscirickettsia salmonis Antibiotic Resistance Prediction and Phenotypes

Previous studies have reported *P. salmonis* resistance to penicillin by disk diffusion assays (Mikalsen et al., 2007), and to penicillin and spectinomycin by MIC assays in cell cultures (Cvitanich et al., 1991). On the other hand, moderate degrees of susceptibility to florfenicol, oxytetracycline, flumequine, and oxalinic acid have been reported in MIC assays using the Austral-SRS media (Yánez et al., 2013; Henríquez et al., 2016; Contreras-Lynch et al., 2017). A controversy was generated regarding the MIC assessment and its relation to the epidemiological cutoff values (ECOFF) for florfenicol and oxytetracycline, both

antibiotics profusely used in Chilean aquaculture (Mancilla, 2018), as two works reported similar MIC values but different interpretation of bacterial population distribution based on MIC results. While Contreras-Lynch et al. (2017) concluded that the *P. salmonis* population did not considerably decrease its susceptibility to florfenicol and oxytetracycline, Henríquez et al. (2016) reported a bacterial population of concern with decreased susceptibility to this antibiotics, although both works reported similar MIC values for the tested *P. salmonis* strains (Henríquez et al., 2016; Contreras-Lynch et al., 2017). Here, we obtained the MIC values for only four strains (in contrast to the 58 and 292 isolates reported previously) (Henríquez et al., 2016; Contreras-Lynch et al., 2017), and based on our cutoff value (10 μg/ml), they were classified as susceptible to the antibiotics used in aquaculture (**Table 2**). Moreover, considering the previously reported MIC values, all *P. salmonis* isolates tested in the Henríquez et al. (2016) and the Contreras-Lynch et al. (2017) reports fall within the susceptible categories defined in this work. On the other hand, when growing in the CMMAB medium, *P. salmonis* prove to be resistant to 9 of the 16 antibiotics tested, and in contrast, the bacterium was resistant to only three antibiotics in the Austral-SRS medium, thus revealing the importance of the culture media composition for antibiotic resistance testing in *P. salmonis*. To our knowledge, differential resistance phenotypes depending on the growth media have not been previously reported in *P. salmonis*.

Gene variations and gene mutations conferring antibiotic resistance have been the primary way to explain bacterial resistance to antibiotics (Espedido and Gosbel, 2012). Here, more than 130 individual genes were predicted as ARGs in the four strains, and 14 of them could be related to ampicillin resistance. Considering that ARG databases have been constructed based on genomes and gene information from human-related pathogens (Feldgarden et al., 2019), discrepancies between predicted ARGs and resistance phenotypes were expected as the search parameters used in this work privileged encountering distant ARG homologs in a fish pathogen. Therefore, this ARG prediction with loose parameters needed an important experimental counterpart to test antibiotic resistance potential. Predicted ARGs belonging to the categories of antibiotic target alteration and antibiotic target replacement resistance mechanism were expressed in all tested media, but with similar expression levels. This was a possible result since these types of ARGs may not be inducible by amp and thus exert their function just by expressing, and not by overexpressing (Munita and Arias, 2016). In contrast, antibiotic inactivation and antibiotic efflux genes were expected to be overexpressed in the CMMAB amp medium; however, gene expression changes were detected only between the bacteria grown in CMMAB medium and not between CMMAB amp and Austral-SRS. Thus, changes in ARG expression levels did not explain the 500- to 2000-fold increase in MIC observed between Austral-SRS and CMMAB media. In addition, the lack of a positive result in the clover-leaf test for ampicillin supports the predicted ARGs gene expression results, and therefore, no phenotypic evidence of antibiotic inactivation was observed in our experimental conditions.

In our conditions, addition of glucose or aa in the nutrient-rich media did not decrease *P. salmonis* susceptibility to amp, suggesting that the presence of these nutrients was not the sole requirement that allowed bacterial growth. On the contrary, nutrient scarcity in the defined CMMAB media seemed to provide the adequate conditions for bacterial growth in the presence of the antibiotic. Media composition for antibiotic susceptibility testing should be considered when studying pathogenic bacteria, as media mimicking host environments (Ersoy et al., 2017) have proven to be more reliable to predict antibiotic efficacy in the host.

Metabolic Resistance as a Mechanism for *Piscirickettsia salmonis* Ampicillin Resistance

Since culture media composition can have a significant impact on bacteria metabolic state and global physiological changes can occur as a consequence of antibiotic exposure (Yang et al., 2017, 2019; Shin et al., 2021), we reasoned that a more global bacterial response, rather than the induction of a few genes, needed to be analyzed in order to elucidate the amp resistance mechanism in *P. salmonis*. Transcriptomic analysis showed that *P. salmonis* growing in the CMMAB medium (and CMM amp medium) senses specific external stimulus, such as particular nutrients, that triggers signal transduction mechanisms. Some of them were chemotaxis-related genes and flagellar- and/or cilium-dependent cell motility. As stated in previous works, *P. salmonis* does not possess a functional flagellum that confers motility in any examined condition (Cvitanich et al., 1991; Mauel and Miller, 2002), although flagellar proteins and genes are expressed during intracellular infection (Ortiz-Severín et al., 2020; Zúñiga et al., 2020), which suggests an alternative role to flagellar structures during infection and intracellular growth (Machuca and Martinez, 2016), and now, during growth in nutrient scarcity conditions in a defined media.

Although CMMAB media contains sufficient nutrients to allow bacterial growth in similar levels to those obtained with the nutrient-rich media (**Figures 2A,B**), results indicate that *P. salmonis* suffers a metabolic downshift when grown in the CMMAB medium that coincides with nutrient deprivation. As Austral-SRS media contains an excess of nutrients with complex carbon sources, including a soybean casein digest and fetal bovine serum, the sole presence of amino acids, glucose, and salts in CMMAB medium constitutes a decrease in nutrient availability for the bacterium. As described for *E. coli* when growth is nutrient-limited in the presence of an excess of energy, nutrient availability is correlated with growth but not with the metabolism (Erickson et al., 2017; Lopatkin et al., 2019), and the excess of available energy goes to cellular activities other than growth. In this condition, *E. coli* survival to treatments with bactericidal antibiotics depends on cellular metabolism irrespective of the growth rate, as accelerated respiratory activity potentiates antibiotic lethality (Lopatkin et al., 2019). Although a link between cell death caused by bactericidal antibiotics and accelerated respiration was previously stablished (Lobritz et al., 2015), the role of growth rate was unclear. Here, we

observed similar growth parameters in Austral-SRS and CMMAB media, but considerably different MIC were observed for several bactericidal antibiotics. Thus, we hypothesize that in *P. salmonis* growing in CMMAB, the increased MIC for amp responds to a change in the metabolic state of the bacterium, although further experiments need to be conducted to support this idea.

Lethality by bactericidal antibiotics, such as amp, has been associated with a build-up of toxic metabolic by-products as a consequence of an overly active central carbon metabolism and increased abundance of central carbon metabolites (Belenky et al., 2015; Stokes et al., 2019). These perturbations led to an oxygen consumption, breakdown of nucleotides, and induction of redox stress (Belenky et al., 2015). In addition, TCA cycle metabolites, aa, and nucleotides activate bacterial metabolism, and in turn, a decreased TCA, aa, and nucleotide metabolism, such as observed in *P. salmonis* grown in CMMAB and CMMAB amp, is correlated with a decreased proton-motive force that can drive antibiotic incorporation by the cell, and overall respiration that increases cell death in the presence of antibiotics (Lobritz et al., 2015; Stokes et al., 2019; Liu et al., 2020).

Recently, Lopatkin et al. (2021) replicated metabolic mutations found in antibiotic resistance *E. coli* strains, obtaining antibiotic-tolerant strains as a result. Two of these metabolic mutations were associated to the TCA cycle [2 oxoglutarate dehydrogenase (AKGD) and isocitrate dehydrogenase (ICDHyr)], and one of them was associated with amino acid metabolism (glutamate synthase). In this work, an overall downregulation of central carbon metabolism is observed in CMMAB media. Particularly, both AKGD (PSLF89_3188, PSLF89_898, and PSLF89_899)- and ICDHyr (PSLF89_2677)-associated transcripts were downregulated compared to the control condition in which antibiotic resistance is not observed. We propose that downregulation of these genes provides a metabolic context, given by nutrient scarcity, that protects *P. salmonis* against the detrimental effects of amp, thus suggesting a metabolic regulation of antibiotic resistance in *P. salmonis*.

MATERIALS AND METHODS

Bacterial Strains

The reference strain LF-89 (ATCC VR-1361) was obtained from the American Type Culture Collection (ATCC), and strain EM-90 was kindly donated by Dr. Sergio Marshall. Strains CGR02 (genogroup LF89-like) and Ps12201A (genogroup EM-90 like) were isolated by Etecma (Puerto Montt, Chile) in 2013 and 2017, respectively. Strains LF-89, EM-90, and CGR02 were previously sequenced by our group, while the Ps12201A strain was sequenced in this work. The genome sequences are available at the NCBI Genome database under the accession numbers SAMN02469424, SAMN10437718, SAMN04309076, and SAMN16064558.

Genome Sequencing and Assembly of Strain Ps12201A

Ps12201A strain was grown to exponential phase in Austral-SRS, and the total DNA was purified with the DNeasy Blood and Tissue Kit for DNA (Qiagen). The bacterial genome was sequenced using Oxford Nanopore version R9.4. DNA library was prepared from 4 μg input of DNA using the 1D Genomic DNA Ligation Sequencing Kit (SQK-LSK108) (Oxford Nanopore Technologies, Oxford, United Kingdom) in accordance with the manufacturer's instructions. Nanopore sequencing was conducted in our lab using FLO-MIN106 (R9.4) flow cells with the software minKNOW version 1.10.11 and the script NC_48Hr_sequencing_FLO-MIN106_SQK-LSK108_plus_Basecaller for 24 h. For Illumina sequencing of Ps12201A strain, DNA library was constructed following the protocol of TruSeq DNA sample preparation (Illumina, Inc.; San Diego, CA, United States). Sequencing was performed by MrDNA Next Generation Sequencing Service Provider (Shallowater, TX, United States) on Illumina HiSeq platform in an overlapping 2 × 250 bp.

For the assembly of Ps12201A strain, Nanopore sequences were trimmed of adaptors using the software Porechop version 0.2.2. Then, they were cleaned of low-quality sequences using Nanofilt version 1.2.0 with a Phred value cutoff of $Q > 13$ and a minimum read length of 500 bp. In the case of Illumina sequences, cleaning of low-quality reads and trimming of adaptors were performed by using Trimmomatic version 0.36 with the following parameters: ILLUMINACLIP:TruSeq3-PE.fa:2:30:10, LEADING:3, TRAILING:3, SLIDINGWINDOW:4:15, and MINLEN:100. To obtain a high-quality genome assembly, the "ONT assembly and Illumina polishing pipeline" was used[1]. This pipeline uses Nanopore reads to build the assembly with Canu software (Koren et al., 2017), and then, these contigs are corrected using Illumina reads with Racon software[2] and Pilon software (Walker et al., 2014). The default parameters were used with an estimated genome size of 3.2 Mb.

Bacterial Growth and Culture Media

The strains were stored at −80°C in cryovials stocks, plated in Austral-SRS agar plates (Mikalsen et al., 2007; Vera et al., 2012), and incubated at 18°C until visible growth. The bacteria were routinely maintained by subculturing in liquid Austral-SRS medium with agitation (180 rpm) at 18°C. The *P. salmonis* culture experiments were carried out in culture broths with different nutrient composition and availabilities: (1) the nutrient-rich medium Austral-SRS; (2) the basal medium described in Cortés et al. (2017), named here CMM1; and (3) CMMAB, a new defined culture medium based on the CMM1 composition that was developed in this work to evaluate antibiotic susceptibility in agreement with the Clinical and Laboratory Standards Institute (CLSI) (Miller et al., 2014; CLSI National Committee for Clinical Laboratory Standards, 2015). All broth compositions and nutrient concentrations are detailed in **Supplementary Table 1**.

Growth Curve Analysis

For growth curve assays, exponentially growing bacteria (OD_{600} = 0.3–0.7) were used as inoculum in Austral-SRS, CMM1,

[1]https://github.com/nanoporetech/ont-assembly-polish

[2]https://github.com/isovic/racon

or CMMAB broths, and 48-well plates were inoculated to a final OD_{600} = 0.01 in 700 μl and incubated at 18°C with agitation. Every growth curve experiment was performed with two or three technical replicates and three biological replicates. Bacterial growth was evaluated periodically by measuring the optical density (OD_{600}) for 7 days in an Infinite® 200 PRO NanoQuant (Tecan®). pH measurements were conducted with an aliquot of the cultures (with or without bacteria), using pH test paper bromocresol purple pH 5.62–7.2 and pH test paper cresol red pH 7.2–8.8 (Thomas Scientific).

The effect of ampicillin in growth curves was evaluated for the LF-89 strain in 48-well plates as before but adding ampicillin to Austral-SRS and CMMAB media to a final concentration of 50 μg/ml.

Growth curve parameters were calculated based on the raw growth data using the R package Growthcurver (Sprouffske and Wagner, 2016). Growth parameters were obtained for each biological replicate, and the data were subsequently processed in Excel to compare replicates separately. GraphPad Prism version 8.0.1 for Windows (GraphPad Software, La Jolla, CA, United States) was used for graphical representation and statistical analysis of the results.

CHSE-214 Infections and MTT Cell Viability Assay

The epithelial-like embryo cell line CHSE-214 (ECACC 91041114), derived from Chinook salmon *Oncorhynchus tshawitscha*, was obtained from the European Collection of Authenticated Cell Cultures and grown in minimum essential medium (MEM) supplemented with 5% FBS (Gibco). Infection with *P. salmonis* was carried out as described previously (Ortiz-Severín et al., 2019) with some modifications. CHSE-214 cells were seeded in T25 flasks and incubated at 20°C until reaching 80% confluency. Grown flasks were used to seed 24-well plates with 75,000 cells per well. Bacteria were grown in liquid broth (Austral-SRS or CMMAB) for 4 days and inoculated at a multiplicity of infection (MOI) of 100. After 3 days of co-incubation, gentamicin was added to a final concentration of 50 μg/ml to kill extracellular bacteria. The antibiotic was incubated for 1 h, washed three times with PBS, and replaced with fresh culture media. Infection was carried out for 14 days at 18°C. MTT cell viability assay was performed as previously described (Mosmann, 1983; Tada et al., 1986). Briefly, cultures were treated with 50 μg/ml gentamicin and PenStrep 1× solution (Gibco) for 1 h and washed with PBS before adding 300 μl of fresh MEM. Next, 30 μl of MTT solution (5 mg/ml in PBS) was added to infected and uninfected cells and plates were incubated for 5 h at 20°C protected from light. After the incubation period, supernatant from each well was carefully removed and placed in a new plate before adding 300 μl of solubilization solution (10% SDS in HCL 0.01 M) directly to the remaining cells. Cells were vigorously suspended, and the plate was incubated at room temperature for 15 min. The 300 μl of MTT supernatant solution was added to each well and mixed thoroughly before reading the absorbance at 570 and 690 nm in an Infinite® 200 PRO NanoQuant (Tecan®) spectrophotometer. Cell viability was calculated as a percent of the control uninfected cell's viability using the following formula: $[(abs_{570nm}\text{sample} - abs_{690nm}\text{sample})/abs_{570nm}\text{control} - abs_{690nm}\text{control}]*100$.

Prediction of Antibiotic Resistance Genes

The online interface of the Resistance Gene Identifier (RGI) version 5.2.0[3] was used. The ARGs selection criteria were set to "Perfect," "Strict," and "Loose" algorithms to search for hits in the curated reference sequences in the Comprehensive Antibiotic Resistance Database (CARD) (Alcock et al., 2020) version 3.1.2. In addition, *P. salmonis* genomes were subjected to ARGs searches employing the SARG collection of hidden Markov models (HMMs) with the online version of SARGfam available in https://smile.hku.hk/SARGs which uses HMMER3 in hmmscan mode (Yin et al., 2018). Hits with an e-value cutoff of 1×10^{-5} were annotated as ARG. Finally, we searched for ARGs using AMRFinder software (Feldgarden et al., 2019) as standalone version[4] and the parameters were set to $i = 0$ and $c = 0$.

Afterward, all results were manually curated, filtered by sequence identity over 35% and coverage over 50%, and categorized by hand using the CARD categories available[5] without incorporating duplicated results. The bar graphs and bubble chart were created using GraphPad Prism version 8.0.1 for Windows; this program was used for graphical representation and statistical analysis of the results. Figures were composed using Adobe Illustrator CS6.

Antibiotic Susceptibility Testing

Minimal inhibitory concentration (MIC) values were determined for four *P. salmonis* strains using two-fold dilutions of the antibiotics tetracycline (10 μg/ml), oxytetracycline (10 μg/ml), flumequine (40 μg/ml), oxolinic acid (10 μg/ml), erythromycin (100 μg/ml), chloramphenicol (20 μg/ml), florfenicol (20 μg/ml), polymyxin B (100 μg/ml), vancomycin (10 mg/ml), ampicillin (800–1000 μg/ml), penicillin G (800 μg/ml), ceftazidime (10 mg/ml), streptomycin (400 μg/ml), spectinomycin (100 μg/ml), trimethoprim (20 mg/ml), and rifampicin (100 μg/ml). Antibiotic stocks were prepared and stored according to the CLSI recommendations (Miller et al., 2014). The antibiotic susceptibility testing was performed according to the CLSI guidelines (Miller et al., 2014), using the Austral-SRS nutrient broth and the defined medium CMMAB in 96-well round-bottom plates. Freshly prepared two-fold dilutions were used in each microplate inoculated with exponentially growing cultures at a final OD_{600} = 0.01. The plates were sealed and incubated statically at 18°C for 7 days (strains LF-89, CRG02) or 10 days (strains EM-90 y Ps12201A). The MIC value was defined as the lowest concentration of the antibiotic that inhibited at least 80% of normal growth, considering the normal growth as a bacterial precipitate with a diameter of >2 mm. Each plate

[3]https://card.mcmaster.ca/analyze/rgi

[4]https://github.com/ncbi/amr/wiki/AMRFinder-database

[5]https://card.mcmaster.ca/

contained three replicates per condition, and every experiment was repeated at least five times.

Clover-Leaf Test

β-Lactamase production was evaluated in *P. salmonis* as described before (Mikalsen et al., 2007). Briefly, *E. coli* DH5α was used as the indicator strain and *P. salmonis* LF-89 as the test strain. Overnight cultures of bacteria grown in Austral-SRS broth were used as inoculum for the Austral-SRS and CMMAB agar plates. *P. salmonis* was streaked over the *E. coli* lawn, and two disks containing 100 or 500 mg of ampicillin were placed over the *P. salmonis* lines. After 10 days of incubation at 18°C, plates were photographed, and the inhibition zones were evaluated.

Bacterial RNA Purification and Transcripts Quantification

Total RNA was purified from *P. salmonis* cultures grown in Austral-SRS, CMMAB, or CMMAB supplemented with 50 μg/ml ampicillin and grown to mid-log phase (OD_{600} ∼ 0.6). *P. salmonis* cells were collected by centrifugation at 8,000 × *g* for 5 min, washed with sterile PBS, and suspended in TRIzol (Thermo Fisher Scientific). Cells were disaggregated and homogenized with a 27G syringe, and RNA was purified following the manufacturer's instructions. RNA was suspended in Ambion® RNAsecure™ (Invitrogen), treated with RQ1 RNase-Free DNase I (Promega) according to standard protocols, and visualized in an RNA denaturing agarose gel. The purified RNA was quantified using a Qubit™ RNA HS Assay kit (Thermo Fischer Scientific), and 2 μg of RNA was used to synthesize cDNA with the M-MLV Reverse Transcriptase using random primers (Promega). Transcripts were quantified using a Takyon qPCR Kit (Eurogentec) with specific primers designed for the predicted *P. salmonis* LF-89 ARGs (**Supplementary Table 5**). Real-time quantitative PCR (qPCR) was performed in an AriaMx 1.0 system (Agilent). The geometric median of the housekeeping genes *glyA* and *pykA* was calculated for each sample and used to calculate the relative expression levels of the *P. salmonis* genes using the method described by Pfaffl (2001).

RNA Sequencing and Analysis

Three independent cultures of *P. salmonis* LF-89 grown in Austral-SRS broth for 2 days were used to inoculate 5-ml cultures of Austral-SRS, CMMAB, and CMMAB supplemented with 50 μg/ml ampicillin, each in triplicate. When cultures reached OD_{600} ∼ 0.6, 2 ml of each culture was collected and centrifuged at 8,000 × *g* for 5 min. As before, bacteria were disaggregated and homogenized with a 27G syringe, and RNA was purified following the manufacturer's instructions using RNeasy kit (Qiagen), suspended in RNA secure (Ambion), treated with RNase-Free DNase I as described before, and frozen at −80°C until use. Water-diluted samples were quantified with Qubit and RNA integrity was analyzed by TapeStation (Agilent). Approximately 20 μg of RNA of each sample was sent to Novogene (United States) for library preparation and Illumina sequencing. Nine libraries (three for each condition) were prepared and sequenced by Novogen Bioinformatics Technology Co., Ltd. (Beijing, China). The libraries were generated using TruSeq Stranded Total RNA Library Prep (Illumina), and RiboZero Magnetic Kit (Illumina) to remove rRNAs. The sizes of inserts selected for amplification were 250–300 bp. The libraries were sequenced in an Illumina Novaseq platform using 150-bp size paired-end reads. A total of 30.5G raw RNA-seq reads per library were obtained. RNA-seq has been submitted to NCBI, accession number PRJNA744511.

Read quality of the three replicates for every medium (nine samples in total) was assessed with the FASTQC software v0.11.5 (Andrews, 2010), and a proper primer quality trimming was performed using BBDUK from the BBTOOLS suit (Bushnell, 2014). Forward and reverse reads were mapped to the latest *P. salmonis* LF-89 assembly (NCBI accession GCF_000300295.4) using BWA v0.7.17 (Li and Durbin, 2009) and the resulting files were converted to a sorted-bam format with the use of Samtools v1.7 (Li et al., 2009). Over 3,000 genes of LF-89 strain were counted using the HTSeq-count script v 0.6.1 from the HTSeq framework (Anders et al., 2015) along with the previous sorted-bam output.

Samples were compared by PCA using their global gene expression patterns with the Prcomp function of the Stats package v3.6.3 in R v3.6.3 (R Core Team, 2015). For visualizations, gene expression levels were normalized using the between-sample normalization method Trimmed Mean of M-values method (TMM), in addition to the inter-sample normalization method Counts per million mapped reads (CPM). Finally, expression levels were transformed with the pseudo-$\log_2$ method.

Gene-counted files for every sample were then analyzed with an in-house R script, using the DESeq2 library for differential expression analysis (Love et al., 2014). Considering sample S (*P. salmonis* grown in Austral-SRS), sample C (*P. salmonis* grown in CMMAB), and sample A (*P. salmonis* grown in CMMAB with ampicillin), the differential expression was tested between A/S and C/S with S as reference, and A/C with C as reference. Only genes detected (>0 counts) in at least two of three biological replicates were analyzed. The complete list with gene counts and annotation is shown in **Supplementary Table 3**.

Annotated genes were classified according to the predicted functions in the Clusters of Orthologous Groups (COGs) database (Tatusov, 2000). GO enrichment analysis was performed using the ClueGO tool (Bindea et al., 2009) in pairwise comparisons (A/S and C/S comparisons against the reference genome). A p-value < 0.05 and kappa coefficient of 0.4 were considered as threshold values, and only unduplicated GO terms from biological processes with p-value < 0.01 were incorporated in the graphs. The complete list of enriched GO terms is found in **Supplementary Table 4**.

Metabolic Pathway Analysis

A preliminary analysis of metabolic pathways linked to differentially expressed genes was carried out by mapping transcriptomic data to the genome-scale model of *P. salmonis* LF-89 (Cortés et al., 2017). Subsystem data were complemented with manually curated pathway information on Metacyc (Karp et al., 2018) to obtain a list of metabolic pathways of interest. These pathways were subsequently represented on a simplified form

using Escher (King et al., 2015) assigning a fold-change value for each reaction according to their associated genes. For reactions associated with multiple transcripts, computation of fold-change values was performed based on their GPR (gene protein reaction) logical rule. If an OR connector was used, then the associated value corresponds to the maximum value of the fold changes. On the other hand, if an AND connector was used, then the associated fold change for this reaction was its minimum. The complete list of genes mapped to the metabolic pathways and their expression levels can be found in **Supplementary Table 4**.

DATA AVAILABILITY STATEMENT

The datasets presented in this study can be found in online repositories. The names of the repository/repositories and accession number(s) can be found below: https://www.ncbi.nlm.nih.gov/bioproject/, PRJNA744511.

AUTHOR CONTRIBUTIONS

JO-S, VC, and AM conceived and designed the study. JO-S developed the defined medium and performed bacterial growth assays. JO-S and CS performed ARG predictions and antibiotic susceptibility testing. JO-S carried out RNA extraction, interpreted the RNA-seq results, and prepared the figures. NJ and MC carried out the analysis of metabolic pathways and prepared the figures. JM and RP performed bioinformatics and statistical analyses. AM and VC contributed with valuable feedback and funding acquisition. JO-S and VC wrote this article with input from all other authors. All authors reviewed the manuscript.

FUNDING

This study was supported by Fondecyt grants 1160802 and 1211893 (VC), ANID/FONDAP/15200002, and Grant Basal ANID AFB170001. JO-S is recipient of an INTA-Nestlé Abraham Stekel fellowship.

ACKNOWLEDGMENTS

The authors would like to thank Alexis Gaete for helping us with the Nanopore sequencing.

SUPPLEMENTARY MATERIAL

The Supplementary Material for this article can be found online at: https://www.frontiersin.org/articles/10.3389/fmicb.2021.734239/full#supplementary-material

REFERENCES

Alcock, B. P., Raphenya, A. R., Lau, T. T. Y., Tsang, K. K., Bouchard, M., Edalatmand, A., et al. (2020). CARD 2020: Antibiotic resistome surveillance with the comprehensive antibiotic resistance database. *Nucleic Acids Res.* 48, D517–D525. doi: 10.1093/nar/gkz935

Al-Younes, H. M., Gussmann, J., Braun, P. R., Brinkmann, V., and Meyer, T. F. (2006). Naturally occurring amino acids differentially influence the development of *Chlamydia trachomatis* and Chlamydia (*Chlamydophila*) pneumoniae. *J. Med. Microbiol.* 55, 879–886. doi: 10.1099/jmm.0.46445-0

Anders, S., Pyl, P. T., and Huber, W. (2015). HTSeq-A Python framework to work with high-throughput sequencing data. *Bioinformatics* 31, 166–169. doi: 10.1093/bioinformatics/btu638

Andrews, S. (2010). *FastQC: A Quality Control Tool For High Throughput Sequence Data*. Available online at: http://www.bioinformatics.babraham.ac.uk/projects/fastqc (accessed October 8, 2020).

Avendaño-Herrera, R. (2018). Proper antibiotics use in the *Chilean salmon* industry: policy and technology bottlenecks. *Aquaculture* 495, 803–805. doi: 10.1016/j.aquaculture.2018.06.072

Belenky, P., Ye, J. D., Porter, C. B. M., Cohen, N. R., Lobritz, M. A., Ferrante, T., et al. (2015). Bactericidal antibiotics induce toxic metabolic perturbations that lead to cellular damage. *Cell Rep.* 13, 968–980. doi: 10.1016/j.celrep.2015.09.059

Bindea, G., Mlecnik, B., Hackl, H., Charoentong, P., Tosolini, M., Kirilovsky, A., et al. (2009). ClueGO: A Cytoscape plug-in to decipher functionally grouped gene ontology and pathway annotation networks. *Bioinformatics* 25, 1091–1093. doi: 10.1093/bioinformatics/btp101

Bravo, S., and Campos, M. (1989). Coho salmon syndrome in Chile. *Am. Fish. Soc. Newsl.* 17:3.

Bushnell, B. (2014). *BBMap: Short Read Aligner for DNA and RNA-seq Data*. Available online at: https://jgi.doe.gov/data-and-tools/bbtools/ (accessed August 10, 2020).

Cartes, C., Isla, A., Lagos, F., Castro, D., Muñoz, M., Yañez, A., et al. (2017). Search and analysis of genes involved in antibiotic resistance in Chilean strains of *Piscirickettsia salmonis*. *J. Fish Dis.* 40, 1025–1039. doi: 10.1111/jfd.12579

Chamberlain, R. E. (1965). Evaluation of live tularemia vaccine prepared in a chemically defined medium. *Appl. Microbiol.* 13, 232–235. doi: 10.1128/aem.13.2.232-235.1965

CLSI National Committee for Clinical Laboratory Standards (2015). *M45. Methods for Antimicrobial Dilution and Disk Susceptibility Testing of Infrequently Isolated or Fastidious Bacteria; Proposed Guideline*. Wayne, PA: Clinical and Laboratory Standards Institute.

Cold Spring Harbor Protocols (2006). *Cold Spring Harbor Protocols: M9 Recipe*. New York, NY: Cold Spring Harbor Protocols.

Contreras-Lynch, S., Smith, P., Olmos, P., Loy, M. E., Finnegan, W., and Miranda, C. D. (2017). A novel and validated protocol for performing MIC tests to determine the susceptibility of *Piscirickettsia salmonis* isolates to florfenicol and oxytetracycline. *Front. Microbiol.* 8:1255. doi: 10.3389/fmicb.2017.01255

Cortés, M. P., Mendoza, S. N., Travisany, D., Gaete, A., Siegel, A., Cambiazo, V., et al. (2017). Analysis of Piscirickettsia salmonis metabolism using genome-scale reconstruction, modeling, and testing. *Front. Microbiol.* 8:2462. doi: 10.3389/fmicb.2017.02462

Cvitanich, J. D. D., Garate, N. O., Smith, C. E. E., Garate, O., and Smith, C. E. E. (1991). The isolation of a rickettsia-like organism causing disease and mortality in Chilean salmonids and its confirmation by Koch's postulate. *J. Fish Dis.* 14, 121–145. doi: 10.1111/j.1365-2761.1991.tb00584.x

Erickson, D. W., Schink, S. J., Patsalo, V., Williamson, J. R., Gerland, U., and Hwa, T. (2017). A global resource allocation strategy governs growth transition kinetics of *Escherichia coli*. *Nature* 551, 119–123. doi: 10.1038/nature24299

Ersoy, S. C., Heithoff, D. M., Barnes, L., Tripp, G. K., House, J. K., Marth, J. D., et al. (2017). Correcting a fundamental flaw in the paradigm for antimicrobial susceptibility testing. *EBioMedicine* 20, 173–181. doi: 10.1016/j.ebiom.2017.05.026

Espedido, B. A., and Gosbel, I. B. (2012). Chromosomal mutations involved in antibiotic resistance in *Staphylococcus aureus*. *Front. Biosci. (Schol. Ed.)* 4:900–915. doi: 10.2741/s307

EUCAST (2019). *EUCAST: Redefining Susceptibility Testing Categories S, I and R*. Available online at: https://eucast.org/fileadmin/src/media/PDFs/EUCAST_

files/EUCAST_Presentations/2018/EUCAST_-_Intermediate_category_-_information_for_all.pdf (accessed November 30, 2020).

Farha, M. A., French, S., Stokes, J. M., and Brown, E. D. (2018). Bicarbonate alters bacterial susceptibility to antibiotics by targeting the proton motive force. *ACS Infect. Dis.* 4, 382–390. doi: 10.1021/acsinfecdis.7b00194

Feldgarden, M., Brover, V., Haft, D. H., Prasad, A. B., Slotta, D. J., Tolstoy, I., et al. (2019). Validating the AMRFINder tool and resistance gene database by using antimicrobial resistance genotype-phenotype correlations in a collection of isolates. *Antimicrob. Agents Chemother.* 63:e00483–19. doi: 10.1128/AAC.00483-19

Figueroa, J., Castro, D., Lagos, F., Cartes, C., Isla, A., Yáñez, A. J., et al. (2019). Analysis of single nucleotide polymorphisms (SNPs) associated with antibiotic resistance genes in Chilean *Piscirickettsia salmonis* strains. *J. Fish Dis.* 42, 1645–1655. doi: 10.1111/jfd.13089

Food and Agriculture Organization of the United Nations FAO (2018). *The state of World Fisheries and Aquaculture*. Rome: FAO.

Fryer, J. L., Lannan, C. N., Giovannoni, S. J., and Wood, N. D. (1992). Piscirickettsia salmonis gen. nov., sp. nov., the causative agent of an epizootic disease in salmonid fishes. *Int. J. Syst. Bacteriol.* 42, 120–126.

Fuentealba, P., Aros, C., Latorre, Y., Martinez, I., Marshall, S., Ferrer, P., et al. (2017). Genome-scale metabolic reconstruction for the insidious bacterium in aquaculture *Piscirickettsia salmonis*. *Bioresour. Technol.* 223, 105–114. doi: 10.1016/j.biortech.2016.10.024

Fuentealba, P., Latorre, Y., González, E., Martínez, I., Soto, C., and Altamirano, C. (2020). Engineering a defined culture medium to grow *Piscirickettsia salmonis* for its use in vaccine formulations. *J. Ind. Microbiol. Biotechnol.* 47, 299–309. doi: 10.1007/s10295-020-02265-9

Hawke, J. P., Reimschuesse, R., Aoki, T., Bell, T. A., Blanc, G., Carson, J., et al. (2005). *Methods for Broth Dilution Susceptibility Testing of Bacteria Isolated from Aquatic Animals; Proposed Guideline*. Wayne, PA: Clinical and Laboratory Standards Institute.

Henríquez, P., Bohle, H., Bustamante, F., Bustos, P., and Mancilla, M. (2014). Polymorphism in gyrA is associated to quinolones resistance in Chilean *Piscirickettsia salmonis* field isolates. *J. Fish Dis.* 38, 415–418. doi: 10.1111/jfd.12255

Henríquez, P., Kaiser, M., Bohle, H., Bustos, P., and Mancilla, M. (2016). Comprehensive antibiotic susceptibility profiling of Chilean *Piscirickettsia salmonis* field isolates. *J. Fish Dis.* 39, 441–448. doi: 10.1111/jfd.12427

Hicks, N. D., Yang, J., Zhang, X., Zhao, B., Grad, Y. H., Ou, X., et al. (2018). Clinically prevalent mutations in *Mycobacterium tuberculosis* alter propionate metabolism and mediate multidrug tolerance. *Nat. Microbiol.* 3, 1032–1042. doi: 10.1038/s41564-018-0218-3.Clinically

Higuera-Llantén, S., Vásquez-Ponce, F., Barrientos-Espinoza, B., Mardones, F. O., Marshall, S. H., and Olivares-Pacheco, J. (2018). Extended antibiotic treatment in salmon farms select multiresistant gut bacteria with a high prevalence of antibiotic resistance genes. *PLoS One* 13:e0203641. doi: 10.1371/journal.pone.0203641

Jia, B., Delphino, M. K. V. C., Awosile, B., Hewison, T., Whittaker, P., Morrison, D., et al. (2020). Review of infectious agent occurrence in wild salmonids in British Columbia, Canada. *J. Fish Dis.* 43, 153–175. doi: 10.1111/jfd.13084

Jones, S. R. M., Long, A., MacWilliams, C., Polinski, M., and Garver, K. (2020). Factors associated with severity of naturally occurring piscirickettsiosis in netpen- and tank-reared juvenile Atlantic salmon at a research aquarium in western Canada. *J. Fish Dis.* 43, 49–55. doi: 10.1111/jfd.13102

Karp, P. D., Billington, R., Caspi, R., Fulcher, C. A., Latendresse, M., Kothari, A., et al. (2018). The BioCyc collection of microbial genomes and metabolic pathways. *Brief. Bioinform.* 20, 1085–1093. doi: 10.1093/bib/bbx085

King, Z. A., Dräger, A., Ebrahim, A., Sonnenschein, N., Lewis, N. E., and Palsson, B. O. (2015). Escher: a web application for building, sharing, and embedding data-rich visualizations of biological pathways. *PLoS Comput. Biol.* 11:e1004321. doi: 10.1371/journal.pcbi.1004321

Koren, S., Walenz, B. P., Berlin, K., Miller, J. R., Bergman, N. H., and Phillippy, A. M. (2017). Canu: Scalable and accurate long-read assembly via adaptive κ-mer weighting and repeat separation. *Genome Res.* 27, 722–736. doi: 10.1101/gr.215087.116

Lannan, C. N., and Fryer, J. L. (1994). Extracellular survival of *Piscirickettsia salmonis*. *J. Fish Dis.* 17, 545–548.

Li, H., and Durbin, R. (2009). Fast and accurate short read alignment with burrows-wheeler transform. *Bioinformatics* 25, 1754–1760. doi: 10.1093/bioinformatics/btp324

Li, H., Handsaker, B., Wysoker, A., Fennell, T., Ruan, J., Homer, N., et al. (2009). The sequence alignment/map format and SAMtools. *Bioinformatics* 25, 2078–2079. doi: 10.1093/bioinformatics/btp352

Liu, Y., Yang, K., Zhang, H., Jia, Y., and Wang, Z. (2020). Combating antibiotic tolerance through activating bacterial metabolism. *Front. Microbiol.* 11:577564. doi: 10.3389/fmicb.2020.577564

Lobritz, M. A., Belenky, P., Porter, C. B. M., Gutierrez, A., Yang, J. H., Schwarz, E. G., et al. (2015). Antibiotic efficacy is linked to bacterial cellular respiration. *Proc. Natl. Acad. Sci. U.S.A.* 112, 8173–8180. doi: 10.1073/pnas.1509743112

Lopatkin, A. J., Bening, S. C., Manson, A. L., Stokes, J. M., Kohanski, M. A., Badran, A. H., et al. (2021). Clinically relevant mutations in core metabolic genes confer antibiotic resistance. *Science* 371:eaba0862. doi: 10.1126/science.aba0862

Lopatkin, A. J., Stokes, J. M., Zheng, E. J., Yang, J. H., Takahashi, M. K., You, L., et al. (2019). Bacterial metabolic state more accurately predicts antibiotic lethality than growth rate. *Nat. Microbiol.* 4, 2109–2117. doi: 10.1038/s41564-019-0536-0

Love, M. I., Huber, W., and Anders, S. (2014). Moderated estimation of fold change and dispersion for RNA-seq data with DESeq2. *Genome Biol.* 15, 1–21. doi: 10.1186/s13059-014-0550-8

Machuca, A., and Martinez, V. (2016). Transcriptome analysis of the intracellular facultative pathogen *Piscirickettsia salmonis*: expression of putative groups of genes associated with virulence and iron metabolism. *PLoS One* 11:e0168855. doi: 10.1371/journal.pone.0168855

Mancilla, M. (2018). Commentary: a novel and validated protocol for performing MIC tests to determine the susceptibility of *Piscirickettsia salmonis* isolates to florfenicol and oxytetracycline. *Front. Microbiol.* 9:483. doi: 10.3389/fmicb.2018.00483

Mardones, F. O., Paredes, F., Medina, M., Tello, A., Valdivia, V., Ibarra, R., et al. (2018). Identification of research gaps for highly infectious diseases in aquaculture: the case of the endemic *Piscirickettsia salmonis* in the Chilean salmon farming industry. *Aquaculture* 482, 211–220. doi: 10.1016/j.aquaculture.2017.09.048

Martínez, J. L., and Rojo, F. (2011). Metabolic regulation of antibiotic resistance. *FEMS Microbiol. Rev.* 35, 768–789. doi: 10.1111/j.1574-6976.2011.00282.x

Mauel, M. J., and Miller, D. L. (2002). Piscirickettsiosis and piscirickettsiosis-like infections in fish: a review. *Vet. Microbiol.* 87, 279–289.

Mikalsen, J., Skjaervik, O., Wiik-Nielsen, J., Wasmuth, M. A., and Colquhoun, D. J. (2007). Agar culture of *Piscirickettsia salmonis*, a serious pathogen of farmed salmonid and marine fish. *FEMS Microbiol. Lett* 278, 43–47. doi: 10.1111/j.1574-6968.2007.00977.x

Miller, R. A., Carson, J., Dalsgaard, I., Gaunt, P. S., Gieseker, C., Hawke, J. P., et al. (2014). *VET04-A2: Methods for Broth Dilution Susceptibility Testing of Bacteria Isolated From Aquatic Animals; Approved Guideline—Second Edition*, 2nd Edn. Wayne, PA: Clinical and Laboratory Standards Institute (CLSI).

Miranda, C. D., and Rojas, R. (2007). Occurrence of florfenicol resistance in bacteria associated with two Chilean salmon farms with different history of antibacterial usage. *Aquaculture* 266, 39–46. doi: 10.1016/j.aquaculture.2007.02.007

Mosmann, T. (1983). Rapid colorimetric assay for cellular growth and survival: application to proliferation and cytotoxicity assays. *J. Immunol. Methods* 65, 55–63.

Munita, J. M., and Arias, C. A. (2016). Mechanisms of antibiotic resistance . *Microbiol. Spectr.* 4, doi: 10.1128/microbiolspec.VMBF-0016-2015

Nikaido, H. (2003). Molecular basis of bacterial outer membrane permeability revisited. *Microbiol. Mol. Biol. Rev.* 67, 593–656. doi: 10.1128/MMBR.67.4.593

Ortiz-Severín, J., Travisany, D., Maass, A., Cambiazo, V., and Chávez, F. P. (2020). Global proteomic profiling of *Piscirickettsia salmonis* and salmon macrophage-like cells during intracellular infection. *Microorganisms* 8:1845. doi: 10.3390/microorganisms8121845

Ortiz-Severín, J., Travisany, D., Maass, A., Chávez, F. P., and Cambiazo, V. (2019). *Piscirickettsia salmonis* cryptic plasmids: source of mobile DNA and virulence factors. *Pathogens* 8:269. doi: 10.3390/pathogens8040269

Pethe, K., Sequeira, P. C., Agarwalla, S., Rhee, K., Kuhen, K., Phong, W. Y., et al. (2010). A chemical genetic screen in Mycobacterium tuberculosis identifies

carbon-source-dependent growth inhibitors devoid of in vivo efficacy. *Nat. Commun.* 1:57. doi: 10.1038/ncomms1060

Pfaffl, M. W. (2001). A new mathematical model for relative quantification in real-time RT-PCR. *Nucleic Acids Res.* 29:e45.

Price, C. T. D., Richards, A. M., Von Dwingelo, J. E., Samara, H. A., and Abu Kwaik, Y. (2014). Amoeba host-Legionella synchronization of amino acid auxotrophy and its role in bacterial adaptation and pathogenic evolution. *Environ. Microbiol.* 16, 350–358. doi: 10.1111/1462-2920.12290

R Core Team (2015). *R: A Language And Environment For Statistical Computing*. Vienna: R Foundation for Statistical Computing.

Rowley, D. (1953). Inhibition of *E. coli* strains by amino-acids. *Nature* 171, 80–81. doi: 10.1038/171080a0

Rozas, M., and Enriquez, R. (2014). *Piscirickettsiosis* and *Piscirickettsia salmonis* in fish: a review. *J. Fish Dis.* 37, 163–188. doi: 10.1111/jfd.12211

Saavedra, J., Grandón, M., Villalobos-González, J., Bohle, H., Bustos, P., and Mancilla, M. (2018). Isolation, functional characterization and transmissibility of p3PS10, a multidrug resistance plasmid of the fish pathogen *Piscirickettsia salmonis*. *Front. Microbiol.* 9:923. doi: 10.3389/fmicb.2018.00923

San Martín, B., Fresno, M., Cornejo, J., Godoy, M., Ibarra, R., Vidal, R., et al. (2019). Optimization of florfenicol dose against *Piscirickettsia salmonis* in *Salmo salar* through PK/PD studies. *PLoS One* 14:e0215174. doi: 10.1371/journal.pone.0215174

Sanders, S., Bartee, D., Harrison, M. J., Phillips, P. D., Koppisch, A. T., and Freel Meyers, C. L. (2018). Growth medium-dependent antimicrobial activity of early stage MEP pathway inhibitors. *PLoS One* 13:e0197638. doi: 10.1371/journal.pone.0197638

Sandoval, R., Oliver, C., Valdivia, S., Valenzuela, K., Haro, R. E., Sánchez, P., et al. (2016). Resistance-nodulation-division efflux pump acrAB is modulated by florfenicol and contributes to drug resistance in the fish pathogen *Piscirickettsia salmonis*. *FEMS Microbiol. Lett.* 363:fnw102. doi: 10.1093/femsle/fnw102

Sandoz, K. M., Beare, P. A., Cockrell, D. C., and Heinzen, R. A. (2016). Complementation of arginine auxotrophy for genetic transformation of *Coxiella burnetii* by use of a defined axenic medium. *Appl. Environ. Microbiol.* 82, 3042–3051. doi: 10.1128/AEM.00261-16

SERNAPESCA (2020). *Informe Sobre Uso De Antimicrobianos En La Salmonicultura Nacional-Año 2019*. Valparaíso Available online at: http://www.sernapesca.cl/sites/default/files/informe_atb_2019_final.pdf (accessed September 13, 2020).

Shah, S. Q. A., Cabello, F. C., L'Abée-Lund, T. M., Tomova, A., Godfrey, H. P., Buschmann, A. H., et al. (2014). Antimicrobial resistance and antimicrobial resistance genes in marine bacteria from salmon aquaculture and non-aquaculture sites. *Environ. Microbiol.* 16, 1310–1320. doi: 10.1111/1462-2920.12421

Shin, J., Choe, D., Ransegnola, B., Hong, H., Onyekwere, I., Cross, T., et al. (2021). A multifaceted cellular damage repair and prevention pathway promotes high-level tolerance to β-lactam antibiotics. *EMBO Rep.* 22, 1–23. doi: 10.15252/embr.202051790

Smith, P. A., Pizarro, P., Ojeda, P., Contreras, J., Oyanedel, S., and Larenas, J. (1999). Routes of entry of *Piscirickettsia salmonis* in rainbow trout *Oncorhynchus mykiss*. *Dis. Aquat. Organ.* 37, 165–172. doi: 10.3354/dao037165

Sprouffske, K., and Wagner, A. (2016). Growthcurver: an R package for obtaining interpretable metrics from microbial growth curves. *BMC Bioinformatics* 17:172. doi: 10.1186/s12859-016-1016-7

Stokes, J. M., Lopatkin, A. J., Lobritz, M. A., and Collins, J. J. (2019). Bacterial metabolism and antibiotic efficacy. *Cell Metab.* 30, 251–259. doi: 10.1016/j.cmet.2019.06.009

Tada, H., Shiho, O., Kuroshima, K., Koyama, M., and Tsukamoto, K. (1986). An improved colorimetric assay for interleukin 2. *J. Immunol. Methods* 93, 157–165.

Tamminen, M., Karkman, A., Lõhmus, A., Muziasari, W. I., Takasu, H., Wada, S., et al. (2011). Tetracycline resistance genes persist at aquaculture farms in the absence of selection pressure. *Environ. Sci. Technol.* 45, 386–391. doi: 10.1021/es102725n

Tatusov, R. L. (2000). The COG database: a tool for genome-scale analysis of protein functions and evolution. *Nucleic Acids Res.* 28, 33–36. doi: 10.1093/nar/28.1.33

Tesh, M. J., and Miller, R. D. (1981). Amino acid requirements for *Legionella pneumophila* growth. *J. Clin. Microbiol.* 13, 865–869. doi: 10.1128/jcm.13.5.865-869.1981

Tomova, A., Ivanova, L., Buschmann, A. H., Rioseco, M. L., Kalsi, R. K., Godfrey, H. P., et al. (2015). Antimicrobial resistance genes in marine bacteria and human uropathogenic *Escherichia coli* from a region of intensive aquaculture. *Environ. Microbiol. Rep.* 7, 803–809. doi: 10.1111/1758-2229.12327

Valenzuela-Miranda, D., and Gallardo-Escárate, C. (2018). Dual RNA-Seq uncovers metabolic amino acids dependency of the intracellular bacterium *Piscirickettsia salmonis* Infecting *Atlantic salmon*. *Front. Microbiol.* 9:2877. doi: 10.3389/fmicb.2018.02877

Vera, T., Isla, A., Cuevas, A., and Figueroa, J. (2012). A new liquid medium for the pathogen *Piscirickettsia salmonis*. *Arch. Med. Vet.* 277, 273–277.

Walker, B. J., Abeel, T., Shea, T., Priest, M., Abouelliel, A., Sakthikumar, S., et al. (2014). Pilon: An integrated tool for comprehensive microbial variant detection and genome assembly improvement. *PLoS One* 9:e112963. doi: 10.1371/journal.pone.0112963

Washburn, M. R., and Niven, C. F. (1948). Amino acid interrelationships in the nutrition of *Streptococcus bovis*. *J. Bacteriol.* 55, 769–776. doi: 10.1128/jb.55.6.769-776.1948

Yánez, A. J., Valenzuela, K., Matzner, C., Olavarría, V., Figueroa, J., Avendaño-Herrera, R., et al. (2013). Broth microdilution protocol for minimum inhibitory concentration (MIC) determinations of the intracellular salmonid pathogen *Piscirickettsia salmonis* to florfenicol and oxytetracycline. *J. Fish Dis.* 37, 505–509. doi: 10.1111/jfd.12144

Yang, J. H., Bening, S. C., and Collins, J. J. (2017). Antibiotic efficacy – context matters. *Curr. Opin. Microbiol.* 39, 73–80. doi: 10.1016/j.mib.2017.09.002

Yang, J. H., Wright, S. N., Hamblin, M., McCloskey, D., Alcantar, M. A., Schrübbers, L., et al. (2019). A white-box machine learning approach for revealing antibiotic mechanisms of action. *Cell* 177, 1649–1661.e9. doi: 10.1016/j.cell.2019.04.016

Yin, X., Jiang, X. T., Chai, B., Li, L., Yang, Y., Cole, J. R., et al. (2018). ARGs-OAP v2.0 with an expanded SARG database and Hidden Markov Models for enhancement characterization and quantification of antibiotic resistance genes in environmental metagenomes. *Bioinformatics* 34, 2263–2270. doi: 10.1093/bioinformatics/bty053

Zúñiga, A., Aravena, P., Pulgar, R., Travisany, D., Ortiz-Severín, J., Chávez, F. P., et al. (2020). Transcriptomic changes of *Piscirickettsia salmonis* during intracellular growth in a salmon macrophage-like cell line. *Front. Cell. Infect. Microbiol.* 9:426. doi: 10.3389/fcimb.2019.00426

Conflict of Interest: The authors declare that the research was conducted in the absence of any commercial or financial relationships that could be construed as a potential conflict of interest.

Publisher's Note: All claims expressed in this article are solely those of the authors and do not necessarily represent those of their affiliated organizations, or those of the publisher, the editors and the reviewers. Any product that may be evaluated in this article, or claim that may be made by its manufacturer, is not guaranteed or endorsed by the publisher.

frontiers in Microbiology

ORIGINAL RESEARCH
published: 24 November 2021
doi: 10.3389/fmicb.2021.742114

Hfq Regulates Efflux Pump Expression and Purine Metabolic Pathway to Increase Trimethoprim Resistance in *Aeromonas veronii*

Dan Wang[1,2], Hong Li[1], Xiang Ma[1], Yanqiong Tang[1], Hongqian Tang[1], Dongyi Huang[2], Min Lin[3] and Zhu Liu[1]**

[1] College of Life Sciences, Hainan University, Haikou, China, [2] College of Tropical Crops Hainan University, Haikou, China, [3] Chinese Academy of Agricultural Science, Beijing, China

OPEN ACCESS

Edited by:
Xinhua Chen,
Fujian Agriculture and Forestry University, China

Reviewed by:
Jose L. Martinez,
Consejo Superior de Investigaciones Científicas (CSIC), Spain
Kunihiko Nishino,
Osaka University, Japan
Yuanhuan Kang,
Shandong University, China

***Correspondence:**
Dongyi Huang
hdongyi@hainanu.edu.cn
Zhu Liu
zhuliu@hainanu.edu.cn

Specialty section:
This article was submitted to Antimicrobials, Resistance and Chemotherapy, a section of the journal Frontiers in Microbiology

Received: 15 July 2021
Accepted: 22 October 2021
Published: 24 November 2021

Citation:
Wang D, Li H, Ma X, Tang Y, Tang H, Huang D, Lin M and Liu Z (2021) Hfq Regulates Efflux Pump Expression and Purine Metabolic Pathway to Increase Trimethoprim Resistance in Aeromonas veronii. Front. Microbiol. 12:742114. doi: 10.3389/fmicb.2021.742114

Aeromonas veronii (A. veronii) is a zoonotic pathogen. It causes clinically a variety of diseases such as dysentery, bacteremia, and meningitis, and brings huge losses to aquaculture. *A. veronii* has been documented as a multiple antibiotic resistant bacterium. Hfq (host factor for RNA bacteriophage Qβ replication) participates in the regulations of the virulence, adhesion, and nitrogen fixation, effecting on the growth, metabolism synthesis and stress resistance in bacteria. The deletion of *hfq* gene in *A. veronii* showed more sensitivity to trimethoprim, accompanying by the upregulations of purine metabolic genes and downregulations of efflux pump genes by transcriptomic data analysis. Coherently, the complementation of efflux pump-related genes *acrA* and *acrB* recovered the trimethoprim resistance in Δ*hfq*. Besides, the accumulations of adenosine and guanosine were increased in Δ*hfq* in metabonomic data. The strain Δ*hfq* conferred more sensitive to trimethoprim after appending 1 mM guanosine to M9 medium, while wild type was not altered. These results demonstrated that Hfq mediated trimethoprim resistance by elevating efflux pump expression and degrading adenosine, and guanosine metabolites. Collectively, Hfq is a potential target to tackle trimethoprim resistance in *A. veronii* infection.

Keywords: *Aeromonas veronii*, Hfq, trimethoprim, antibiotic resistance, *acrA*/*acrB*, purine pathway

INTRODUCTION

Aeromonas veronii (A. veronii) is a rod-shaped gram-negative pathogen found in diseased grass fish, tilapia, and turtles. It can cause huge losses in the aquaculture industry but also infect humans (Liu et al., 2015; Wang et al., 2019). *A. veronii* performs multiple drug resistance to antibiotics such as ampicillin, kanamycin, streptomycin, and gentamycin, resulting in the increased risk of human diseases and the greater losses to the fishery (Liu et al., 2017; Wang et al., 2019; Zhang et al., 2019). Hfq is a relatively common molecular chaperone that interacts with small RNAs to mediate the binding of small RNA to mRNA and assists in the post-transcriptional regulation of bacterial genes. Hfq participates in several regulatory pathways as a global regulator (Kakoschke et al., 2016).

TABLE 1 | Strains and plasmids used in this paper.

Strains or plasmids	Traits	Sources
E. coli WM3064	Gene cloning strain	Liu et al., 2016
Aeromonas veronii	Wild type strain	Liu et al., 2016
Δ*hfq*	*hfq* deletion mutant	Zhang et al., 2019
Δ*hfq::hfq*	*hfq* complement strain	Zhang et al., 2019
Δ*hfq::acrAB*	acrAB overexpression in hfqmutant strain	This paper
pBBR1MCS-2	Gene cloning vector	Zhang et al., 2019
pBBR *acrAB*	acrA/B overexpression vector	This paper

Deletion of *hfq* reduces tolerance to harsh environments in Escherichia *coli, Salmonella enterica*, and *Vibrio hollisae* (Yamada et al., 2010; Hayashi-Nishino et al., 2012; Azam and Vanderpool, 2018). Hfq is involved in regulating the virulence of *Aeromonas hydrophila*, the adhesion of *Vibrio alginolyticus*, and the nitrogen fixation efficiency and plant interactions of *Pseudomonas stutzeri* (Hayashi-Nishino et al., 2012; Kakoschke et al., 2016; Azam and Vanderpool, 2018; Santiago-Frangos and Woodson, 2018).

Albeit there are few studies on Hfq-related drug resistance, Hfq is documented to affect multidrug resistance of *E. coli* (Yamada et al., 2010). In this study, the *hfq* knockout strain (Δ*hfq*) of *A. veronii* conferred more sensitive to trimethoprim. Trimethoprim is a broad-spectrum antibacterial that inhibits the activity of dihydrofolate reductase and the synthesis of tetrahydrofolate (Stepanek et al., 2016). Tetrahydrofolate is a one-carbon unit donor that provides the raw materials needed to synthesize purine nucleotides and thymidine nucleotides *in vivo*. Tetrahydrofolate is concerned with the regulation of purine metabolism and is closely related to bacterial nucleic acid synthesis, energy metabolism, ion transport and signal transduction (Jinnah et al., 2013; Vazquez-Salazar et al., 2018).

In addition, the absence of *hfq* affects the expression of the efflux pump gene *acrAB* (Spaniol et al., 2015). AcrB belongs to the resistance-nodulation-cell division superfamily (RND). The substrates for the AcrAB-TolC efflux pump include a variety of antibiotics, detergents, bactericides, fuels, and free fatty acids (Li et al., 2015; Phetsang et al., 2016). The efflux pump can excrete trimethoprim, affecting the antibacterial effect of trimethoprim (Köhler et al., 1996; Podnecky et al., 2013). The efflux pump AcrAB accounts for a large proportion of the mechanisms of bacterial antibiotic resistance (Elsby et al., 2017; Zwama et al., 2018). Therefore, it is hypothesized that the sensitivity of *A. veronii* to trimethoprim may be related to the expression of the efflux pump. In summary, Hfq indirectly affects the sensitivity of trimethoprim by affecting purine metabolism and efflux pumping; these effects are important for further understanding of the molecular mechanisms of multidrug resistance.

MATERIALS AND METHODS

Strains and Culture

The strain information was listed in **Table 1**. The derivative *A. veronii* strains included wild-type, Δ*hfq*, Δ*hfq:hfq*, and Δ*hfq:acrAB*. The strains were cultured in M9 minimal medium (M9) at 30°C, 150 r/min, supplemented with 50 μg/mL ampicillin. Δ*hfq* represents the *hfq* knockout strain (Zhang et al., 2019). Δ*hfq:acrAB* overexpresses the *acrAB* gene in the *hfq* knockout strain. The strain *E. coli* WM 3064 was applied to assist in the introduction of the plasmids into *A. veronii* by tri-parent conjugation (Simon et al., 1983; Ferrieres et al., 2010). For the culture of strain WM3064, 0.3 mM diaminopimelic acid was supplemented in LB at 37°C.

Vector and Primers

The vector and primers were listed in **Table 2**. For the construction of the expression vector of the efflux pump-associated gene *acrAB*, the *acrA* and *acrB* genes were inserted into the plasmid pBBR1MCS-2, wherein the enzyme cleavage sites were *Sal*I and *Eco*RI. The upstream and downstream primers required for the construction were *acrA* F 5′-ACGCGTCGACTTGGTATCGGCTGGGGATTG-3′ and *acrB* 5′-CCGGAATTCATGAGCGTCGGGAGAG-3′.

Minimum Inhibitory Concentration Test

Antibiotics were added to sterile 96-well plates at final concentrations of 64, 32, 16, 8, 4, 2, 1, 0.5, 0.25, and 0.125 μg/mL (Andrews, 2001). Then, 10^6 CFU broth was added to each well to a final volume of 200 μL. The 96-well plate was sealed with parafilm and cultured at 30°C with shaking at 150 r/min for 24 h. The experiment was repeated for 3 times.

Transcriptomic Analysis

The wild type and Δ*hfq* strain were cultured in M9 medium containing 50 μg/mL ampicillin, cultured at 30°C and 150 r/min for 20 h, centrifuged to remove the culture medium, and washed with sterile PBS for transcriptomic analysis. The sequencing was carried out by BGI (Beijing Genomics Institution). The cells were collected and lysed, and the sample RNA was extracted with

TABLE 2 | Primers used in this paper.

Names of primers	Sequences (5′-3′)	Usage
WP_041202667.1-F	ATGGTCGCAGAGCTTGTC	Strain validation
WP_041202667.1-R	CAGCACAATAGAACACCAGAC	Strain validation
*acrA Sal*I F	ACGCGTCGACTTGGTATCG GCTGGGGATTG	*acrAB* vector construction
*acrB Eco*RI R	CCGGAATTCATGAGCGTCGGGAGAG	*acrAB* vector construction
pBBR1MCS-2 F	GGCACCCCAGGCTTTACACT	Complement plasmid validation
pBBR1MCS-2 R	GATGTGCTGCAAGGCGATTAAG	Complement plasmid validation

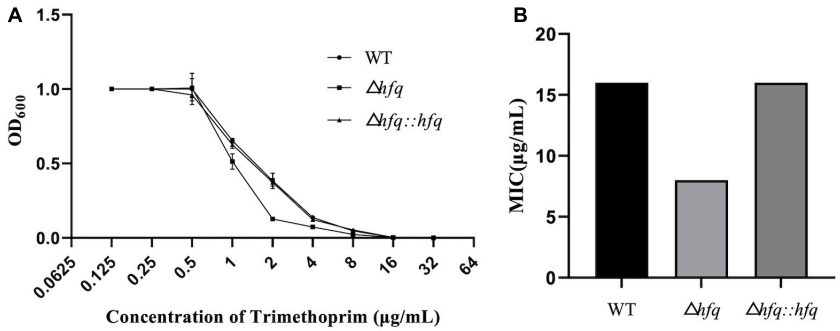

FIGURE 1 | Growth and Minimum inhibitory concentration (MIC) of trimethoprim. **(A)** The growth of three *A. veronii* strain: wildtype, Δ*hfq,* and Δ*hfq:hfq*. **(B)** The MIC of trimethoprim of wildtype, Δ*hfq,* and Δ*hfq:hfq.*

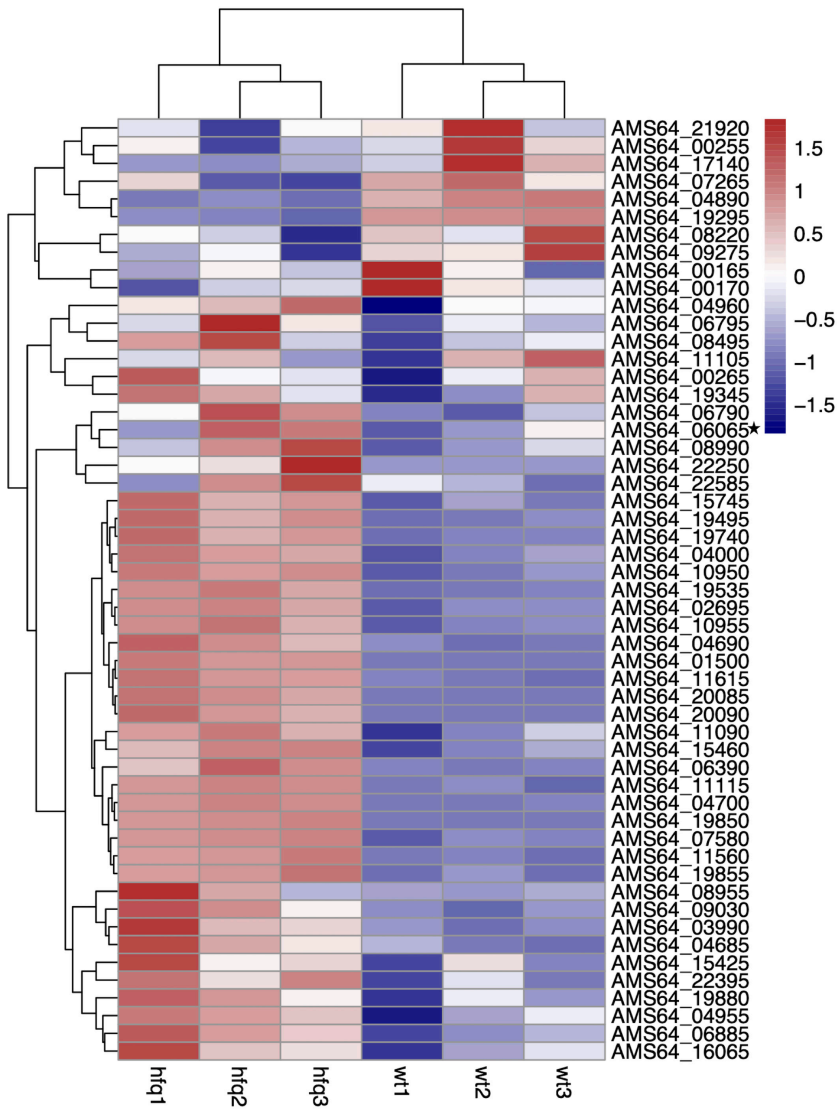

FIGURE 2 | Transcriptomic data of *Aeromonas veronii*. Heat map of expression levels of genes involved in purine metabolism and efflux pump synthesis of wild-type and Δ*hfq* strains.

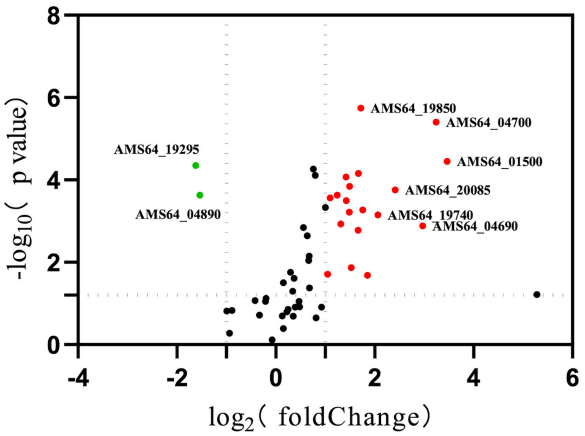

FIGURE 3 | Expression of genes related to purine metabolism. Green represents down-regulated genes with significant differences. Red indicates up-regulated genes with a significant difference. *represents $p < 0.05$.

phenol-chloroform. The concentration and quality of the RNA samples were tested with the Agilent 2100. DNase I was used to remove double-stranded DNA, and a Ribo-Zero Magnetic Kit was used to remove ribosome RNA. Reverse transcription was performed with random primers and first strand cDNA as a template to synthesize the second strand. The linker sequence was attached to the 3′ end of the cDNA fragment. The cDNA sequence was amplified with a primer cocktail, and the purified product was sequenced on a HiSeq Xten (Illumina, San Diego, CA, United States) platform. The sequencing depth was chain-specific sequencing for 2 Gb of clean data. HISAT was attempted for genome assembly, potential coding sequence analysis and new transcript identification that may be present. The transcriptional differences between wild-type and *hfq* knockout were analyzed by Bowtie 2, and FPKM was used to normalize gene expression levels. Each gene expression was calculated using the Benjamini-Hochberg false discovery rate (FDR). The differential transcripts were tested for log-fold change, and the *p* value was corrected with FDR < 0.001. The differential genes were analyzed using GO classification, and disparity expression in the pathway was compared with the entire genomic background using hypergeometric analysis $p \leq 0.05$ was a differential metabolic pathway. GEO accession number was GSE120603, and the URL of accession website was displayed as https://submit.ncbi.nlm.nih.gov/subs/sra/SUB6133286. The DESeq. 2 packages in R were applied to estimate the fold changes and perform other analysis. *A. veronii* TH0426 genome (Genomic Sequence: NZ_CP012504.1) was referenced for transcriptome analysis (Kang et al., 2016).

Metabolomics Analysis

The non-target metabolomic and lipidomic detection platform (UHPLC-QTOF-MS) was applied to metabolomics for the detection of *A. veronii* samples. UHPLC-QTOF-MS included Ultra-Performance Liquid Chromatography 1290UHPLC

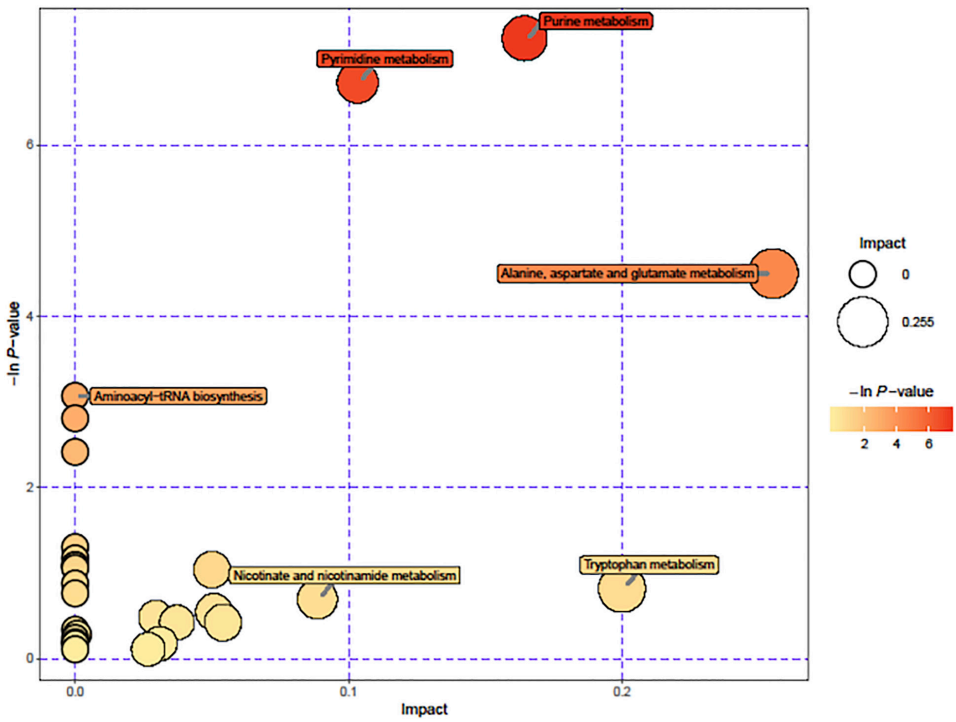

FIGURE 4 | Pathways affected by *hfq* knockout. The circle diameter indicates the degree of influence of the pathway, and the –ln (*p* value) and color indicate the significant difference in the number of genes regulated by the pathway for the entire genomic background.

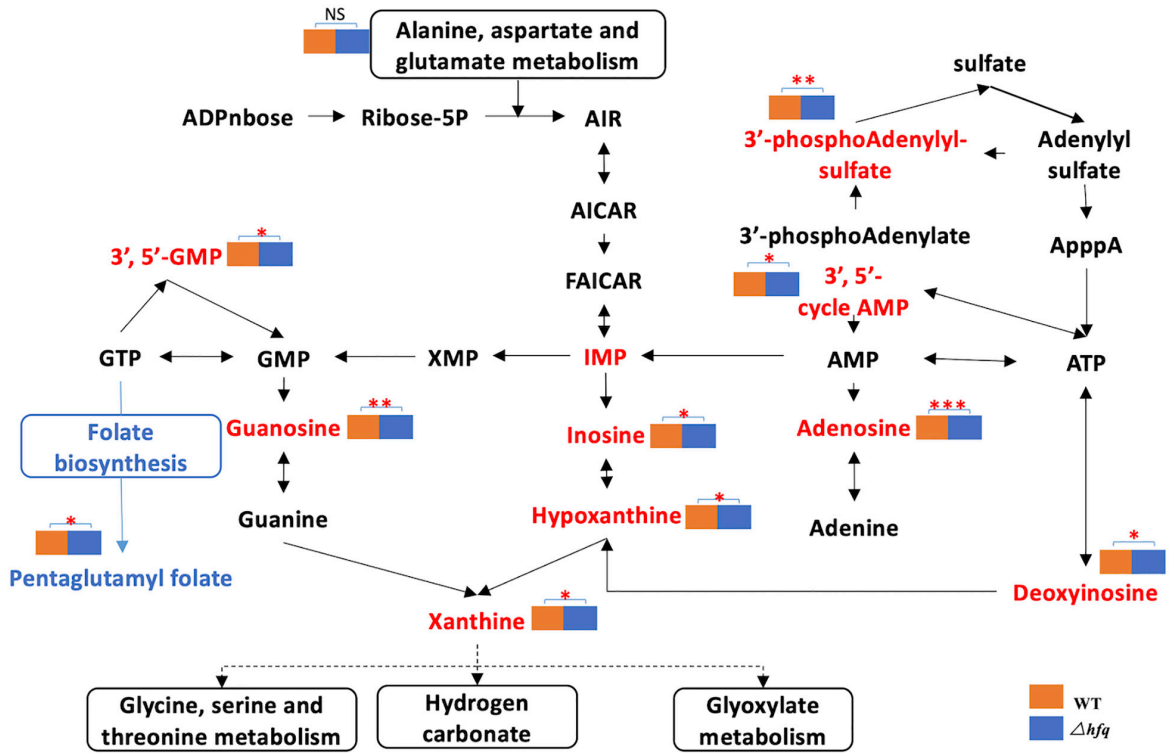

FIGURE 5 | Metabolites of the purine metabolic pathway of *Aeromonas veronii*. The red font indicates the increased metabolites, and the blue color indicates the decreased metabolites. The metabolic pathway is framed by a solid line. * represents the difference between Δ*hfq* and wild-type metabolites. * represents $p < 0.05$, ** represents $p < 0.005$, and *** represents $p < 0.001$.

(Agilent), ACQUITY UPLC BEH Amide column 1.7 μm, 2.1 × 100 mm (Waters) and High-Resolution Mass Spectrometry Triple TOF 6600 (AB Sciex). The original mass spectrum was converted to the mzXML format using Proteo Wizard software, and the peaks were identified using the R Programming Language package (Version 3.2) and self-built secondary mass spectrometry data. URL of accession website was displayed as www.ebi.ac.uk/metabolights/MTBLS1411.

Statistical Analysis

Statistical data were analyzed using the statistical Package for the Social Science (SPSS) version 20.0 (SPSS, Chicago, IL, United States) and GraphPad Prism version 8.0 (GraphPad, San Diego, CA, United States). The results are presented as the mean values of three independent experiments with standard deviation using one-way analysis of variance. $p < 0.05$ or 0.01 were represented as significant or extremely significant, respectively.

RESULTS

Hfq Deletion Reduces Multiple Resistance to Antibiotics Including Trimethoprim

According to previous studies, *A. veronii* were resistant to gentamycin, kanamycin, streptomycin, and were sensitive to chloramphenicol, ciprofloxacin (Liu et al., 2018). Trimethoprim, as an antibiotic that inhibits folic acid metabolism, has a strong inhibitory effect on a variety of bacteria. Resistance to trimethoprim was found to be altered in the absence of hfq (**Figure 1A**). The mutant Δ*hfq* was more sensitive to trimethoprim than wild type, which exhibited with a minimum inhibitory concentration (MIC) of 8 μg/mL in contrast to 16 μg/mL of wild type. The complemented strain attenuated the sensitivity of Δ*hfq* to trimethoprim, and the MIC was the same as that of wild type (**Figure 1B**).

Upregulation of Purine Metabolic Gene Expression and Downregulation of Efflux Pump-Related Genes in Δ*hfq* Strain

To understand the changes of drug resistance in Δ*hfq* strains, transcriptome sequencing was used to compare metabolic pathways with significant variations in expression levels and to analyze their relationship with trimethoprim resistance. The clustering analysis revealed that many genes related to purine metabolism and efflux pump synthesis were expressed differently (**Figure 2**). Although the direct target of trimethoprim was dihydrofolate reductase, the transcriptions of dihydrofolate reductase were not significantly different between Δ*hfq* and wild type (**Figure 2** marked with star). However, the expression of 53 genes was affected in purine metabolism, which functioned

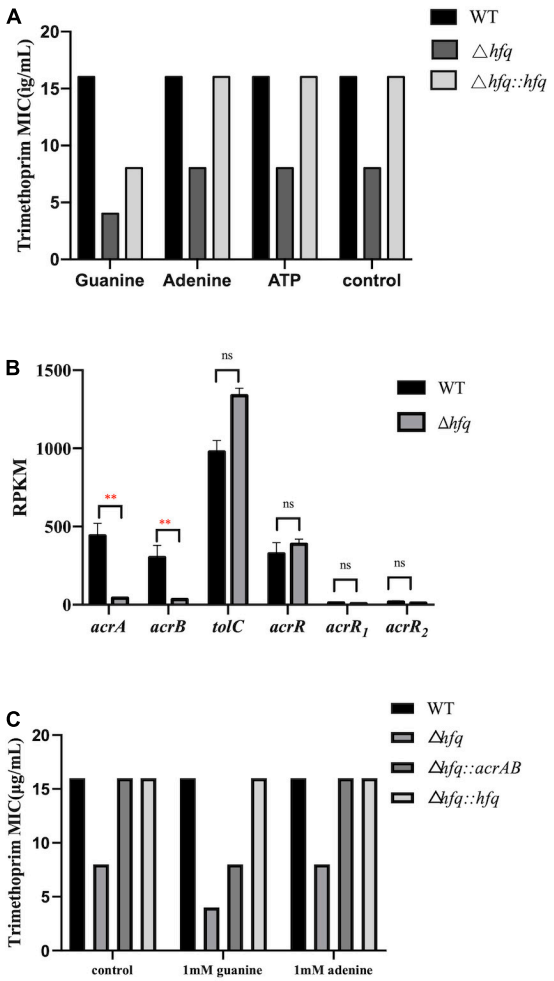

FIGURE 6 | MIC of trimethoprim under conditions of exogenous purine metabolites and overexpressed AcrAB. **(A)** The concentrations of exogenous products are 1 mM for adenosine, guanosine, and adenosine triphosphate, and ATP. Equal volume of ddH_2O was added as a control group **(B)**. Expression of key genes in the efflux pump. The rpkm of three *acrR* copies was presented separately. **(C)** MIC of trimethoprim to *Aeromonas veronii* overexpressing *acrAB*. * represents $p < 0.05$, ** represents $p < 0.01$, and ns represents no significant difference.

as the downstream of folate metabolism (**Figure 3**). There were 21 genes marked with red were up-regulated which led to purine accumulation. Two genes marked with green, as purine consuming enzymes including xanthine nucleic acid transferase and hypoxanthine nucleic acid transferase, were significantly down-regulated.

Metabolomics Analysis Displays That Δ*hfq* Enhances Purine Metabolism

Due to the significant changes of transcription in metabolic pathways, variant metabolites of these pathways have been hypothesized to be responsible for trimethoprim resistance. The differential metabolites of wild-type and Δ*hfq* were screened, analyzed, and classified into metabolic pathways (**Figure 4**). Purine metabolism, pyrimidine metabolism, and alanine, aspartate, and glutamic acid metabolism were greatly affected by the deletion of *hfq*, of which the effects on purine metabolism and pyrimidine metabolism were prominent. The deletion of Hfq incurred a significant increase of purine metabolites including adenosine, guanosine, and xanthine (**Figure 5**).

The Accumulation of Purine Metabolites Enhances the Sensitivity of Δ*hfq* to Trimethoprim

The purine metabolites, such as guanosine and adenosine, were significantly increased in Δ*hfq* compared with wild type (**Figure 3**). To understand whether the accumulation of metabolites changed the trimethoprim sensitivity of *hfq* knockout, the downstream products such as 1 mM adenine, 1 mM guanine, and 1 mM ATP were added to the M9 medium to evaluate the MIC separately (Yang et al., 2019). The MIC of wild type was not altered when supplemented with 1 mM guanosine (**Figure 6A**), while that of Δ*hfq* was decreased. There had little evident changes both in wild type and Δ*hfq* after appending with 1 mM adenine or ATP. The above results suggested that the additional guanine enhanced the sensitivity of Δ*hfq* to trimethoprim.

Overexpression of *acrAB* Enhances the Tolerance to Trimethoprim

AcrAB-TolC is capable of actively transporting antibiotics (Li et al., 2015), and trimethoprim can be transported outside the cell membrane by an efflux pump of *P. aeruginosa*. According to the transcriptomic data, the mRNA levels of *acrA* and *acrB* in Δ*hfq* were significantly reduced (by 9.30-fold and 9.34-fold) compared with wild type, but those of three copies of transcriptional repressor *acrR,* and that of component *tolC* (by 1.35-fold) were transcribed consistently (**Figure 6B**). The *acrAB* overexpression vector was constructed and transferred into the Δ*hfq* strain. The overexpression strain Δ*hfq*:*acrAB* showed an increased MIC and enhanced tolerance compared with Δ*hfq*. Overexpression of *acrAB* reversed the loss of *hfq*, resulting in inefficient discharge of trimethoprim (**Figure 6C**).

DISCUSSION

As a small chaperone protein, Hfq regulates gene expression by binding to sRNA and mRNA in response to external stress and environmental changes. Previous studies revealed that Hfq acts on a variety of membrane-associated protein genes, affecting bacterial growth, cell membrane formation, virulence, drug resistance, stress tolerance, and retention of retained bacteria (Hayashi-Nishino et al., 2012; Zhang et al., 2019).

Aeromonas *veronii* is highly resistant to ampicillin, kanamycin, gentamicin, streptomycin, and spectinomycin (Liu et al., 2016; Zhang et al., 2019). Previously the MIC of *hfq* knockout strain is significantly lower than that of wild type under the treatment of antibiotics (Zhang et al., 2019). As the substrate of nucleotide, the related genes and products

of purine pathway showed significant differences in Hfq mutant strain (**Figures 3**, **5**).But in fact, the productions of purines and nucleotides are affected by one carbon unit carrier tetrahydrofolate, and the latter is controlled by dihydrofolate reductase in turn (Paulsen et al., 2013). Since antibiotic trimethoprim targets dihydrofolate reductase specifically (Darrell et al., 1968; Bourne, 2014; Toulouse et al., 2020), trimethoprim is treated for Hfq knockout instead of other antibiotics. There are many mechanisms for resistance, of which efflux pump is important for multidrug resistance in bacteria (Elsby et al., 2017). The active transport function of the efflux pump is one of the main reasons for the decreased resistance to antibiotics (Abdali et al., 2017). The efflux pump AcrAB-TolC is an RND-type efflux pump that transports antibiotics through the inner membrane, periplasmic cavity, and outer membrane to the outside of the bacteria (Wang et al., 2017; Shi et al., 2019). The downregulations of the efflux pump-related genes *acrA* and *acrB* interfere with the assembly of the efflux pump, which reduce the ability of the efflux pump to bind and transport antibiotics and increase the sensitivity of the bacteria to trimethoprim (Cunrath et al., 2019). As a negative regulator of *acrAB*, the transcription level of *acrR* maintained a consistent in Δ*hfq*, indicating that *acrAB* was regulated independently by Hfq rather than AcrR.

The enzymes of purine metabolism were enhanced in Δ*hfq* strain, companying with the augmented productions of intermediate metabolites guanosine and adenosine. However, the quantities of downstream metabolites including glutamine, serine, threonine and glyoxylate were not significantly altered (**Figure 3**). In this study, metabolomics data showed that the deletion of *hfq* gene influenced on the basal metabolic pathways such as bacterial energy metabolism, hydrazine, and pyrimidine anabolism (**Figures 4**, **5**).

Our experimental results demonstrated that Hfq affected the sensitivity of *A. veronii* to trimethoprim through different pathways. The downregulation of efflux pump system genes reduced the assembly of the efflux pump complex and decreased the ability of the cell to export trimethoprim. The transcriptional upregulation of many genes in purine metabolic pathway recruited the accumulation of metabolites, making *A. veronii* more sensitive to trimethoprim.

DATA AVAILABILITY STATEMENT

The datasets presented in this study can be found in online repositories. The names of the repository/repositories and accession number(s) can be found in the article/supplementary material.

AUTHOR CONTRIBUTIONS

ZL, XM, ML, DH, and DW contributed the conception and design of the study. DW, HL, YT, and HT performed the statistical analysis. DW and ZL drafted the manuscript. All authors contributed to manuscript revision, read, and approved the submitted version.

FUNDING

This work was supported by the grants from the National Natural Science Foundation of China Nos. 31772887 (to ZL) and 32060153 (to HL).

REFERENCES

Abdali, N., Parks, J. M., Haynes, K. M., Chaney, J. L., Green, A. T., Wolloscheck, D., et al. (2017). Reviving antibiotics: efflux pump inhibitors that interact with AcrA, a membrane fusion protein of the AcrAB-TolC multidrug efflux pump. *ACS Infect. Dis.* 3, 89–98. doi: 10.1021/acsinfecdis.6b00167

Andrews, J. M. (2001). Determination of minimum inhibitory concentrations. *J. Antimicrob. Chemother.* 48(Suppl. 1), 5–16. doi: 10.1093/jac/48.suppl_1.5

Azam, M. S., and Vanderpool, C. K. (2018). Translational regulation by bacterial small RNAs via an unusual Hfq-dependent mechanism. *Nucleic Acids Res.* 46, 2585–2599. doi: 10.1093/nar/gkx1286

Bourne, C. R. (2014). Utility of the biosynthetic folate pathway for targets in antimicrobial discovery. *Antibiotics (Basel).* 3, 1–28. doi: 10.3390/antibiotics3010001

Cunrath, O., Meinel, D. M., Maturana, P., Fanous, J., Buyck, J. M., Saint Auguste, P., et al. (2019). Quantitative contribution of efflux to multi-drug resistance of clinical *Escherichia coli* and *Pseudomonas aeruginosa* strains. *EBioMedicine* 41, 479–487. doi: 10.1016/j.ebiom.2019.02.061

Darrell, J. H., Garrod, L. P. and Waterworth P. M. (1968). Trimethoprim: laboratory and clinical studies. *J. Clin. Pathol.* 21, 202–209. doi: 10.1136/jcp.21.2.202

Elsby, R., Chidlaw, S., Outteridge, S., Pickering, S., Radcliffe, A., Sullivan, R., et al. (2017). Mechanistic in vitro studies confirm that inhibition of the renal apical efflux transporter multidrug and toxin extrusion (MATE) 1, and not altered absorption, underlies the increased metformin exposure observed in clinical interactions with cimetidine, trimethoprim or pyrimethamine. *Pharmacol. Res. Perspect.* 5:e00357. doi: 10.1002/prp2.357

Ferrieres, L., Hemery, G., Nham, T., Guerout, A.-M., Mazel, D., Beloin, C., et al. (2010). Silent mischief: bacteriophage mu insertions contaminate products of *Escherichia coli* random mutagenesis performed using suicidal transposon delivery plasmids mobilized by broad-host-range RP4 conjugative machinery. *J. Bacteriol.* 192, 6418–6427. doi: 10.1128/jb.00621-10

Hayashi-Nishino, M., Fukushima, A., and Nishino, K. (2012). Impact of hfq on the intrinsic drug resistance of *salmonella enterica* serovar typhimurium. *Front. Microbiol.* 3:205. doi: 10.3389/fmicb.2012.00205

Jinnah, H. A., Sabina, R. L., and Van Den Berghe, G. (2013). Metabolic disorders of purine metabolism affecting the nervous system. *Handb. Clin. Neurol.* 113, 1827–1836. doi: 10.1016/B978-0-444-59565-2.00052-6

Kakoschke, T. K., Kakoschke, S. C., Zeuzem, C., Bouabe, H., Adler, K., Heesemann, J., et al. (2016). The RNA chaperone Hfq is essential for virulence and modulates the expression of four adhesins in *Yersinia Enterocolitica*. *Sci. Rep.* 6:29275. doi: 10.1038/srep29275

Kang, Y., Pan, X., Xu, Y., Siddiqui, S. A., Wang, C., Shan, X., et al. (2016). Complete genome sequence of the fish pathogen *Aeromonas veronii* TH0426 with potential application in biosynthesis of pullulanase and chitinase. *J. Biotechnol.* 227, 81–82. doi: 10.1016/j.jbiotec.2016.04.009

Köhler, T., Kok, M., Michea-Hamzehpour, M., Plesiat, P., Gotoh, N., Nishino, T., et al. (1996). Multidrug efflux in intrinsic resistance to trimethoprim and sulfamethoxazole in *Pseudomonas aeruginosa*. *Antimicrob. Agents Chemother.* 40, 2288–2290. doi: 10.1128/aac.40.10.2288

Li, X. Z., Plesiat, P., and Nikaido, H. (2015). The challenge of efflux-mediated antibiotic resistance in gram-negative bacteria. *Clin. Microbiol. Rev.* 28, 337–418. doi: 10.1128/CMR.00117-14

Liu, P., Chen, Y., Wang, D., Tang, Y., Tang, H., Song, H., et al. (2016). Genetic selection of peptide aptamers that interact and inhibit both small protein b and alternative ribosome-rescue factor a of *Aeromonas veronii* C4. *Front. Microbiol.* 7:1228. doi: 10.3389/fmicb.2016.01228

Liu, P., Huang, D., Hu, X., Tang, Y., Ma, X., Yan, R., et al. (2017). Targeting Inhibition of SmpB by peptide aptamer attenuates the virulence to protect zebrafish against *Aeromonas veronii* infection. *Front. Microbiol.* 8:1766. doi: 10.3389/fmicb.2017.01766

Liu, Z., Hu, K., Tang, Y., Li, H., Tang, H., Hu, X., et al. (2018). SmpB down-regulates proton-motive force for the persister tolerance to aminoglycosides in *Aeromonas veronii*. *Biochem. Biophys. Res. Commun.* 507, 407–413. doi: 10.1016/j.bbrc.2018.11.052

Liu, Z., Liu, P., Liu, S., Song, H., Tang, H., and Hu, X. (2015). Small protein B upregulates sensor kinase bvgS expression in *Aeromonas veronii*. *Front. Microbiol.* 6:579. doi: 10.3389/fmicb.2015.00579

Paulsen, J. L., Viswanathan, K., Wright, D. L., and Anderson, A. C. (2013). Structural analysis of the active sites of dihydrofolate reductase from two species of Candida uncovers ligand-induced conformational changes shared among species. *Bioorg. Med. Chem. Lett.* 23, 1279–1284. doi: 10.1016/j.bmcl.2013.01.008

Phetsang, W., Pelingon, R., Butler, M. S., Kc, S., Pitt, M. E., Kaeslin, G., et al. (2016). Fluorescent trimethoprim conjugate probes to assess drug accumulation in wild type and mutant *Escherichia coli*. *ACS Infect. Dis.* 2, 688–701. doi: 10.1021/acsinfecdis.6b00080

Podnecky, N. L., Wuthiekanun, V., Peacock, S. J., and Schweizer, H. P. (2013). The BpeEF-OprC efflux pump is responsible for widespread trimethoprim resistance in clinical and environmental *Burkholderia pseudomallei* Isolates. *Antimicrob. Agents Chemother.* 57, 4381–4386. doi: 10.1128/aac.00660-13

Santiago-Frangos, A., and Woodson, S. A. (2018). Hfq chaperone brings speed dating to bacterial sRNA. *Wiley Interdiscip. Rev. RNA* 9:e1475. doi: 10.1002/wrna.1475

Shi, X., Chen, M., Yu, Z., Bell, J. M., Wang, H., Forrester, I., et al. (2019). In situ structure and assembly of the multidrug efflux pump AcrAB-TolC. *Nat. Commun.* 10:2635. doi: 10.1038/s41467-019-10512-6

Simon, R., Priefer, U., and Pühler, A. (1983). A broad host range mobilization system for in vivo genetic engineering: transposon mutagenesis in gram negative bacteria. *Naturebiotechnology* 1, 784–791. doi: 10.1038/nbt1183-784

Spaniol, V., Bernhard, S., and Aebi, C. (2015). *Moraxella catarrhalis* AcrAB-OprM efflux pump contributes to antimicrobial resistance and is enhanced during cold shock response. *Antimicrob. Agents Chemother.* 59, 1886–1894. doi: 10.1128/AAC.03727-14

Stepanek, J. J., Schäkermann, S., Wenzel, M., Prochnow, P., and Bandow, J. E. (2016). Purine biosynthesis is the bottleneck in trimethoprim-treatedBacillus subtilis. *Proteomics Clin. Appl.* 10, 1036–1048. doi: 10.1002/prca.201600039

Toulouse, J. L., Shi, G., Lemay-St-Denis, C., Ebert, M. C. C. J. C., Deon, D., Gagnon, M., et al. (2020). Dual-Target inhibitors of the folate pathway inhibit intrinsically trimethoprim-resistant DfrB dihydrofolate reductases. *ACS Med. Chem. Lett.* 11, 2261–2267. doi: 10.1021/acsmedchemlett.0c00393

Vazquez-Salazar, A., Becerra, A., and Lazcano, A. (2018). Evolutionary convergence in the biosyntheses of the imidazole moieties of histidine and purines. *PLoS One* 13:e0196349. doi: 10.1371/journal.pone.0196349

Wang, D., Li, H., Ma, X., Tang, Y., Tang, H., Hu, X., et al. (2019). Small RNA AvrA regulates IscR to increase the stress tolerances in SmpB deficiency of *Aeromonas veronii*. *Front. Cell Infect. Microbiol.* 9:142. doi: 10.3389/fcimb.2019.00142

Wang, Z., Fan, G., Hryc, C. F., Blaza, J. N., Serysheva, I. I., Schmid, M. F., et al. (2017). An allosteric transport mechanism for the AcrAB-TolC multidrug efflux pump. *Elife* 6:e24905. doi: 10.7554/eLife.24905

Yamada, J., Yamasaki, S., Hirakawa, H., Hayashi-nishino, M., Yamaguchi, A., and Nishino, K. (2010). Impact of the RNA chaperone HFQ on multidrug resistance in *Escherichia coli*. *J. Antimicrob. Chemother.* 65, 853–858. doi: 10.1093/jac/dkq067

Yang, J. H., Wright, S. N., Hamblin, M., McCloskey, D., Alcantar, M. A., Schrübbers, L., et al. (2019). A white-box machine learning approach for revealing antibiotic mechanisms of action. *Cell* 177, 1649.e–1661.e. doi: 10.1016/j.cell.2019.04.016

Zhang, L., Yu, W., Tang, Y., Li, H., Ma, X., and Liu, Z. (2019). RNA chaperone hfq mediates persistence to multiple antibiotics in *Aeromonas veronii*. *Microb. Pathog.* 132, 124–128. doi: 10.1016/j.micpath.2019.04.045

Zwama, M., Yamasaki, S., Nakashima, R., Sakurai, K., Nishino, K., and Yamaguchi, A. (2018). Multiple entry pathways within the efflux transporter AcrB contribute to multidrug recognition. *Nat. Commun.* 9:124. doi: 10.1038/s41467-017-02493-1

Conflict of Interest: The authors declare that the research was conducted in the absence of any commercial or financial relationships that could be construed as a potential conflict of interest.

Publisher's Note: All claims expressed in this article are solely those of the authors and do not necessarily represent those of their affiliated organizations, or those of the publisher, the editors and the reviewers. Any product that may be evaluated in this article, or claim that may be made by its manufacturer, is not guaranteed or endorsed by the publisher.

Advantages of publishing in Frontiers

OPEN ACCESS
Articles are free to read for greatest visibility and readership

FAST PUBLICATION
Around 90 days from submission to decision

HIGH QUALITY PEER-REVIEW
Rigorous, collaborative, and constructive peer-review

TRANSPARENT PEER-REVIEW
Editors and reviewers acknowledged by name on published articles

Frontiers
Avenue du Tribunal-Fédéral 34
1005 Lausanne | Switzerland

Visit us: www.frontiersin.org
Contact us: frontiersin.org/about/contact

REPRODUCIBILITY OF RESEARCH
Support open data and methods to enhance research reproducibility

DIGITAL PUBLISHING
Articles designed for optimal readership across devices

FOLLOW US
@frontiersin

IMPACT METRICS
Advanced article metrics track visibility across digital media

EXTENSIVE PROMOTION
Marketing and promotion of impactful research

LOOP RESEARCH NETWORK
Our network increases your article's readership